UNIVERSITY OF CALIFORNIA,
IRVINE

Effects of Charge and Hydrophobicity on the Oligomerization of Macrocyclic β-Sheet Peptides derived from Islet Amyloid Polypeptide

DISSERTATION

submitted in partial satisfaction of the requirements
for the degree of

DOCTOR OF PHILOSOPHY

in Chemistry

by

Yilin Wang

Dissertation Committee:
Professor James Nowick, Chair
Associate Professor Jennifer Prescher
Professor David Van Vranken

2017

DEDICATION

To

my grandparents and parents

for supporting me,

even when it meant that I was not by their side.

TABLE OF CONTENTS

LIST OF FIGURES

LIST OF TABLES

ACKNOWLEDGMENTS

I would like to express my deepest gratitude to my committee chair, Professor James Nowick, who is the best mentor a graduate student could hope for. In science, his unmatched attention to detail and passionate pursuit of scientific discussions motivated me to better myself. In everyday life, his respect for diversity, patience for his students, and willingness to put others before himself leaves me humbled. Without his support, I would not be the scientist and teacher that I am today.

I would like to thank my committee members, Professor Jennifer Prescher and Professor David Van Vranken, for mentoring me these past few years. Professor Jennifer Prescher was incredibly helpful with guiding me through my orals proposal and her chemical biology class was essential towards my development as a teacher. Without the knowledge from her class, I would not have been able to instruct the Chem 128 course. Professor David Van Vranken provided unparallel support in my teaching career. When he discovered that I was teaching Chem 128 and Chem 51C, he allowed me to learn from the material that he prepared. I loved the Chem 201 class that he taught and have since applied the collaborative learning activities to my own classes.

I would like to thank the Nowick lab for being an inclusive and fun learning environment. I want to especially thank Nicholas Truex for his assistance with NMR spectroscopy and Adam Kreutzer for his assistance in X-ray crystallography. Nick and Adam provided me with support throughout my graduate career and I sincerely appreciate it. The Nowick lab is a wonderful group where ideas and creativity flourish due to constant communication, I could not have found a better lab.

I would like to thank all of the professors and staff in the UCI Department of chemistry. I thank Professor Greg Weiss for helping me grow as a teacher. I thank Dr. Phil Dennison for providing support for the NMR experiments. I will also like to thank the National Institute of Health and the National Science Foundation for supporting these projects.

Last, but not least, I would like to thank my family and my fiancé for their constant support. My family supported my decision to pursue my studies in a foreign country, even when it meant that I would be far away. My fiancé, Alexander Thuy-Boun, provided me with emotional support even when things were tough. It is thanks to them that I have the opportunity to grow and develop as a scientist.

CURRICULUM VITAE

Yilin Wang

Education

University of California, Irvine Irvine, CA
Ph.D. Department of Chemistry. (Sep 2012- present)
Thesis: Effects of Charge and Hydrophobicity on the Oligomerization of IAPP-Derived Peptides

University of Tennessee, Knoxville Knoxville, TN
Master of Science. Department of Chemistry (Aug 2012)
Thesis: Design and Synthesis of Boronic Acid-Based Sensors to Study Carbohydrates

University of Florida Gainesville, FL
Bachelor of Science, Biochemistry (Dec 2009)

Santa Fe College Gainesville, FL
Associate of Arts (April 2007)

Teaching Experience

University of California, Irvine
Instructor, Organic Chemistry, Chem 51C Spring 2017
Lecture enrollment: 370 students

- Designed and taught two one-hour-and-twenty-minutes lectures a week to sophmore students.
- Integrated active learning activities applicable to large lecture sizes such as iClicker problems to address SLOs and think-pair-share to encourage discussions for collaborative learning.
- Prepared biweekly online homework sets to keep students apprised of their progress.
- Introduced Biology and Chemistry Online Notes (BACON) tutorials so students can relate course material to real world applications.
- Prepared weekly worksheets for discussion sections led by two teaching assistants.

Instructor, Introduction to Chemical Biology, Chem 128 Summer 2016
Lecture enrollment: 26 students

- Designed and taught three two-hour lectures a week to junior and senior students.
- Began each class with a list of Student Learning Objectives (SLOs) and installed example problems addressing SLOs throughout lecture
- Integrated active learning activities such as semi-flipped classroom to encourage student participation.
- Prepared weekly problem sets and quizzes to keep students apprised of their progress.
- Emphasized relevance of course material in real world applications with relatable examples.

- Designed end-of-term project to encourage students to explore scientific literature online and develop crucial scientific communications skills.
- Worked with a diverse population of students including international and ESL students, and taught strategies for reading scientific articles.
- Nominated to instruct Organic Chemistry, Chem 51C, in Spring 2017 due to glowing student evaluations.

Graduate Course Teaching Assistant, Chemical Biology, Chem 219 Winter, 2016
Lecture and Discussion enrollment: 19 students
- Guest lectured two one-hour sessions during this course.
- Prepared biweekly problem sets derived from current, prominent publications.
- Led weekly discussions of hot topics in Chemical Biology.
- Assisted students in the construction of an original proposal in chemical biology.

Laboratory Course Teaching Assistant, Chemistry 1LD, 1LC, 51LB, 51LC Spring, 2016
Lab enrollment: 20 students Summer, 2013
- Taught students to keep complete and accurate scientific records. Fall, 2012
- Supervised and instructed students in general and organic chemistry lab techniques.
- Held weekly student-led presentations to consolidate lab materials from the previous week.
- Began each lab section with a comprehensive overview of laboratory techniques, objectives, and safety precautions.

Lecture Course Teaching Assistant, General Chemistry 1A and 1C Fall, 2015
Lecture enrollment: >300 students Discussion enrollment: 70 students Summer, 2014
- Head TA for Chem 1A, with duties such as supervising graders and one other teaching assistant.
- Prepared weekly problem sets in Chem 1A and contributed exam problems.
- Led discussions and assisted students individually with understanding concepts and homework problems.
- Held reviews for students and graded exams to provide students with helpful feedback.

Lecture Course Teaching Assistant, Organic Chemistry 51B and 51C Spring, 2013
Lecture enrollment: >200 students Discussion enrollment: 25 students Winter, 2017
- Assisted in the preparation of teaching materials such as problem sets and exams.
- Led discussions of problems relating to organic chemistry topics using collaborative learning techniques.
- Held reviews for students and graded exams to provide students with helpful feedback.

University of Tennessee, Knoxville
Lecture and Laboratory Course Teaching Assistant, Chemistry 100 and 110
Fall 2010—Spring, 2012
Lecture enrollment: >150 students Discussion enrollment: 30 students Lab enrollment: 22 students
- Led weekly discussions and supervised nursing students in basic chemistry lab techniques for Principles of Chemistry 100 and Introduction to Organic and Biochemistry 110.

- Prepared weekly worksheets for discussions to help students understand course material.
- Held reviews for students and graded exams to provide students with helpful feedback.

University and Community Services

Safety Representative June 2014 — July 2017
University of California, Irvine, Department of Chemistry
- Achieved zero injury rate during this period with a lab of approximately 15 members.
- Conducted safety inspections to OSHA standards and reported findings at weekly safety meetings.
- Ensured safe practices in lab by verifying PPE compliance and updating SOPs.
- Worked closely with the Environmental Health & Safety department to implement new safety regulations.

Chemistry Outreach Participant Jan 2016 — Jan 2017
University of California, Irvine, Department of Chemistry
- Visited K-12 schools to perform demonstration and talk about chemistry with a team of graduate students.
- Assisted with the preparation of chemicals required for conducting demonstrations.
- Increased the relevance of chemistry to students using lively demonstrations and interesting experiments.

Professional Development

Course Design Certificate Nov 2016
University of California, Irvine, Center of Engaged Instruction
- This is a 3-week program that covers the foundations of successful course design with a focus on student learning outcomes (SLO).
- Practiced "backwards, integrated course design" by establishing goals for student learning and aligning assignments and assessments with these goals.

University Studies 390A, Advanced Pedagogy and Academic Job Preparation Winter 2017
University of California, Irvine, Center of Engaged Instruction
- Introduction to principles of course design and instructional development.
- This course covers topics on active learning, learning through diversity, and educational research.

University Studies 390B, Advanced Pedagogy and Academic Job Preparation Spring 2017
University of California, Irvine, Center of Engaged Instruction
- Application of US 390A material in the design and implementation of the Teaching Assistant Professional Development Program.
- Fellows design a workshop meant to model best teaching practices as well as introduce new TAs to their roles and responsibilities.

Center for Integration of Research, Teaching, and Learning Associate Winter 2017
University of California, Irvine, Center of Engaged Instruction

- This program teaches graduate students and faculty to effectively implement research based practices in different learning environments.
- Participants are taught the importance of learning through diversity, learning communities and teaching as research.
- Designed a potential teaching as research project with definable goals and outcomes.

Research Experience

Graduate Research Assistant Jan 2013 – Present
University of California, Irvine, Department of Chemistry
Advisor: James Nowick
Currently developing β-sheet chemical models to study oligomers of human islet amyloid polypeptide, an amyloidgenic peptide that is associated in the pathology of type 2 diabetes.

Graduate Research Assistant Jan 2010 – Aug 2012
University of Tennessee, Knoxville, Department of Chemistry
Advisor: Michael Best
Worked on the design and synthesis of boronic acid-based sensors for microarray analysis and FRET-detection to study carbohydrates. (Jan 2011- Aug 2012)

Undergraduate Research Assistant Sep 2008 – Nov 2009
University of Florida, Department of Chemistry
Advisor: Marta Wayne
Worked on the study of virulence evolution in a host-parasite system in the absence of viral evolution.

Undergraduate Summer Researcher June 2007—Sep 2007
University of Florida, Department of Chemistry
Advisor: Eileen Buss
Explored the effects of different pesticides to billbugs and turfgrass population.

Presentations

5. **Wang, Y.** Mar 2016. Protein domains have structural and functional roles. Chem 219, Chemical Biology for graduate students.

4. **Wang, Y.** Feb 2016. RNA structure and synthesis. Chem 219, Chemical Biology for graduate students.

3. Truex, N. L.; **Wang, Y.**; Nowick, J. S. July, 2016. Assembly and Coassembly of Peptides Derived from β-Amyloid. 2016 Graduate Research Symposium of the ACS Division of Organic Chemistry. Bryn Mawr, PA.

2. **Wang, Y**.; Truex, N.; Nowick, J. S. November, 2015. Effect of hydrophobicity and charge in the oligomerization of amyloidogenic peptides and the design of a pH-switchable oligomer. Western ACS Regional Conference, San Marcos, CA.

1. Brusini, J.; **Wang, Y**.; Matos, L. F.; Sylvestre, L.S.; Bolker, B.M.; Wayne, M. L. November, 2013. Virulence evolution in a host parasite system in the absence of viral evolution. ESA Annual Meetings, Austin, TX.

Publications

5. **Wang, Y**.; Truex, N.; Nowick, J. S. Effects of Charge and Hydrophobicity on the Oligomerization of a Peptide Derived from IAPP. *Manuscript in preparation*.

4. **Wang, Y.**; Kreutzer, A. G.; Truex, N. L.; Nowick, J. S. A Tetramer Derived from Islet Amyloid Polypeptide. *J. Org. Chem.* **2017**, *82*, 7905-7912.

3. Truex, N.; **Wang, Y.**; Nowick, J. S. Assembly of peptides derived from β-sheet regions of β-amyloid. *J. Am. Chem. Soc.* **2016**, *138*, 13882-13890.

2. Chen, J.; Lambert, J.; Buonaugurio, A.; Bowen, K. H.*; Do-Thanh, C.-L.; **Wang, Y**.; Best, M.D.; Compton, B.; Sommerfeld, T. Combined photoelectron, collision-induced dissociation, and computational studies of parent and fragment anions of N-paranitrosulfophenysulfonylalanine and N-paranitrophenylalanine. *J. Chem. Phys.* **2013**, *139*, 224-308.

1. Brusini, J.; **Wang, Y**.; Matos, L. F.; Sylvestre, L. S.; Bolker, B. M.; Wayne, M. L. Virulence evolution in a host-parasite system in the absence of viral evolution. *Evol. Ecol. Res.* **2013.** *15,* 883-901.

Honors and Awards

Most Promising Future Faculty May 2017

- This competitive award honors one graduate student for a record of distinguished teaching, and promising research.

Pedagogical Fellowship Nov 2016

- This competitive program is based on a record of excellent teaching, promising scholarship, and service to the University, department, and the disciplines' professional community. The program is designed to provide Fellows with advanced pedagogical, pre-professional, and program development through course work, practice, and feedback.

First Year Achievement Award, University of Tennessee, Knoxville Aug 2010

- This competitive award honors three first year students for excellent teaching and distinguished academic performance.

Dean's Honor List (Santa Fe College) Aug 2005— Apr 2007

ABSTRACT OF THE DISSERTATION

Effects of Charge and Hydrophobicity on the Oligomerization of
Macrocyclic β-Sheet Peptides derived from Islet Amyloid Polypeptide

By

Yilin Wang

Doctor of Philosophy in Chemistry

University of California, Irvine, 2017

Professor James Nowick, Chair

Aggregation of the islet amyloid polypeptide (IAPP) to form fibrils and oligomers is important in the progression of type 2 diabetes. This dissertation describes the effects of charge and hydrophobicity on the oligomerization of macrocyclic β-sheet peptides derived from IAPP. Incorporation of residues 11–17 of IAPP (RLANFLV) into a macrocyclic β-sheet peptide results in a monomeric peptide that does not self-assemble to form oligomers. Mutation of Arg_{11} to the uncharged isostere citrulline gives peptide homologues that assemble to form tetramers in both the crystal state and in aqueous solution (peptide $\mathbf{1_{Cit}}$). The tetramers consist of hydrogen-bonded dimers that sandwich together through hydrophobic interactions. This dissertation also probes the role of charge and hydrophobicity by changing residue 11 to glutamic acid (peptide $\mathbf{1_{Glu}}$) and leucine (peptide $\mathbf{1_{Leu}}$). Diffusion ordered spectroscopy (DOSY) studies show that peptides $\mathbf{1_{Glu}}$ and $\mathbf{1_{Leu}}$ form tetramers in solution. NOESY studies confirm that both peptides formed the same sandwich-like tetramer as peptide $\mathbf{1_{Cit}}$. ^{1}H NMR spectroscopy at various concentrations reveal that peptide $\mathbf{1_{Leu}}$ has the highest propensity to form tetramers due to the leucine residue at

position 11 which contributes to packing. The effects of pH and charge on oligomerization are further probed by incorporation of histidine at position 11 (peptide $\mathbf{1}_{\mathbf{His}}$). DOSY studies show that peptide $\mathbf{1}_{\mathbf{His}}$ forms a tetramer at high pH. At low pH, peptide $\mathbf{1}_{\mathbf{His}}$ forms a new species that has not been observed by our group — a dimer. These studies demonstrate the importance of charge and hydrophobicity in the oligomerization of IAPP-derived peptides.

Chapter 1

Introduction

Interaction among β-sheets is important in the formation of amyloid oligomers, which are implicated in approximately 50 disorders.[1-4] Tremendous interest in type II diabetes and Alzheimer's disease has emerged in recent years as they become increasingly common in the modern world.[2,5-7] Islet amyloid polypeptide (IAPP) in type II diabetes and β-amyloid peptide (Aβ) in Alzheimer's disease aggregate to form toxic oligomers that are central to the progression of the diseases.[8-10] Unfortunately, not much is known about the structure of the oligomers because high-resolution characterization proves challenging due to their polymorphic and heterogeneous nature.

To gain insight into the assembly of amyloid oligomers, research groups developed structural models by studying segments of full-length amyloidogenic peptides and proteins.[11-14] Eisenberg and coworkers proposed an oligomeric assembly derived from αB crystallin, forming a barrel of six antiparallel β-sheets.[11] Surewicz and coworkers described a hexameric oligomer derived from prion protein that assembled to form three four-stranded, antiparallel β-sheets arranged like the edges of a triangle.[12] In the Nowick lab, we use macrocyclic β-sheet peptides containing fragments of amyloidogenic peptides and proteins as chemical models to study β-sheet interactions.[15-21] Nicholas Truex of our group reported the solution phase assembly of Aβ homotetramers and heterotetramers using Hao-containing macrocyclic β-sheets.[18,19] Adam Kreutzer of our group proposed the X-ray crystallographic structure of Aβ trimers and dodecamers using *N*-methyl macrocyclic β-sheet peptides (Figure 1.1).[20] My research has focused on using these chemical model systems to gain insight into the structure of IAPP oligomers at high-resolution using NMR spectroscopy and X-ray crystallography.[22]

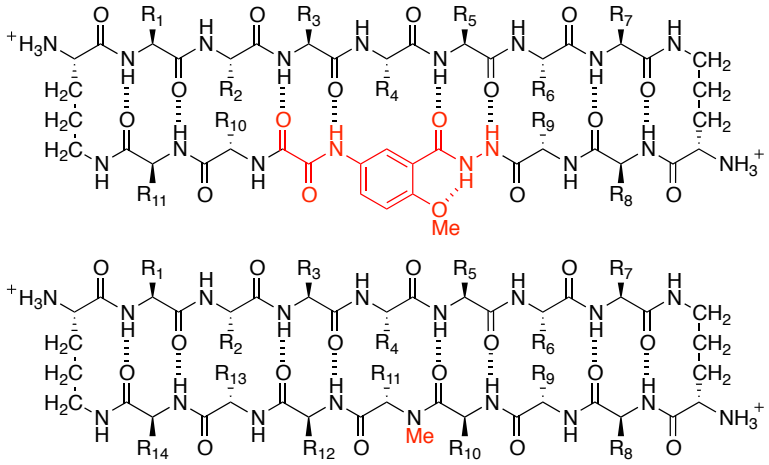

Figure 1.1. Chemical structures of Hao-containing macrocyclic β-sheet peptides (top) and *N*-methyl macrocyclic β-sheet peptides (bottom).

In selecting the fragment of IAPP to study, I took into account its relevance to toxic oligomers and its β-sheet forming propensity.[23,24] A proposed model on IAPP cytotoxicity shows that residues 1–19 are important as they are responsible for disrupting the lipid membrane.[25,26] Although there are no high-resolution structures of the amyloid oligomers, they appear to be composed of β-sheets. Hoyer and coworkers proposed an NMR-based structure of an IAPP:affibody complex and suggested that the IAPP β-hairpin structure might be involved in IAPP aggregation.[27] The β-hairpin comprises residues 12–28 where residues 12–18 and residues 22–28 form β-strands. Structural models of the IAPP fibrils also provide insight into IAPP sequences that have β-sheet forming propensities. Various research groups proposed structural models of IAPP fibrils where central residues 12–17 and C-terminal residues 31–36 are typically involved in β-strand formation.[28-30] I began my research by incorporating residues 11–17 of IAPP into a Hao-containing macrocyclic β-sheet peptide.

The macrocyclic β-sheet peptide contains the heptapeptide strand from IAPP (RLANFLV) and a template strand that are connected by two δ-linked ornithine ($^{\delta}$Orn) turn units (Figure 1.2).[31] The template strand contains the unnatural amino acid Hao, which mimics a

tripeptide β-strand, templates β-sheet formation, and blocks uncontrolled aggregation.[32] The template strand also contains four additional α-amino acids, with two residues flanking each side of Hao. These four residues are used to reinforce the hydrophobic surface and increase solubility of the macrocyclic β-sheet peptide. In the current study, my original aim was to study the interaction of amyloid oligomers of IAPP.

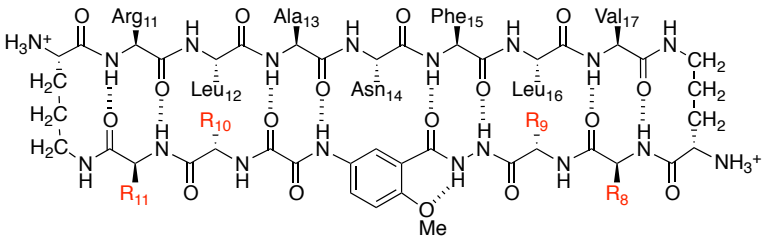

Figure 1.2. Chemical structure of macrocyclic β-sheet peptides incorporating residues 11 – 17 IAPP. Bottom strand residues R_8–R_{11} are highlighted in red to show that they are modified to manipulate properties of the peptide.

Initial studies of the IAPP-derived macrocyclic β-sheet peptides with varying R_8-R_{11} residues show no oligomer information (Chapter 2). The lack of oligomerization was surprising as a homologous region of Aβ residues 17–23, LVFFAED, forms a tetramer when constrained in a macrocyclic β-sheet peptide. The tetramer consists of a sandwich of hydrogen bonded dimers that pack on their hydrophobic surface containing leucine, phenylalanine, alanine, and aspartic acid. Both heptapeptide sequences contain three nonpolar residues and an additional polar residue on the hydrophobic surface. The tetramerization of Aβ-derived macrocyclic β-sheet peptide sparked my curiosity as to why the IAPP-derived macrocyclic β-sheet peptides were not self assembling.

I focused my attention on the arginine residue as it has a positive charge that is not present on the Aβ sequence. To study the effects of arginine on oligomerization, I mutated it to the neutral isostere citrulline that contains a urea group in place of the guanidinium group

(Chapter 3).[22] NMR spectroscopy shows that the mutant peptide, like the Aβ-derived peptide, forms a tetramer in solution. The formation of a tetramer was interesting, as it demonstrated that charge can modulate oligomerization. To gain further insight into the structure of the tetramer, I decided to pursue X-ray crystallography of the mutant peptide. Obtaining a suitable crystal offered some unique challenges. Screening the peptide in 864 conditions revealed one promising condition with cubic crystal growth. Incorporation of a heavy atom in the form of *p*-iodo-phenylalanine at position 15 for single-wavelength anomalous dispersion phasing led to poor crystal quality. I hypothesized that the poor crystal quality is due to the importance of the phenylalanine residue in assembly. Therefore, I opted to use (2-bromoallyl)glycine to replace the isoleucine residue on the template strand which yielded a suitable crystal.[11] In chapter 3, I describe the assembly of the crystal structure and correlated it to the assembly of the mutant peptide in solution.

Inspired by the role of charge in oligomerization, I wanted to ask two questions: Can pH modulate oligomerization and does hydrophobicity affect oligomerization? In many biological processes, pH triggers a conformational change in protein structure. Histidine residues are often involved because their protonation state changes near physiological pH.[33-37] I designed a macrocyclic β-sheet peptide that incorporates residues 11–17 of IAPP with a histidine mutation at position 11. I detail the studies of the His-containing peptide in Chapter 4, showing that charge can modulate oligomerization. To probe the effects of hydrophobicity on oligomerization, I designed additional mutants containing either glutamic acid or leucine at position 11. NMR studies show that both of these mutant peptides form tetramers, but there are differences in their propensities to form tetramers. I compare and contrast the properties of the mutant peptides in Chapter 4, offering insight into the interaction of β-sheets.

The study of IAPP-derived macrocyclic β-sheet peptides demonstrated that charge and hydrophobicity are important in oligomerization. Additional studies of other sequences of IAPP using Hao-containing macrocyclic β-sheets and *N*-methyl macrocyclic β-sheets shows no formation of discrete oligomers at low millimolar concentrations. The lack of self-assembly may be due to the many hydrophilic residues that are present in the IAPP sequence. Unlike Aβ, IAPP does not have long consecutive sequences of hydrophobic residues. In the future, one could envision increasing the number of residues incorporated as a potential modification to our current chemical model for the study of IAPP.

References

(1) Knowles, T. P. J.; Vendruscolo, M.; Dobson, C. M. *Nat. Rev. Mol. Cell. Bio.* **2014**, *15*, 384-396.

(2) Chiti, F.; Dobson, C. M. *Annu. Rev. Biochem.* **2006**, *75*, 333-366.

(3) Caughey, B.; Lansbury, P. T. *Annu. Rev. Neurosci.* **2003**, *26*, 267-298.

(4) Campioni, S.; Mannini, B.; Zampagni, M.; Pensalfini, A.; Parrini, C.; Evangelisti, E.; Relini, A.; Stefani, M.; Dobson, C. M.; Cecchi, C.; Chiti, F. *Nat. Chem. Biol.* **2010**, *6*, 140-147.

(5) Hu, F. B. *Diabetes Care* **2011**, *34*, 1249-1257.

(6) Dobson, C. M. *Nature* **2003**, *426*, 884-890.

(7) Olshansky, S. J.; Passaro, D. J.; Hershow, R. C.; Layden, J.; Carnes, B. A.; Brody, J.; Hayflick, L.; Butler, R. N.; Allison, D. B.; Ludwig, D. S. *N. Engl. J. Med.* **2005**, *352*, 1138-1145.

(8) Benilova, I.; Karran, E.; De Strooper, B. *Nat. Neurosci.* **2012**, *15*, 349-357.

(9) Meier, J. J.; Kayed, R.; Lin, C. Y.; Gurlo, T.; Haataja, L.; Jayasinghe, S.; Langen, R.; Glabe, C. G.; Butler, P. C. *Am. J. Physiol. Endocrinol. Metab.* **2006**, *291*, E1317-E1324.

(10) Haass, C.; Selkoe, D. J. *Nat. Rev. Mol. Cell. Bio.* **2007**, *8*, 101-112.

(11) Laganowsky, A.; Liu, C.; Sawaya, M. R.; Whitelegge, J. P.; Park, J.; Zhao, M. L.; Pensalfini, A.; Soriaga, A. B.; Landau, M.; Teng, P. K.; Cascio, D.; Glabe, C.; Eisenberg, D. *Science* **2012**, *335*, 1228-1231.

(12) Apostol, M. I.; Perry, K.; Surewicz, W. K. *J. Am. Chem. Soc.* **2013**, *135*, 10202-10205.

(13) Do, T. D.; LaPointe, N. E.; Nelson, R.; Krotee, P.; Hayden, E. Y.; Ulrich, B.; Quan, S.; Feinstein, S. C.; Teplow, D. B.; Eisenberg, D.; Shea, J. E.; Bowers, M. T. *J. Am. Chem. Soc.* **2016**, *138*, 549-557.

(14) Teoh, C. L.; Su, D. D.; Sahu, S.; Yun, S. W.; Drummond, E.; Prelli, F.; Lim, S.; Cho, S.; Ham, S.; Wisniewski, T.; Chang, Y. T. *J. Am. Chem. Soc.* **2015**, *137*, 13503-13509.

(15) Pham, J. D.; Chim, N.; Goulding, C. W.; Nowick, J. S. *J. Am. Chem. Soc.* **2013**, *135*, 12460-12467.

(16) Salveson, P. J.; Spencer, R. K.; Nowick, J. S. *J. Am. Chem. Soc.* **2016**, *138*, 4458-4467.

(17) Spencer, R. K.; Kreutzer, A. G.; Salveson, P. J.; Li, H.; Nowick, J. S. *J. Am. Chem. Soc.* **2015**, *137*, 6304-6311.

(18) Truex, N. L.; Wang, Y. L.; Nowick, J. S. *J. Am. Chem. Soc.* **2016**, *138*, 13882-13890.

(19) Truex, N. L.; Nowick, J. S. *J. Am. Chem. Soc.* **2016**, *138*, 13891-13900.

(20) Kreutzer, A. G.; Hamza, I. L.; Spencer, R. K.; Nowick, J. S. *J. Am. Chem. Soc.* **2016**, *138*, 4634-4642.

(21) Spencer, R. K.; Li, H.; Nowick, J. S. *J. Am. Chem. Soc.* **2014**, *136*, 5595-5598.

(22) Wang, Y.; Kreutzer, A. G.; Truex, N. L.; Nowick, J. S. *J. Org. Chem.* **2017**, *82*, 7905-7912.

(23) Dupuis, N. F.; Wu, C.; Shea, J. E.; Bowers, M. T. *J. Am. Chem. Soc.* **2011**, *133*, 7240-7243.

(24) Dupuis, N. F.; Wu, C.; Shea, J. E.; Bowers, M. T. *J. Am. Chem. Soc.* **2009**, *131*, 18283-18292.

(25) Engel, M. F. M.; Khemtemourian, L.; Kleijer, C. C.; Meeldijk, H. J. D.; Jacobs, J.; Verkleij, A. J.; de Kruijff, B.; Killian, J. A.; Hoppener, J. W. M. *Proc. Natl. Acad. Sci. U.S.A.* **2008**, *105*, 6033-6038.

(26) Engel, M. F. M.; Yigittop, H.; Elgersma, R. C.; Rijkers, D. T. S.; Liskamp, R. M. J.; de Kruijff, B.; Hoppener, J. W. M.; Killian, J. A. *J. Mol. Biol.* **2006**, *356*, 783-789.

(27) Mirecka, E. A.; Feuerstein, S.; Gremer, L.; Schroder, G. F.; Stoldt, M.; Willbold, D.; Hoyer, W. *Sci. Rep.* **2016**, *6*.

(28) Luca, S.; Yau, W. M.; Leapman, R.; Tycko, R. *Biochemistry* **2007**, *46*, 13505-13522.

(29) Wiltzius, J. J. W.; Sievers, S. A.; Sawaya, M. R.; Cascio, D.; Popov, D.; Riekel, C.; Eisenberg, D. *Protein Sci.* **2008**, *17*, 1467-1474.

(30) Bedrood, S.; Li, Y. Y.; Isas, J. M.; Hegde, B. G.; Baxa, U.; Haworth, I. S.; Langen, R. *J. Biol. Chem.* **2012**, *287*, 5235-5241.

(31) Nowick, J. S.; Brower, J. O. *J. Am. Chem. Soc.* **2003**, *125*, 876-877.

(32) Nowick, J. S.; Lam, K. S.; Khasanova, T. V.; Kemnitzer, W. E.; Maitra, S.; Mee, H. T.; Liu, R. W. *J. Am. Chem. Soc.* **2002**, *124*, 4972-4973.

(33) Kampmann, T.; Mueller, D. S.; Mark, A. E.; Young, P. R.; Kobe, B. *Structure* **2006**, *14*, 1481-1487.

(34) Fritz, R.; Stiasny, K.; Heinz, F. X. *J. Cell Biol.* **2008**, *183*, 353-361.

(35) Anderson, J. M.; Andersen, N. H. *Angew. Chem. Int. Ed.* **2017**, *56*, 7074-7077.

(36) Kilmartin, J. V.; Breen, J. J.; Roberts, G. C. K.; Ho, C. *Proc. Natl. Acad. Sci. U.S.A.* **1973**, *70*, 1246-1249.

(37) Eaton, W. A.; Henry, E. R.; Hofrichter, J.; Mozzarelli, A. *Nat. Struct. Mol. Biol.* **1999**, *6*, 351-358.

Chapter 2

Design of Macrocyclic β-Sheet Peptides Associated with Amyloid β and Islet Amyloid Polypeptide

Introduction

The accumulation of misfolded β-sheet into protein aggregates has been associated with the pathology of over 20 diseases, such as Alzheimer's disease and diabetes mellitus type 2.[1-3] In Alzheimer's disease, the β-amyloid peptide (Aβ) causes neuronal death in brain tissues.[4-6] In diabetes mellitus type II, the misfolded human islet amyloid polypeptide (IAPP or amylin) results in β-cell death in the pancreas.[7-10] In all these diseases, the aggregation process involves the formation of insoluble amyloid fibrils and cytotoxic amyloid oligomers.[4,10,11] Studies show that patients with type 2 diabetes have a higher chance of developing Alzheimer's disease and vice versa.[12-16] The process of cross seeding, the aggregation of one protein promoting the aggregation of another, could be because Aβ and IAPP exhibit 25% sequence identity and 50% sequence similarity. The specificity in cross seeding may be the consequence of biomolecular recognition resulting from the hydrophobic interactions and hydrogen bonding between protein β-sheets.

Extensive research efforts have been made over the past several years to comprehend the biomolecular basis of amyloid diseases.[17-19] In amyloidogenic diseases, the respective peptide misfolds and forms the toxic oligomers, which are in equilibrium with the fibers.[4] Despite decades of research, it is not yet clear how these oligomers result in disorders and understanding these amyloid interactions is necessary for therapeutic advances. To shed light on the assembly of the oligomers, the Nowick lab uses chemical models (Figure 2.1) to study particular amyloidogenic segments with a propensity to form intermolecular β-sheet network.[20-30] The upper strand ($R_{1\text{-}7}$) of the macrocycle contains a heptapeptide sequence that is often a native amyloidogenic sequence. The lower strand contains the molecular template "Hao" a tripeptide β-sheet mimic, which prevents uncontrollable aggregation, and effectively induces β-sheet

interactions.[31] Two ornithine turn-units connect the upper and lower strands and the macrocycle comes together with intramolecular hydrogen bonding.[32] This chapter describes the design of macrocyclic β-sheet peptides to study the assembly of amyloidogenic sequences.

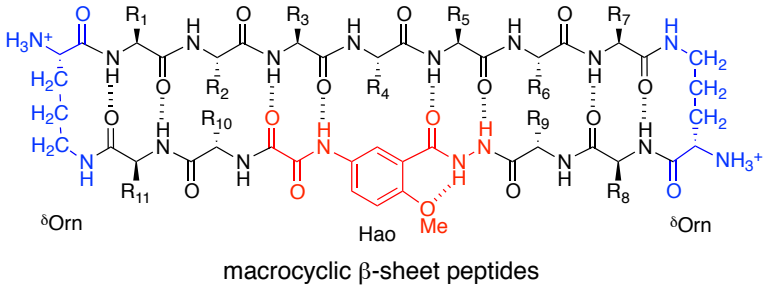

Figure 2.1. 54-membered macrocyclic peptide designed by the Nowick lab to study amyloidogenic sequences.

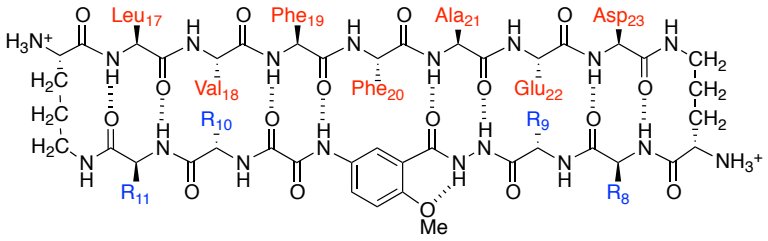

Table 2.1. Macrocyclic β-sheet peptides **1a** and **1b** with $A\beta_{17-23}$ as the heptapeptide top strand. The bottom strand shows the swapping of the hydrophobic/ hydrophilic residue positions. Peptide **1b** is designed as a defined oligomer to study $A\beta_{17-23}$ interactions. Peptide **1a** has been previously published.

	R_8	R_9	R_{10}	R_{11}
1a	Lys	Leu	Ile	Glu
1b	Ile	Lys	Lys	Ile

Former Nowick group member, Dr. Pin-Nan Cheng developed the 54-membered macrocyclic peptide chemical model, peptide **1a**, to study its ability to inhibit amyloid aggregation (Table 2.1).[20] The upper strand (R_{1-7}) of the macrocycle contains the native heptapeptide sequence LVFFAED derived from $A\beta_{17-23}$ as the sequence of interest. The Lys_8 and Glu_{11} on the bottom strand of **1a** are hydrophilic residues that reduce oligomerization. Structural studies with NMR spectroscopy show that the macrocycle exists in solution as a monomer.

Modifications of this design to form defined oligomers turned into an exciting project to study the molecular recognition between the N- terminus and C-terminus of the Aβ protein. For this project we incorporate $A\beta_{17-23}$ sequence LVFFAED and $A\beta_{30-36}$ sequence AIIGLMV into macrocyclic β-sheets to study their propensity to homo- and hetereooligomerize. We have developed these macrocyclic β-sheets as chemical models for the oligomerization of amyloidogenic sequences.

My involvement in the project focuses on the design, synthesis, and characterization of peptide **1b** (Table 2.1).[27] In order to promote oligomerization, I placed hydrophobic residues at R_8 and R_{11} instead of at R_9 and R_{10}. This switch places upper strand Leu_{17}, Phe_{19}, Ala_{21}, and Glu_{23} residues and bottom strand Ile_8 and Ile_{11} residues on the same hydrophobic surface for molecular recognition. This peptide and its derivatives were used for NMR analysis to study homo- and heterooligomerization of the N- and C-terminal regions of Aβ.[27,28]

To study the fundamental principles in the molecular recognition of amyloidogenic sequences of IAPP, I designed macrocyclic β-sheet peptides containing a heptapeptide segment of IAPP. Previously, Dr. Pin-nan Cheng designed peptide **2a** as a monomer to study its properties as an amyloid inhibitor (Table 2.2).[20] The upper strand of the peptide contains the central native heptapeptide sequence RLANFLV derived from $IAPP_{11-17}$ as the sequence of

interest. I made a series of macrocycles based on peptide **2a** to study the self-assembly of $IAPP_{11-17}$ into an oligomer.

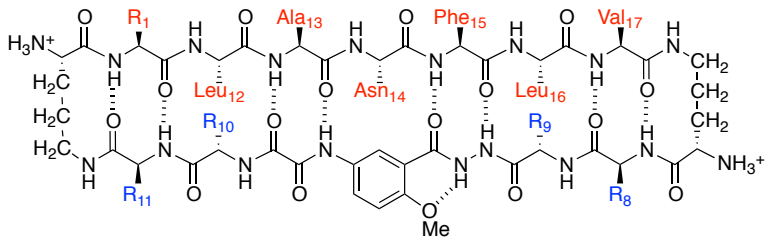

Table 2.2. Macrocyclic β-sheet peptides **2a** and **2i**, with $IAPP_{11-17}$ and a one-residue mutation of $IAPP_{11}$ as the heptapeptide top strand. The bottom strand shows the swapping of the hydrophobic/ hydrophilic residue positions. **2i** was designed to be a defined oligomer to study the effect of arginine. Peptide **2a** has been previously published.

	R_1	R_8	R_9	R_{10}	R_{11}
2a	Arg	Lys	Phe	Tyr	Lys
2i	Leu	Ile	Lys	Val	Ile

Results and Discussion

I carried out the synthesis and purification of macrocycles according to published procedures.[33] The corresponding linear peptides were synthesized using standard Fmoc-based solid phase peptide synthesis (SPPS) on 2-chlorotrityl resin. The protected linear peptides were cleaved from the resin, cyclized in solution, then globally deprotected to generate the 54-membered macrocyclic β-sheet peptide. The peptides were purified by reversed-phase high-performance liquid chromatography (RP-HPLC) and lyophilized to give 10-40 mg of the peptide as a TFA salt. Analysis by mass spectrometry and HPLC show that the purity was >95%.

^{1}H NMR structural studies in aqueous solutions provide detailed knowledge on oligomerization and β-sheet properties. ^{1}H NMR and the accompanying 2D NMR results provide assignment of the respective peptide residues. The ^{1}H NMR of peptide **1b** at 4 mM shows that the resonances are broader and the α-protons are shifted downfield by 0.4–1.0 ppm from their

random coil values. The large downfield chemical shifts of the α-protons in peptide **1b** demonstrates packing of the macrocyclic β-sheet peptides. In addition, the upfield shifting of the aromatic resonances of the Phe residue from its random coil values indicates aromatic packing.

In the ^{1}H NMR spectrum, the difference in the chemical shifts of the diastereotopic δ-protons of an ornithine turn unit ($\Delta\delta^{\delta}$Orn) is an indication of the degree of folding of the peptide. Previous studies of homologous macrocycles have shown that a value of 0.6 ppm indicates complete folding in water.[21] The average $\Delta\delta^{\delta}$Orn value of peptide **1b** is 0.68 ppm, indicating a β-sheet structure.

NOESY studies of the macrocycle oligomer display a network of NOEs that show an in-register edge-to-edge dimerization through antiparallel β-sheet formation. Intramolecular NOEs (Figure 2.2) are observed between the α-proton of Glu_{22} and Lys, between the α-proton of Phe_{19} and the proton at the 6-position of Hao, and between the α-proton of Val_{18} and Lys indicating formation of a β-sheet. Intermolecular NOEs are observed between the α-proton of Leu_{17} and Asp_{23}, and between the α-proton of Phe_{19} and Ala_{21} indicating edge-to-edge, in-register, antiparallel dimerization.

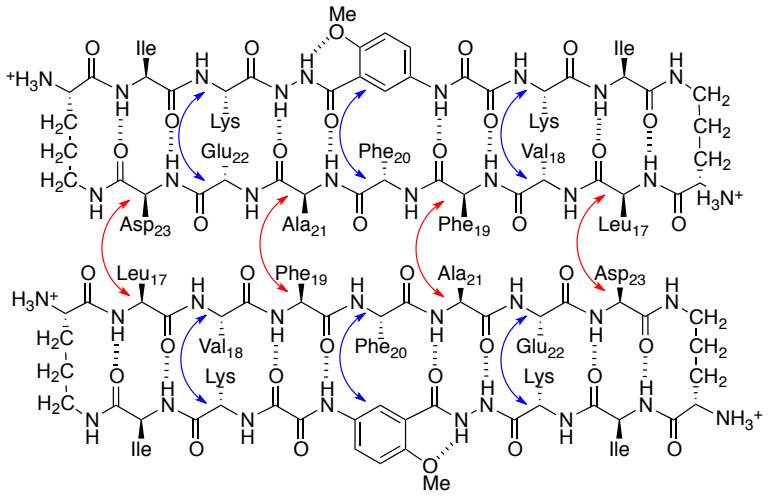

Figure 2.2. Chemdraw of peptide **1b** dimer assembling in a non-shifted, antiparallel fashion as derived from the NOESY spectroscopy.

NMR diffusion experiments such as DOSY provide a way to distinguish between the different species based on the diffusion coefficient peptides. The ratio of the diffusion coefficient of the oligomer to the monomer ($D_{oligomer}$/ $D_{monomer}$) is a representation of the oligomerization state.[23,27,28] For a tetramer, this value is approximately 0.58–0.63 and for a dimer, this value is approximately 0.75–0.79. Measurement of the diffusion coefficients taken from DOSY experiments of peptide **1b** indicates the presence of a single oligomeric species. The $D_{oligomer}$ of peptide **1b** is (11.1 ± 1.0) × 10^{-7} m^2/s but $D_{monomer}$ cannot be obtained, as peptide **1b** forms a tetramer even at low concentrations. The diffusion coefficient of a monomeric control macrocyclic peptide within 10% molecular weight of peptide **1b** is used. $D_{monomer}$ is (17.6 ± 1.0) × 10^{-11} m^2/s. The ratio of diffusion coefficients for peptide **1b** is 0.63 suggesting that it is a tetrameric oligomer in water.

X-ray crystallography is a viable platform for crystal-state structural determination complementary to NMR in solution-state structural determination. Based on previous studies in our lab, an X-ray crystallographic structure can offer more information about the solution-phase structure in addition to NMR.[34] Phase determination of the X-ray crystallography is done by single anomalous dispersion (SAD), which requires the incorporation of a heavy atom to solve the crystal structure.[22] The heavy atom is incorporated hboin the form of 4-iodophenylalanine in position R_3 to give peptide **1c**.

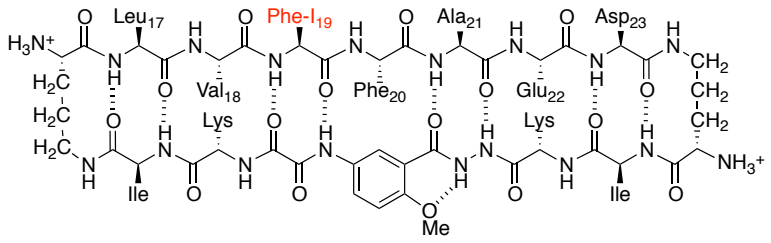

Figure 2.3. Macrocyclic β-sheet peptides **1c** incorporating 4-iodophenylalanine for X-ray crystallography.

The process of finding a crystal suitable for X-ray crystallography can be the hardest step. The synthesized peptide undergoes pre-crystallization test (PCT) to determine the optimum concentration for crystal formation followed by high-throughput screening with 288 conditions such as buffers and polyethylene glycol (PEG) at different pH and concentrations. Select conditions that yield crystal growth were then optimized for best crystal growth by varying the concentration of salts and pH. Peptide **1c** was synthesized because peptide **1b** was believed to assemble on the L_{17}, F_{19}, A_{21}, and D_{23} hydrophobic face in solution-state and having the heavy atom on the hydrophobic face would cause less interference (Figure 2.3). The morphology of the crystals obtained from screening of peptide **1c** showed poor growth with needles of various sizes. These crystals presented poor X-ray diffraction patterns, indicating that peptide **1c** is not an appropriate candidate for X-ray crystallography. For future studies, 4-iodophenylalanine can replace the Phe_{20} residue to screen for suitable x-ray crystallography candidates.

The macrocyclic β-sheet peptides can be extended to the study of the oligomerization of IAPP-derived macrocyles, which can provide valuable insight on IAPP oligomers. When I first joined the lab, I designed peptides **2b**-**2d** by transposing different residues in the bottom strand of **2a** to promote oligomerization and learn about β-sheet folding (Table 2.3). ^{1}H NMR spectroscopic data of the peptides provide detailed knowledge on oligomerization and β-sheet properties. A signature pattern of an oligomer is to have a series of α-protons peaks downfield of the HOD and the spectra peaks are generally much broader. The ^{1}H NMR spectrum of each of the above compounds at 4 mM in D_2O showed that there were hardly any change in chemical shifts of their α-protons from their random coil values and the peaks were sharp and distinct, indicating that they were monomers. Peptide **2a** has hydrophilic residues at R_8 and R_{11} that promote the formation of a monomer. Thus, it is not surprising that peptide **2b** and **2c**, which

both have hydrophilic edge-residues, were monomers. On the other hand, the lower strand of peptide **2d** is flanked by 2 hydrophobic residues, Tyr_8 and Phe_{11}, which can promote oligomerization. The lack of oligomer formation suggests that aromatic residues do not pack well with the upper strand for the formation of an oligomer.

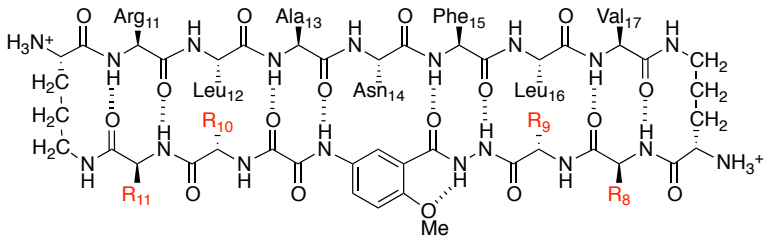

Table 2.3. Macrocyclic β-sheet peptides **2a**–**2g**, with $IAPP_{11-17}$ as the heptapeptide top strand. The bottom strand shows the transposing of the hydrophobic/ hydrophilic residue positions. Peptide **2a** has been previously published.

	R_8	R_9	R_{10}	R_{11}	Δ^{δ}Orn (ppm)	β-sheet folding
2a*	Lys	Phe	Tyr	Lys	0.50	+
2b	Lys	Tyr	Lys	Phe	0.44	+
2c	Tyr	Lys	Phe	Lys	0.16	-
2d	Tyr	Lys	Lys	Phe	0.19	-
2e	Ile	Lys	Lys	Ile	0.26	-
2f	Ile	Lys	Thr	Ile	0.37	+
2g	Ile	Thr	Val	Ile	0.60	++

Applying the same oligomerizing principles from peptide **1b** containing $A\beta_{17-23}$, I decided to use the same bottom strand from peptide **1b** to promote oligomerization by eliminating the aromatic residues (peptide **2e**). Previous macrocyles that oligomerized are relatively hydrophobic, so I mutated R_{10} from Lys to Thr (peptide **2f**) to increase the hydrophobicity by removing a positive charge. To further investigate the effect of bottom strand hydrophobicity on oligomerization, I removed another charge by doubly mutating the Lys of peptide **2e** at positions R_9 and R_{10} to Thr and Val respectively (peptide **2g**). The NMR spectrum of each of the compounds at 4 mM in D_2O showed sharp and distinct peaks, and the chemical shifts of their α-

protons showed only small shifts from their random coil values, indicating that they are monomers. Tabulation of Δ^{δ}Orn values shows that a more hydrophobic bottom strand promotes better folding of macrocyclic β-sheets. In peptides **2e**-**2g**, the Arg_1, Ala_3, Phe_5, Val_7, Ile_8, and Ile_{10} are on the same face but they do not pack appropriately to form a hydrophobic core that promotes oligomerization. The only hydrophilic residue on this surface is Arg and I postulate that the positive charge on the residue may be the cause of the monomeric nature of peptides **2b**-**2g.**

To corroborate the above hypothesis that the upper strand was not suitable for the formation of an oligomer, the top strand native heptapeptide sequence was shifted one residue towards the N-terminus to give QRLANFL as the native heptapeptide upper strand (Table 2.4). The removal of a charge in the outer edge of the top strand may promote oligomerization. The NMR spectrum of peptide **2h** at 4 mM in D_2O showed that there were generally only small changes in chemical shifts of its α-protons from their random coil values and the peaks were sharp and distinct, indicating that peptide **2h** is a monomer. In peptide **2h**, Gln_{10}, Leu_{12}, Asn_{14}, Leu_{16}, Ile_8, and Ile_{11} are on the same face and this arrangement places two polar hydrophilic residues on the hydrophobic face as opposed to one charged hydrophilic residue on the hydrophobic face. The lack of oligomer formation suggests that removal of a charge in the form of Arg_{11} by shifting the heptapeptide sequence is insufficient because this introduces 2 hydrophilic residues, Gln_1 and Asn_5, to the packing surface.

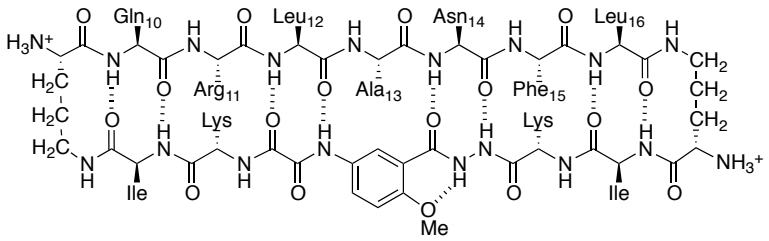

macrocyclic β-sheet peptides **2h**

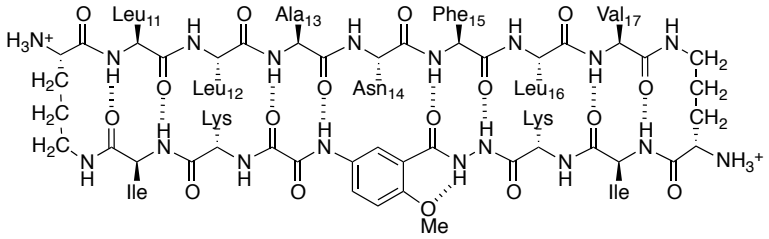

macrocyclic β-sheet peptides **2i**

Table 2.4. Macrocyclic β-sheet peptide **2h** with $IAPP_{10-16}$ as the heptapeptide top strand and peptide **2i** with $IAPP_{11-17}$ as the heptapeptide top strand with a leucine mutation at Arg_{11}. Peptide **2h** is a monomer whereas peptide **2i** is an oligomer.

	Δ^{δ}Orn (ppm)	β-sheet folding	Oligomer Formation
2h	0.13	-	No
2i	0.68	+++	Yes

To better understand the effect of the positive charge on the upper strand, I modified the native IAPP sequence by mutating the Arg_{11} residue to Leu_{11} (peptide **2i**). The Leu_{11} residue lacks the positive charge of the Arg_{11} residue, which I believe is preventing the formation of oligomers. The ^{1}H NMR spectrum at 4 mM in D_2O shows that the α-protons peaks are shifted downfield of the HOD and the spectra is much broader with less distinct sharp peaks. This shift indicates that peptide **1b** is an oligomer and assumes a β-sheet structure. Oligomerization of peptide **2h** supports my hypothesis that the Arg residue is inhibiting self-association of peptides.

Conclusions

The solution-state assembly of peptide **1b** provided interesting insights into the formation of oligomers using our chemical models. By swapping the hydrophobic residues and hydrophilic residues in the lower strand of peptide **1a**, peptide **1b** promoted the formation of an oligomer for molecular recognition. Structural analysis using ^{1}H NMR show that peptide **1b** is a well-behaved, edge-to-edge, in-register, antiparallel tetramer that assembles on the hydrophobic surface.

Peptides **2b**-**2i** were synthesized to study the central residue of IAPP, $IAPP_{11-17}$, and the original purpose of the project is to understand the biomolecular recognition by the formation of an oligomer. However, this proves to be challenging as the charged Arg residue in the upper strand is preventing oligomerization. The mutation of the Arg amino acid to Leu resulted in the formation of an oligomer, further supporting my hypothesis that the Arg residue is inhibiting oligomerization. Chapters 3 and 4 further explores this interesting hypothesis.

As mentioned in the introduction, patients with Alzheimer's are more likely to contract type 2 diabetes and vice versa. Thus, future studies of this biomolecular interaction could possibly help us better understand the cross-fibrillation of Aβ peptide and IAPP.

References

(1) Knowles, T. P. J.; Vendruscolo, M.; Dobson, C. M. *Nat. Rev. Mol. Cell. Bio.* **2014**, *15*, 384-396.

(2) Chiti, F.; Dobson, C. M. *Annu. Rev. Biochem.* **2006**, *75*, 333-366.

(3) Li, L.; Hoelscher, C. *Brain Res. Rev.* **2007**, *56*, 384-402.

(4) Benilova, I.; Karran, E.; De Strooper, B. *Nat. Neurosci.* **2012**, *15*, 349-357.

(5) Lesne, S.; Koh, M. T.; Kotilinek, L.; Kayed, R.; Glabe, C. G.; Yang, A.; Gallagher, M.; Ashe, K. H. *Nature* **2006**, *440*, 352-357.

(6) Lesne, S. E.; Sherman, M. A.; Grant, M.; Kuskowski, M.; Schneider, J. A.; Bennett, D. A.; Ashe, K. H. *Brain* **2013**, *136*, 1383-1398.

(7) Zhang, S. P.; Liu, J. X.; Dragunow, M.; Cooper, G. J. S. *J. Biol. Chem.* **2003**, *278*, 52810-52819.

(8) Bram, Y.; Frydman-Marom, A.; Yanai, I.; Gilead, S.; Shaltiel-Karyo, R.; Amdursky, N.; Gazit, E. *Sci. Rep.* **2014**, *4*.

(9) Tenidis, K.; Waldner, M.; Bernhagen, J.; Fischle, W.; Bergmann, M.; Weber, M.; Merkle, M. L.; Voelter, W.; Brunner, H.; Kapurniotu, A. *J. Mol. Biol.* **2000**, *295*, 1055-1071.

(10) Meier, J. J.; Kayed, R.; Lin, C. Y.; Gurlo, T.; Haataja, L.; Jayasinghe, S.; Langen, R.; Glabe, C. G.; Butler, P. C. *Am. J. Physiol. Endocrinol. Metab.* **2006**, *291*, E1317-E1324.

(11) Harrison, R. S.; Sharpe, P. C.; Singh, Y.; Fairlie, D. P. *Rev. Physiol. Bioch.. P.* **2007**, *159*, 1-77.

(12) Nicolls, M. R. *Curr. Alzheimer Res.* **2004**, *1*, 47-54.

(13) Yan, L. M.; Velkova, A.; Tatarek-Nossol, M.; Andreetto, E.; Kapurniotu, A. *Angew. Chem. Int. Ed.* **2007**, *46*, 1246-1252.

(14) Andreetto, E.; Yan, L. M.; Tatarek-Nossol, M.; Velkova, A.; Frank, R.; Kapurniotu, A. *Angew. Chem. Int. Ed.* **2010**, *49*, 3081-3085.

(15) O'Nuallain, B.; Williams, A. D.; Westermark, P.; Wetzel, R. *J. Biol. Chem.* **2004**, *279*, 17490-17499.

(16) Berhanu, W. M.; Yasar, F.; Hansmann, U. H. E. *ACS Chem. Neurosci.* **2013**, *4*, 1488-1500.

(17) Kepp, K. P. *Chem. Rev.* **2012**, *112*, 5193-5239.

(18) Stefani, M. *Prog. Neurobiol.* **2012**, *99*, 226-245.

(19) Olzscha, H.; Schermann, S. M.; Woerner, A. C.; Pinkert, S.; Hecht, M. H.; Tartaglia, G. G.; Vendruscolo, M.; Hayer-Hartl, M.; Hartl, F. U.; Vabulas, R. M. *Cell* **2011**, *144*, 67-78.

(20) Cheng, P. N.; Liu, C.; Zhao, M. L.; Eisenberg, D.; Nowick, J. S. *Nat. Chem.* **2012**, *4*, 927-933.

(21) Khakshoor, O.; Demeler, B.; Nowick, J. S. *J. Am. Chem. Soc.* **2007**, *129*, 5558-5569.

(22) Pham, J. D.; Chim, N.; Goulding, C. W.; Nowick, J. S. *J. Am. Chem. Soc.* **2013**, *135*, 12460-12467.

(23) Pham, J. D.; Demeler, B.; Nowick, J. S. *J. Am. Chem. Soc.* **2014**, *136*, 5432-5442.

(24) Pham, J. D.; Spencer, R. K.; Chen, K. H.; Nowick, J. S. *J. Am. Chem. Soc.* **2014**, *136*, 12682-12690.

(25) Salveson, P. J.; Spencer, R. K.; Nowick, J. S. *J. Am. Chem. Soc.* **2016**, *138*, 4458-4467.

(26) Kreutzer, A. G.; Hamza, I. L.; Spencer, R. K.; Nowick, J. S. *J. Am. Chem. Soc.* **2016**, *138*, 4634-4642.

(27) Truex, N. L.; Wang, Y. L.; Nowick, J. S. *J. Am. Chem. Soc.* **2016**, *138*, 13882-13890.

(28) Truex, N. L.; Nowick, J. S. *J. Am. Chem. Soc.* **2016**, *138*, 13891-13900.

(29) Spencer, R. K.; Li, H.; Nowick, J. S. *J. Am. Chem. Soc.* **2014**, *136*, 5595-5598.

(30) Wang, Y.; Kreutzer, A. G.; Truex, N. L.; Nowick, J. S. *J. Org. Chem.* **2017**, *82*, 7905-7912.

(31) Nowick, J. S.; Lam, K. S.; Khasanova, T. V.; Kemnitzer, W. E.; Maitra, S.; Mee, H. T.; Liu, R. W. *J. Am. Chem. Soc.* **2002**, *124*, 4972-4973.

(32) Nowick, J. S.; Brower, J. O. *J. Am. Chem. Soc.* **2003**, *125*, 876-877.

(33) Spencer, R.; Chen, K. H.; Manuel, G.; Nowick, J. S. *Eur. J. Org. Chem.* **2013**, 3523-3528.

(34) Khakshoor, O.; Lin, A. J.; Korman, T. P.; Sawaya, M. R.; Tsai, S. C.; Eisenberg, D.; Nowick, J. S. *J. Am. Chem. Soc.* **2010**, *132*, 11622-11628.

Material and Methods

Fmoc-protected amino acids, 2-chlorotrityl resin, and coupling reagents— HOBT, HBTU, HCTU, HATU, were purchased from GL Biosciences Shanghai, LC Science, AnaSpec, Chem Impex, and Novabiochem. NMR solvents, D_2O, DMSO, and $CDCl_3$ were purchased from Cambridge Isotope Laboratories. HPLC grade solvents— acetonitrile, dichloromethane, hexanes, and tetrahydrofuran, were purchased from Fisher Scientific. Triisopropylsilane, N-methylmorpholine, trifluoroacetic acid, diisopropylethylamine (DIPEA), and 2,4,6-trimethylpyridine were purchased from Sigma-Aldrich. Polyprep chromatography columns were purchased from Bio-Rad. Fmoc-Hao-OH was synthesized based on published procedures.[1]

Synthesis of macrocyclic peptides

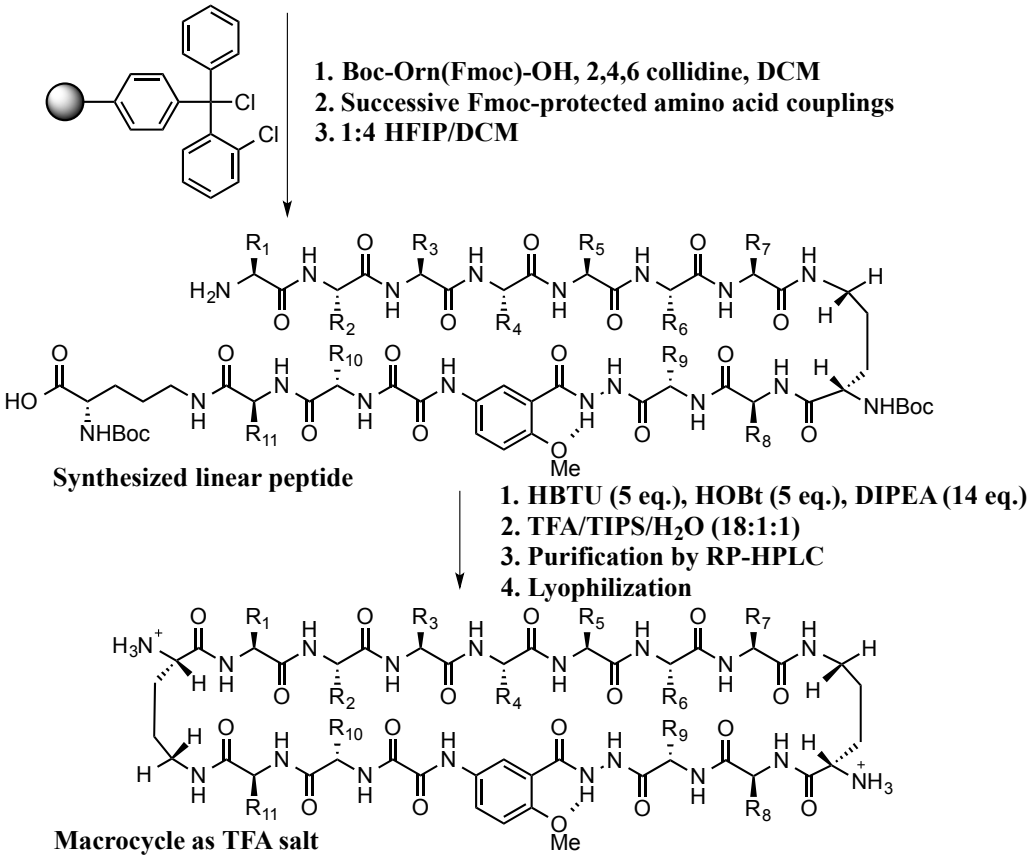

2-Chlorotrityl resin (0.300 g, 1.14 mmol/g, 0.100 mmol) was added to a polyprep column and swelled in dichloromethane (DCM) for 30 minutes before the solution was drained. The resin was then loaded overnight with Boc-Orn(Fmoc)-OH (81.8 mg, 0.18 mmol) dissolved in 5% 2,4,6-collidine in DCM (10 mL). 8 hours later, the resin was drained and capped with 17:2:1 DCM/MeOH/DIPEA. The resin was then used for automated peptide synthesis on the PS-3 Peptide Synthesizer from Protein Technologies, Inc. Each vial used for automated synthesis contained Fmoc-protected amino acid (0.468 mmol, 4.00 equiv) and HCTU (0.468 mmol, 4 equiv). Cleavage of the synthesized linear peptide from the resin was done using 1:4 HFIP/ DCM. The linear peptide was then cyclized for 12 hours using HBTU (5 equiv), HBTU (5 equiv), and diisopropylethylamine (14 equiv) at around 1 mM in DMF to give the protected cyclized peptide. A 18:1:1 TFA/TIPS/H_2O mixture was used to globally deprotect the macrocyle.

Purification

Peptides were analyzed for purity using analytical reversed-phase HPLC in an Agilent Zorbax SB-C18 column (50 mm x 4.6 mm), detection was set to 214 nm. A gradient of 5-95% CH_3CN with 0.1% TFA in H_2O with 0.085% TFA with a flow of 1.0 mL/min over 20 min was the method used for analysis. The peptides were purified using preparative reverse-phased HPLC on a Zorbox SB-C18 PrepHT (21.2 mm × 250 mm, 7 μm particle size) column from Agilent with the Beckmann system, detection is also set to 214 nm. H_2O and CH_3CN both contains 1% TFA. Mass spectrometry (MS) using electrospray ionization (ESI) is used to confirm the identity of the peptide.

Characterization

HPLC, mass spectrometry, and NMR spectroscopy are used in the characterization of macrocyles (HPLC and mass spectrometry described in the purification section). ^{1}H, TOCSY, NOESY, ROESY were recorded on a Varian 800 MHz spectrometer. The ^{1}H spectra were taken with 128 scans and with preset conditions as needed. The TOCSY and ROESY were acquired with 70 ms mixing time and NOESY was acquired with 150 ms mixing time. Diffusion-Ordered Spectroscopy was performed using a Bruker 500 MHz cryoprobe instrument. Data was processed using XwinNMR and TopSpin.

References

(1) Nowick, J. S.; Chung, D. M.; Maitra, K.; Maitra, S.; Stigers, K. D.; Sun, Y. *J. Am. Chem. Soc.* **2000**, *122*, 7654-7661.

HPLC , MS ESI$^+$ TOF, and NMR (^{1}H, TOCSY and NOESY) of peptide **1b**

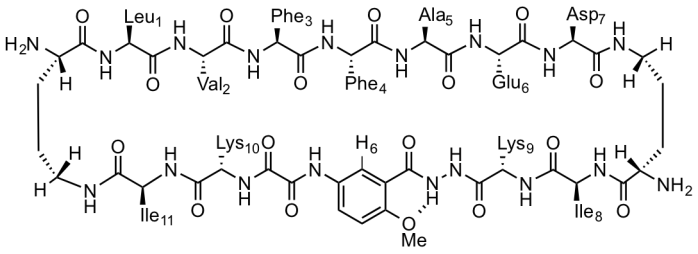

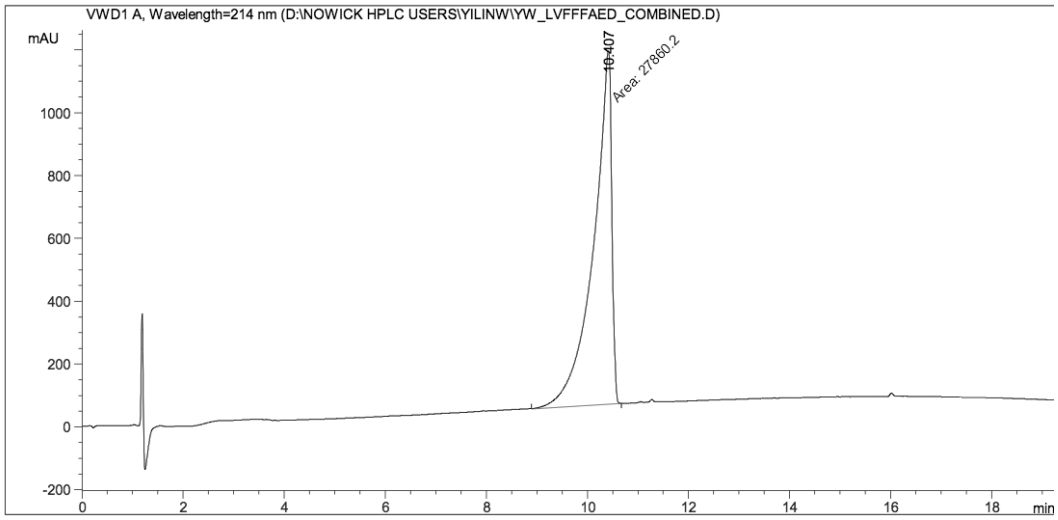

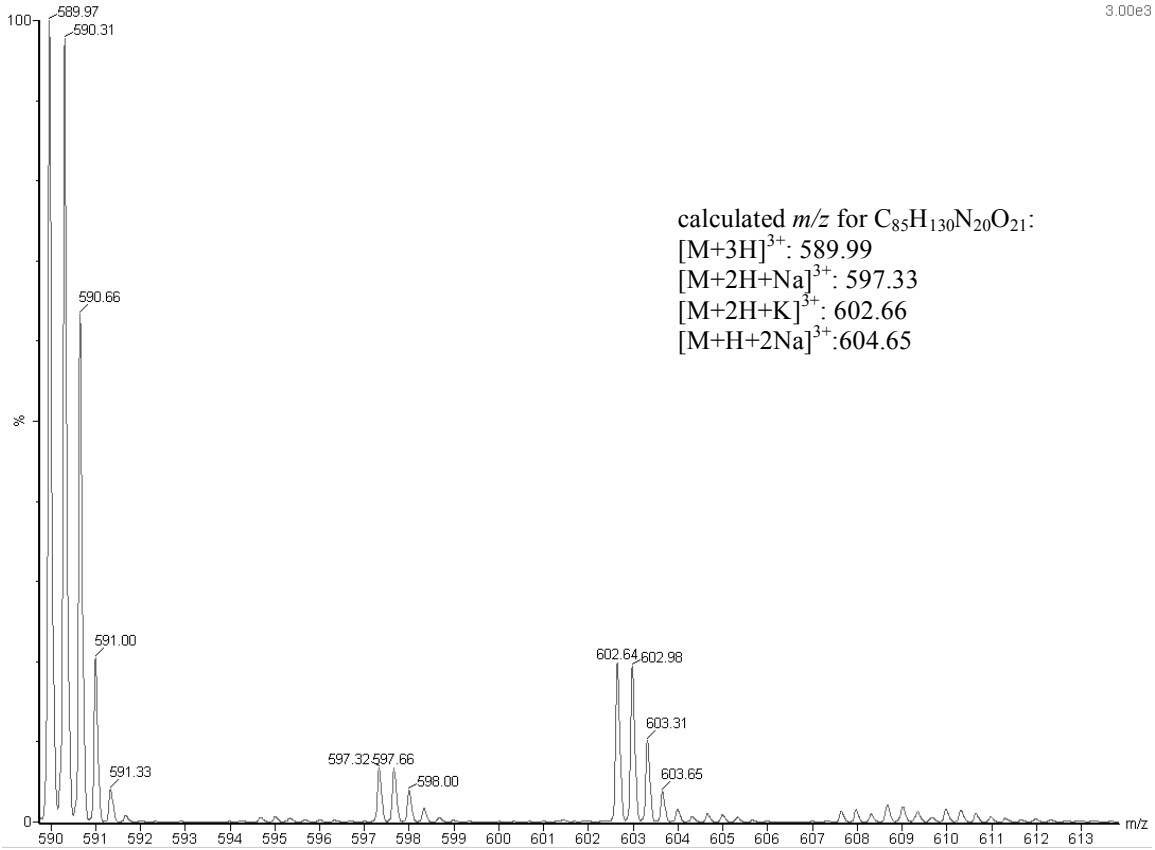

calculated *m/z* for $C_{85}H_{130}N_{20}O_{21}$:
$[M+3H]^{3+}$: 589.99
$[M+2H+Na]^{3+}$: 597.33
$[M+2H+K]^{3+}$: 602.66
$[M+H+2Na]^{3+}$:604.65

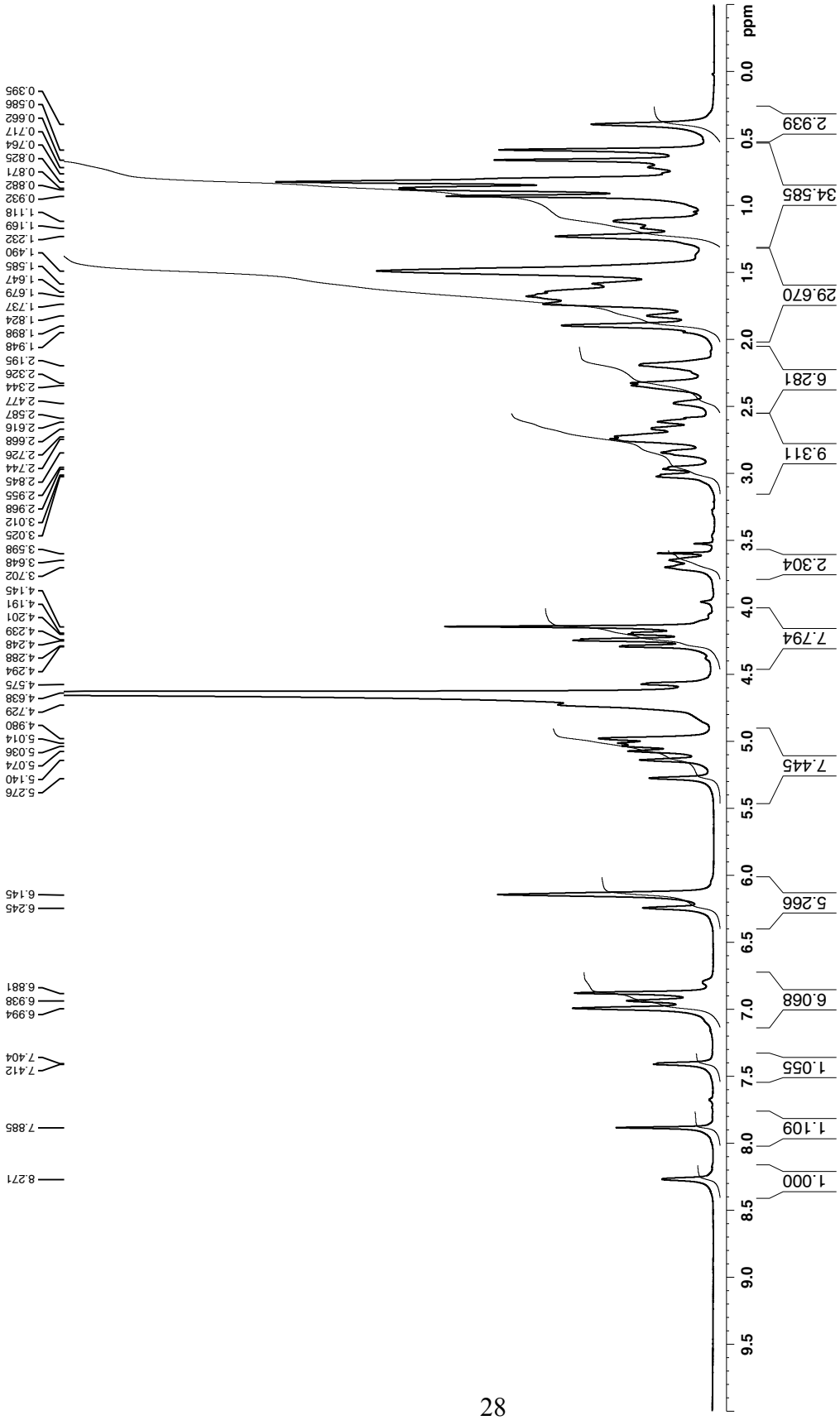
ppm
0.0
0.5
1.0
1.5
2.0
2.5
3.0
3.5
4.0
4.5
5.0
5.5
6.0
6.5
7.0
7.5
8.0
8.5
9.0
9.5
2.939
34.585
29.670
6.281
9.311
2.304
7.794
7.445
5.266
6.068
1.055
1.109
1.000
8.271
7.885
7.412
7.404
6.994
6.938
6.881
6.245
6.145
5.276
5.140
5.074
5.036
5.014
4.980
4.729
4.638
4.575
4.294
4.288
4.248
4.239
4.201
4.191
4.145
3.702
3.648
3.598
3.025
3.012
2.968
2.955
2.845
2.744
2.726
2.668
2.616
2.587
2.477
2.344
2.326
2.195
1.948
1.898
1.824
1.737
1.679
1.647
1.585
1.490
1.232
1.169
1.118
0.932
0.882
0.871
0.825
0.764
0.717
0.662
0.586
0.395

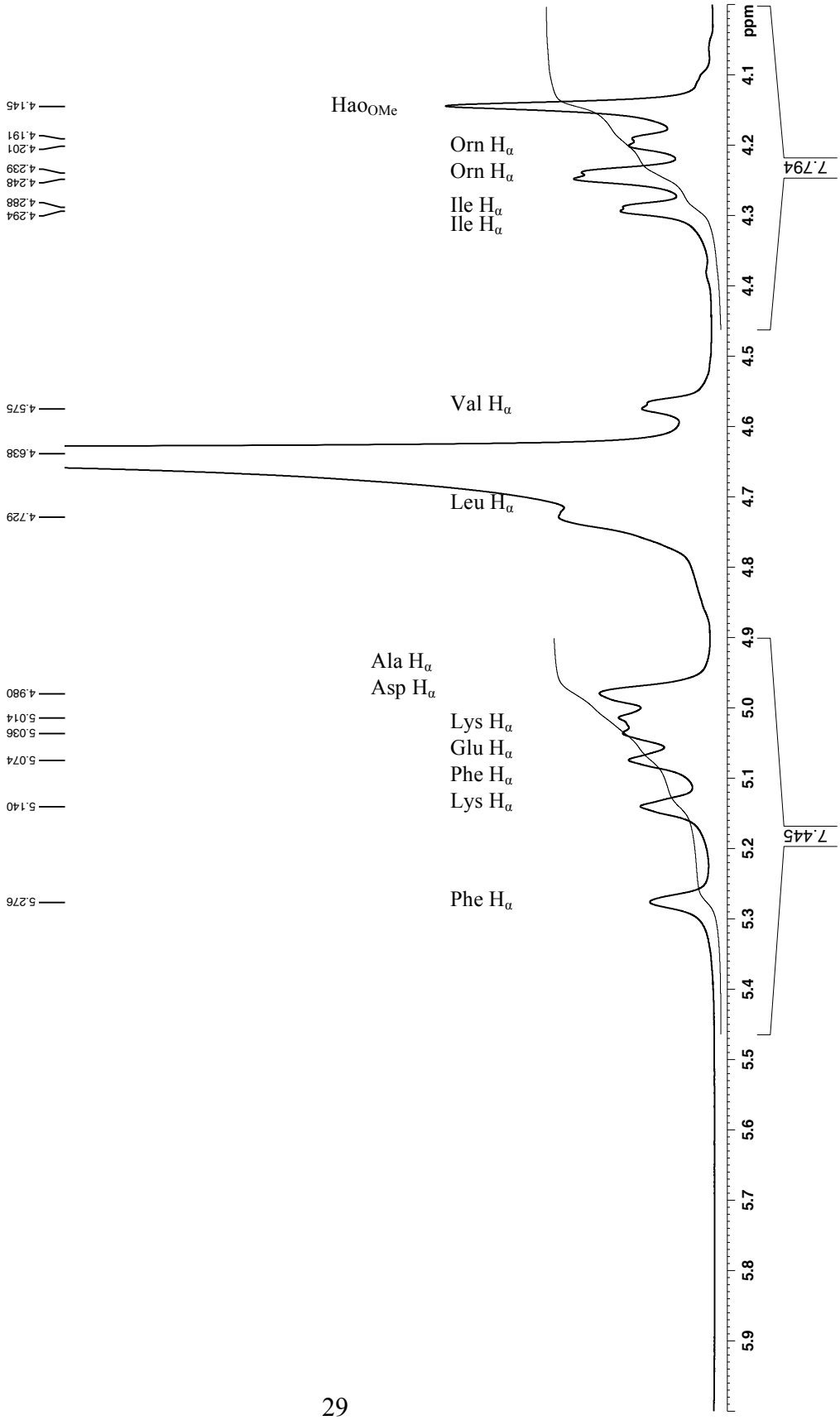
Hao$_{OMe}$
Orn H$_\alpha$
Orn H$_\alpha$
Ile H$_\alpha$
Ile H$_\alpha$
Val H$_\alpha$
Leu H$_\alpha$
Ala H$_\alpha$
Asp H$_\alpha$
Lys H$_\alpha$
Glu H$_\alpha$
Phe H$_\alpha$
Lys H$_\alpha$
Phe H$_\alpha$
4.145
4.191
4.201
4.239
4.248
4.288
4.294
4.575
4.638
4.729
4.980
5.014
5.036
5.074
5.140
5.276
7.794
7.445
ppm


20130701_YW_1_38_DOSY_cryo 2 1 /v/data/yilinw/nmr
F1 [log(m2/s)]
- 8
- 9
- 10
- 11
F2 [ppm]
2
4
6
8

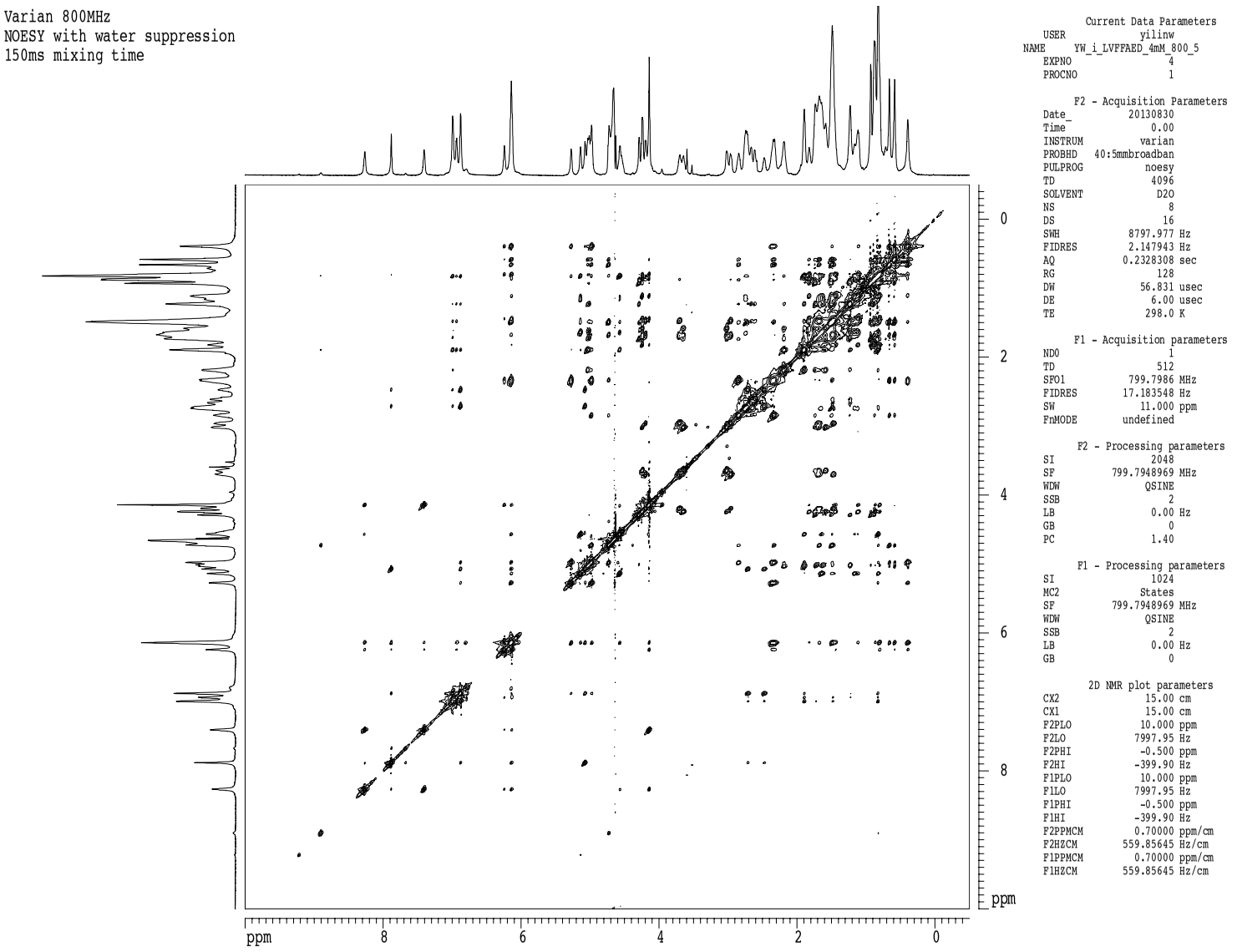

Current Data Parameters

USER	yilinw
NAME	YW_i_LVFFAED_4mM_800_5
EXPNO	4
PROCNO	1

F2 - Acquisition Parameters

Date_	20130830
Time	0.00
INSTRUM	varian
PROBHD	40:5mmbroadban
PULPROG	noesy
TD	4096
SOLVENT	D2O
NS	8
DS	16
SWH	8797.977 Hz
FIDRES	2.147943 Hz
AQ	0.2328308 sec
RG	128
DW	56.831 usec
DE	6.00 usec
TE	298.0 K

F1 - Acquisition parameters

ND0	1
TD	512
SFO1	799.7986 MHz
FIDRES	17.183548 Hz
SW	11.000 ppm
FnMODE	undefined

F2 - Processing parameters

SI	2048
SF	799.7948969 MHz
WDW	QSINE
SSB	2
LB	0.00 Hz
GB	0
PC	1.40

F1 - Processing parameters

SI	1024
MC2	States
SF	799.7948969 MHz
WDW	QSINE
SSB	2
LB	0.00 Hz
GB	0

2D NMR plot parameters

CX2	15.00 cm
CX1	15.00 cm
F2PLO	10.000 ppm
F2LO	7997.95 Hz
F2PHI	-0.500 ppm
F2HI	-399.90 Hz
F1PLO	10.000 ppm
F1LO	7997.95 Hz
F1PHI	-0.500 ppm
F1HI	-399.90 Hz
F2PPMCM	0.70000 ppm/cm
F2HZCM	559.85645 Hz/cm
F1PPMCM	0.70000 ppm/cm
F1HZCM	559.85645 Hz/cm

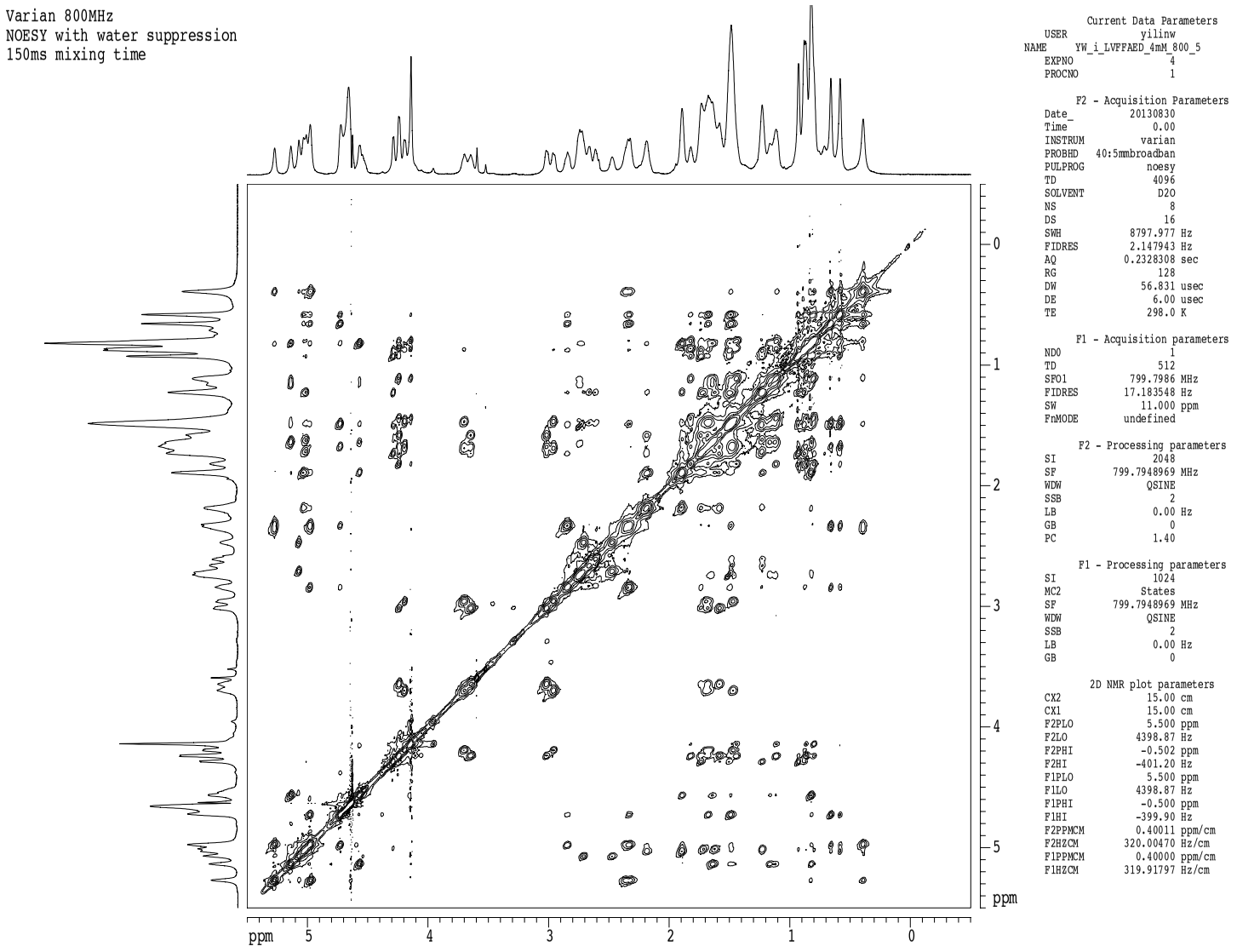

Current Data Parameters

USER	yilinw
NAME	YW_i_LVFFAED_4mM_800_5
EXPNO	4
PROCNO	1

F2 - Acquisition Parameters

Date_	20130830
Time	0.00
INSTRUM	varian
PROBHD	40:5mmbroadban
PULPROG	noesy
TD	4096
SOLVENT	D2O
NS	8
DS	16
SWH	8797.977 Hz
FIDRES	2.147943 Hz
AQ	0.2328308 sec
RG	128
DW	56.831 usec
DE	6.00 usec
TE	298.0 K

F1 - Acquisition parameters

ND0	1
TD	512
SFO1	799.7986 MHz
FIDRES	17.183548 Hz
SW	11.000 ppm
FnMODE	undefined

F2 - Processing parameters

SI	2048
SF	799.7948969 MHz
WDW	QSINE
SSB	2
LB	0.00 Hz
GB	0
PC	1.40

F1 - Processing parameters

SI	1024
MC2	States
SF	799.7948969 MHz
WDW	QSINE
SSB	2
LB	0.00 Hz
GB	0

2D NMR plot parameters

CX2	15.00 cm
CX1	15.00 cm
F2PLO	5.500 ppm
F2LO	4398.87 Hz
F2PHI	-0.502 ppm
F2HI	-401.20 Hz
F1PLO	5.500 ppm
F1LO	4398.87 Hz
F1PHI	-0.500 ppm
F1HI	-399.90 Hz
F2PPMCM	0.40011 ppm/cm
F2HZCM	320.00470 Hz/cm
F1PPMCM	0.40000 ppm/cm
F1HZCM	319.91797 Hz/cm

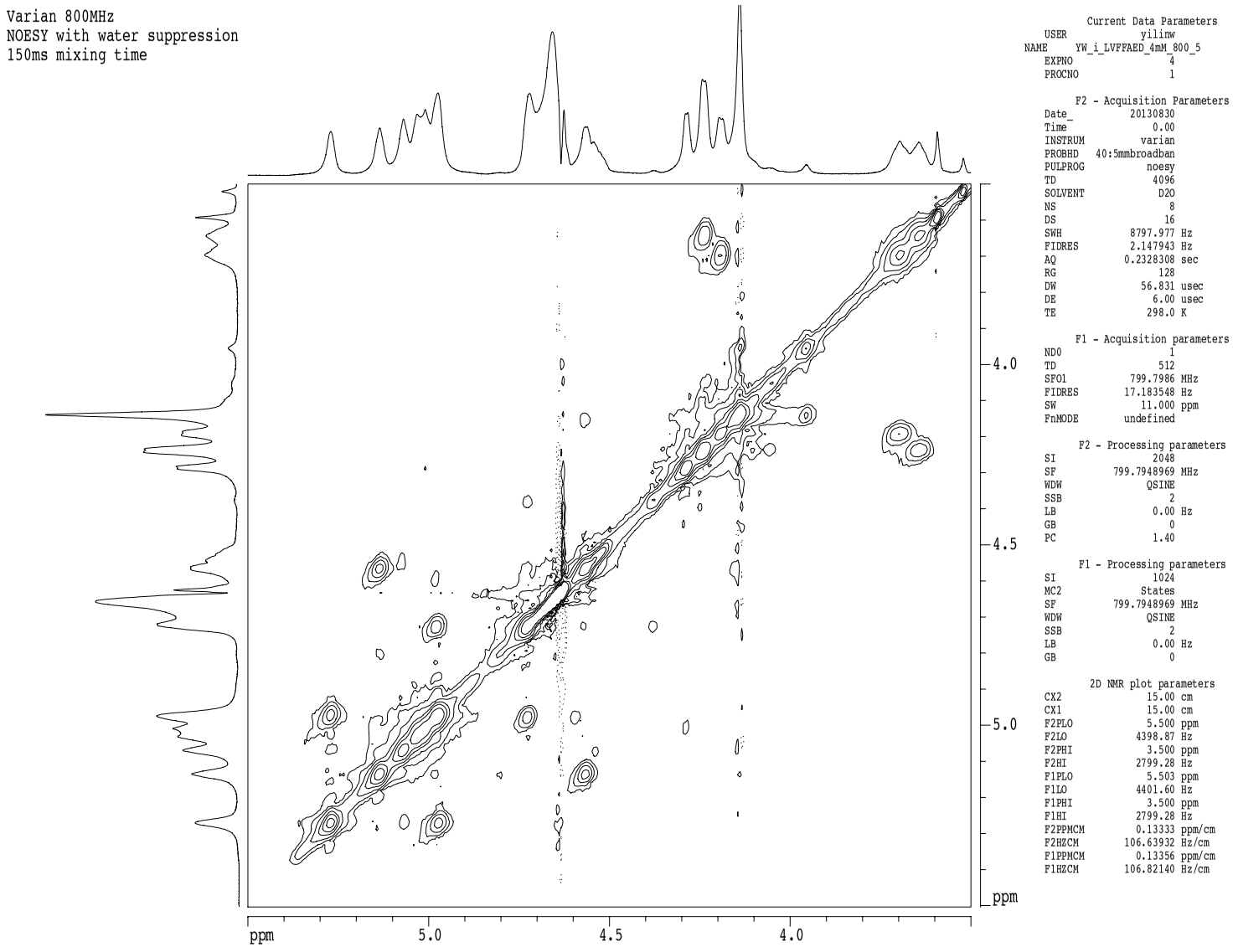

Current Data Parameters

USER	yilinw
NAME	YW_i_LVFFAED_4mM_800_5
EXPNO	4
PROCNO	1

F2 - Acquisition Parameters

Date_	20130830
Time	0.00
INSTRUM	varian
PROBHD	40:5mmbroadban
PULPROG	noesy
TD	4096
SOLVENT	D2O
NS	8
DS	16
SWH	8797.977 Hz
FIDRES	2.147943 Hz
AQ	0.2328308 sec
RG	128
DW	56.831 usec
DE	6.00 usec
TE	298.0 K

F1 - Acquisition parameters

ND0	1
TD	512
SFO1	799.7986 MHz
FIDRES	17.183548 Hz
SW	11.000 ppm
FnMODE	undefined

F2 - Processing parameters

SI	2048
SF	799.7948969 MHz
WDW	QSINE
SSB	2
LB	0.00 Hz
GB	0
PC	1.40

F1 - Processing parameters

SI	1024
MC2	States
SF	799.7948969 MHz
WDW	QSINE
SSB	2
LB	0.00 Hz
GB	0

2D NMR plot parameters

CX2	15.00 cm
CX1	15.00 cm
F2PLO	5.500 ppm
F2LO	4398.87 Hz
F2PHI	3.500 ppm
F2HI	2799.28 Hz
F1PLO	5.503 ppm
F1LO	4401.60 Hz
F1PHI	3.500 ppm
F1HI	2799.28 Hz
F2PPMCM	0.13333 ppm/cm
F2HZCM	106.63932 Hz/cm
F1PPMCM	0.13356 ppm/cm
F1HZCM	106.82140 Hz/cm

HPLC , MS ESI$^+$ TOF, and NMR (^{1}H, TOCSY and ROESY) of peptide **1c**

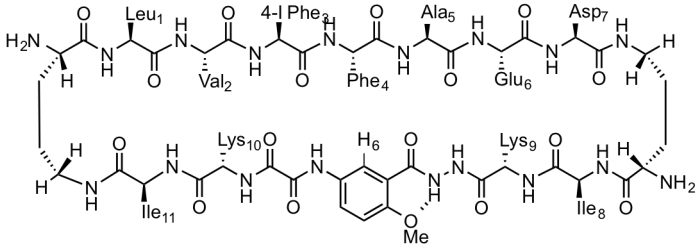

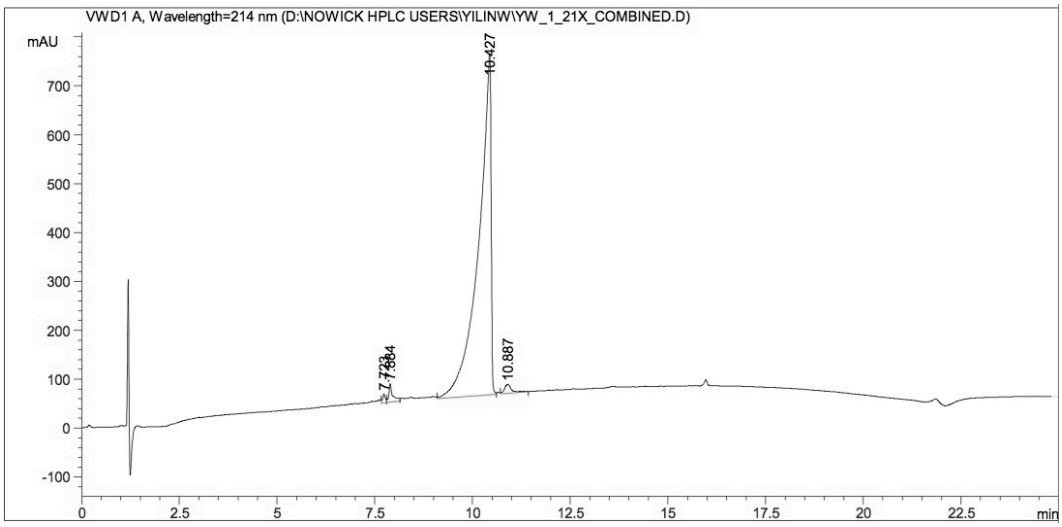

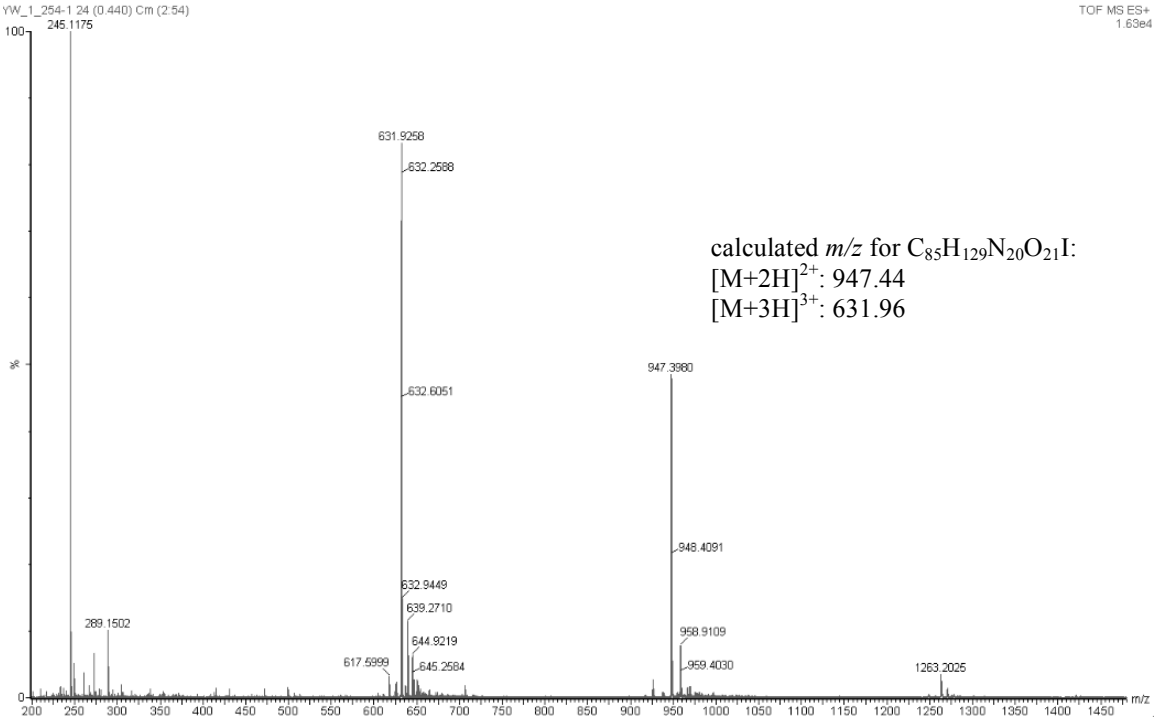

calculated *m/z* for $C_{85}H_{129}N_{20}O_{21}I$:
$[M+2H]^{2+}$: 947.44
$[M+3H]^{3+}$: 631.96

ppm
9.5
9.0
8.5
8.0
7.5
7.0
6.5
6.0
5.5
5.0
4.5
4.0
3.5
3.0
2.5
2.0
1.5
1.0
0.5
0.0
1.041
1.056
1.017
5.470
1.647
1.734
1.000
5.252
2.025
1.616
7.551
1.690
9.969
2.707
1.797
35.696
27.464
3.026
8.062
7.513
6.925
6.678
6.582
5.968
5.639
4.950
4.778
4.740
4.689
4.475
4.240
4.032
3.832
3.719
3.279
3.222
2.603
2.549
2.448
2.187
2.120
1.988
1.691
1.532
1.424
1.310
1.268
1.167
1.107
0.915
0.786
0.710
0.465
0.439
0.383
0.328
0.255
0.213
0.002

HPLC , MS ESI$^+$ TOF, and NMR (^{1}H, TOCSY and ROESY) of peptide **2b**

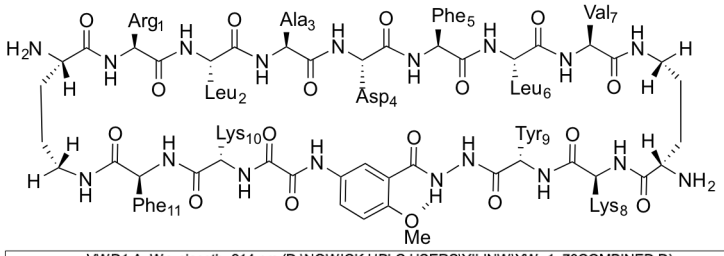

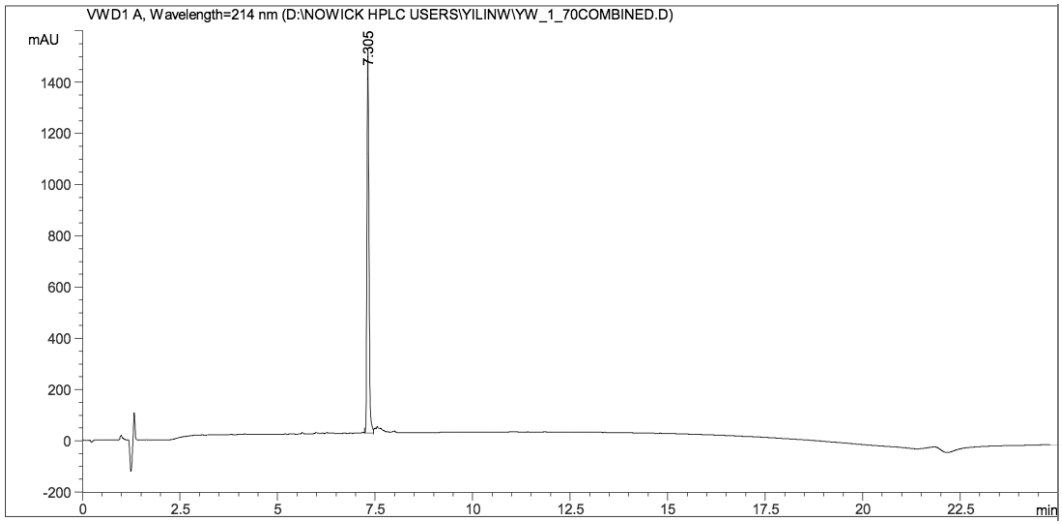

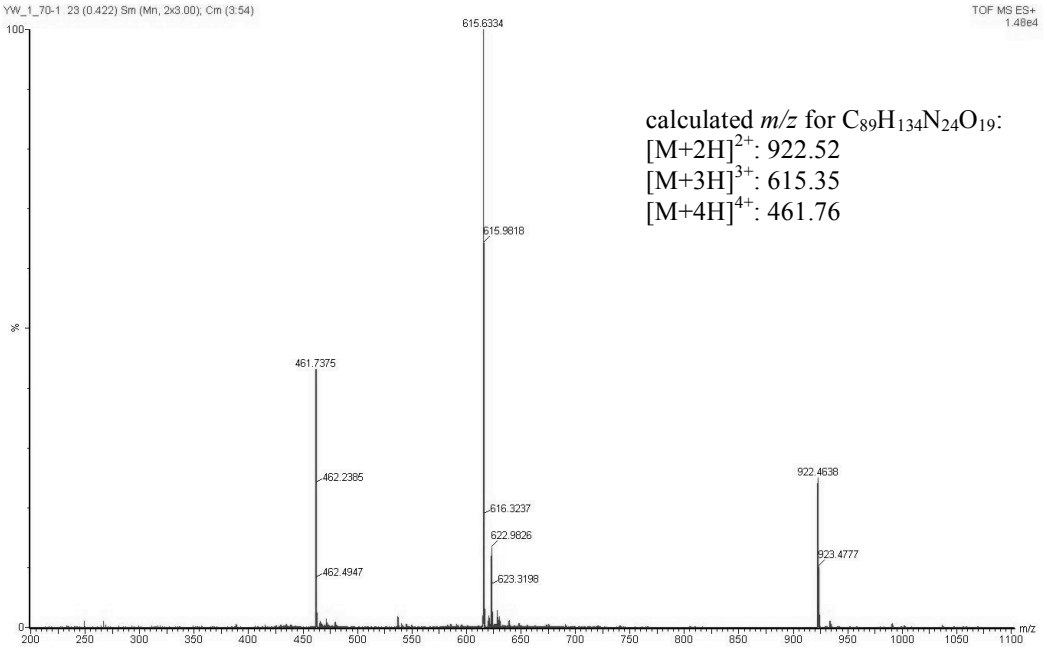

calculated *m/z* for $C_{89}H_{134}N_{24}O_{19}$:
$[M+2H]^{2+}$: 922.52
$[M+3H]^{3+}$: 615.35
$[M+4H]^{4+}$: 461.76

8.069
7.931
7.922
7.367
7.358
7.324
7.316
7.295
7.286
7.263
7.274
7.179
7.127
7.118
7.088
7.078
7.019
7.010
6.782
6.772
4.879
4.861
4.768
4.664
4.656
4.648
4.557
4.546
4.538
4.447
4.437
4.427
4.418
4.381
4.372
4.342
4.364
4.261
4.253
4.125
4.118
4.111
4.104
4.014
4.005
3.994
3.963
3.367
3.359
3.351
3.283
3.274
3.253
3.246
3.236
3.229
3.167
3.157
3.130
3.097
3.080
3.053
3.043
2.955
2.944
2.935
2.917
2.908
2.896
2.879
2.667
2.660
2.647
2.640
2.629
2.620
2.610
1.990
1.984
1.975
1.967
1.834
1.815
1.805
1.783
1.774
1.756
1.749
1.657
1.649
1.639
1.628
1.617
1.570
1.548
1.542
1.524
1.517
1.373
1.365
1.314
1.292
1.284
ppm
9.5
9.0
8.5
8.0
7.5
7.0
6.5
6.0
5.5
5.0
4.5
4.0
3.5
3.0
2.5
2.0
1.5
1.0
0.5
0.0
16.536
34.769
1.003
1.976
15.837
0.981
3.988
1.841
1.071
4.757
1.384
1.255
1.299
2.000
7.016
5.964
0.827
0.896

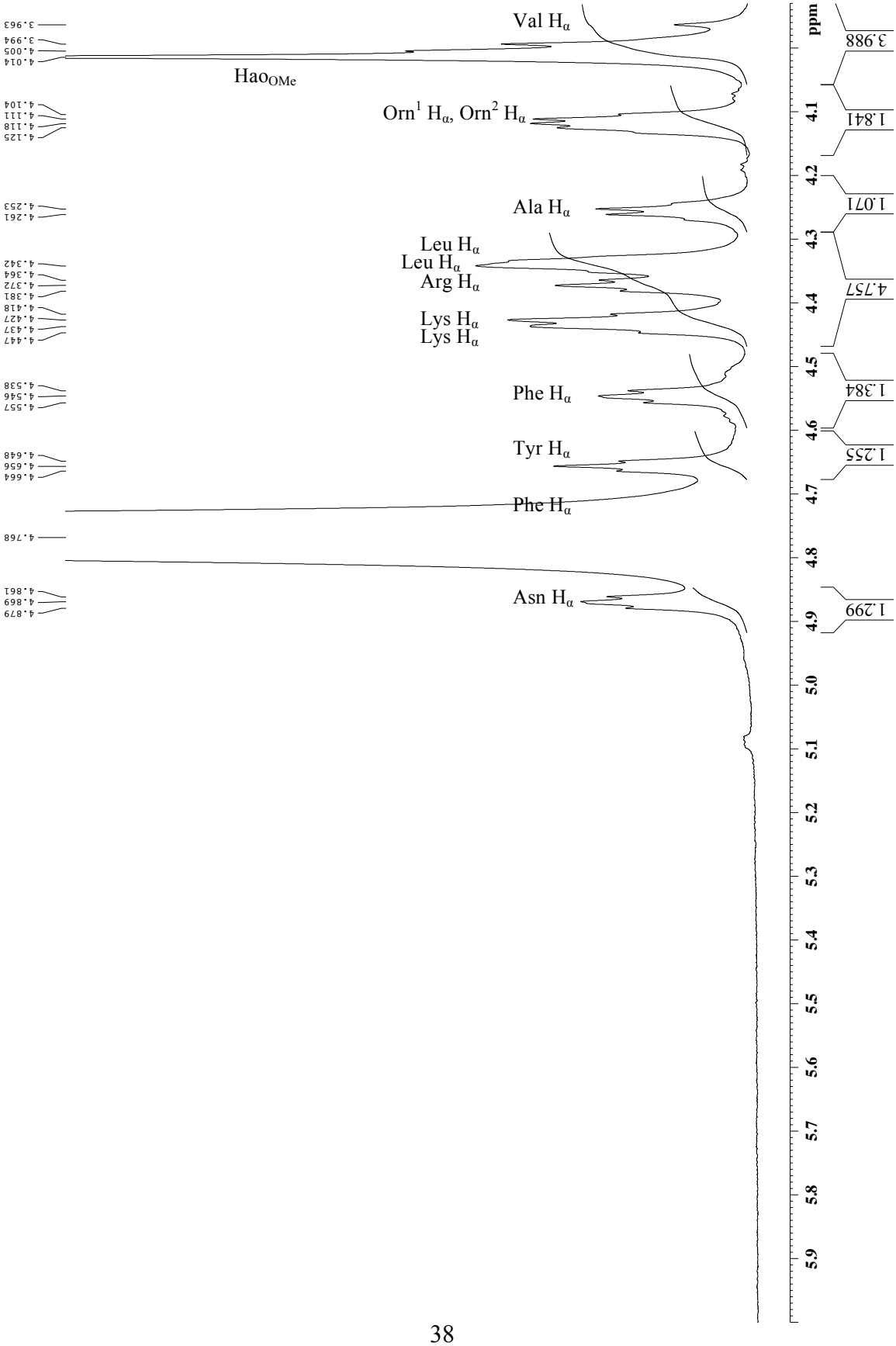
Val Hα
Haoome
Orn1 Hα, Orn2 Hα
Ala Hα
Leu Hα
Leu Hα
Arg Hα
Lys Hα
Lys Hα
Phe Hα
Tyr Hα
Phe Hα
Asn Hα
ppm
3.988
1.841
1.071
4.757
1.384
1.255
1.299

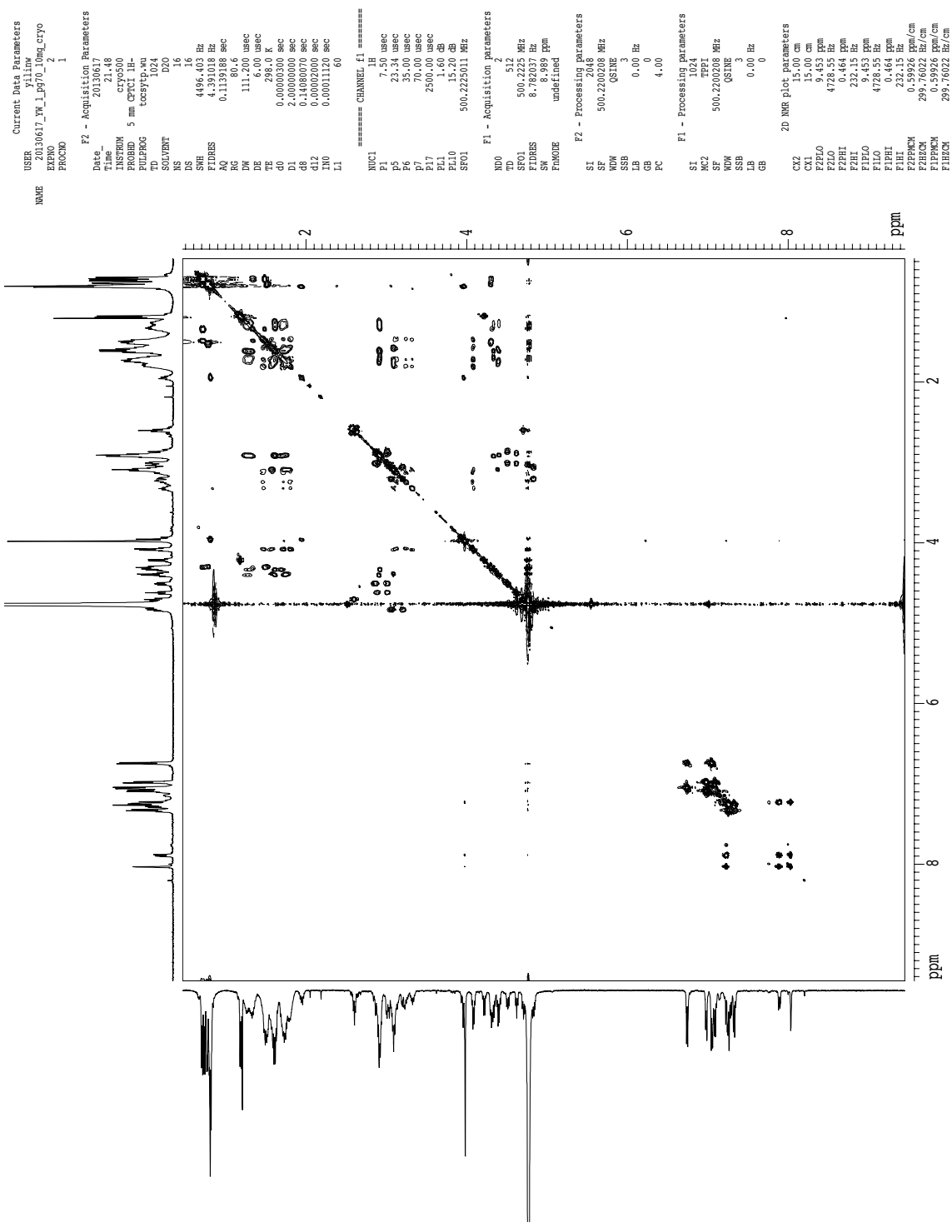
Current Data Parameters
NAME yilinw
EXPNO 2
PROCNO 1
F2 - Acquisition Parameters
Date_ 20130617
Time 21.48
INSTRUM cryo500
PROBHD 5 mm CPTCI 1H-
PULPROG tocsytp.wu
TD 1024
SOLVENT D2O
NS 16
DS 16
SWH 4496.403 Hz
FIDRES 4.391018 Hz
AQ 0.1139188 sec
RG 80.6
DW 111.200 usec
DE 6.00 usec
TE 298.0 K
d0 0.00000300 sec
D1 2.00000000 sec
d8 0.14080070 sec
d12 0.00002000 sec
IN0 0.00011120 sec
L1 60
======== CHANNEL f1 ========
NUC1 1H
P1 7.50 usec
p5 23.34 usec
P6 35.00 usec
p7 70.00 usec
P17 2500.00 usec
PL1 1.60 dB
PL10 15.20 dB
SFO1 500.2225011 MHz
F1 - Acquisition parameters
2
TD 512
SFO1 500.2225 MHz
FIDRES 8.782037 Hz
SW 8.999 ppm
FnMODE undefined
F2 - Processing parameters
SI 1024
SF 500.2200208 MHz
WDW QSINE
SSB 3
LB 0.00 Hz
GB 0
PC 4.00
F1 - Processing parameters
SI 1024
MC2 TPPI
SF 500.2200208 MHz
WDW QSINE
SSB 3
LB 0.00 Hz
GB 0
2D NMR plot parameters
CX2 15.00 cm
CX1 15.00 cm
F2PLO 9.453 ppm
F2LO 4728.55 Hz
F2PHI 0.464 ppm
F2HI 232.15 Hz
F1PLO 9.453 ppm
F1LO 4728.55 Hz
F1PHI 0.464 ppm
F1HI 232.15 Hz
F2PPMCM 0.59926 ppm/cm
F2HZCM 299.76022 Hz/cm
F1PPMCM 0.59926 ppm/cm
F1HZCM 299.76022 Hz/cm
2
4
6
8
ppm
2
4
6
8
ppm

presat ROESY

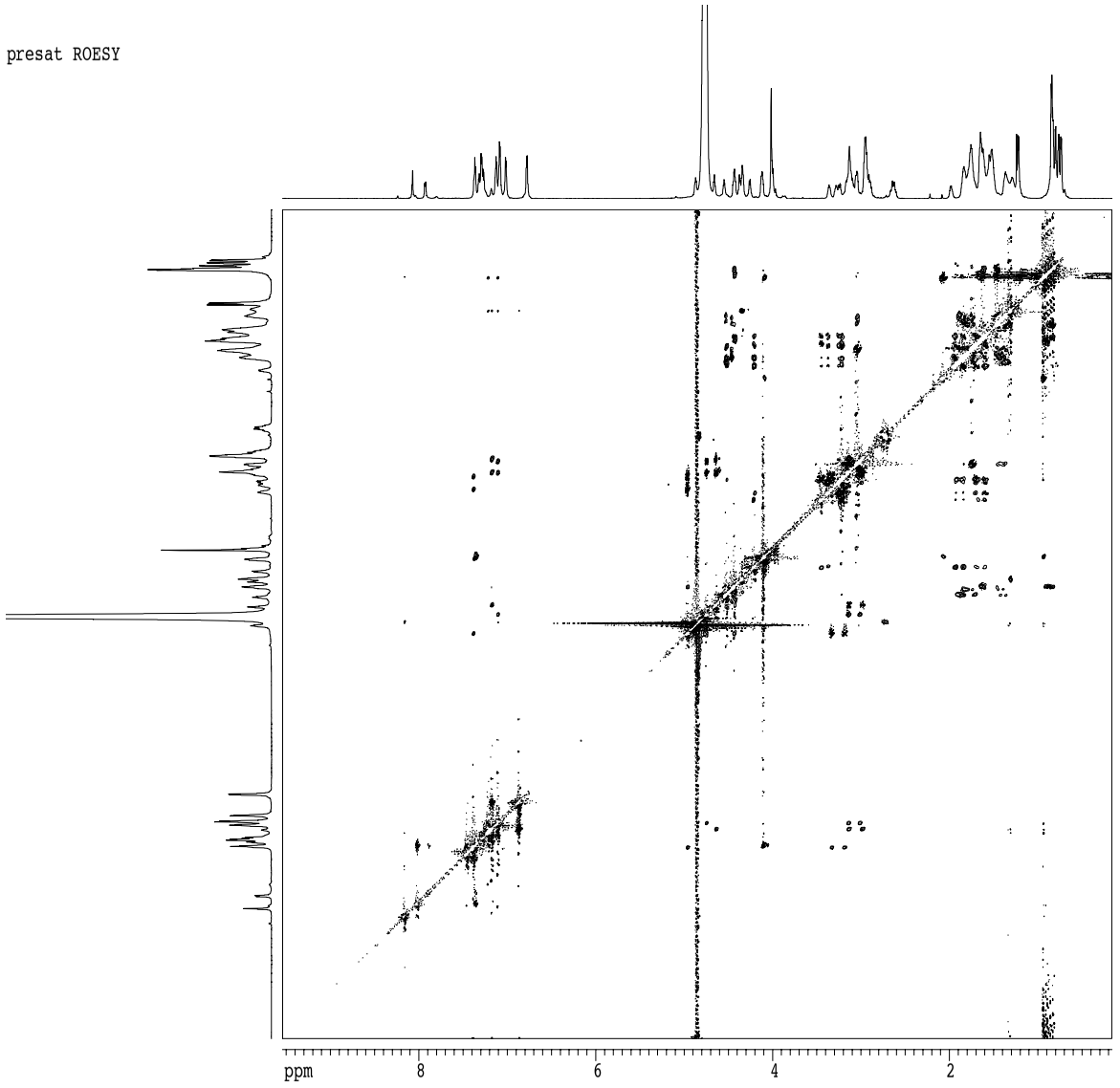

Current Data Parameters

USER	yilinw
NAME	20130720_YW_1_70_800
EXPNO	3
PROCNO	1

F2 - Acquisition Parameters

Date_	20130701
Time	0.00
INSTRUM	varian
PROBHD	40:5mmbroadban
PULPROG	roesy
TD	2048
SOLVENT	D2O
NS	8
DS	16
SWH	7499.766 Hz
FIDRES	3.661995 Hz
AQ	0.1365876 sec
RG	128
DW	66.669 usec
DE	6.00 usec
TE	298.0 K

F1 - Acquisition parameters

ND0	1
TD	512
SFO1	799.7986 MHz
FIDRES	14.647980 Hz
SW	9.377 ppm
FnMODE	undefined

F2 - Processing parameters

SI	2048
SF	799.7947056 MHz
WDW	QSINE
SSB	2
LB	0.00 Hz
GB	0
PC	1.40

F1 - Processing parameters

SI	1024
MC2	States
SF	799.7947056 MHz
WDW	QSINE
SSB	2
LB	0.00 Hz
GB	0

2D NMR plot parameters

CX2	15.00 cm
CX1	15.00 cm
F2PLO	9.540 ppm
F2LO	7630.04 Hz
F2PHI	0.163 ppm
F2HI	130.28 Hz
F1PLO	9.540 ppm
F1LO	7630.04 Hz
F1PHI	0.163 ppm
F1HI	130.28 Hz
F2PPMCM	0.62514 ppm/cm
F2HZCM	499.98434 Hz/cm
F1PPMCM	0.62514 ppm/cm
F1HZCM	499.98434 Hz/cm

HPLC , MS ESI^{+} TOF, and NMR (^{1}H, TOCSY and ROESY) of peptide **2c**

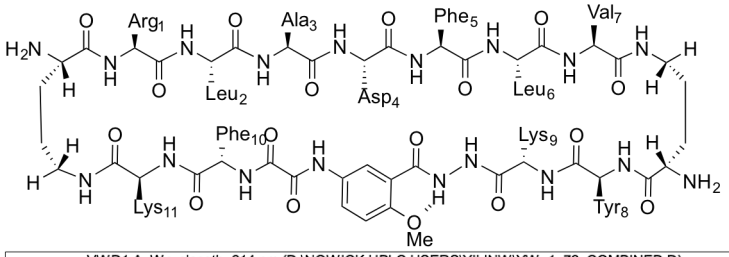

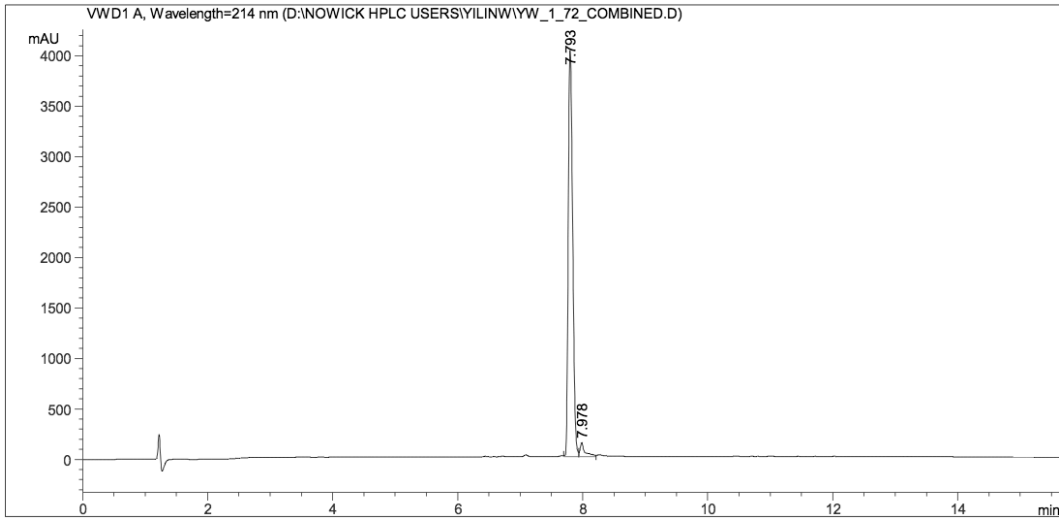

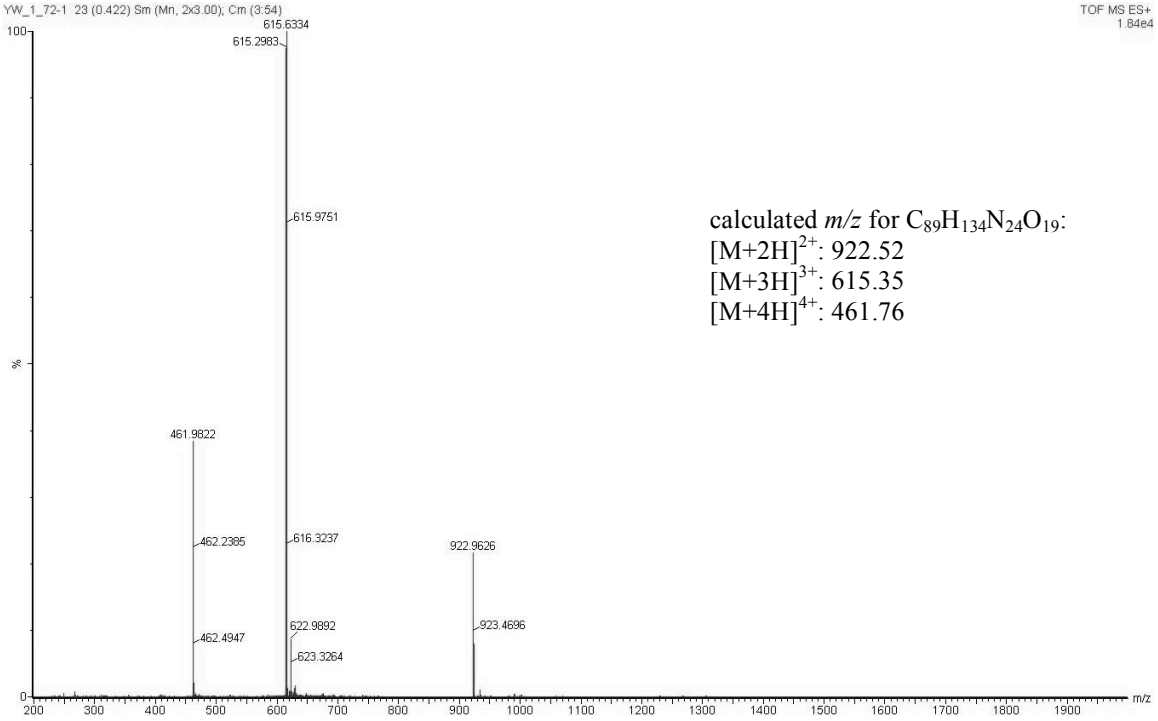

calculated *m/z* for $C_{89}H_{134}N_{24}O_{19}$:
$[M+2H]^{2+}$: 922.52
$[M+3H]^{3+}$: 615.35
$[M+4H]^{4+}$: 461.76

8.219
8.211
8.042
7.367
7.343
7.281
7.040
7.032
6.928
6.858
6.777
5.186
4.858
4.768
4.590
4.566
4.543
4.490
4.378
4.263
4.209
4.141
4.071
4.060
3.541
3.528
3.513
3.178
3.089
3.043
3.007
2.923
2.883
2.852
2.717
2.701
2.587
2.575
2.558
1.862
1.786
1.749
1.688
1.638
1.625
1.563
1.553
1.522
1.489
1.463
1.431
1.342
0.859
0.853
0.840
0.796
0.727
1.240
1.530
3.987
2.102
2.035
2.096
2.888
1.879
1.037
5.578
1.385
3.358
2.955
1.066
0.407
2.000
3.714
6.870
5.809
1.151
0.933
39.612
17.828
ppm

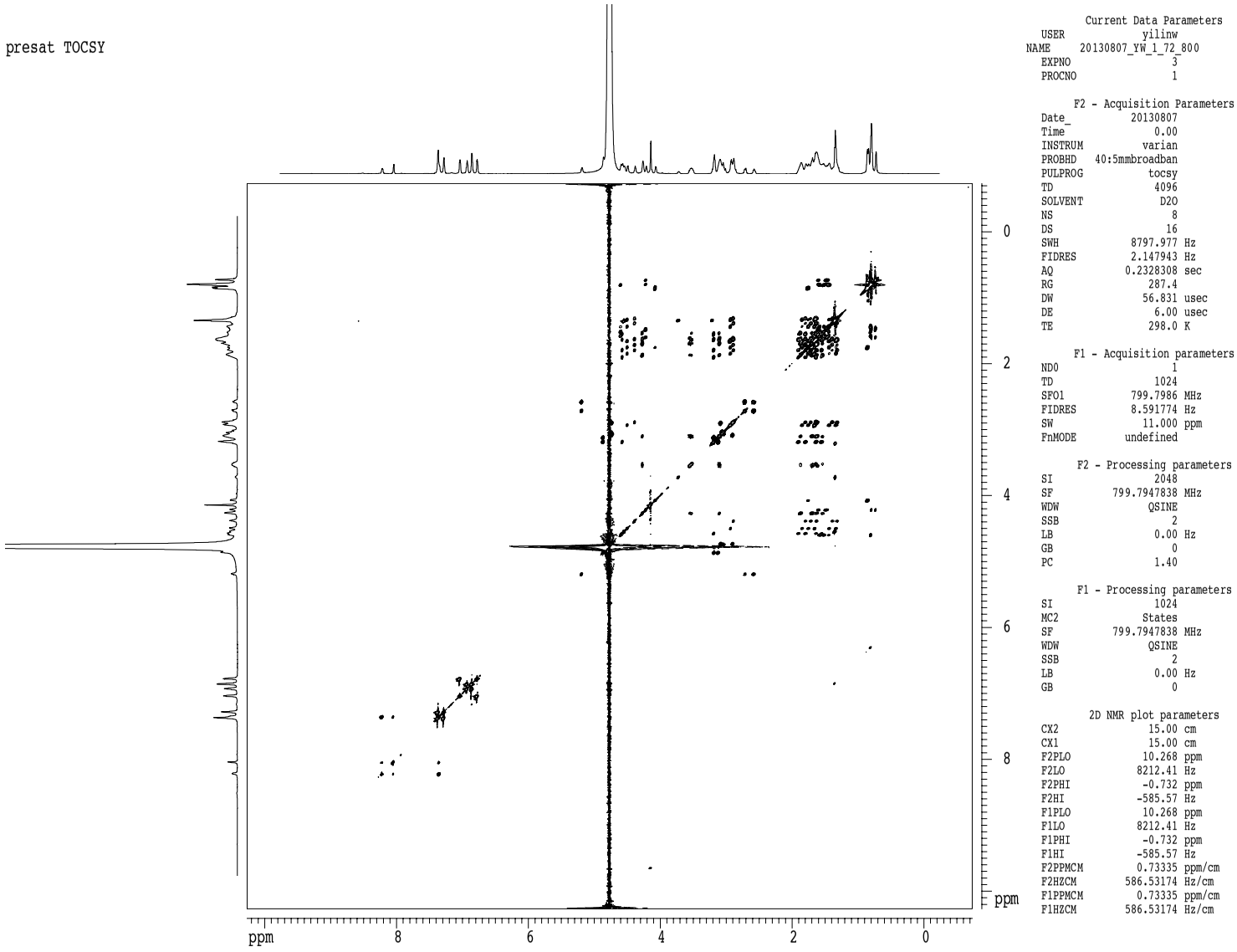

Current Data Parameters

USER	yilinw
NAME	20130807_YW_1_72_800
EXPNO	3
PROCNO	1

F2 - Acquisition Parameters

Date_	20130807
Time	0.00
INSTRUM	varian
PROBHD	40:5mmbroadban
PULPROG	tocsy
TD	4096
SOLVENT	D2O
NS	8
DS	16
SWH	8797.977 Hz
FIDRES	2.147943 Hz
AQ	0.2328308 sec
RG	287.4
DW	56.831 usec
DE	6.00 usec
TE	298.0 K

F1 - Acquisition parameters

ND0	1
TD	1024
SFO1	799.7986 MHz
FIDRES	8.591774 Hz
SW	11.000 ppm
FnMODE	undefined

F2 - Processing parameters

SI	2048
SF	799.7947838 MHz
WDW	QSINE
SSB	2
LB	0.00 Hz
GB	0
PC	1.40

F1 - Processing parameters

SI	1024
MC2	States
SF	799.7947838 MHz
WDW	QSINE
SSB	2
LB	0.00 Hz
GB	0

2D NMR plot parameters

CX2	15.00 cm
CX1	15.00 cm
F2PLO	10.268 ppm
F2LO	8212.41 Hz
F2PHI	-0.732 ppm
F2HI	-585.57 Hz
F1PLO	10.268 ppm
F1LO	8212.41 Hz
F1PHI	-0.732 ppm
F1HI	-585.57 Hz
F2PPMCM	0.73335 ppm/cm
F2HZCM	586.53174 Hz/cm
F1PPMCM	0.73335 ppm/cm
F1HZCM	586.53174 Hz/cm

presat TOCSY

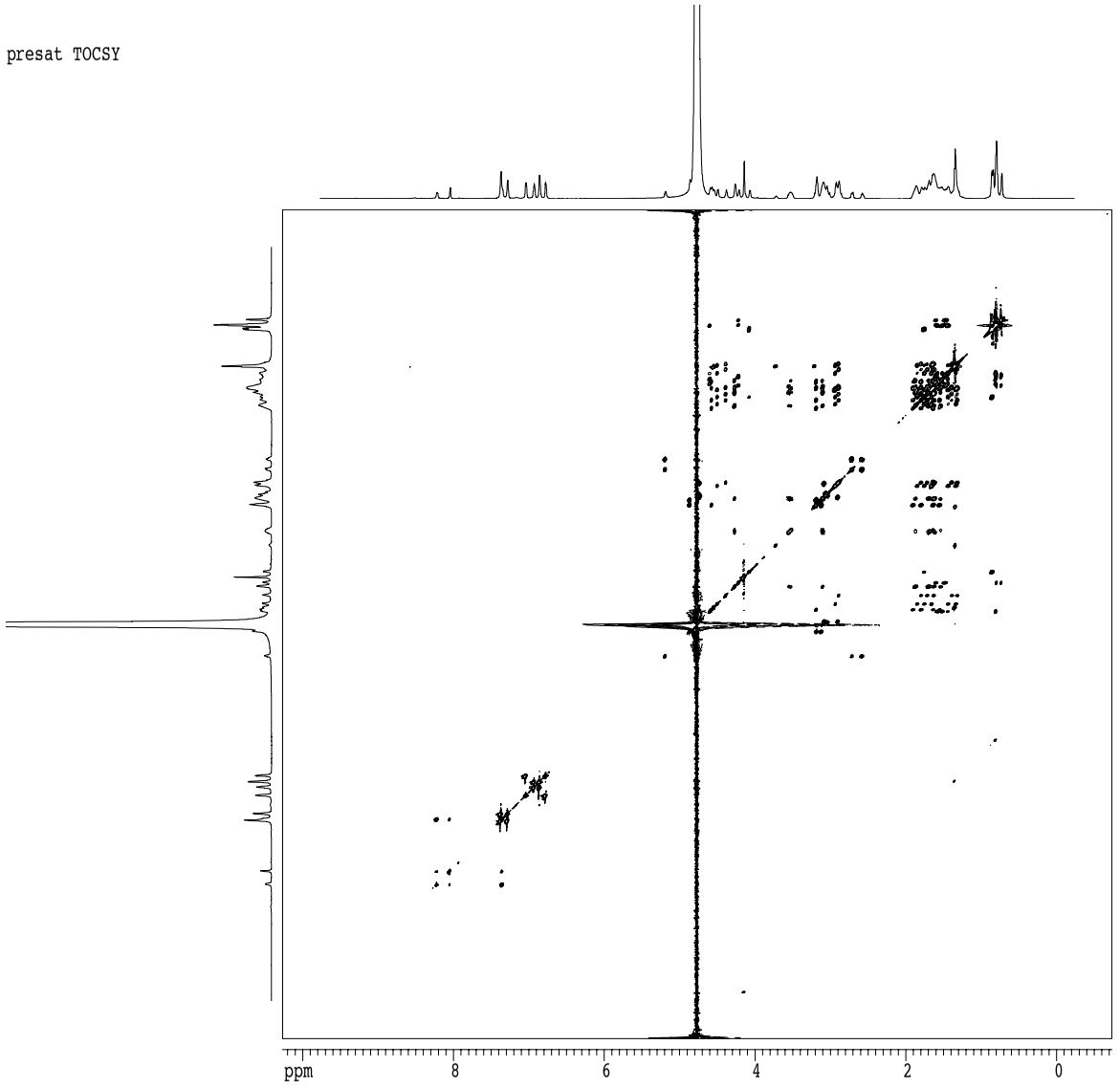

Current Data Parameters

USER	yilinw
NAME	20130807_YW_1_72_800
EXPNO	3
PROCNO	1

F2 - Acquisition Parameters

Date_	20130807
Time	0.00
INSTRUM	varian
PROBHD	40:5mmbroadban
PULPROG	tocsy
TD	4096
SOLVENT	D2O
NS	8
DS	16
SWH	8797.977 Hz
FIDRES	2.147943 Hz
AQ	0.2328308 sec
RG	287.4
DW	56.831 usec
DE	6.00 usec
TE	298.0 K

F1 - Acquisition parameters

ND0	1
TD	1024
SFO1	799.7986 MHz
FIDRES	8.591774 Hz
SW	11.000 ppm
FnMODE	undefined

F2 - Processing parameters

SI	2048
SF	799.7947838 MHz
WDW	QSINE
SSB	2
LB	0.00 Hz
GB	0
PC	1.40

F1 - Processing parameters

SI	1024
MC2	States
SF	799.7947838 MHz
WDW	QSINE
SSB	2
LB	0.00 Hz
GB	0

2D NMR plot parameters

CX2	15.00 cm
CX1	15.00 cm
F2PLO	10.268 ppm
F2LO	8212.41 Hz
F2PHI	-0.732 ppm
F2HI	-585.57 Hz
F1PLO	10.268 ppm
F1LO	8212.41 Hz
F1PHI	-0.732 ppm
F1HI	-585.57 Hz
F2PPMCM	0.73335 ppm/cm
F2HZCM	586.53174 Hz/cm
F1PPMCM	0.73335 ppm/cm
F1HZCM	586.53174 Hz/cm

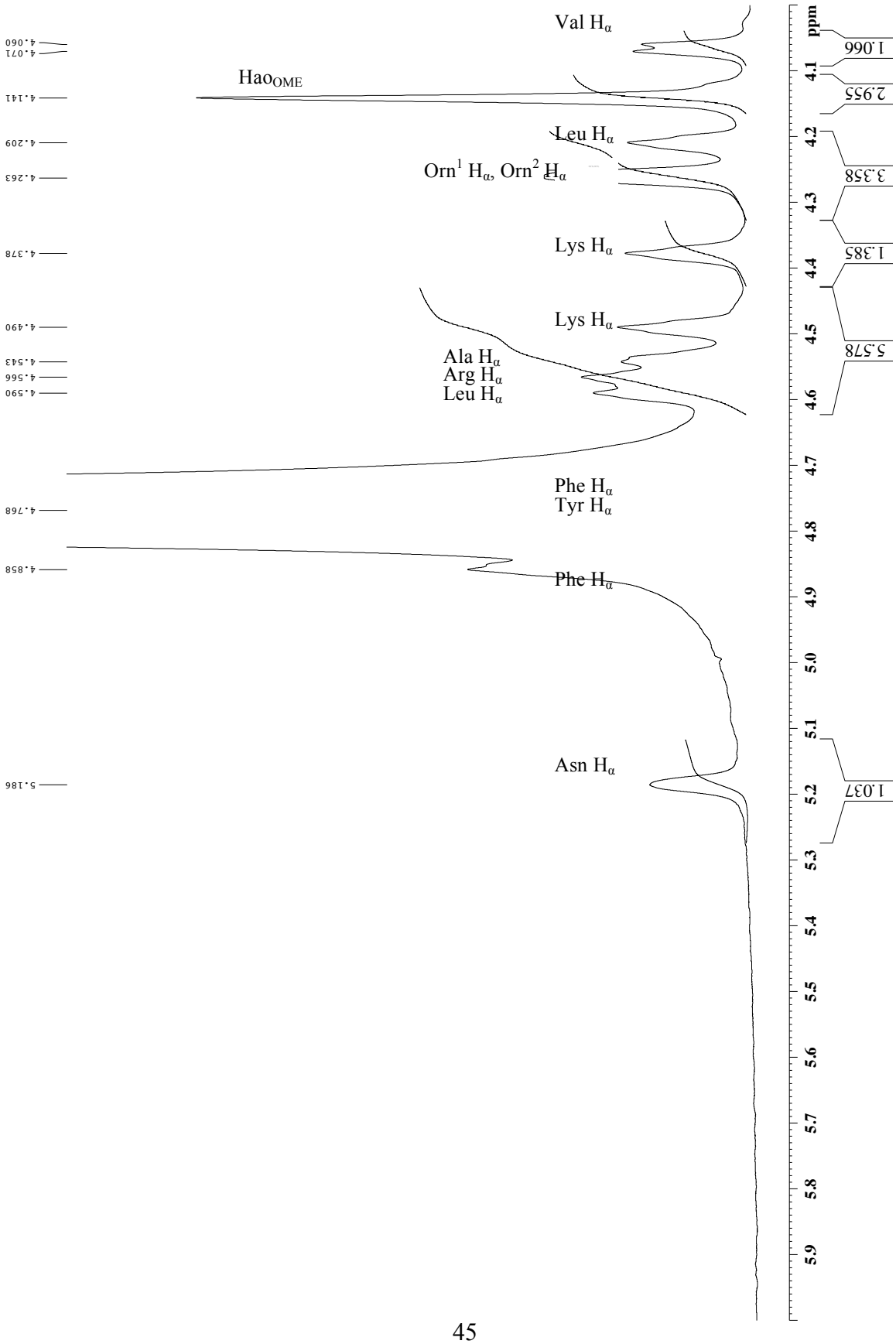
Val Hα
Haoome
Leu Hα
Orn1 Hα, Orn2 Hα
Lys Hα
Lys Hα
Ala Hα
Arg Hα
Leu Hα
Phe Hα
Tyr Hα
Phe Hα
Asn Hα
4.060
4.071
4.141
4.209
4.263
4.378
4.490
4.543
4.566
4.590
4.768
4.858
5.186
ppm
4.1
4.2
4.3
4.4
4.5
4.6
4.7
4.8
4.9
5.0
5.1
5.2
5.3
5.4
5.5
5.6
5.7
5.8
5.9
1.066
2.955
3.358
1.385
5.578
1.037

HPLC , MS ESI$^+$ TOF, and NMR (^{1}H, TOCSY and ROESY) of peptide **2d**

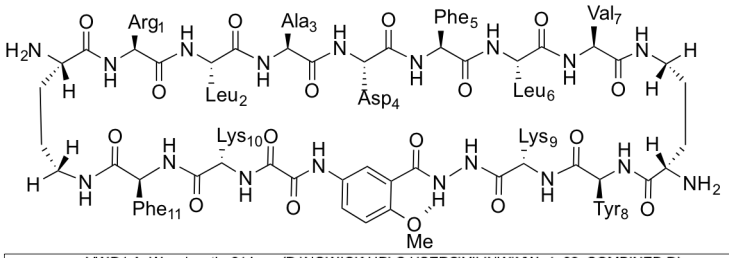

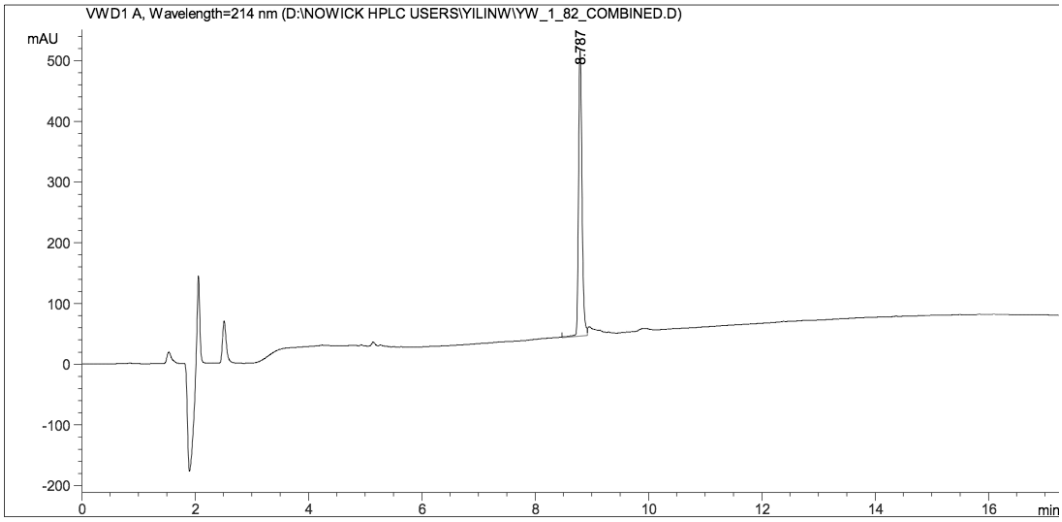

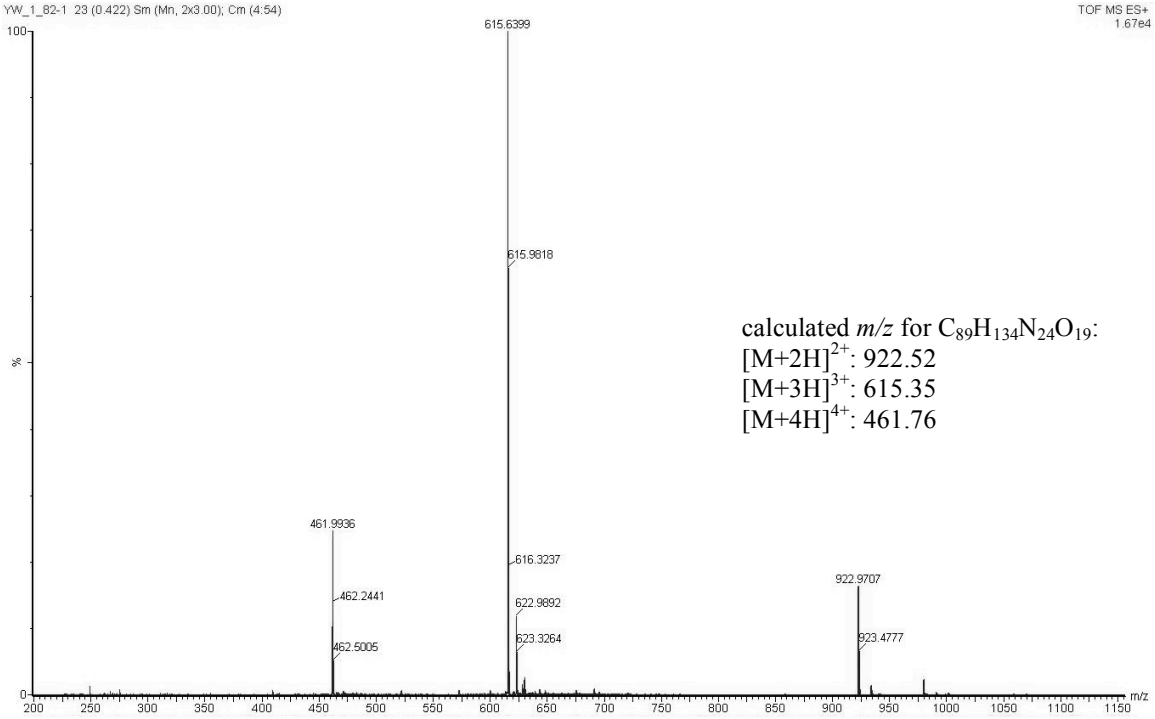

calculated *m/z* for $C_{89}H_{134}N_{24}O_{19}$:
$[M+2H]^{2+}$: 922.52
$[M+3H]^{3+}$: 615.35
$[M+4H]^{4+}$: 461.76

8.060
7.988
7.978
7.360
7.352
7.327
7.319
7.310
7.292
7.284
7.094
7.085
7.075
7.052
7.044
6.995
6.988
6.780
6.771
4.768
4.645
4.563
4.457
4.449
4.419
4.347
4.280
4.272
4.112
4.107
4.074
4.009
3.999
3.298
3.132
3.060
3.044
3.007
2.966
2.955
2.944
2.935
2.919
2.908
2.852
2.714
2.695
2.641
2.632
1.868
1.821
1.797
1.672
1.663
1.653
1.634
1.624
1.616
1.570
1.562
1.526
1.443
1.376
1.336
1.286
1.224
1.217
0.872
0.865
0.842
0.809
ppm
9.5
9.0
8.5
8.0
7.5
7.0
6.5
6.0
5.5
5.0
4.5
4.0
3.5
3.0
2.5
2.0
1.5
1.0
0.5
0.0
1.000
1.015
14.246
2.134
2.609
4.049
1.225
1.048
6.257
1.042
1.135
17.273
2.343
37.346
17.930

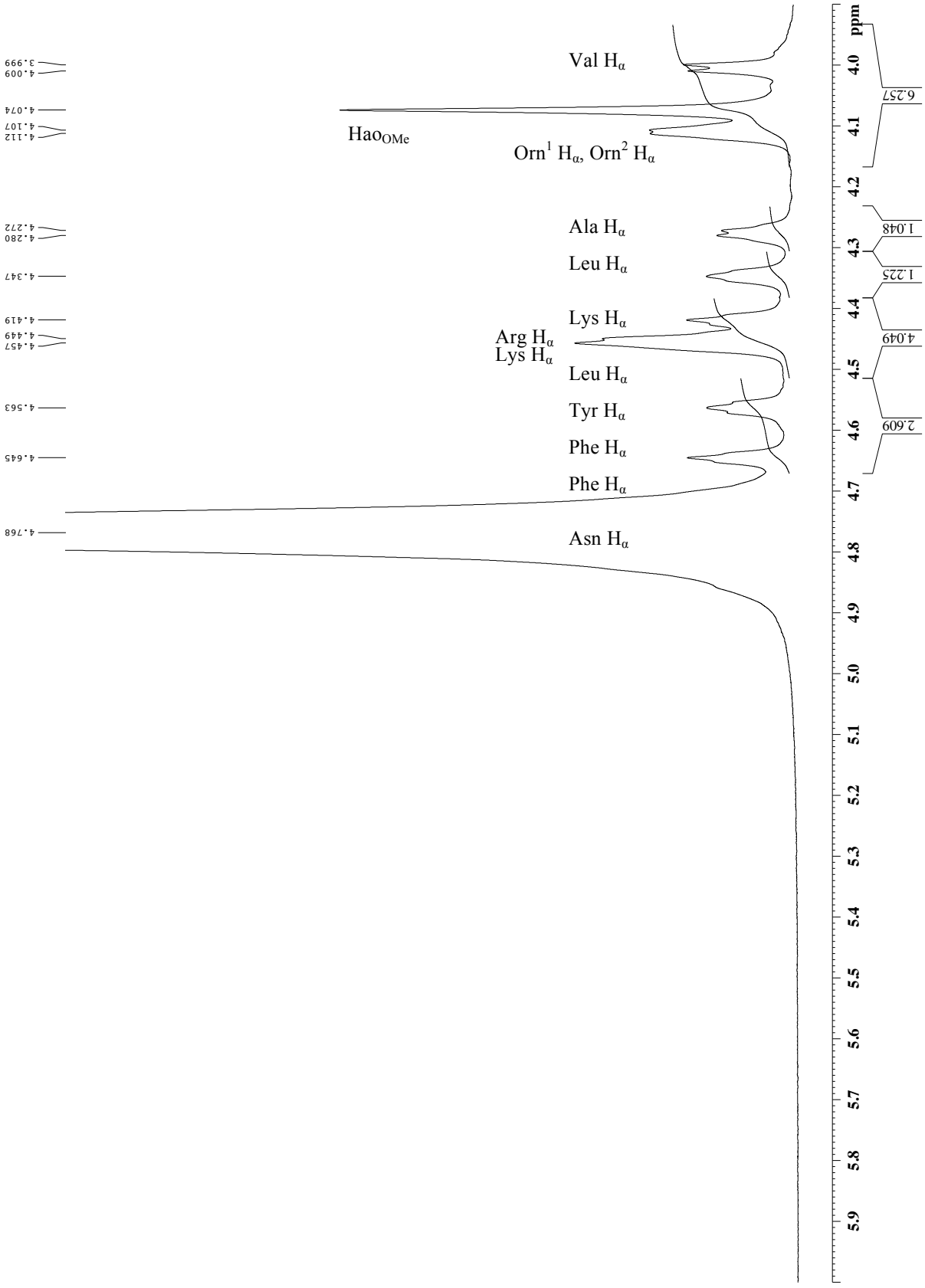
Val Hα
Haoome
Orn1 Hα, Orn2 Hα
Ala Hα
Leu Hα
Lys Hα
Arg Hα
Lys Hα
Leu Hα
Tyr Hα
Phe Hα
Phe Hα
Asn Hα
ppm
6.257
1.048
1.225
4.049
2.609

HPLC , MS ESI$^+$ TOF, and NMR (^{1}H, TOCSY and ROESY) of peptide **2e**

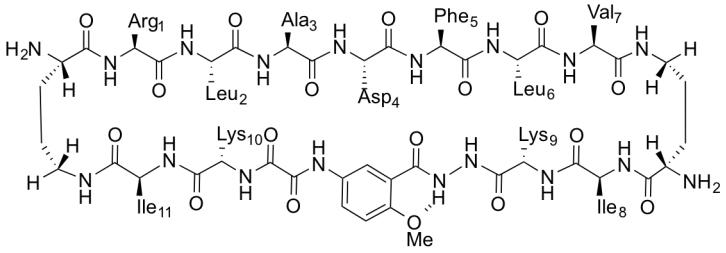

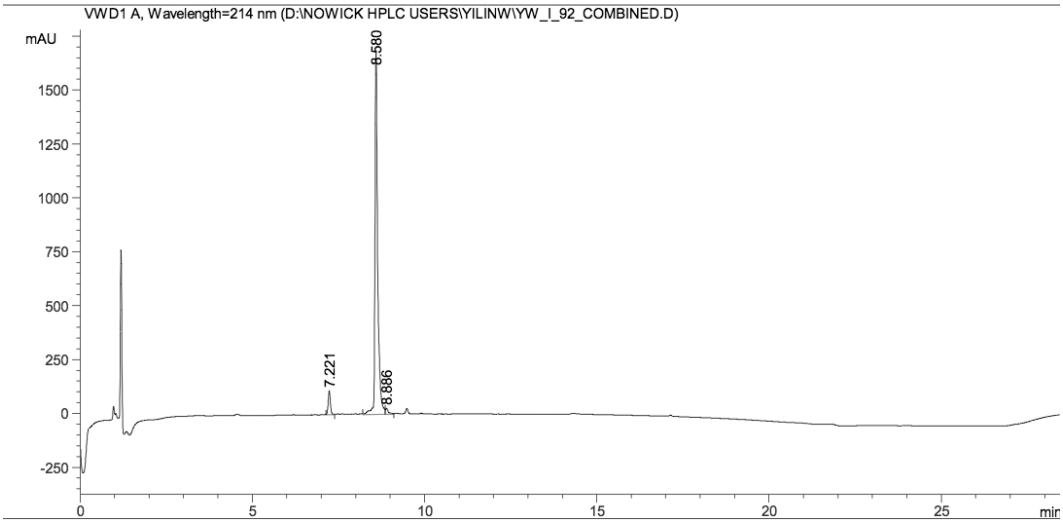

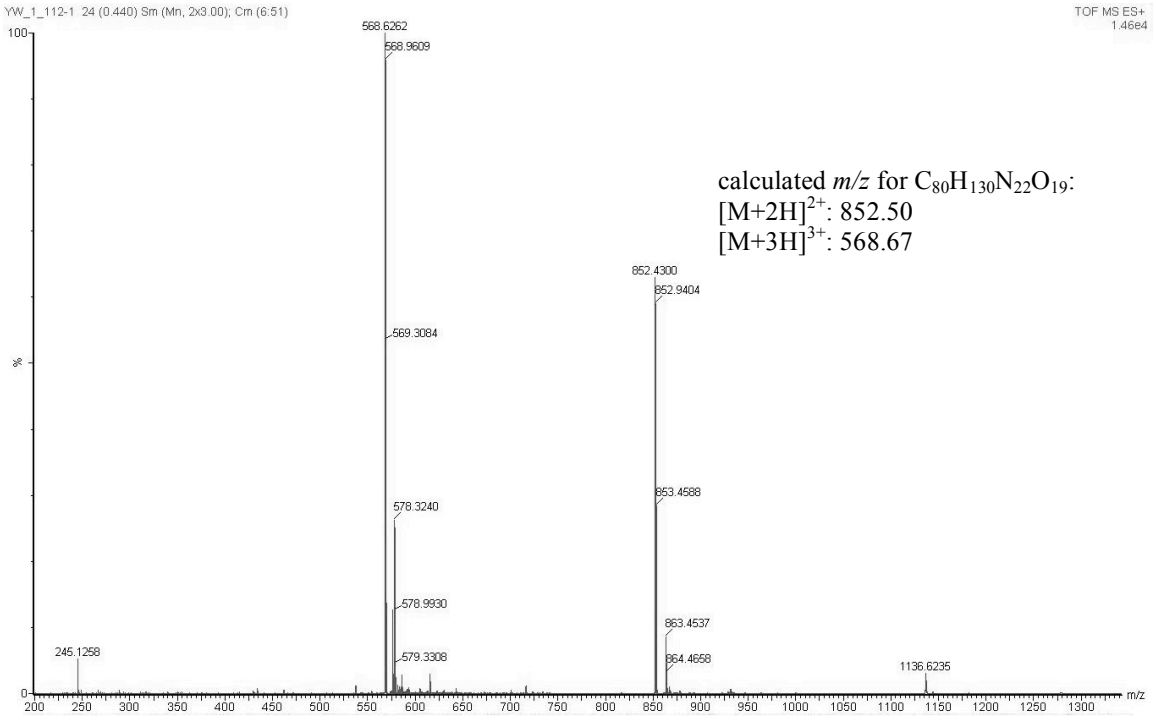

calculated *m/z* for $C_{80}H_{130}N_{22}O_{19}$:
$[M+2H]^{2+}$: 852.50
$[M+3H]^{3+}$: 568.67

8.682
8.328
8.046
8.035
7.923
7.833
7.736
7.725
7.688
7.489
7.375
7.367
7.328
7.319
7.266
7.256
7.180
7.057
7.049
7.007
6.999
6.965
6.957
6.865
4.892
4.769
4.682
4.650
4.641
4.596
4.508
4.497
4.487
4.478
4.467
4.388
4.378
4.374
4.366
4.356
4.343
4.335
4.281
4.276
4.242
4.203
4.129
4.118
4.061
4.051
4.020
3.971
3.961
3.870
3.771
3.734
3.646
3.635
3.560
3.553
3.487
3.438
3.429
3.334
3.277
3.260
3.252
3.232
3.219
3.187
3.169
3.146
3.138
3.087
3.079
3.072
3.062
3.037
2.998
2.989
2.979
2.970
2.962
2.924
2.916
2.907
2.854
2.804
2.777
2.725
2.716
2.682
2.673
2.649
2.639
2.631
2.620
2.234
2.044
2.036
1.898
1.890
1.850
1.780
1.710
1.701
1.683
1.587
1.547
1.537
1.530
1.521
1.513
1.500
ppm
9.5
9.0
8.5
8.0
7.5
7.0
6.5
6.0
5.5
5.0
4.5
4.0
3.5
3.0
2.5
2.0
1.5
1.0
0.5
0.0
1.000
0.976
3.566
4.801
1.384
3.645
3.355
4.437
0.468
2.476
1.273
5.579
0.357
2.098
6.934
2.003
7.529
3.202
1.581
58.760
44.279

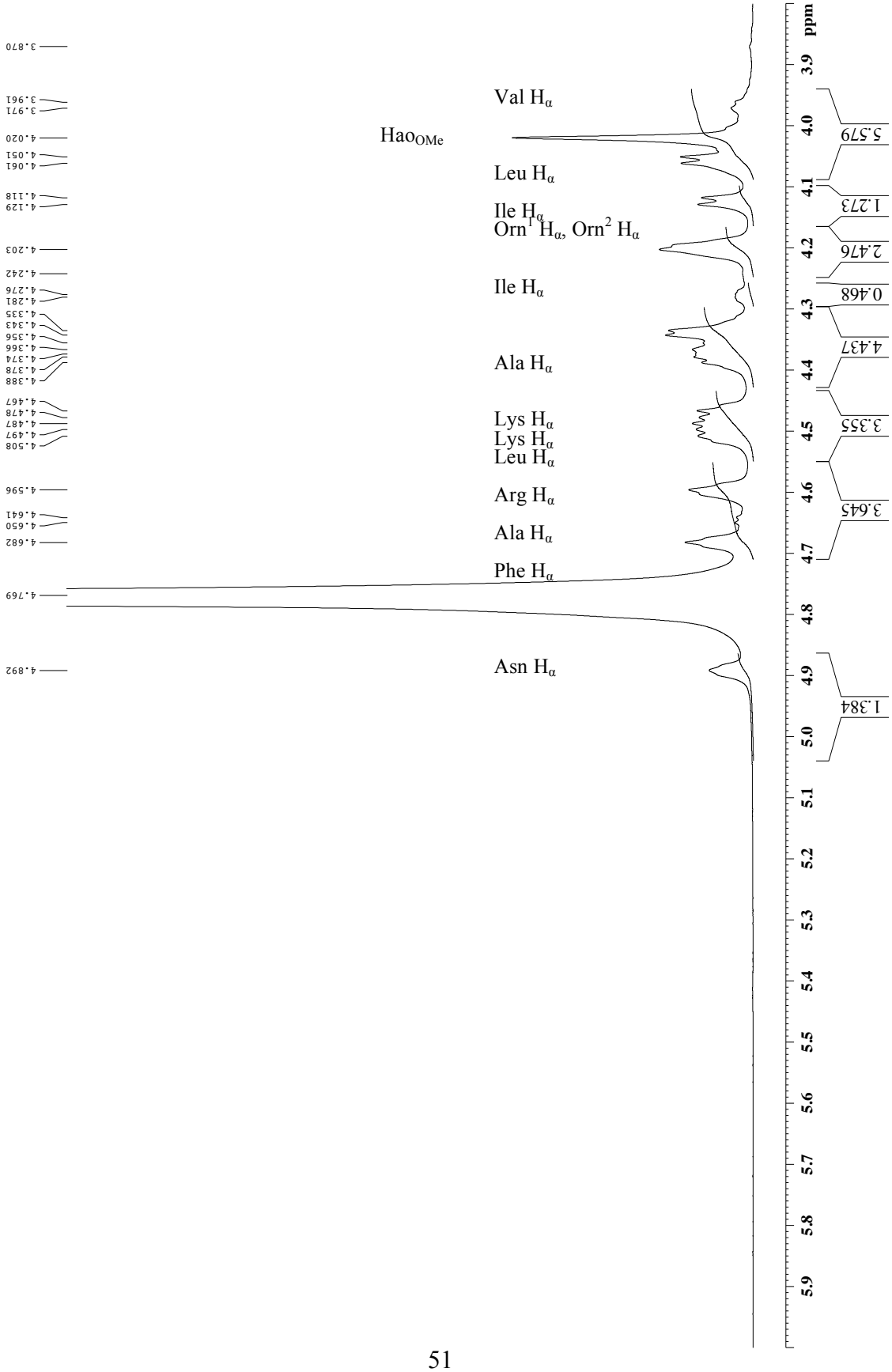
Val Hα
Haoome
Leu Hα
Ile Hα
Orn1 Hα, Orn2 Hα
Ile Hα
Ala Hα
Lys Hα
Lys Hα
Leu Hα
Arg Hα
Ala Hα
Phe Hα
Asn Hα
ppm

presat TOCSY

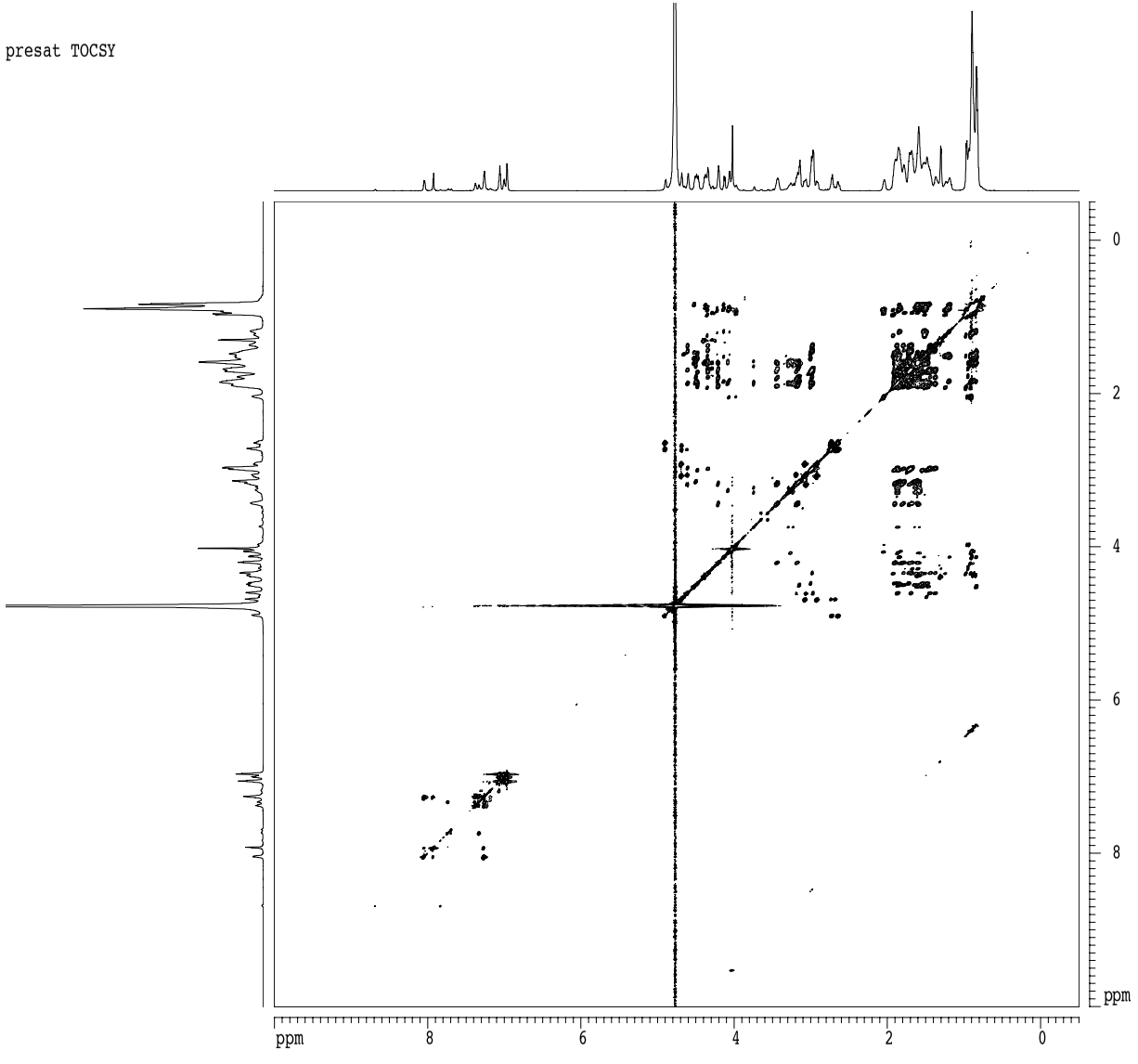

Current Data Parameters

USER	yilinw
NAME	20130730_YW_1_92
EXPNO	3
PROCNO	1

F2 - Acquisition Parameters

Date_	20130729
Time	0.00
INSTRUM	varian
PROBHD	40:5mmbroadban
PULPROG	tocsy
TD	4506
SOLVENT	D2O
NS	8
DS	16
SWH	8797.977 Hz
FIDRES	1.952502 Hz
AQ	0.2561316 sec
RG	287.4
DW	56.831 usec
DE	6.00 usec
TE	298.0 K

F1 - Acquisition parameters

ND0	1
TD	1024
SFO1	799.7986 MHz
FIDRES	8.591774 Hz
SW	11.000 ppm
FnMODE	undefined

F2 - Processing parameters

SI	2048
SF	799.7947935 MHz
WDW	QSINE
SSB	2
LB	0.00 Hz
GB	0
PC	1.40

F1 - Processing parameters

SI	1024
MC2	States
SF	799.7947935 MHz
WDW	QSINE
SSB	2
LB	0.00 Hz
GB	0

2D NMR plot parameters

CX2	15.00 cm
CX1	15.00 cm
F2PLO	10.003 ppm
F2LO	8000.25 Hz
F2PHI	-0.503 ppm
F2HI	-402.50 Hz
F1PLO	10.003 ppm
F1LO	8000.25 Hz
F1PHI	-0.503 ppm
F1HI	-402.50 Hz
F2PPMCM	0.70041 ppm/cm
F2HZCM	560.18365 Hz/cm
F1PPMCM	0.70041 ppm/cm
F1HZCM	560.18365 Hz/cm

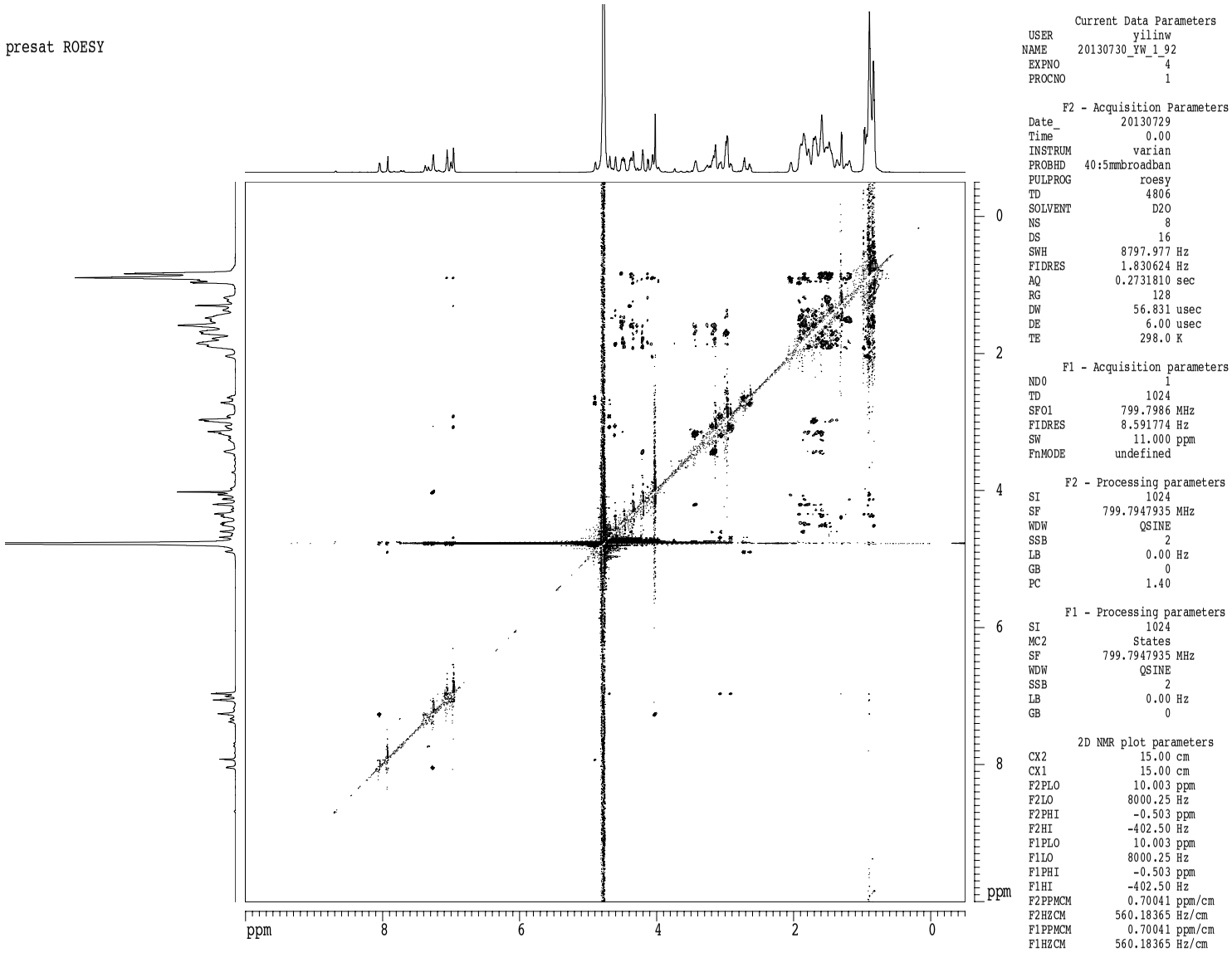
presat ROESY
ppm
8
6
4
2
0
ppm
0
2
4
6
8
Current Data Parameters
USER yilinw
NAME 20130730_YW_1_92
EXPNO 4
PROCNO 1
F2 - Acquisition Parameters
Date_ 20130729
Time 0.00
INSTRUM varian
PROBHD 40:5mmbroadban
PULPROG roesy
TD 4806
SOLVENT D2O
NS 8
DS 16
SWH 8797.977 Hz
FIDRES 1.830624 Hz
AQ 0.2731810 sec
RG 128
DW 56.831 usec
DE 6.00 usec
TE 298.0 K
F1 - Acquisition parameters
ND0 1
TD 1024
SFO1 799.7986 MHz
FIDRES 8.591774 Hz
SW 11.000 ppm
FnMODE undefined
F2 - Processing parameters
SI 1024
SF 799.7947935 MHz
WDW QSINE
SSB 2
LB 0.00 Hz
GB 0
PC 1.40
F1 - Processing parameters
SI 1024
MC2 States
SF 799.7947935 MHz
WDW QSINE
SSB 2
LB 0.00 Hz
GB 0
2D NMR plot parameters
CX2 15.00 cm
CX1 15.00 cm
F2PLO 10.003 ppm
F2LO 8000.25 Hz
F2PHI -0.503 ppm
F2HI -402.50 Hz
F1PLO 10.003 ppm
F1LO 8000.25 Hz
F1PHI -0.503 ppm
F1HI -402.50 Hz
F2PPMCM 0.70041 ppm/cm
F2HZCM 560.18365 Hz/cm
F1PPMCM 0.70041 ppm/cm
F1HZCM 560.18365 Hz/cm

HPLC , MS ESI$^+$ TOF, and NMR (^{1}H, TOCSY and ROESY) of peptide **2f**

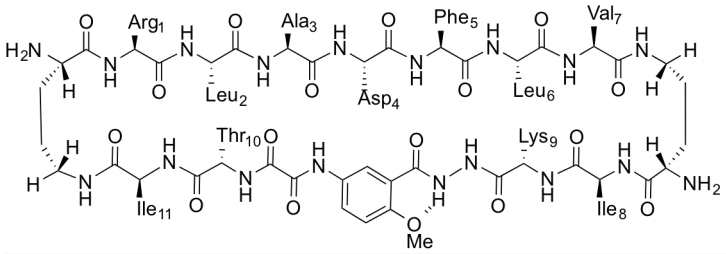

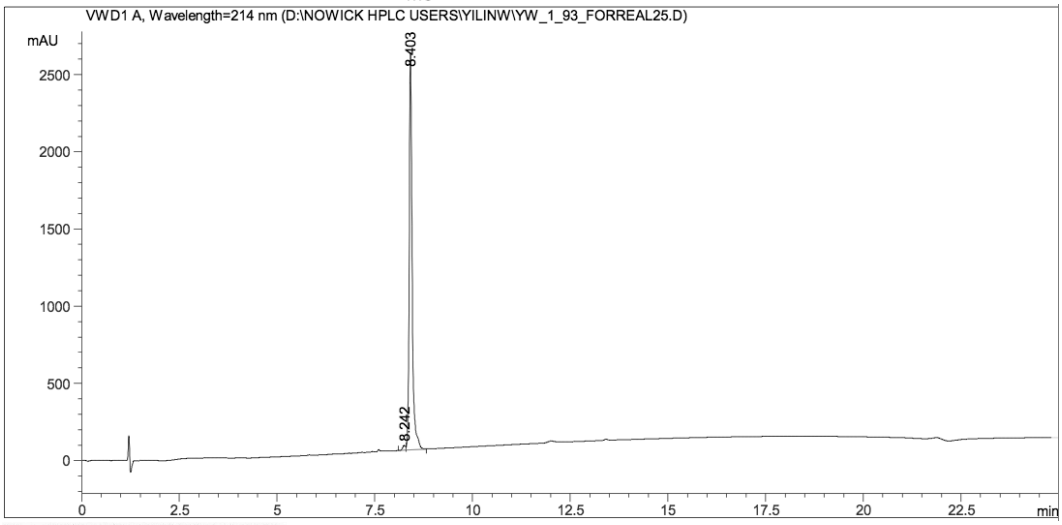

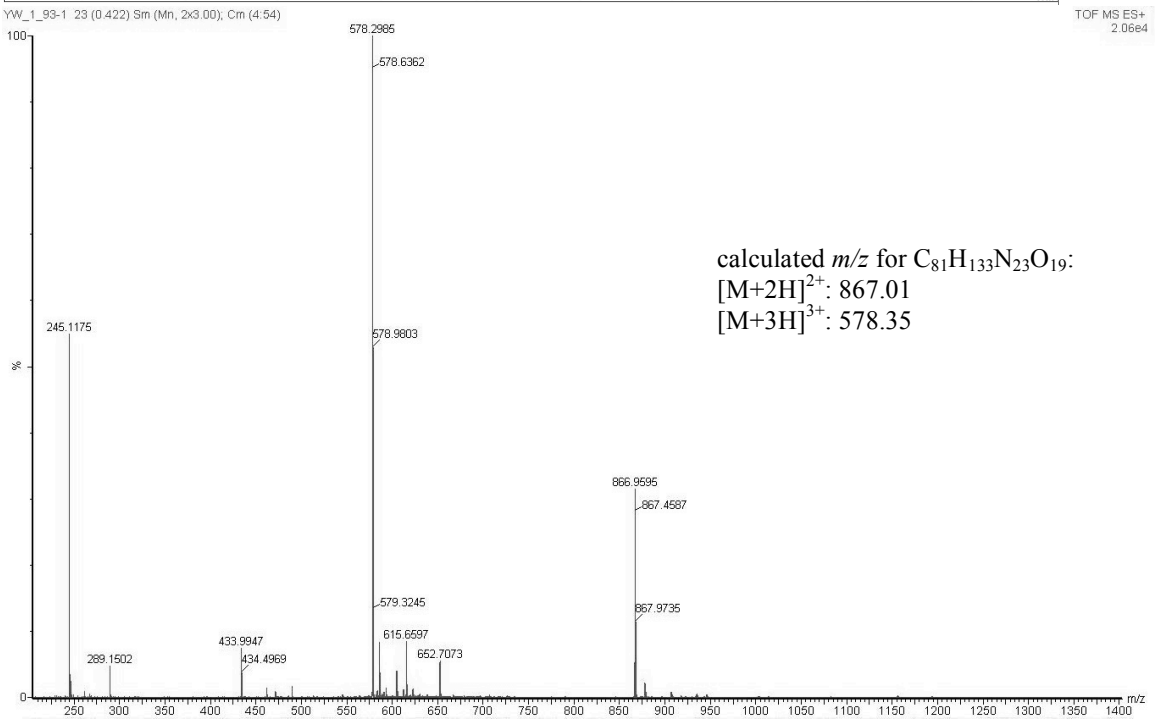

calculated *m/z* for $C_{81}H_{133}N_{23}O_{19}$:
$[M+2H]^{2+}$: 867.01
$[M+3H]^{3+}$: 578.35

8.337
8.120
8.074
7.975
7.927
7.744
7.695
7.370
7.266
7.259
7.179
7.057
6.994
6.920
5.013
4.906
4.889
4.882
4.768
4.711
4.599
4.554
4.511
4.447
4.400
4.367
4.243
4.189
4.088
4.026
3.871
3.843
3.690
3.657
3.620
3.525
3.481
3.377
3.344
3.290
3.154
3.071
3.058
3.008
2.969
2.886
2.707
2.619
2.465
2.360
2.234
2.051
1.991
1.877
1.849
1.793
1.695
1.573
1.507
1.444
1.387
1.317
1.235
1.163
0.964
0.890
0.821
0.740
0.653
0.111
0.675
0.700
5.044
1.000
3.616
2.791
7.399
1.851
7.821
1.975
27.343
34.750
9.5
9.0
8.5
8.0
7.5
7.0
6.5
6.0
5.5
5.0
4.5
4.0
3.5
3.0
2.5
2.0
1.5
1.0
0.5
0.0
ppm

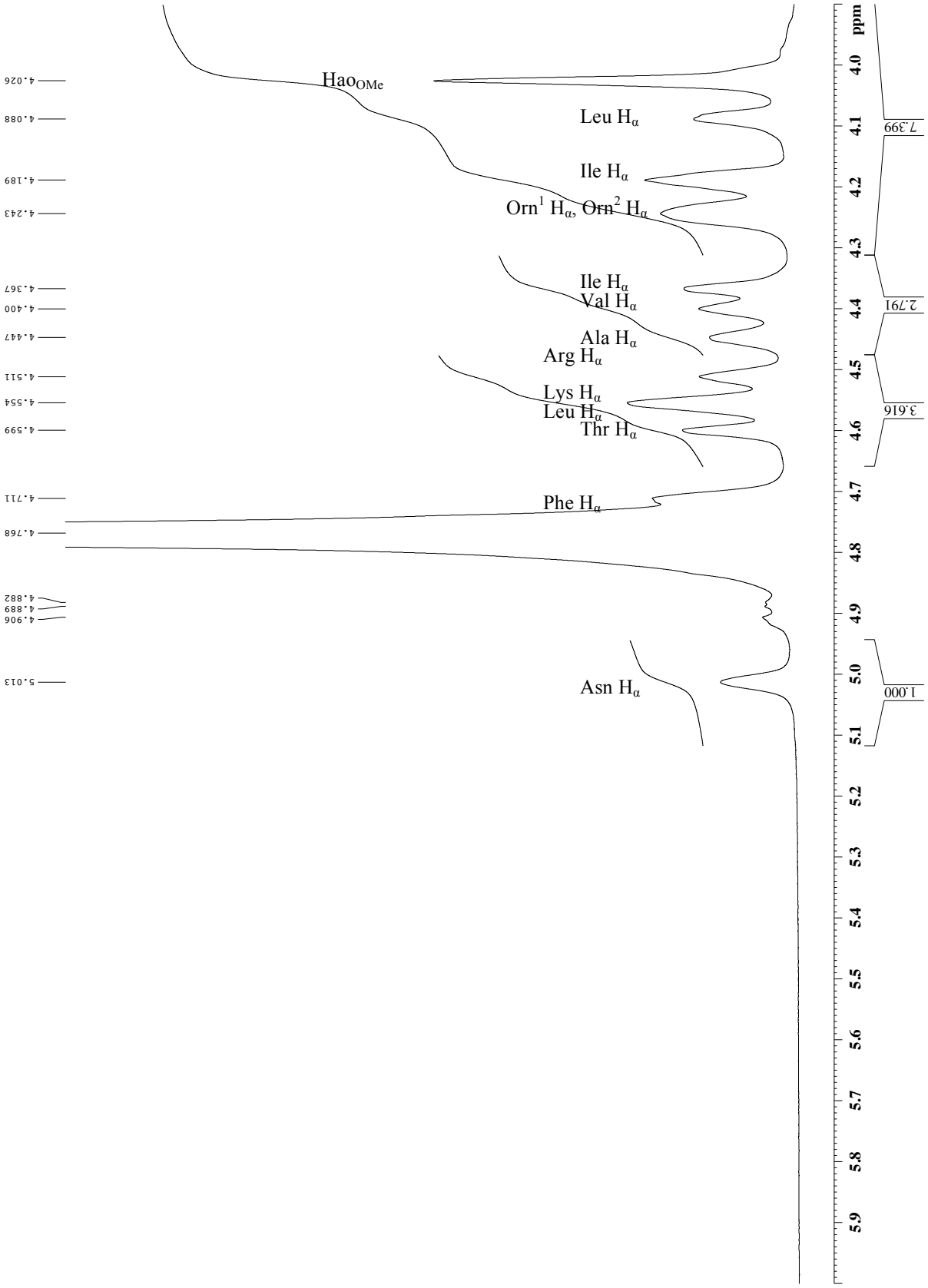
Hao$_{OMe}$
Leu H_α
Ile H_α
Orn^1 H_α, Orn^2 H_α
Ile H_α
Val H_α
Ala H_α
Arg H_α
Lys H_α
Leu H_α
Thr H_α
Phe H_α
Asn H_α
4.026
4.088
4.189
4.243
4.367
4.400
4.447
4.511
4.554
4.599
4.711
4.768
4.882
4.889
4.906
5.013
ppm
7.399
2.791
3.616
1.000

presat TOCSY

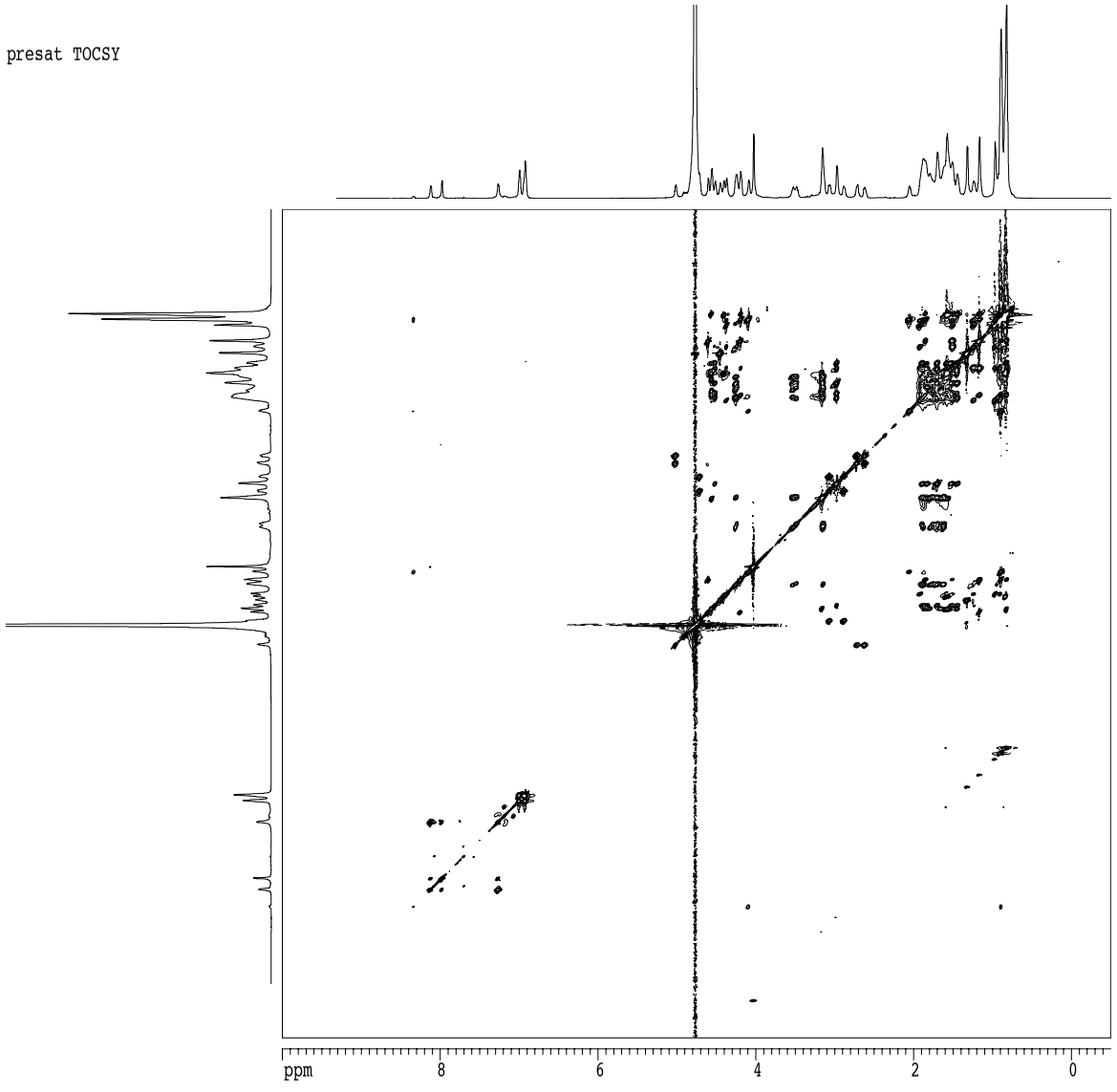

Current Data Parameters

USER	yilinw
NAME	20130805_YW_1_93
EXPNO	4
PROCNO	1

F2 - Acquisition Parameters

Date_	20130804
Time	0.00
INSTRUM	varian
PROBHD	40:5mmbroadban
PULPROG	tocsy
TD	4096
SOLVENT	D2O
NS	8
DS	16
SWH	8797.977 Hz
FIDRES	2.147943 Hz
AQ	0.2328308 sec
RG	287.4
DW	56.831 usec
DE	6.00 usec
TE	298.0 K

F1 - Acquisition parameters

ND0	1
TD	1024
SFO1	799.7986 MHz
FIDRES	8.591774 Hz
SW	11.000 ppm
FnMODE	undefined

F2 - Processing parameters

SI	1024
SF	799.7947904 MHz
WDW	QSINE
SSB	2
LB	0.00 Hz
GB	0
PC	1.40

F1 - Processing parameters

SI	1024
MC2	States
SF	799.7947904 MHz
WDW	QSINE
SSB	2
LB	0.00 Hz
GB	0

2D NMR plot parameters

CX2	15.00 cm
CX1	15.00 cm
F2PLO	10.000 ppm
F2LO	7997.95 Hz
F2PHI	-0.500 ppm
F2HI	-399.90 Hz
F1PLO	10.000 ppm
F1LO	7997.95 Hz
F1PHI	-0.500 ppm
F1HI	-399.90 Hz
F2PPMCM	0.70000 ppm/cm
F2HZCM	559.85638 Hz/cm
F1PPMCM	0.70000 ppm/cm
F1HZCM	559.85638 Hz/cm

presat ROESY

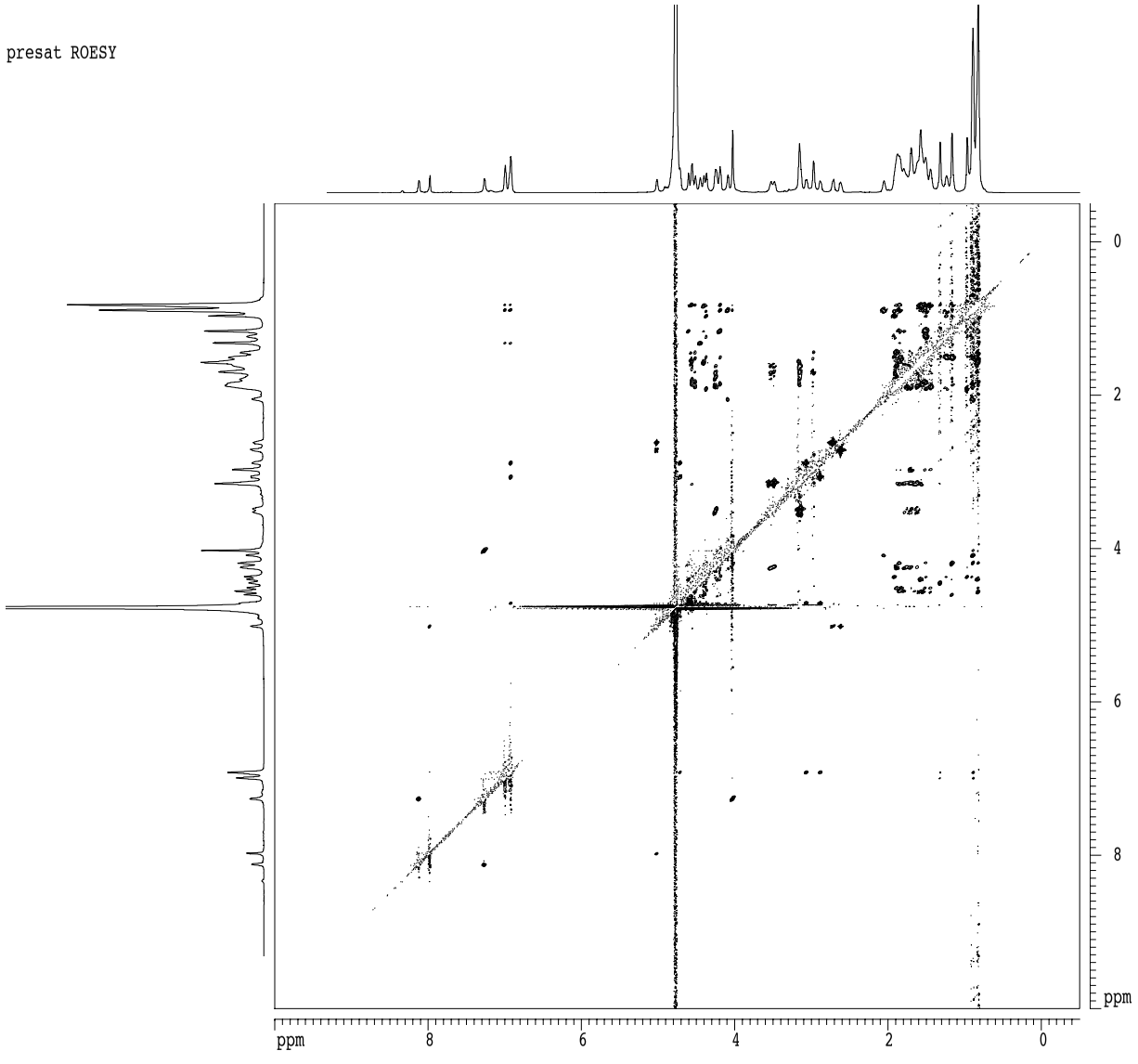

Current Data Parameters

USER	yilinw
NAME	20130805_YW_1_93
EXPNO	3
PROCNO	1

F2 - Acquisition Parameters

Date_	20130804
Time	0.00
INSTRUM	varian
PROBHD	40:5mmbroadban
PULPROG	roesy
TD	4096
SOLVENT	D2O
NS	8
DS	16
SWH	8797.977 Hz
FIDRES	2.147943 Hz
AQ	0.2328308 sec
RG	128
DW	56.831 usec
DE	6.00 usec
TE	298.0 K

F1 - Acquisition parameters

ND0	1
TD	1024
SFO1	799.7986 MHz
FIDRES	8.591774 Hz
SW	11.000 ppm
FnMODE	undefined

F2 - Processing parameters

SI	1024
SF	799.7947904 MHz
WDW	QSINE
SSB	2
LB	0.00 Hz
GB	0
PC	1.40

F1 - Processing parameters

SI	1024
MC2	States
SF	799.7947904 MHz
WDW	QSINE
SSB	2
LB	0.00 Hz
GB	0

2D NMR plot parameters

CX2	15.00 cm
CX1	15.00 cm
F2PLO	10.000 ppm
F2LO	7997.95 Hz
F2PHI	-0.500 ppm
F2HI	-399.90 Hz
F1PLO	10.000 ppm
F1LO	7997.95 Hz
F1PHI	-0.500 ppm
F1HI	-399.90 Hz
F2PPMCM	0.70000 ppm/cm
F2HZCM	559.85638 Hz/cm
F1PPMCM	0.70000 ppm/cm
F1HZCM	559.85638 Hz/cm

HPLC , MS ESI$^+$ TOF, and NMR (^{1}H, TOCSY and ROESY) of peptide **2g**

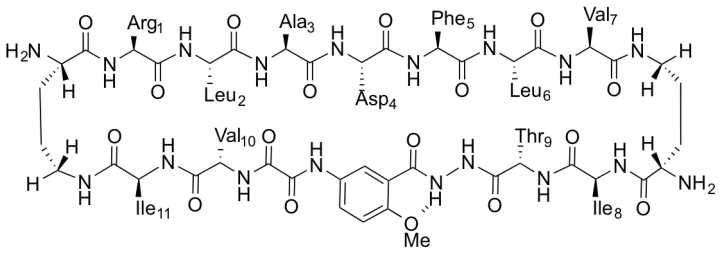

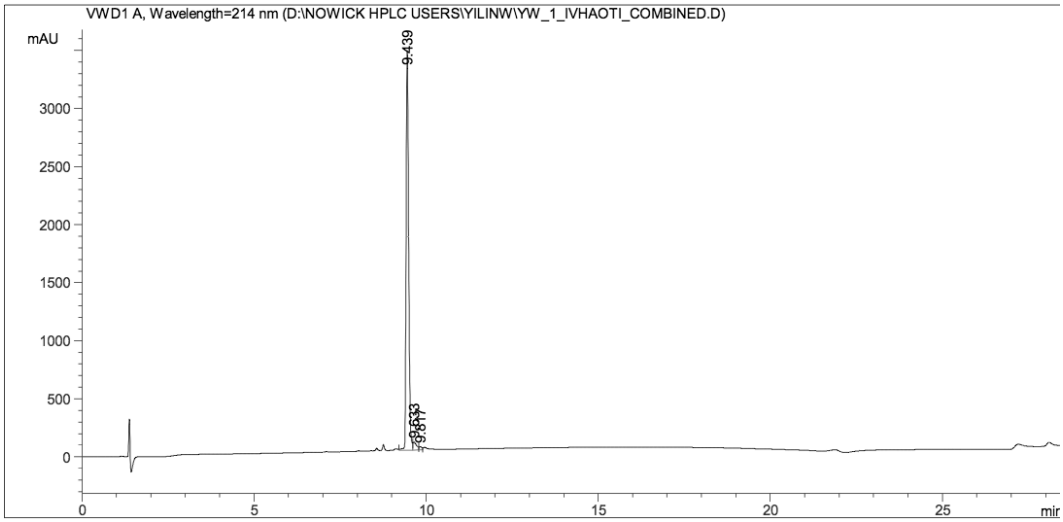

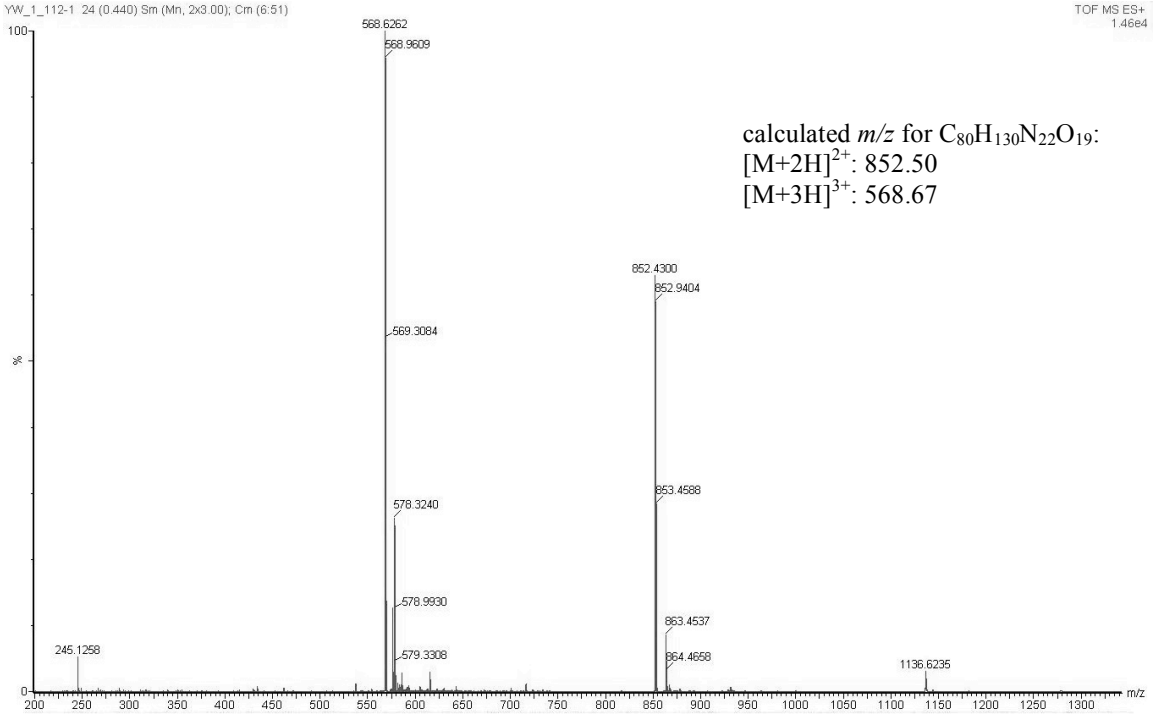

calculated *m/z* for $C_{80}H_{130}N_{22}O_{19}$:
$[M+2H]^{2+}$: 852.50
$[M+3H]^{3+}$: 568.67

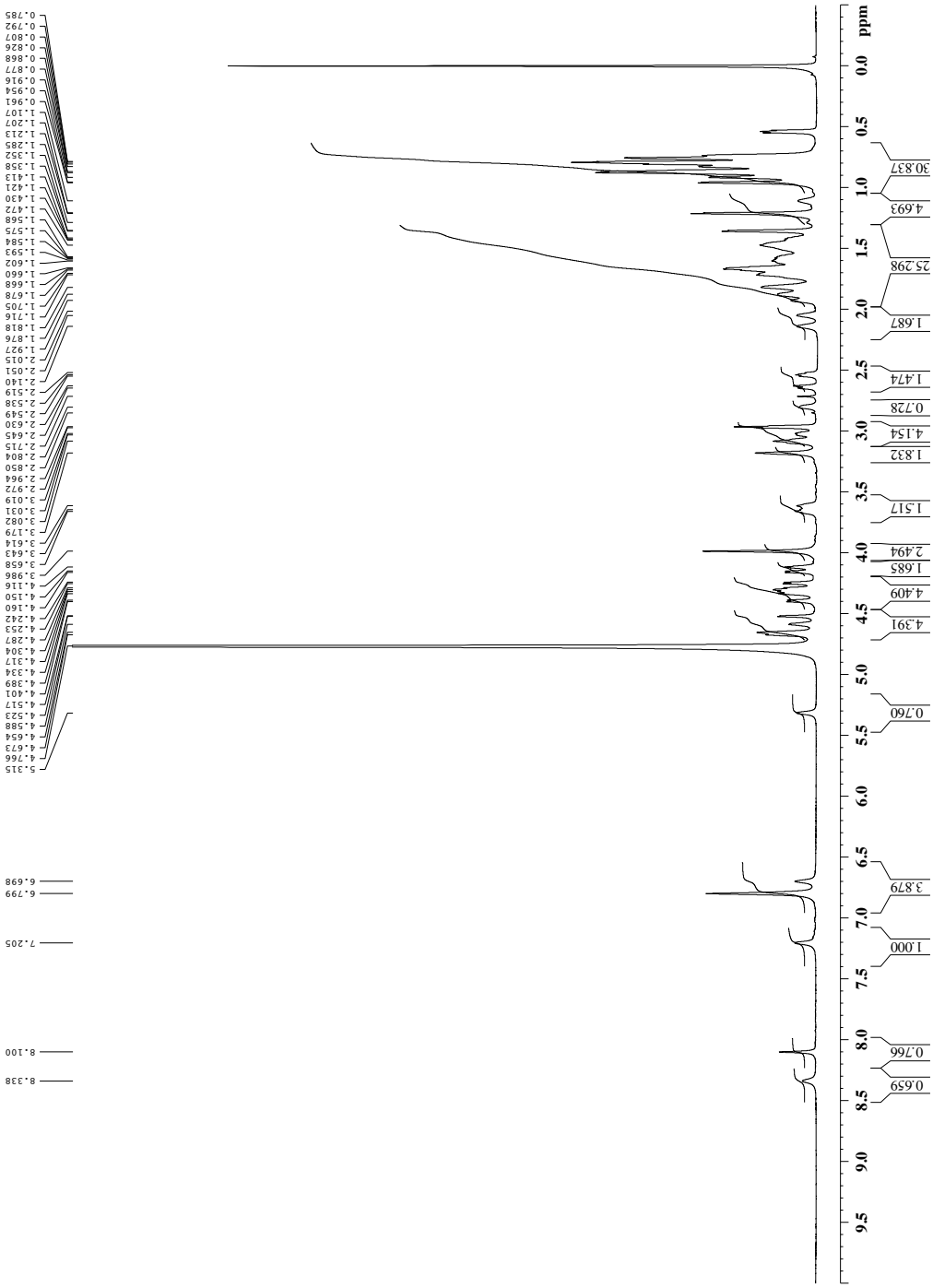
ppm
0.0
0.5
1.0
1.5
2.0
2.5
3.0
3.5
4.0
4.5
5.0
5.5
6.0
6.5
7.0
7.5
8.0
8.5
9.0
9.5
30.837
4.693
25.298
1.687
1.474
0.728
4.154
1.832
1.517
2.494
1.685
4.409
4.391
0.760
3.879
1.000
0.766
0.659
0.785
0.792
0.807
0.826
0.868
0.877
0.916
0.954
0.961
1.107
1.207
1.213
1.285
1.352
1.358
1.413
1.421
1.430
1.472
1.568
1.575
1.584
1.593
1.602
1.660
1.668
1.678
1.705
1.716
1.818
1.876
1.927
2.015
2.051
2.140
2.519
2.538
2.549
2.630
2.645
2.715
2.804
2.850
2.964
2.972
3.019
3.031
3.082
3.179
3.614
3.643
3.658
3.986
4.116
4.150
4.160
4.242
4.253
4.287
4.304
4.317
4.334
4.389
4.401
4.517
4.523
4.588
4.654
4.673
4.766
5.315
6.698
6.799
7.205
8.100
8.338

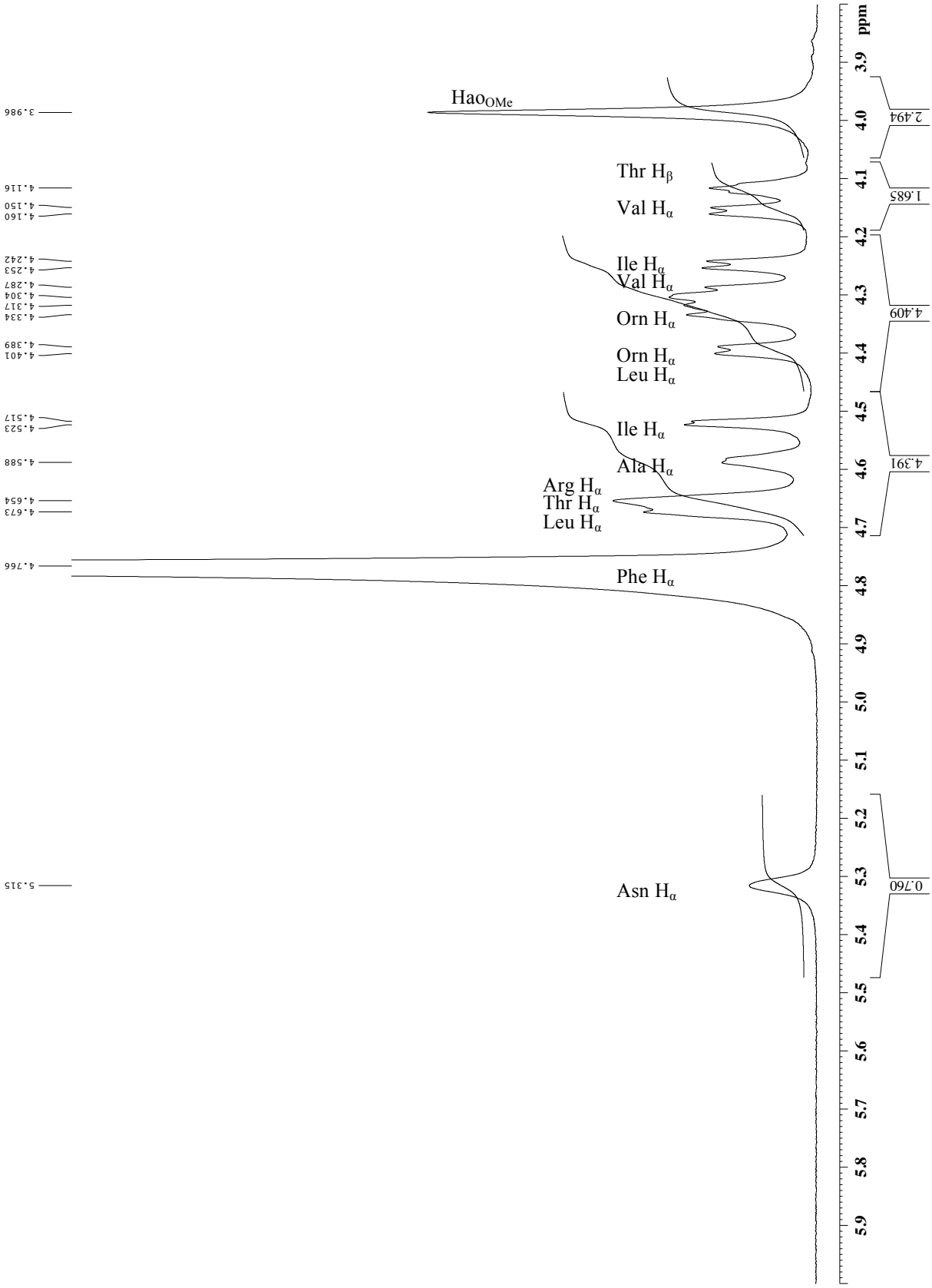
Hao$_{OMe}$
Thr H$_\beta$
Val H$_\alpha$
Ile H$_\alpha$
Val H$_\alpha$
Orn H$_\alpha$
Orn H$_\alpha$
Leu H$_\alpha$
Ile H$_\alpha$
Ala H$_\alpha$
Arg H$_\alpha$
Thr H$_\alpha$
Leu H$_\alpha$
Phe H$_\alpha$
Asn H$_\alpha$
3.986
4.116
4.150
4.160
4.242
4.253
4.287
4.304
4.317
4.334
4.389
4.401
4.517
4.523
4.588
4.654
4.673
4.766
5.315
2.494
1.685
4.409
4.391
0.760
ppm

Varian 800MHz
TOCSY with water suppression
70ms spinlock mix time

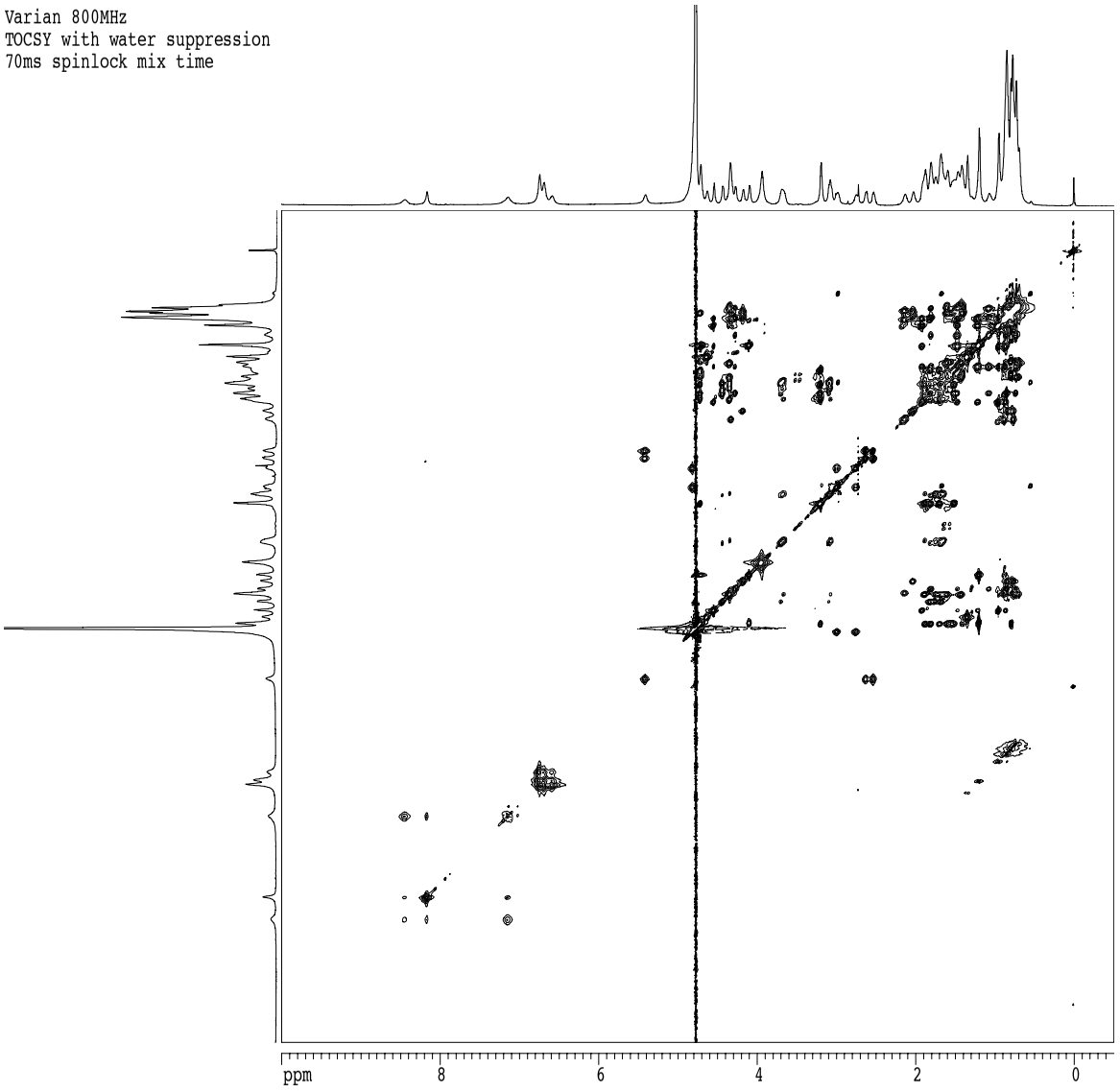

Current Data Parameters

USER	yilinw
NAME	YW_1_112_8mM_800_25C
EXPNO	3
PROCNO	1

F2 - Acquisition Parameters

Date_	20130930
Time	0.00
INSTRUM	varian
PROBHD	40:5mmbroadban
PULPROG	tocsy
TD	4096
SOLVENT	D2O
NS	4
DS	16
SWH	8797.977 Hz
FIDRES	2.147943 Hz
AQ	0.2328308 sec
RG	287.4
DW	56.831 usec
DE	6.00 usec
TE	298.0 K

F1 - Acquisition parameters

ND0	1
TD	512
SFO1	799.7986 MHz
FIDRES	17.183548 Hz
SW	11.000 ppm
FnMODE	undefined

F2 - Processing parameters

SI	2048
SF	799.7947757 MHz
WDW	QSINE
SSB	2
LB	0.00 Hz
GB	0
PC	1.40

F1 - Processing parameters

SI	1024
MC2	States
SF	799.7947757 MHz
WDW	QSINE
SSB	2
LB	0.00 Hz
GB	0

2D NMR plot parameters

CX2	15.00 cm
CX1	15.00 cm
F2PLO	10.000 ppm
F2LO	7997.95 Hz
F2PHI	-0.500 ppm
F2HI	-399.90 Hz
F1PLO	10.000 ppm
F1LO	7997.95 Hz
F1PHI	-0.500 ppm
F1HI	-399.90 Hz
F2PPMCM	0.70000 ppm/cm
F2HZCM	559.85638 Hz/cm
F1PPMCM	0.70000 ppm/cm
F1HZCM	559.85638 Hz/cm

Varian 800MHz
ROESY with presaturation

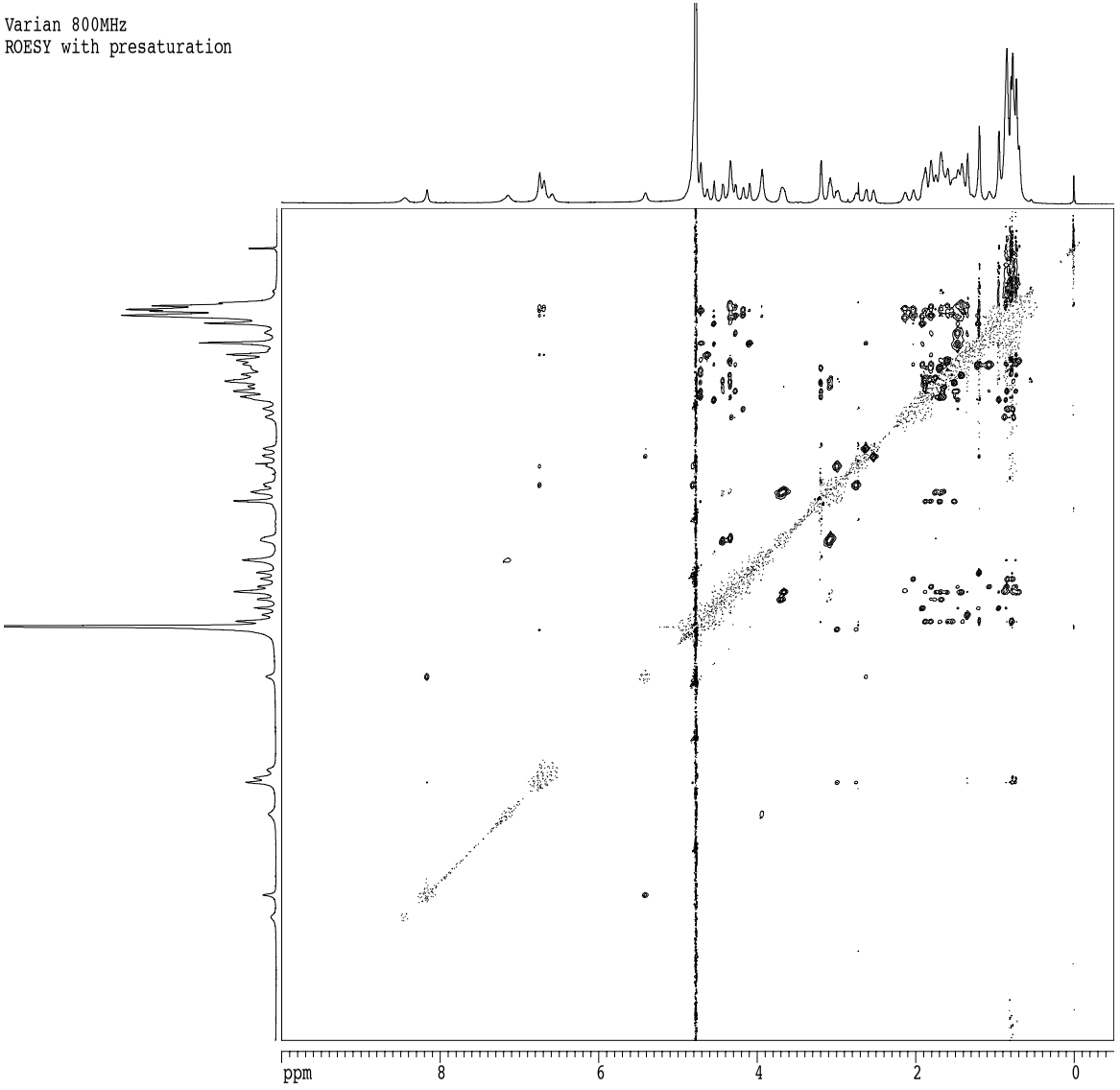

Current Data Parameters

USER	yilinw
NAME	YW_1_112_8mM_800_25C
EXPNO	4
PROCNO	1

F2 - Acquisition Parameters

Date_	20130930
Time	0.00
INSTRUM	varian
PROBHD	40:5mmbroadban
PULPROG	roesy
TD	4096
SOLVENT	D2O
NS	8
DS	16
SWH	8797.977 Hz
FIDRES	2.147943 Hz
AQ	0.2328308 sec
RG	128
DW	56.831 usec
DE	6.00 usec
TE	298.0 K

F1 - Acquisition parameters

ND0	1
TD	512
SFO1	799.7986 MHz
FIDRES	17.183548 Hz
SW	11.000 ppm
FnMODE	undefined

F2 - Processing parameters

SI	2048
SF	799.7947757 MHz
WDW	QSINE
SSB	2
LB	0.00 Hz
GB	0
PC	1.40

F1 - Processing parameters

SI	1024
MC2	States
SF	799.7947757 MHz
WDW	QSINE
SSB	2
LB	0.00 Hz
GB	0

2D NMR plot parameters

CX2	15.00 cm
CX1	15.00 cm
F2PLO	10.000 ppm
F2LO	7997.95 Hz
F2PHI	-0.500 ppm
F2HI	-399.90 Hz
F1PLO	10.000 ppm
F1LO	7997.95 Hz
F1PHI	-0.500 ppm
F1HI	-399.90 Hz
F2PPMCM	0.70000 ppm/cm
F2HZCM	559.85638 Hz/cm
F1PPMCM	0.70000 ppm/cm
F1HZCM	559.85638 Hz/cm

HPLC , MS ESI$^+$ TOF, and NMR (^{1}H, TOCSY and ROESY) of peptide **2h**

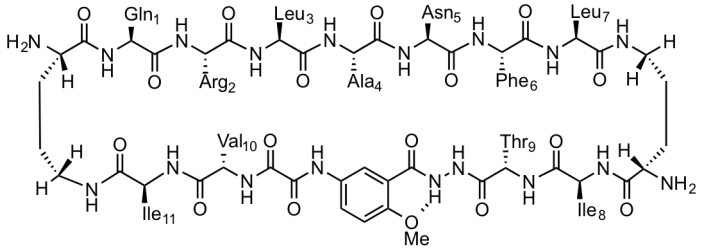

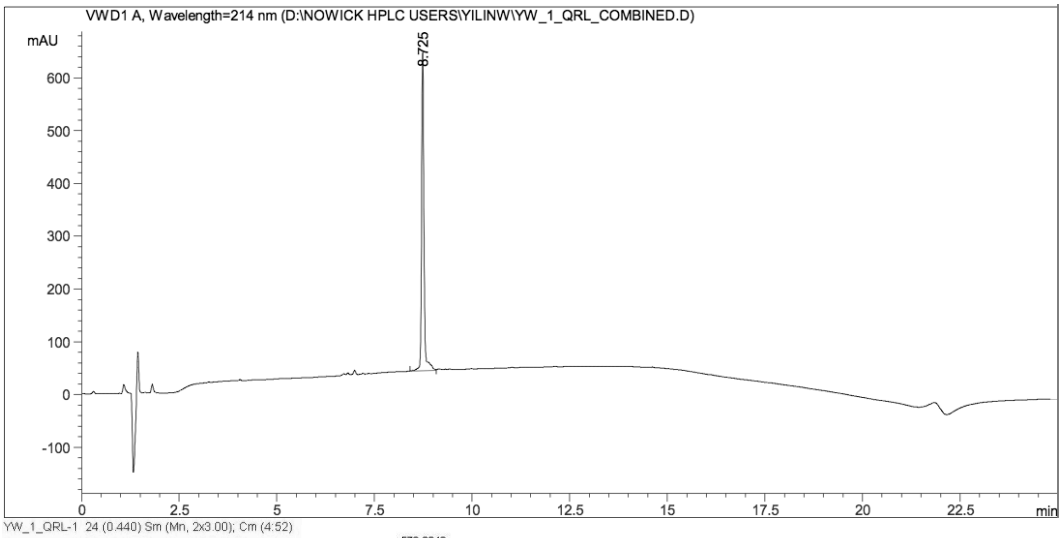

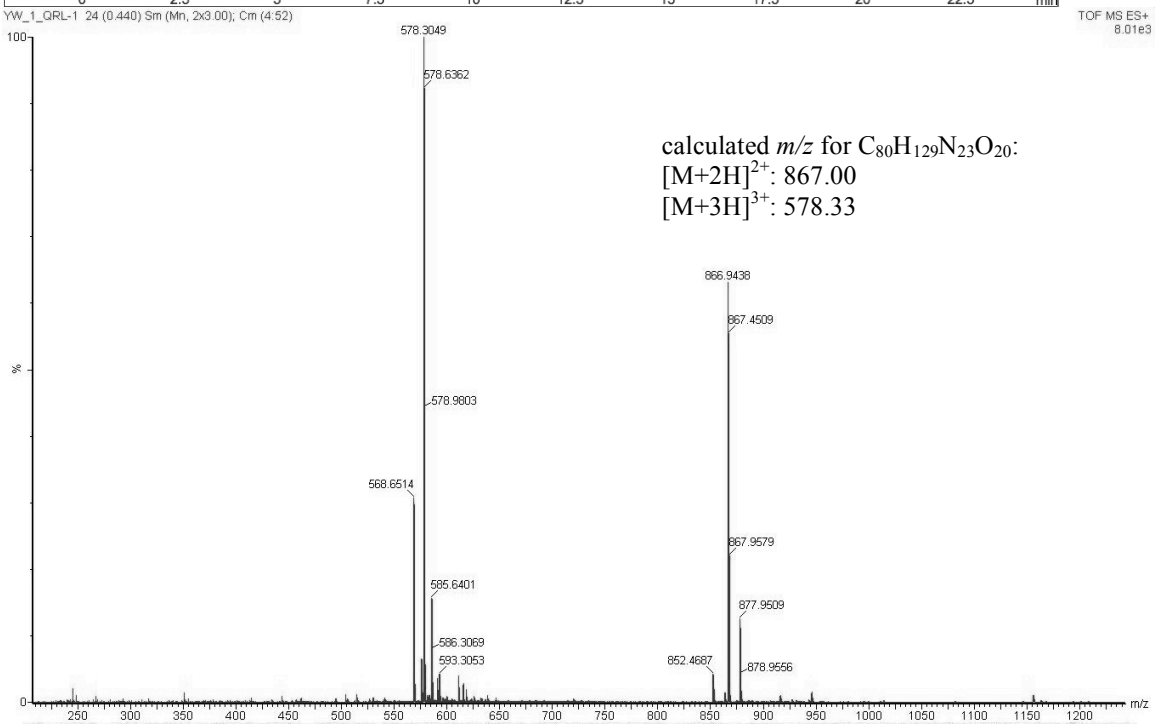

calculated *m/z* for $C_{80}H_{129}N_{23}O_{20}$:
$[M+2H]^{2+}$: 867.00
$[M+3H]^{3+}$: 578.33

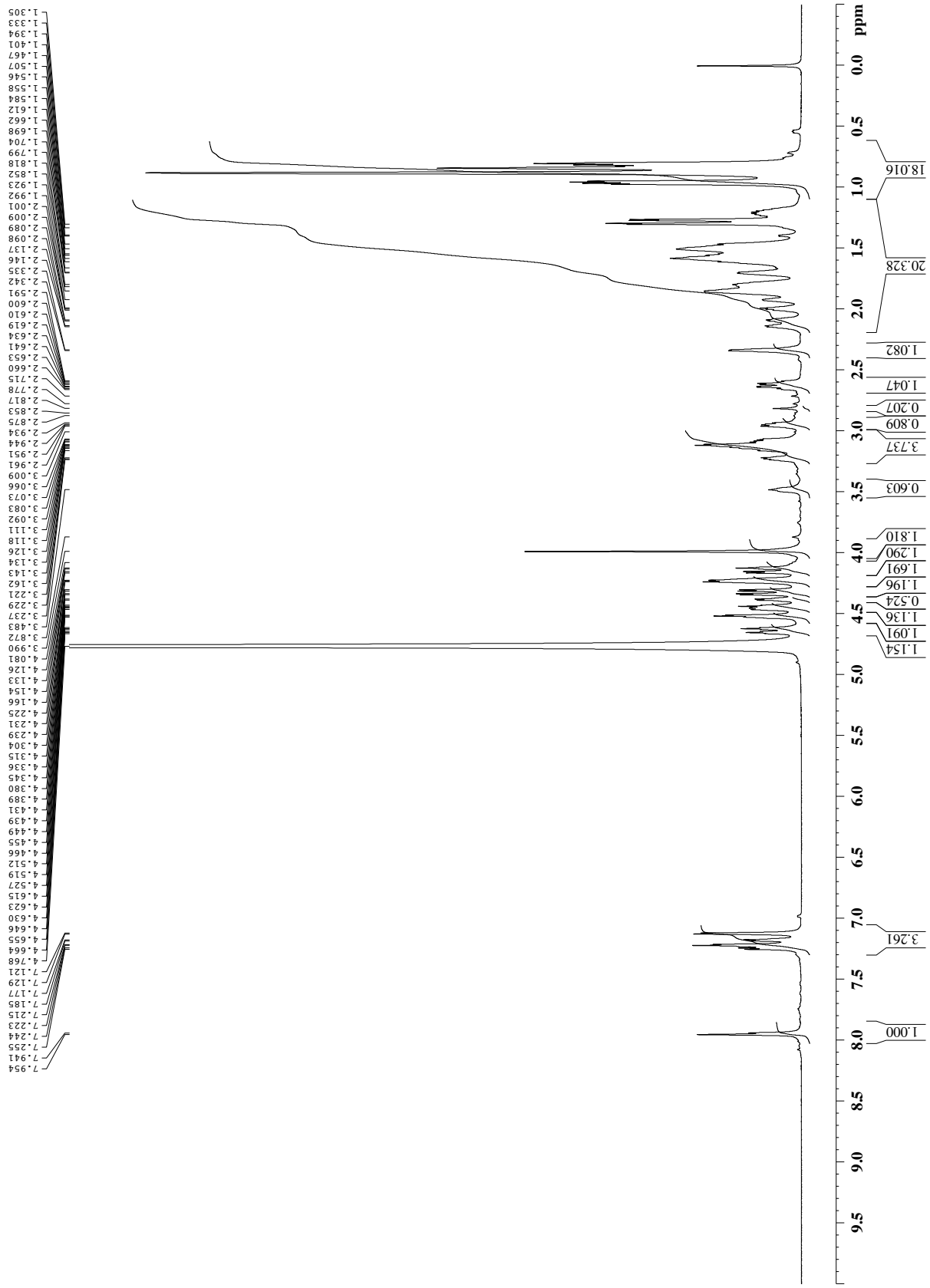
ppm
18.016
20.328
1.082
1.047
0.207
0.809
3.737
0.603
1.810
1.290
1.691
1.196
0.524
1.136
1.091
1.154
3.261
1.000

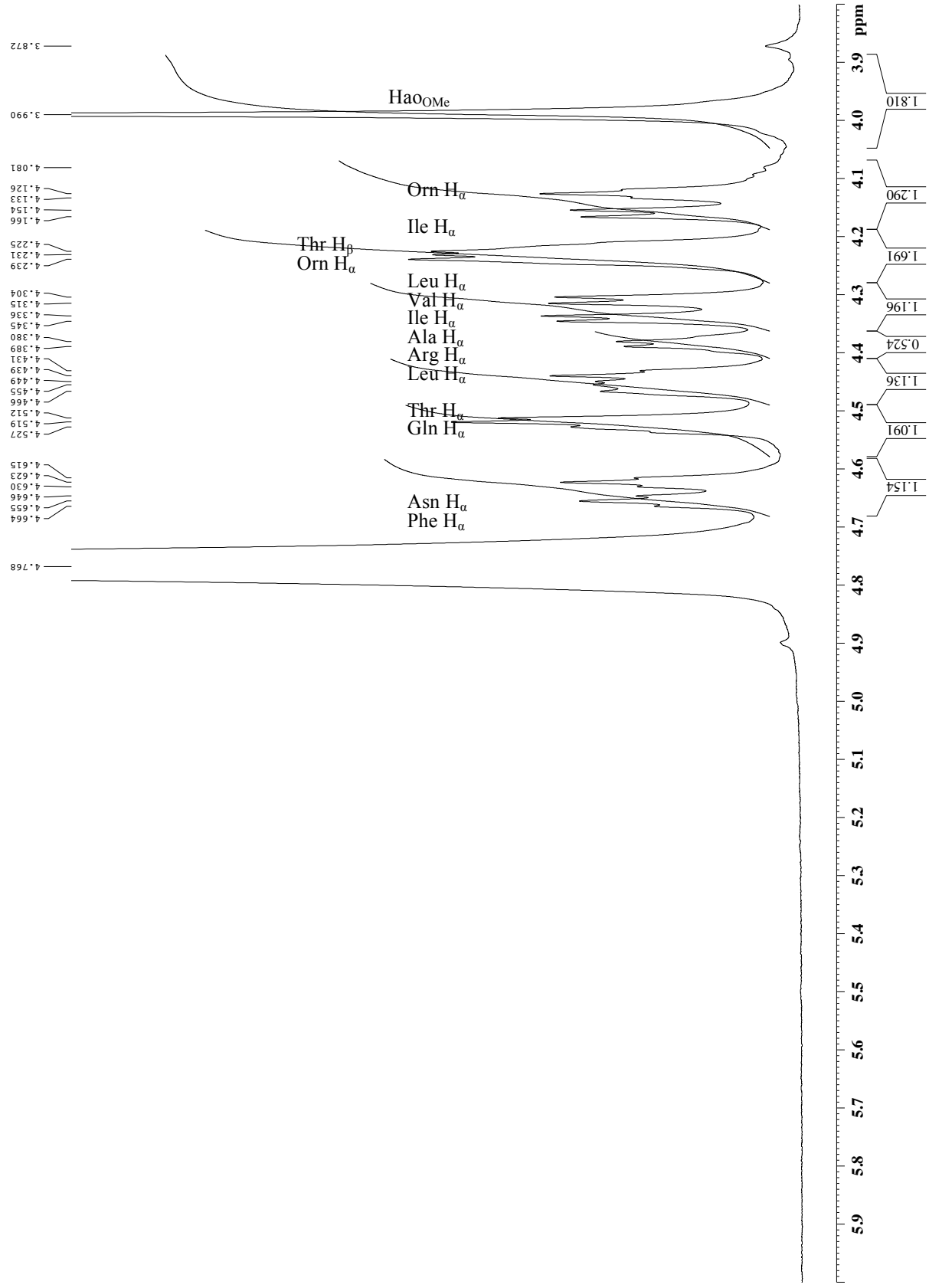
Hao$_{OMe}$
Orn H$_\alpha$
Ile H$_\alpha$
~~Thr H$_\beta$~~
Orn H$_\alpha$
Leu H$_\alpha$
Val H$_\alpha$
Ile H$_\alpha$
Ala H$_\alpha$
Arg H$_\alpha$
Leu H$_\alpha$
~~Thr H$_\alpha$~~
Gln H$_\alpha$
Asn H$_\alpha$
Phe H$_\alpha$
ppm
1.810
1.290
1.691
1.196
0.524
1.136
1.091
1.154

Varian 800MHz
TOCSY with water suppression
70ms spinlock mix time

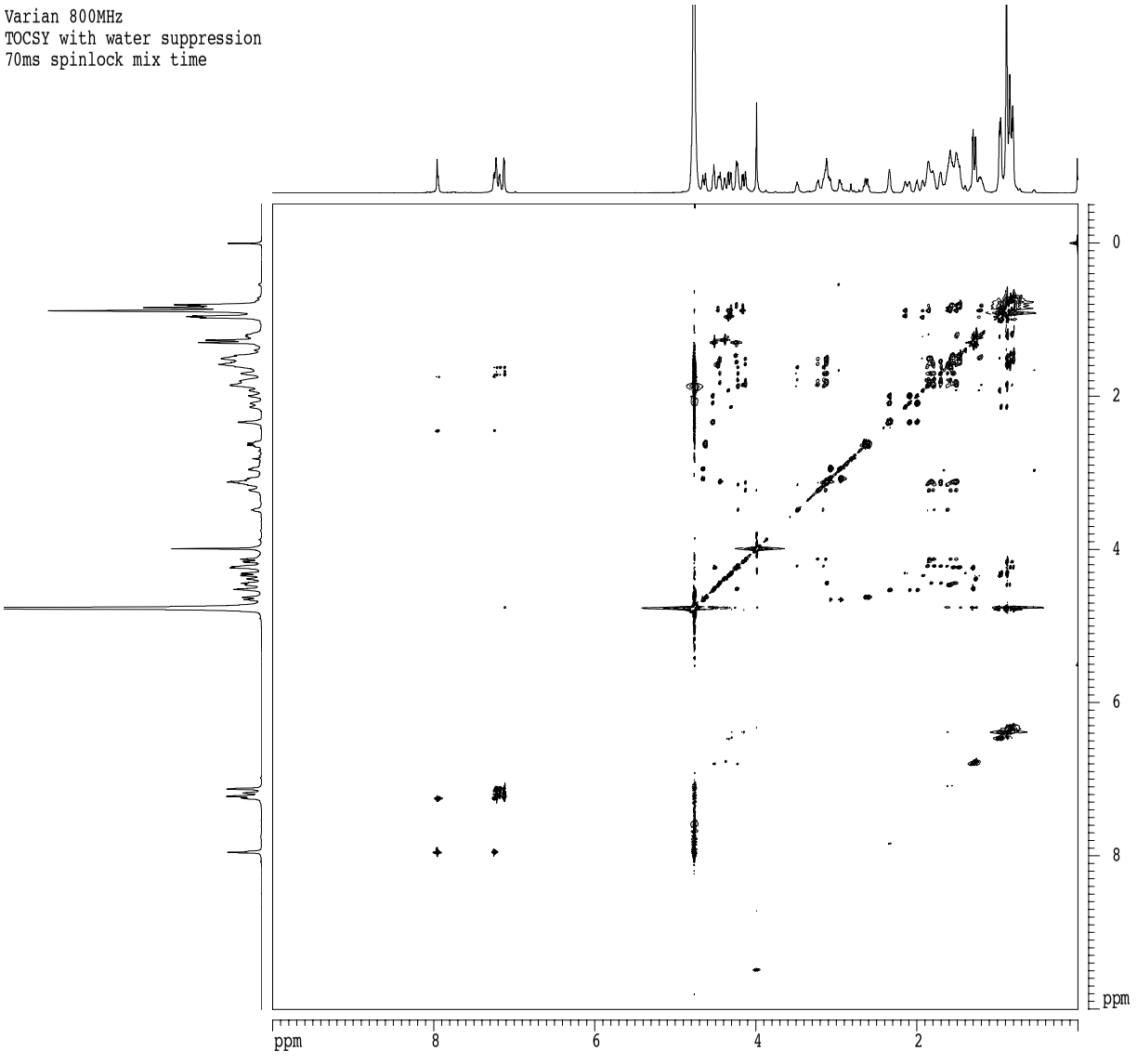

Current Data Parameters

USER	yilinw
NAME	131110_YW_1_QRL
EXPNO	3
PROCNO	1

F2 - Acquisition Parameters

Date_	20131110
Time	0.00
INSTRUM	varian
PROBHD	40:5mmbroadban
PULPROG	tocsy
TD	5212
SOLVENT	D2O
NS	4
DS	16
SWH	11196.641 Hz
FIDRES	2.148243 Hz
AQ	0.2327984 sec
RG	287.4
DW	44.656 usec
DE	6.00 usec
TE	298.0 K

F1 - Acquisition parameters

ND0	1
TD	512
SFO1	799.7986 MHz
FIDRES	17.183548 Hz
SW	11.000 ppm
FnMODE	undefined

F2 - Processing parameters

SI	2048
SF	799.7947714 MHz
WDW	QSINE
SSB	2
LB	0.00 Hz
GB	0
PC	1.40

F1 - Processing parameters

SI	1024
MC2	States
SF	799.7947714 MHz
WDW	QSINE
SSB	2
LB	0.00 Hz
GB	0

2D NMR plot parameters

CX2	15.00 cm
CX1	15.00 cm
F2PLO	10.000 ppm
F2LO	7997.96 Hz
F2PHI	-0.001 ppm
F2HI	-0.42 Hz
F1PLO	10.006 ppm
F1LO	8002.94 Hz
F1PHI	-0.511 ppm
F1HI	-408.41 Hz
F2PPMCM	0.66670 ppm/cm
F2HZCM	533.22546 Hz/cm
F1PPMCM	0.70113 ppm/cm
F1HZCM	560.75647 Hz/cm

Varian 800MHz
ROESY with presaturation

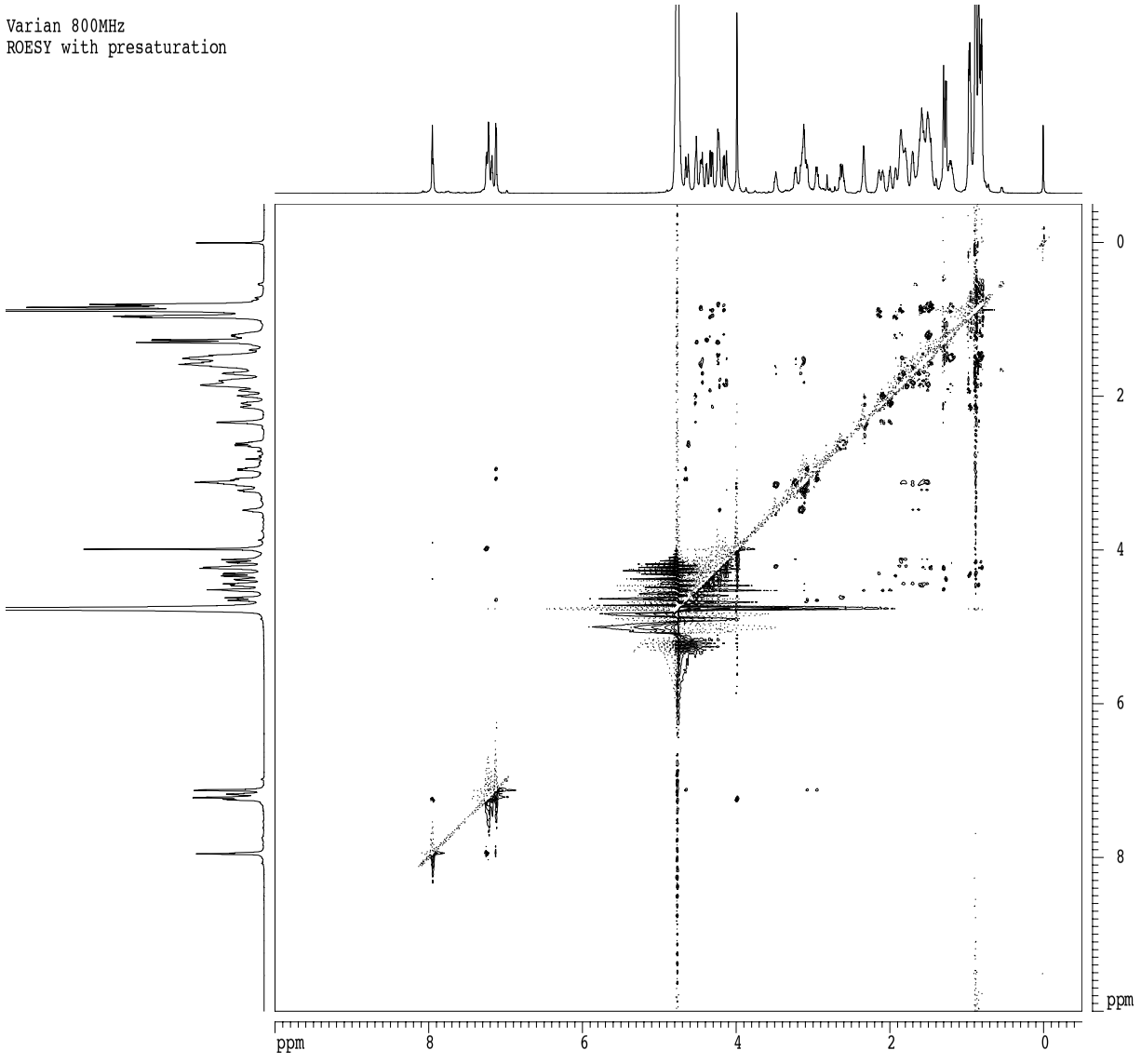

Current Data Parameters

USER	yilinw
NAME	131110_YW_1_QRL
EXPNO	4
PROCNO	1

F2 - Acquisition Parameters

Date_	20131110
Time	0.00
INSTRUM	varian
PROBHD	40:5mmbroadban
PULPROG	roesy
TD	5212
SOLVENT	D2O
NS	8
DS	16
SWH	11196.641 Hz
FIDRES	2.148243 Hz
AQ	0.2327984 sec
RG	128
DW	44.656 usec
DE	6.00 usec
TE	298.0 K

F1 - Acquisition parameters

ND0	1
TD	512
SFO1	799.7986 MHz
FIDRES	17.183548 Hz
SW	11.000 ppm
FnMODE	undefined

F2 - Processing parameters

SI	1024
SF	799.7947714 MHz
WDW	QSINE
SSB	2
LB	0.00 Hz
GB	0
PC	1.40

F1 - Processing parameters

SI	512
MC2	States
SF	799.7947714 MHz
WDW	QSINE
SSB	2
LB	0.00 Hz
GB	0

2D NMR plot parameters

CX2	15.00 cm
CX1	15.00 cm
F2PLO	10.000 ppm
F2LO	7997.95 Hz
F2PHI	-0.500 ppm
F2HI	-399.90 Hz
F1PLO	10.000 ppm
F1LO	7997.95 Hz
F1PHI	-0.500 ppm
F1HI	-399.90 Hz
F2PPMCM	0.70000 ppm/cm
F2HZCM	559.85638 Hz/cm
F1PPMCM	0.70000 ppm/cm
F1HZCM	559.85638 Hz/cm

HPLC , MS ESI$^+$ TOF, and NMR (^{1}H, TOCSY and ROESY) of peptide **2i**

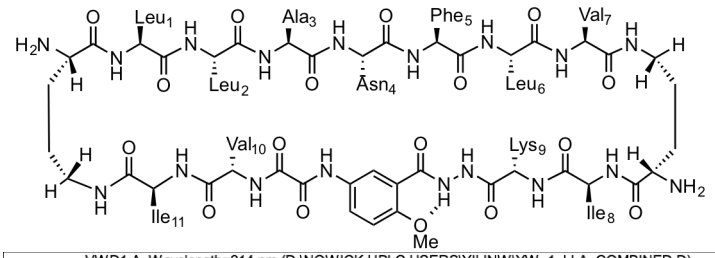

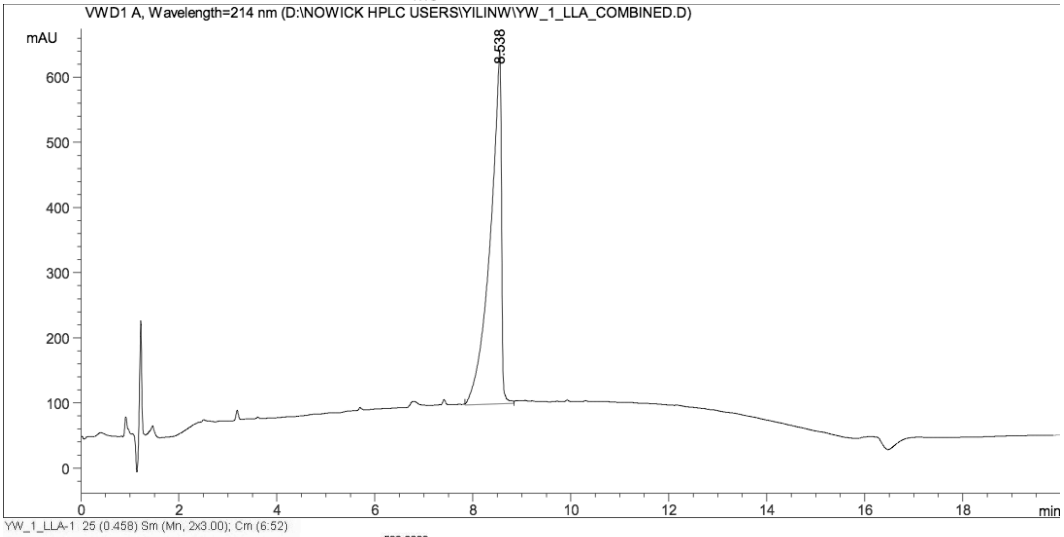

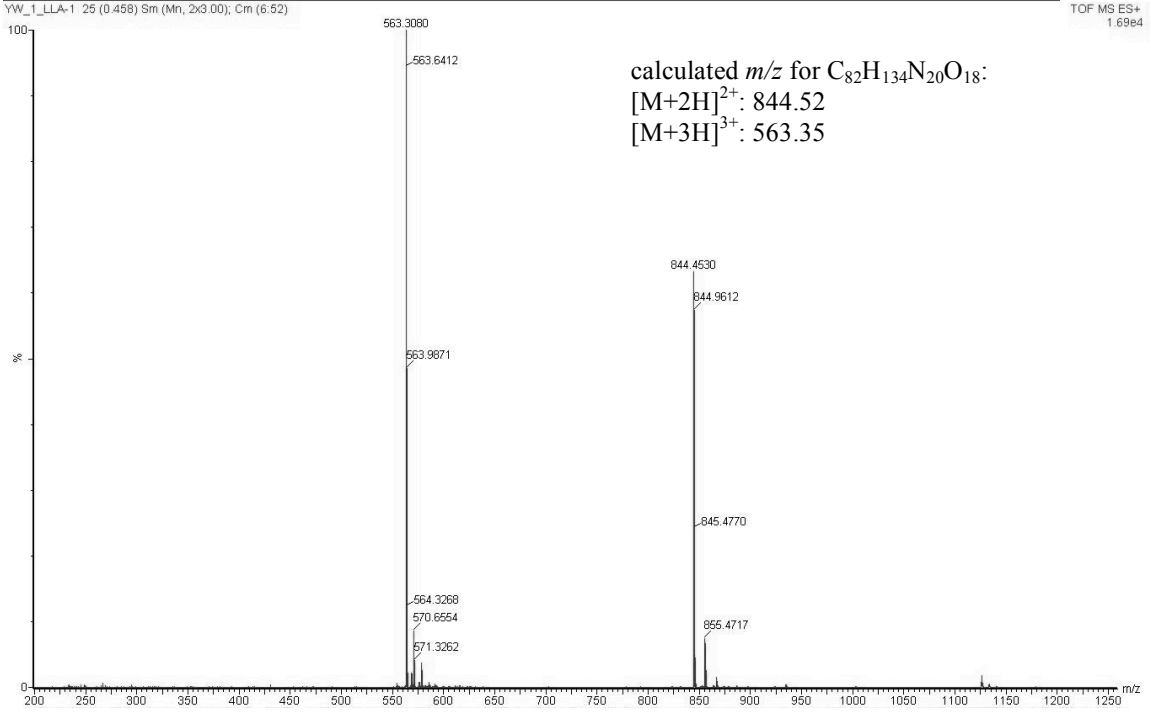

calculated *m/z* for $C_{82}H_{134}N_{20}O_{18}$:
$[M+2H]^{2+}$: 844.52
$[M+3H]^{3+}$: 563.35

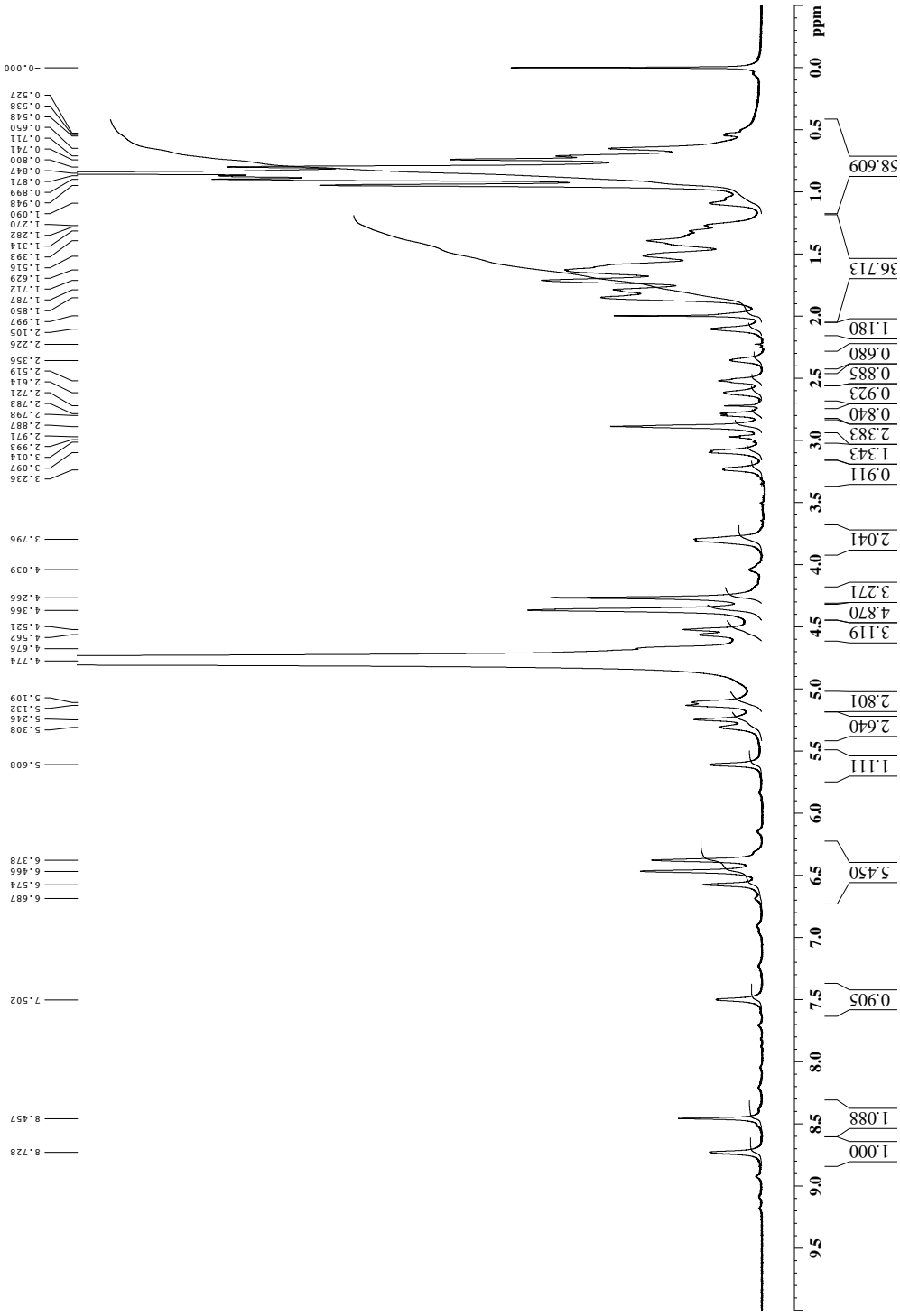

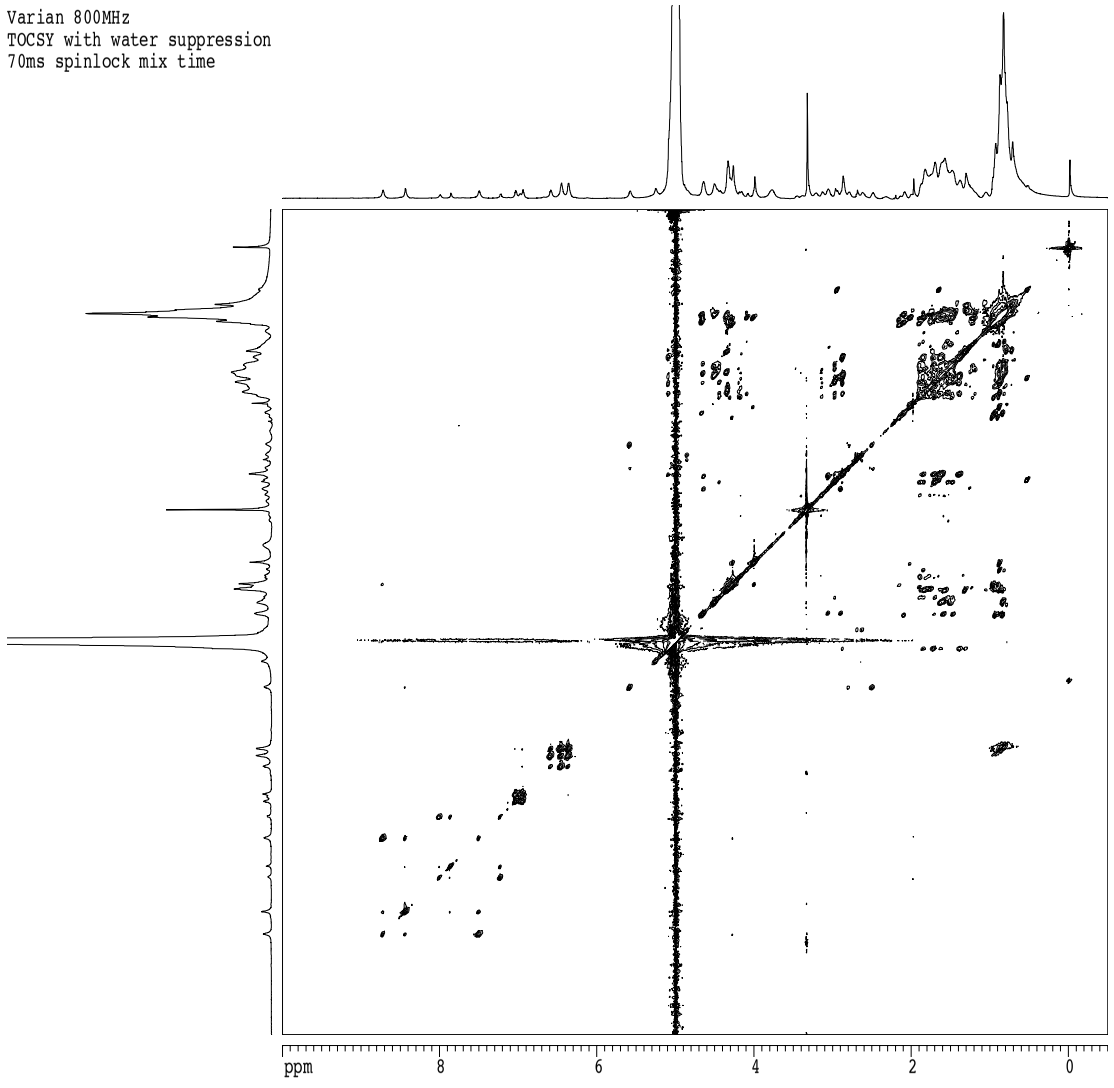

Current Data Parameters

USER	yilinw
NAME	LLA_4mM_800_5C
EXPNO	3
PROCNO	1

F2 - Acquisition Parameters

Date_	20131125
Time	0.00
INSTRUM	varian
PROBHD	40:5mmbroadban
PULPROG	tocsy
TD	4096
SOLVENT	D2O
NS	4
DS	16
SWH	8797.977 Hz
FIDRES	2.147943 Hz
AQ	0.2328308 sec
RG	287.4
DW	56.831 usec
DE	6.00 usec
TE	278.0 K

F1 - Acquisition parameters

ND0	1
TD	512
SFO1	799.7986 MHz
FIDRES	17.183548 Hz
SW	11.000 ppm
FnMODE	undefined

F2 - Processing parameters

SI	2048
SF	799.7945677 MHz
WDW	QSINE
SSB	2
LB	0.00 Hz
GB	0
PC	1.40

F1 - Processing parameters

SI	1024
MC2	States
SF	799.7945677 MHz
WDW	QSINE
SSB	2
LB	0.00 Hz
GB	0

2D NMR plot parameters

CX2	15.00 cm
CX1	15.00 cm
F2PLO	10.000 ppm
F2LO	7997.95 Hz
F2PHI	-0.500 ppm
F2HI	-400.10 Hz
F1PLO	10.000 ppm
F1LO	7997.95 Hz
F1PHI	-0.500 ppm
F1HI	-400.10 Hz
F2PPMCM	0.70002 ppm/cm
F2HZCM	559.86981 Hz/cm
F1PPMCM	0.70002 ppm/cm
F1HZCM	559.86981 Hz/cm

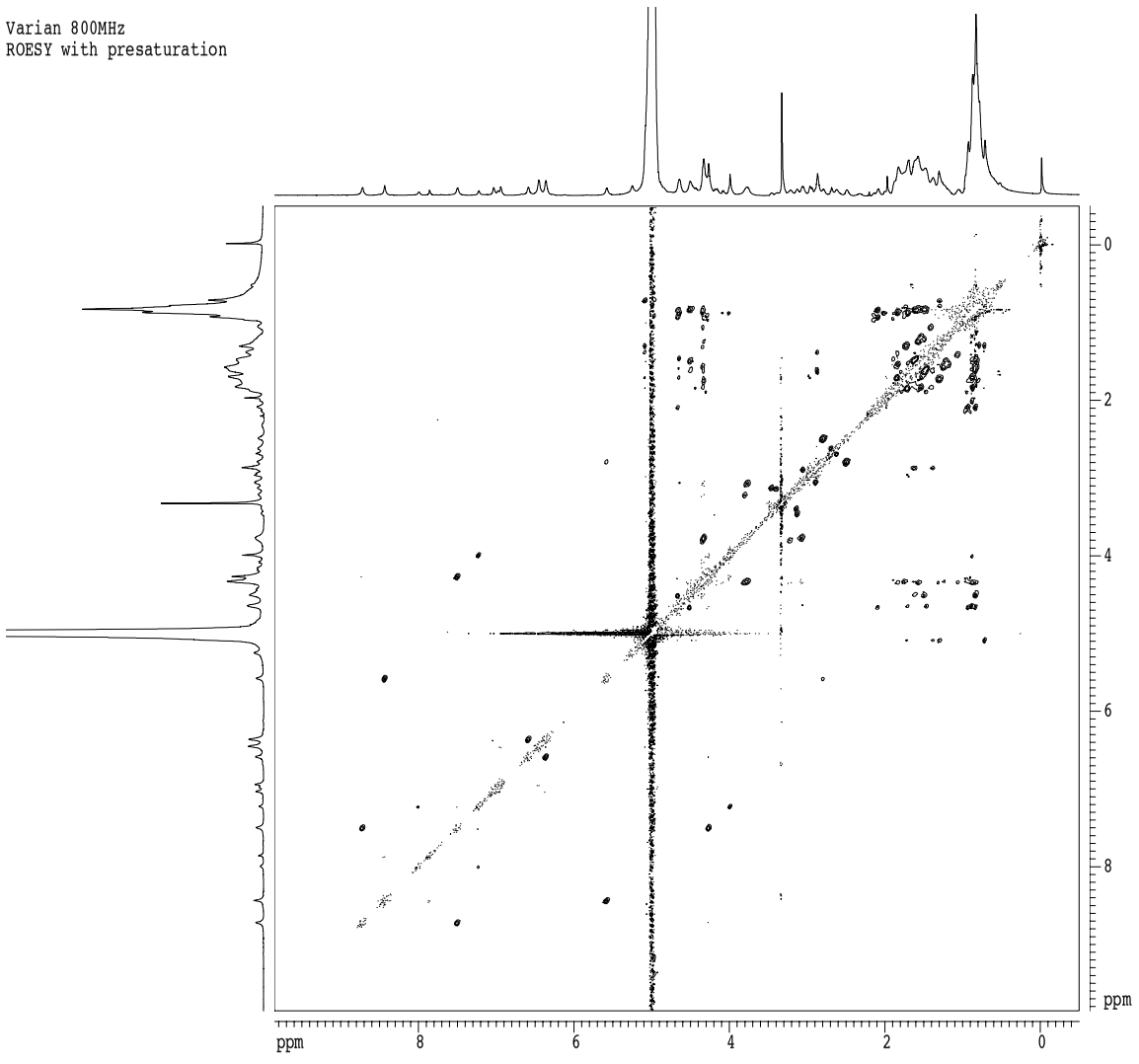

Current Data Parameters

USER	yilinw
NAME	LLA_4mM_800_5C
EXPNO	4
PROCNO	1

F2 - Acquisition Parameters

Date_	20131125
Time	0.00
INSTRUM	varian
PROBHD	40:5mmbroadban
PULPROG	roesy
TD	4096
SOLVENT	D2O
NS	8
DS	16
SWH	8797.977 Hz
FIDRES	2.147943 Hz
AQ	0.2328308 sec
RG	128
DW	56.831 usec
DE	6.00 usec
TE	278.0 K

F1 - Acquisition parameters

ND0	1
TD	512
SFO1	799.7986 MHz
FIDRES	17.183548 Hz
SW	11.000 ppm
FnMODE	undefined

F2 - Processing parameters

SI	1024
SF	799.7945677 MHz
WDW	QSINE
SSB	2
LB	0.00 Hz
GB	0
PC	1.40

F1 - Processing parameters

SI	512
MC2	States
SF	799.7945677 MHz
WDW	QSINE
SSB	2
LB	0.00 Hz
GB	0

2D NMR plot parameters

CX2	15.00 cm
CX1	15.00 cm
F2PLO	9.855 ppm
F2LO	7881.74 Hz
F2PHI	-0.500 ppm
F2HI	-399.90 Hz
F1PLO	9.855 ppm
F1LO	7881.74 Hz
F1PHI	-0.500 ppm
F1HI	-399.90 Hz
F2PPMCM	0.69031 ppm/cm
F2HZCM	552.10913 Hz/cm
F1PPMCM	0.69031 ppm/cm
F1HZCM	552.10913 Hz/cm

Chapter 3

A Tetramer Derived from Islet Amyloid Polypeptide

Introduction

Interactions among β-sheets are central to the misfolding and aggregation of peptides and proteins that form toxic oligomers and insoluble fibrils in over 40 amyloid diseases, including type 2 diabetes, Alzheimer's disease, and Parkinson's disease.[1,2] The fibrils share the common feature of an extended network of hydrogen-bonded β-sheets that are further stabilized through hydrophobic packing.[3-11] Less is known about the structures of the smaller, often metastable and polymorphic oligomers, but β-sheets and hydrophobic interactions appear to be important in oligomer formation.[12-17]

The 37-residue islet amyloid polypeptide (IAPP) aggregates to form fibrils and oligomers that are central to islet β-cell death in the progression of type 2 diabetes.[18-23] Tycko and coworkers proposed structural models of IAPP fibrils using constraints from solid-state NMR spectroscopy.[4] In these models, a fibril consists of layers of parallel, in-register β-sheets that run perpendicular to the length of the fibril. β-Strands consisting of central residues 8–17 form one of the layers, while β-strands comprising C-terminal residues 28–36 form the other layer. A loop region containing residues 18–27 connects the two β-strands. Using X-ray crystallographic structures derived from fragments of IAPP, Eisenberg and coworkers constructed a similar fibril model in which the side chains are more tightly packed.[5,24] Langen and coworkers proposed a model of IAPP fibrils using constraints from EPR spectroscopy in which the β-strands pack more loosely.[25] The residues involved in β-sheet formation vary slightly among these different models, but central residues 12–17 and C-terminal residues 31–36 are generally thought to be involved in β-strand formation.

Although the structures of IAPP oligomers are not known at high resolution, they appear to be composed of β-sheets. Through ion mobility-mass spectrometry (IM-MS) studies in conjunction with replica exchange molecular dynamics (REMD), Bowers and coworkers proposed β-hairpin building blocks for human IAPP oligomers.[26,27] Hoyer and coworkers obtained an NMR-based structure of IAPP in a β-hairpin conformation bound to an affibody and suggested that this β-hairpin might be involved in IAPP aggregation.[23] The β-hairpin comprises residues 12–28; residues 12–18 and residues 22–28 form β-strands, while residues 19–21 form a turn. In a separate study, Zanni and coworkers used 2D IR spectroscopy to show that residues 23–27 have β-sheet structure in the oligomer but form a disordered loop in the fibril.[28]

Our laboratory recently introduced macrocyclic β-sheet peptides as a platform to explore the interactions among β-sheets in amyloidogenic peptides and proteins (Figure 3.1).[28,29] The macrocyclic β-sheet peptides contain a peptide strand and a template strand that are connected by two δ-linked ornithine ($^{\delta}$Orn) turn units.[30,31] The peptide strand contains a heptapeptide sequence derived from an amyloidogenic peptide or protein. The template strand contains four additional α-amino acids and the unnatural amino acid Hao, which mimics a tripeptide β-strand, templates β-sheet formation, and blocks uncontrolled aggregation.[32] Our laboratory has used macrocyclic β-sheet peptides containing heptapeptide segments from the β-amyloid peptide Aβ, β_2-microglobulin, and α-synuclein as inhibitors to control amyloid aggregation and reduce amyloid toxicity.[29] Recently, Nicholas Truex and I used NMR spectroscopy to study the homotetramers and heterotetramers formed by macrocyclic β-sheet peptides containing residues 17–23 and 30–36 from Aβ.[33,34]

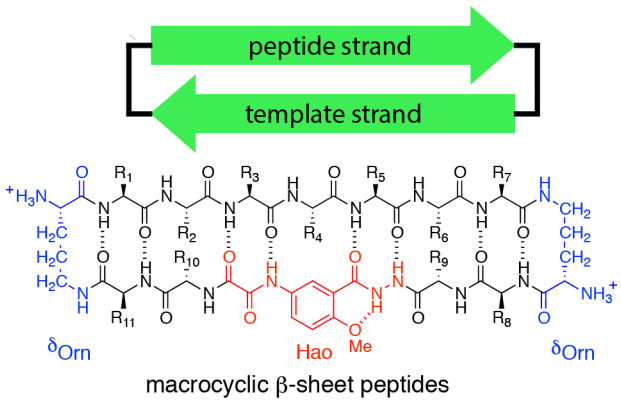

Figure 3.1. Cartoon representation (top) and chemical structure (bottom) of macrocyclic β-sheet **1**. The macrocyclic β-sheet consists of a heptapeptide strand (R_1–R_7) connected by two ornithine turn units to a template strand containing the tripeptide mimic Hao flanked by two α-amino acid residues on each side.

In the current study, I use macrocyclic β-sheet peptides as a platform to explore assembly of the central region of IAPP. I designed peptide $\mathbf{1}_{\mathbf{Arg}}$ to contain central residues 11–17 of IAPP (RLANFLV). I chose the $IAPP_{11–17}$ heptapeptide for its propensity to form a β-strand in fibrils and β-hairpin monomers. I also designed homologue peptide $\mathbf{1}_{\mathbf{Cit}}$, in which I mutated Arg_{11} to the uncharged isostere of arginine, citrulline (Figure 3.2). Here I describe NMR spectroscopic studies of peptides $\mathbf{1}_{\mathbf{Arg}}$ and $\mathbf{1}_{\mathbf{Cit}}$, report the X-ray crystallographic structure of a tetramer formed by a homologue of peptide $\mathbf{1}_{\mathbf{Cit}}$, and correlate the X-ray crystallographic structure with the solution-phase assembly of the IAPP-derived peptides.

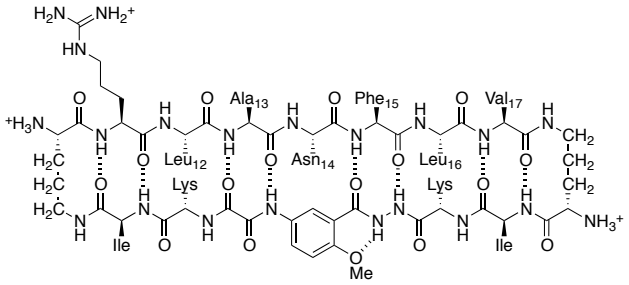

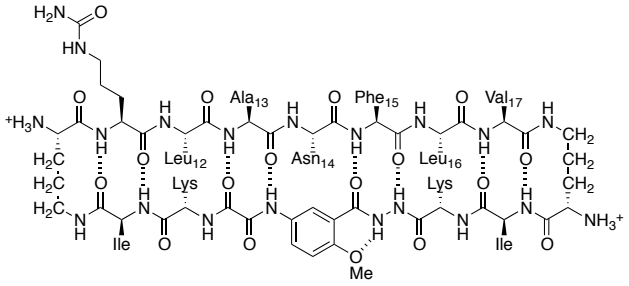

Figure 3.2. Chemical structures of peptides $\mathbf{1_{Arg}}$ (top) and $\mathbf{1_{Cit}}$ (bottom).

Results and Discussion

The β-strand formed by $IAPP_{11–17}$ displays a hydrophobic surface comprising the side chains of Ala_{13}, Phe_{15}, and Val_{17}, as well as Arg_{11}. To reinforce the hydrophobicity of this surface, I incorporated isoleucine residues at positions R_8 and R_{11} of the template strand. I incorporated lysine residues at positions R_9 and R_{10} to increase solubility of the peptide and render the surface displaying the side chains of Leu_{12}, Asn_{14}, and Leu_{16} hydrophilic.

In aqueous solution, peptide $\mathbf{1_{Arg}}$ is monomeric. The ^{1}H NMR spectrum of peptide $\mathbf{1_{Arg}}$ at 4 mM exhibits a single set of sharp resonances, associated with the monomeric peptide (Figure 3.3 and 3.4). The resonances associated with the α-protons are in the 4–5 ppm range, showing little to no downfield shifting relative to the typical values for the corresponding residues in a random coil conformation (Figure 3.5).[35] At 8 mM, I observe

broadening of the resonances but no additional peaks associated with assembly of the peptide (Figure 3.3). I hypothesized that the positive charge on Arg_{11} may prevent peptide $\mathbf{1_{Arg}}$ from oligomerizing. To explore this hypothesis, I replaced Arg_{11} with the neutrally charged isostere citrulline, reducing the net charge from +5 to +4.

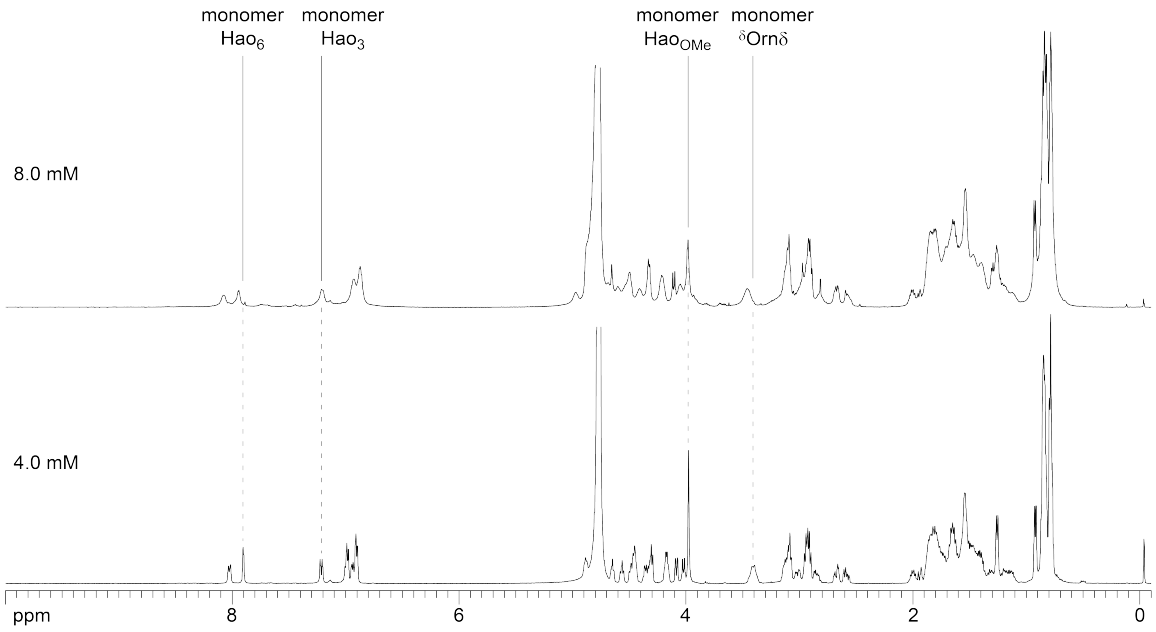

Figure 3.3. ^{1}H NMR spectra of peptide $\mathbf{1_{Arg}}$ at 4 mM and 8 mM and 50 mM CD_3COOD and 50 mM CD_3COONa buffer in D_2O at 500 MHz and 298K.

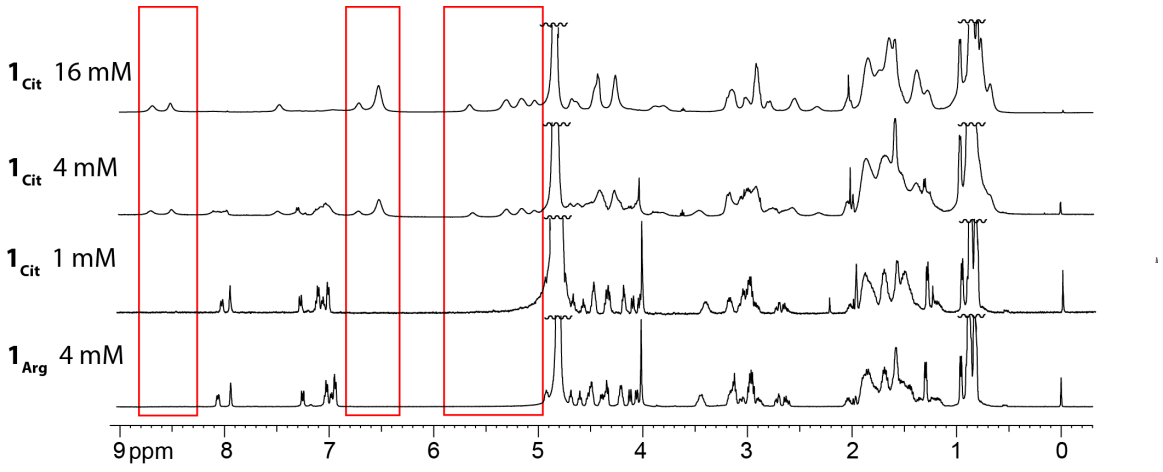

Figure 3.4. ^{1}H NMR spectra of macrocyclic β-sheet peptides $\mathbf{1}_{\mathbf{Arg}}$ and $\mathbf{1}_{\mathbf{Cit}}$ in 50 mM CD_3COOD and 50 mM CD_3COONa buffer in D_2O at 298 K. The red boxes highlight noteworthy resonances of the tetramer.

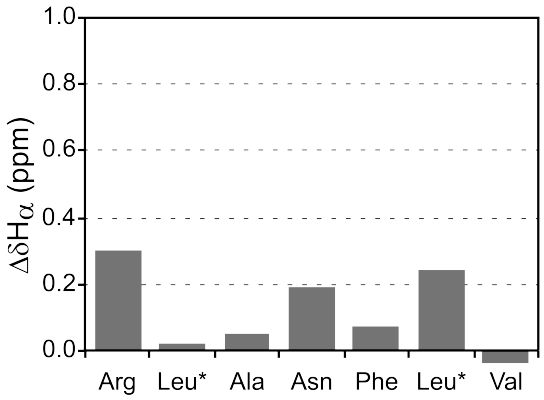

Figure 3.5. Downfield shifting of the α-protons of peptide $\mathbf{1}_{\mathbf{Arg}}$ at 4 mM relative to those of random coil chemical shifts.*Leucine residues are not assigned in a sequence specific fashion.

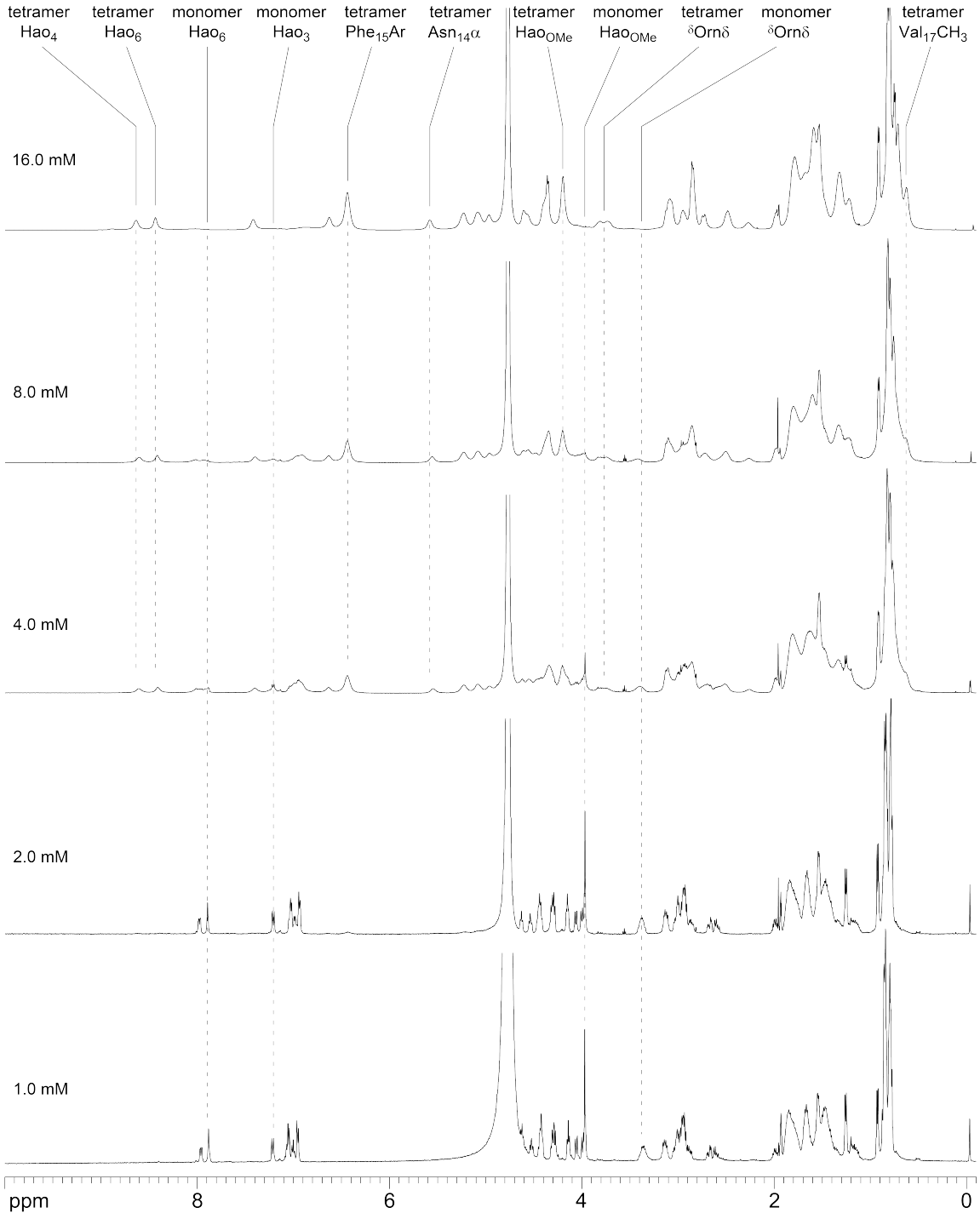

Figure 3.6. ^{1}H NMR spectra of peptide $\mathbf{1_{Cit}}$ various concentrations and 50 mM CD_3COOD and 50 mM CD_3COONa buffer in D_2O at 500 MHz and 298K.

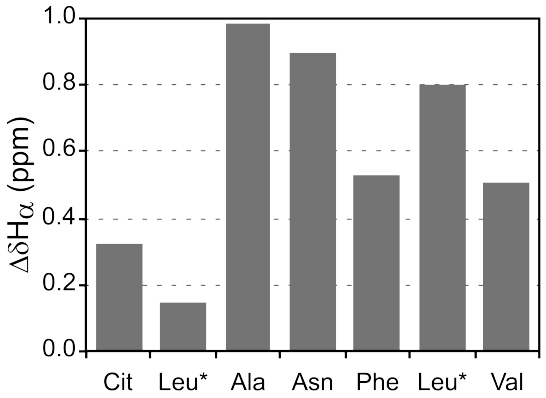

Figure 3.7. Downfield shifting of the α-protons of peptide $\mathbf{1_{Cit}}$ at 16 mM relative to those of random coil chemical shifts.*Leucine residues are not assigned in a sequence specific fashion.

Peptide $\mathbf{1_{Cit}}$ is monomeric at low concentrations but forms a tetramer at higher concentrations. At 1 mM, the spectrum is similar to that of peptide $\mathbf{1_{Arg}}$ (Figure 3.4 and 3.6). At 4 mM, peptide $\mathbf{1_{Cit}}$ displays two sets of broad resonances associated with the monomer and the tetramer. At 16 mM, only the resonances associated with the tetramer are visible. The resonances associated with the α-protons of the tetramer are shifted downfield by up to 1 ppm relative to those of random coil values (Figure 3.7).[35] This downfield shifting reflects the folding and assembly of the peptide into the tetramer. The aromatic resonances associated with the Phe_{15} side chain are shifted upfield by approximately 0.5 ppm, to 6.5 ppm, suggesting that the side chains of Phe_{15} pack to form a hydrophobic core within the tetramer.

Comparison of ^{1}H NMR spectra of peptide $\mathbf{1_{Cit}}$ at 1 mM and 16 mM shows that folding accompanies oligomerization. The magnetic anisotropy of the diastereotopic δ-protons of the $^{\delta}$Orn turn units reflects β-sheet folding in macrocyclic β-sheet peptides.[30,31] In a well-folded macrocyclic β-sheet peptide, each diastereotopic *pro-S* δ-proton resonance is about 0.6 ppm downfield of the corresponding *pro-R* δ-proton resonance. The monomer subunits of the tetramer formed by peptide $\mathbf{1_{Cit}}$ are well folded, with the

difference in chemical shifts of the diastereotopic *pro-S* and *pro-R* δ-protons being 0.66 and 0.70 ppm. In contrast, monomeric peptide $\mathbf{1}_{\mathbf{Cit}}$ is partially folded, with the difference in chemical shifts of the diastereotopic *pro-S* and *pro-R* δ-protons being 0.19 and 0.29 ppm.

To further characterize the structure of the tetramer formed by peptide $\mathbf{1}_{\mathbf{Cit}}$, I turned to X-ray crystallography. To facilitate X-ray crystallographic phase determination, I designed and synthesized homologue peptide $\mathbf{2}_{\mathbf{Cit}}$ (Figure 3.8). Peptide $\mathbf{2}_{\mathbf{Cit}}$ contains the leucine isostere, (2-bromoallyl)glycine, in place of one of the isoleucines in the template strand to allow X-ray crystallographic phase determination by means of single-wavelength anomalous diffraction phasing.[13] Peptide $\mathbf{2}_{\mathbf{Cit}}$ afforded crystals suitable for X-ray diffraction in conditions containing sodium citrate buffer, isopropanol, and poly(ethylene glycol) (PEG) 4,000.

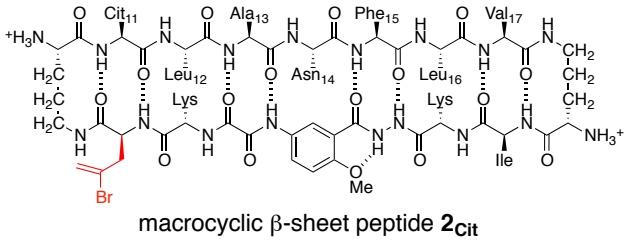

macrocyclic β-sheet peptide $\mathbf{2}_{\mathbf{Cit}}$

Figure 3.8. Chemical structure of peptide $\mathbf{2}_{\mathbf{Cit}}$ with the leucine isostere, (2-bromoallyl)glycine residue in red.

The asymmetric unit contains four folded macrocyclic β-sheets, which pack to form a tetramer. The heptapeptide β-strand of each monomer subunit is hydrogen bonded to the template strand through a network of eight hydrogen bonds (Figure 3.9A). The monomers in the asymmetric unit are similar in conformation with little variation in the

side chains. One notable difference is in the Phe_{15} residues, which exhibit two rotamers (Figure 3.9B).

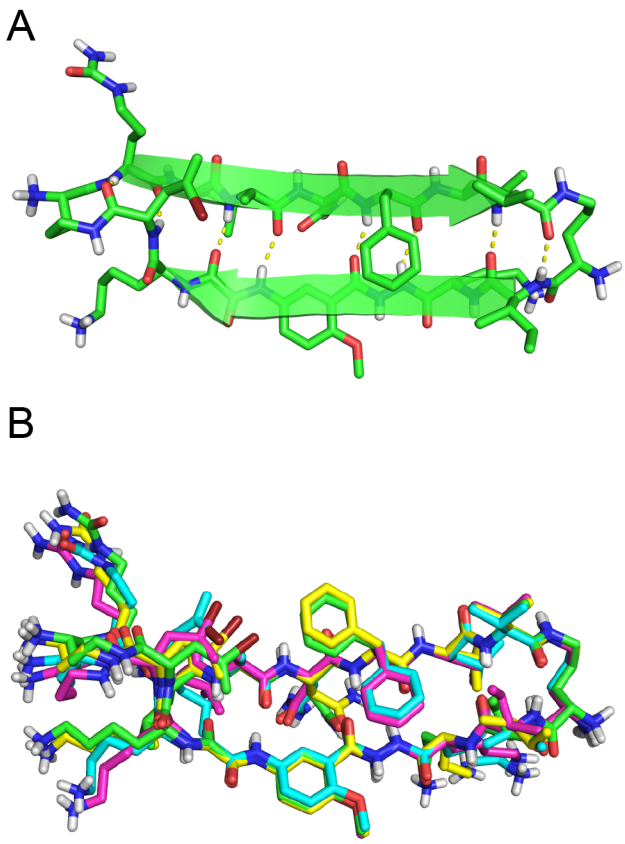

Figure 3.9. X-ray crystallographic structure of peptide $\mathbf{2_{Cit}}$ (PDB 5UHR). (A) Representative monomer subunit. (B) Overlay of the four monomers in the asymmetric unit.

The monomer subunits pair through edge-to-edge hydrogen bonding to form antiparallel β-sheet dimers (Figure 3.10). The two heptapeptide β-strands in the dimer are shifted by two residues towards the C-termini. Six intermolecular hydrogen bonds form between the two monomers. The dimer presents two surfaces. One surface is hydrophobic and displays the side chains of Cit_{11}, Ala_{13}, Phe_{15}, and Val_{17} of the peptide strand, as well as the Ile and (2-bromoallyl)glycine of the template strand (Figure 3.10A). The two Phe_{15} side chains on the hydrophobic surface adopt different rotamers. The other surface is

hydrophilic and displays the Leu_{12}, Asn_{14}, and Leu_{16} side chains of the peptide strand, as well as the two Lys residues of the template strand (Figure 3.10B).

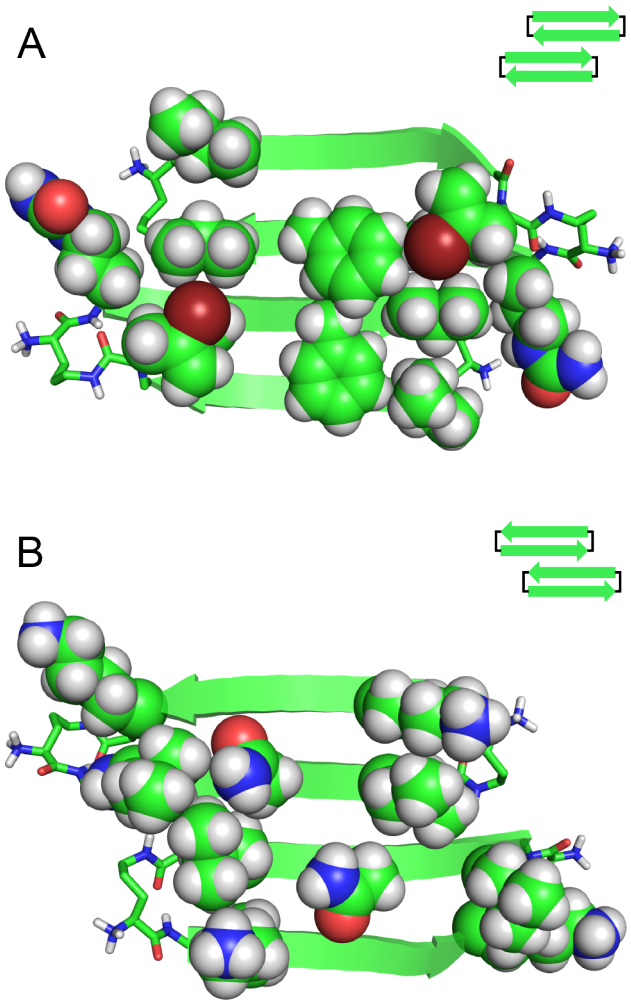

Figure 3.10. X-ray crystallographic structure of the dimer formed by peptide $\mathbf{2}_{\mathbf{Cit}}$. (A) View of the hydrophobic surface with side chains shown as spheres. (B) View of the hydrophilic surface with side chains shown as spheres.

Two hydrogen-bonded dimers sandwich together on their hydrophobic surfaces to form a tetramer (Figure 3.11). In the tetramer, the β-sheets of the dimers are nearly orthogonal. The side chains of Ala_{13}, Phe_{15}, Val_{17}, Ile, and (2-bromoallyl)glycine create a hydrophobic core within the sandwich, with the four phenyl groups packing at the center

of the sandwich. The two rotamers of the Phe_{15} side chains allow the phenyl groups to pack together tightly through hydrophobic interactions and aromatic stacking at the center of the hydrophobic core. The side chains of Ala_{13}, Val_{17}, Ile, and (2-bromoallyl)glycine surround the four Phe_{15} side chains, packing through hydrophobic interaction to stabilize the tetramer. The hydrophilic side chain of Cit_{11} extends out of the hydrophobic core. The hydrophilic surfaces of the dimer subunits that comprise the tetramer are exposed to solvent.

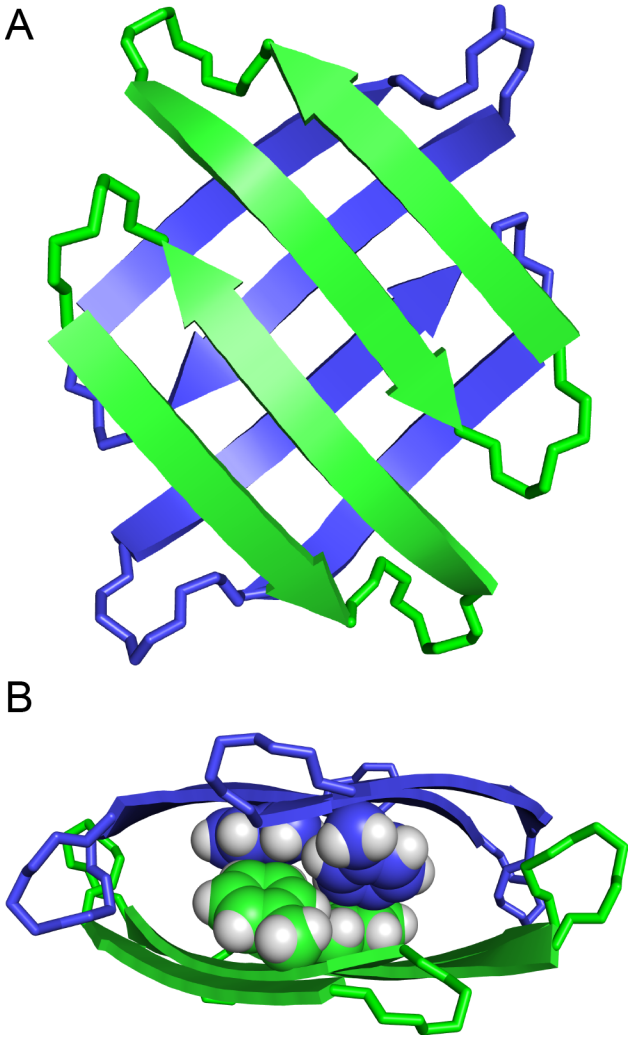

Figure 3.11. X-ray crystallographic structure of the tetramer of peptide $\mathbf{2_{Cit}}$. (A) Top view. (B) Side view. Sphere representations of Phe_{15} show packing of the aromatic side chains in the hydrophobic core.

Diffusion-ordered spectroscopy (DOSY) provides a useful tool for assessing the relative oligomerization state of macrocyclic β-sheets peptides.[33,34,36,37] Oligomers diffuse more slowly than the monomers, with dimers having a diffusion coefficient of about 0.75–0.79 times that of the monomer and tetramers having a diffusion coefficient of about 0.58–0.63 times that of the monomer.[33,37,38] At 298 K, the diffusion coefficient of peptide $\mathbf{1}_{\mathbf{Arg}}$ is 19.6 × 10^{-7} cm^2/s in deuterioacetate buffered D_2O (Table 3.1). At 1 mM, peptide $\mathbf{1}_{\mathbf{Cit}}$ is monomeric, with a diffusion coefficient of 20.0 × 10^{-7} cm^2/s, which is the same as peptide $\mathbf{1}_{\mathbf{Arg}}$ within the limits of experimental error. At 2 mM, peptide $\mathbf{1}_{\mathbf{Cit}}$ is largely monomeric, with a diffusion coefficient of 18.9 × 10^{-7} cm^2/s.

As the concentration is increased and the resonances from the oligomer grow in, the diffusion coefficient of peptide $\mathbf{1}_{\mathbf{Cit}}$ decreases. At 4 mM and 8 mM, discrete diffusion coefficients cannot be measured for the resonances associated with the monomer and the oligomer, because exchange occurs at a rate similar to the 75-ms time scale of the experiment. Instead, an averaged diffusion coefficient for the mixture is observed. At 4 mM, the diffusion coefficient is 17.4 × 10^{-7} cm^2/s, and at 8 mM the diffusion coefficient is 14.2 × 10^{-7} cm^2/s. At 16 mM, the oligomer predominates vastly, and only resonances for the oligomer are observed. At 16 mM, the diffusion coefficient is 12.4 × 10^{-7} cm^2/s. This value is about 0.6 times that of the monomer of peptide $\mathbf{1}_{\mathbf{Cit}}$, and is consistent with a tetramer.

Table 3.1. Diffusion coefficients (*D*) of peptides $\mathbf{1}_{\mathbf{Arg}}$ and $\mathbf{1}_{\mathbf{Cit}}$ in 50 mM CD_3COOD and 50 mM CD_3COONa buffer in D_2O at 298 K.

	$MW_{monomer}$ (Da)	$MW_{tetramer}$ (Da)	Conc. (mM)	*D* ($\times 10^{-7}$ cm^2/s)	oligomer state
$\mathbf{1}_{\mathbf{Arg}}$	1759	7036	4	19.6 ± 0.6	monomer
$\mathbf{1}_{\mathbf{Cit}}$	1760	7040	1	20.0 ± 2.0	monomer
$\mathbf{1}_{\mathbf{Cit}}$	1760	7040	2	18.9 ± 1.2	monomer
$\mathbf{1}_{\mathbf{Cit}}$	1760	7040	4	17.4 ± 1.2	mixture
$\mathbf{1}_{\mathbf{Cit}}$	1760	7040	8	14.2 ± 0.3	mixture
$\mathbf{1}_{\mathbf{Cit}}$	1760	7040	16	12.4 ± 0.3	tetramer

NOESY NMR spectroscopy establishes that the structure of the tetramer formed by peptide $\mathbf{1}_{\mathbf{Cit}}$ in aqueous solution is similar to the tetramer observed for peptide $\mathbf{2}_{\mathbf{Cit}}$ in the crystal. I observe NOEs from the folding of the monomers and formation of the dimers. Two strong crosspeaks in the NOESY spectrum reflect folding of macrocyclic β-sheet peptide $\mathbf{1}_{\mathbf{Cit}}$, one between the α-protons of Leu and Lys, and one between the α-proton of Asn_{14} and the proton at the 6-position of the unnatural amino acid Hao (Figure 3.12). NOEs between the α-proton and *pro-S* δ-proton of the $^{\delta}$Orn turn units further reflect folding of the macrocycle. A strong crosspeak between the α-protons of Ala_{13} and Val_{17} reflect shifted antiparallel dimer formation. An additional NOE between the methoxy protons of Hao and the Ile side chain reflect packing of the dimers in a sandwich-like fashion (Figure 3.13). The interlayer NOE between the Hao-methoxy and Ile side chain is characteristic of sandwich-like tetramers of Hao-containing macrocyclic β-sheet peptides.[33] These NOEs associated with folding, dimerization, and packing reflect the congruence of the X-ray crystallographic and solution-state tetramers.

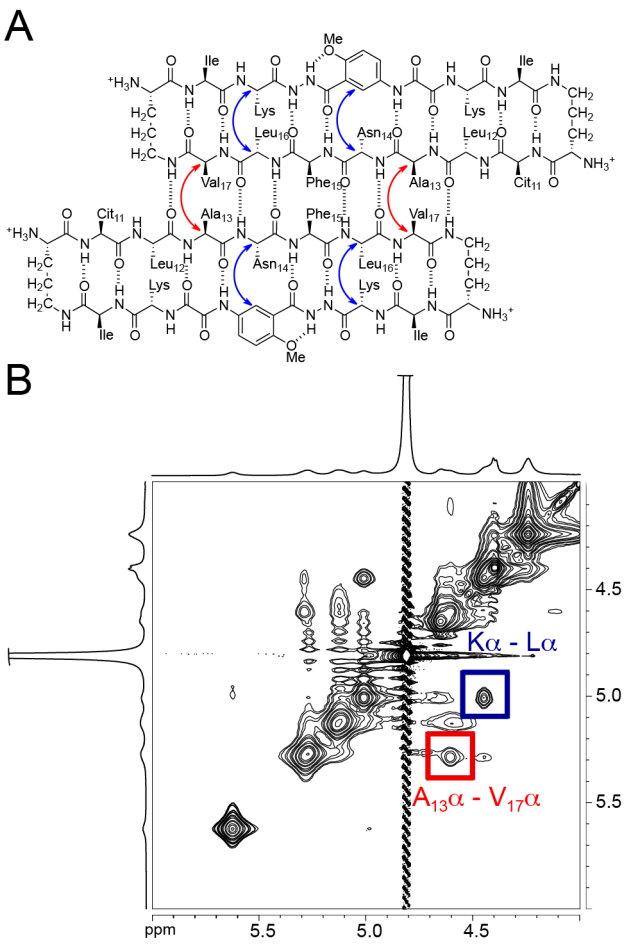

Figure 3.12. NOEs associated with the dimer subunit of peptide $\mathbf{1}_{\mathbf{Cit}}$. (A) Shifted, antiparallel hydrogen-bonded dimer. Blue arrows indicate intramolecular NOEs and red arrows indicate intermolecular NOE observed in the NOESY spectrum. (B) Expansion of the NOESY spectrum showing selected intramolecular (blue) and intermolecular (red) NOE crosspeaks.

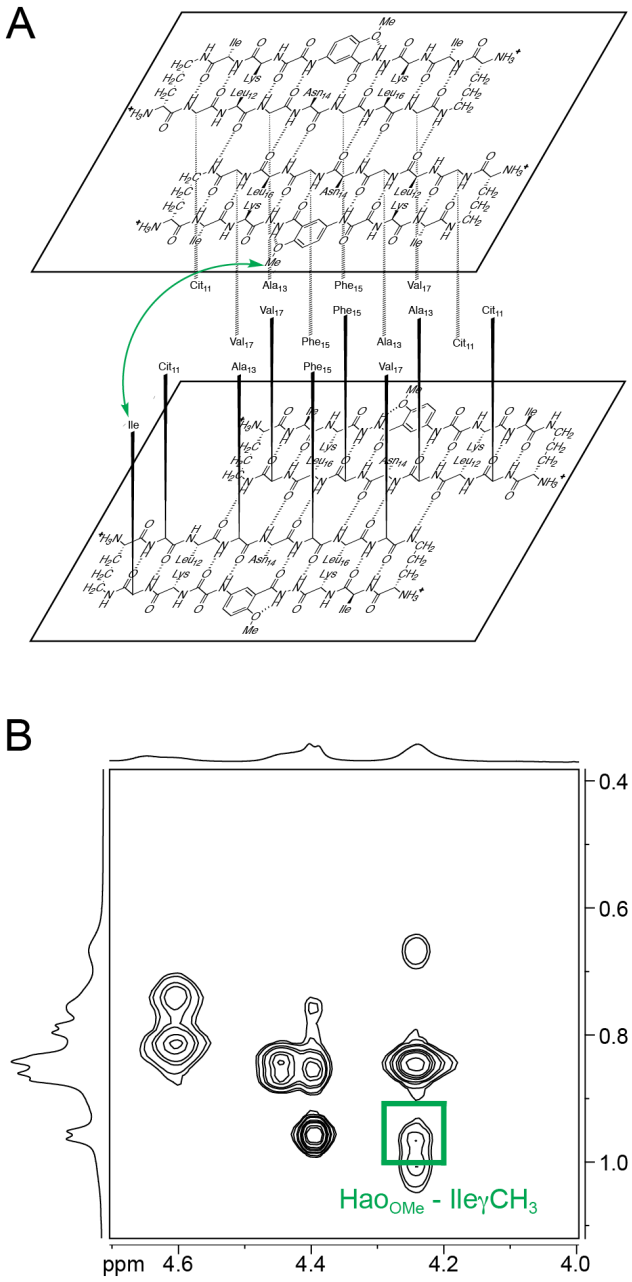

Figure 3.13. NOE associated with the tetramer of peptide $\mathbf{1}_{\mathbf{Cit.}}$ (A) Green arrow indicates interlayer NOE observed in the NOESY spectrum. (B) NOE crosspeak between the Ile side chain and the methoxy protons of the unnatural amino acid Hao.

To understand why peptide $\mathbf{1}_{\mathbf{Cit}}$ forms tetramers but peptide $\mathbf{1}_{\mathbf{Arg}}$ does not, I used the X-ray crystallographic structure of peptide $\mathbf{2}_{\mathbf{Cit}}$ to generate molecular models of tetramers of peptides $\mathbf{1}_{\mathbf{Cit}}$ and $\mathbf{1}_{\mathbf{Arg}}$. I modeled the tetramer formed by peptide $\mathbf{1}_{\mathbf{Cit}}$ by

mutating the (2-bromoallyl)glycine residue to isoleucine and minimizing the resulting structure in MacroModel with the MMFFs force field with GB/SA water solvation (Figure 3.14). I modeled a tetramer of peptide $\mathbf{1}_{\mathbf{Arg}}$ in a similar fashion, mutating both the (2-bromoallyl)glycine and the citrulline residues. Both molecular models overlay well with the X-ray crystallographic structure of the tetramer of peptide $\mathbf{2}_{\mathbf{Cit}}$ (RMSD ~1 Å). Inspection of the dimer subunits suggests an explanation of the differing stabilities of the $\mathbf{1}_{\mathbf{Cit}}$ and $\mathbf{1}_{\mathbf{Arg}}$ tetramers (Figure 3.15). In the dimer subunit of peptide $\mathbf{1}_{\mathbf{Arg}}$, the cationic guanidinium group of each arginine is near the ammonium group of one of the $^{\delta}$Orn turn units, while in the dimer subunit of peptide $\mathbf{1}_{\mathbf{Cit}}$, the neutral urea group of citrulline is near the ammonium group. Thus, it appears that charge-charge repulsion destabilizes the dimer and hence the tetramer of peptide $\mathbf{1}_{\mathbf{Arg}}$.

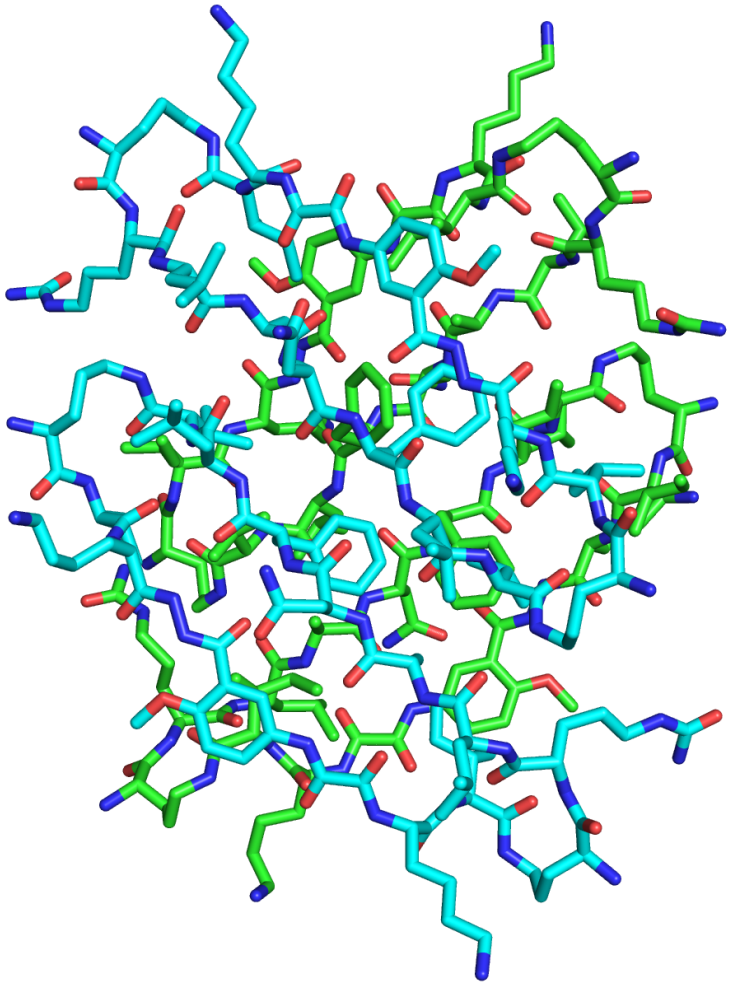

Figure 3.14. Crystographically based molecular model of the tetramer formed by peptide $\mathbf{1}_{Cit}$. The model was generated in MacroModel with the MMFFs force field with GB/SA water solvation.

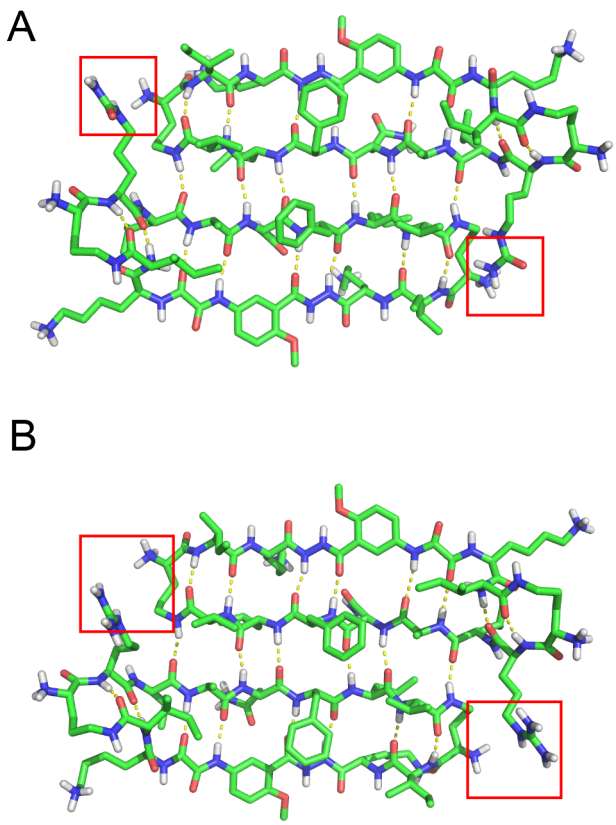

Figure 3.15. Crystallographically based molecular models of the dimer subunits of the tetramers of peptide $\mathbf{1}_{\mathbf{Cit}}$ (A) and $\mathbf{1}_{\mathbf{Arg}}$ (B). The red boxes highlight interactions between the ammonium groups of the $^{\delta}$Orn turn units and the Arg_{11} or Cit_{11} side chains.

The X-ray crystallographic structure and molecular model of the tetramers formed by peptides $\mathbf{2}_{\mathbf{Cit}}$ and $\mathbf{1}_{\mathbf{Cit}}$ share several features with structures reported for IAPP fibrils. Like the tetramers, the full atomic models of IAPP described by Tycko and coworkers consist of layered β-sheets in which hydrophobic interactions stabilize the layered structure. In contrast to the tetramers of peptides $\mathbf{2}_{\mathbf{Cit}}$ and $\mathbf{1}_{\mathbf{Cit}}$, the fibrils consist of parallel β-sheets formed by IAPP rather than antiparallel β-sheets. In the two different fibril models proposed by Tycko and coworkers, the Phe_{15} side chains are on either the interior or the exterior of the layers. The fragment-based model of IAPP fibrils proposed by Eisenberg and coworkers also consists of layered parallel β-sheets, with the side

chains of Phe_{15} on the exterior of the layers. Recently, Eisenberg and coworkers reported that $IAPP_{15–25}$ forms fibrils consisting of loosely laminated antiparallel β-sheets.[39] Hydrophobic interactions of Phe_{15} appear to be more important in the NMR structure of the IAPP β-hairpin bound to an affibody reported by Hoyer et *al*., in which the Phe_{15} and Phe_{23} pack tightly against one of the phenylalanine residues in the affibody to form a central core.[23] This mode of assembly is similar to the packing of Phe_{15} in the tetramers formed by peptides $\mathbf{1}_{\mathbf{Cit}}$ and $\mathbf{2}_{\mathbf{Cit}}$.

The tetramers formed by peptides $\mathbf{1}_{\mathbf{Cit}}$ and $\mathbf{2}_{\mathbf{Cit}}$ share common features with assemblies formed by other Hao-containing macrocyclic β-sheet peptides that our laboratory has studied (Figure 3.16). Several Hao-containing macrocyclic β-sheet peptides containing heptapeptide sequences from various amyloidogenic peptides and proteins form hydrogen-bonded assemblies laminated through hydrophobic interactions in the crystal state.[29,40] I have also identified two Hao-containing macrocyclic β-sheet peptides containing heptapeptide sequences from the β-amyloid peptide Aβ, which assemble to form tetramers in solution.[33,34] The flat, hydrophobic Hao group appears to facilitate the formation of these layered structures. These structures differ from those that I have observed for *N*-methylated macrocyclic β-sheet peptides, which I have also studied (Figure 3.16). Most of the *N*-methylated macrocyclic β-sheet peptides containing sequences from various amyloidogenic peptides and proteins that I have observed in the crystal state form compact higher-order oligomers, such as hexamers, octamers, nonamers, and dodecamers.[15,16,41,42] The *N*-methylated macrocyclic β-sheet peptides are generally more twisted than the Hao-containing macrocyclic β-sheet peptides. This twisting appears to facilitate assembly through interactions between curved hydrophobic

surfaces, in addition to hydrogen bonding. The flat sandwich-like structures formed by the Hao-containing macrocyclic β-sheets resemble the laminated structures of amyloid fibrils, while the compact globular structures formed by the *N*-methylated macrocyclic β-sheets might offer a glimpse into the structures of amyloid oligomers.

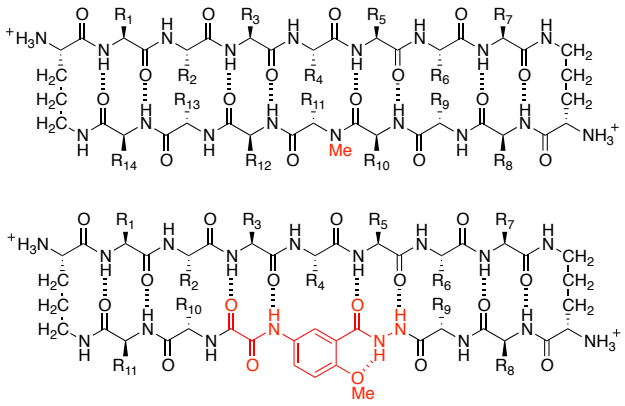

Figure 3.16. Chemical structures of *N*-methylated macrocyclic β-sheet peptides (top) and Hao-based macrocyclic β-sheet peptides (bottom).

Conclusion

The ^{1}H NMR, X-ray crystallographic, and molecular modeling studies of peptides $\mathbf{1}_{\mathbf{Arg}}$, $\mathbf{1}_{\mathbf{Cit}}$, and $\mathbf{2}_{\mathbf{Cit}}$ described above demonstrate the importance of hydrogen bonding and hydrophobic interactions in the oligomerization of IAPP-derived peptides. Peptide $\mathbf{1}_{\mathbf{Arg}}$ remains monomeric in aqueous solution, whereas peptides $\mathbf{1}_{\mathbf{Cit}}$ and $\mathbf{2}_{\mathbf{Cit}}$ assemble to form tetramers in aqueous solution and in the crystal state. The differences between peptides $\mathbf{1}_{\mathbf{Arg}}$ and $\mathbf{1}_{\mathbf{Cit}}$ suggest that charge-charge interactions can modulate oligomer formation.

Our laboratory has previously used NMR spectroscopy and X-ray crystallography as complimentary techniques to investigate the assembly of different macrocyclic β-sheet peptides derived from Aβ.[37,43] In these studies, the macrocyclic β-sheet peptides assembled to form tetramers both in solution and in the crystal, but the structure of the

tetramer formed in solution differed from the structure formed in the crystal. The findings of the current paper are significant because they demonstrate that macrocyclic β-sheet peptides can assemble to form the same structure in solution and in the crystal state. Furthermore, the tetramer described here might serve as a structural model for understanding important contacts within oligomers and fibrils formed by full-length IAPP.

References

(1) Chiti, F.; Dobson, C. M. *Annu. Rev. Biochem.* **2006**, *75*, 333-366.

(2) Knowles, T. P. J.; Vendruscolo, M.; Dobson, C. M. *Nat. Rev. Mol. Cell. Biol.* **2014**, *15*, 384-396.

(3) Nelson, R.; Sawaya, M. R.; Balbirnie, M.; Madsen, A. O.; Riekel, C.; Grothe, R.; Eisenberg, D. *Nature* **2005**, *435*, 773-778.

(4) Luca, S.; Yau, W. M.; Leapman, R.; Tycko, R. *Biochemistry* **2007**, *46*, 13505-13522.

(5) Wiltzius, J. J. W.; Sievers, S. A.; Sawaya, M. R.; Cascio, D.; Popov, D.; Riekel, C.; Eisenberg, D. *Protein Sci.* **2008**, *17*, 1467-1474.

(6) Lu, J. X.; Qiang, W.; Yau, W. M.; Schwieters, C. D.; Meredith, S. C.; Tycko, R. *Cell* **2013**, *154*, 1257-1268.

(7) Xiao, Y. L.; Ma, B. Y.; McElheny, D.; Parthasarathy, S.; Long, F.; Hoshi, M.; Nussinov, R.; Ishii, Y. *Nat. Struct. Mol. Biol.* **2015**, *22*, 499-505

.

(8) Lendel, C.; Bjerring, M.; Dubnovitsky, A.; Kelly, R. T.; Filippov, A.; Antzutkin, O. N.; Nielsen, N. C.; Hard, T. *Angew. Chem. Int. Ed.* **2014**, *53*, 12756-12760.

(9) Xiao, Y. L.; Ma, B. Y.; McElheny, D.; Parthasarathy, S.; Long, F.; Hoshi, M.; Nussinov, R.; Ishii, Y. *Nat. Struct. Mol. Biol.* **2015**, *22*, 499-505.

(10) Walti, M. A.; Ravotti, F.; Arai, H.; Glabe, C. G.; Wall, J. S.; Bockmann, A.; Guntert, P.; Meier, B. H.; Riek, R. *Proc. Natl. Acad. Sci. U.S.A.* **2016**, *113*, E4976-E4984.

(11) Colvin, M. T.; Silvers, R.; Ni, Q. Z.; Can, T. V.; Sergeyev, I.; Rosay, M.; Donovan, K. J.; Michael, B.; Wall, J.; Linse, S.; Griffin, R. G. *J. Am. Chem. Soc.* **2016**, *138*, 9663-9674.

(12) Sandberg, A.; Luheshi, L. M.; Sollvander, S.; de Barros, T. P.; Macao, B.; Knowles, T. P. J.; Biverstal, H.; Lendel, C.; Ekholm-Petterson, F.; Dubnovitsky, A.; Lannfelt, L.; Dobson, C. M.; Hard, T. *Proc. Natl. Acad. Sci. U.S.A.* **2010**, *107*, 15595-15600.

(13) Laganowsky, A.; Liu, C.; Sawaya, M. R.; Whitelegge, J. P.; Park, J.; Zhao, M. L.; Pensalfini, A.; Soriaga, A. B.; Landau, M.; Teng, P. K.; Cascio, D.; Glabe, C.; Eisenberg, D. *Science* **2012**, *335*, 1228-1231.

(14) Mirecka, E. A.; Shaykhalishahi, H.; Gauhar, A.; Akgul, S.; Lecher, J.; Willbold, D.; Stoldt, M.; Hoyer, W. *Angew. Chem. Int. Ed.* **2014**, *53*, 4227-4230.

(15) Spencer, R. K.; Kreutzer, A. G.; Salveson, P. J.; Li, H.; Nowick, J. S. *J. Am. Chem. Soc.* **2015**, *137*, 6304-6311.

(16) Salveson, P. J.; Spencer, R. K.; Nowick, J. S. *J. Am. Chem. Soc.* **2016**, *138*, 4458-4467.

(17) Kreutzer, A. G.; Hamza, I. L.; Spencer, R. K.; Nowick, J. S. *J. Am. Chem. Soc.* **2016**, *138*, 4634-4642.

(18) Janson, J.; Ashley, R. H.; Harrison, D.; McIntyre, S.; Butler, P. C. *Diabetes* **1999**, *48*, 491-498.

(19) Meier, J. J.; Kayed, R.; Lin, C. Y.; Gurlo, T.; Haataja, L.; Jayasinghe, S.; Langen, R.; Glabe, C. G.; Butler, P. C. *Am. J. Physiol. Endocrinol. Metab.* **2006**, *291*, E1317-E1324.

(20) Konarkowska, B.; Aitken, J. F.; Kistler, J.; Zhang, S. P.; Cooper, G. J. S. *Febs Journal* **2006**, *273*, 3614-3624.

(21) Westermark, P.; Andersson, A.; Westermark, G. T. *Physiol. Rev.* **2011**, *91*, 795-826.

(22) Bram, Y.; Frydman-Marom, A.; Yanai, I.; Gilead, S.; Shaltiel-Karyo, R.; Amdursky, N.; Gazit, E. *Sci. Rep.* **2014**, *4*.

(23) Mirecka, E. A.; Feuerstein, S.; Gremer, L.; Schroder, G. F.; Stoldt, M.; Willbold, D.; Hoyer, W. *Sci. Rep.* **2016**, *6*.

(24) Soriaga, A. B.; Sangwan, S.; Macdonald, R.; Sawaya, M. R.; Eisenberg, D. *J. Phys. Chem. B* **2016**, *120*, 5810-5816.

(25) Bedrood, S.; Li, Y. Y.; Isas, J. M.; Hegde, B. G.; Baxa, U.; Haworth, I. S.; Langen, R. *J. Biol. Chem.* **2012**, *287*, 5235-5241.

(26) Dupuis, N. F.; Wu, C.; Shea, J. E.; Bowers, M. T. *J. Am. Chem. Soc.* **2009**, *131*, 18283-18292.

(27) Dupuis, N. F.; Wu, C.; Shea, J. E.; Bowers, M. T. *J. Am. Chem. Soc.* **2011**, *133*, 7240-7243.

(28) Buchanan, L. E.; Dunkelberger, E. B.; Tran, H. Q.; Cheng, P. N.; Chiu, C. C.; Cao, P.; Raleigh, D. P.; de Pablo, J. J.; Nowick, J. S.; Zanni, M. T. *Proc. Natl. Acad. Sci. U.S.A.* **2013**, *110*, 19285-19290.

(29) Cheng, P. N.; Liu, C.; Zhao, M. L.; Eisenberg, D.; Nowick, J. S. *Nat. Chem.* **2012**, *4*, 927-933.

(30) Nowick, J. S.; Lam, K. S.; Khasanova, T. V.; Kemnitzer, W. E.; Maitra, S.; Mee, H. T.; Liu, R. W. *J. Am. Chem. Soc.* **2002**, *124*, 4972-4973.

(31) Nowick, J. S.; Brower, J. O. *J. Am. Chem. Soc.* **2003**, *125*, 876-877.

(32) Nowick, J. S.; Chung, D. M.; Maitra, K.; Maitra, S.; Stigers, K. D.; Sun, Y. *J. Am. Chem. Soc.* **2000**, *122*, 7654-7661.

(33) Truex, N. L.; Wang, Y. L.; Nowick, J. S. *J. Am. Chem. Soc.* **2016**, *138*, 13882-13890.

(34) Truex, N. L.; Nowick, J. S. *J. Am. Chem. Soc.* **2016**, *138*, 13891-13900.

(35) Wishart, D. S.; Sykes, B. D. *Methods Enzymol.* **1994**, *239*, 363-392.

(36) Khakshoor, O.; Demeler, B.; Nowick, J. S. *J. Am. Chem. Soc.* **2007**, *129*, 5558-5569.

(37) Pham, J. D.; Demeler, B.; Nowick, J. S. *J. Am. Chem. Soc.* **2014**, *136*, 5432-5442.

(38) Polson, A. *J. Phys. Colloid Chem.* **1950**, *54*, 649-652.

(39) Krotee, P.; Rodriguez, J. A.; Sawaya, M. R.; Cascio, D.; Reyes, F. E.; Shi, D.; Hattne, J.; Nannenga, B. L.; Oskarsson, M. E.; Philipp, S.; Griner, S.; Jiang, L.; Glabe, C. G.; Westermark, G. T.; Gonen, T.; Eisenberg, D. S. *Elife* **2017**, *6*.

(40) Liu, C.; Zhao, M. L.; Jiang, L.; Cheng, P. N.; Park, J.; Sawaya, M. R.; Pensalfini, A.; Gou, D. W.; Berk, A. J.; Glabe, C. G.; Nowick, J.; Eisenberg, D. *Proc. Natl. Acad. Sci. U.S.A.* **2012**, *109*, 20913-20918.

(41) Spencer, R. K.; Li, H.; Nowick, J. S. *J. Am. Chem. Soc.* **2014**.

(42) Yoo, S.; Kreutzer, A. G.; Truex, N. L.; Nowick, J. S. *Chem Sci* **2016**, *7*, 6946-6951.

(43) Pham, J. D.; Chim, N.; Goulding, C. W.; Nowick, J. S. *J. Am. Chem. Soc.* **2013**, *135*, 12460-12467.

Material and Methods

Synthesis of Macrocyclic β-Sheet Peptides. Synthesis and purification of the macrocyclic β-sheet peptides were performed as previously described.[1] The peptides were purified by reverse-phase HPLC and the pure fractions were lyophilized to give 22 mg of peptide $\mathbf{1}_{\mathbf{Arg}}$, 37 mg of peptide $\mathbf{1}_{\mathbf{Cit}}$, and 19 mg of $\mathbf{2}_{\mathbf{Cit}}$. Based on resin loading, the yields are 9%, 14%, and 7%, respectively.

Macrocyclic β-Sheet peptide $\mathbf{1}_{\mathbf{Arg}}$: HRMS (ESI-TOF) *m/z*: $[M + H]^+$ Calcd for $C_{83}H_{139}N_{24}O_{18}$ 1760.0699; Found 1760.0710.

Macrocyclic β-Sheet peptide $\mathbf{1}_{\mathbf{Cit}}$: HRMS (ESI-TOF) *m/z*: $[M + Na]^+$ Calcd for $C_{83}H_{137}N_{23}O_{19}Na$ 1783.0359; Found 1783.0337.

Macrocyclic β-Sheet peptide $\mathbf{2}_{\mathbf{Cit}}$: HRMS (ESI-TOF) *m/z*: $[M + H]^+$ Calcd for $C_{82}H_{132}N_{23}O_{19}Br$ 1822.9331; Found 1822.9333.

NMR Spectroscopy of the Macrocyclic β-Sheet Peptides

Sample Preparation. NMR spectroscopy of the macrocyclic β-sheet peptides was performed in D_2O (D, 99.96%; Cambridge Isotope Laboratories, Inc.) with 50 mM CD_3COOD (D, 99.5%; Cambridge Isotope Laboratories, Inc.) and 50 mM CD_3COONa (D, 99%; Cambridge Isotope Laboratories, Inc.). The solutions were prepared by dissolving a weighed portion of the peptide in the appropriate volume of solvent. The molecular weights of the peptides were calculated as the TFA salts with all amino groups assumed to be protonated ($\mathbf{1}_{\mathbf{Arg}}$, M.W. 2330.24, $\mathbf{1}_{\mathbf{Cit}}$, M.W. 2331.24, and $\mathbf{2}_{\mathbf{Cit}}$, M.W. 2394.10). Each solution contained 4,4-dimethyl-4-silapentane-1-ammonium trifluoroacetate (DSA) as an internal standard for referencing chemical shifts.[2] The

solutions were allowed to stand for 24 h to allow complete hydrogen to deuterium exchange of the amide NH protons.

^{1}H NMR, TOCSY, ROESY, and NOESY Data Collection. NMR spectra were recorded on a Bruker 500 MHz spectrometer with a TCI cryoprobe. TOCSY spectra were recorded with 2048 points in the f_2 dimension and 512 increments in the f_1 dimension with a 150-ms spin-lock mixing time. TOCSY spectra were recorded with 2048 points in the f_2 dimension and 512 increments in the f_1 dimension with either a 100- or 150-ms spin-lock mixing time. NOESY spectra were recorded with 2048 points in the f_2 dimension and 512 increments in the f_1 dimension with a 150-ms mixing time.

^{1}H NMR, TOCSY, and NOESY Data Processing. NMR spectra were processed with BrukerXwinNMR software. Automatic baseline correction was applied in both dimensions after phasing the spectra. TOCSY spectra were Fourier transformed to a final matrix size of 4096 x 1024 real points using a Qsine weighting function and forward linear prediction. NOESY and ROESY spectra were Fourier transformed to a final matrix size of 4096 x 2048 real points using a Qsine weighting functionand forward linear prediction.

Diffusion-Ordered Spectroscopy (DOSY) Experiments. DOSY experiments were performed on a Bruker 500 MHz spectrometer equipped with a TCI cryoprobe, with a diffusion delay (Δ) of 75-ms and a diffusion gradient length (δ) of 2.5-ms. Sixteen sets of FIDs were recorded with the gradient strength incremented from 5%–95% using a linear ramp. The combined FIDs were Fourier transformed in Bruker's TopSpin^{TM} software to give a pseudo-2D spectrum. After phasing and performing baseline correction, each pseudo-2D spectrum was processed with logarithmic scaling on the Y-axis. The Y-axis

was calibrated to the diffusion coefficient of the residual HOD peak in D_2O (1.9×10^{-9} m^2/s at 298 K).[3] The diffusion coefficients of the peptides were read and converted from logarithmic values to linear values.

Crystallization of Peptide $\mathbf{2_{Cit}}$

The procedures in this section follow closely to those our laboratory has previously published.[4] Initial crystallization conditions for peptide $\mathbf{2_{Cit}}$ were determined using the hanging-drop vapor-diffusion method. Crystallization conditions were screened using three crystallization kits in a 96-well plate format (Hampton Index, PEG/Ion, and Crystal Screen). Three 150 nL hanging drops that differed in the ratio of peptide to well solution were made per condition in each 96-well plate for a total of 864 experiments. Hanging drops were made by combining an appropriate volume of peptide $\mathbf{2_{Cit}}$ (10 mg/mL in deionized water) with an appropriate volume of well solution to create three 150-nL hanging drops with 1:1, 1:2, and 2:1 peptide:well solution. The hanging drops were made using a TTP LabTech Mosquito nanodisperse instrument. Crystals of peptide $\mathbf{2_{Cit}}$ grew in ~48 h in a solution of 0.1 M sodium citrate at pH 5.0, 20% (v/v) isopropanol, and 18% PEG 4000.

Crystallization conditions for peptide $\mathbf{2_{Cit}}$ were optimized using a 4x6 matrix Hampton VDX 24-well plate. The sodium citrate pH was varied in each row in increments of 0.5 pH units (4.0, 4.5, 5.0, and 5.5) and the isopropanol concentration in each column in increments of 2% (26%, 24%, 22%, 20%, 18%, 16%). The first well in the 4x6 matrix was prepared by combined 100 μL of 1 M sodium citrate at pH 4.0, 260 μL of isopropanol, 360 μL of 50% (w/v) PEG 4000, and 280 μL of deionized water. The

other wells were prepared in analogous fashion, by combining 100 μL of sodium citrate of varying pH, 360 μL of 50% (w/v) PEG 4000, isopropanol in varying amounts, and deionized water for a total volume of 1 mL in each well.

Three hanging-drops were prepared per borosilicate glass slide by combining a solution of peptide $\mathbf{2}_{\mathbf{Cit}}$ (10 mg/mL in deionized water) and the well solution in the following amounts: 1 μL:1 μL, 2 μL:1 μL, and 1 μL:2 μL. Slides were inverted and pressed firmly against the silicone grease surrounding each well. Crystals of peptide $\mathbf{2}_{\mathbf{Cit}}$ suitable for X-ray diffraction grew in ~3 days. Crystallization conditions were further optimized using smaller variations in sodium citrate pH (in increments of 0.2 pH units) and isopropanol concentrations (in increments of 1%). Crystals were harvested with a nylon loop attached to a copper or steel pin and flash frozen in liquid nitrogen prior to data collection. The optimized crystallization conditions for peptide $\mathbf{2}_{\mathbf{Cit}}$ are summarized in the supplementary information.

Diffraction data for peptide $\mathbf{2}_{\mathbf{Cit}}$ were collected at the Stanford Synchrotron Radiation Lightsource (SSRL) with a synchrotron source at 0.92-Å wavelength. Diffraction data were scaled and merged using XDS.[5] Coordinates for the anomalous signal were determined by HySS in the Phenix software suite 1.10.1.[6] The electron density map was generated in Phaser using the coordinates of the bromine anomalous signal. Molecular manipulation of the model was performed with Coot. Coordinates were refined with phenix.refine.

Molecular Modeling of the Macrocyclic β-Sheet Peptides

Molecular models of the tetramers of peptides $\mathbf{1}_{\mathbf{Arg}}$ and $\mathbf{1}_{\mathbf{Cit}}$ were generated from the X-ray crystallographic structure of the homologous peptide $\mathbf{2}_{\mathbf{Cit}}$ (PDB: 5UHR). I

modeled the tetramer formed by peptides $\mathbf{1}_{\mathbf{Cit}}$ by mutating the (2-bromoallyl)glycine residue to isoleucine and the side chain torsion angles were adjusted to match the resulting NOE. I modeled a tetramer of peptide $\mathbf{1}_{\mathbf{Arg}}$ in a similar fashion, mutating both the (2-bromoallyl)glycine and the citrulline residues. The coordinates were exported from PyMOL and the file was imported into MacroModel with the Maestro user interface. Atom types and bond orders were edited as needed to correct errors in bond type and charge. Minimization was performed with the MMFFs force field and GB/SA water solvation.

References

(1) Truex, N. L.; Wang, Y. L.; Nowick, J. S. *J. Am. Chem. Soc.* **2016**, *138*, 13882-13890.

(2) Nowick, J. S.; Khakshoor, O.; Hashemzadeh, M.; Brower, J. O. *Org Lett.* **2003**, *5*, 3511-3513.

(3) Longsworth, L. G. *J. Phys. Chem.* **1960**, *64*, 1914-1917.

(4) Spencer, R. K.; Kreutzer, A. G.; Salveson, P. J.; Li, H.; Nowick, J. S. *J. Am. Chem. Soc.* **2015**, *137*, 6304-6311.

(5) Kabsch, W. *Acta Crystallogr., Sect. D: Biol. Crystallogr.* **2010**, *66*, 125-132.

(6) Adams, P. D.; Afonine, P. V.; Bunkoczi, G.; Chen, V. B.; Davis, I. W.; Echols, N.; Headd, J. J.; Hung, L. W.; Kapral, G. J.; Grosse-Kunstleve, R. W.; McCoy, A. J.; Moriarty, N. W.; Oeffner, R.; Read, R. J.; Richardson, D. C.; Richardson, J. S.; Terwilliger, T. C.; Zwart, P. H. *Acta Crystallogr., Sect. D: Biol. Crystallogr.* **2010**, *66*, 213-221.

RP-HPLC of Macrocyclic β-Sheet **1_{Arg}**

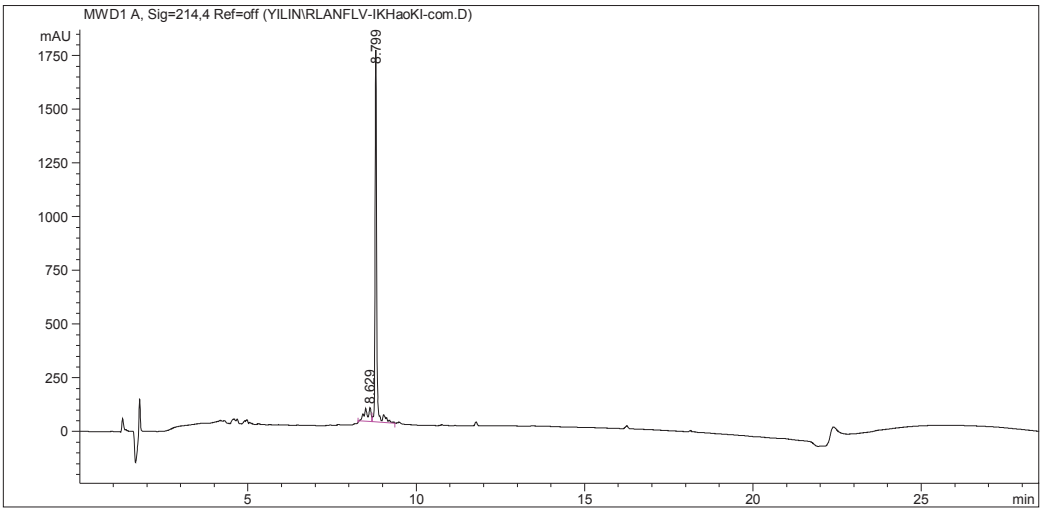

Peak #	RetTime [min]	Type	Width [min]	Area mAU *s	Height [mAU]	Area %
1	8.629	MF	0.1768	685.6629	64.6265	10.0330
2	8.799	FM	0.0584	6148.4335	1756.0099	89.9670

column: Aeris XB-C18 2.6µ
dimensions: 150 mm x 4.6 mm
mobile phase: A: H_2O, 0.1% TFA
B: CH_3CN, 0.1% TFA
gradient: A/B (95:5) to (0:100) in 20 min
flow rate: 1.0 mL/min
detection: VWD, wavelength = 214 nm
temperature: 298 K

MS (ESI) of Macrocyclic β-Sheet **1_{Arg}**

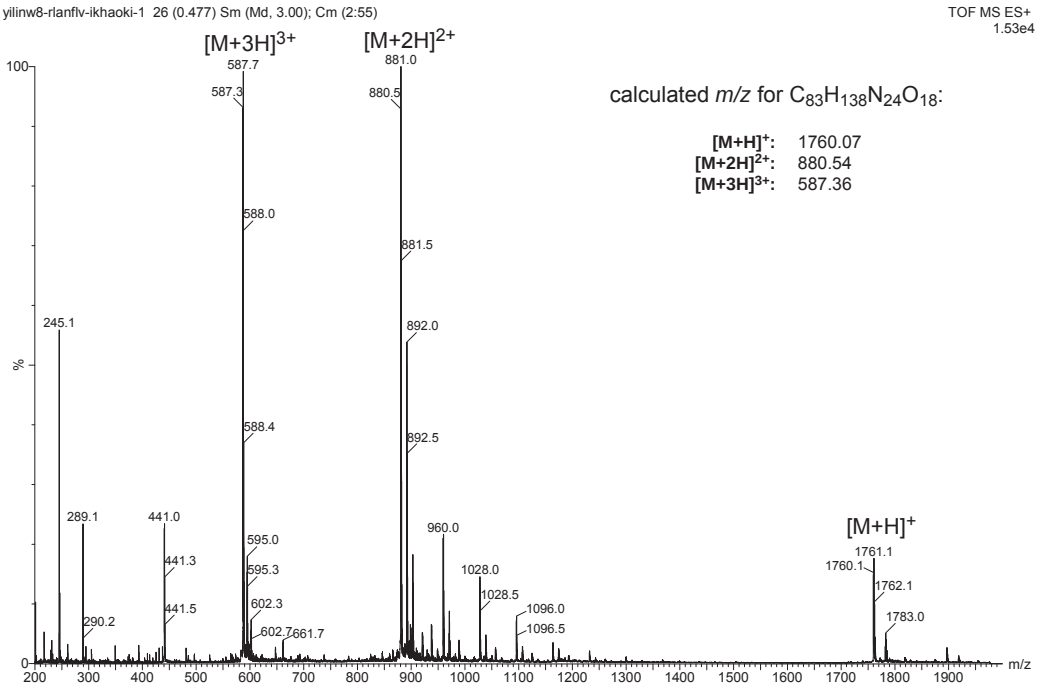

calculated *m/z* for $C_{83}H_{138}N_{24}O_{18}$:

$[M+H]^+$: 1760.07
$[M+2H]^{2+}$: 880.54
$[M+3H]^{3+}$: 587.36

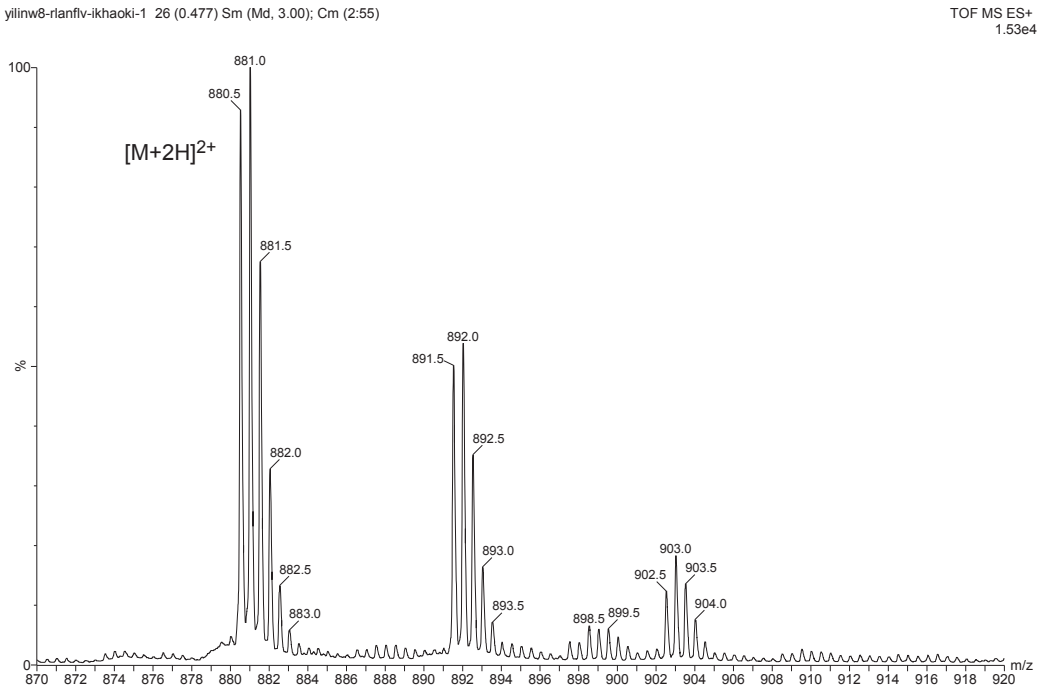
yilinw8-rlanflv-ikhaoki-1 26 (0.477) Sm (Md, 3.00); Cm (2:55)
TOF MS ES+
1.53e4
[M+2H]2+
881.0
880.5
881.5
882.0
882.5
883.0
892.0
891.5
892.5
893.0
893.5
898.5
899.5
902.5
903.0
903.5
904.0
100
%
0
m/z
870 872 874 876 878 880 882 884 886 888 890 892 894 896 898 900 902 904 906 908 910 912 914 916 918 920

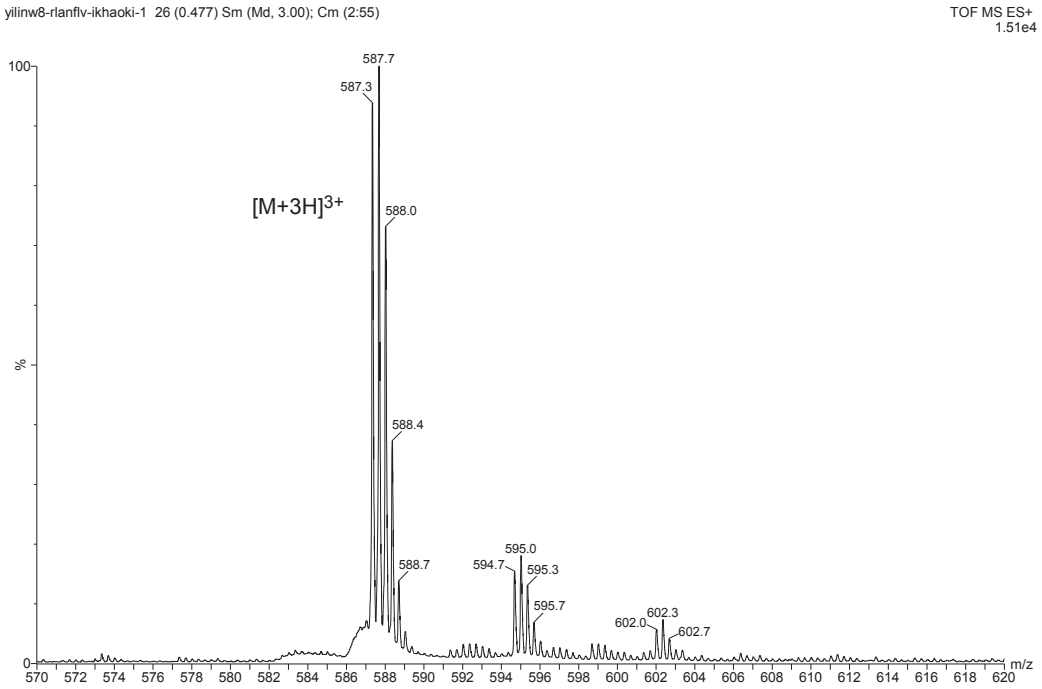
yilinw8-rlanflv-ikhaoki-1 26 (0.477) Sm (Md, 3.00); Cm (2:55)
TOF MS ES+
1.51e4
[M+3H]3+
587.7
587.3
588.0
588.4
588.7
594.7
595.0
595.3
595.7
602.0
602.3
602.7
100
%
0
m/z
570 572 574 576 578 580 582 584 586 588 590 592 594 596 598 600 602 604 606 608 610 612 614 616 618 620

^{1}H NMR of macrocyclic β-sheet peptide **1$_{Arg}$**, 4 mM in 100 mM deuterioacetate buffer in D_2O at 500 MHz and 298 K

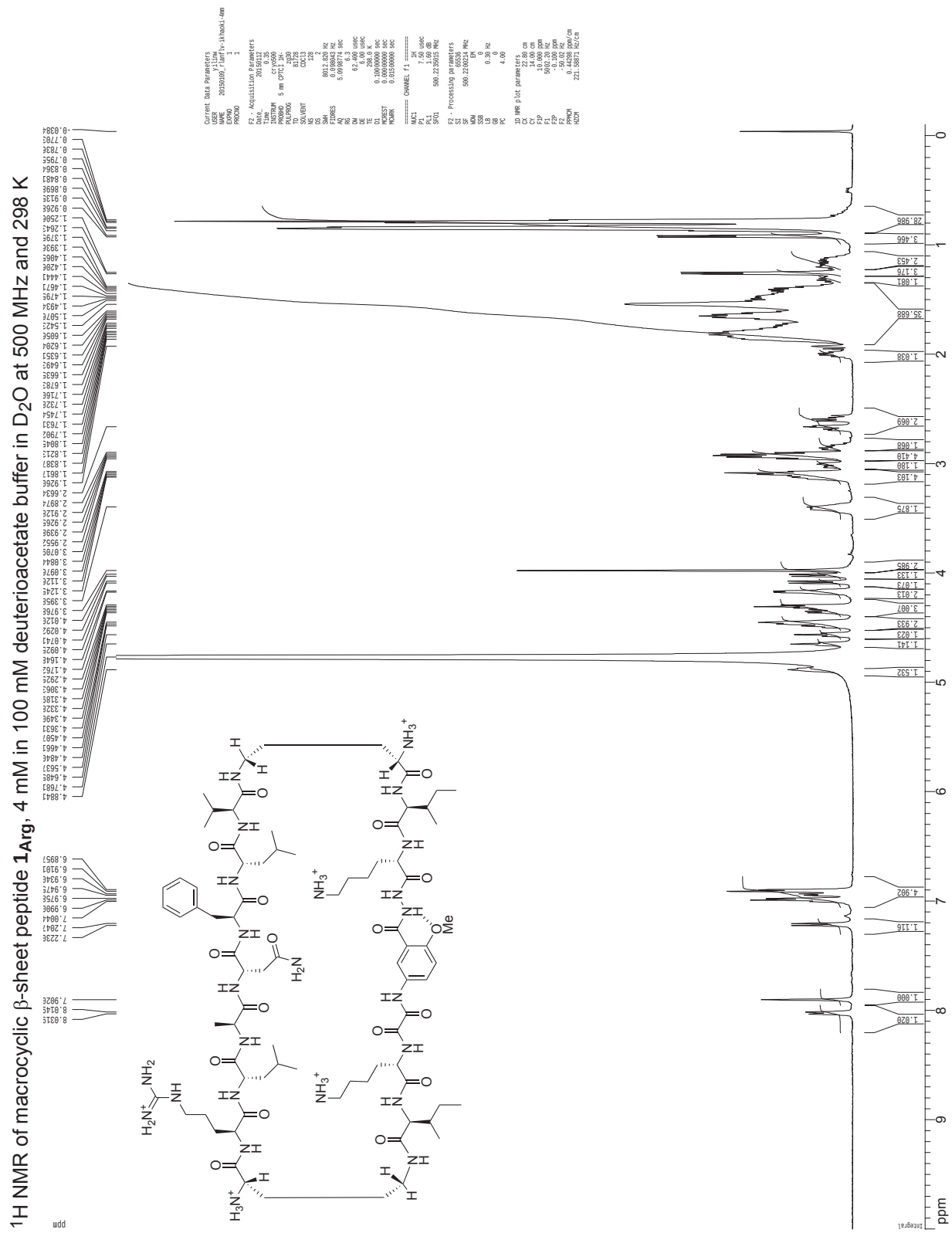

^{1}H NMR of macrocyclic β-sheet peptide **1$_{Arg}$**, 4 mM in 100 mM deuterioacetate buffer in D_2O at 500 MHz and 298 K

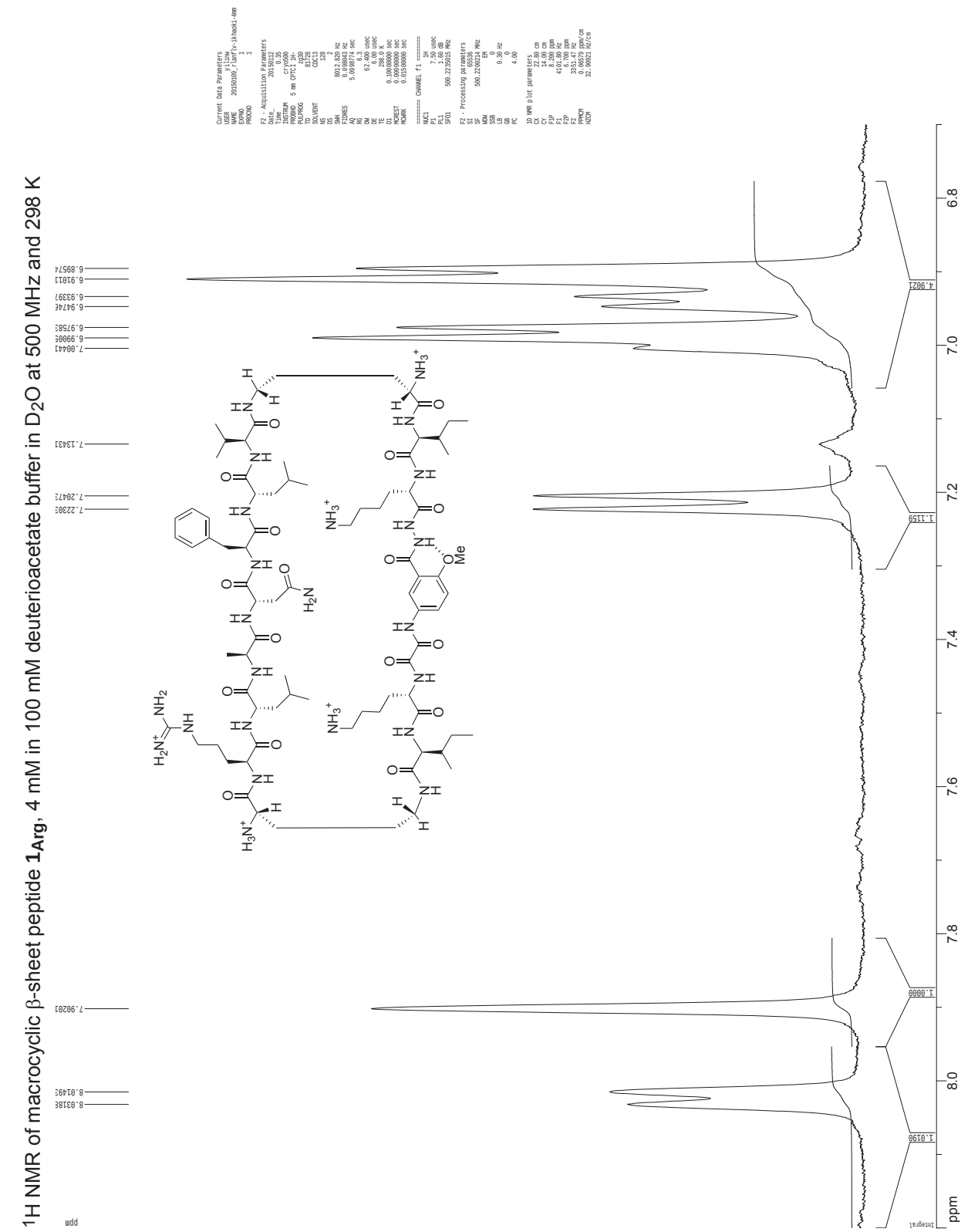

^{1}H NMR of macrocyclic β-sheet peptide **1$_{Arg}$**, 4 mM in 100 mM deuterioacetate buffer in D_2O at 500 MHz and 298 K

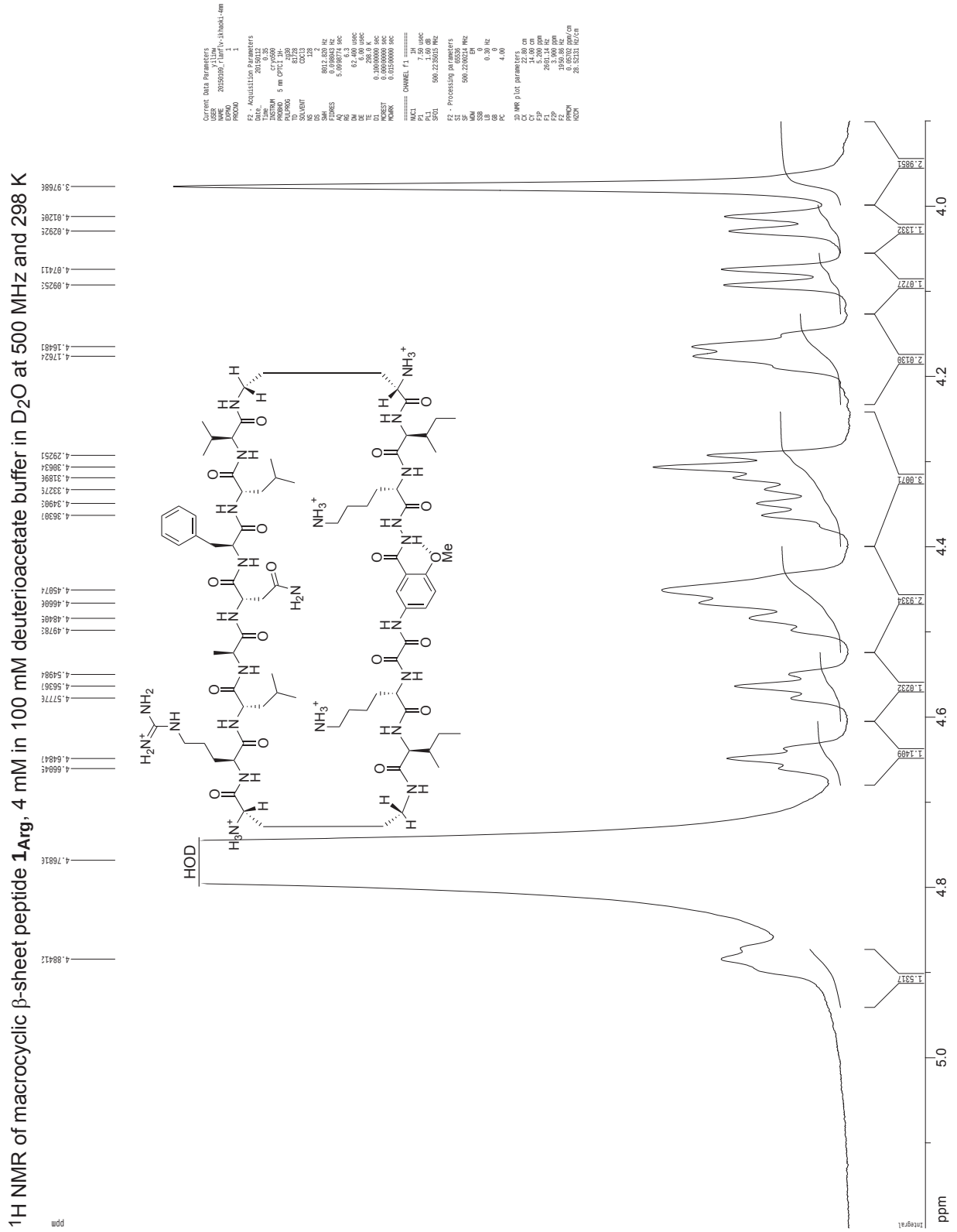

^{1}H NMR of macrocyclic β-sheet peptide **1$_{Arg}$**, 4 mM in 100 mM deuterioacetate buffer in D_2O at 500 MHz and 298 K

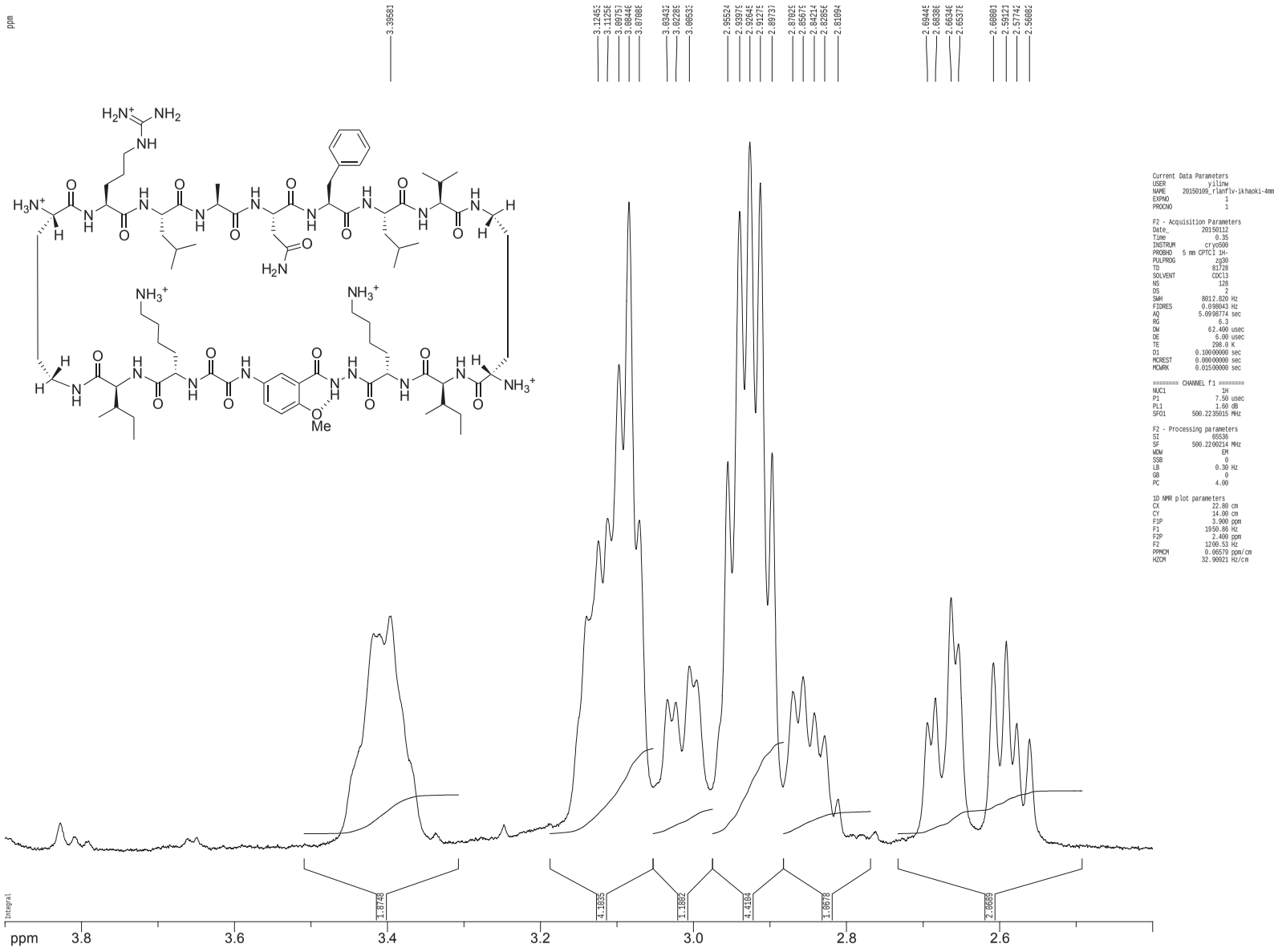

^{1}H NMR of macrocyclic β-sheet peptide **1$_{Arg}$**, 4 mM in 100 mM deuterioacetate buffer in D_2O at 500 MHz and 298 K

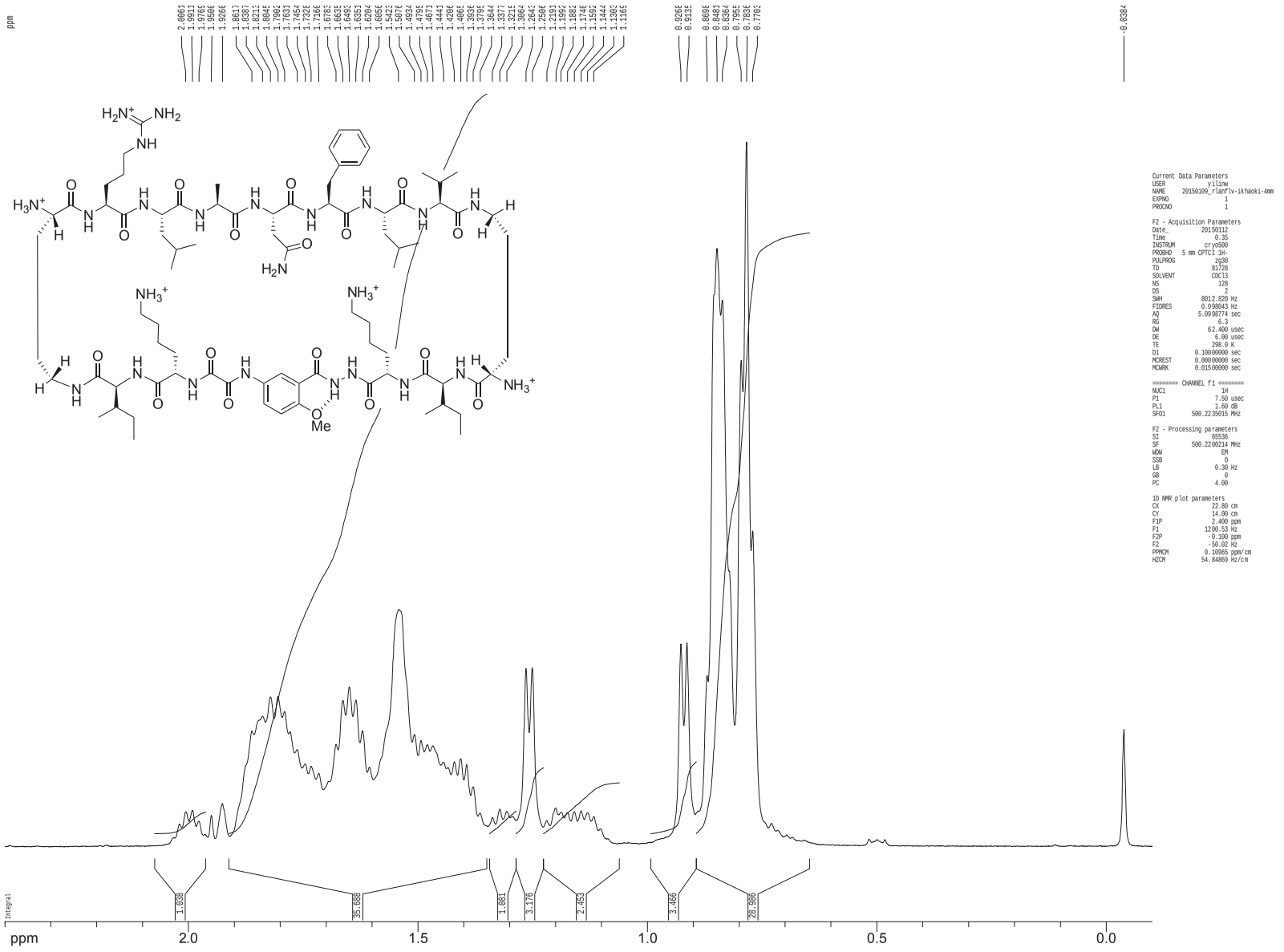

Current Data Parameters
USER yilinw
NAME 20150109_rlanflv-ikhaoki-4mm
EXPNO 1
PROCNO 1

F2 - Acquisition Parameters
Date_ 20150112
Time 0.35
INSTRUM cryo500
PROBHD 5 mm CPTCI 1H-
PULPROG zg30
TD 81728
SOLVENT CDCl3
NS 128
DS 2
SWH 8012.820 Hz
FIDRES 0.098043 Hz
AQ 5.0898774 sec
RG 6.3
DW 62.400 usec
DE 6.00 usec
TE 298.0 K
D1 0.10000000 sec
MCREST 0.00000000 sec
MCWRK 0.01500000 sec

======== CHANNEL f1 ========
NUC1 1H
P1 7.50 usec
PL1 1.60 dB
SFO1 500.2235015 MHz

F2 - Processing parameters
SI 65536
SF 500.2200214 MHz
WDW EM
SSB 0
LB 0.30 Hz
GB 0
PC 4.00

1D NMR plot parameters
CY 22.80 cm
CY 14.00 cm
F1P 2.400 ppm
F1 1200.53 Hz
F2P -0.100 ppm
F2 -50.02 Hz
PPMCM 0.10965 ppm/cm
HZCM 54.84869 Hz/cm

^{1}H NMR 2D TOCSY of macrocyclic β-sheet peptide **$\mathbf{1_{Arg}}$** with 150-ms spin-lock mixing time
4 mM in 100 mM deuterioacetate buffer in D_2O at 500 MHz and 298 K

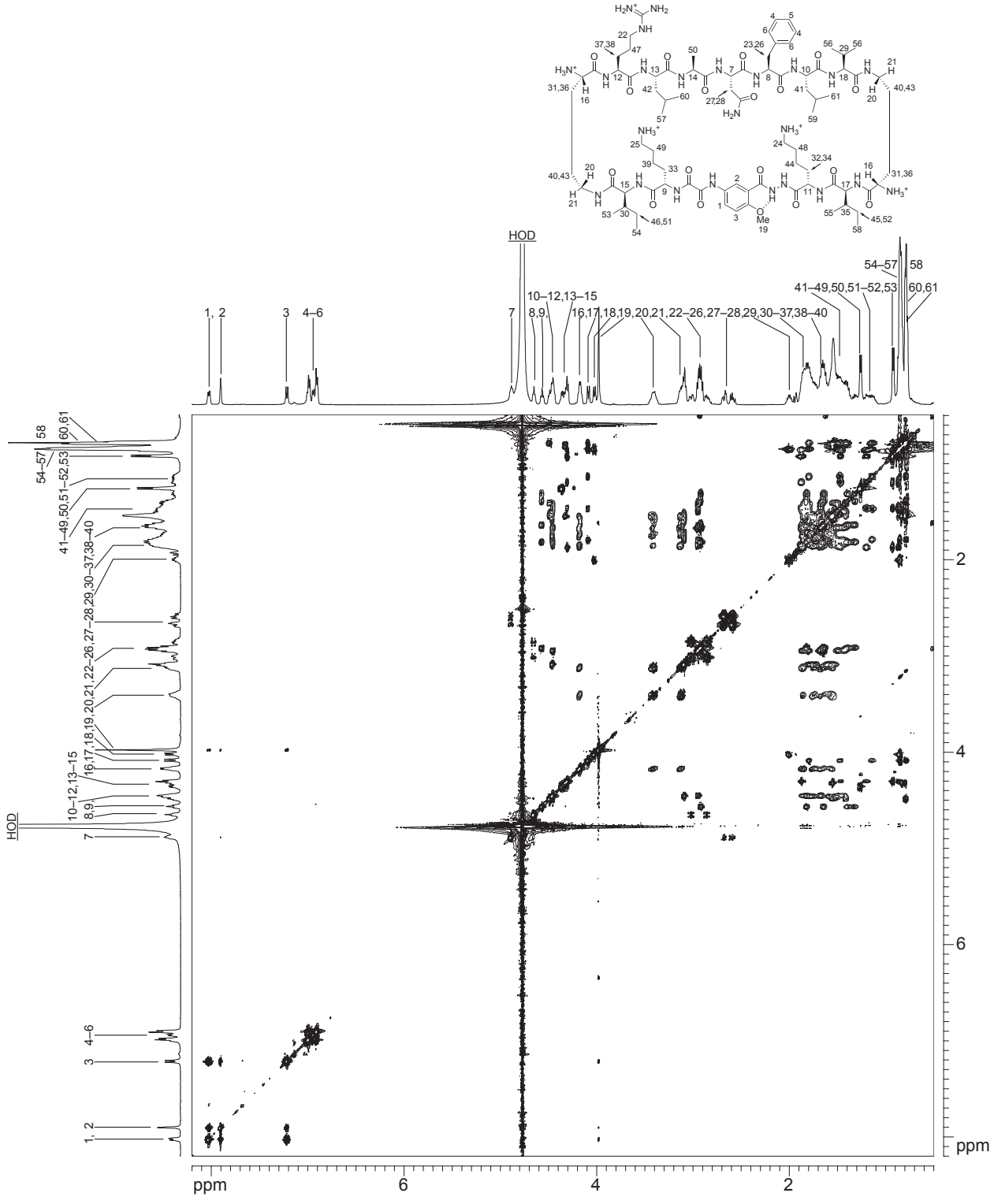

^{1}H NMR 2D TOCSY of macrocyclic β-sheet peptide **1_{Arg}** with 150-ms spin-lock mixing time
4 mM in 100 mM deuterioacetate buffer in D_2O at 500 MHz and 298 K

^{1}H NMR 2D ROESY of macrocyclic β-sheet peptide **1_{Arg}** with 150-ms spin-lock mixing time
4 mM in 100 mM deuterioacetate buffer in D_2O at 500 MHz and 298 K

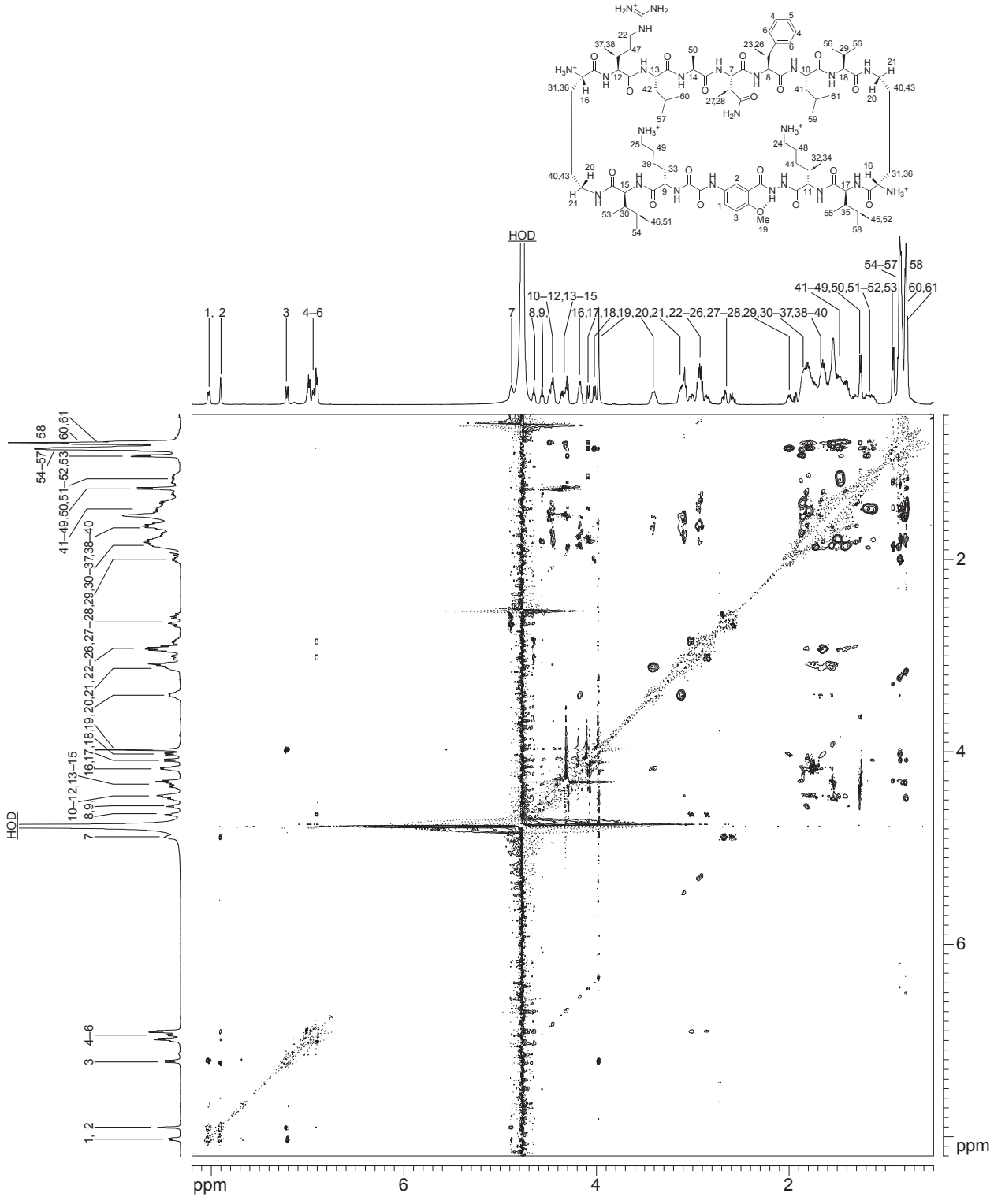

^{1}H NMR 2D ROESY of macrocyclic β-sheet peptide **1_{Arg}** with 150-ms spin-lock mixing time
4 mM in 100 mM deuterioacetate buffer in D_2O at 500 MHz and 298 K

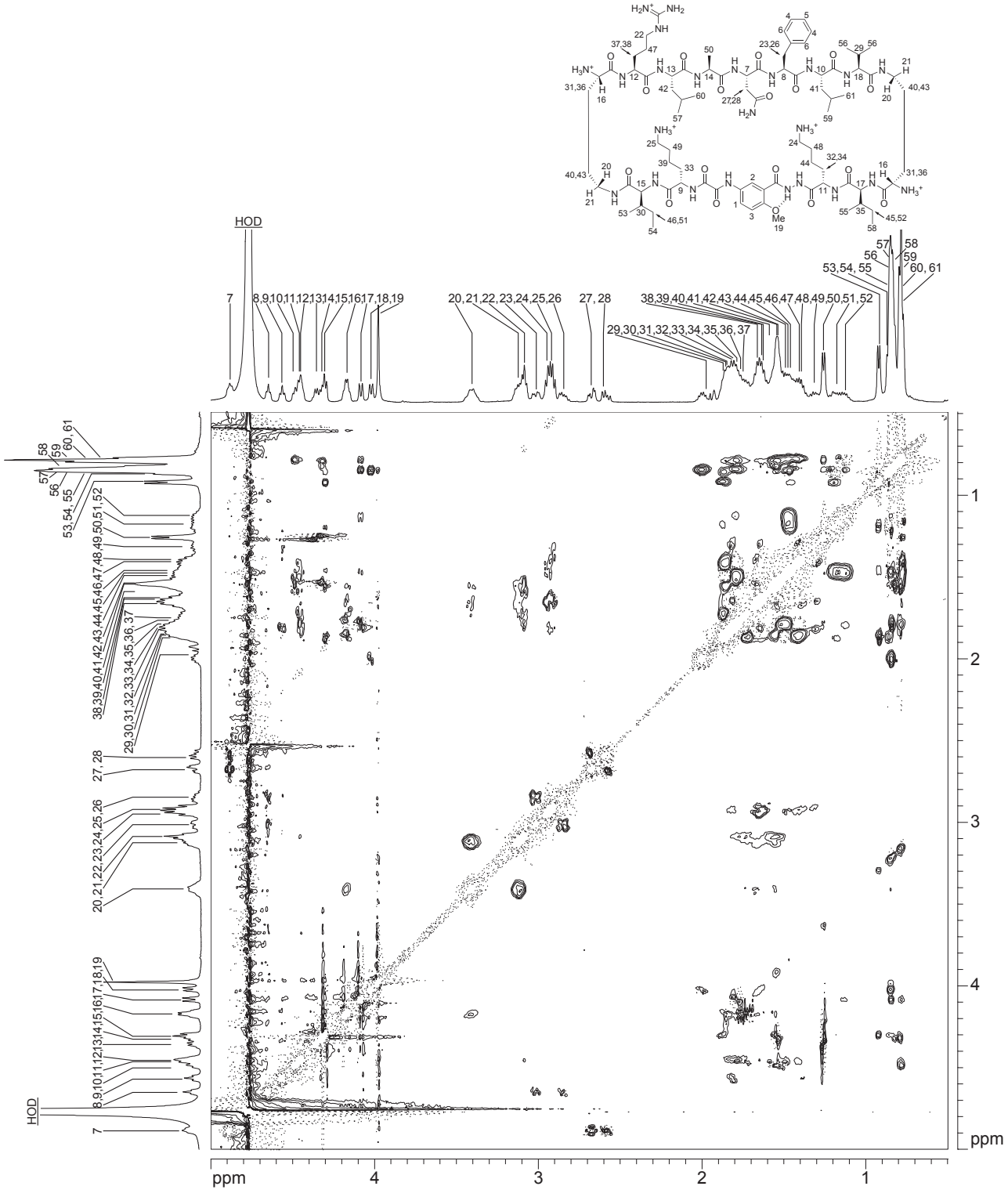

^{1}H NMR DOSY of macrocyclic β-sheet peptide **1$_{Arg}$** at 500 MHz and 298 K
4 mM in 100 mM deuterioacetate buffer in D_2O

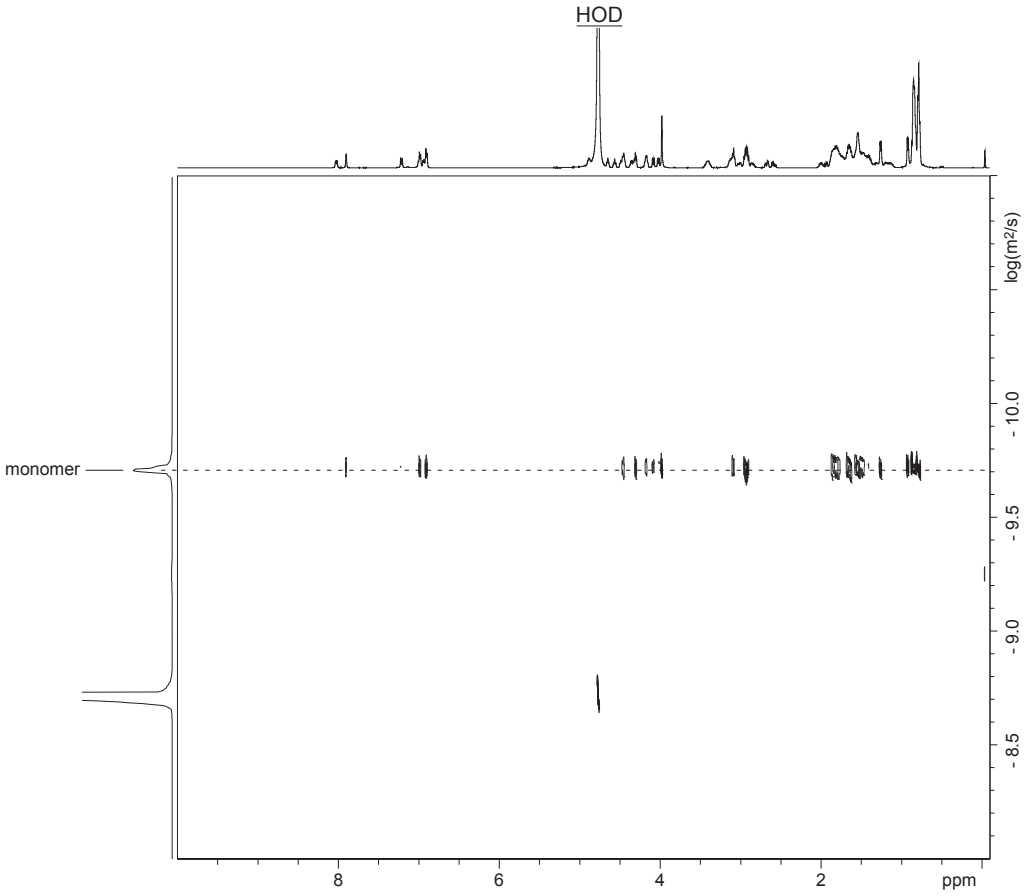

Calculations for macrocyclic β-sheet peptide **1$_{Arg}$** at 4 mM

D_{HOD} = 19.0 x 10^{-10} m^2/s [a]
log (D_{HOD}) = -8.721

$D_{monomer}$: log(D) = -9.708; D = $10^{-9.708}$ = 19.6 ± 0.6 x 10^{-11} m^2/s

[a]Longsworth, L. G. *J. Phys. Chem.* **1960**, *64*, 1914−1917.

RP-HPLC of Macrocyclic β-Sheet **1_{Cit}**

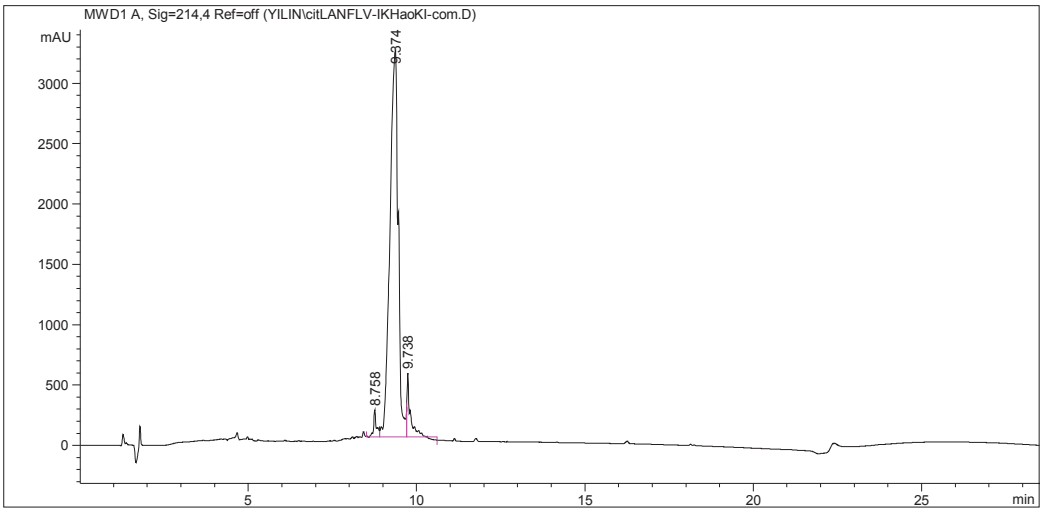

Peak #	RetTime [min]	Type	Width [min]	Area mAU *s	Height [mAU]	Area %
1	8.758	MF	0.0983	1323.3335	224.3247	2.2091
2	9.374	FM	0.2858	5.4981e4	3206.0356	91.7819
3	9.738	FM	0.1130	3599.7199	530.8340	6.0090

column:	Aeris XB-C18 2.6µ
dimensions:	150 mm x 4.6 mm
mobile phase:	A: H_2O, 0.1% TFA B: CH_3CN, 0.1% TFA
gradient:	A/B (95:5) to (0:100) in 20 min
flow rate:	1.0 mL/min
detection:	VWD, wavelength = 214 nm
temperature:	298 K

MS (ESI) of Macrocyclic β-Sheet **1_{Cit}**

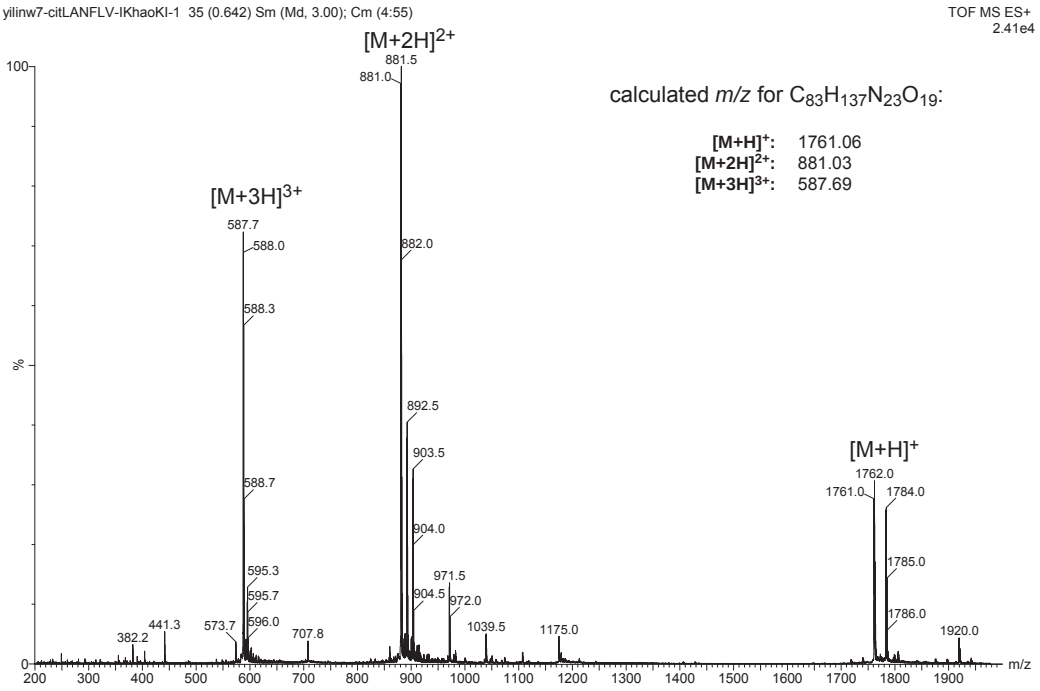

calculated *m/z* for $C_{83}H_{137}N_{23}O_{19}$:

$[M+H]^+$:	1761.06
$[M+2H]^{2+}$:	881.03
$[M+3H]^{3+}$:	587.69

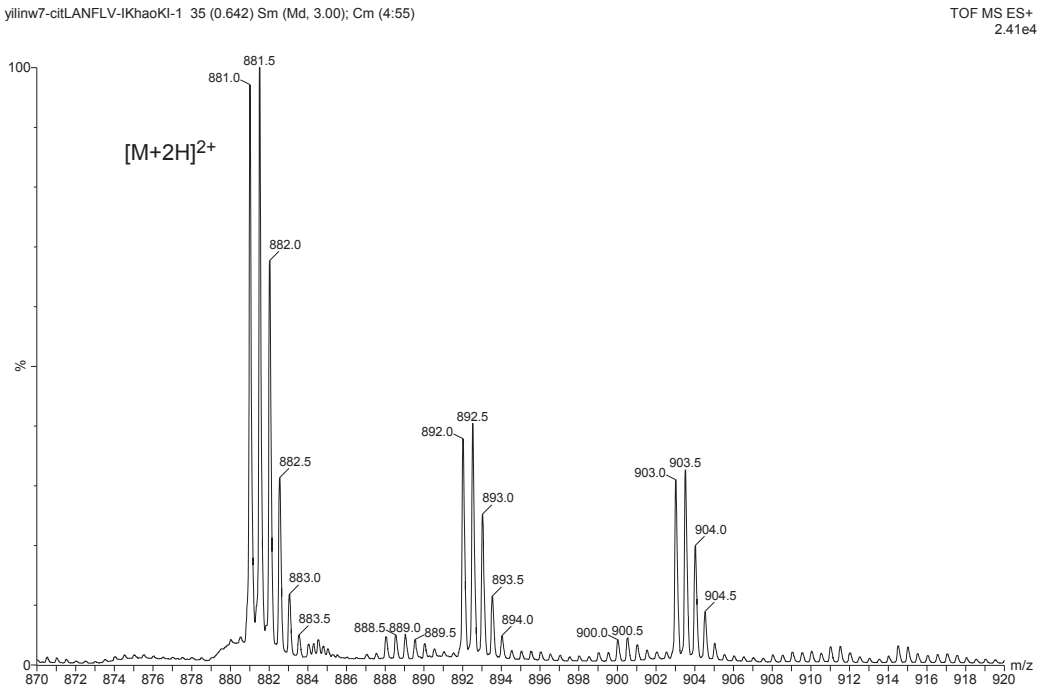
yilinw7-citLANFLV-IKhaoKI-1 35 (0.642) Sm (Md, 3.00); Cm (4:55)
TOF MS ES+
2.41e4
[M+2H]2+
881.5
881.0
882.0
882.5
883.0
883.5
888.5
889.0
889.5
892.5
892.0
893.0
893.5
894.0
900.0
900.5
903.0
903.5
904.0
904.5
%
m/z

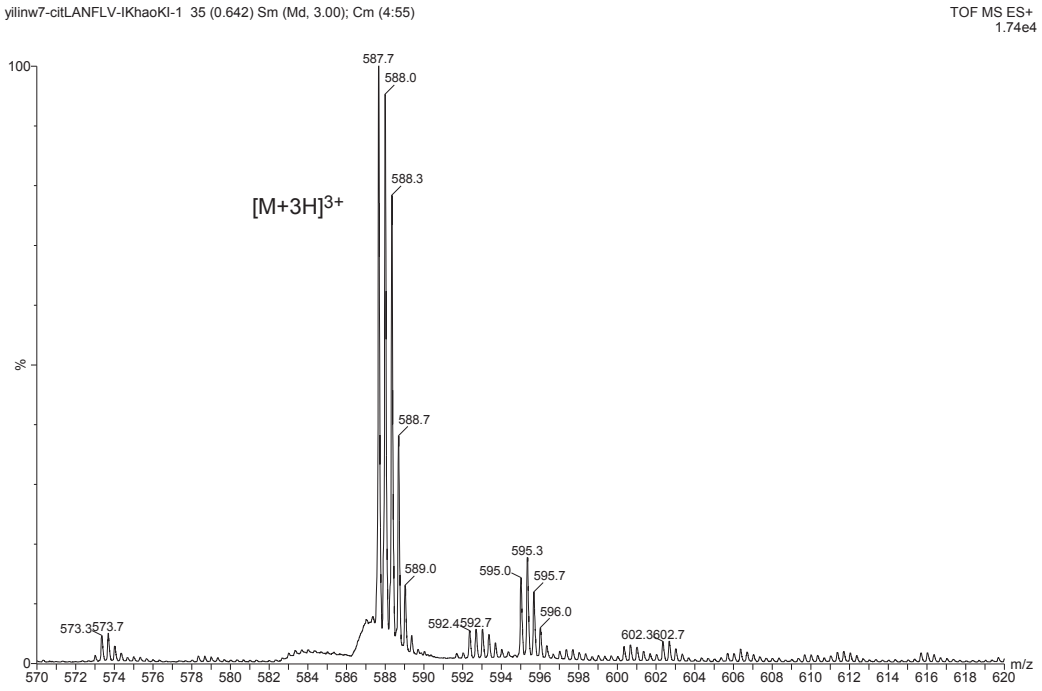
yilinw7-citLANFLV-IKhaoKI-1 35 (0.642) Sm (Md, 3.00); Cm (4:55)
TOF MS ES+
1.74e4
[M+3H]3+
587.7
588.0
588.3
588.7
589.0
573.3
573.7
592.4
592.7
595.0
595.3
595.7
596.0
602.3
602.7
%
m/z

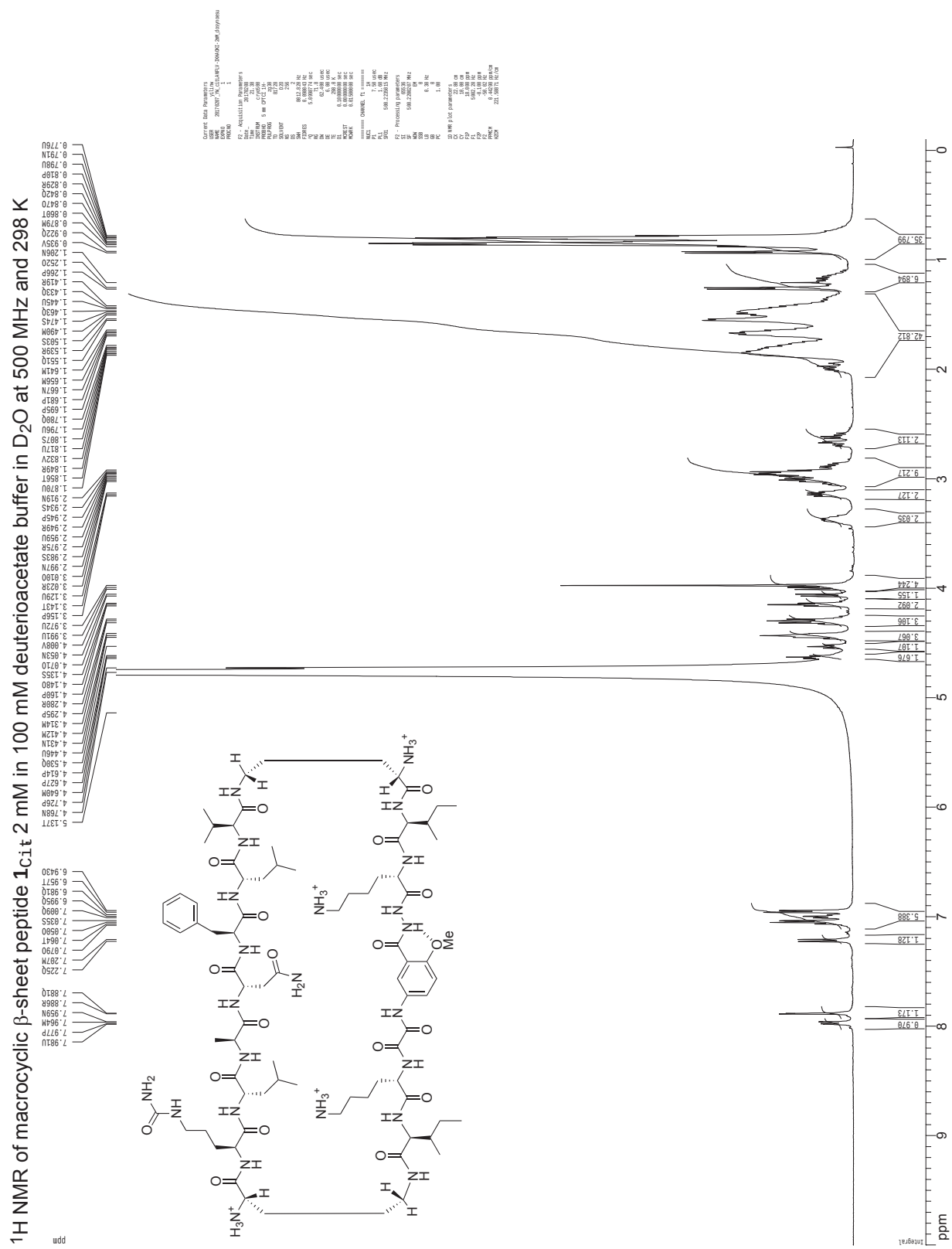
1H NMR of macrocyclic β-sheet peptide 1cit 2 mM in 100 mM deuterioacetate buffer in D2O at 500 MHz and 298 K
ppm

^{1}H NMR of macrocyclic β-sheet peptide **1$_{Cit}$**, 2 mM in 100 mM deuterioacetate buffer in D_2O at 500 MHz and 298 K

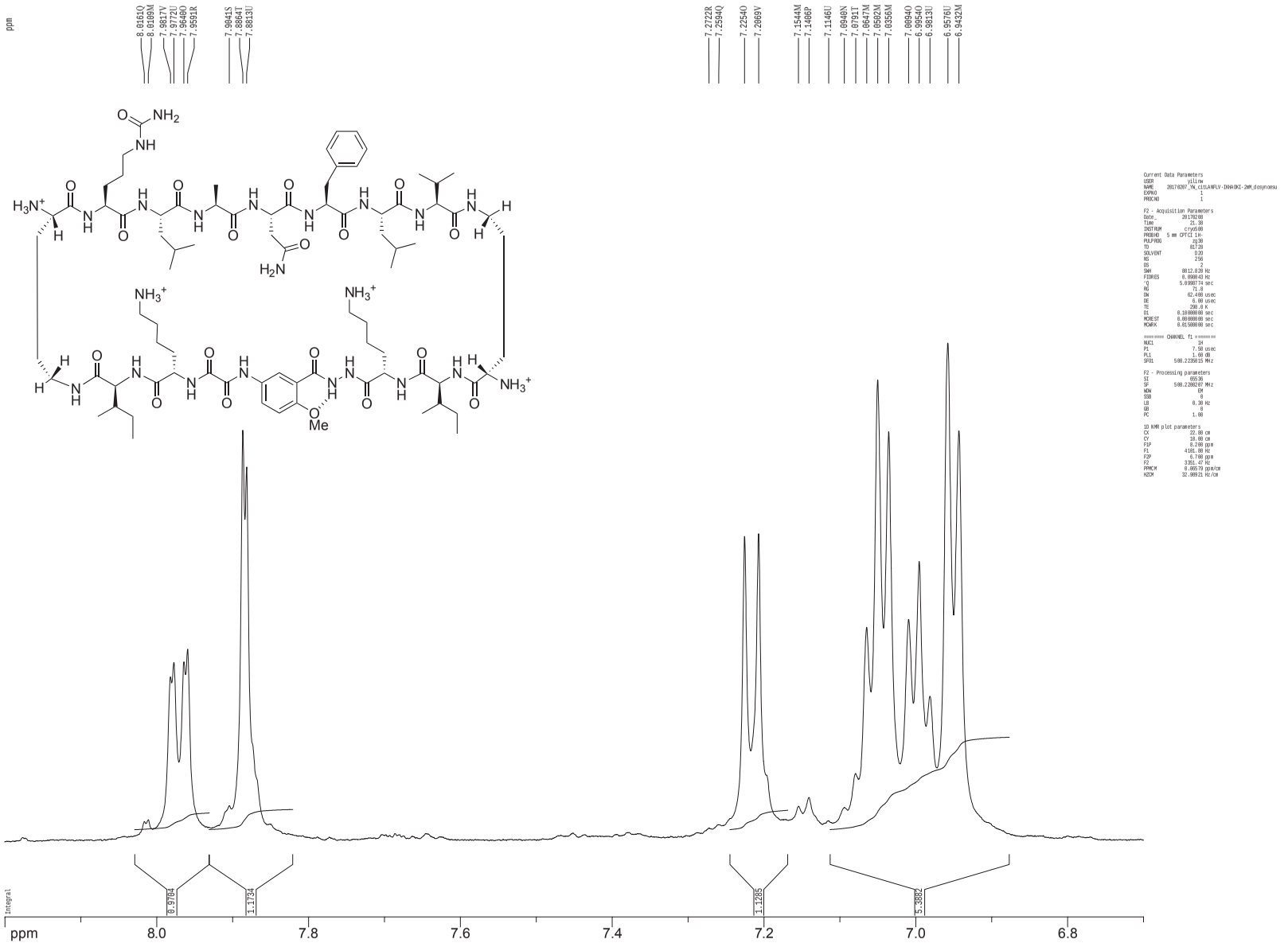

^{1}H NMR of macrocyclic β-sheet peptide **1$_{Cit}$**, 2 mM in 100 mM deuterioacetate buffer in D_2O at 500 MHz and 298 K

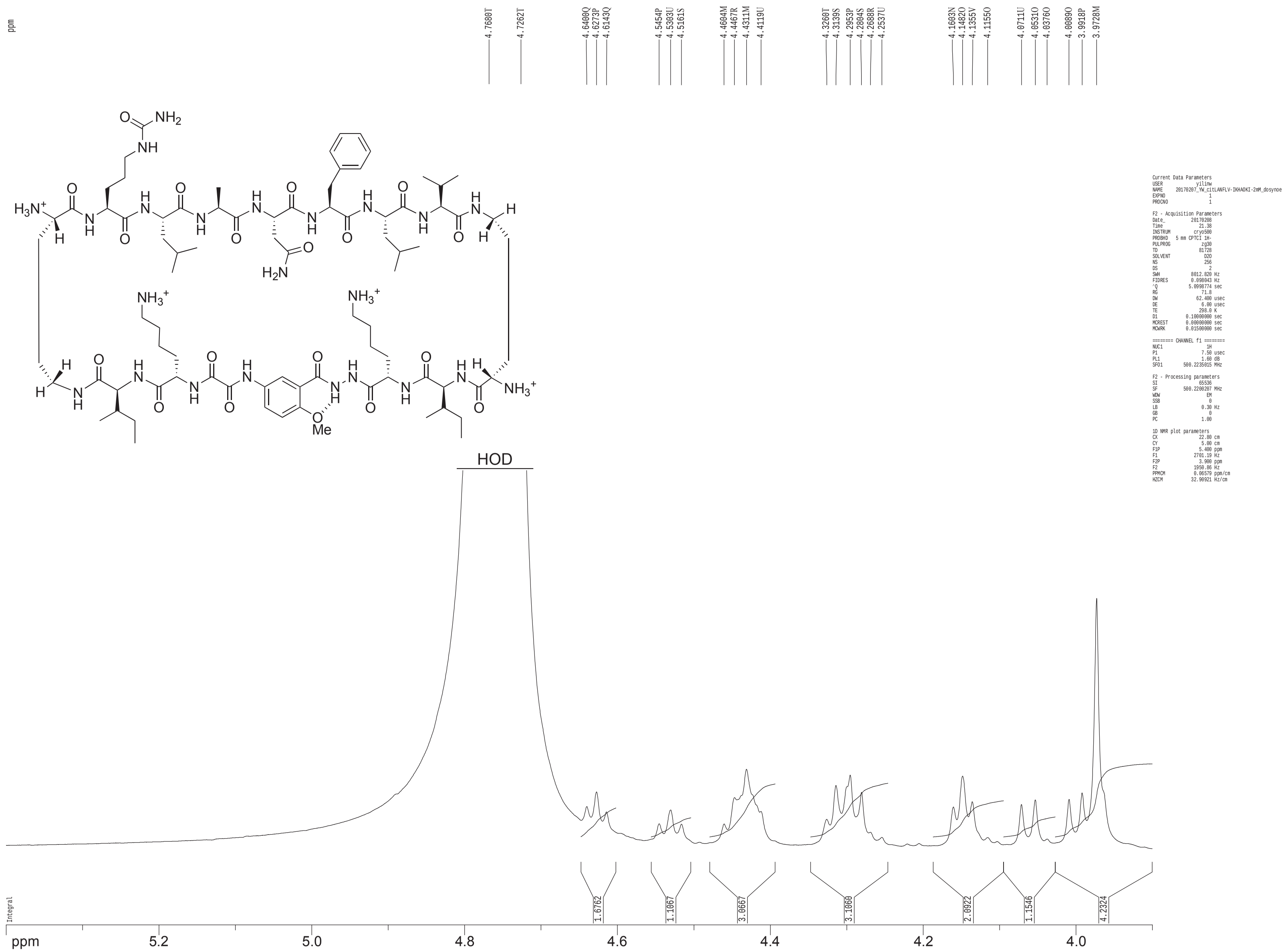

^{1}H NMR of macrocyclic β-sheet peptide **1$_{Cit}$**, 2 mM in 100 mM deuterioacetate buffer in D_2O at 500 MHz and 298 K

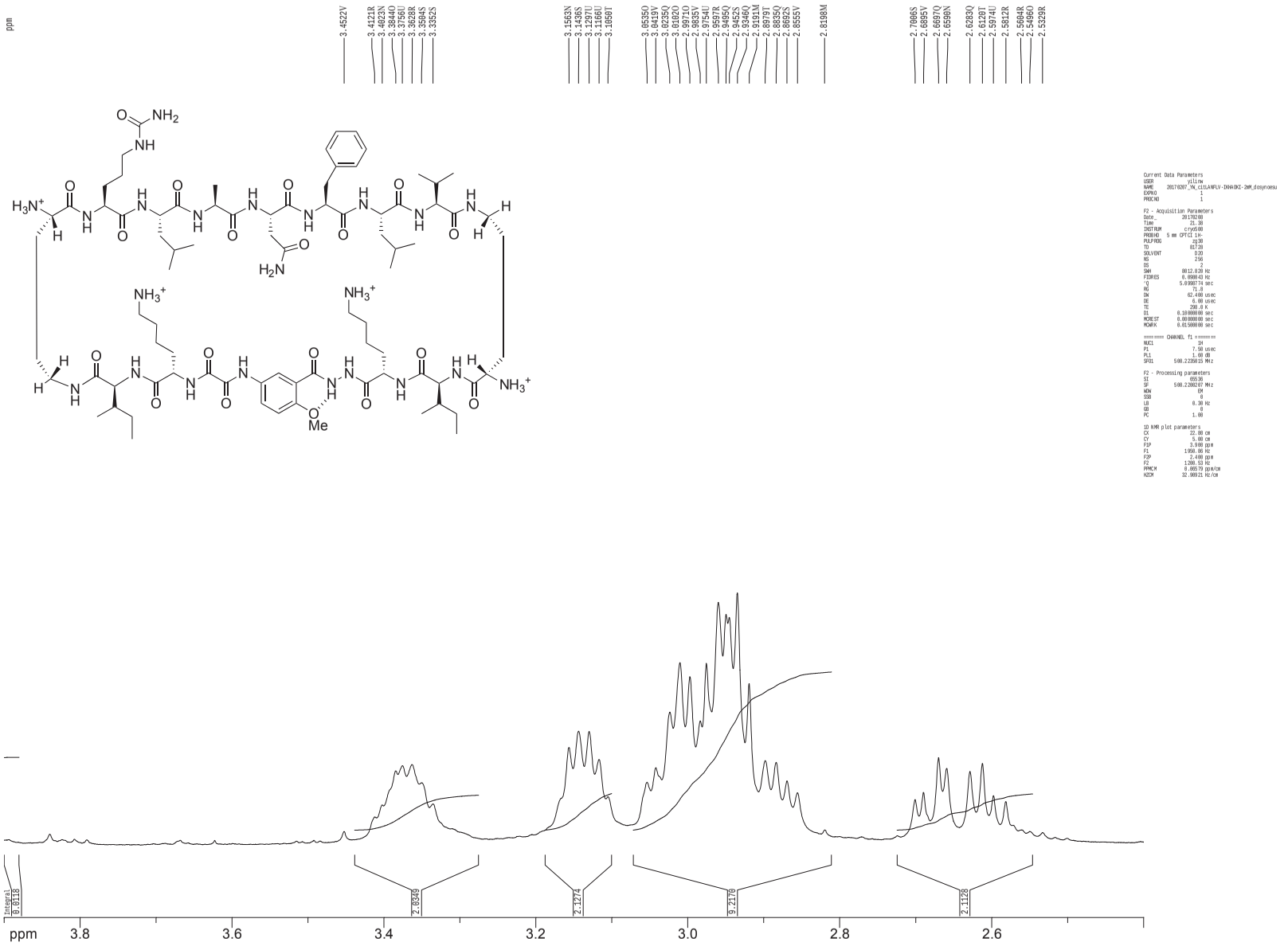

[1]H NMR of macrocyclic β-sheet peptide **1$_{Cit}$**, 2 mM in 100 mM deuterioacetate buffer in D_2O at 500 MHz and 298 K

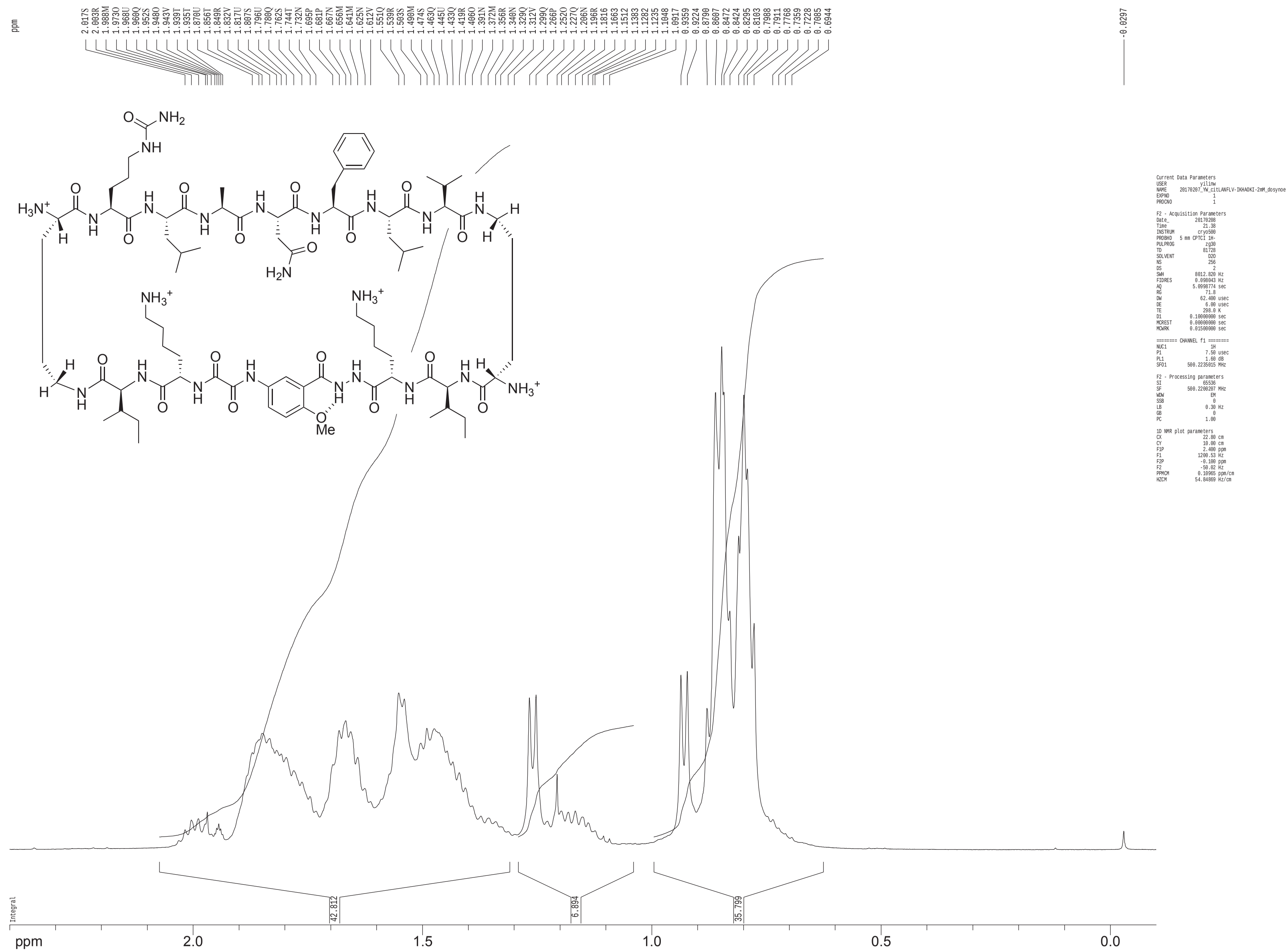

^{1}H NMR 2D TOCSY of macrocyclic β-sheet peptide **1_{Cit}** with 150-ms spin-lock mixing time
2 mM in 100 mM deuterioacetate buffer in D_2O at 500 MHz and 298 K

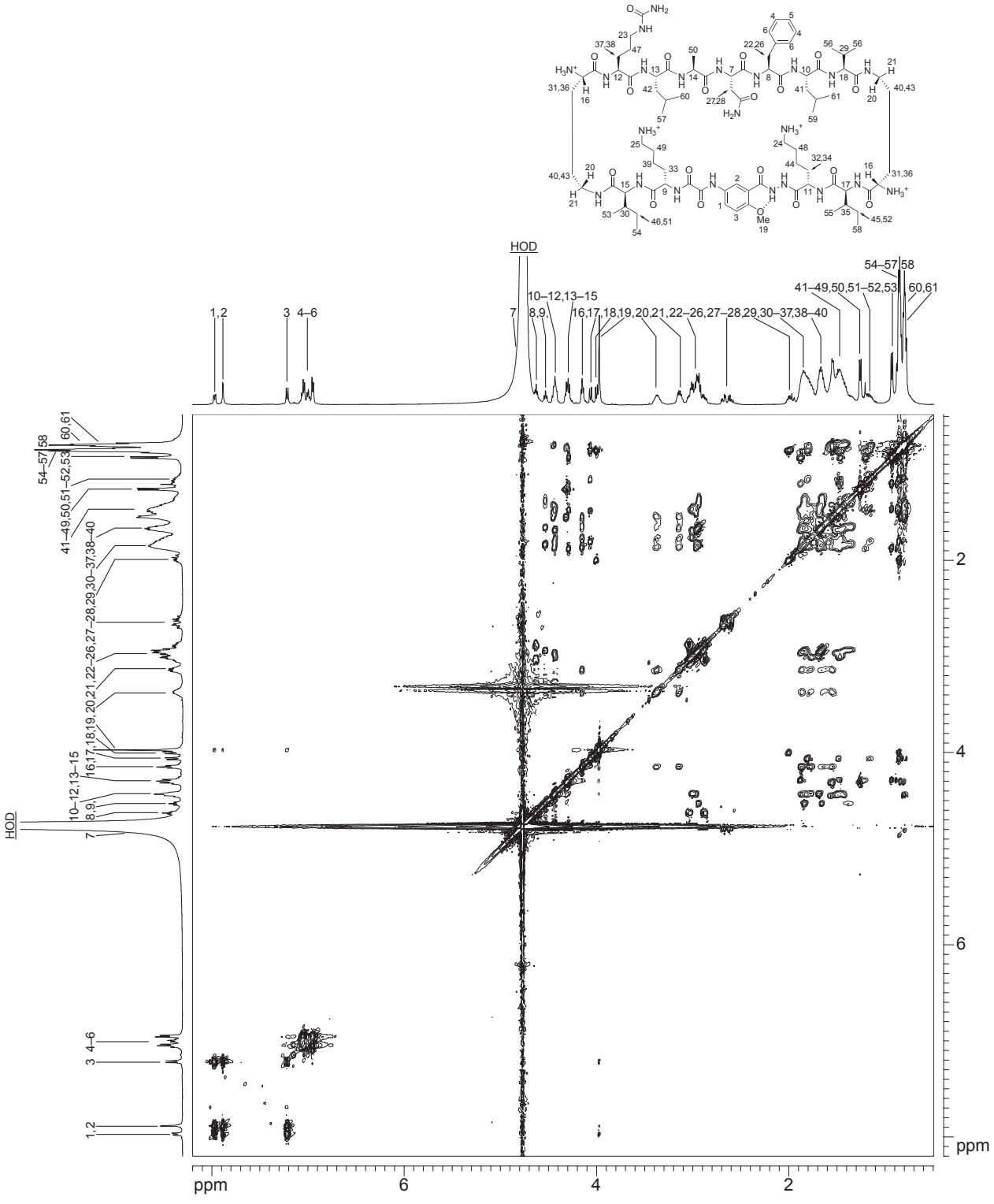

^{1}H NMR 2D TOCSY of macrocyclic β-sheet peptide **$\mathbf{1_{Cit}}$** with 150-ms spin-lock mixing time
2 mM in 100 mM deuterioacetate buffer in D_2O at 500 MHz and 298 K

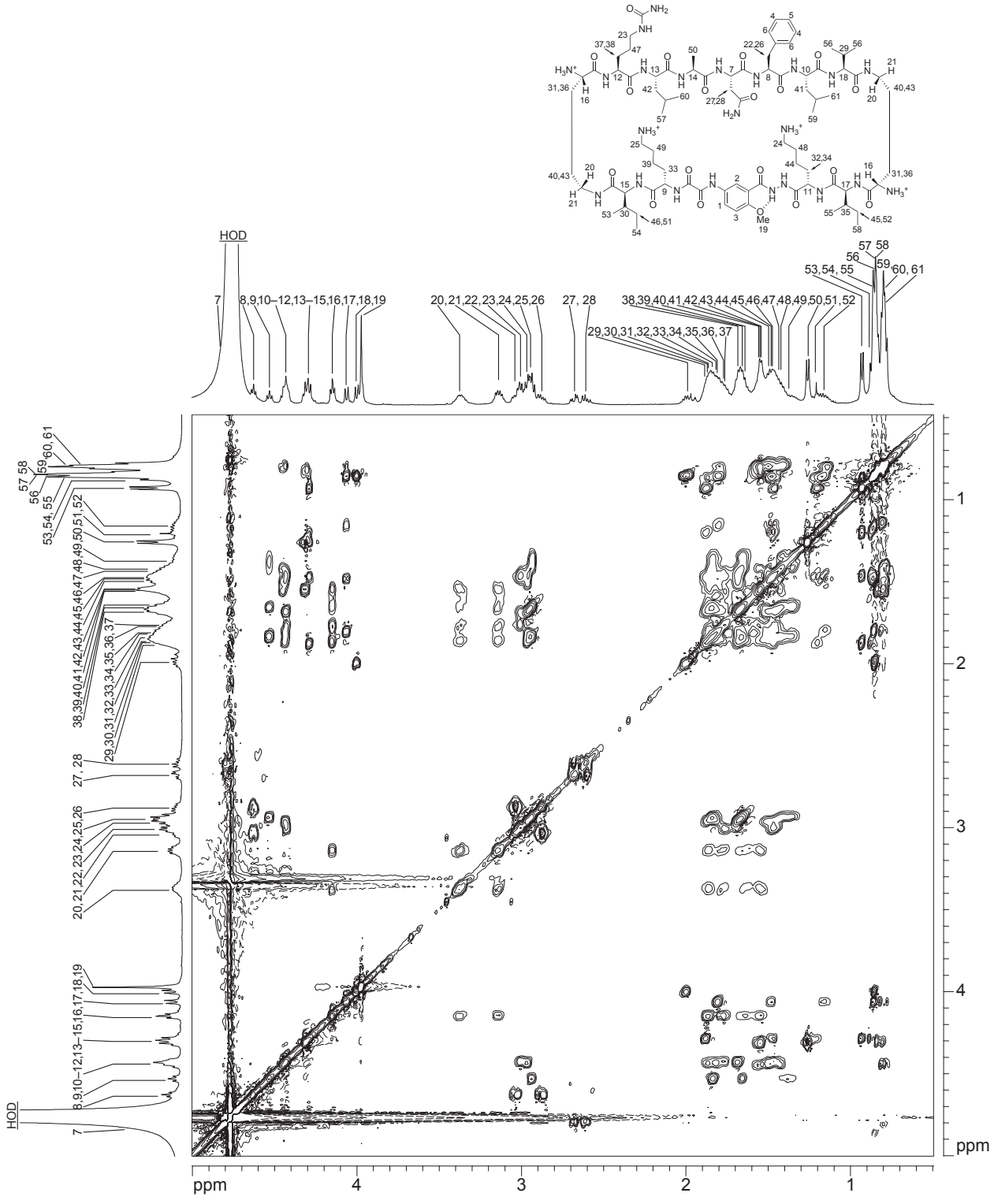

^{1}H NMR 2D ROESY of macrocyclic β-sheet peptide **1_{Cit}** with 100-ms spin-lock mixing time
2 mM in 100 mM deuterioacetate buffer in D_2O at 500 MHz and 298 K

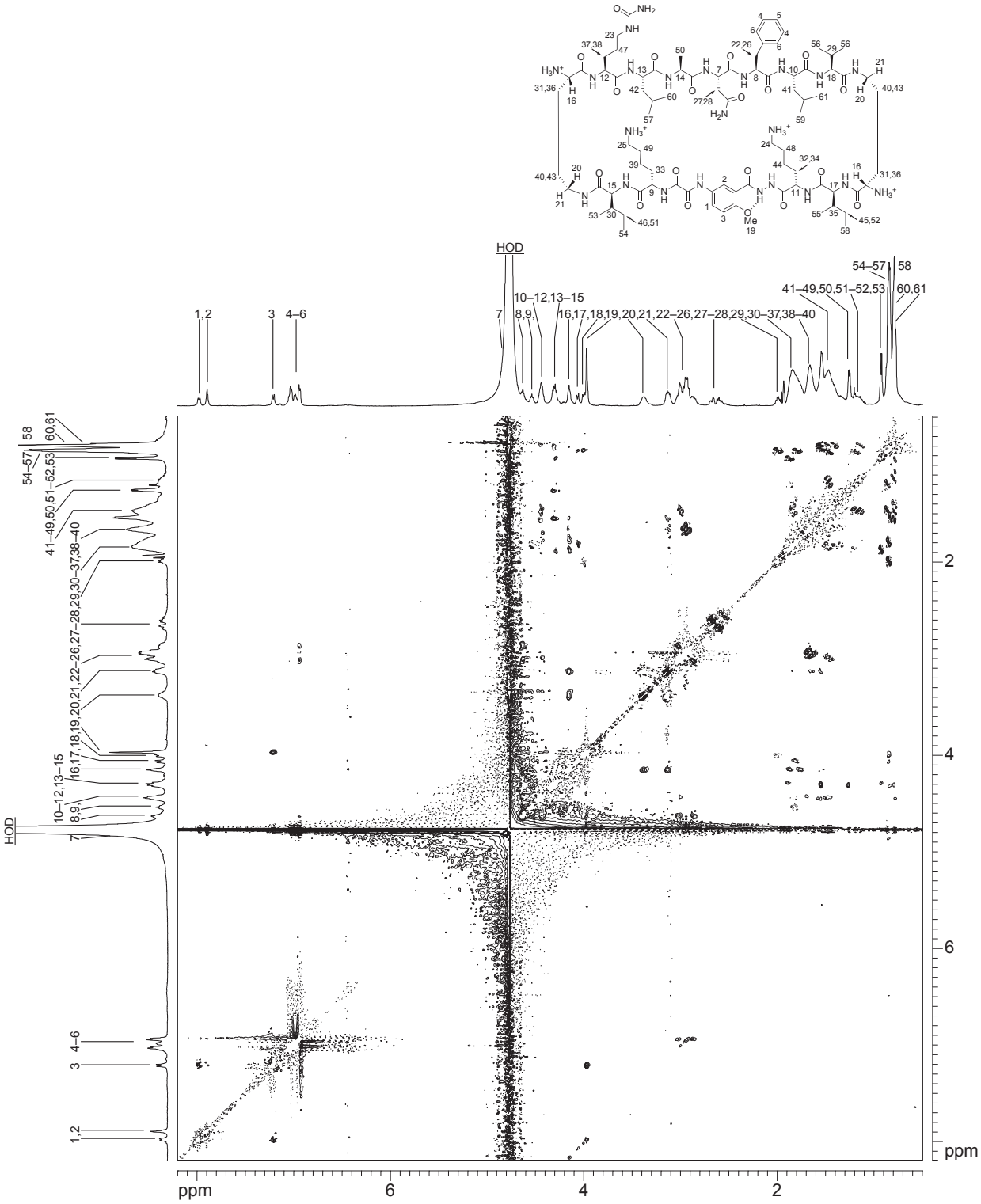

^{1}H NMR 2D ROESY of macrocyclic β-sheet peptide **1_{Cit}** with 100-ms spin-lock mixing time
2 mM in 100 mM deuterioacetate buffer in D_2O at 500 MHz and 298 K

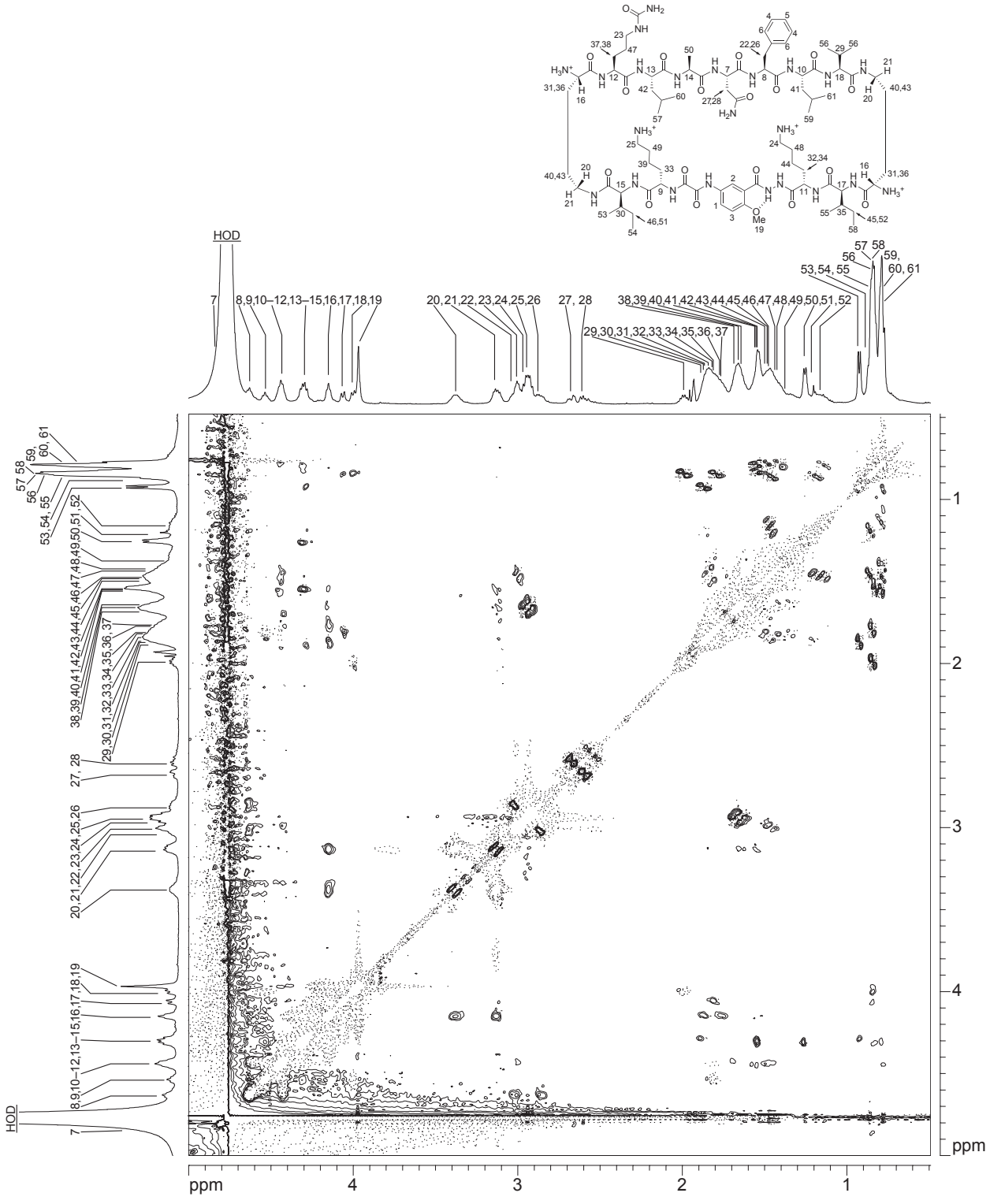

^{1}H NMR of macrocyclic β-sheet peptide **1$_{Cit}$**, 16 mM in 100 mM deuterioacetate buffer in D_2O at 500 MHz and 298 K

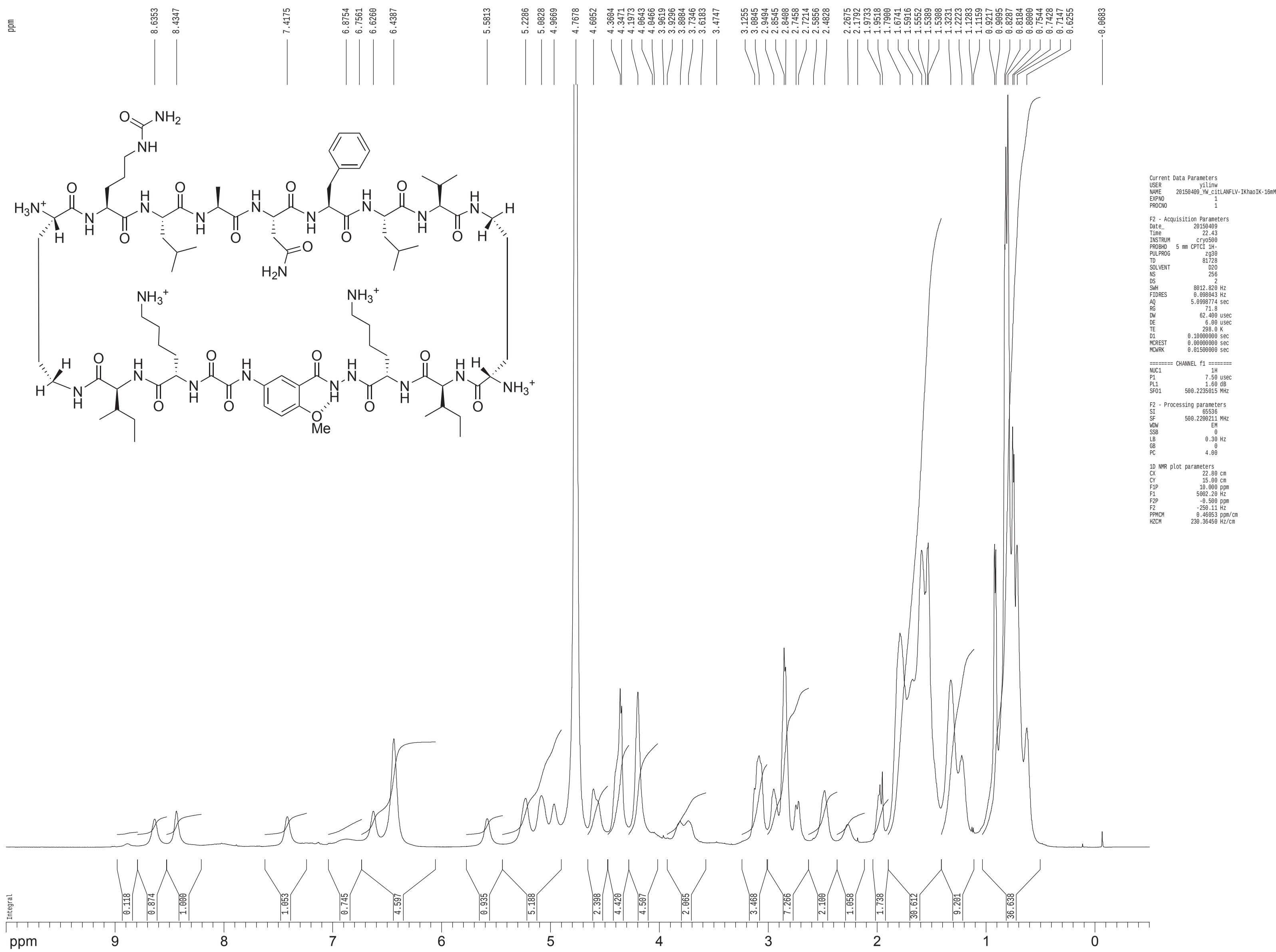

^{1}H NMR of macrocyclic β-sheet peptide **1_{Cit}**, 16 mM in 100 mM deuterioacetate buffer in D_2O at 500 MHz and 298 K

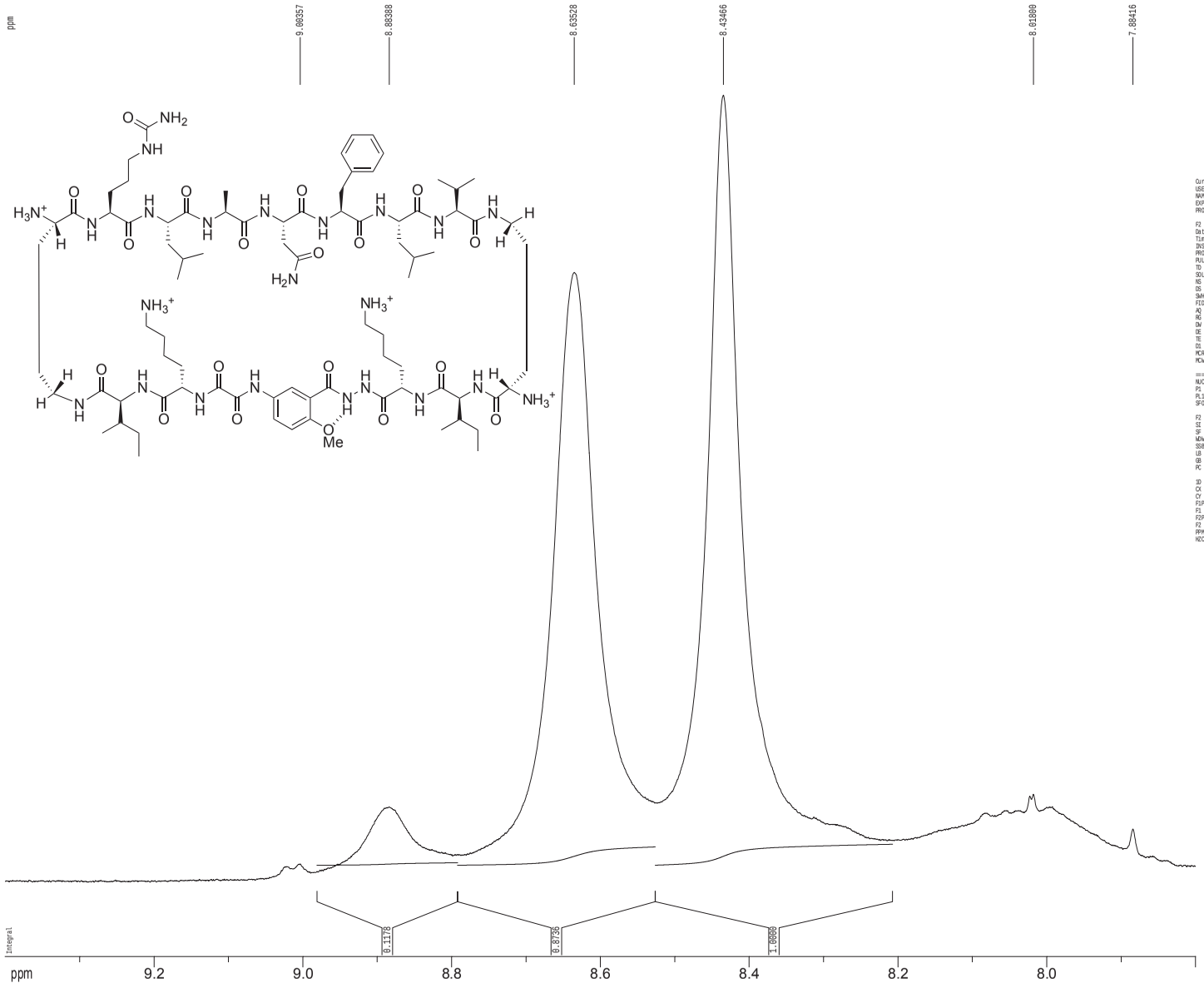

^{1}H NMR of macrocyclic β-sheet peptide **1_{Cit}**, 16 mM in 100 mM deuterioacetate buffer in D_2O at 500 MHz and 298 K

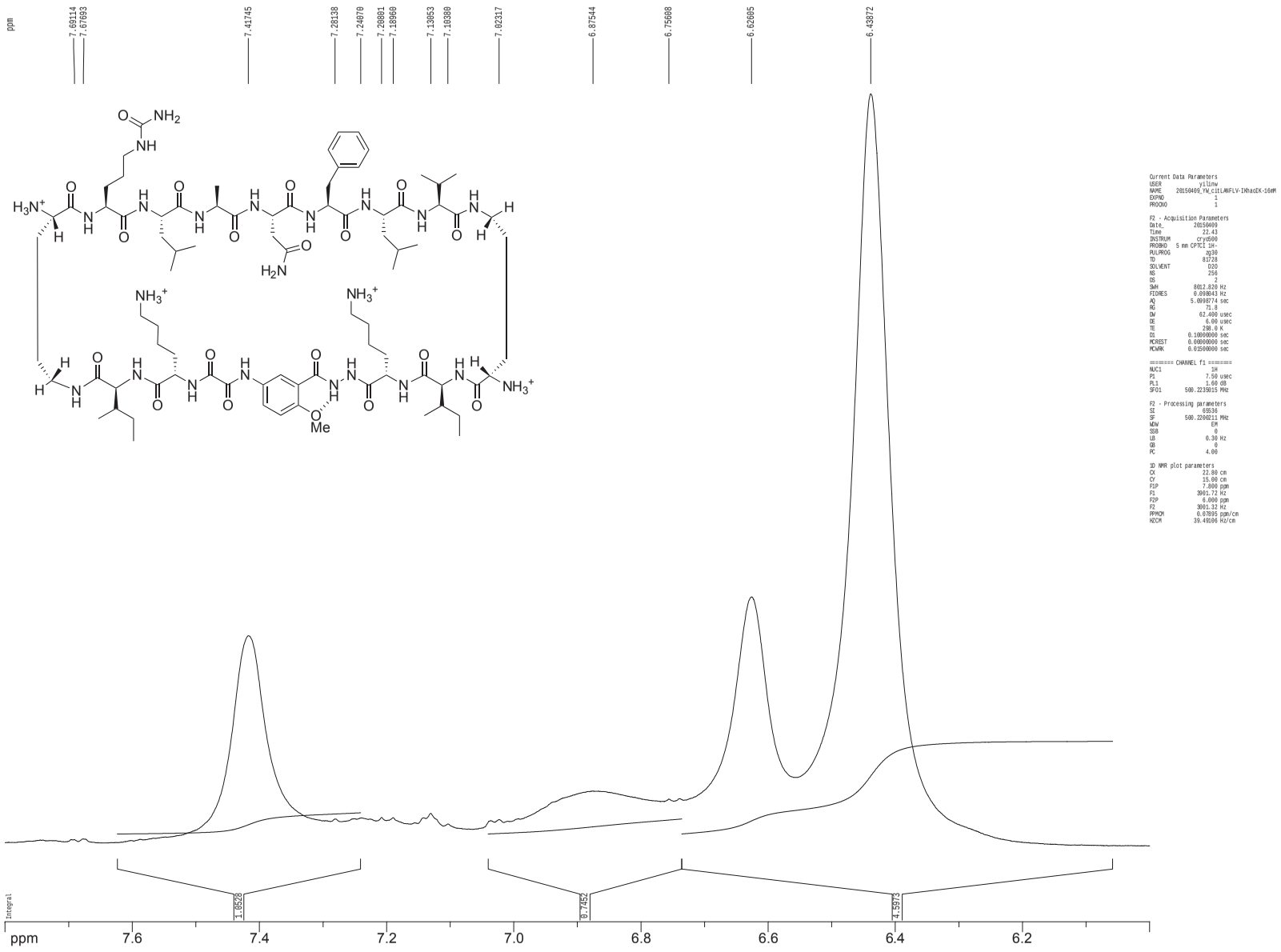

Current Data Parameters
USER yilinw
NAME 20150409_YW_citLWNFLV-IKhaoDK-16mM
EXPNO 1
PROCNO 1

F2 - Acquisition Parameters
Date_ 20150409
Time 22.43
INSTRUM cryo500
PROBHD 5 mm CPTCI 1H-
PULPROG zg30
TD 81728
SOLVENT D2O
NS 256
DS 2
SWH 8012.820 Hz
FIDRES 0.098043 Hz
AQ 5.0998774 sec
RG 71.8
DW 62.400 usec
DE 6.00 usec
TE 298.0 K
D1 0.10000000 sec
MCREST 0.00000000 sec
MCWRK 0.03500000 sec

====== CHANNEL f1 ======
NUC1 1H
P1 7.50 usec
PL1 1.60 dB
SFO1 500.2239015 MHz

F2 - Processing parameters
SI 65536
SF 500.2200211 MHz
WDW EM
SSB 0
LB 0.30 Hz
GB 0
PC 4.00

1D NMR plot parameters
CX 22.80 cm
CY 15.00 cm
F1P 7.800 ppm
F1 3901.72 Hz
F2P 6.000 ppm
F2 3001.32 Hz
PPMCM 0.07895 ppm/cm
HZCM 39.49186 Hz/cm

^{1}H NMR of macrocyclic β-sheet peptide **1**$_{Cit}$, 16 mM in 100 mM deuterioacetate buffer in D_2O at 500 MHz and 298 K

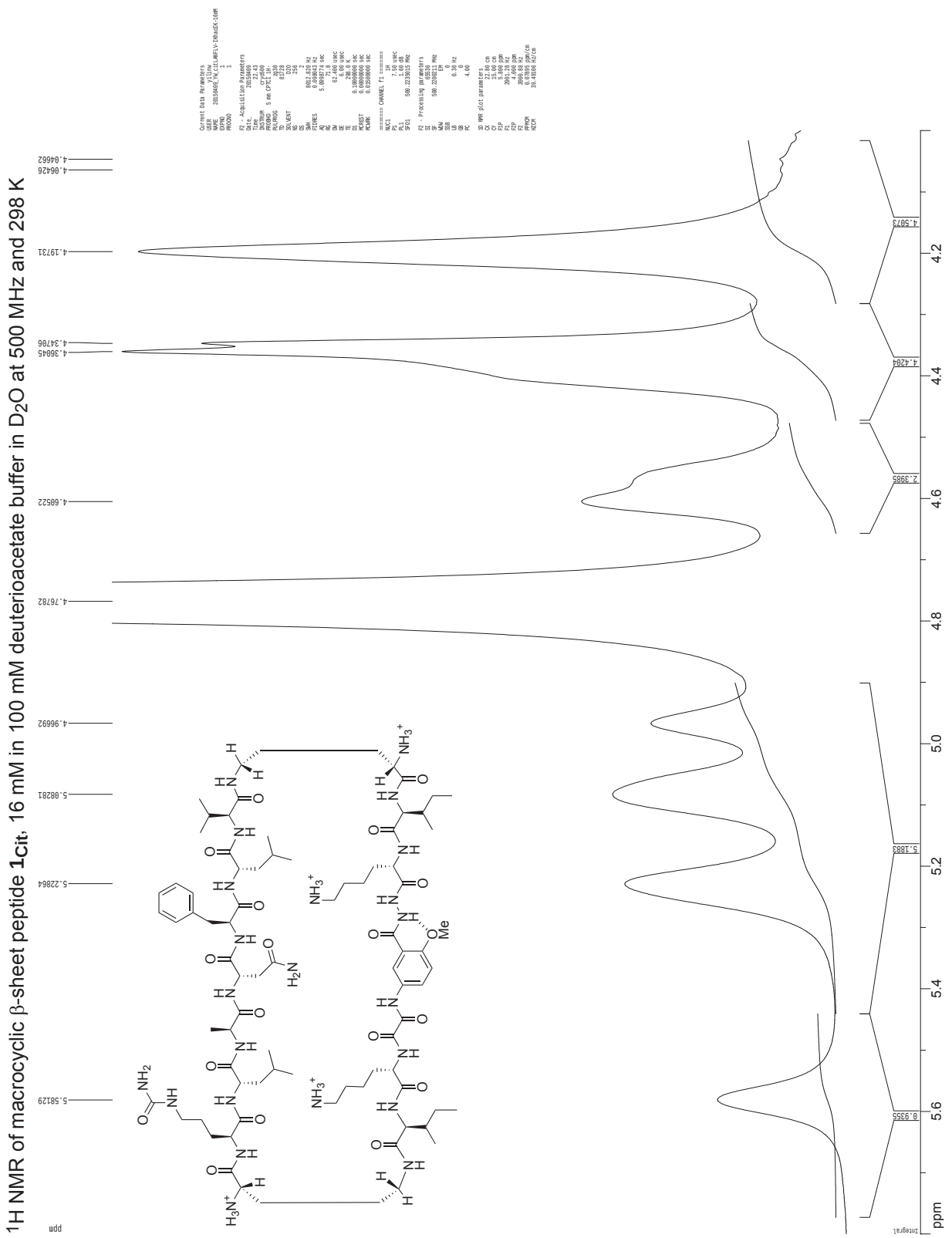

^{1}H NMR of macrocyclic β-sheet peptide **1_{Cit}**, 16 mM in 100 mM deuterioacetate buffer in D_2O at 500 MHz and 298 K

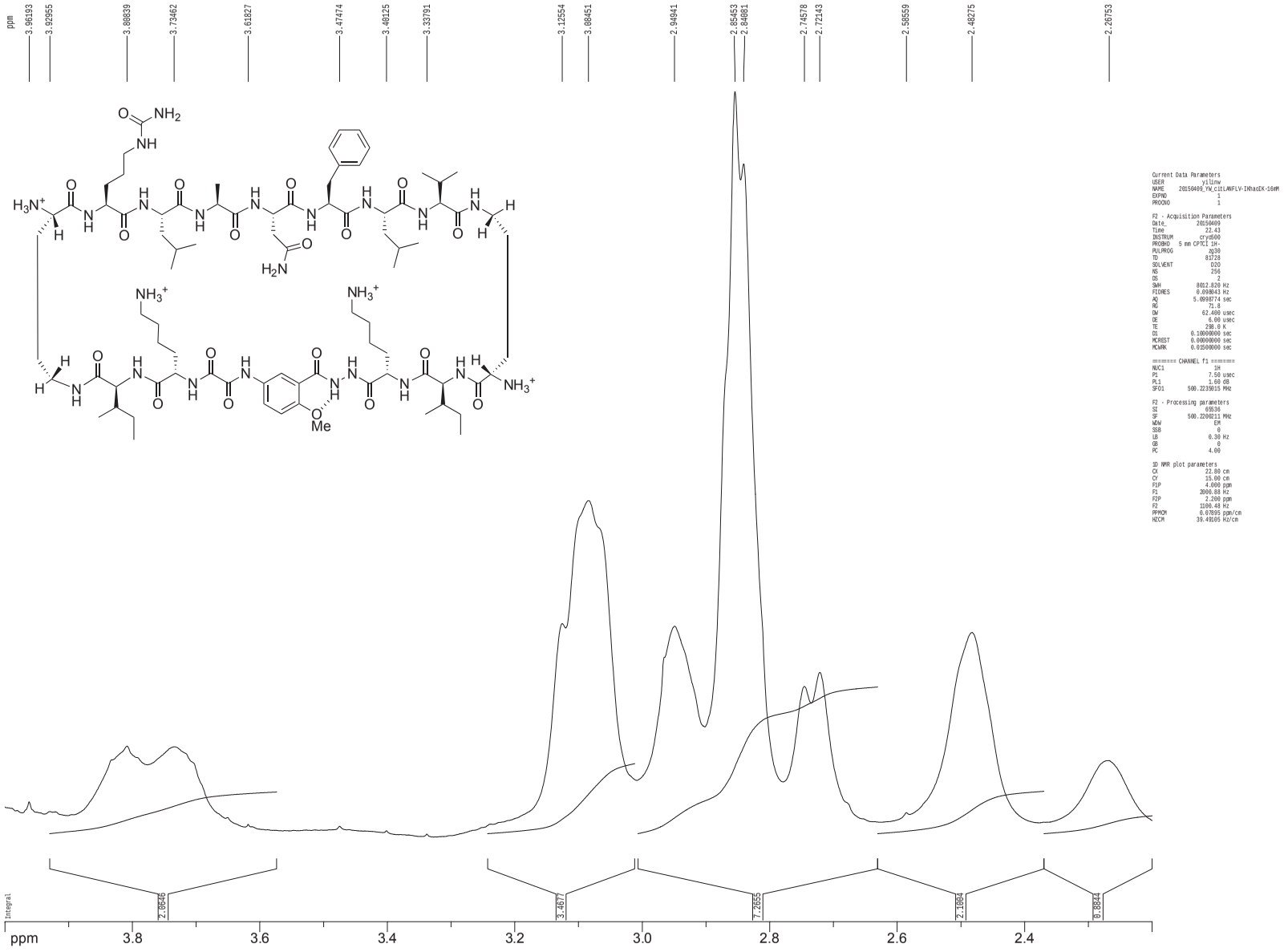

Current Data Parameters
USER yilinw
NAME 20150409_YW_citLWFLV-IKhaoDK-16mM
EXPNO 1
PROCNO 1

F2 - Acquisition Parameters
Date_ 20150409
Time 22.43
INSTRUM cryo500
PROBHD 5 mm CPTCI 1H-
PULPROG zg30
TD 81728
SOLVENT D2O
NS 256
DS 2
SWH 8012.820 Hz
FIDRES 0.098043 Hz
AQ 5.0998774 sec
RG 71.8
DW 62.400 usec
DE 6.00 usec
TE 298.0 K
D1 0.10000000 sec
MCREST 0.00000000 sec
MCWRK 0.03500000 sec

======= CHANNEL f1 ======
NUC1 1H
P1 7.50 usec
PL1 1.60 dB
SFO1 500.2239015 MHz

F2 - Processing parameters
SI 65536
SF 500.2200211 MHz
WDW EM
SSB 0
LB 0.30 Hz
GB 0
PC 4.00

1D NMR plot parameters
CX 22.80 cm
CY 15.00 cm
F1P 4.000 ppm
F1 2000.88 Hz
F2P 2.200 ppm
F2 1100.48 Hz
PPMCM 0.07895 ppm/cm
HZCM 39.49105 Hz/cm

^{1}H NMR of macrocyclic β-sheet peptide **1_{Cit}**, 16 mM in 100 mM deuterioacetate buffer in D_2O at 500 MHz and 298 K

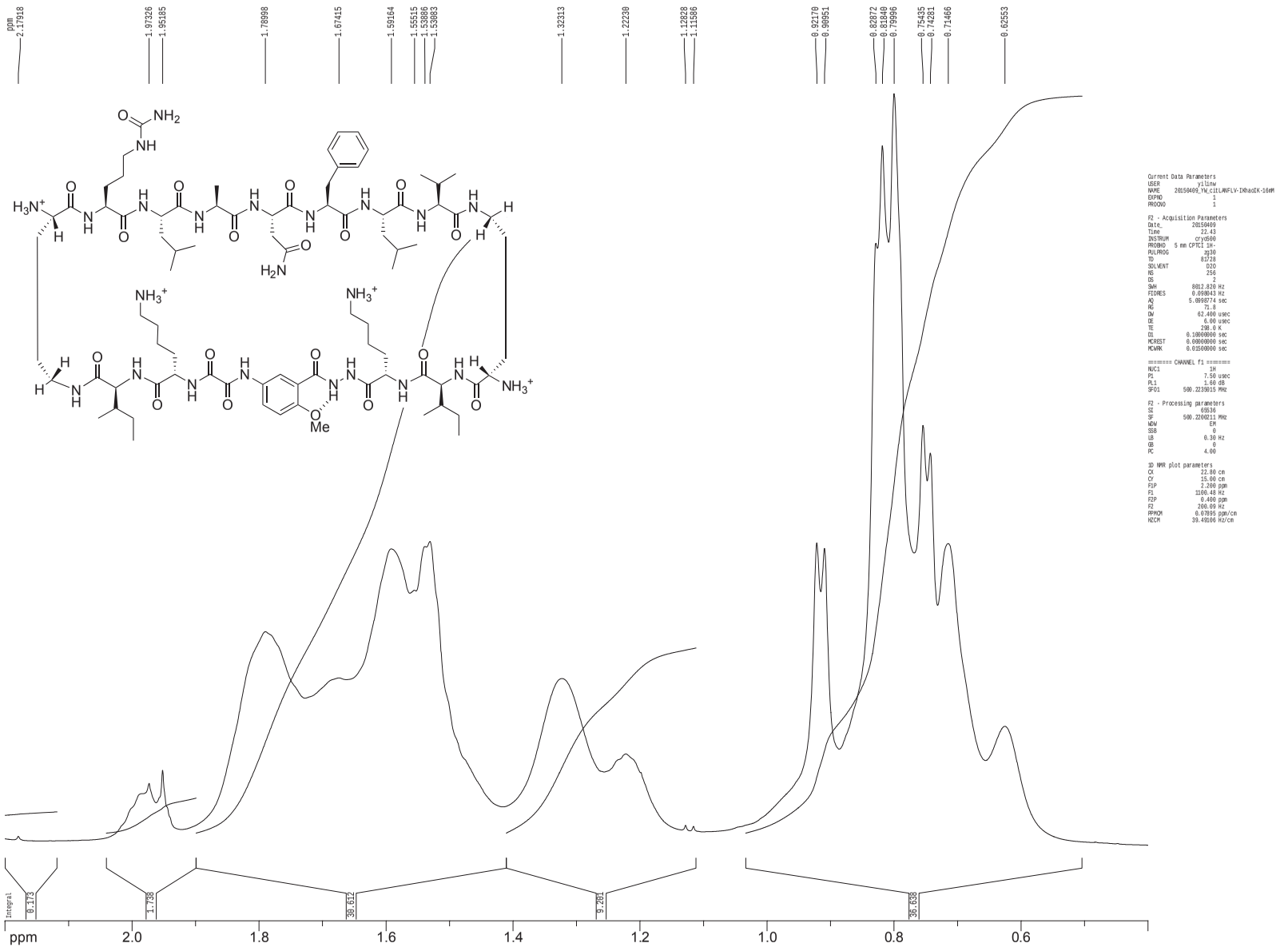

Current Data Parameters
USER yilinw
NAME 20150409_YW_citLWVFLV-IKhaoDK-16mM
EXPNO 1
PROCNO 1

F2 - Acquisition Parameters
Date_ 20150409
Time 22.43
INSTRUM cryo500
PROBHD 5 mm CPTCI 1H-
PULPROG zg30
TD 81728
SOLVENT D2O
NS 256
DS 2
SWH 8012.820 Hz
FIDRES 0.098043 Hz
AQ 5.0998774 sec
RG 71.8
DW 62.400 usec
DE 6.00 usec
TE 298.0 K
D1 0.10000000 sec
MCREST 0.00000000 sec
MCWRK 0.03500000 sec

====== CHANNEL f1 ======
NUC1 1H
P1 7.50 usec
PL1 1.60 dB
SFO1 500.2239015 MHz

F2 - Processing parameters
SI 65536
SF 500.2200211 MHz
WDW EM
SSB 0
LB 0.30 Hz
GB 0
PC 4.00

1D NMR plot parameters
CX 22.80 cm
CY 15.00 cm
F1P 2.200 ppm
F1 1100.48 Hz
F2P 0.400 ppm
F2 200.09 Hz
PPMCM 0.07895 ppm/cm
HZCM 39.49186 Hz/cm

^{1}H NMR 2D TOCSY of macrocyclic β-sheet peptide **$\mathbf{1_{Cit}}$** with 150-ms spin-lock mixing time
16 mM in 100 mM deuterioacetate buffer in D_2O at 500 MHz and 298 K

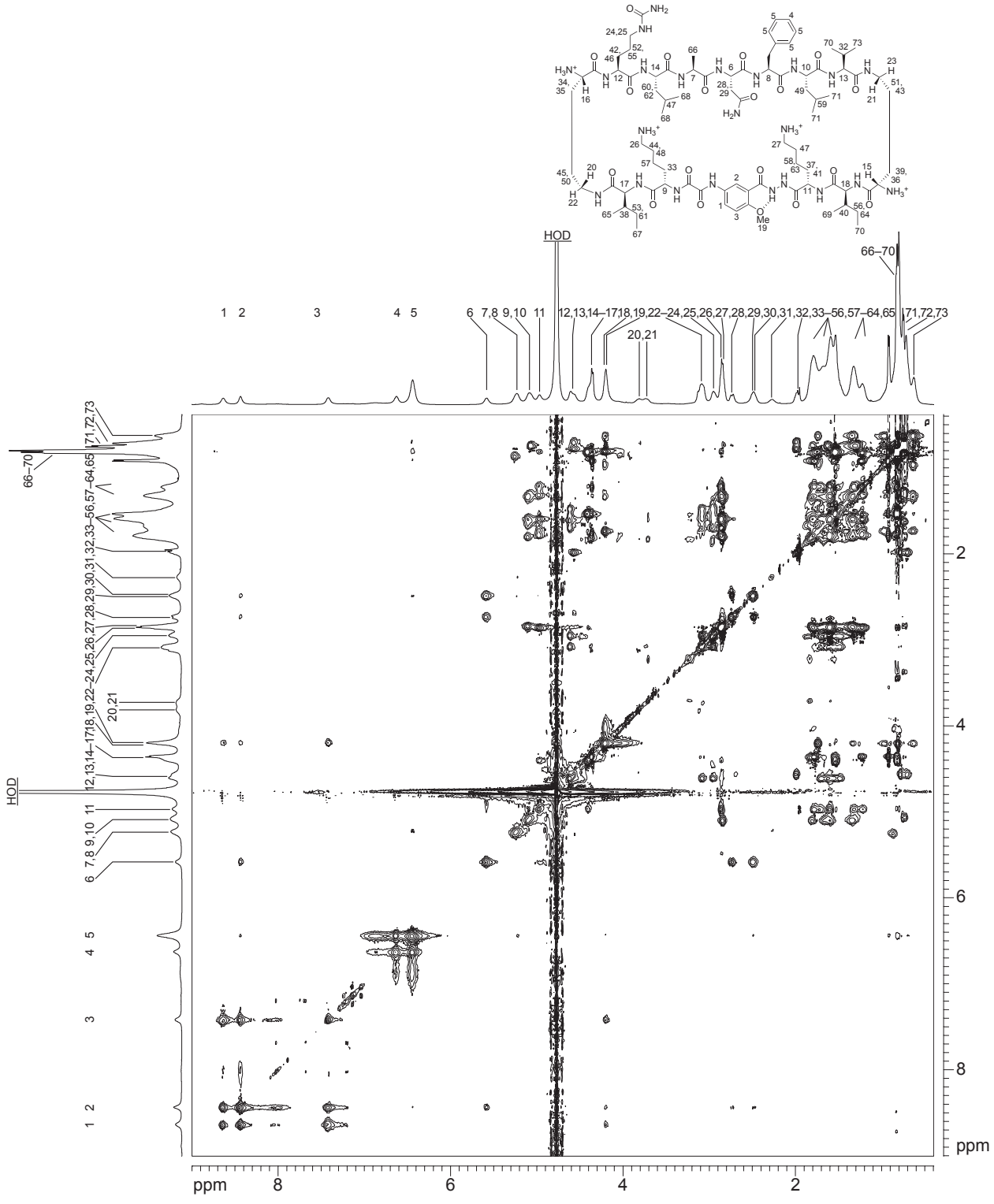

^{1}H NMR 2D TOCSY of macrocyclic β-sheet peptide **1$_{Cit}$** with 150-ms spin-lock mixing time
16 mM in 100 mM deuterioacetate buffer in D_2O at 500 MHz and 298 K

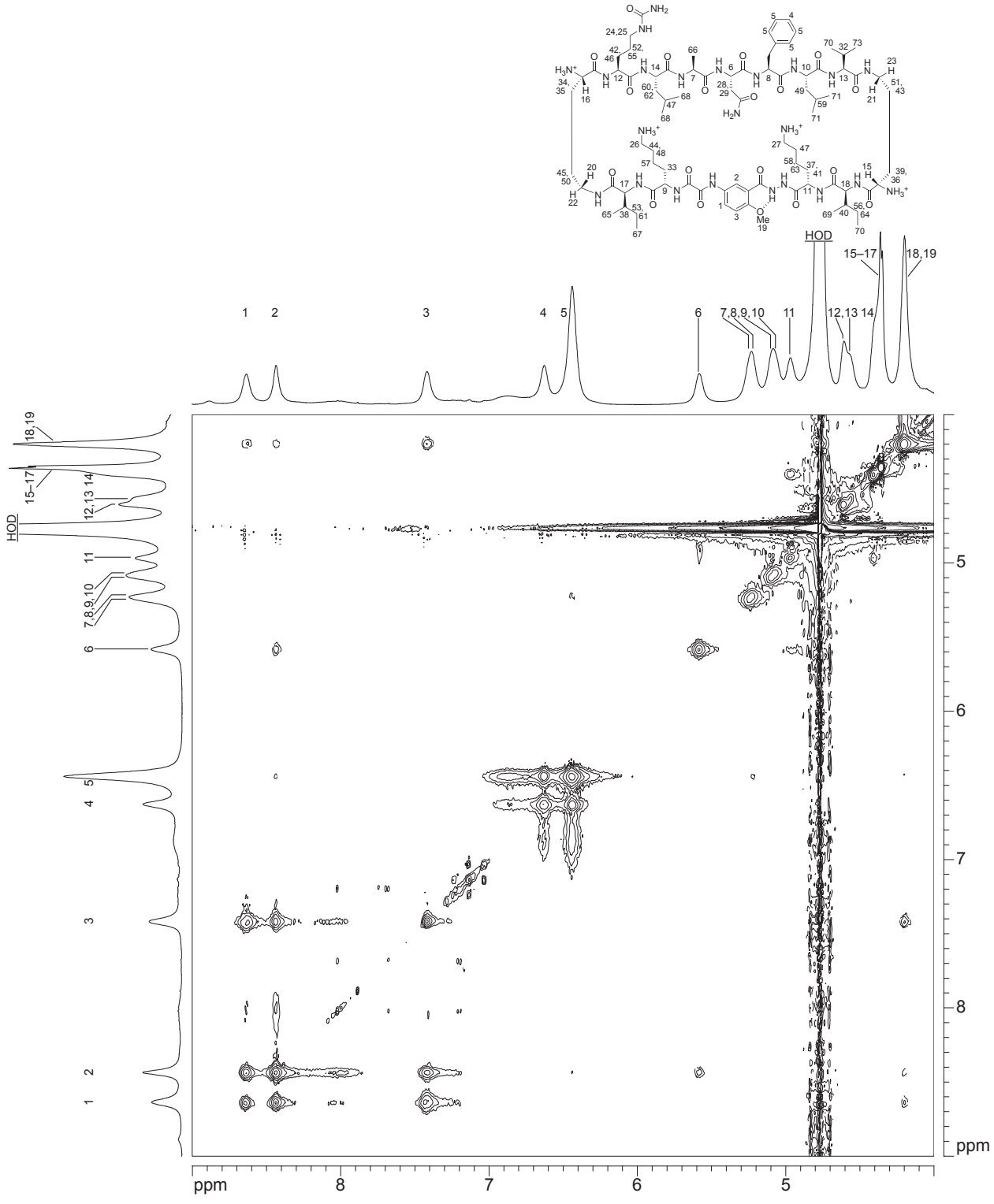

^{1}H NMR 2D TOCSY of macrocyclic β-sheet peptide **1$_{Cit}$** with 150-ms spin-lock mixing time
16 mM in 100 mM deuterioacetate buffer in D_2O at 500 MHz and 298 K

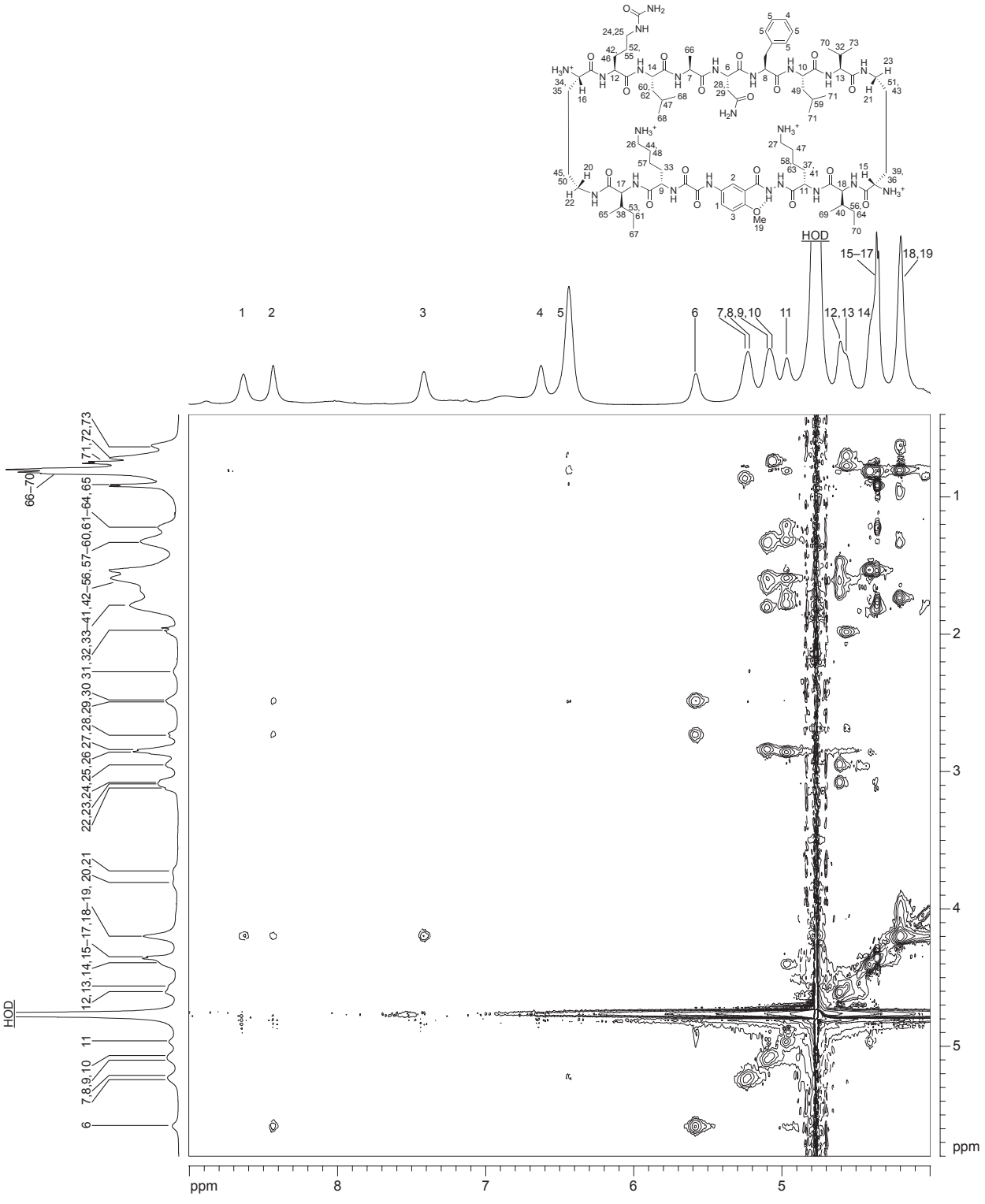

^{1}H NMR 2D TOCSY of macrocyclic β-sheet peptide **1_{Cit}**
16 mM in D_2O at 500 MHz and 298 K with 150-ms spin-lock mixing time

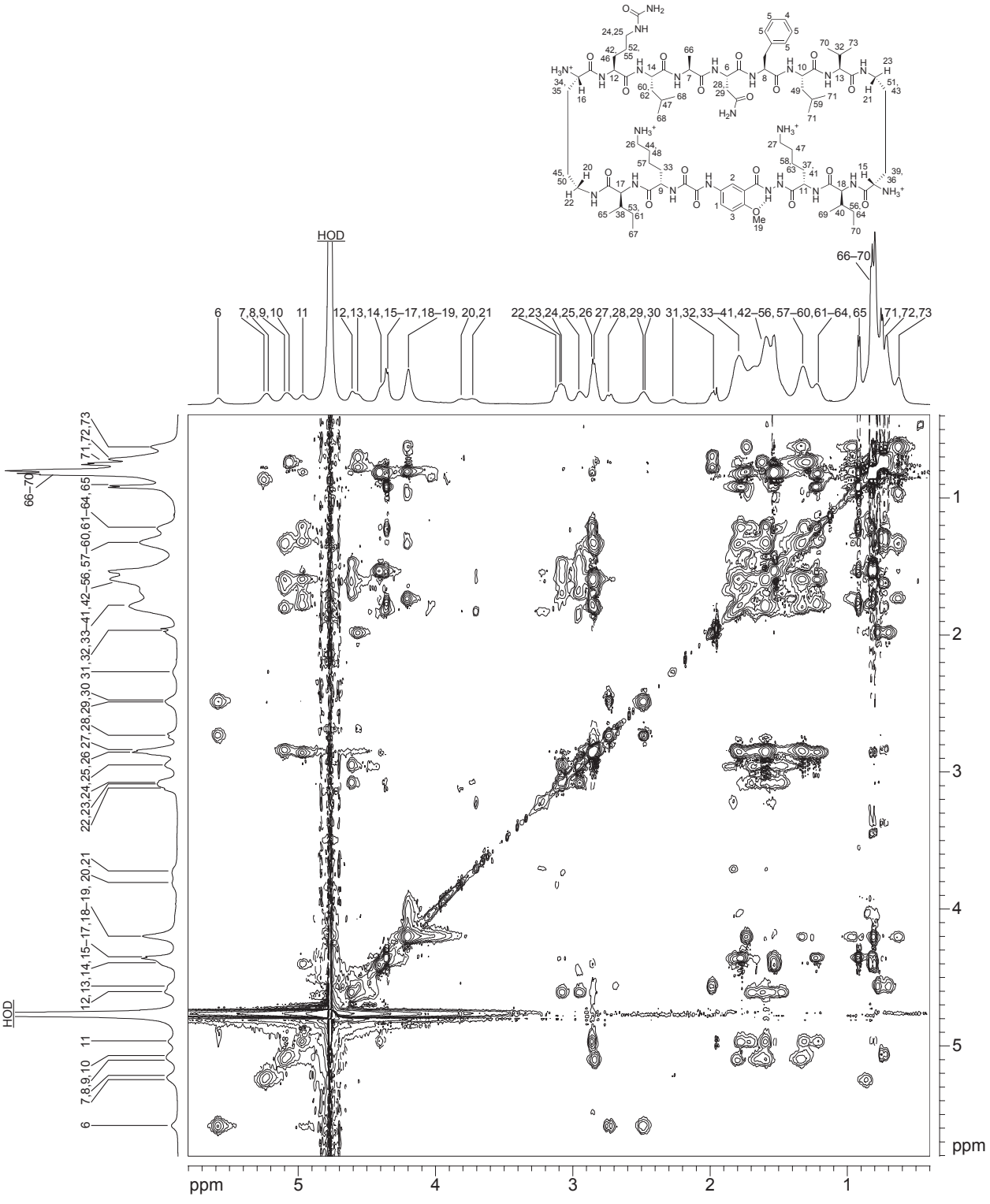

^{1}H NMR 2D NOESY of macrocyclic β-sheet peptide **1_{Cit}** with 150-ms mixing time
16 mM in 100 mM deuterioacetate buffer in D_2O at 500 MHz and 298 K

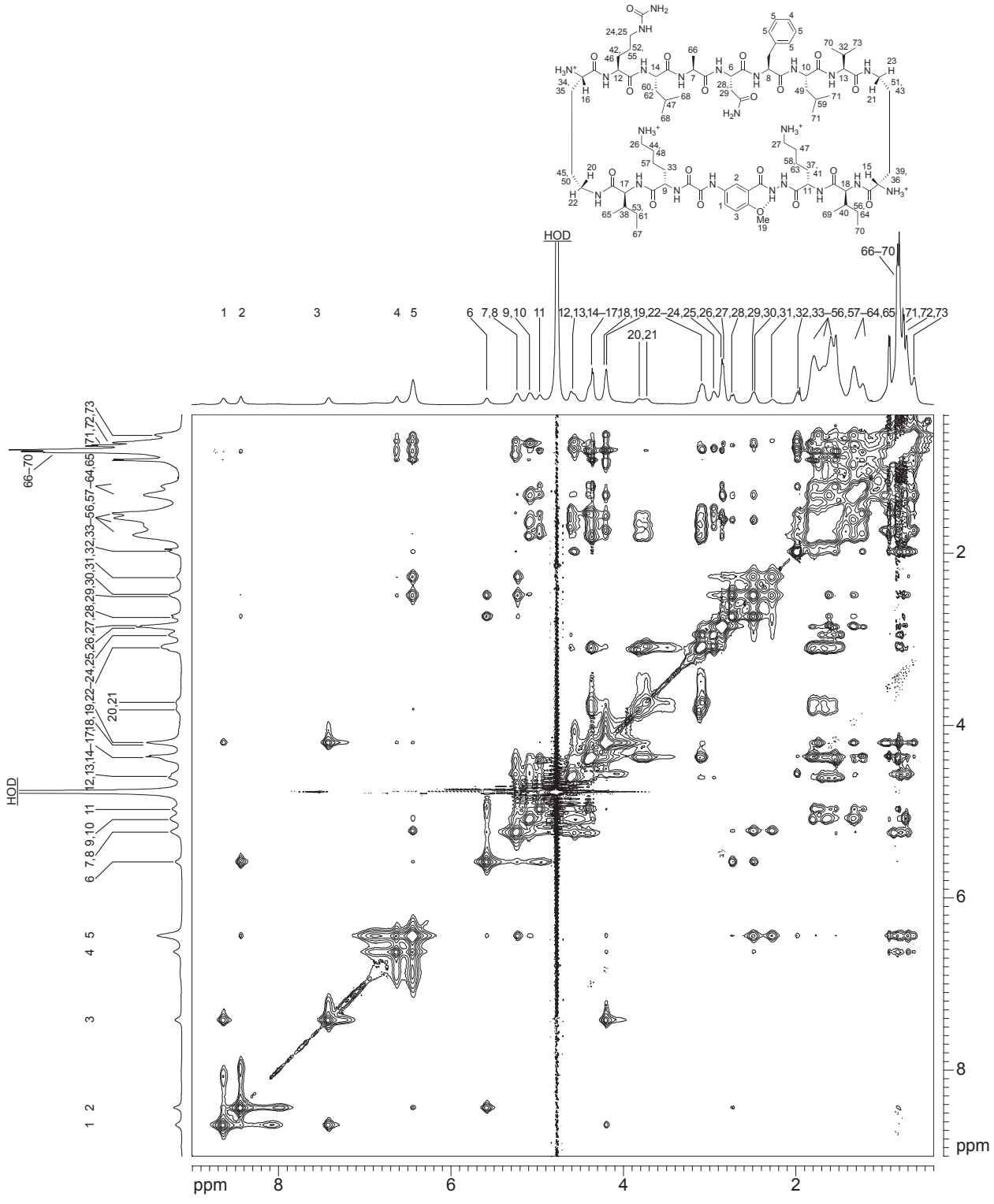

^{1}H NMR 2D NOESY of macrocyclic β-sheet peptide **$\mathbf{1_{Cit}}$** with 150-ms mixing time
16 mM in 100 mM deuterioacetate buffer in D_2O at 500 MHz and 298 K

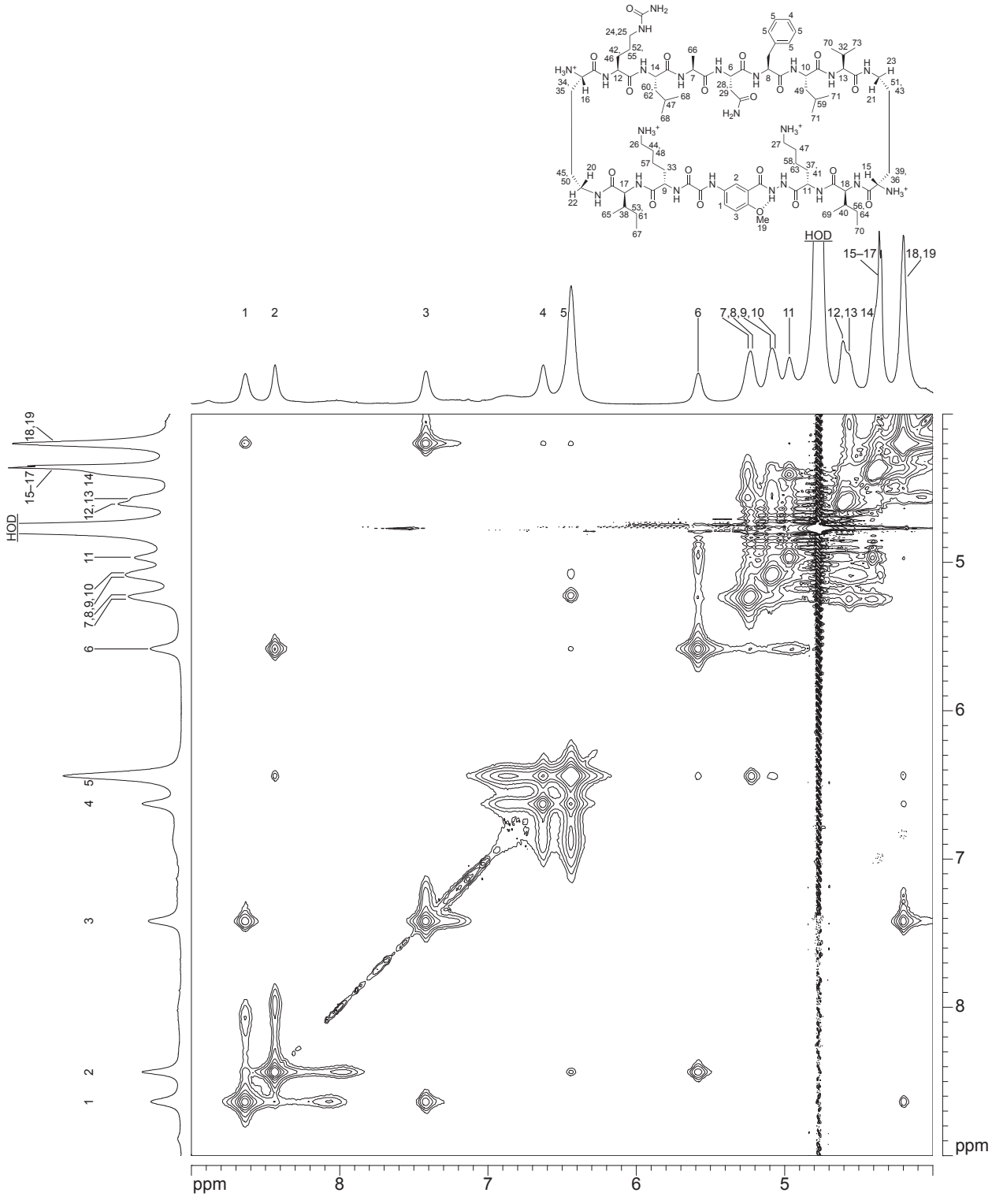

^{1}H NMR 2D NOESY of macrocyclic β-sheet peptide **1_{Cit}** with 150-ms mixing time
16 mM in 100 mM deuterioacetate buffer in D_2O at 500 MHz and 298 K

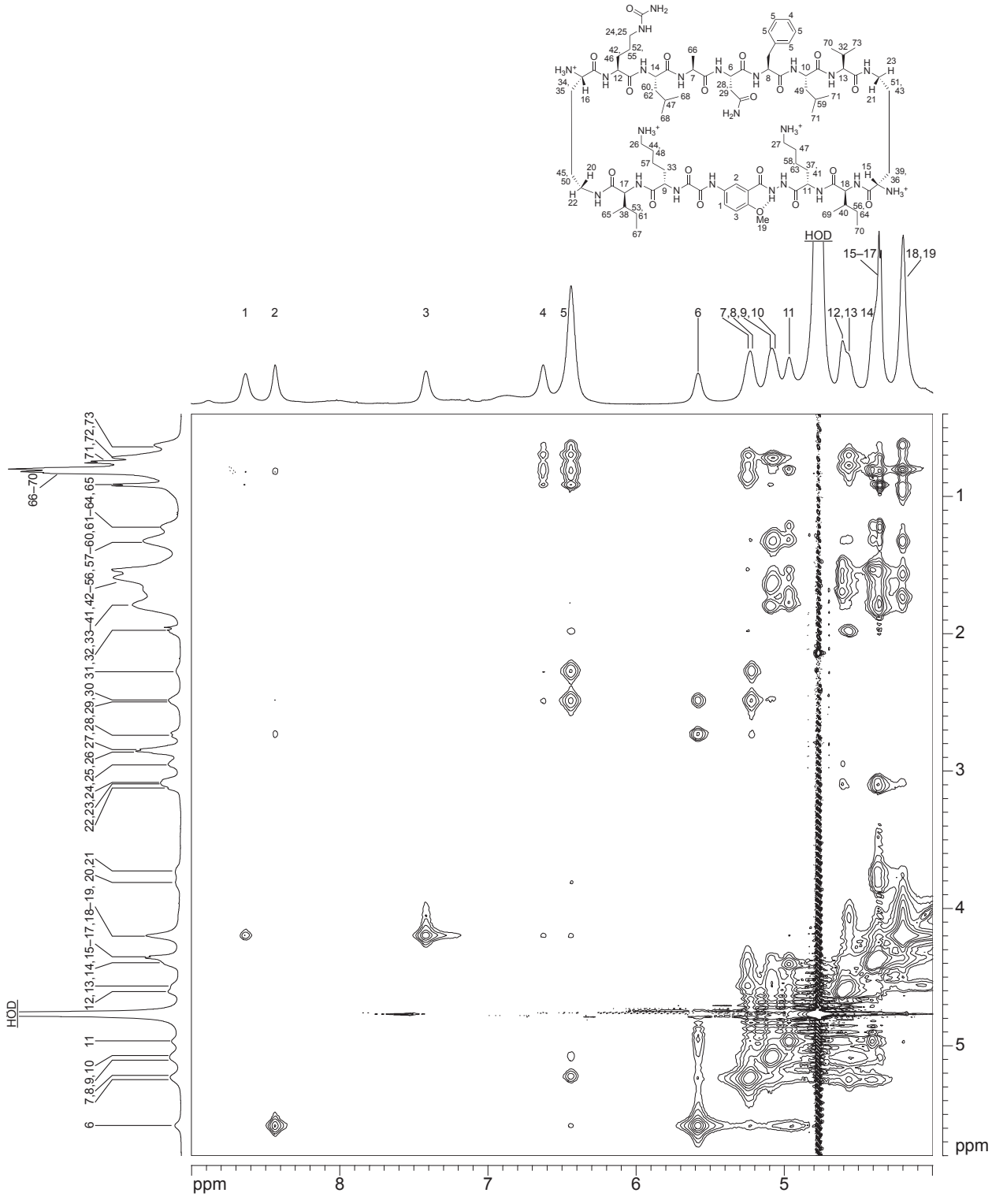

^{1}H NMR 2D NOESY of macrocyclic β-sheet peptide **$\mathbf{1_{Cit}}$** with 150-ms mixing time
16 mM in 100 mM deuterioacetate buffer in D_2O at 500 MHz and 298 K

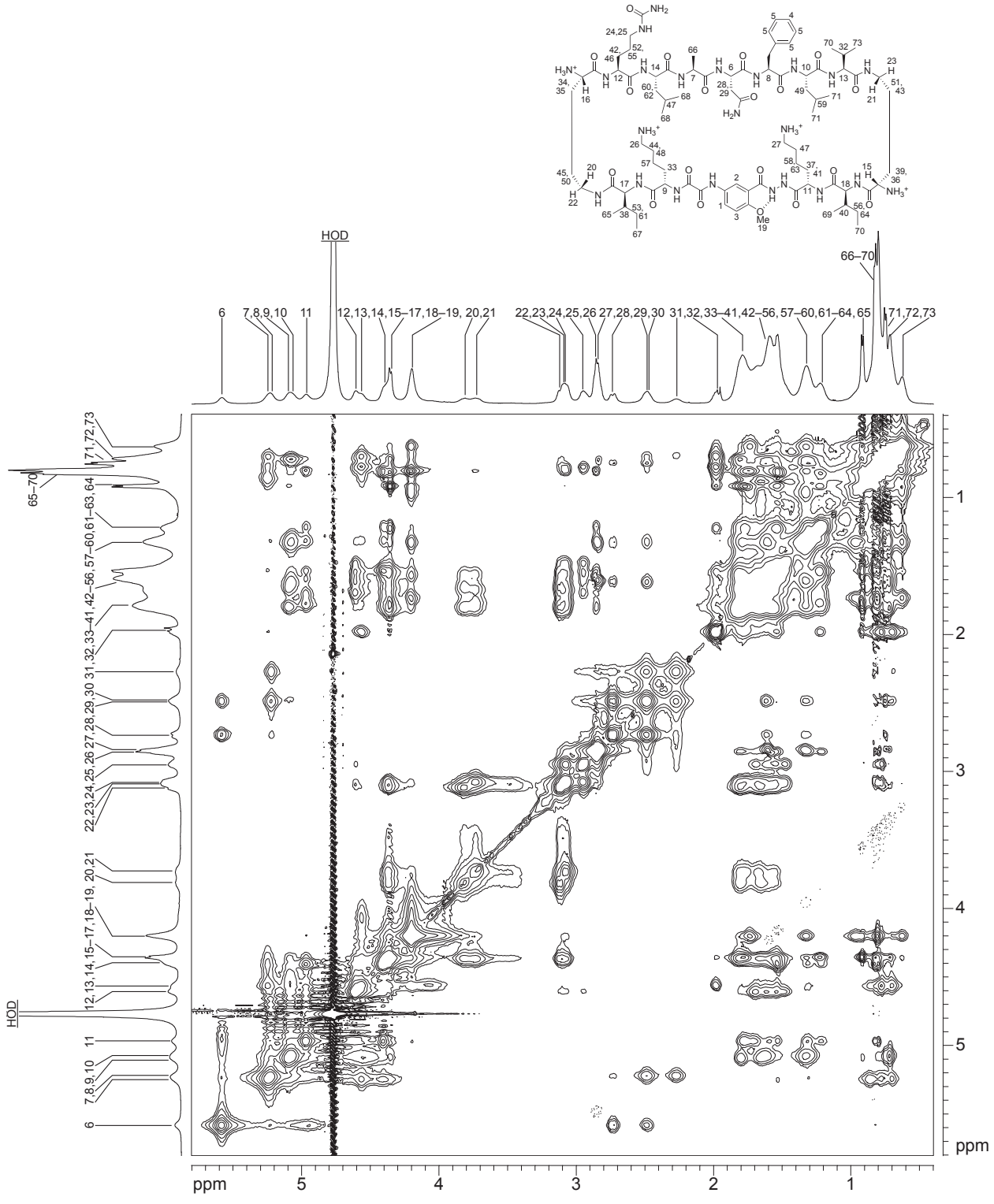

^{1}H NMR DOSY of macrocyclic β-sheet peptide **1$_{Cit}$** at 500 MHz and 298 K
1 mM in 100 mM deuterioacetate buffer in D_2O

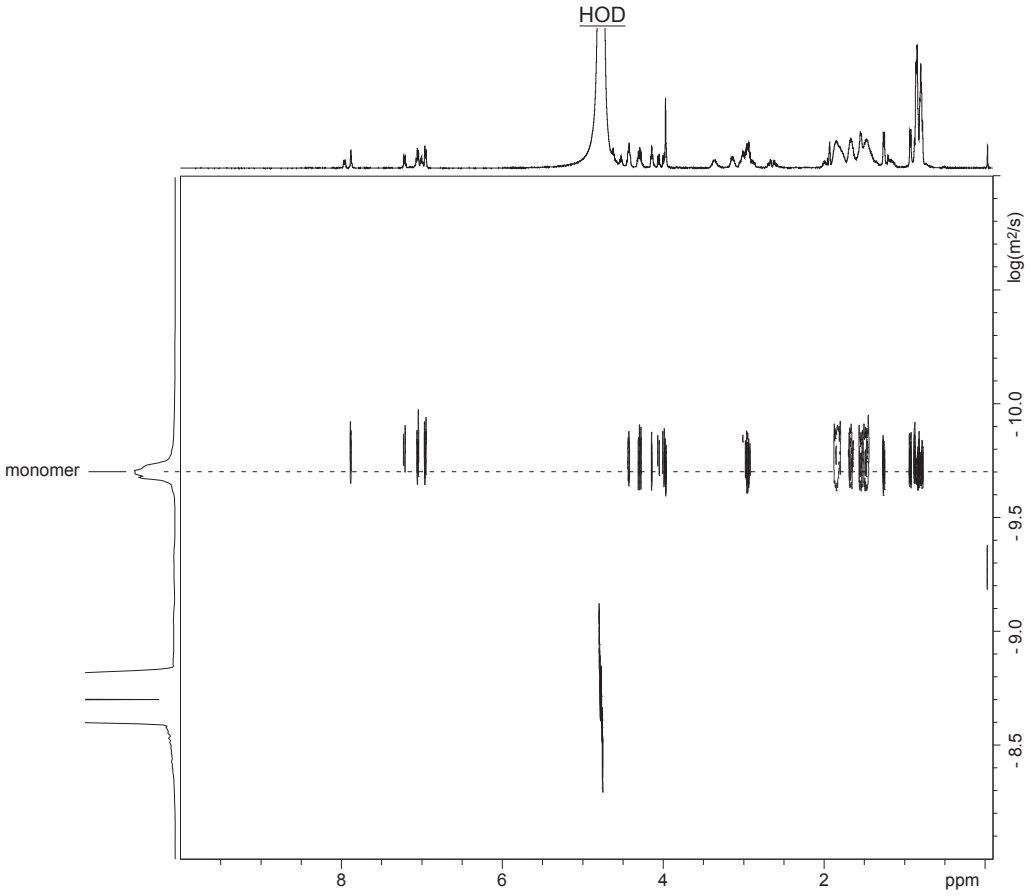

Calculations for macrocyclic β-sheet peptide **1$_{Cit}$** at 1 mM

D_{HOD} = 19.0 x 10^{-10} m^2/s [a]
log (D_{HOD}) = -8.721

$D_{monomer}$: log(D) = -9.700; D = $10^{-9.700}$ = 20.0 ± 2.0 x 10^{-11} m^2/s

[a]Longsworth, L. G. *J. Phys. Chem.* **1960**, *64*, 1914−1917.

^{1}H NMR DOSY of macrocyclic β-sheet peptide **1$_{Cit}$** at 500 MHz and 298 K
2 mM in 100 mM deuterioacetate buffer in D_2O

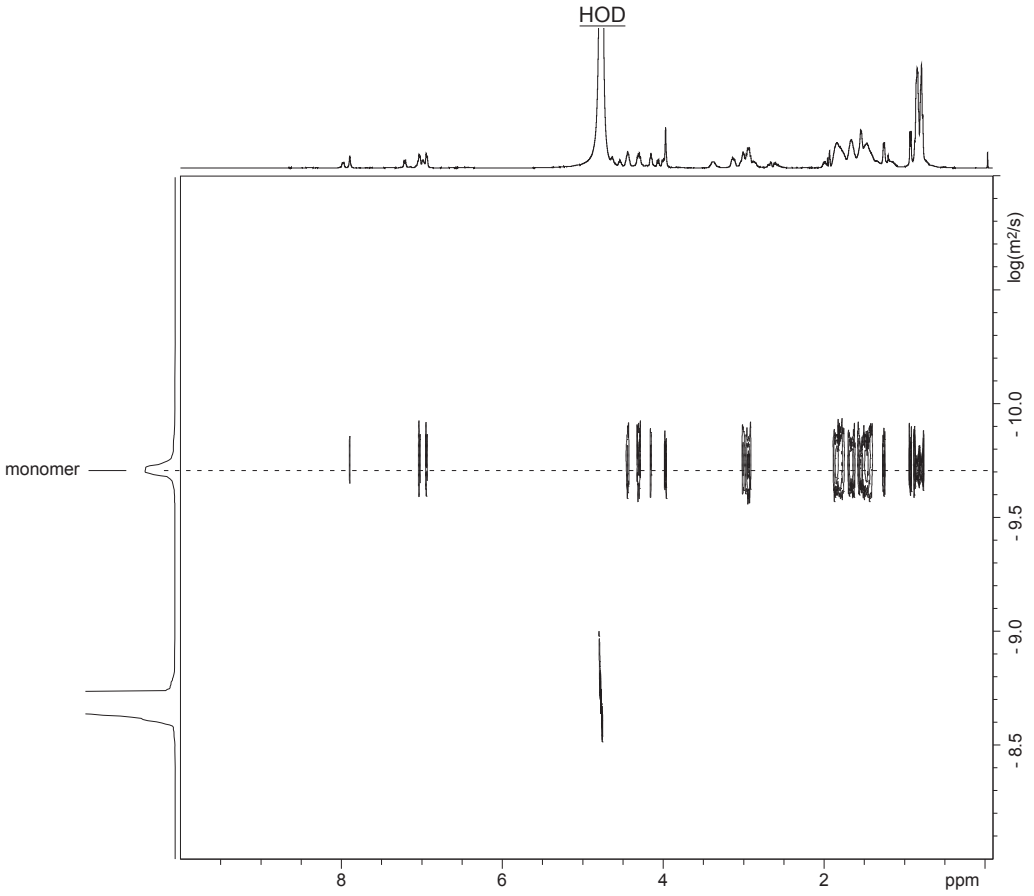

Calculations for macrocyclic β-sheet peptide **1$_{Cit}$** at 2 mM

D_{HOD} = 19.0 x 10^{-10} m^2/s [a]
log (D_{HOD}) = -8.721

$D_{monomer}$: log(D) = -9.723; D = $10^{-9.723}$ = 18.9 ± 1.2 x 10^{-11} m^2/s

[a]Longsworth, L. G. *J. Phys. Chem.* **1960**, *64*, 1914−1917.

^{1}H NMR DOSY of macrocyclic β-sheet peptide **1$_{Cit}$** at 500 MHz and 298 K
4 mM in 100 mM deuterioacetate buffer in D_2O

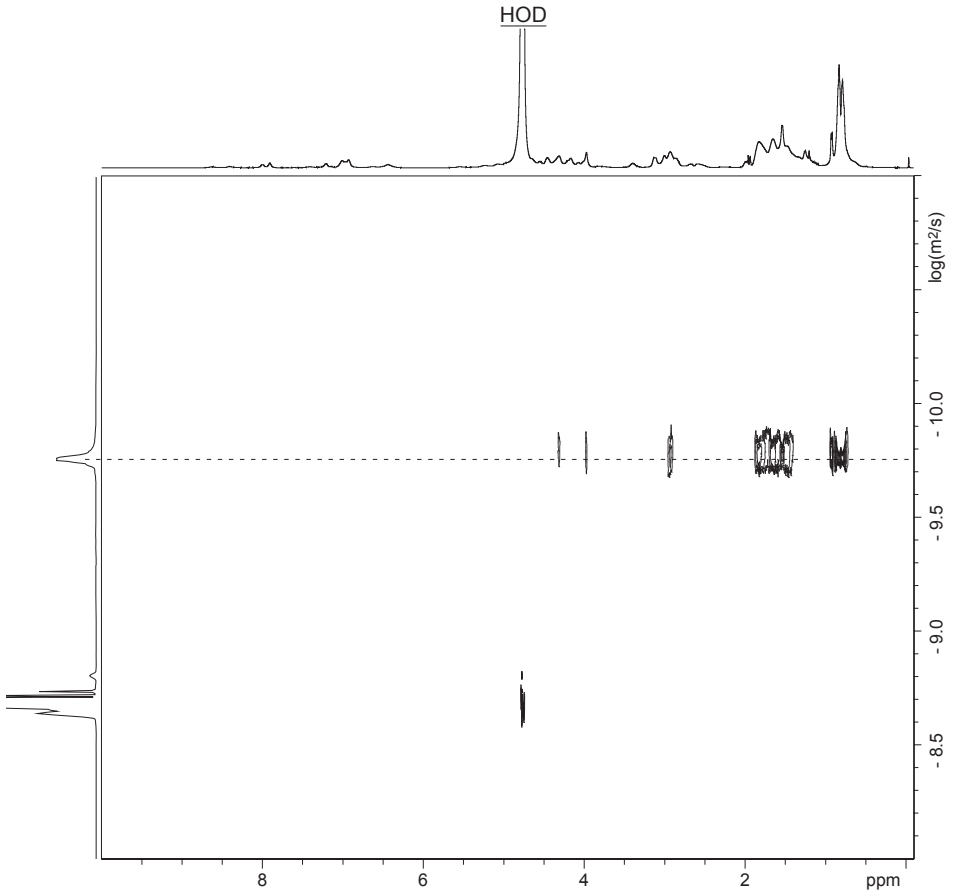

Calculations for macrocyclic β-sheet peptide **1$_{Cit}$** at 4 mM

D_{HOD} = 19.0 x 10^{-10} m^2/s [a]
log (D_{HOD}) = -8.721

$D_{monomer}$: log(D) = -9.759; D = $10^{-9.759}$ = 17.4 ± 1.2 x 10^{-11} m^2/s

[a]Longsworth, L. G. *J. Phys. Chem.* **1960**, *64*, 1914−1917.

^{1}H NMR DOSY of macrocyclic β-sheet peptide **1$_{Cit}$** at 500 MHz and 298 K
8 mM in 100 mM deuterioacetate buffer in D_2O

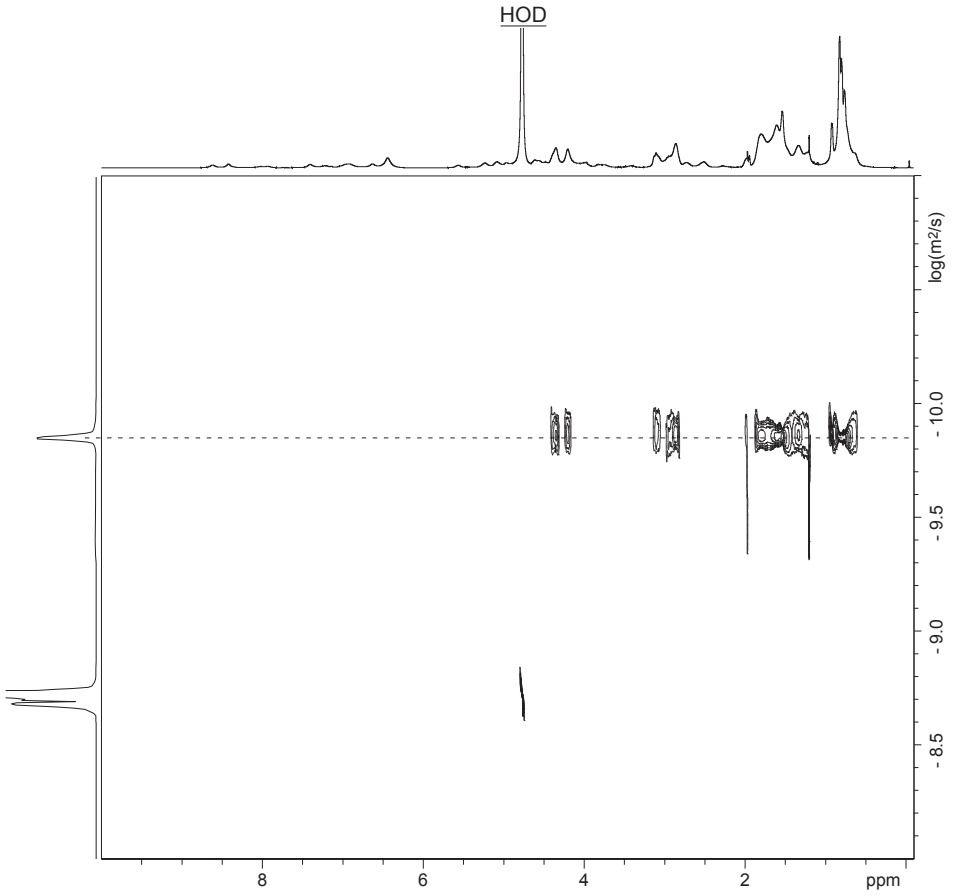

Calculations for macrocyclic β-sheet peptide **1$_{Cit}$** at 8 mM

D_{HOD} = 19.0 x 10^{-10} m^2/s [a]
log (D_{HOD}) = -8.721

$D_{monomer}$: log(D) = -9.849; D = $10^{-9.849}$ = 14.2 ± 0.3 x 10^{-11} m^2/s

[a]Longsworth, L. G. *J. Phys. Chem.* **1960**, *64*, 1914−1917.

^{1}H NMR DOSY of macrocyclic β-sheet peptide **1$_{Cit}$** at 500 MHz and 298 K
16 mM in 100 mM deuterioacetate buffer in D_2O

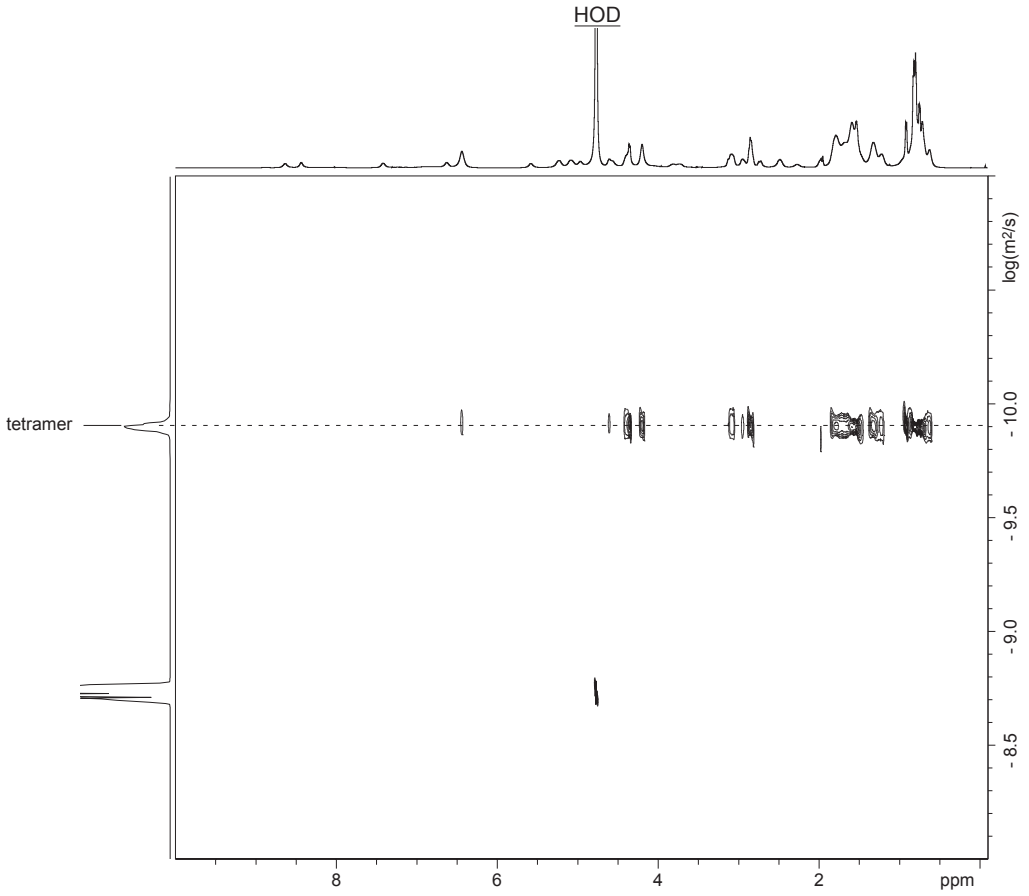

Calculations for macrocyclic β-sheet peptide **1$_{Cit}$** at 16 mM

D_{HOD} = 19.0 x 10^{-10} m^2/s [a]
log (D_{HOD}) = -8.721

$D_{monomer}$: log(D) = -9.905; D = $10^{-9.905}$ = 12.4 ± 0.3 x 10^{-11} m^2/s

[a]Longsworth, L. G. *J. Phys. Chem.* **1960**, *64*, 1914−1917.

RP-HPLC of Macrocyclic β-Sheet **2_{Cit}**

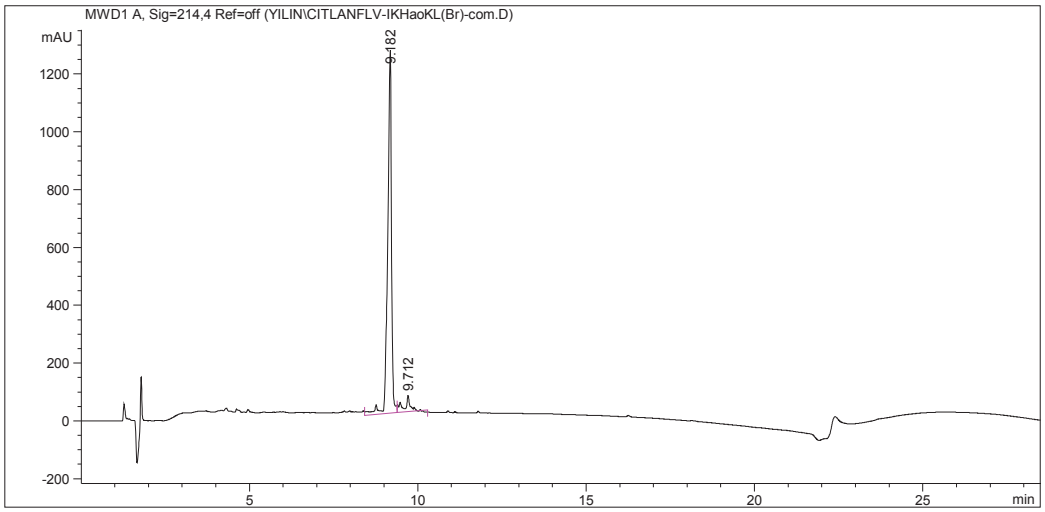

Peak #	RetTime [min]	Type	Width [min]	Area mAU *s	Height [mAU]	Area %
1	9.182	MF	0.1294	9766.9707	1258.4011	93.6334
2	9.712	FM	0.1955	664.1050	56.6224	6.3666

column: Aeris XB-C18 2.6µ
dimensions: 150 mm x 4.6 mm
mobile phase: A: H_2O, 0.1% TFA
B: CH_3CN, 0.1% TFA
gradient: A/B (95:5) to (0:100) in 20 min
flow rate: 1.0 mL/min
detection: VWD, wavelength = 214 nm
temperature: 298 K

MS (ESI) of Macrocyclic β-Sheet **2_{Cit}**

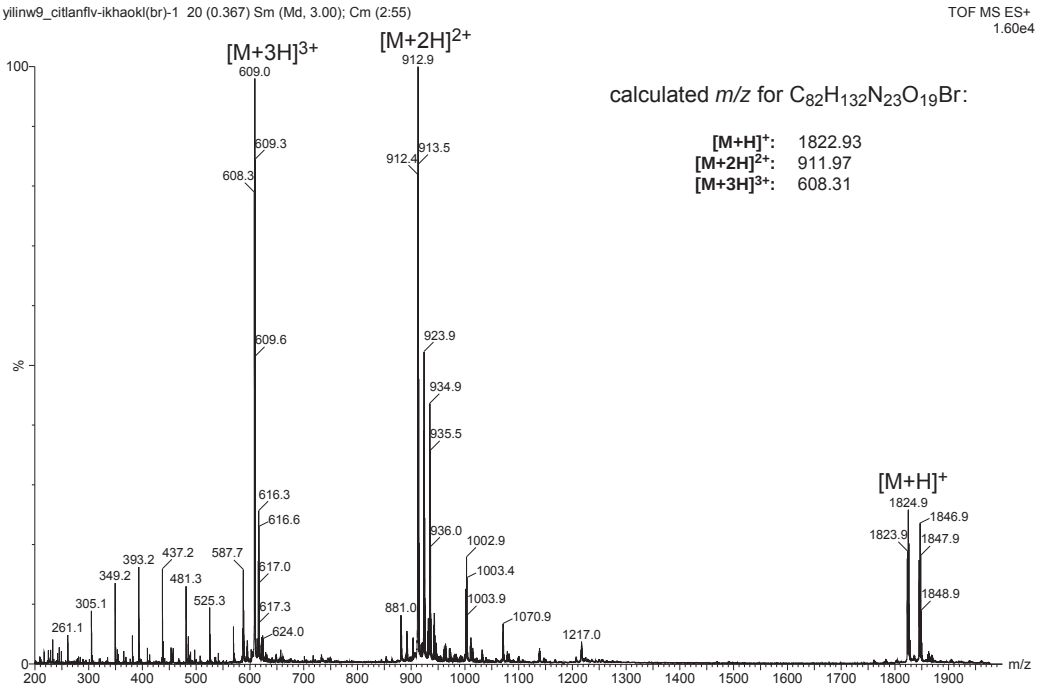

calculated *m/z* for $C_{82}H_{132}N_{23}O_{19}Br$:

$[M+H]^+$: 1822.93
$[M+2H]^{2+}$: 911.97
$[M+3H]^{3+}$: 608.31

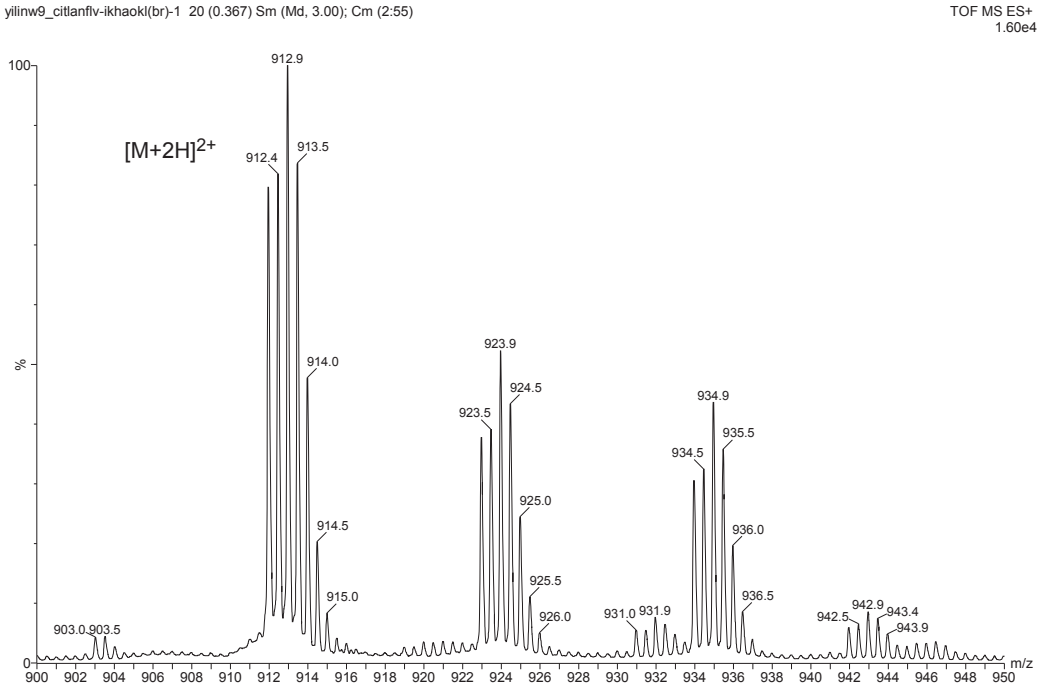
yilinw9_citlanflv-ikhaokl(br)-1 20 (0.367) Sm (Md, 3.00); Cm (2:55)
TOF MS ES+
1.60e4
[M+2H]2+
912.9
912.4
913.5
914.0
914.5
915.0
903.0
903.5
923.9
923.5
924.5
925.0
925.5
926.0
931.0
931.9
934.9
934.5
935.5
936.0
936.5
942.5
942.9
943.4
943.9
%
m/z

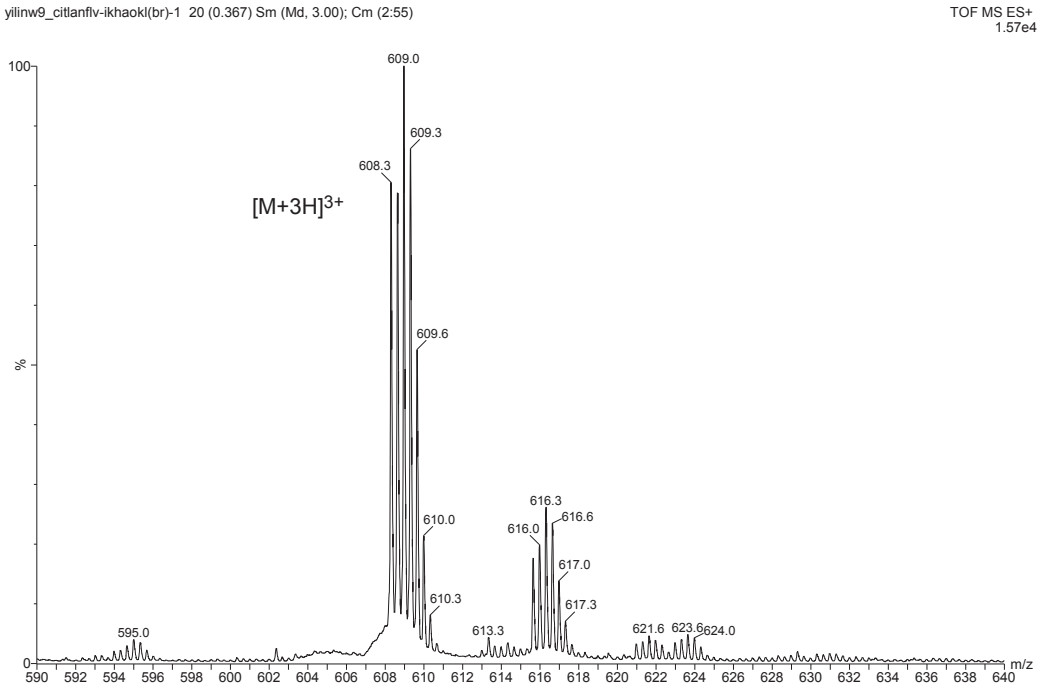
yilinw9_citlanflv-ikhaokl(br)-1 20 (0.367) Sm (Md, 3.00); Cm (2:55)
TOF MS ES+
1.57e4
[M+3H]3+
609.0
609.3
608.3
609.6
610.0
610.3
595.0
613.3
616.3
616.6
616.0
617.0
617.3
621.6
623.6
624.0
%
m/z

^{1}H NMR of macrocyclic β-sheet peptide **2cit**, 1 mM in 100 mM deuterioacetate buffer in D_2O at 500 MHz and 298 K

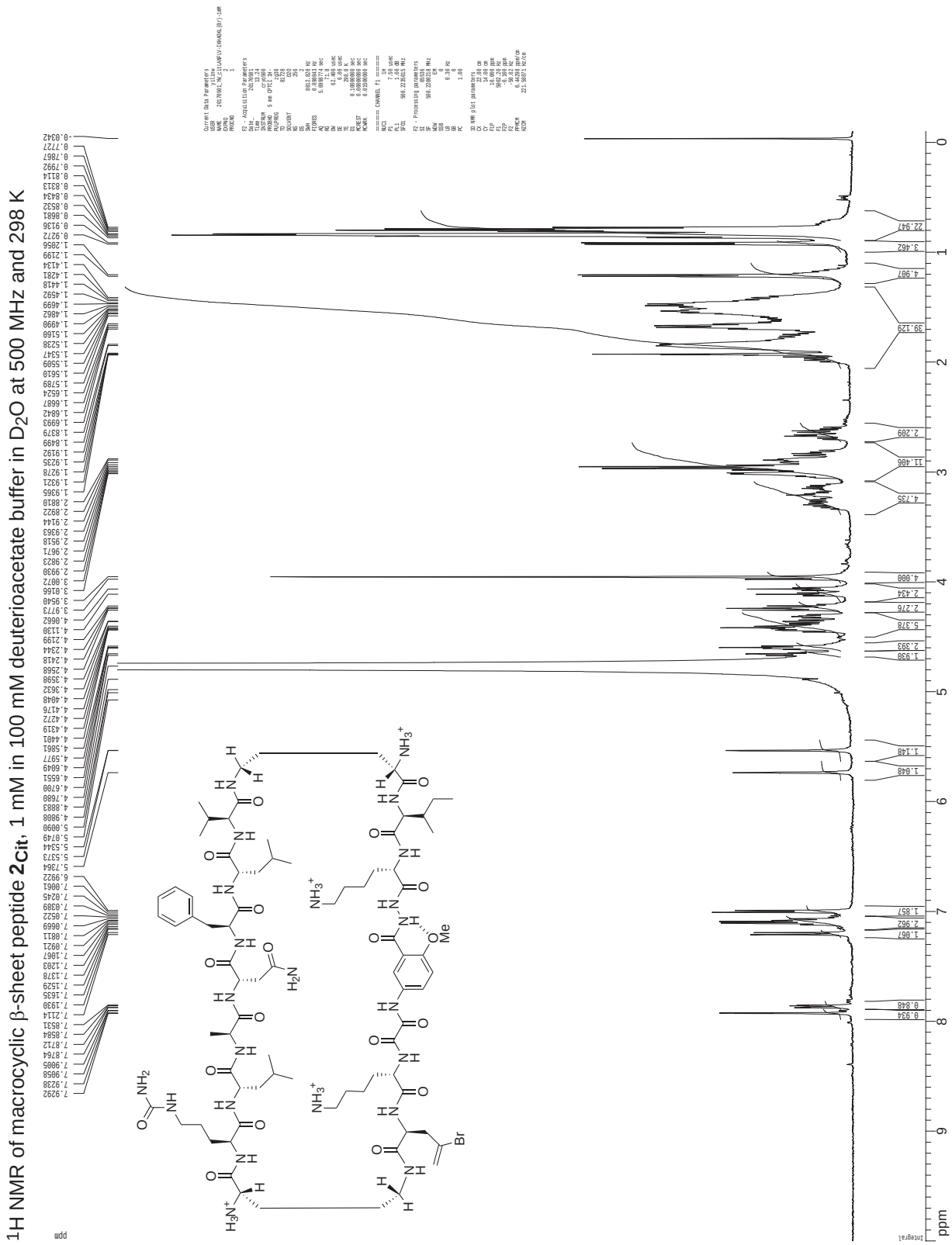

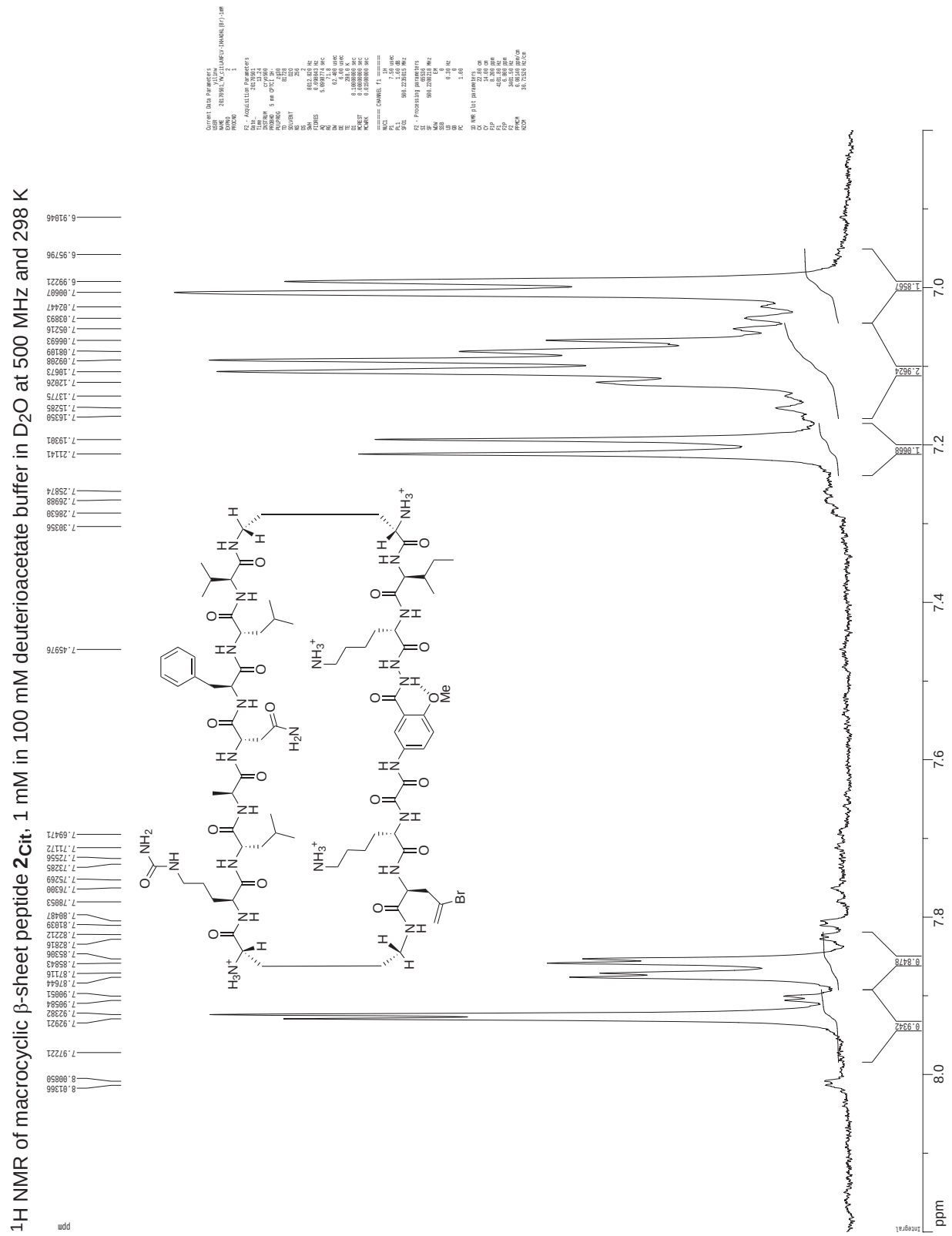
1H NMR of macrocyclic β-sheet peptide 2Cit, 1 mM in 100 mM deuterioacetate buffer in D2O at 500 MHz and 298 K
ppm
integral
7.0
7.2
7.4
7.6
7.8
8.0
1.8567
2.9624
1.0868
0.8478
0.9342
Br
Me
NH2
NH3+

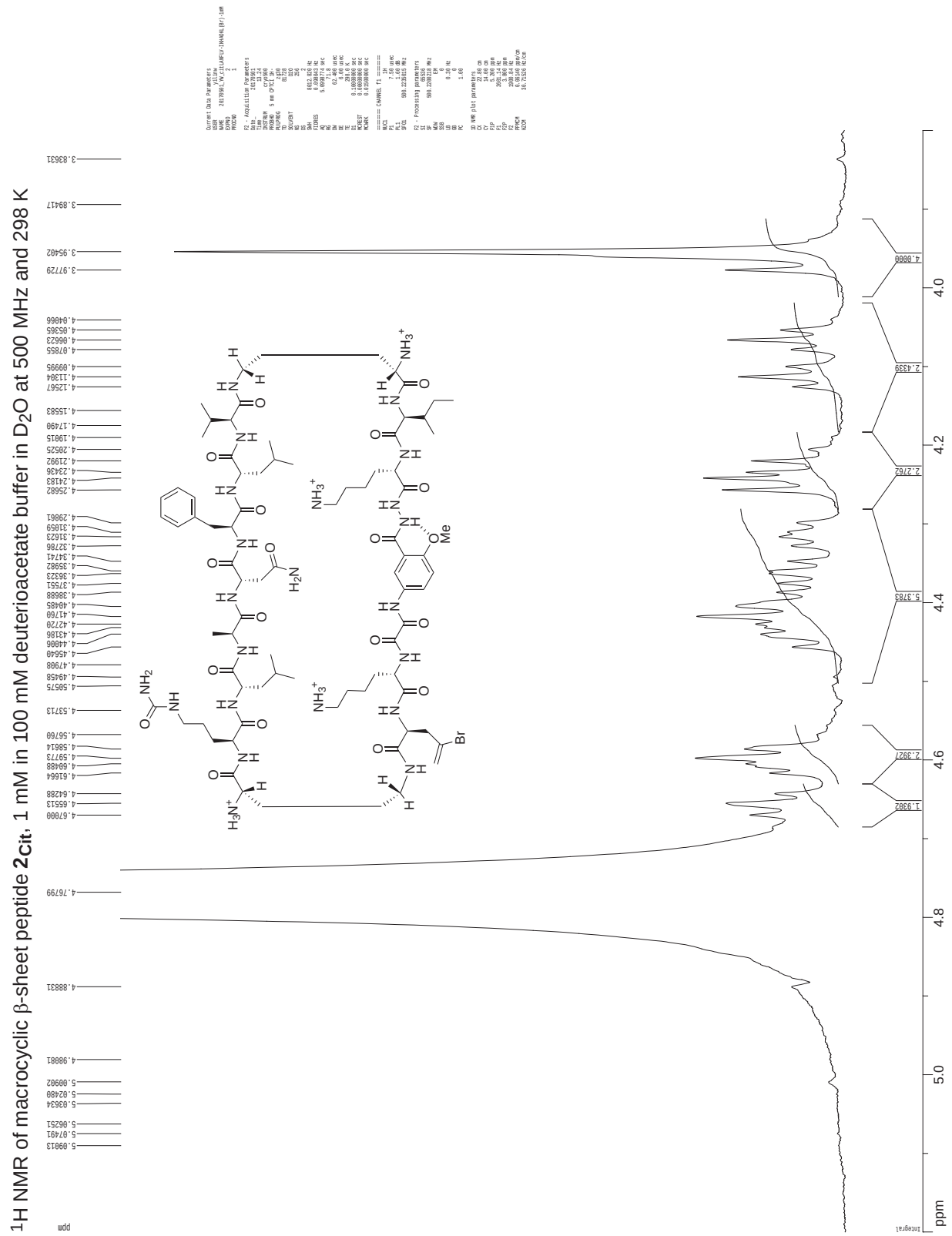
1H NMR of macrocyclic β-sheet peptide 2cit, 1 mM in 100 mM deuterioacetate buffer in D2O at 500 MHz and 298 K
ppm
5.09013
5.07491
5.06251
5.03634
5.02480
5.00902
4.98081
4.88831
4.76799
4.67000
4.65513
4.64288
4.61664
4.60488
4.59773
4.58614
4.56760
4.53713
4.50575
4.49458
4.47908
4.45640
4.44006
4.43186
4.42270
4.41760
4.40485
4.38688
4.37551
4.36323
4.35982
4.34741
4.32786
4.31623
4.31059
4.29861
4.25662
4.24183
4.23436
4.21992
4.20525
4.19015
4.17490
4.15583
4.12567
4.11304
4.09995
4.07855
4.06623
4.05365
4.04866
3.97729
3.95402
3.89417
3.83631
Integral
1.9382
2.3927
5.3783
2.2762
2.4339
4.0000
ppm
5.0
4.8
4.6
4.4
4.2
4.0

^{1}H NMR of macrocyclic β-sheet peptide **2$_{Cit}$**, 1 mM in 100 mM deuterioacetate buffer in D_2O at 500 MHz and 298 K

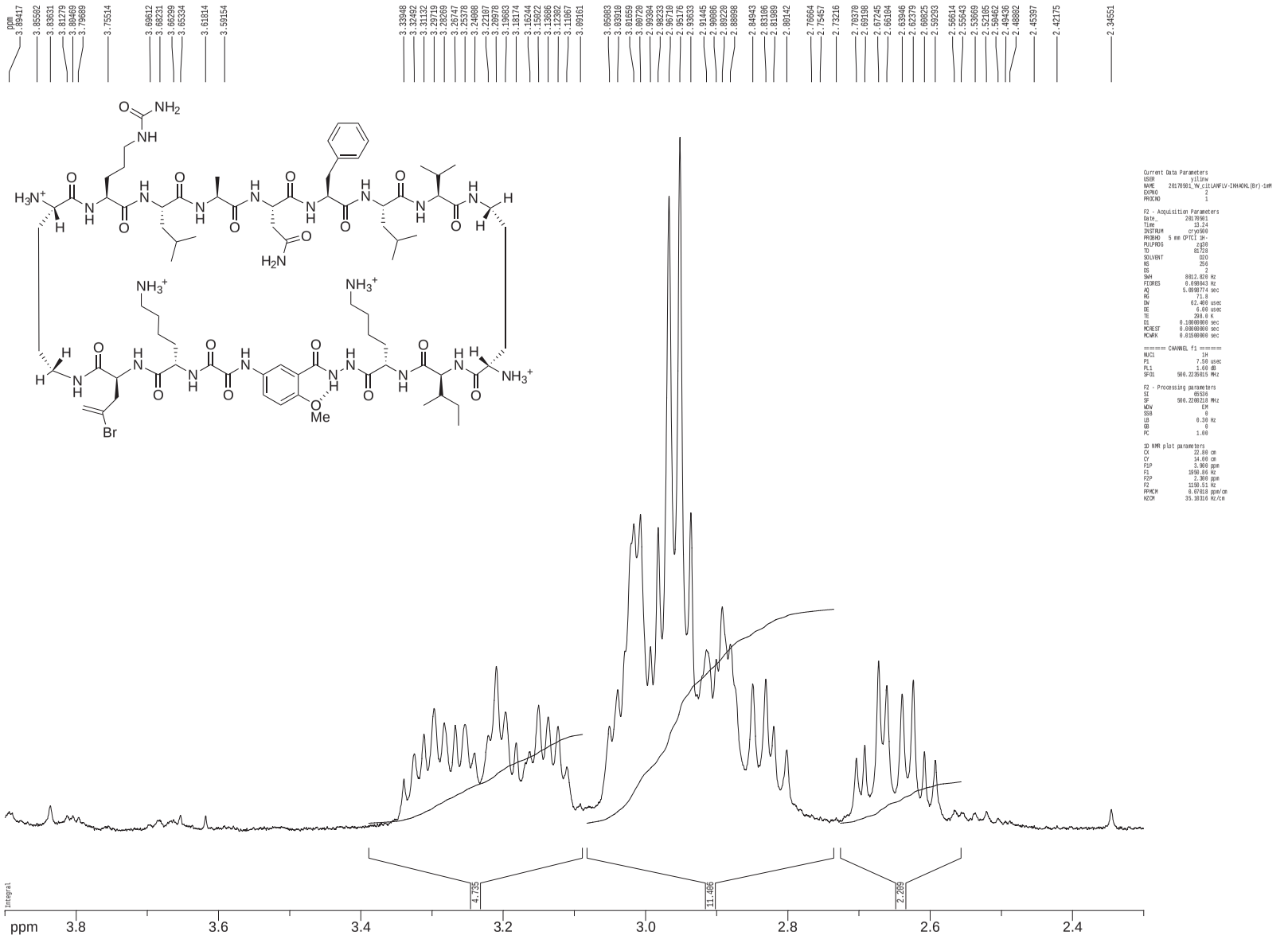

^{1}H NMR of macrocyclic β-sheet peptide **2$_{Cit}$**, 1 mM in 100 mM deuterioacetate buffer in D_2O at 500 MHz and 298 K

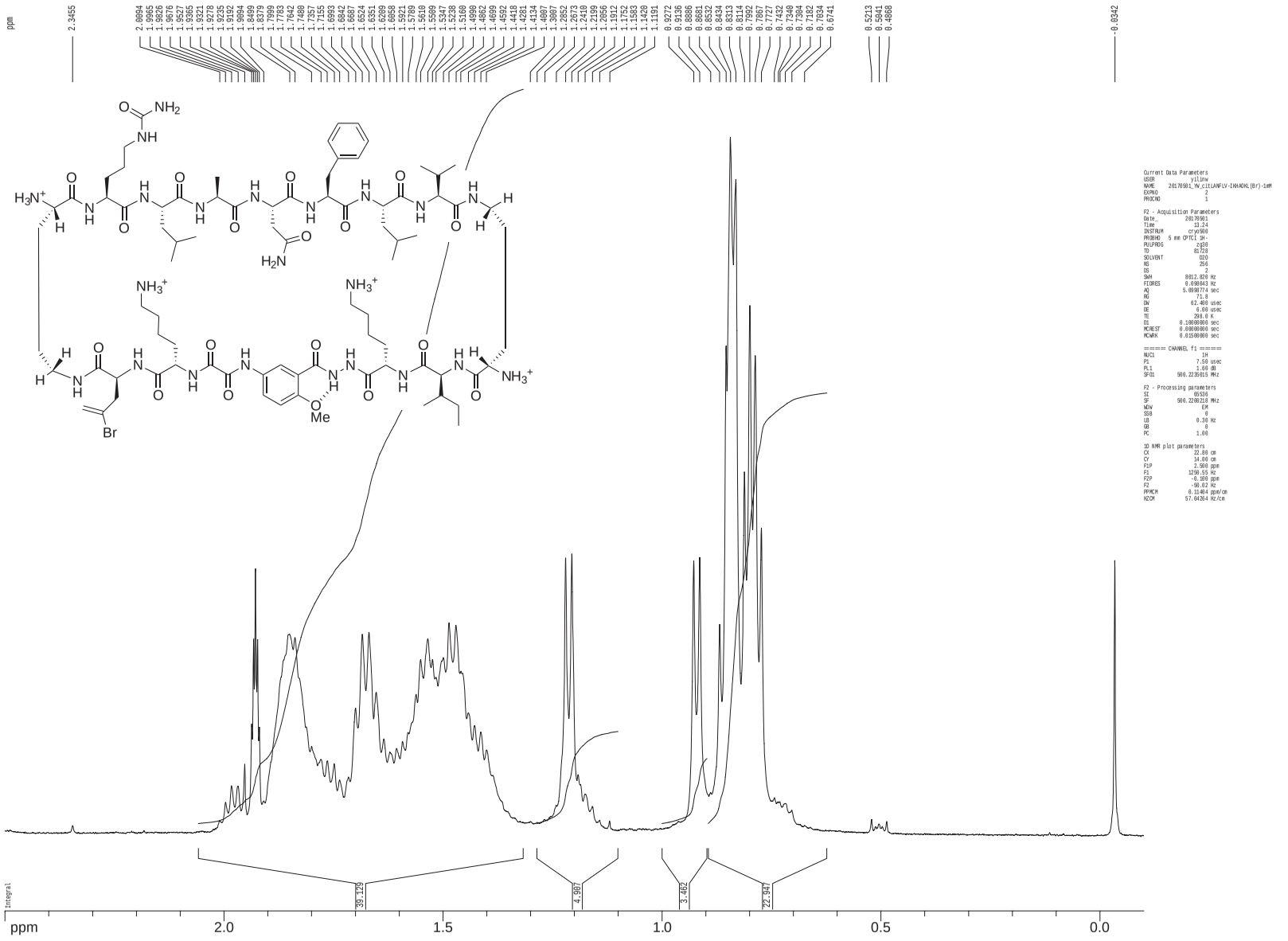

Chapter 4

Effects of Charge and Hydrophobicity on the Oligomerization of a Peptide Derived from IAPP

Introduction

pH provides a critical trigger for changes in protein conformation and structure. Decreases in pH trigger the release of oxygen from hemoglobin in the bloodstream to tissues where it is needed.[1] The cooperative protonation of histidine residues in the hemoglobin tetramer provide the trigger mechanism.[2,3] Decreases in pH also trigger fusion of the endosomal and viral membranes in the transmission of influenza A viruses. This process occurs through the protonation of histidine residues in influenza hemagglutinin, which causes refolding and binding to receptors on the host cells, which then induce endocytosis of the virus.[4-6] Researchers have also exploited variations in pH for drug delivery to environments where there are subtle pH changes.[7-11] Polyhistidine-based micelles were designed to respond to acidic tumour microenvironments and a copolymer nanoparticle incorporating a polyhistidine sequence was designed to increase uptake of antibiotic through acidic bacterial cell walls.[7,8] pH can also provide a conformational switch in the folding of synthetic macromolecules.[12-14] In a recent study, Andersen and coworkers designed a pH switch for β-sheet folding in which the hexapeptide sequence HPATGK switches from unstructured to a turn at physiological and higher pH.[13] Histidine residues provide a good trigger for these biological and biomimetic processes because its protonation state changes near physiological pH.

In the current study, I set out to explore the role of charge and hydrophobicity in peptide self-assembly and ask whether pH can modulate assembly. I performed these studies with a well-characterized peptide model system that assembles to form tetramers in both aqueous solution and in the crystal state.[15,16] The model system consists of macrocyclic β-sheet peptides containing residues 11–17 of the islet amyloid polypeptide (IAPP). Peptides $\mathbf{1}_{\mathbf{Arg}}$ and $\mathbf{1}_{\mathbf{Cit}}$ (Figure 4.2), which I had previously characterized, are representative of the model system. Peptide $\mathbf{1}_{\mathbf{Arg}}$

consists of a peptide strand and a template strand that are connected by two δ-linked ornithine ($^{\delta}$Orn) turn units.[17,18] The peptide strand of $\mathbf{1_{Arg}}$ contains the $IAPP_{11–17}$ heptapeptide sequence RLANFLV, and the template strand contains isoleucine and lysine residues to reinforce hydrophobicity and increase solubility respectively. The unnatural amino acid Hao is centered within the template strand and mimics a tripeptide β-strand, templates β-sheet formation, and blocks uncontrolled aggregation.[19] Peptide $\mathbf{1_{Cit}}$ is a homologue, in which cationic Arg_{11} is replaced by the neutral isostere citrulline. Citrulline contains a urea group in place of the guanidinium group. Peptide $\mathbf{1_{Cit}}$ assembles to form tetramers at low millimolar concentrations in aqueous solution (Figure 4.1), whereas Peptide $\mathbf{1_{Arg}}$ is monomeric under these conditions.

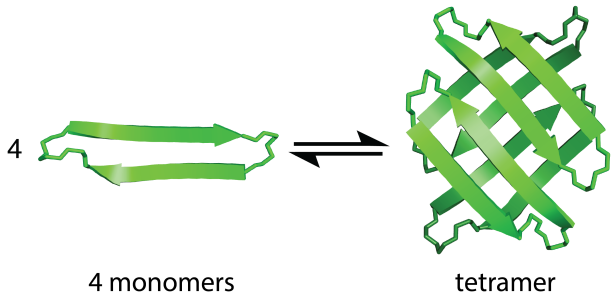

Figure 4.1. Tetramer formation of peptide $\mathbf{1_{Cit}}$. X-ray crystallographic structure of the tetramer and of the monomer subunit of a heavy atom derivative of peptide $\mathbf{1_{Cit}}$ (PDB 5UHR). The tetramer consists of a sandwich of hydrogen-bonded dimers laminated through hydrophobic interactions.

Inspired by my previous results and by the role of pH in protein interactions, I further explored the role of charge and hydrophobicity in the assembly of macrocyclic β-sheet peptides derived from $IAPP_{11–17}$. I incorporated glutamic acid at position 11 to create peptide $\mathbf{1_{Glu}}$, and leucine at position 11 to create peptide $\mathbf{1_{Leu}}$, and I studied the assembly of the peptides by NMR spectroscopy (Figure 4.2). My efforts culminated in peptide $\mathbf{1_{His}}$, a macrocyclic β-sheet peptide that changes oligomerization state in response to pH.

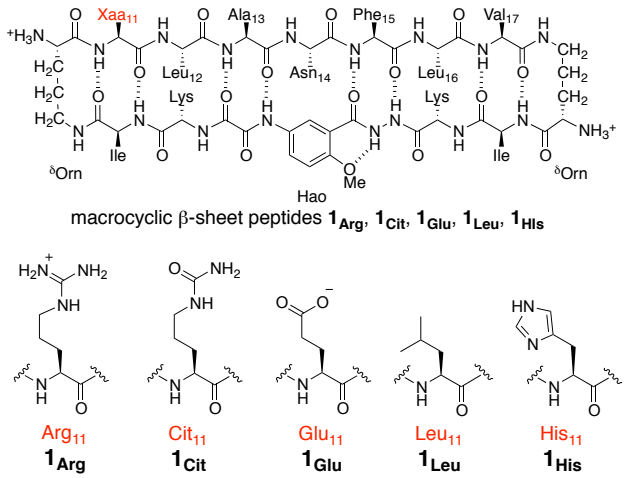

Figure 4.2. Chemical structure of macrocyclic β-sheet peptides peptides $\mathbf{1}_{\mathbf{Arg}}$, $\mathbf{1}_{\mathbf{Cit}}$, $\mathbf{1}_{\mathbf{Glu}}$, $\mathbf{1}_{\mathbf{Leu}}$, and $\mathbf{1}_{\mathbf{His}}$ with different residues at position 11.

Results and Discussion

The ^{1}H NMR spectrum of macrocyclic β-sheet peptides reflects their oligomerization state.[15,16,20-22] In the monomeric state, resonances are sharp and are generally at values typical of the corresponding random coil amino acids.[23] In the tetrameric state, resonances are often broader, the resonances of the α-protons are generally shifted downfield and the aromatic resonances are often shifted upfield.

In aqueous solution at 298 K, ^{1}H NMR spectrum of peptide $\mathbf{1}_{\mathbf{Arg}}$ at 4 mM displays a single set of sharp resonances, indicating that the peptide is monomeric (Figure 4.3). The resonances associated with the α-protons are upfield of the HOD peak at around 4–5 ppm and the resonances associated with the Phe_{15} side chain are at around 7 ppm, showing little to no shifting relative to the typical values for the corresponding residues in a random coil confirmation.[23] At 8 mM, the ^{1}H NMR spectrum of peptide $\mathbf{1}_{\mathbf{Arg}}$ shows broadening of the resonances but no additional peaks associated with the onset of peptide self association. ^{1}H NMR spectrum of peptide $\mathbf{1}_{\mathbf{Cit}}$ at 1 mM resembles the ^{1}H spectrum of peptide $\mathbf{1}_{\mathbf{Arg}}$ and displays a single set of sharp resonances, indicating that the peptide is monomeric. At 4 mM, peptide $\mathbf{1}_{\mathbf{Cit}}$ displays two sets of broad

resonances associated with the monomer and the tetramer, and at 16 mM only the resonances associated with the tetramer are visible. The tetramer resonances associated with the α-protons are shifted downfield by up to 1 ppm relative to those of random coil α-protons. The aromatic resonances associated with the Phe_{15} side chain are shifted upfield from 7.0 to 6.5 ppm. The shifting of the resonances reflects the folding and assembly of the peptide into a tetramer.

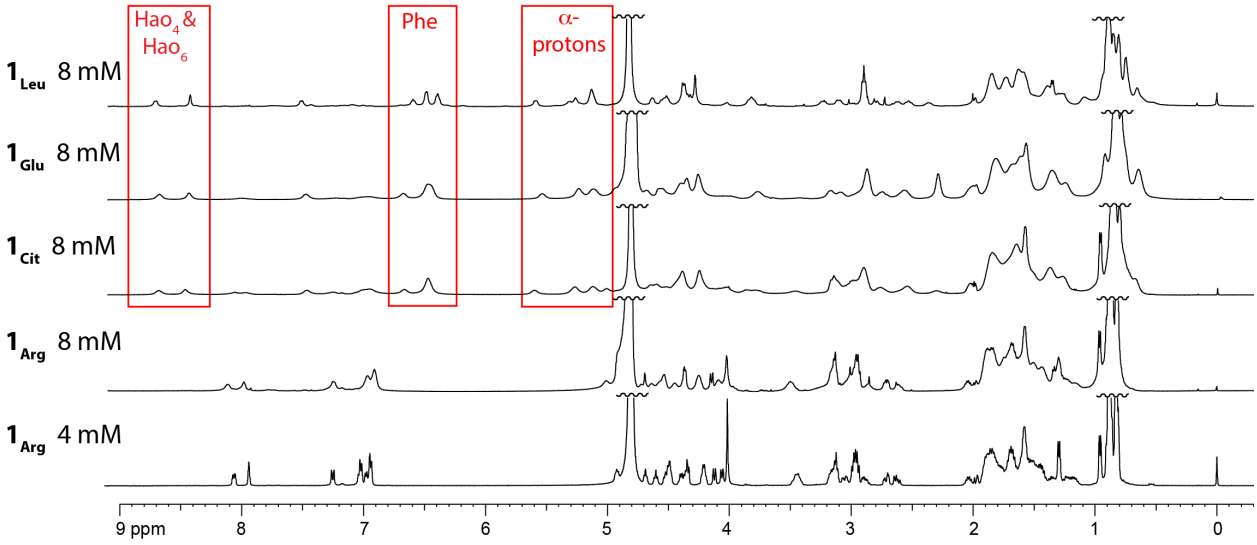

Figure 4.3. ^{1}H NMR spectra of macrocyclic β-sheet peptides $\mathbf{1}_{Arg}$, $\mathbf{1}_{Cit}$, $\mathbf{1}_{Glu}$, and $\mathbf{1}_{Leu}$ in 50 mM CD_3COOD and 50 mM CD_3COONa buffer in D_2O at 298 K. The red boxes highlight key resonances in the tetramer.

The magnetic anisotropy of the diastereotopic δ-protons of the $^{\delta}$Orn turn units reflects β-sheet folding in macrocyclic β-sheet peptides.[18] Previous studies in our laboratory have shown that complete folding accompanies oligomerization.[15,20,21] In a well-folded macrocyclic β-sheet peptide, each diastereotopic *pro-S* δ-proton resonance is about 0.6 ppm downfield of the corresponding *pro-R* δ-proton resonance. The ^{1}H NMR spectrum of monomeric peptide $\mathbf{1}_{Arg}$ shows that it is partially folded, with average difference in chemical shifts being 0.31 ppm. In contrast, the monomer subunits of the tetramer formed by peptides $\mathbf{1}_{Cit}$, $\mathbf{1}_{Glu}$, and $\mathbf{1}_{Leu}$ are well folded with average differences in chemical shifts being 0.68, 0.64, 0.66 ppm, respectively (Table 4.1).

Table 4.1. $\Delta\delta^{\delta}$Orn values of peptides $\mathbf{1}_{\mathbf{Arg}}$, $\mathbf{1}_{\mathbf{Cit}}$, $\mathbf{1}_{\mathbf{Glu}}$, $\mathbf{1}_{\mathbf{Leu}}$, $\mathbf{1}_{\mathbf{His}}$ in D_2O at 298 K.

	pH	Conc (mM)	$\Delta\delta^{\delta}$Orn (ppm)	$\Delta\delta^{\delta}$Orn (ppm)	average $\Delta\delta^{\delta}$Orn (ppm)
$\mathbf{1}_{\mathbf{Arg}}$	4.7 [a]	4	0.31	0.31	0.31
$\mathbf{1}_{\mathbf{Cit}}$	4.7 [a]	16	0.70	0.66	0.68
$\mathbf{1}_{\mathbf{Glu}}$	4.7 [a]	16	0.69	0.59	0.64
$\mathbf{1}_{\mathbf{Leu}}$	4.7 [a]	16	0.71	0.60	0.66
$\mathbf{1}_{\mathbf{His}}$	2.5 [b]	1	0.29	0.29	0.29
$\mathbf{1}_{\mathbf{His}}$	2.5 [b]	16	0.47	0.47	0.47
$\mathbf{1}_{\mathbf{His}}$	4.7 [a]	16	0.51	0.51	0.51
$\mathbf{1}_{\mathbf{His}}$	7.2 [c]	16	0.57	0.77	0.67

[a] 50 mM CD_3COOD and 50 mM CD_3COONa buffered D_2O.
[b] Unbuffered peptide in D_2O.
[c] 50 mM CD_3COOD and 50 mM CD_3COONa buffered D_2O with the pH adjusted to 7.2 with NaOD.

To better understand how charge and hydrophobicity affect oligomerization, I compared homologues $\mathbf{1}_{\mathbf{Cit}}$, $\mathbf{1}_{\mathbf{Glu}}$, and $\mathbf{1}_{\mathbf{Leu}}$ and evaluated the effects of the respective polar, acidic, and hydrophobic residues at position 11. Peptides $\mathbf{1}_{\mathbf{Cit}}$, $\mathbf{1}_{\mathbf{Glu}}$, and $\mathbf{1}_{\mathbf{Leu}}$ are monomeric at submillimolar concentrations in aqueous solution, but form tetramers at millimolar concentrations (Figure 4.5 and 4.6). The ^{1}H NMR spectra of peptides $\mathbf{1}_{\mathbf{Cit}}$, $\mathbf{1}_{\mathbf{Glu}}$, and $\mathbf{1}_{\mathbf{Leu}}$ show only single sets of sharp resonances associated with the monomer at 0.1 mM. The chemical shifts of the α-proton and aromatic resonances are similar to those of peptide $\mathbf{1}_{\mathbf{Arg}}$, reflecting the monomeric state of the peptides at low concentrations (Figure 4.3). At 8 mM, each of the three peptides display two sets of resonances, which correspond to the monomer and the tetramer (Figure 4.2, 4.5, and 4.6). The ^{1}H NMR spectra of the three peptides are broad, and key resonances appear at similar positions, with the α-proton resonances of the tetramers being shifted downfield and the aromatic resonances shifted upfield.

To assess the propensities of peptides $\mathbf{1}_{\mathbf{Cit}}$, $\mathbf{1}_{\mathbf{Glu}}$, and $\mathbf{1}_{\mathbf{Leu}}$ to form tetramers, I measured the monomer–tetramer ratios at 1, 2, 4, and 8 mM by ^{1}H NMR spectroscopy. Integration of the Hao_6

and Hao_4 resonances permits the measurement of the monomer and the tetramer ratio (Figure 4.4). Peptide $\mathbf{1}_{Cit}$ is about 50% tetrameric at 4 mM, peptide $\mathbf{1}_{Glu}$ is 50% tetrameric at 2 mM, and peptide $\mathbf{1}_{Leu}$ is 50% tetrameric at just above 1 mM. These studies show the following propensities for these peptides to form tetramers: $\mathbf{1}_{Leu} > \mathbf{1}_{Glu} > \mathbf{1}_{Cit} >> \mathbf{1}_{Arg}$.

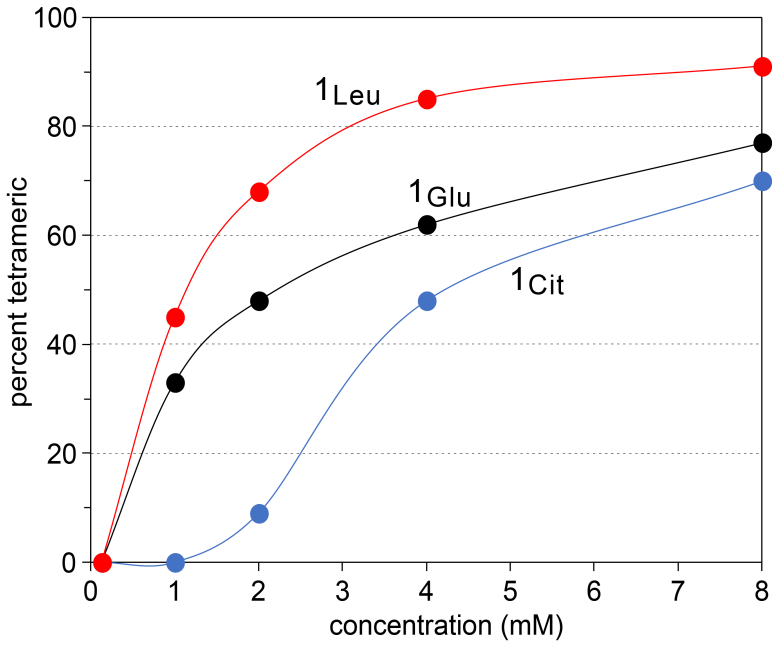

Figure 4.4. Percentage of tetrameric peptides $\mathbf{1}_{Cit}$, $\mathbf{1}_{Glu}$, and $\mathbf{1}_{Leu}$ at 1, 2, 4, and 8 mM. The values are derived from integrations of the Hao_4 and Hao_6 resonances of the tetramer and the monomer.

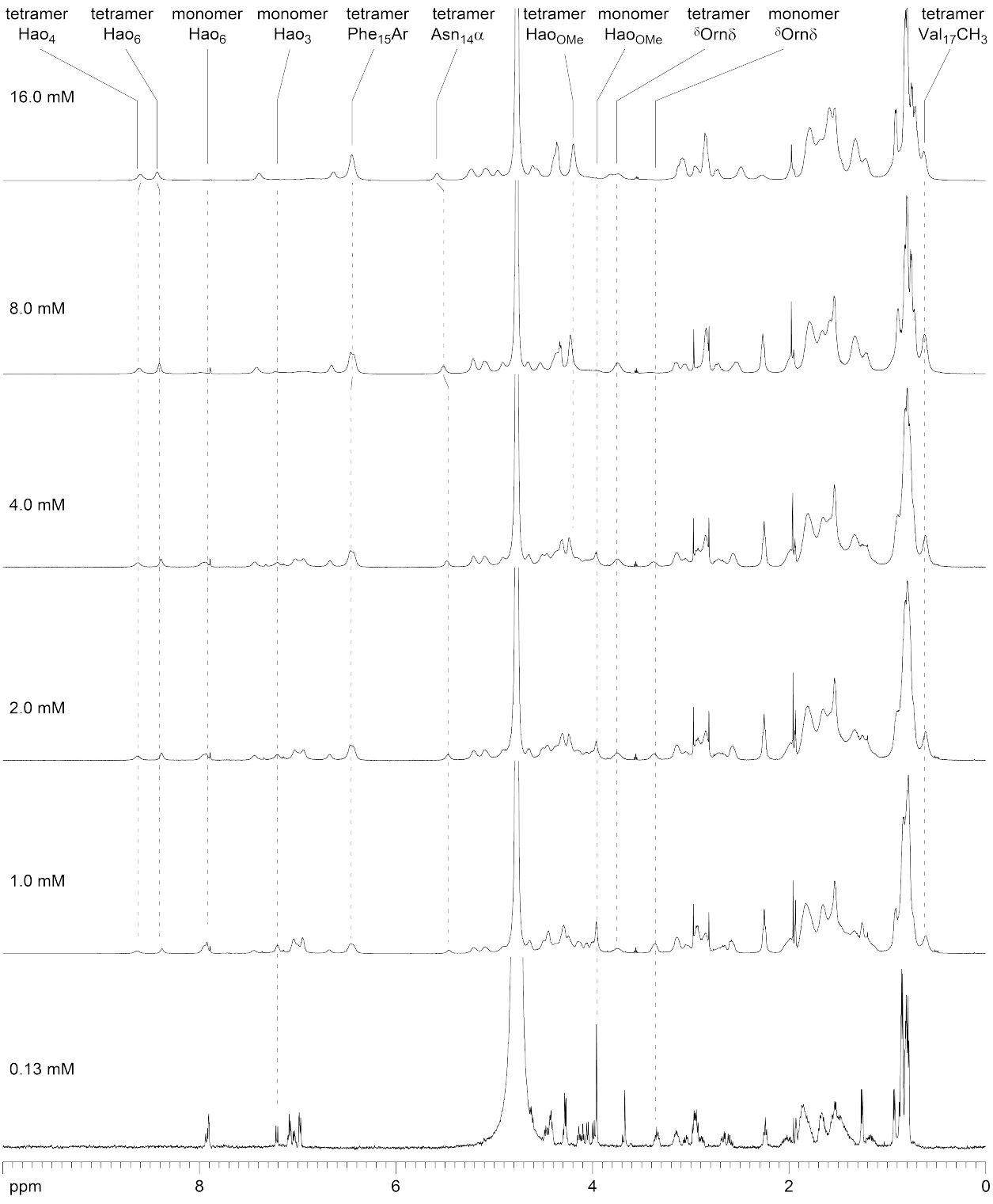

Figure 4.5. ^{1}H NMR spectra of peptide $\mathbf{1_{Glu}}$ various concentrations and 50 mM CD_3COOD and 50 mM CD_3COONa buffer in D_2O at 500 MHz and 298K.

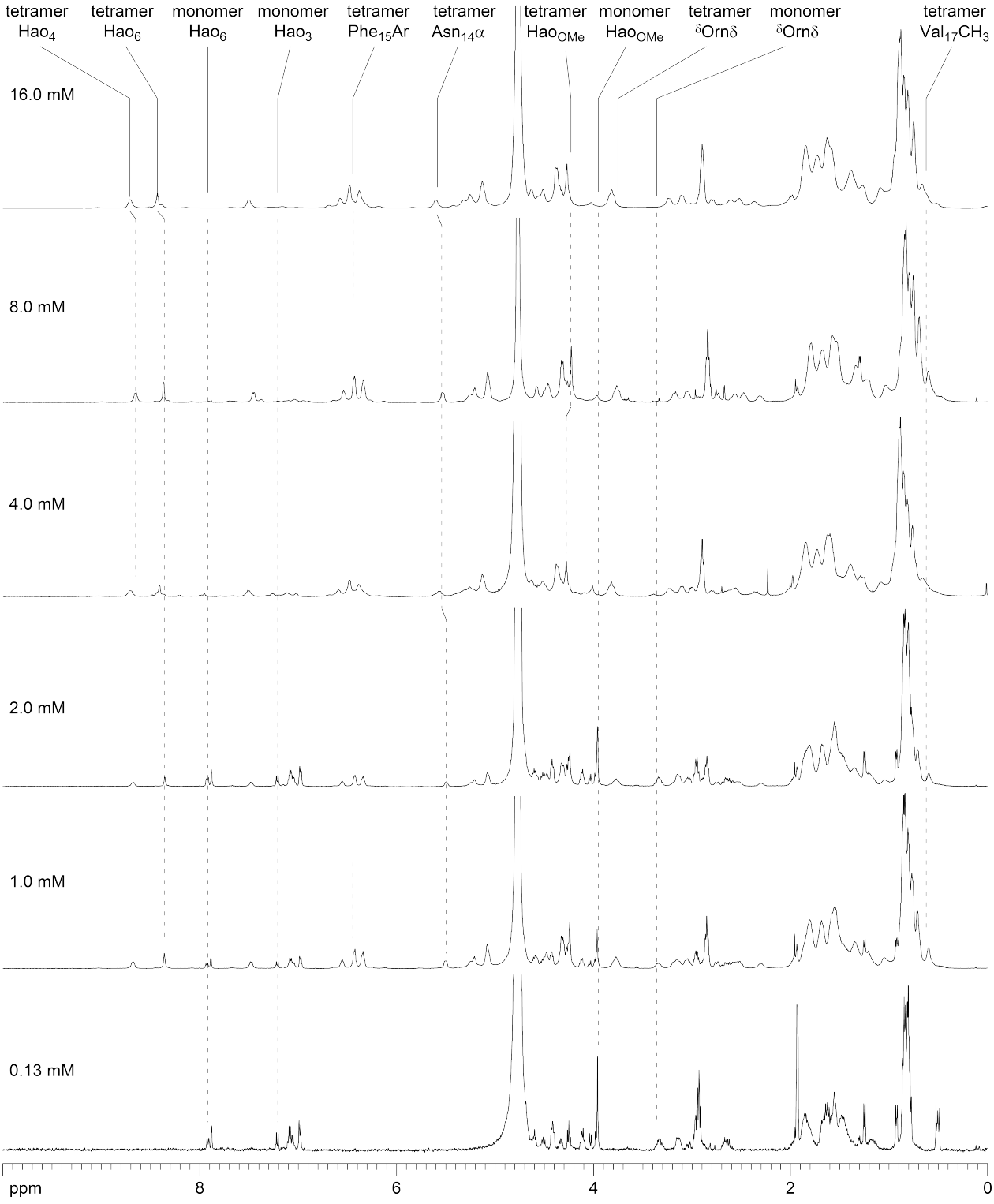

Figure 4.6. ^{1}H NMR spectra of peptide $\mathbf{1_{Glu}}$ various concentrations and 50 mM CD_3COOD and 50 mM CD_3COONa buffer in D_2O at 500 MHz and 298K.

Electrostatic and hydrophobic interactions explain the relative propensities of peptides $\mathbf{1}_{\mathbf{Cit}}$, $\mathbf{1}_{\mathbf{Glu}}$, $\mathbf{1}_{\mathbf{Leu}}$, and $\mathbf{1}_{\mathbf{Arg}}$ to form tetramers in aqueous solution. I previously observed that a derivative of peptide $\mathbf{1}_{\mathbf{Cit}}$ containing a heavy atom forms sandwich like tetramers (Figure 4.1). The crystallographic structure (PDB 5UHR) shows the side chain of Cit_{11} is proximal to the protonated α-amine of Orn in the dimer subunits of the tetramer. This interaction is crucial to the propensity of tetramer formation. Peptide $\mathbf{1}_{\mathbf{Leu}}$ has the highest propensity to oligomerize as it has a non-polar residue at position 11, which can further contribute to the hydrophobic core. Peptide $\mathbf{1}_{\mathbf{Glu}}$ has the second highest propensity to oligomerize as it has a negatively charged, polar residue at position 11, which allows for electrostatic attraction or the formation of a salt bridge with the α-amine of ^{s}Orn. Peptide $\mathbf{1}_{\mathbf{Cit}}$ has the lowest propensity to oligomerize as it has a polar, neutral side chain. In contrast, peptide $\mathbf{1}_{\mathbf{Arg}}$ does not oligomerize as the electrostatic repulsion of the positively charged side chain of Arg_{11} and the protonated α-amine of ^{s}Orn inhibits the formation of the dimer.

Diffusion-ordered spectroscopy (DOSY) provides a convenient method to assess the relative oligomerization state of macrocyclic β-sheet peptides **1**. Dimers typically have a diffusion coefficient of about 0.75–0.79 times that of monomers, and tetramers have a diffusion coefficient of about 0.58–0.63 times that of monomers.[15,16,20,24,25] We have previously observed that monomers exhibit a diffusion coefficient of about 20×10^{-7} cm^2/s, while tetramers exhibit a diffusion coefficient of about 12×10^{-7} cm^2/s in deuterioacetate buffered D_2O at 298 K. At 16 mM, diffusion coefficient of peptides $\mathbf{1}_{\mathbf{Glu}}$ and $\mathbf{1}_{\mathbf{Leu}}$ are consistent with that of tetramers. In deuterioacetate buffer at pH 4.7 and 7.2, the diffusion coefficient of peptide $\mathbf{1}_{\mathbf{Glu}}$ are 12.1 and 12.4×10^{-7} cm^2/s, respectively (Table 4.2). At pH 4.7 and 7.2 in deuterioacetate buffer, the diffusion coefficient of peptide $\mathbf{1}_{\mathbf{Leu}}$ are 11.4 and 12.3×10^{-7} cm^2/s, respectively.

Table 4.2. Diffusion coefficients (*D*) of peptides $\mathbf{1_{Glu}}$, $\mathbf{1_{Leu}}$, $\mathbf{1_{His}}$ in D_2O at 298 K.

	conc (mM)	pH	*D* (10^{-7} cm^2/s)	oligomer state
$\mathbf{1_{Glu}}$	16	4.7[a]	12.1 ± 0.6	tetramer
$\mathbf{1_{Glu}}$	16	7.2[c]	12.4 ± 0.3	tetramer
$\mathbf{1_{Leu}}$	16	4.7[a]	11.4 ± 0.5	tetramer
$\mathbf{1_{Leu}}$	16	7.2[c]	12.3 ± 1.3	tetramer
$\mathbf{1_{His}}$	1	2.5[b]	19.8 ± 0.8	monomer
$\mathbf{1_{His}}$	4	2.5[b]	16.8 ± 0.6	dimer
$\mathbf{1_{His}}$	8	2.5[b]	16.4 ± 0.9	dimer
$\mathbf{1_{His}}$	16	2.5[b]	16.4 ± 0.3	dimer
$\mathbf{1_{His}}$	16	4.7[a]	16.0 ± 0.3	dimer
$\mathbf{1_{His}}$	16	7.2[c]	12.3 ± 1.2	tetramer

[a] 50 mM CD_3COOD and 50 mM CD_3COONa buffered D_2O.
[b] Unbuffered peptide in D_2O.
[c] 50 mM CD_3COOD and 50 mM CD_3COONa buffered D_2O with the pH adjusted to 7.2 with NaOD.

NOESY NMR spectroscopy establishes that the structure of the tetramer formed by peptides $\mathbf{1_{Leu}}$ and $\mathbf{1_{Glu}}$ in aqueous solution is similar to the tetramer previously observed for peptide $\mathbf{1_{Cit}}$.[22] The spectrum exhibits NOEs that correspond to the intramolecular contacts of the monomer, intermolecular contact of the dimer, and intermolecular contact of the tetramer. Three strong crosspeaks in the NOESY spectrum of peptides $\mathbf{1_{Leu}}$ indicate that the macrocyclic β-sheet monomers are well-folded, one between the α-protons of Leu_{12} and Lys, one between the α-protons of Leu_{16} and Lys, and one between the α-proton of Asn_{14} and the proton at the 6-position of the tripeptide mimic Hao (Figure 4.8). In addition, a strong crosspeak between the α-protons of Ala_{13} and Val_{17} reflect a shifted, antiparallel dimer formation where the two heptapeptide β-strands are shifted by two residues towards the C-termini (Figure 4.7). A characteristic NOE between the methoxy group of Hao and the Ile side chain reflects packing of the dimers to form a sandwich like tetramer. The NOESY of peptide $\mathbf{1_{Glu}}$ exhibits the same NOE crosspeaks with the exception of one of the Leu-Lys crosspeaks that is buried due to overlap. These NOEs associated with the folded monomer, dimer, and tetramer indicate that peptides $\mathbf{1_{Leu}}$ and $\mathbf{1_{Glu}}$ form the same tetramer structure as peptide $\mathbf{1_{Cit}}$ in solution.

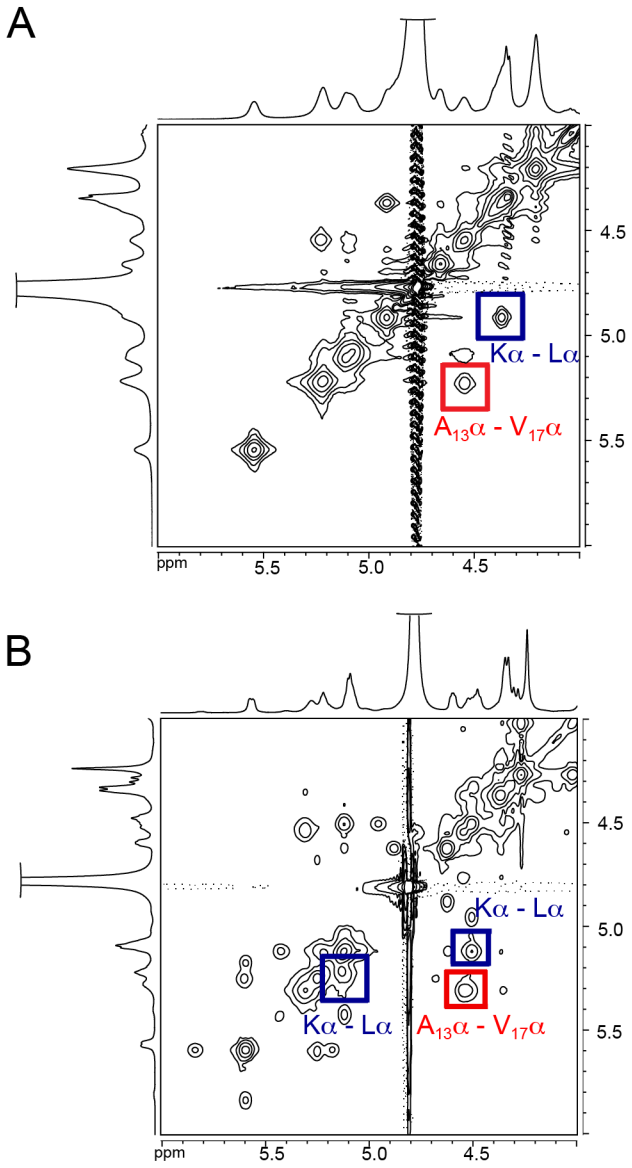

Figure 4.7. NOEs associated with the dimer subunit of peptide $\mathbf{1}_{\mathbf{Glu}}$ and $\mathbf{1}_{\mathbf{Leu}}$ (A) Expansion of the NOESY spectrum of peptide $\mathbf{1}_{\mathbf{Glu}}$ showing selected intramolecular (blue) and intermolecular (red) NOE crosspeaks. (B) Expansion of the NOESY spectrum of peptide $\mathbf{1}_{\mathbf{Leu}}$ showing selected intramolecular (blue) and intermolecular (red) NOE crosspeaks.

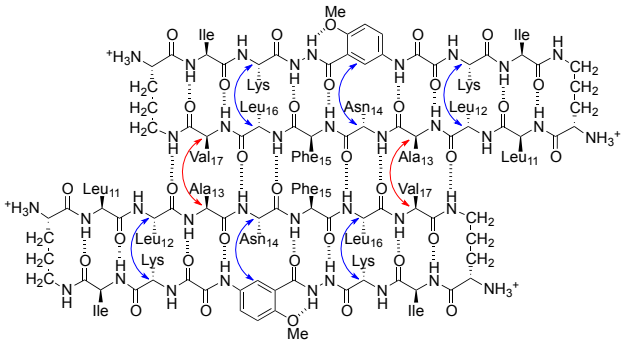

Figure 4.8. Shifted, antiparallel hydrogen-bonded dimer of peptide $\mathbf{1_{Leu}}$. Blue arrows indicate intramolecular NOEs and red arrows indicate intermolecular NOEs observed in the NOESY spectrum. For peptide $\mathbf{1_{Glu}}$, the Leu-Lys crosspeak cannot be observed due to overlap.

Inspired by these results and the role of pH in triggering changes in protein structure and interactions, I incorporated a histidine residue at position 11. I envisioned that peptide $\mathbf{1_{His}}$ would change oligomerization state when triggered by the protonation of histidine ($pK_a \sim 6$). Below pH 6, it would form a monomer as the imidazole side chain is predominantly protonated, making it cationic like arginine. As the pH increases above 6, it would form a tetramer as the imidazole side chain loses a proton, making it neutral, like citrulline and leucine.

At pH 2.5, peptide $\mathbf{1_{His}}$ is monomeric at 1 mM. The ^{1}H NMR spectrum of peptide $\mathbf{1_{His}}$ exhibits a single set of sharp resonances, associated with the monomer (Figure 4.8). Similar to previous results, the resonances associated with the α-protons are in the 4–5 ppm range, showing little to no downfield shifting relative to the typical values of the corresponding residues in a random coil conformation. The aromatic resonances of the Phe_{15} side chains are at approximately 7 ppm, corresponding to typical random coil chemical shifts. The diffusion coefficient at 1 mM and pH 2.5 is 20.1×10^{-7} cm^2/s, congruent with the diffusion coefficient of the monomeric peptide $\mathbf{1_{Arg}}$.

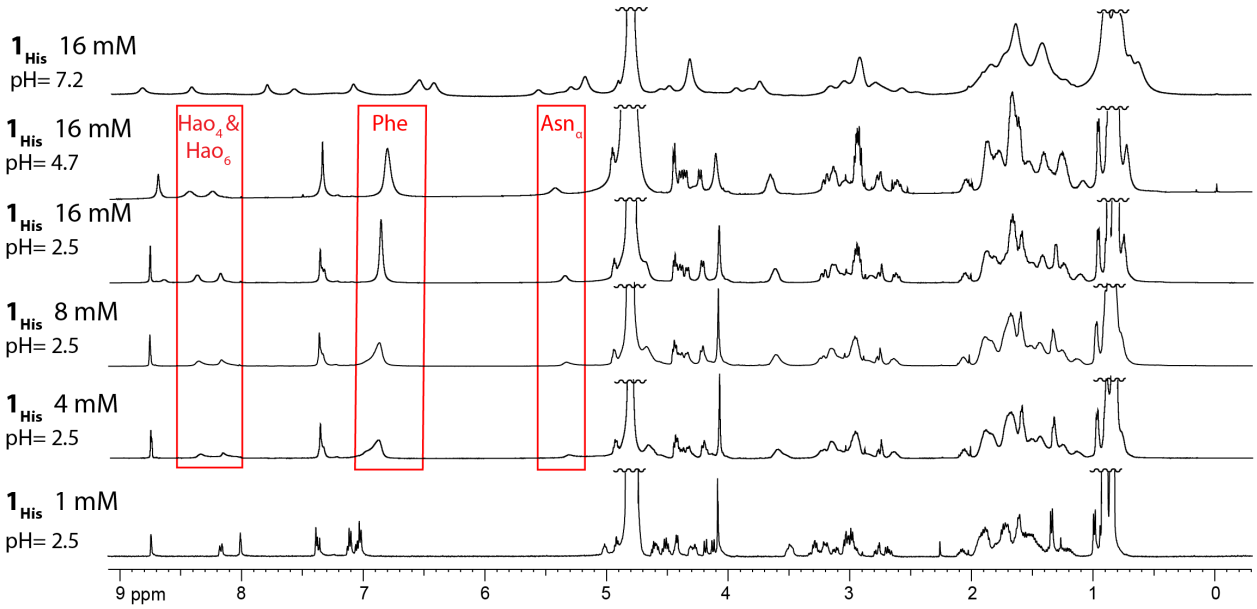

Figure 4.9. ^{1}H NMR spectra of macrocyclic β-sheet peptides $\mathbf{1}_{\mathbf{His}}$. Spectra at pH 2.5 are in D_2O. Spectrum at pH 4.7 are in 50 mM CD_3COOD and 50 mM CD_3COONa buffer in D_2O at 298 K. Spectrum at pH 7.2 are in 50 mM CD_3COOD and 50 mM CD_3COONa buffer adjusted to pH 7.2 with NaOD in D_2O at 298 K. The red boxes highlight key resonances in the dimer.

At higher concentrations at pH 2.5, peptide $\mathbf{1}_{\mathbf{His}}$ forms a dimer—an oligomerization state that the Nowick group has not previously observed in Hao-containing macrocyclic β-sheet peptides. The ^{1}H NMR resonances are somewhat broadened at 4 and 8 mM, but are sharp at 16 mM (Figure 4.9). The diffusion coefficients at 4 mM, 8 mM, and 16 mM are 16.8, 16.4, and 16.4 $\times 10^{-7}$ cm^2/s respectively (Table 4.2). These values are 0.84–0.82 times that of the monomer, best matching a dimer and not matching a tetramer. The lack of change in diffusion coefficient from 8 mM to 16 mM indicates that the observed spectrum does not correspond to a rapid monomer-tetramer equilibrium, but instead represents a unique species — a dimer.

The spectrum of the dimer differs from that of the monomer and those of the other tetramers. The aromatic resonances of Phe_{15} are shifted upfield by 0.2 ppm to 6.8 ppm, and the Hao_4 and Hao_6 resonances are shifted downfield by 0.2 ppm to 8.3 and 8.1 ppm respectively. The monomer subunit of the dimer folds better than the free monomer with the average difference in

chemical shifts of the diastereotopic *pro-S* and *pro-R* δ-protons of the δ-linked ornithine turn units increasing from 0.29 ppm at 1 mM to 0.47 ppm at 16 mM.

NOESY spectroscopy reveals relatively little about the structure of the dimer. The NOESY spectrum of peptide $\mathbf{1_{His}}$ at pH 2.5 and 16 mM shows negative NOEs, as would be expected for an oligomer but not a monomer. A crosspeak between the α-protons of Leu and Lys and a crosspeak between the α-proton of Asn_{14} and the proton at the 6-position of the Hao residue shows that the monomer subunit is folded into a β-sheet. No additional NOE crosspeaks between α-protons are observed, which may reflect overlap of resonances or the lack of edge-to-edge contacts between the folded monomer subunits. NOE crosspeaks between the side chain of Phe_{15} and one of the isoleucine residues suggest hydrophobic packing, as do weaker NOE crosspeaks between the isoleucine side chain and the methoxy group of Hao.

Upon increasing the pH to pH 7.2, the ^{1}H NMR spectrum changes dramatically. At pH 4.7 and 16 mM, the spectrum largely resembles that at pH 2.5, it is slightly broadened and the diffusion coefficient is 16.0×10^{-7} cm^2/s, suggesting the onset of further self association. At pH 7.2, the diffusion coefficient of peptide $\mathbf{1_{His}}$ at 16 mM is 12.3×10^{-7} cm^2/s, congruent with the formation of a tetramer. The ^{1}H NMR spectrum is broad and new resonances appear in the α-region and aromatic region, indicating the formation of a new species (Figure 4.9). The monomer subunits are fully folded with the average difference in chemical shifts of the diastereotopic *pro-S* and *pro-R* δ-protons of the δ-linked ornithine turn units at 0.67 ppm. The resonances associated with the α-protons of the tetramer are shifted downfield of the HOD peak, reflecting the folding and assembly of the peptide. The aromatic resonances of the Phe_{15} side chains are shifted upfield to reflect packing of the aromatic side chains to form a hydrophobic core. The dimer resonances are no longer present at higher pH, showing a pH-dependent response.

The observation of a stable dimer of peptide $\mathbf{1}_{\mathbf{His}}$ under acidic condition is interesting, because I do not observe dimer formation for peptides $\mathbf{1}_{\mathbf{Cit}}$, $\mathbf{1}_{\mathbf{Glu}}$, or $\mathbf{1}_{\mathbf{Leu}}$. In all conditions studied, I observe only monomer or tetramer for these peptides. The absence of observed dimer for these peptides does not mean that no dimer forms, but rather that under all conditions studied the monomer or tetramer predominates and that tetramer formation must be cooperative.

The formation of a dimer by peptide $\mathbf{1}_{\mathbf{His}}$ under acidic conditions suggests that some feature or features of the protonated imidazole group stabilize the dimer, while destabilizing the tetramer. The extra charge of the protonated peptide $\mathbf{1}_{\mathbf{His}}$ likely disrupts tetramer formation. The protonated imidazole group of peptide $\mathbf{1}_{\mathbf{His}}$ is less hydrophilic than the guanidinium group of peptide $\mathbf{1}_{\mathbf{Arg}}$, which likely facilitates hydrophobic packing of the dimer. It is also interesting that the ^{1}H NMR spectrum of $\mathbf{1}_{\mathbf{Arg}}$ broadens slightly at 8 mM, indicating the onset of self association. It is likely that this hint of self association reflects the onset of dimerization, rather than tetramerization.

Conclusion

The NMR studies of macrocyclic β-sheet peptides $\mathbf{1}_{\mathbf{Arg}}$, $\mathbf{1}_{\mathbf{Cit}}$, $\mathbf{1}_{\mathbf{Glu}}$, $\mathbf{1}_{\mathbf{Leu}}$, and $\mathbf{1}_{\mathbf{His}}$ show that modulation of charge can manipulate oligomerization state and variations in hydrophobicity can affect oligomerization propensity. These results demonstrate that an increase in positive charge on the hydrophobic surface led to an absence of tetramer formation and that an increase in hydrophobicity on the hydrophobic surface led to an increase in propensity to form tetramers. Installment of the histidine residue at position 11 provided a convenient pH trigger for modulating the overall charge of the hydrophobic surface, and NMR studies at various pH further corroborates that charge is important in oligomerization.

References

(1) Kilmartin, J. V.; Breen, J. J.; Roberts, G. C. K.; Ho, C. *Proc. Natl. Acad. Sci. U.S.A.* **1973**, *70*, 1246-1249.

(2) Eaton, W. A.; Henry, E. R.; Hofrichter, J.; Mozzarelli, A. *Nat. Struct. Mol. Biol.* **1999**, *6*, 351-358.

(3) Edelstein, S. J. *Annu. Rev. Biochem.* **1975**, *44*, 209-232.

(4) Kampmann, T.; Mueller, D. S.; Mark, A. E.; Young, P. R.; Kobe, B. *Structure* **2006**, *14*, 1481-1487.

(5) Fritz, R.; Stiasny, K.; Heinz, F. X. *J. Cell Biol.* **2008**, *183*, 353-361.

(6) Kalani, M. R.; Moradi, A.; Moradi, M.; Tajkhorshid, E. *Biophys. J.* **2013**, *105*, 993-1003.

(7) Lee, E. S.; Gao, Z. G.; Kim, D.; Park, K.; Kwon, I. C.; Bae, Y. H. *J. Control. Release* **2008**, *129*, 228-236.

(8) Radovic-Moreno, A. F.; Lu, T. K.; Puscasu, V. A.; Yoon, C. J.; Langer, R.; Farokhzad, O. C. *ACS Nano.* **2012**, *6*, 4279-4287.

(9) Griset, A. P.; Walpole, J.; Liu, R.; Gaffey, A.; Colson, Y. L.; Grinstaff, M. W. *J. Am. Chem. Soc.* **2009**, *131*, 2469-2471.

(10) Qu, W.; Li, Y.; Hovgaard, L.; Li, S.; Dai, W. B.; Wang, J. C.; Zhang, X.; Zhang, Q. *Int. J. Nanomed.* **2012**, *7*, 4983-4994.

(11) Yang, Y. Q.; Zheng, L. S.; Guo, X. D.; Qian, Y.; Zhang, L. J. *Biomacromolecules* **2011**, *12*, 116-122.

(12) Wada, K.; Mizuno, T.; Oku, J.; Tanaka, T. *Protein Peptide Lett.* **2003**, *10*, 27-33.

(13) Anderson, J. M.; Andersen, N. H. *Angew. Chem. Int. Ed.* **2017**, *56*, 7074-7077.

(14) Jones, I. M.; Lingard, H.; Hamilton, A. D. *Angew. Chem. Int. Ed.* **2011**, *50*, 12569-12571.

(15) Truex, N. L.; Wang, Y. L.; Nowick, J. S. *J. Am. Chem. Soc.* **2016**, *138*, 13882-13890.

(16) Truex, N. L.; Nowick, J. S. *J. Am. Chem. Soc.* **2016**, *138*, 13891-13900.

(17) Nowick, J. S.; Lam, K. S.; Khasanova, T. V.; Kemnitzer, W. E.; Maitra, S.; Mee, H. T.; Liu, R. W. *J. Am. Chem. Soc.* **2002**, *124*, 4972-4973.

(18) Nowick, J. S.; Brower, J. O. *J. Am. Chem. Soc.* **2003**, *125*, 876-877.

(19) Nowick, J. S.; Chung, D. M.; Maitra, K.; Maitra, S.; Stigers, K. D.; Sun, Y. *J. Am. Chem. Soc.* **2000**, *122*, 7654-7661.

(20) Khakshoor, O.; Demeler, B.; Nowick, J. S. *J. Am. Chem. Soc.* **2007**, *129*, 5558-5569.

(21) Pham, J. D.; Demeler, B.; Nowick, J. S. *J. Am. Chem. Soc.* **2014**, *136*, 5432-5442.

(22) Wang, Y.; Kreutzer, A. G.; Truex, N. L.; Nowick, J. S. *J. Org. Chem.* **2017**, *82*, 7905-7912.

(23) Wishart, D. S.; Sykes, B. D. *Methods Enzymol.* **1994**, *239*, 363-392.

(24) Pham, J. D.; Chim, N.; Goulding, C. W.; Nowick, J. S. *J. Am. Chem. Soc.* **2013**, *135*, 12460-12467.

(25) Polson, A. *J. Phys. Colloid Chem.* **1950**, *54*, 649-652.

Material and Methods

Synthesis of Macrocyclic β-Sheet Peptides. Synthesis of the macrocyclic β-sheet peptides were performed as previously published.[1] The peptides were purified by reverse-phase HPLC and the pure fractions were lyophilized to give 19 mg of peptide $\mathbf{1}_{\mathbf{Glu}}$, 22 mg of peptide $\mathbf{1}_{\mathbf{Leu}}$, and 8 mg of $\mathbf{1}_{\mathbf{His}}$. Based on resin loading, the yields are 7%, 9%, and 4%, respectively.

Macrocyclic β-Sheet peptide $\mathbf{1}_{\mathbf{Glu}}$: HRMS (ESI-TOF) *m/z*: $[M + H]^+$ Calcd for $C_{82}H_{134}N_{21}O_{20}$ 1733.0114; Found 1733.0093.

Macrocyclic β-Sheet peptide $\mathbf{1}_{\mathbf{Leu}}$: HRMS (ESI-TOF) *m/z*: $[M + Na]^+$ Calcd for $C_{83}H_{137}N_{21}O_{18}Na$ 1739.0348; Found 1739.0363.

Macrocyclic β-Sheet peptide $\mathbf{1}_{\mathbf{His}}$: HRMS (ESI-TOF) *m/z*: $[M + H]^+$ Calcd for $C_{83}H_{134}N_{23}O_{18}$ 1741.0277; Found 1741.0278.

NMR Spectroscopy of the Macrocyclic β-Sheet Peptides

Sample Preparation. NMR spectroscopy of the macrocyclic β-sheet peptides at pH 2.5 was performed in D_2O (D, 99.96%; Cambridge Isotope Laboratories, Inc.). NMR spectroscopy of the macrocyclic β-sheet peptides at pH 4.7 was performed in D_2O with 50 mM CD_3COOD (D, 99.5%; Cambridge Isotope Laboratories, Inc.) and 50 mM CD_3COONa (D, 99%; Cambridge Isotope Laboratories, Inc.). NMR spectroscopy of the macrocyclic β-sheet peptides at pH 7.2 was performed in D_2O with 50 mM CD_3COOD and 50 mM CD_3COONa with the pH adjusted using NaOD (D, 99.5%; Cambridge Isotope Laboratories, Inc.). The solutions were prepared by dissolving a weighed portion of the peptide in the appropriate volume of solvent. The molecular weights of the peptides were calculated as the TFA salts with all amino groups assumed to be protonated ($\mathbf{1}_{\mathbf{Glu}}$, M.W. 2188.87, $\mathbf{1}_{\mathbf{Leu}}$, M.W. 2172.93, and $\mathbf{1}_{\mathbf{His}}$, M.W. 2310.90). The solutions at

pH 4.7 and 7.2 contained 4,4-dimethyl-4-silapentane-1-ammonium trifluoroacetate (DSA) as an internal standard for referencing chemical shifts.[2] The solutions were prepared and left for 24 h to allow complete hydrogen to deuterium exchange of the amide NH protons.

^{1}H NMR, TOCSY, ROESY, and NOESY Data Collection. NMR spectra were recorded on a Bruker 500 MHz spectrometer with a TCI cryoprobe. TOCSY spectra were recorded with 2048 points in the f_2 dimension and 512 increments in the f_1 dimension with a 150-ms spin-lock mixing time. TOCSY spectra were recorded with 2048 points in the f_2 dimension and 512 increments in the f_1 dimension with either a 100- or 150-ms spin-lock mixing time. NOESY spectra were recorded with 2048 points in the f_2 dimension and 512 increments in the f_1 dimension with a 150-ms mixing time.

^{1}H NMR, TOCSY, and NOESY Data Processing. NMR spectra were processed with BrukerXwinNMR software. Automatic baseline correction was applied in both dimensions after phasing the spectra. TOCSY spectra were Fourier transformed to a final matrix size of 4096 x 1024 real points using a Qsine weighting function and forward linear prediction. NOESY and ROESY spectra were Fourier transformed to a final matrix size of 4096 x 2048 real points using a Qsine weighting functionand forward linear prediction.

Diffusion-Ordered Spectroscopy (DOSY) Experiments. DOSY experiments were performed on a Bruker 500 MHz spectrometer equipped with a TCI cryoprobe, with a diffusion delay (Δ) of 75-ms and a diffusion gradient length (δ) of 2.5-ms. Sixteen sets of FIDs were recorded with the gradient strength incremented from 5%–95% using a linear ramp. The combined FIDs were Fourier transformed in Bruker's TopSpin™ software to give a pseudo-2D spectrum. After phasing and performing baseline correction, each pseudo-2D spectrum was processed with logarithmic scaling on the Y-axis. The Y-axis was calibrated to the diffusion

coefficient of the residual HOD peak in D_2O (1.9×10^{-9} m^2/s at 298 K).[3] The diffusion coefficients of the peptides were read and converted from logarithmic values to linear values.

References

(1) Truex, N. L.; Wang, Y. L.; Nowick, J. S. *J. Am. Chem. Soc.* **2016**, *138*, 13882-13890.

(2) Nowick, J. S.; Khakshoor, O.; Hashemzadeh, M.; Brower, J. O. *Org Lett.* **2003**, *5*, 3511-3513.

(3) Longsworth, L. G. *J. Phys. Chem.* **1960**, *64*, 1914-1917.

RP-HPLC of Macrocyclic β-Sheet $\mathbf{1_{Glu}}$

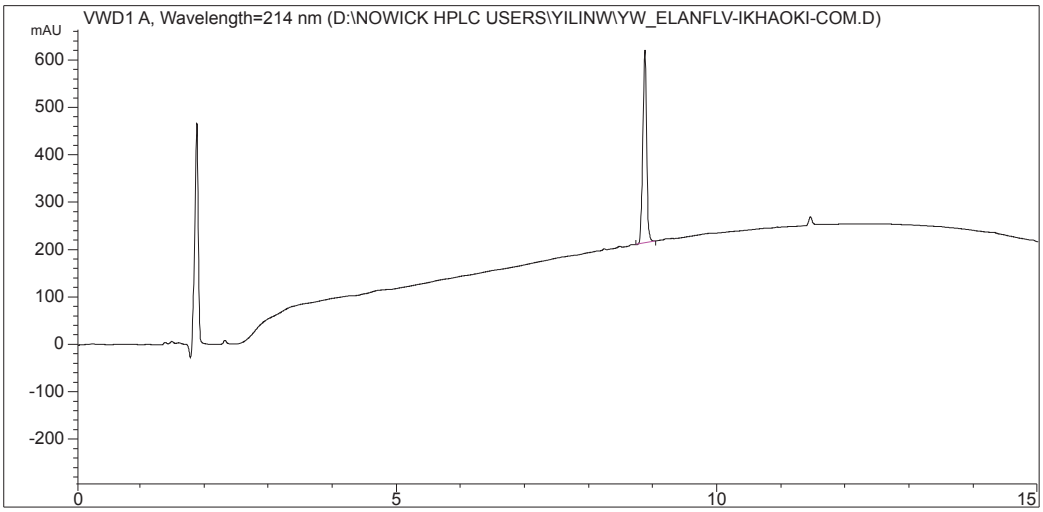

Peak #	RetTime [min]	Type	Width [min]	Area mAU *s	Height [mAU]	Area %
1	8.861	MM	0.0677	1665.86951	410.1195	100.000

column: Aeris XB-C18 2.6µ
dimensions: 150 mm x 4.6 mm
mobile phase: A: H_2O, 0.1% TFA
B: CH_3CN, 0.1% TFA
gradient: A/B (95:5) to (0:100) in 20 min
flow rate: 1.0 mL/min
detection: VWD, wavelength = 214 nm
temperature: 298 K

MS (ESI) of Macrocyclic β-Sheet $\mathbf{1_{Glu}}$

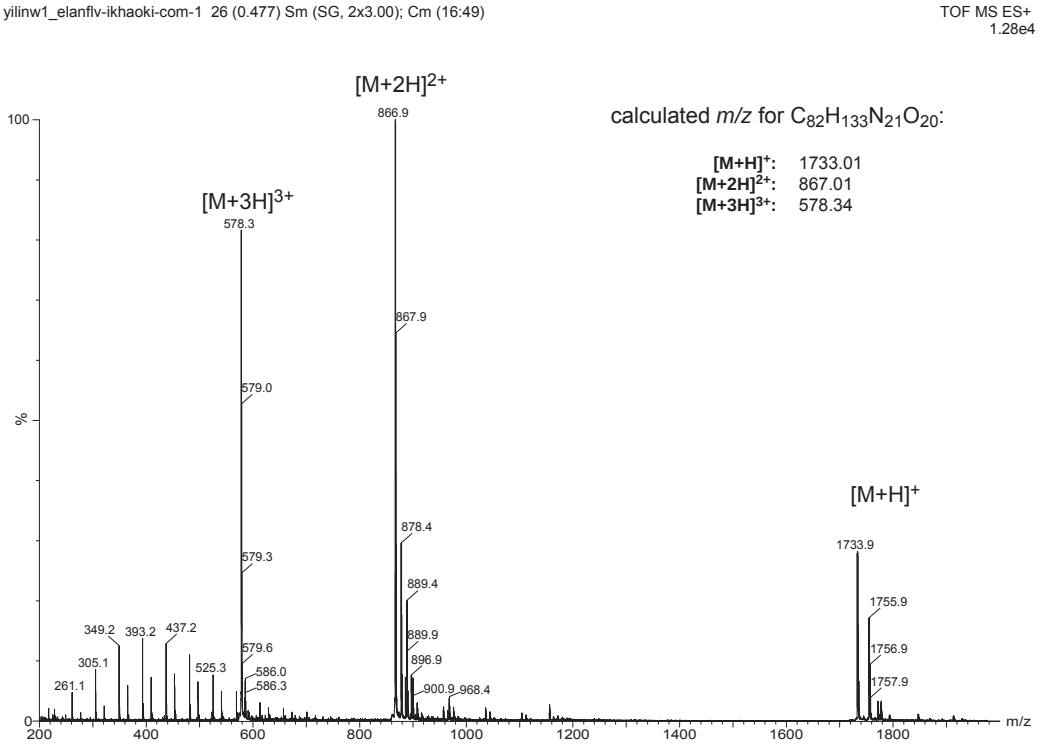

calculated *m/z* for $C_{82}H_{133}N_{21}O_{20}$:

$[M+H]^+$: 1733.01
$[M+2H]^{2+}$: 867.01
$[M+3H]^{3+}$: 578.34

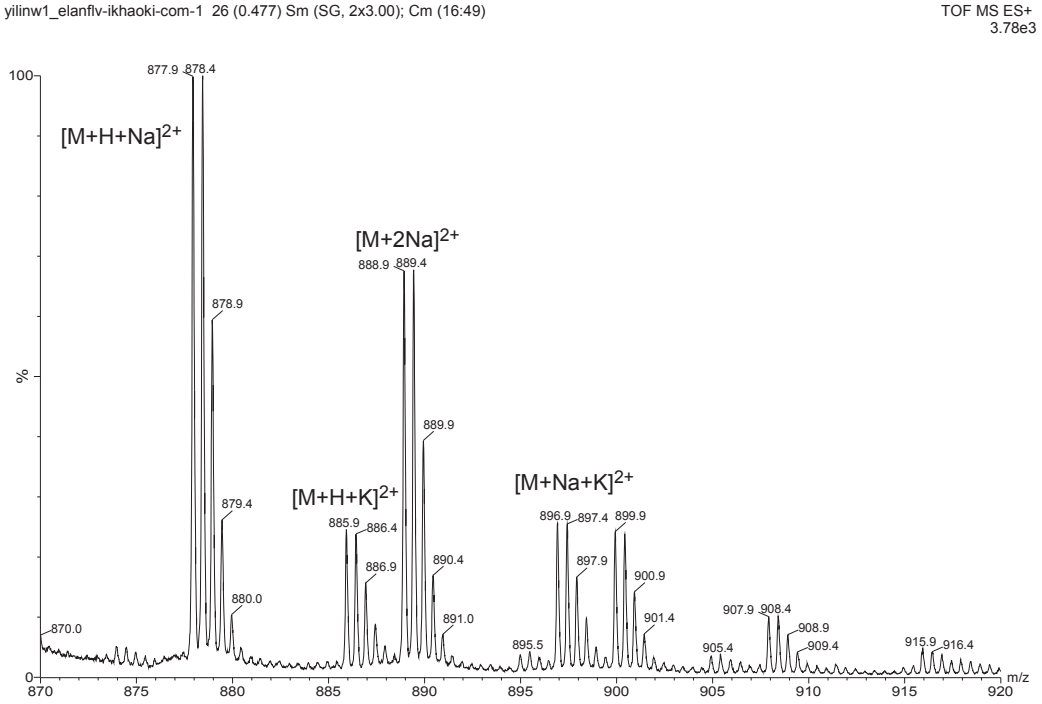
yilinw1_elanflv-ikhaoki-com-1 26 (0.477) Sm (SG, 2x3.00); Cm (16:49)
TOF MS ES+
3.78e3
100
%
0
[M+H+Na]2+
[M+2Na]2+
[M+H+K]2+
[M+Na+K]2+
877.9
878.4
878.9
879.4
880.0
870.0
885.9
886.4
886.9
888.9
889.4
889.9
890.4
891.0
895.5
896.9
897.4
897.9
899.9
900.9
901.4
905.4
907.9
908.4
908.9
909.4
915.9
916.4
870
875
880
885
890
895
900
905
910
915
920
m/z

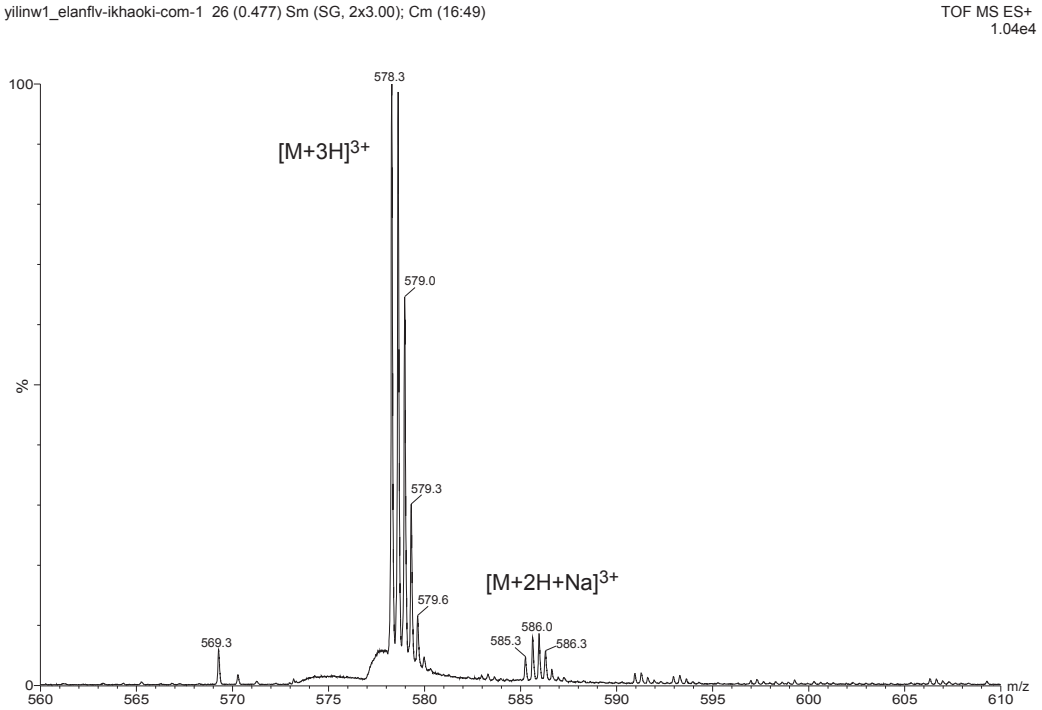
yilinw1_elanflv-ikhaoki-com-1 26 (0.477) Sm (SG, 2x3.00); Cm (16:49)
TOF MS ES+
1.04e4
100
%
0
[M+3H]3+
[M+2H+Na]3+
578.3
579.0
579.3
579.6
569.3
585.3
586.0
586.3
560
565
570
575
580
585
590
595
600
605
610
m/z

^{1}H NMR of macrocyclic β-sheet peptide **1$_{Leu}$**, 1 mM in 100 mM deuterioacetate buffer in D_2O at 500 MHz and 298 K

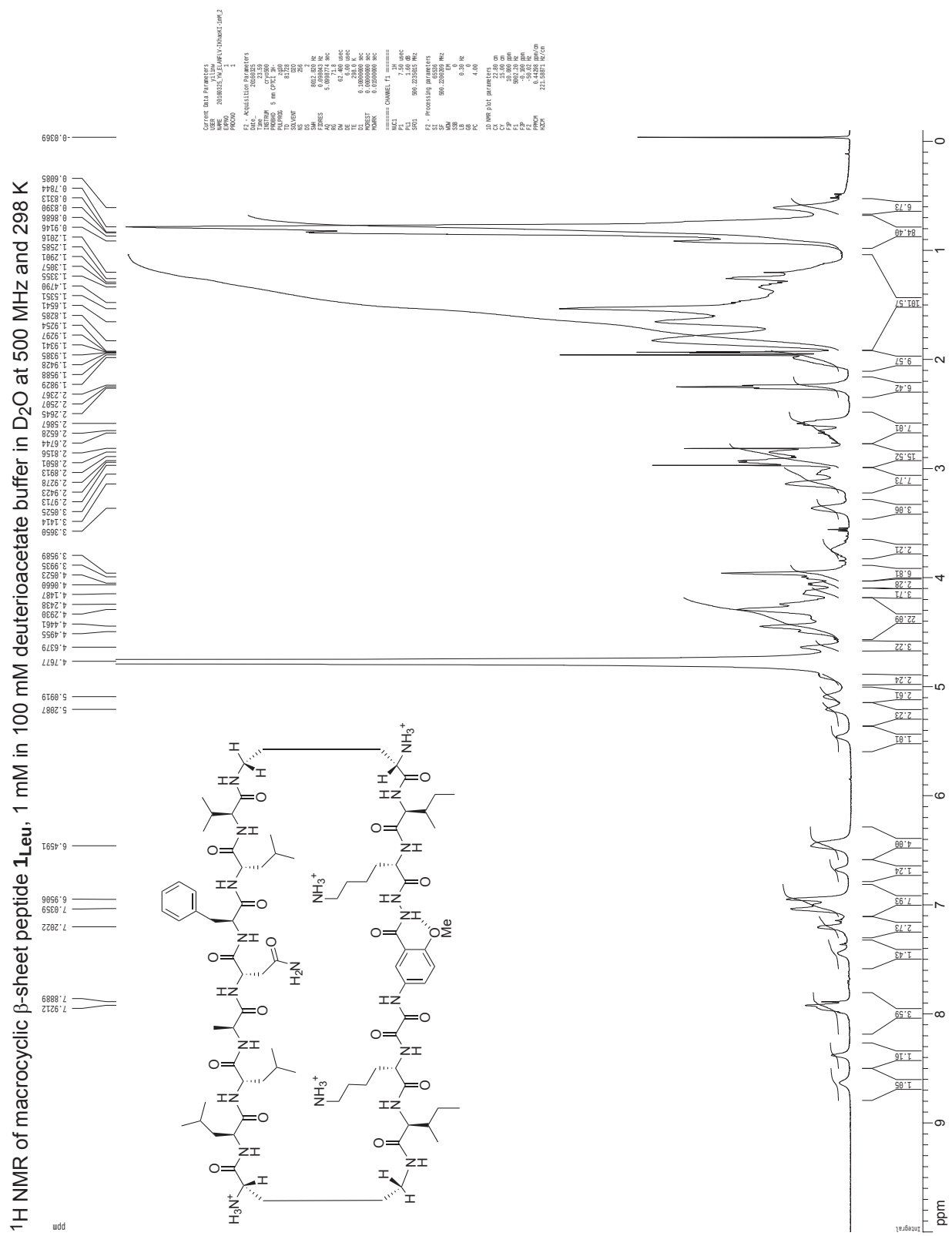

^{1}H NMR of macrocyclic β-sheet peptide **$\mathbf{1}_{\mathbf{Leu}}$**, 1 mM in 100 mM deuterioacetate buffer in D_2O at 500 MHz and 298 K

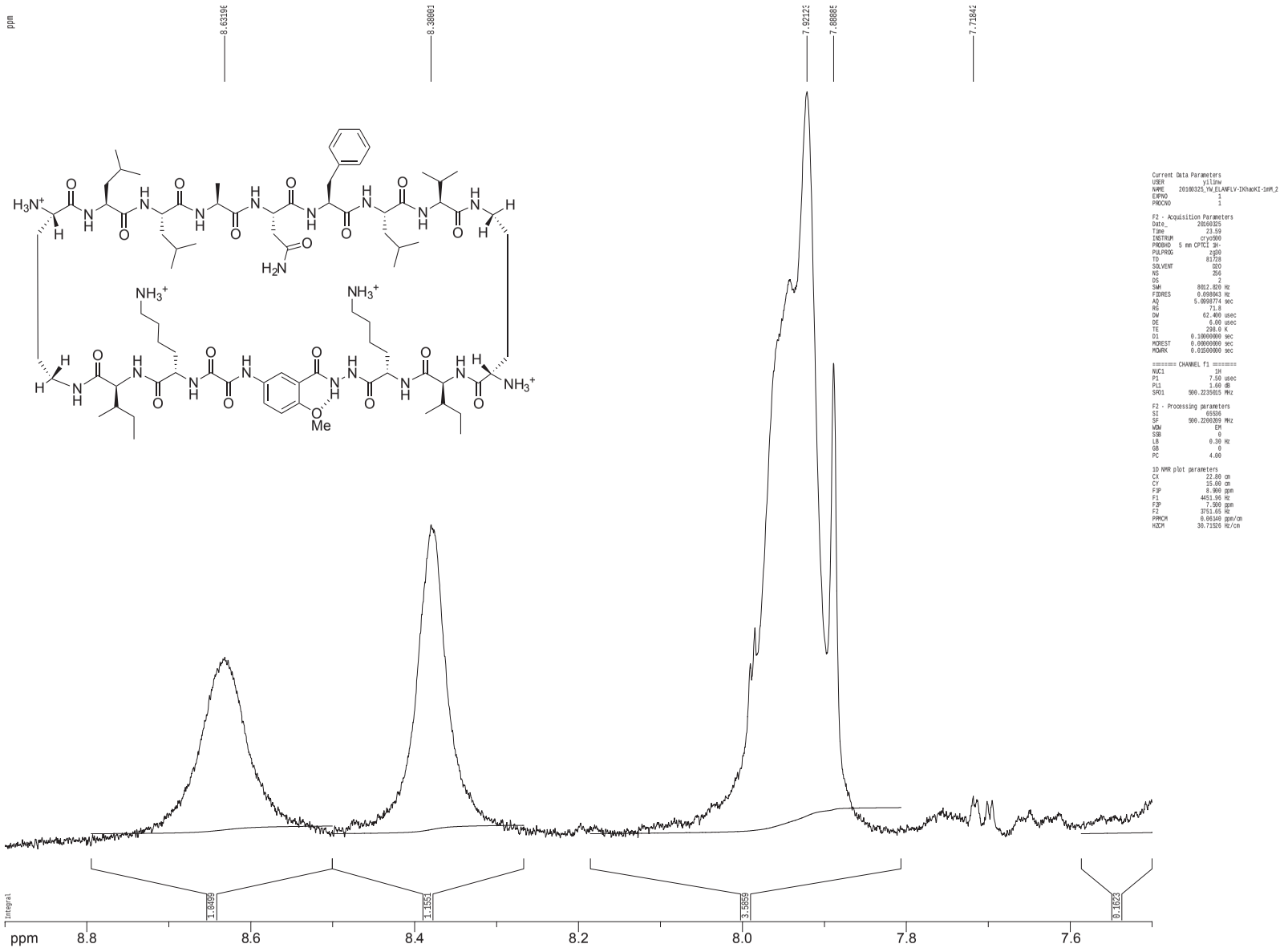

Current Data Parameters
USER yilizw
NAME 20100325_YW_ELANFLV-IKhaoKI-1mM_2
EXPNO 1
PROCNO 1

F2 - Acquisition Parameters
Date_ 20100325
Time 23.59
INSTRUM cryo600
PROBHD 5 mm CPTCI 1H-
PULPROG zg30
TD 81728
SOLVENT D2O
NS 256
DS 2
SWH 8012.820 Hz
FIDRES 0.098043 Hz
AQ 5.0998774 sec
RG 71.8
DW 62.400 usec
DE 6.00 usec
TE 298.0 K
D1 0.10000000 sec
MOREST 0.00000000 sec
MOWRK 0.01500000 sec

======= CHANNEL f1 =======
NUC1 1H
P1 7.50 usec
PL1 1.60 dB
SFO1 500.2235015 MHz

F2 - Processing parameters
SI 65536
SF 500.2200309 MHz
WDW EM
SSB 0
LB 0.30 Hz
GB 0
PC 4.00

1D NMR plot parameters
CX 22.80 cm
CY 15.00 cm
F1P 8.900 ppm
F1 4451.96 Hz
F2P 7.900 ppm
F2 3751.65 Hz
PPMCM 0.06340 ppm/cm
HZCM 30.71520 Hz/cm

^{1}H NMR of macrocyclic β-sheet peptide **1$_{Leu}$**, 1 mM in 100 mM deuterioacetate buffer in D_2O at 500 MHz and 298 K

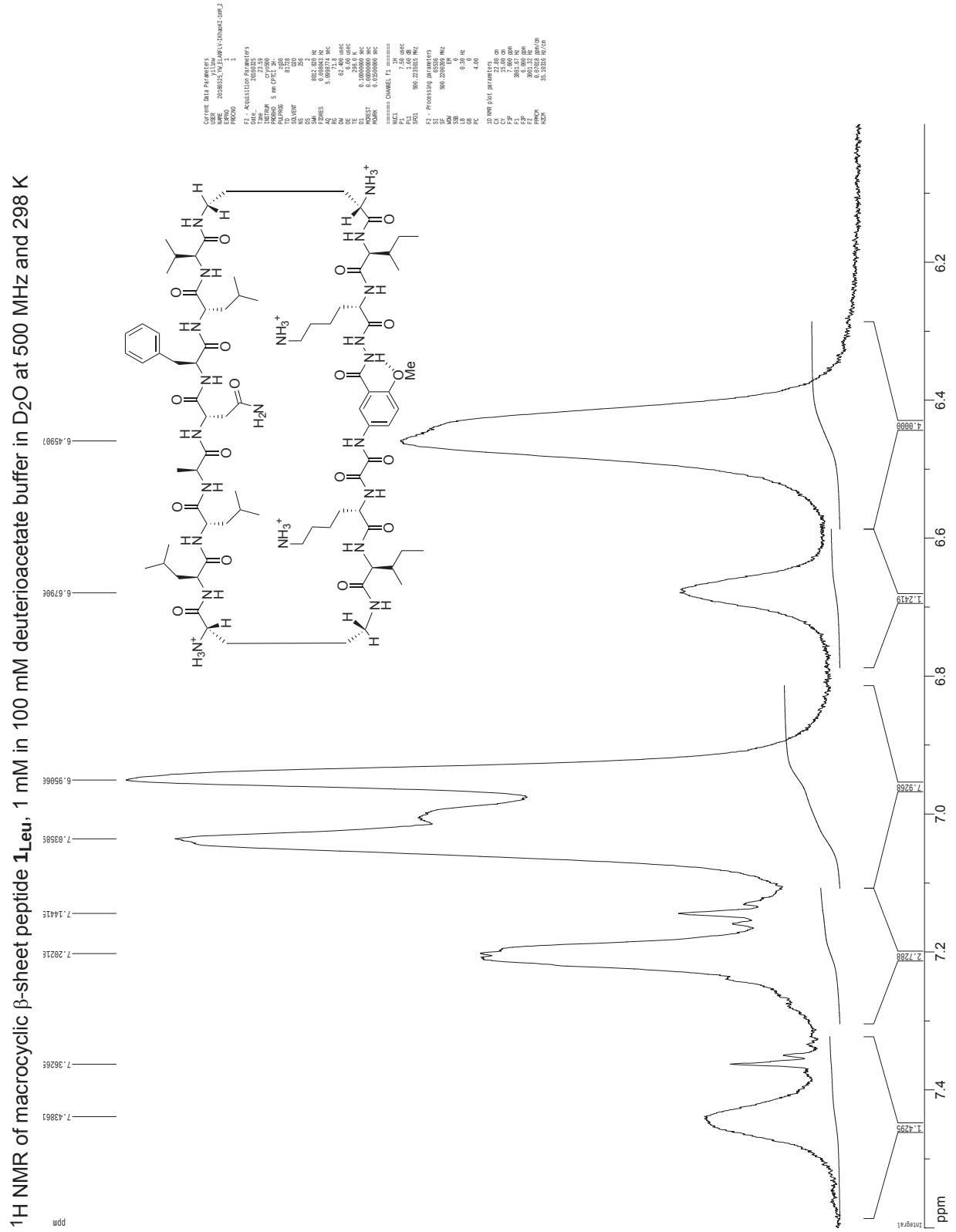

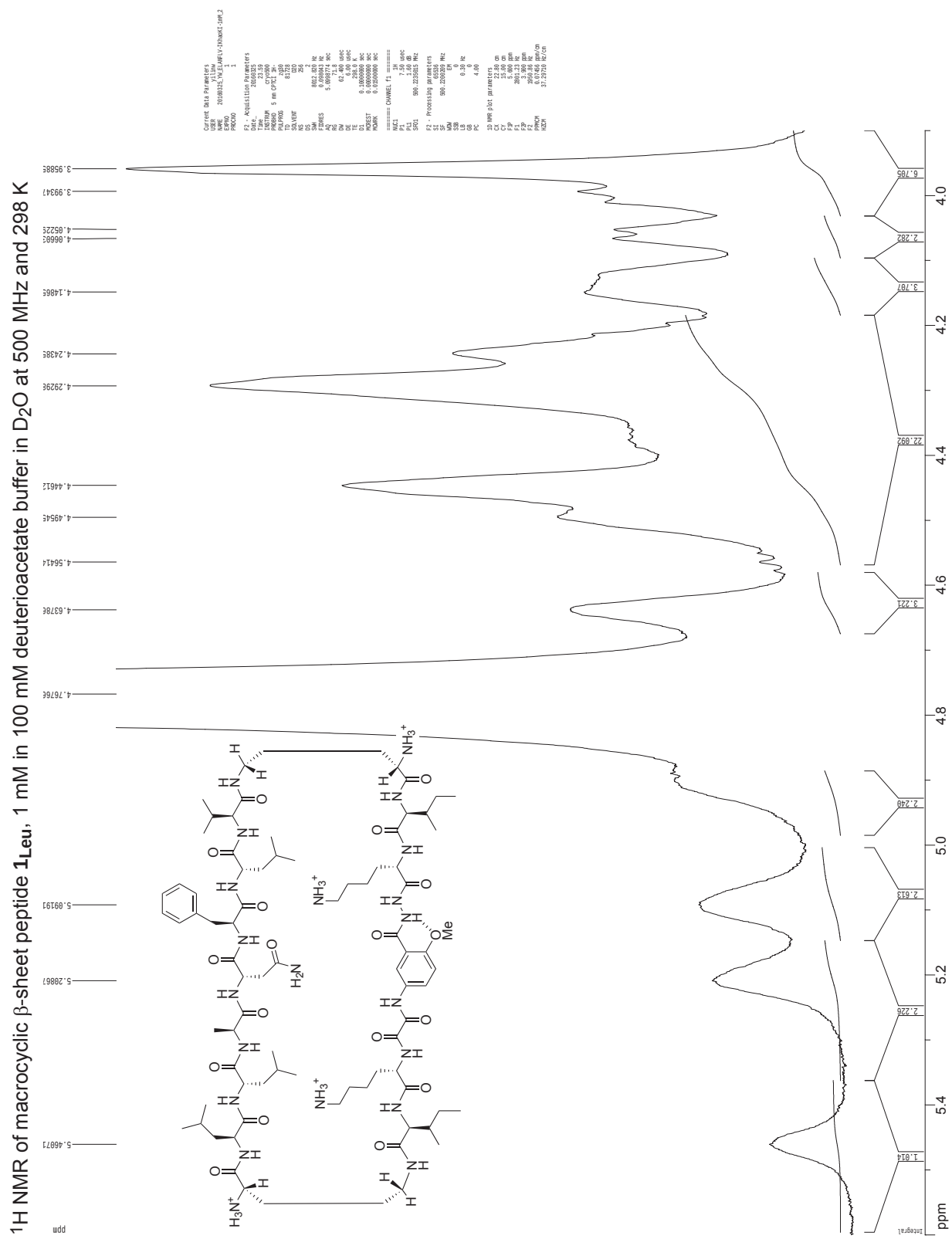
1H NMR of macrocyclic β-sheet peptide 1Leu, 1 mM in 100 mM deuterioacetate buffer in D2O at 500 MHz and 298 K
ppm
integral
Me
H2N
NH3+

^{1}H NMR of macrocyclic β-sheet peptide **1**$_{\mathbf{Leu}}$, 1 mM in 100 mM deuterioacetate buffer in D_2O at 500 MHz and 298 K

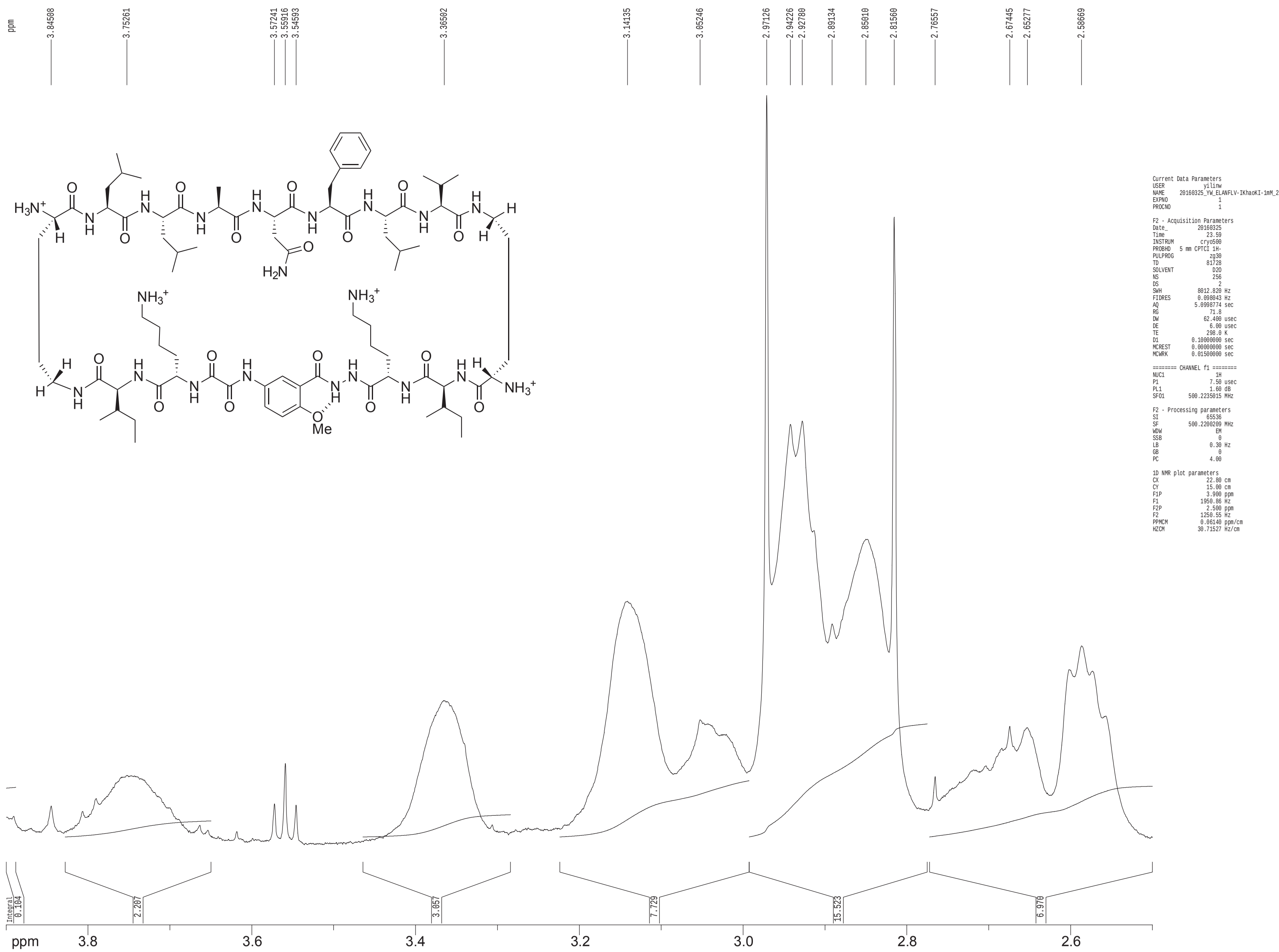

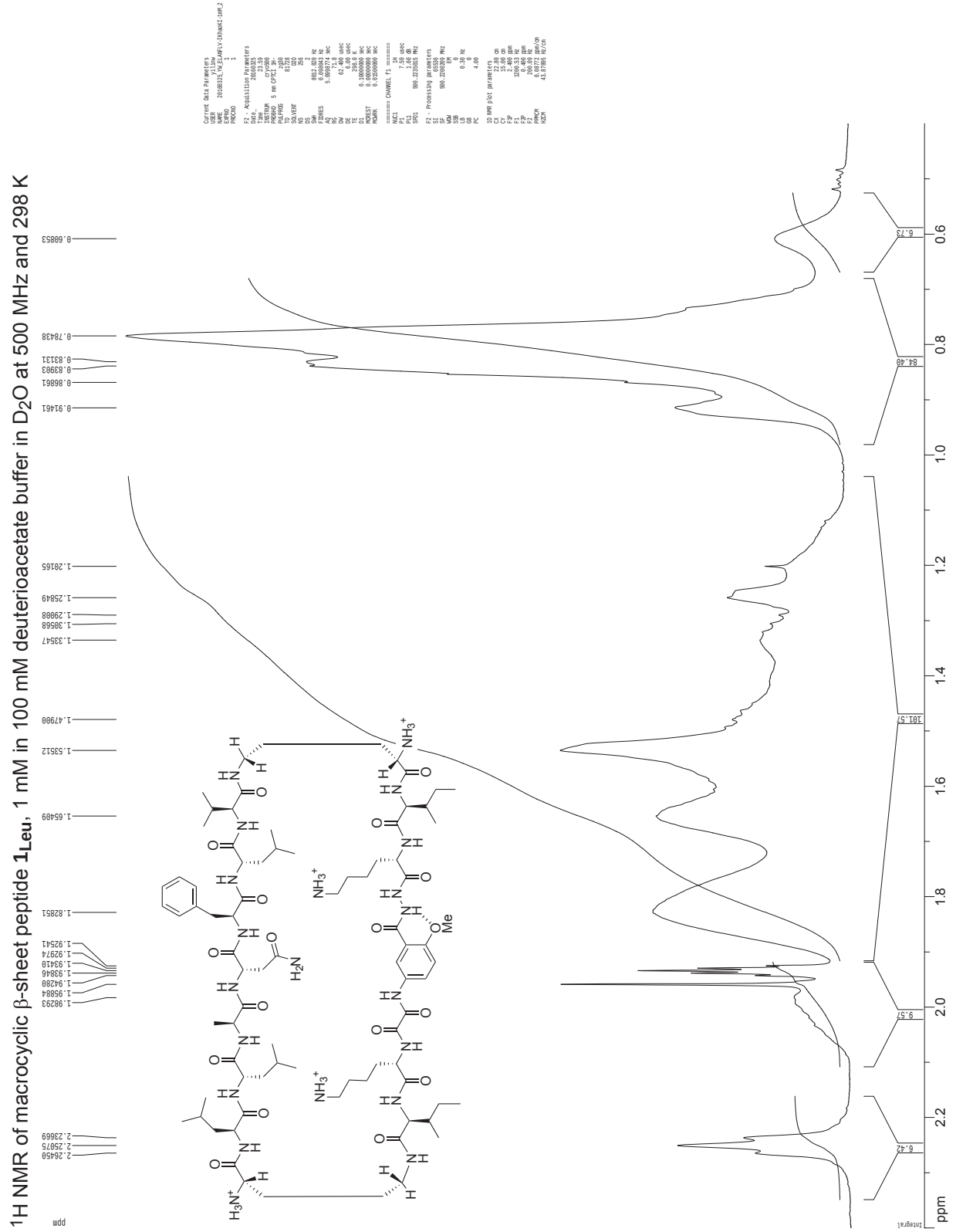
1H NMR of macrocyclic β-sheet peptide 1Leu, 1 mM in 100 mM deuterioacetate buffer in D2O at 500 MHz and 298 K
ppm
Integral
NH3+
H2N
Me

^{1}H NMR 2D TOCSY of macrocyclic β-sheet peptide **1$_{Glu}$** with 150-ms spin-lock mixing time
1 mM in 100 mM deuterioacetate buffer in D_2O at 500 MHz and 298 K

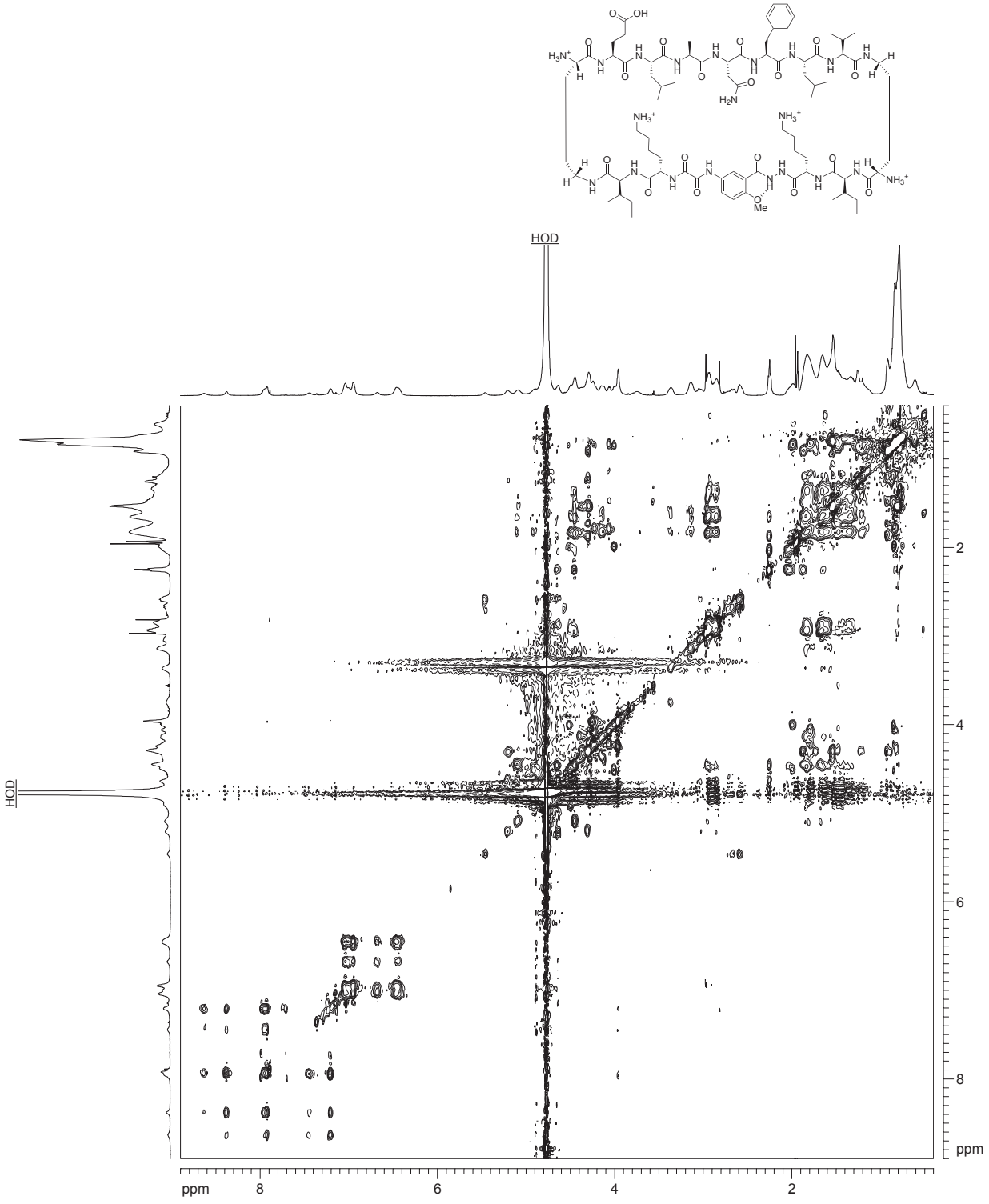

^{1}H NMR 2D TOCSY of macrocyclic β-sheet peptide **1$_{Glu}$** with 150-ms spin-lock mixing time
1 mM in 100 mM deuterioacetate buffer in D_2O at 500 MHz and 298 K

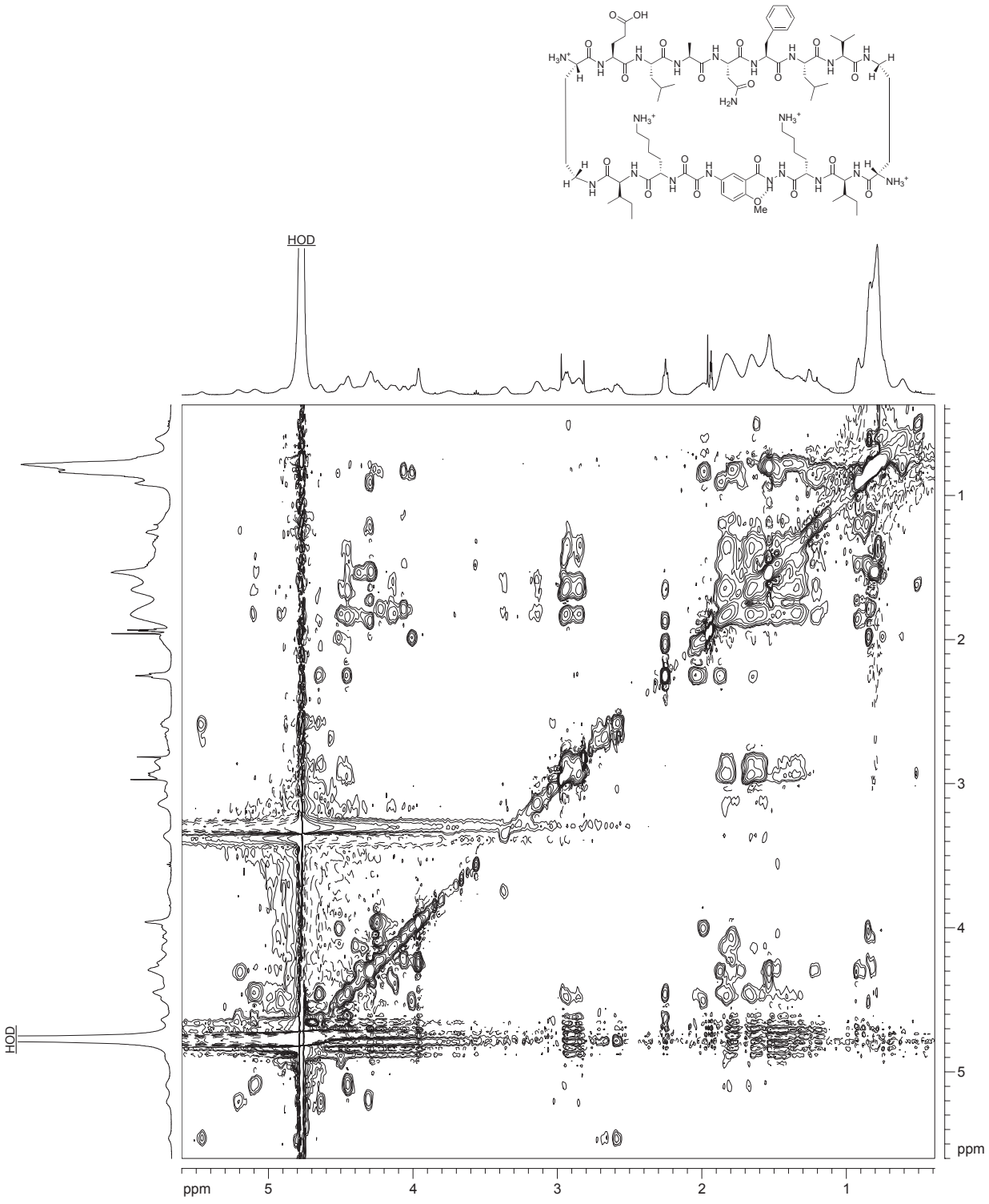

^{1}H NMR 2D ROESY of macrocyclic β-sheet peptide **1_{Glu}** with 150-ms spin-lock mixing time
1 mM in 100 mM deuterioacetate buffer in D_2O at 500 MHz and 298 K

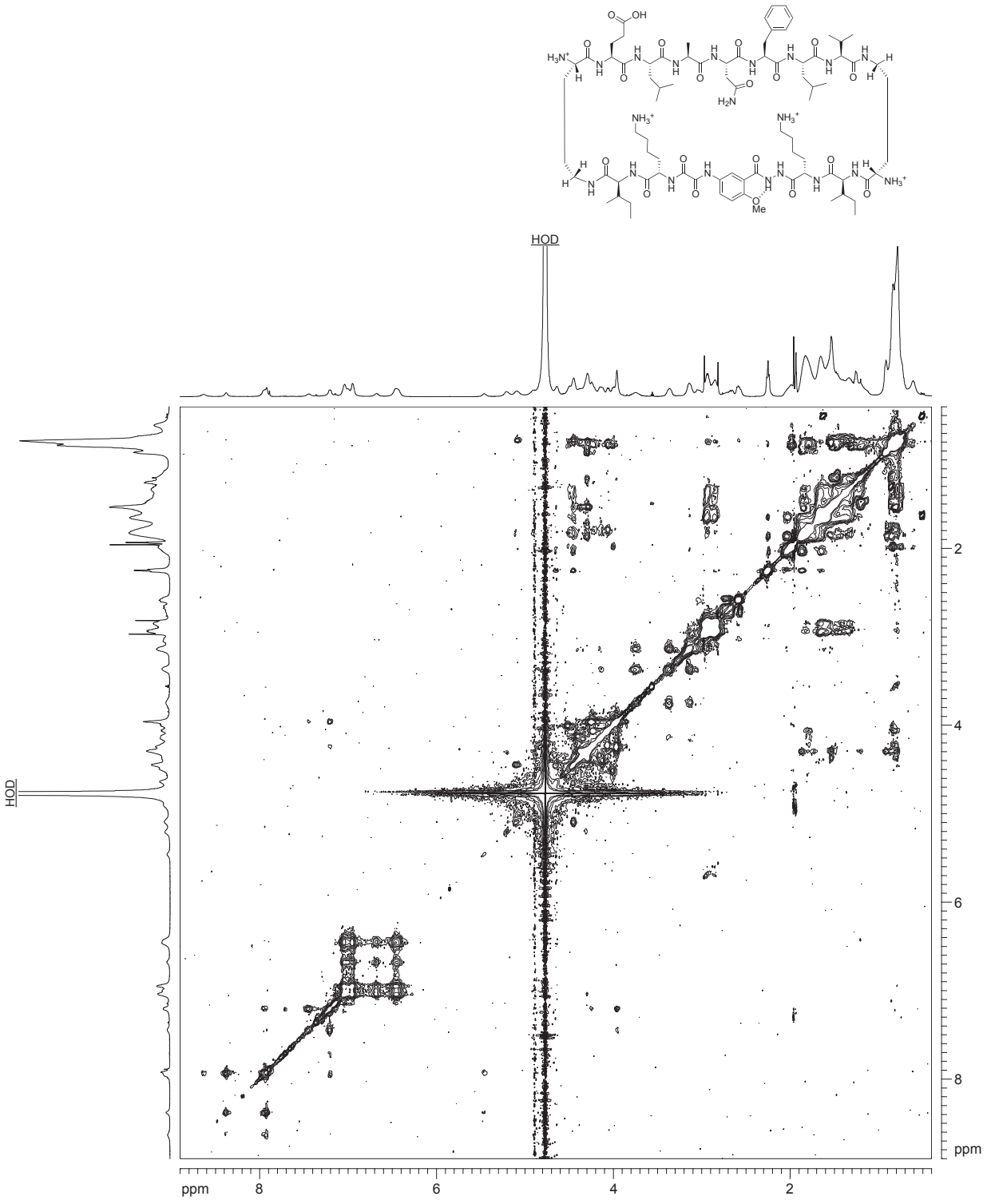

^{1}H NMR 2D ROESY of macrocyclic β-sheet peptide **1_{Glu}** with 150-ms spin-lock mixing time
1 mM in 100 mM deuterioacetate buffer in D_2O at 500 MHz and 298 K

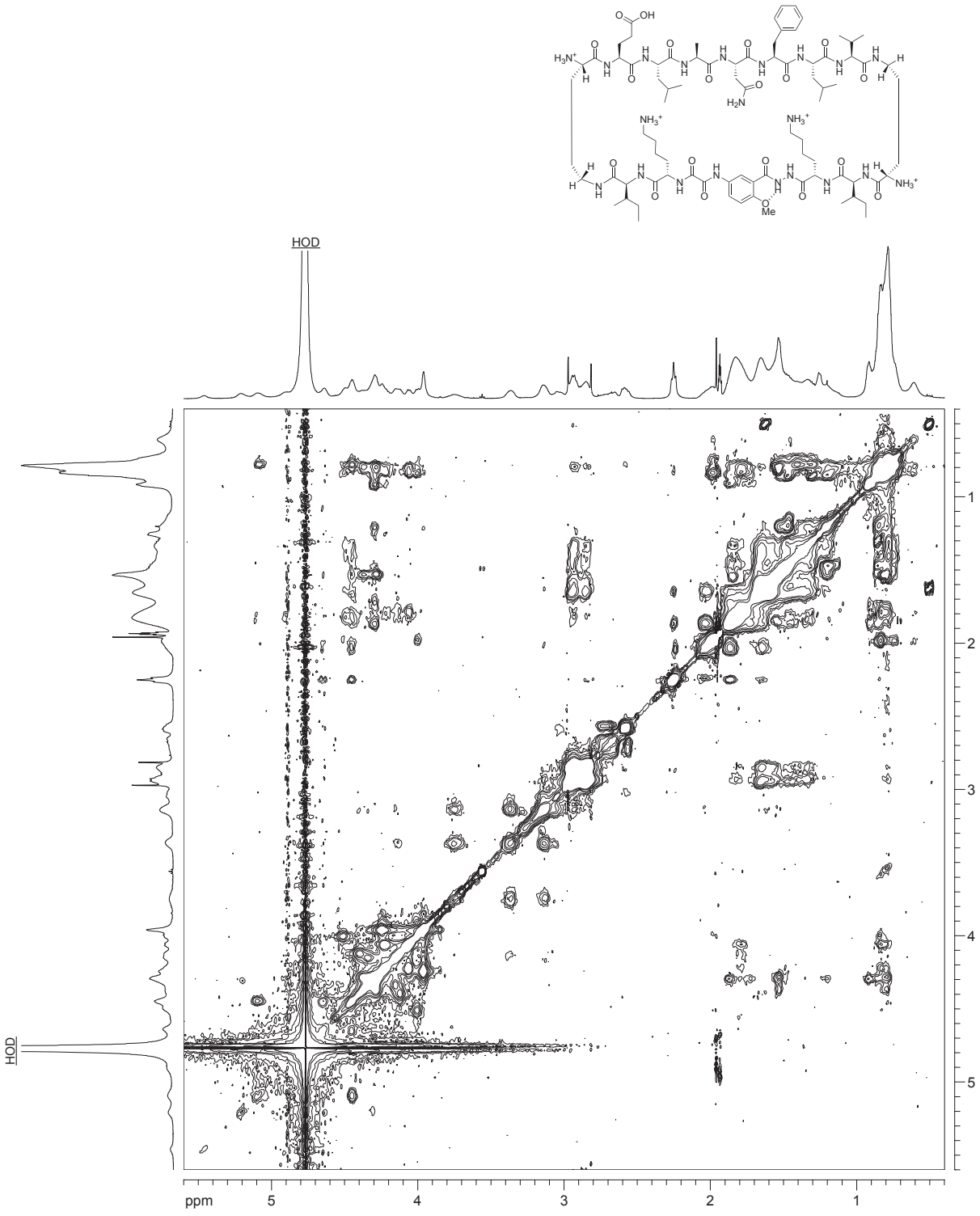

^{1}H NMR of macrocyclic β-sheet peptide **1$_{GIu}$**, 16 mM in 100 mM deuterioacetate buffer in D_2O at 500 MHz and 298 K

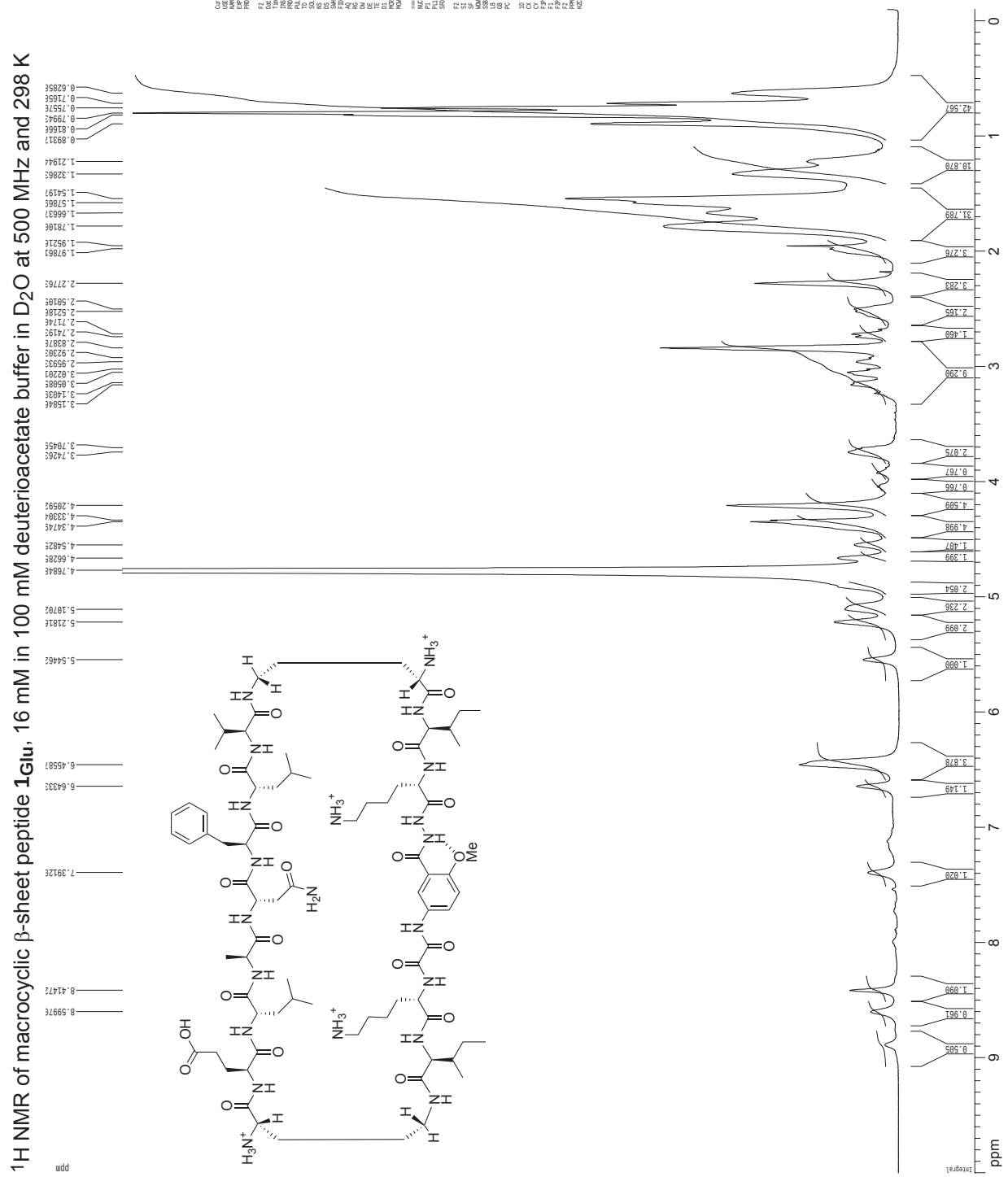

^{1}H NMR of macrocyclic β-sheet peptide **$\mathbf{1_{Glu}}$**, 16 mM in 100 mM deuterioacetate buffer in D_2O at 500 MHz and 298 K

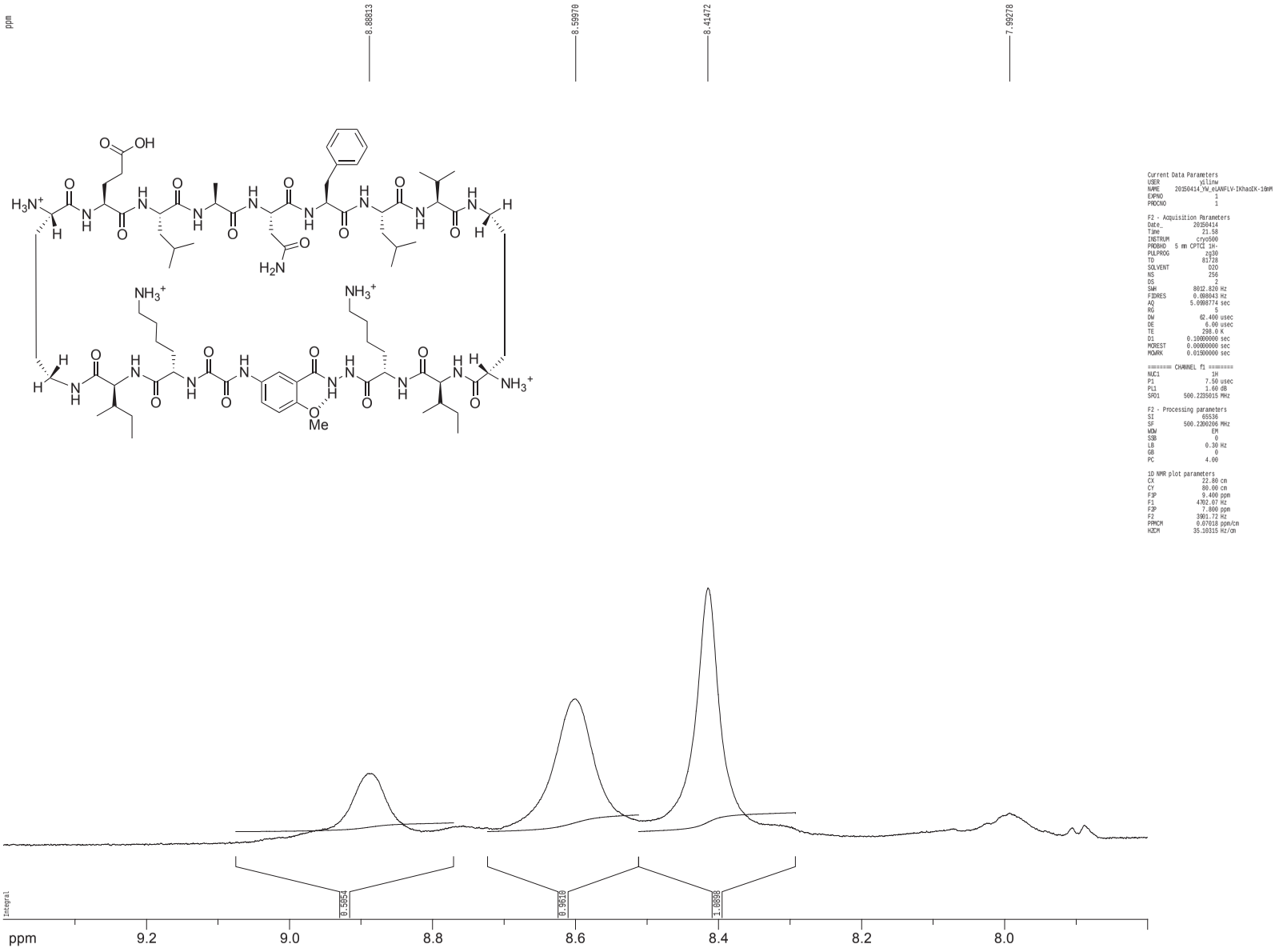

^{1}H NMR of macrocyclic β-sheet peptide **$\mathbf{1_{Glu}}$**, 16 mM in 100 mM deuterioacetate buffer in D_2O at 500 MHz and 298 K

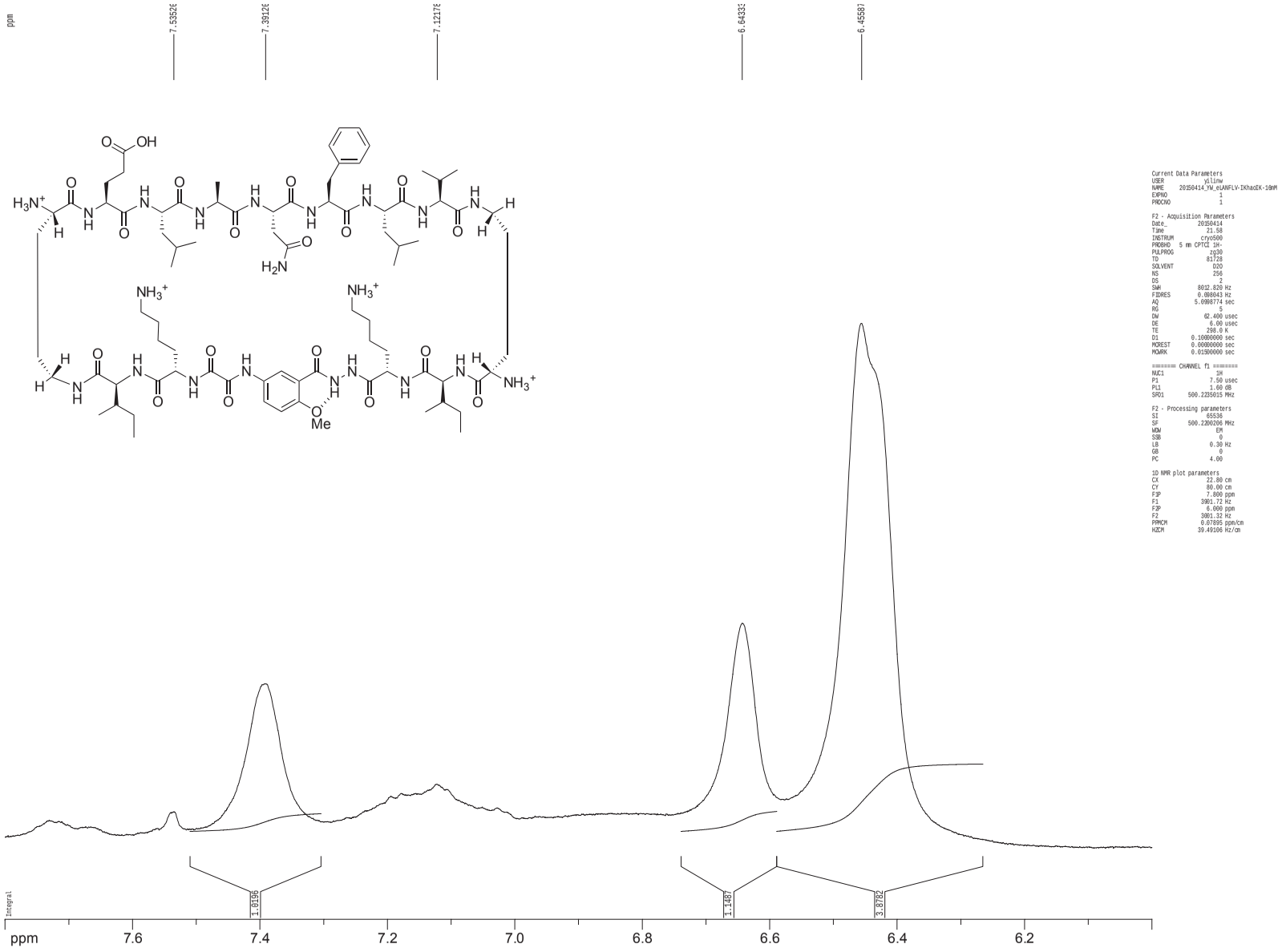

Current Data Parameters
USER yilinw
NAME 20150414_YW_eLWNFLV-IKhaoIK-16mM
EXPNO 1
PROCNO 1

F2 - Acquisition Parameters
Date_ 20150414
Time 21.58
INSTRUM cryo500
PROBHD 5 mm CPTCI 1H-
PULPROG zg30
TD 81728
SOLVENT D2O
NS 256
DS 2
SWH 8012.820 Hz
FIDRES 0.098043 Hz
AQ 5.0908774 sec
RG 5
DW 62.400 usec
DE 6.00 usec
TE 298.0 K
D1 0.10000000 sec
MCREST 0.00000000 sec
MCWRK 0.01500000 sec

======= CHANNEL f1 =======
NUC1 1H
P1 7.50 usec
PL1 1.60 dB
SFO1 500.2235015 MHz

F2 - Processing parameters
SI 65536
SF 500.2200200 MHz
WDW EM
SSB 0
LB 0.30 Hz
GB 0
PC 4.00

1D NMR plot parameters
CX 22.80 cm
CY 80.00 cm
F1P 7.800 ppm
F1 3901.72 Hz
F2P 6.000 ppm
F2 3001.32 Hz
PPMCM 0.07895 ppm/cm
HZCM 39.49106 Hz/cm

^{1}H NMR of macrocyclic β-sheet peptide **1$_{GIu}$**, 16 mM in 100 mM deuterioacetate buffer in D_2O at 500 MHz and 298 K

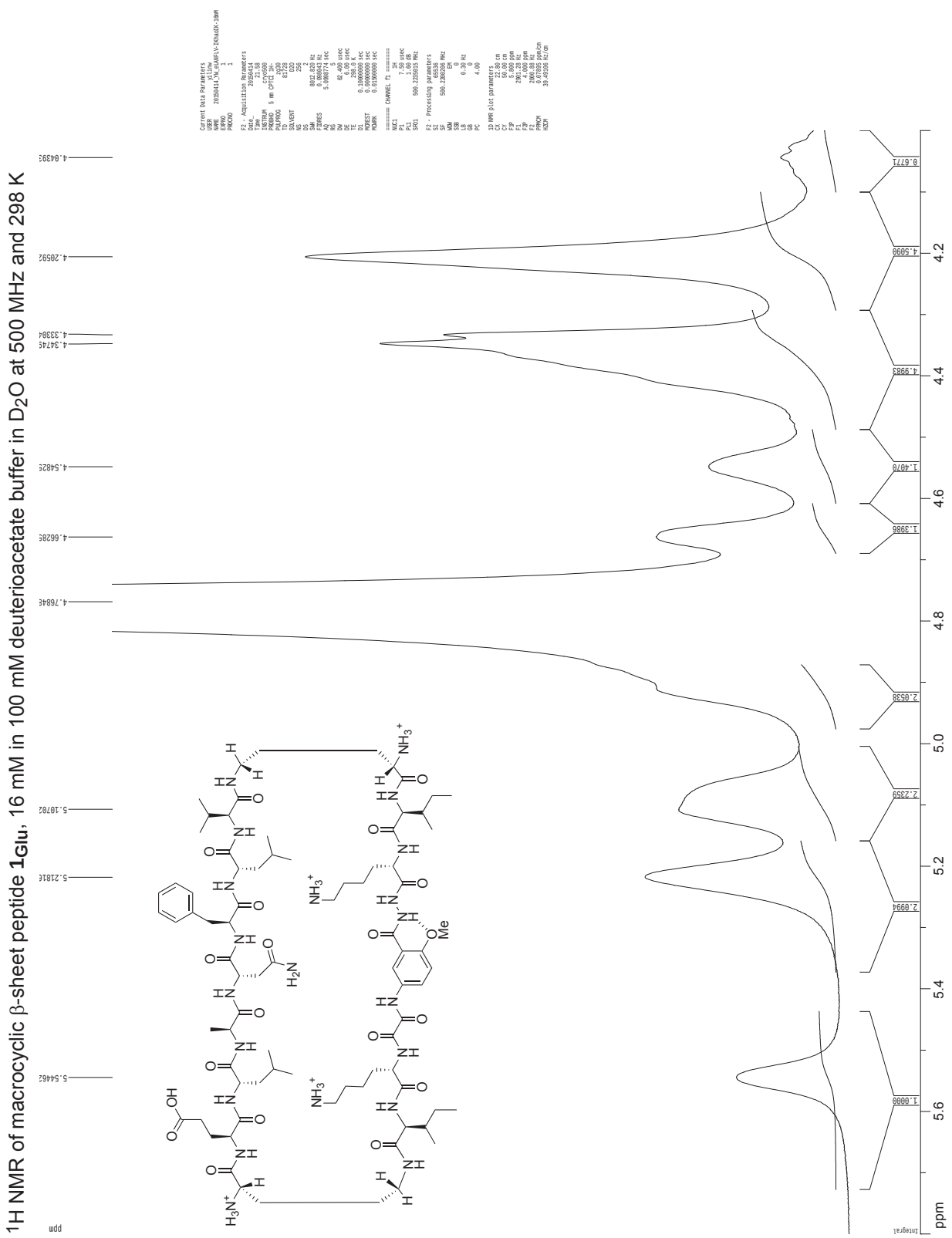

^{1}H NMR of macrocyclic β-sheet peptide **1_{Glu}**, 16 mM in 100 mM deuterioacetate buffer in D_2O at 500 MHz and 298 K

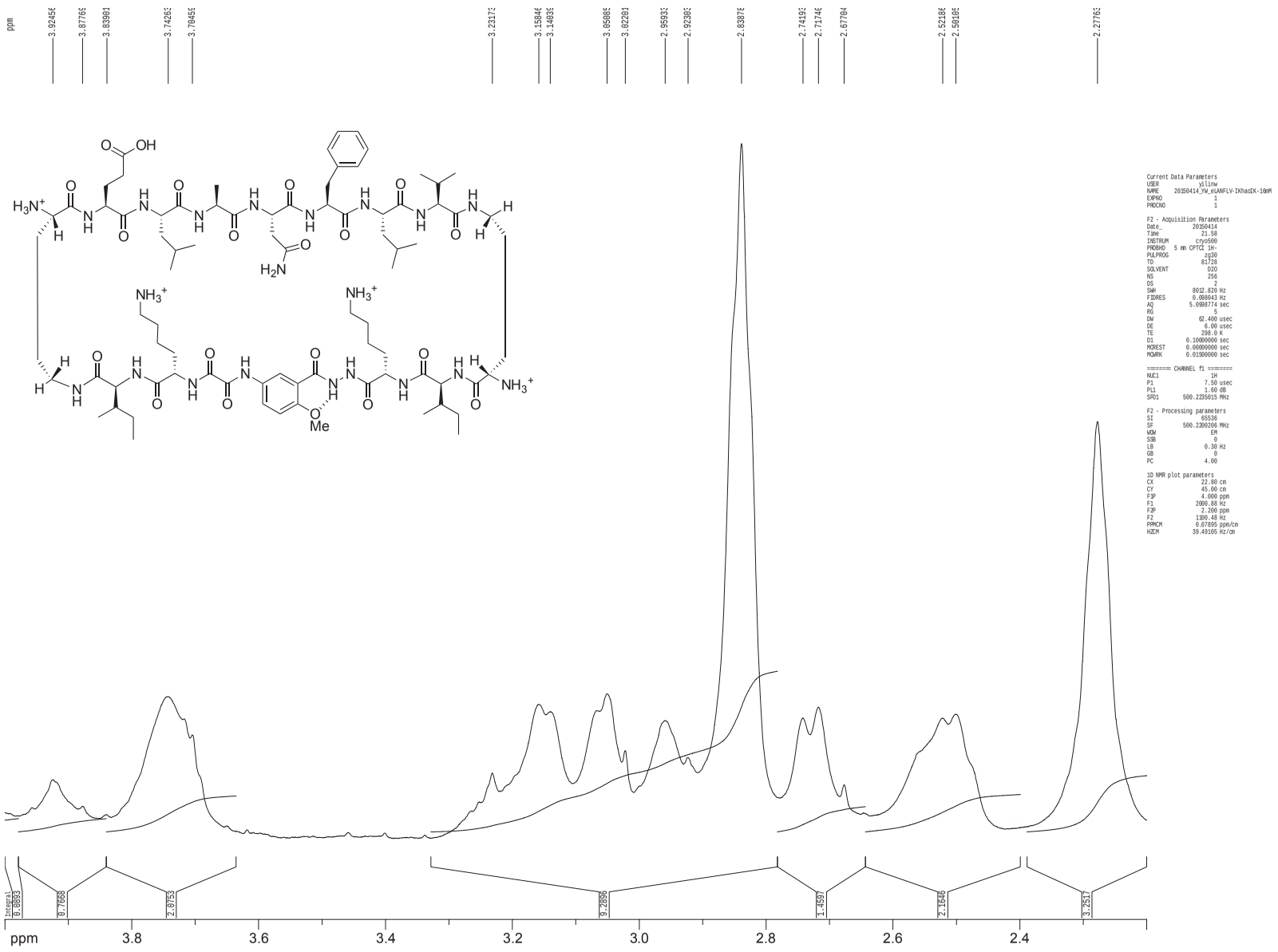

Current Data Parameters
USER yiliu
NAME 20150414_YW_eUANFLV-IKhacIK-16mM
EXPNO 1
PROCNO 1

F2 - Acquisition Parameters
Date_ 20150414
Time 21.58
INSTRUM cryo500
PROBHD 5 mm CPTCI 1H-
PULPROG zg30
TD 81728
SOLVENT D2O
NS 256
DS 2
SWH 8012.820 Hz
FIDRES 0.098043 Hz
AQ 5.0908774 sec
RG 5
DW 62.400 usec
DE 6.00 usec
TE 298.0 K
D1 0.10000000 sec
MCREST 0.00000000 sec
MCWRK 0.01500000 sec

======= CHANNEL f1 =======
NUC1 1H
P1 7.50 usec
PL1 1.60 dB
SFO1 500.2235015 MHz

F2 - Processing parameters
SI 65536
SF 500.2200200 MHz
WDW EM
SSB 0
LB 0.30 Hz
GB 0
PC 4.00

1D NMR plot parameters
CX 22.80 cm
CY 45.00 cm
F1P 4.000 ppm
F1 2000.88 Hz
F2P 2.200 ppm
F2 1100.48 Hz
PPMCM 0.07895 ppm/cm
HZCM 39.49105 Hz/cm

^{1}H NMR of macrocyclic β-sheet peptide **1$_{Glu}$**, 16 mM in 100 mM deuterioacetate buffer in D_2O at 500 MHz and 298 K

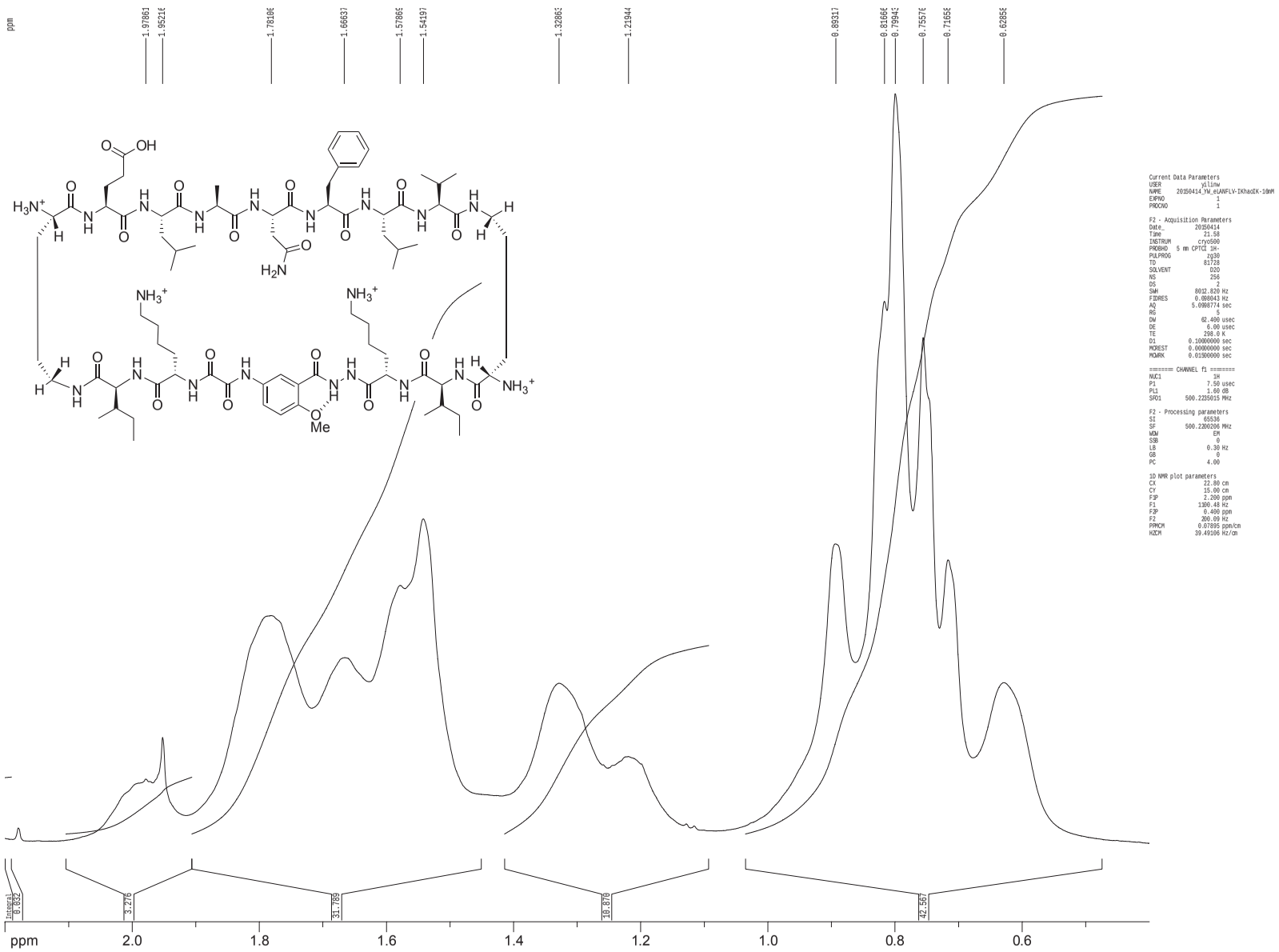

Current Data Parameters
USER yilinw
NAME 20150414_YW_eLANFLV-IKhacIK-16mM
EXPNO 1
PROCNO 1

F2 - Acquisition Parameters
Date_ 20150414
Time 21.58
INSTRUM cryo500
PROBHD 5 mm CPTCI 1H-
PULPROG zg30
TD 81728
SOLVENT D2O
NS 256
DS 2
SWH 8012.820 Hz
FIDRES 0.098043 Hz
AQ 5.0908774 sec
RG 5
DW 62.400 usec
DE 6.00 usec
TE 298.0 K
D1 0.10000000 sec
MCREST 0.00000000 sec
MCWRK 0.01500000 sec

======= CHANNEL f1 =======
NUC1 1H
P1 7.50 usec
PL1 1.60 dB
SFO1 500.2235015 MHz

F2 - Processing parameters
SI 65536
SF 500.2200200 MHz
WDW EM
SSB 0
LB 0.30 Hz
GB 0
PC 4.00

1D NMR plot parameters
CX 22.00 cm
CY 15.00 cm
F1P 2.200 ppm
F1 1100.48 Hz
F2P 0.400 ppm
F2 200.09 Hz
PPMCM 0.07895 ppm/cm
HZCM 39.49106 Hz/cm

^{1}H NMR 2D TOCSY of macrocyclic β-sheet peptide **$\mathbf{1_{Glu}}$** with 150-ms spin-lock mixing time
16 mM in 100 mM deuterioacetate buffer in D_2O at 500 MHz and 298 K

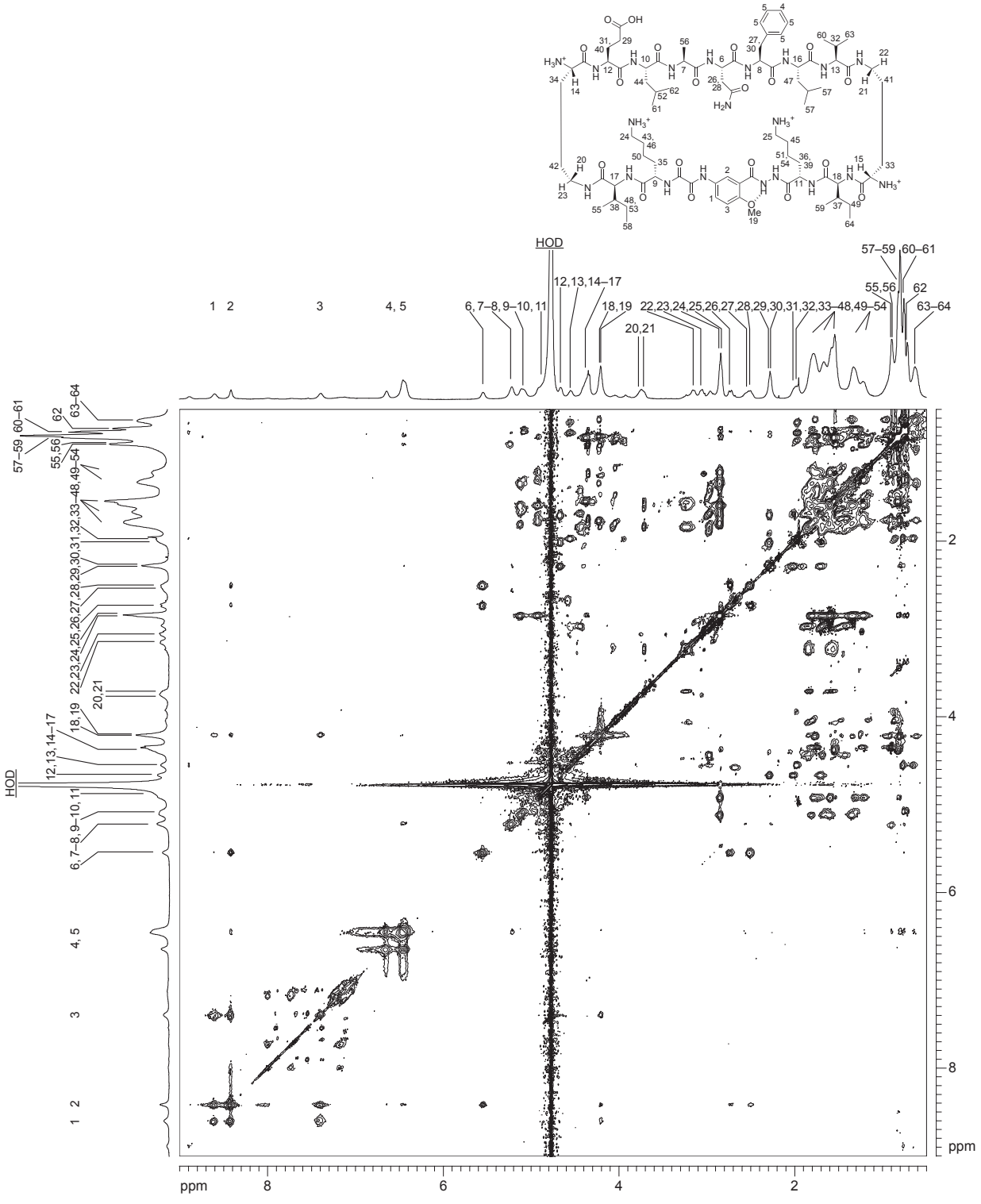

^{1}H NMR 2D TOCSY of macrocyclic β-sheet peptide **1$_{Glu}$** with 150-ms spin-lock mixing time
16 mM in 100 mM deuterioacetate buffer in D_2O at 500 MHz and 298 K

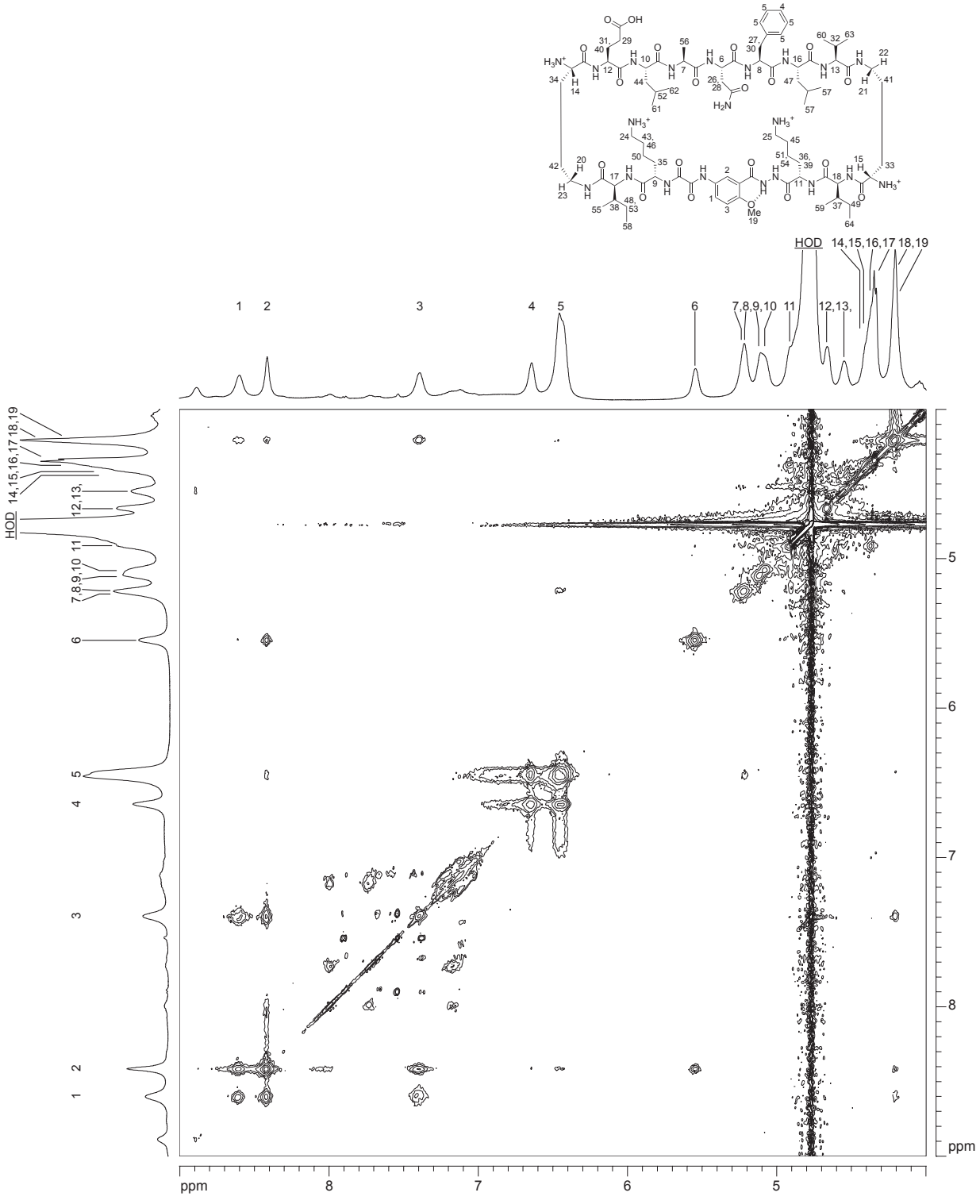

^{1}H NMR 2D TOCSY of macrocyclic β-sheet peptide **$\mathbf{1_{Glu}}$** with 150-ms spin-lock mixing time
16 mM in 100 mM deuterioacetate buffer in D_2O at 500 MHz and 298 K

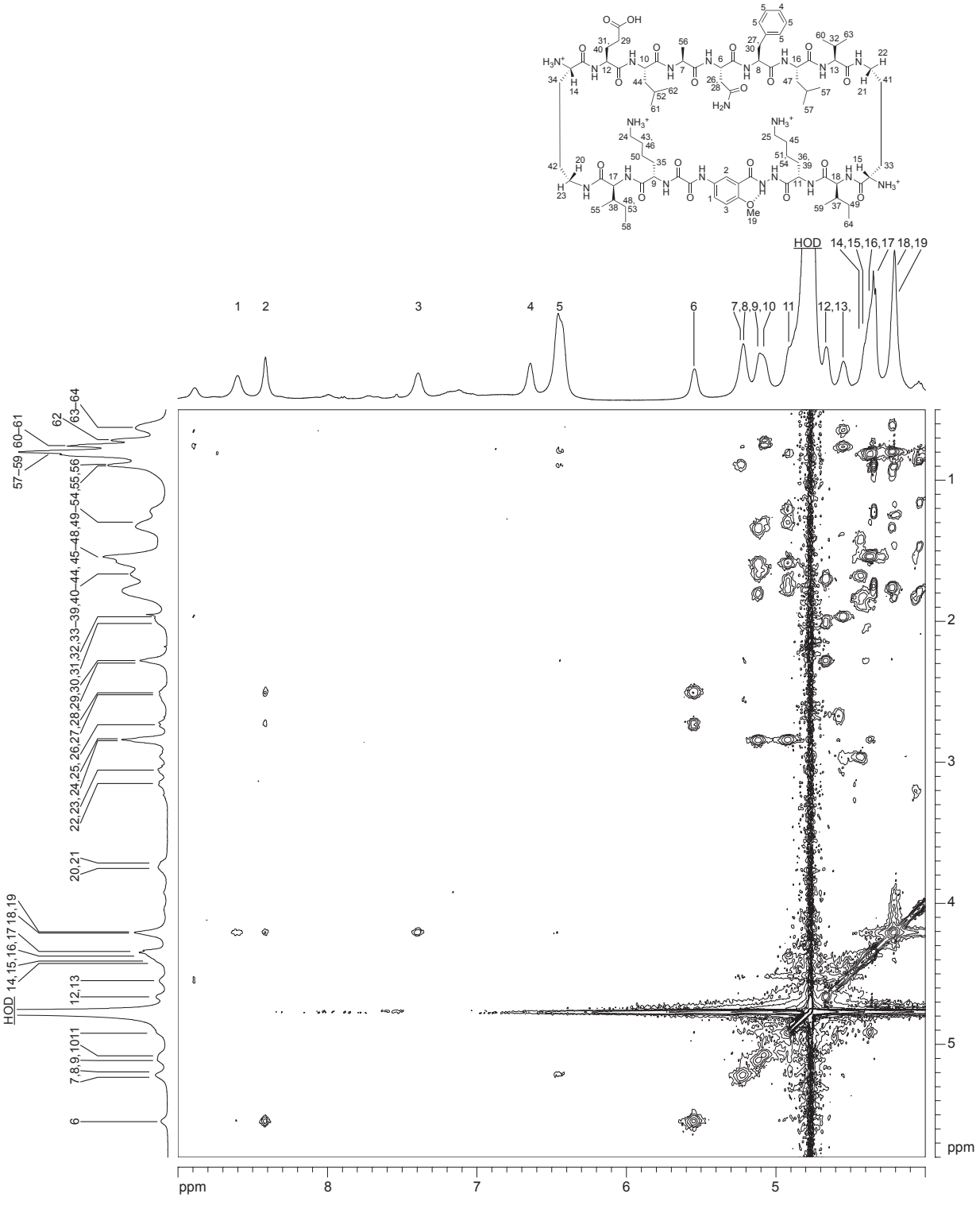

^{1}H NMR 2D TOCSY of macrocyclic β-sheet peptide **1$_{Glu}$** with 150-ms spin-lock mixing time
16 mM in 100 mM deuterioacetate buffer in D_2O at 500 MHz and 298 K

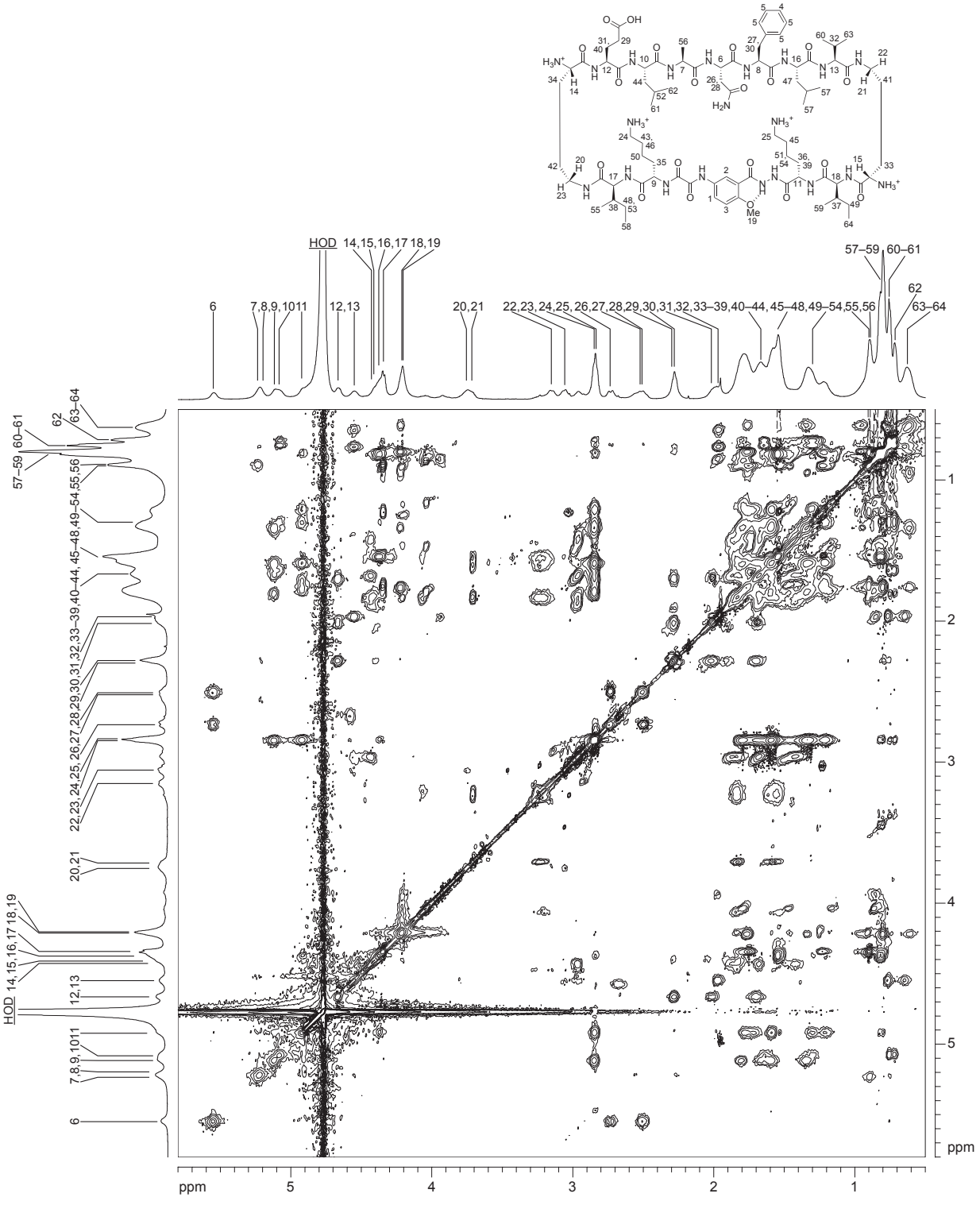

^{1}H NMR 2D NOESY of macrocyclic β-sheet peptide **1_{Glu}** with 150-ms mixing time
16 mM in 100 mM deuterioacetate buffer in D_2O at 500 MHz and 298 K

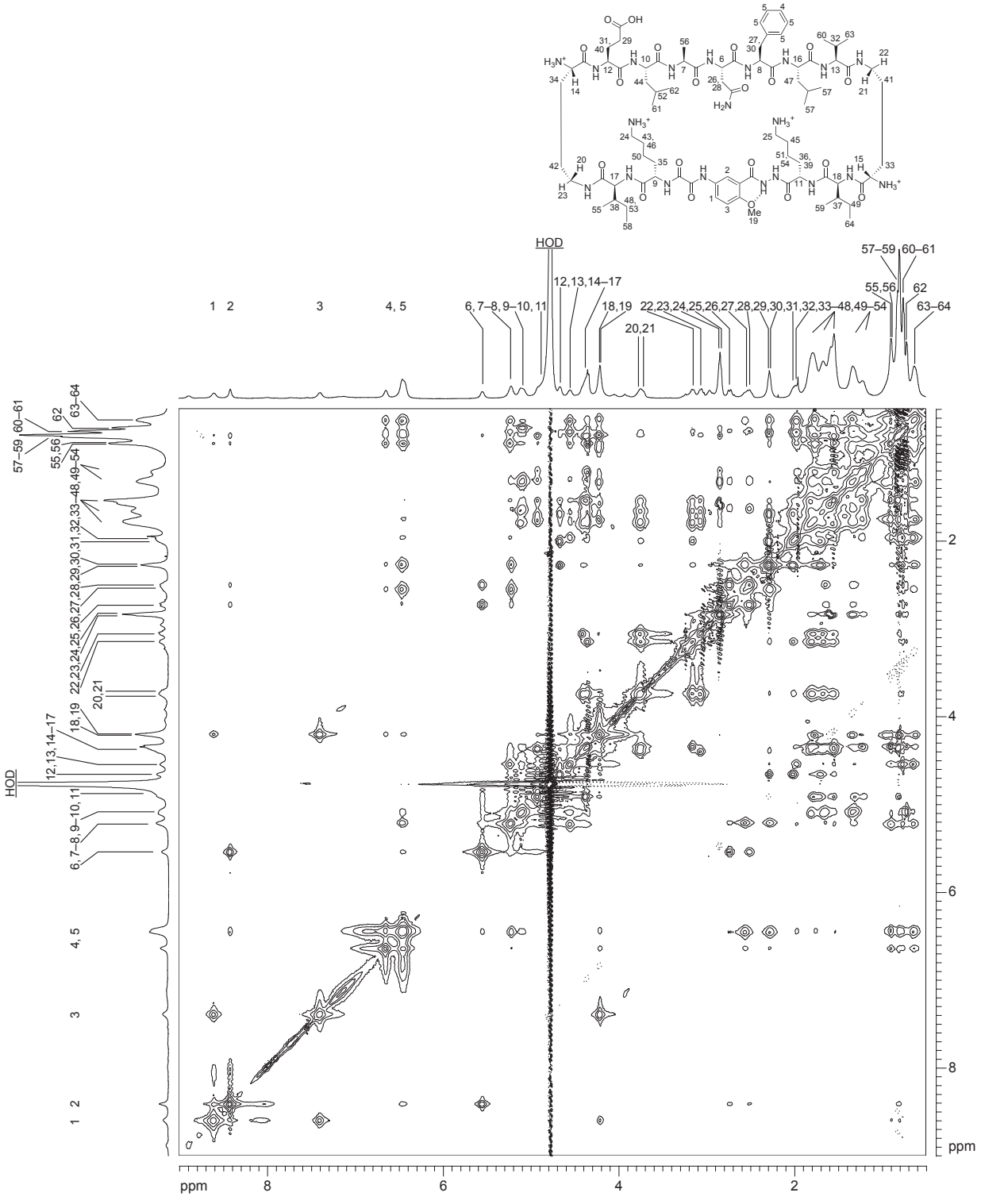

^{1}H NMR 2D NOESY of macrocyclic β-sheet peptide **1$_{Glu}$** with 150-ms mixing time
16 mM in 100 mM deuterioacetate buffer in D_2O at 500 MHz and 298 K

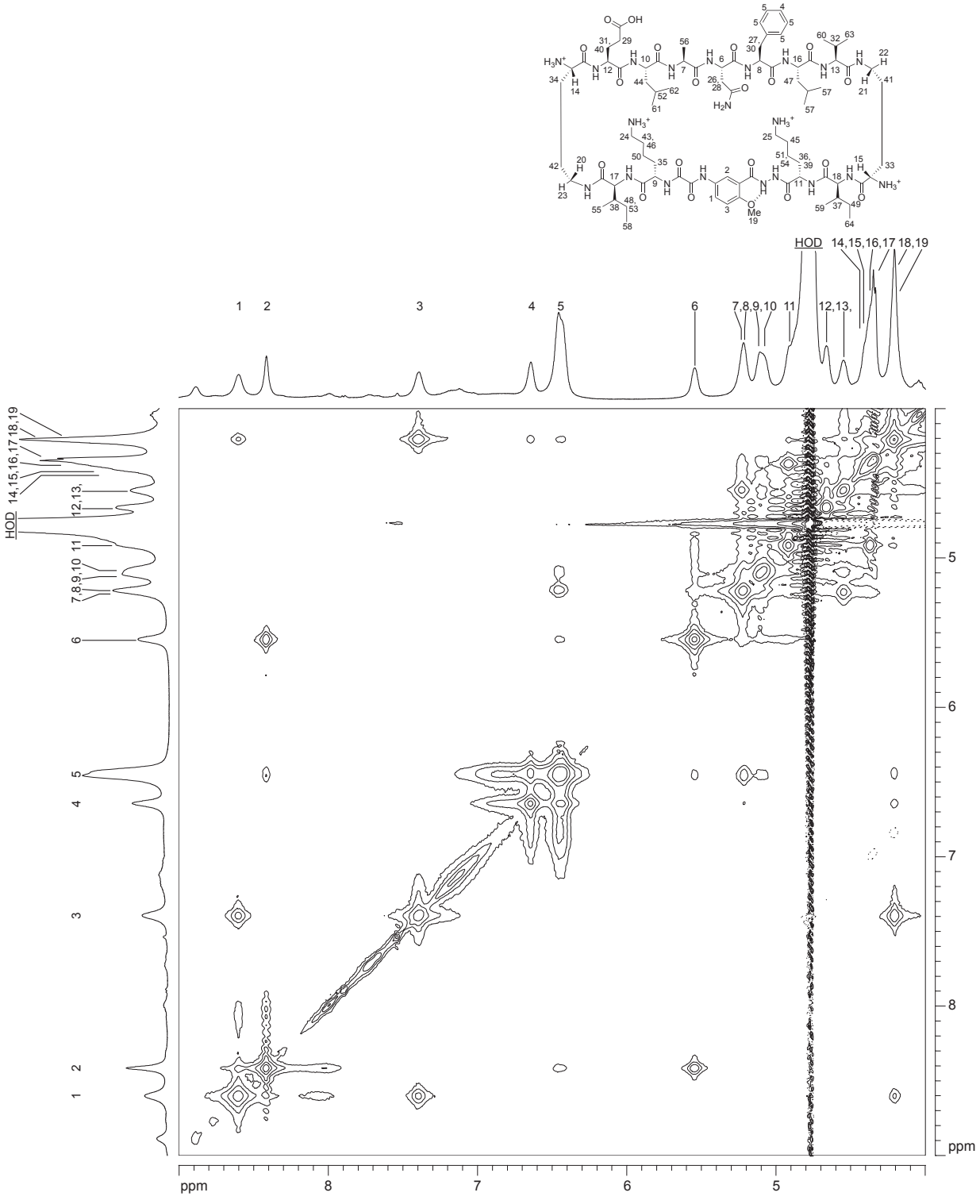

^{1}H NMR 2D NOESY of macrocyclic β-sheet peptide **$\mathbf{1_{Glu}}$** with 150-ms mixing time
16 mM in 100 mM deuterioacetate buffer in D_2O at 500 MHz and 298 K

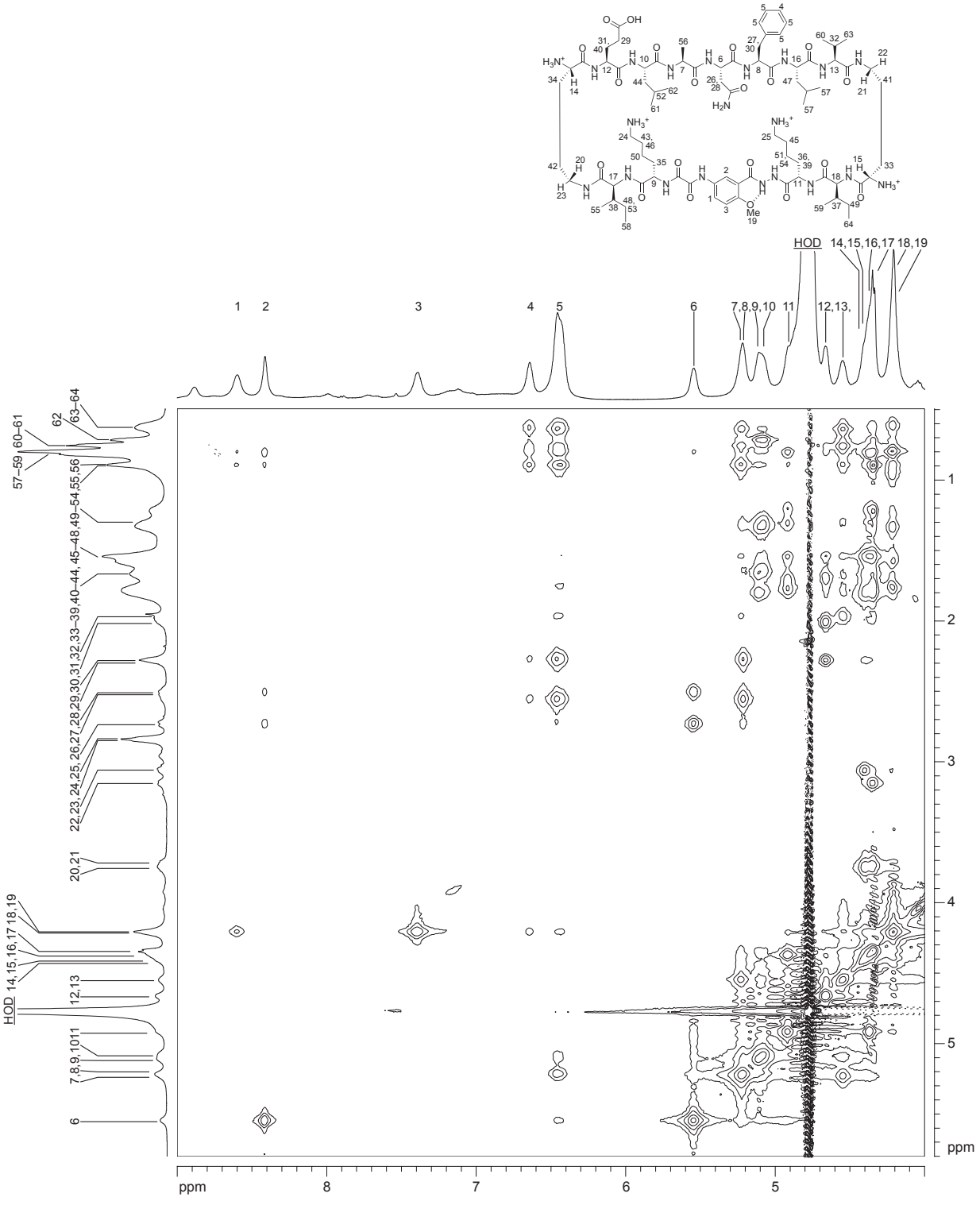

^{1}H NMR 2D NOESY of macrocyclic β-sheet peptide **1_{Glu}** with 150-ms mixing time
16 mM in 100 mM deuterioacetate buffer in D_2O at 500 MHz and 298 K

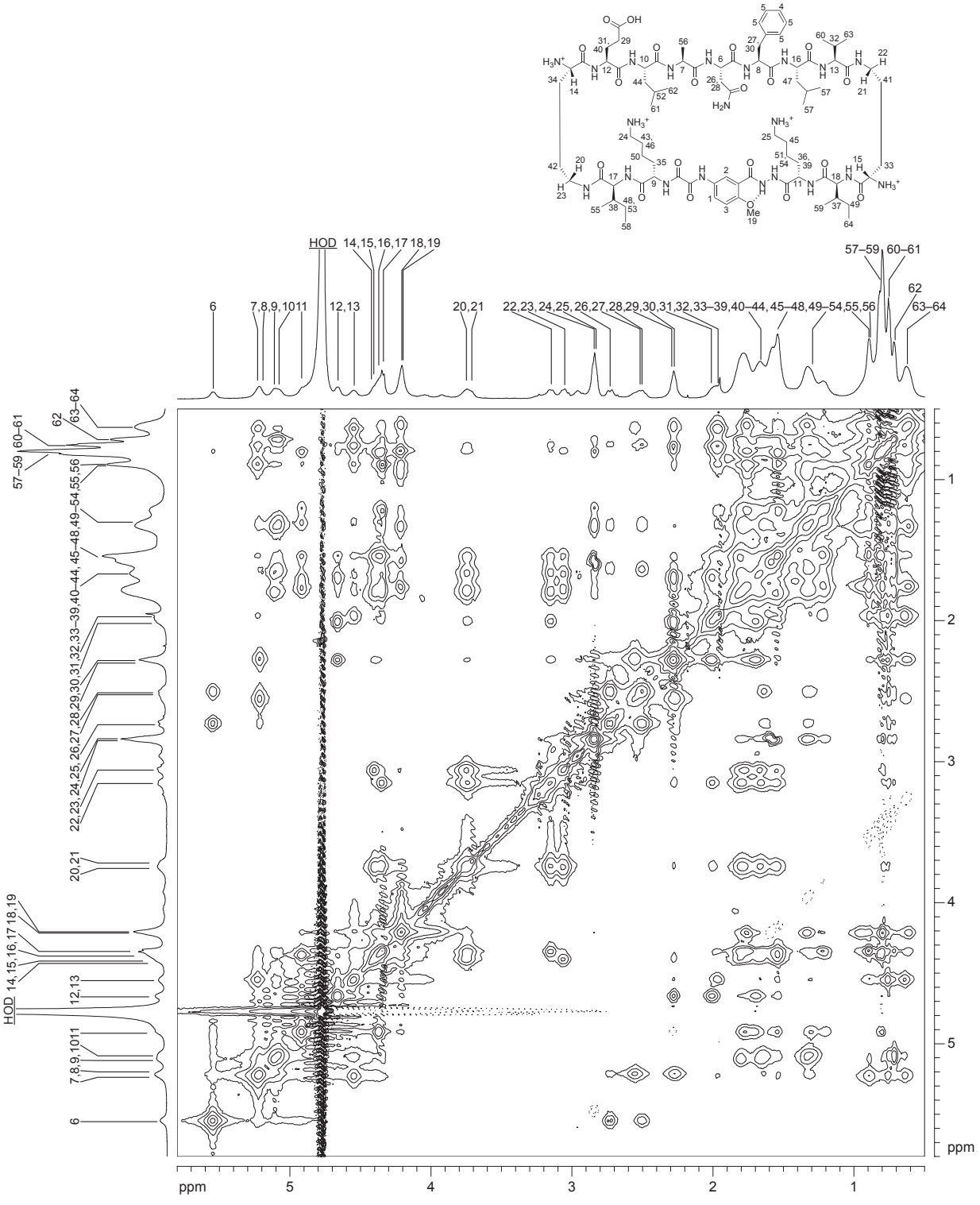

^{1}H NMR DOSY of macrocyclic β-sheet peptide **1$_{Glu}$** at 500 MHz and 298 K
16 mM in 100 mM deuterioacetate buffer in D_2O

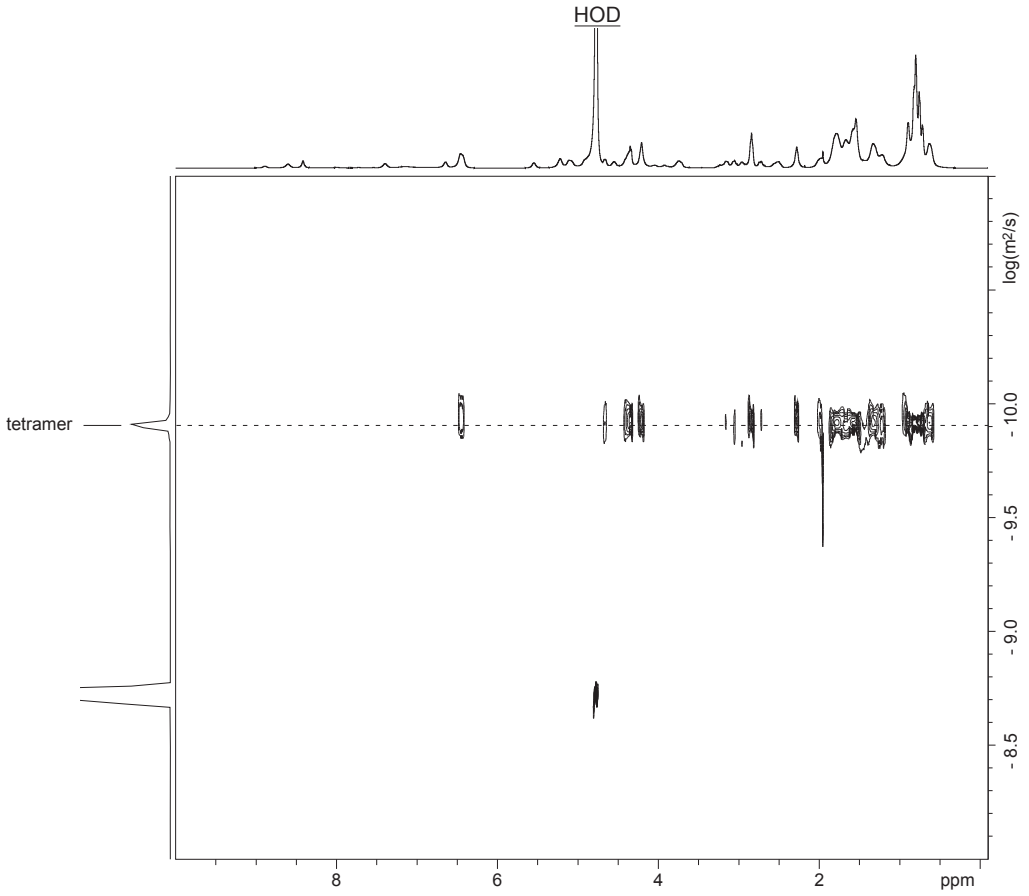

Calculations for macrocyclic β-sheet peptide **1$_{Glu}$** at 16 mM

D_{HOD} = 19.0 x 10^{-10} m^2/s [a]
log (D_{HOD}) = -8.721

$D_{tetramer}$: log(D) = -9.917; D = $10^{-9.917}$ = 12.1 ± 0.6 x 10^{-11} m^2/s

[a]Longsworth, L. G. *J. Phys. Chem.* **1960**, *64*, 1914−1917.

^{1}H NMR DOSY of macrocyclic β-sheet peptide **1$_{Glu}$** at 500 MHz and 298 K
16 mM at pH 7.2 in D_2O

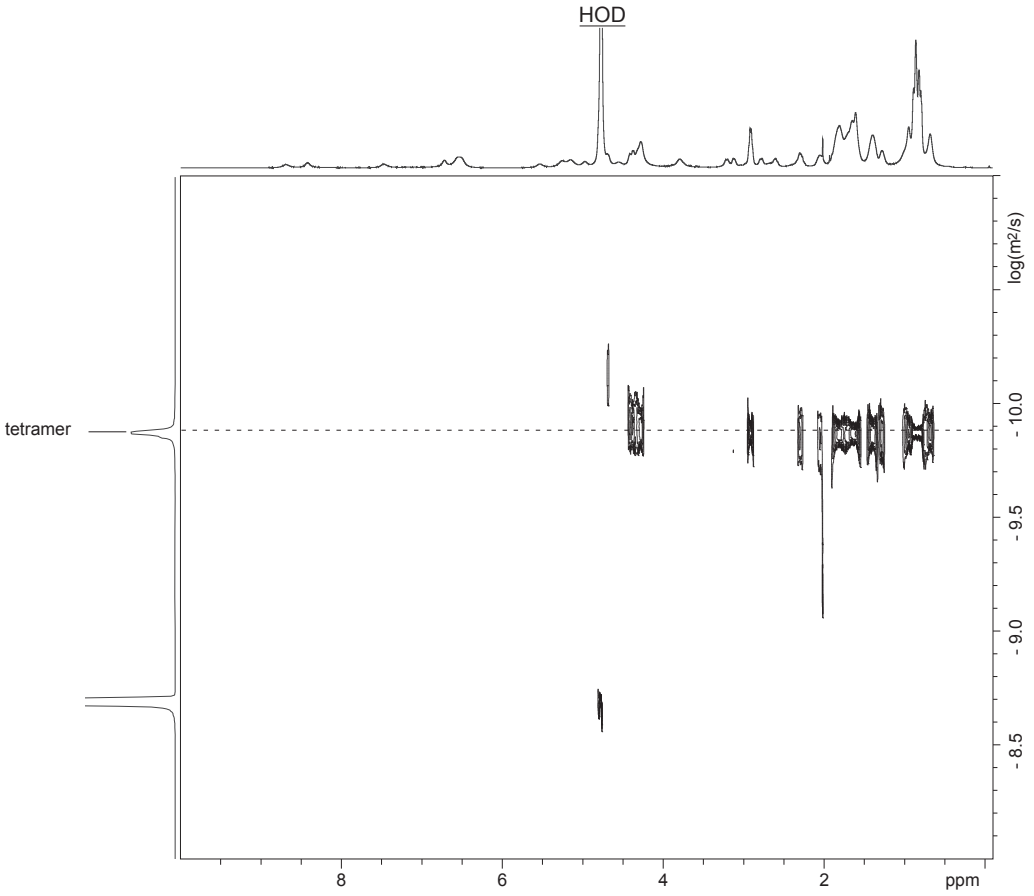

Calculations for macrocyclic β-sheet peptide **1$_{Glu}$** at 16 mM and pH 7.2

D_{HOD} = 19.0 x 10^{-10} m^2/s [a]
log (D_{HOD}) = -8.721

$D_{tetramer}$: log(D) = -9.907; D = $10^{-9.907}$ = 12.4 ± 0.3 x 10^{-11} m^2/s

[a]Longsworth, L. G. *J. Phys. Chem.* **1960**, *64*, 1914−1917.

RP-HPLC of Macrocyclic β-Sheet $\mathbf{1_{Leu}}$

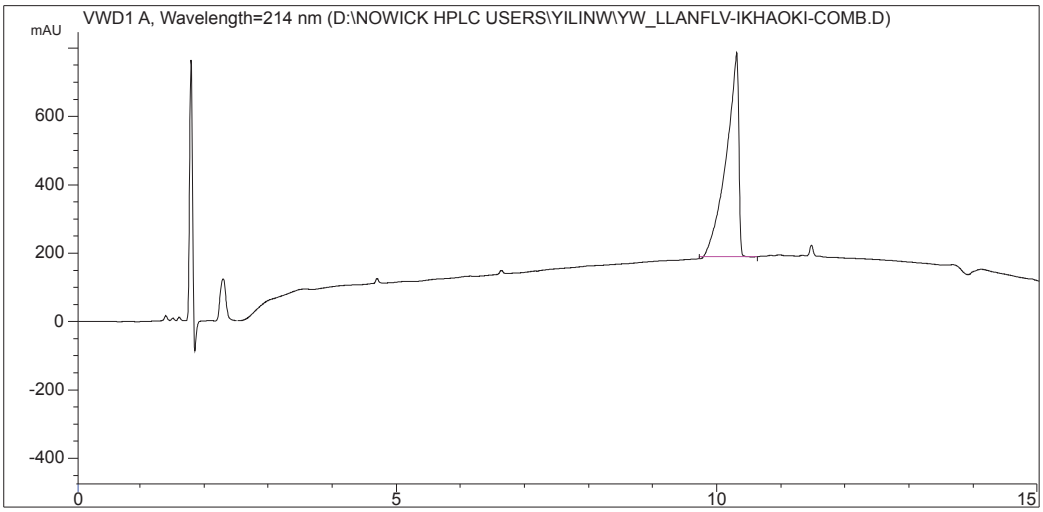

Peak #	RetTime [min]	Type	Width [min]	Area mAU *s	Height [mAU]	Area %
1	10.274	MM	0.2254	8094.08105	598.6033	100.000

column:	Aeris XB-C18 2.6µ
dimensions:	150 mm x 4.6 mm
mobile phase:	A: H_2O, 0.1% TFA
	B: CH_3CN, 0.1% TFA
gradient:	A/B (95:5) to (0:100) in 20 min
flow rate:	1.0 mL/min
detection:	VWD, wavelength = 214 nm
temperature:	298 K

MS (ESI) of Macrocyclic β-Sheet $\mathbf{1_{Leu}}$

yilinw2-llanflv-ikhaoki-com-1 26 (0.477) Sm (SG, 2x3.00); Cm (6:40)

TOF MS ES+
1.29e4

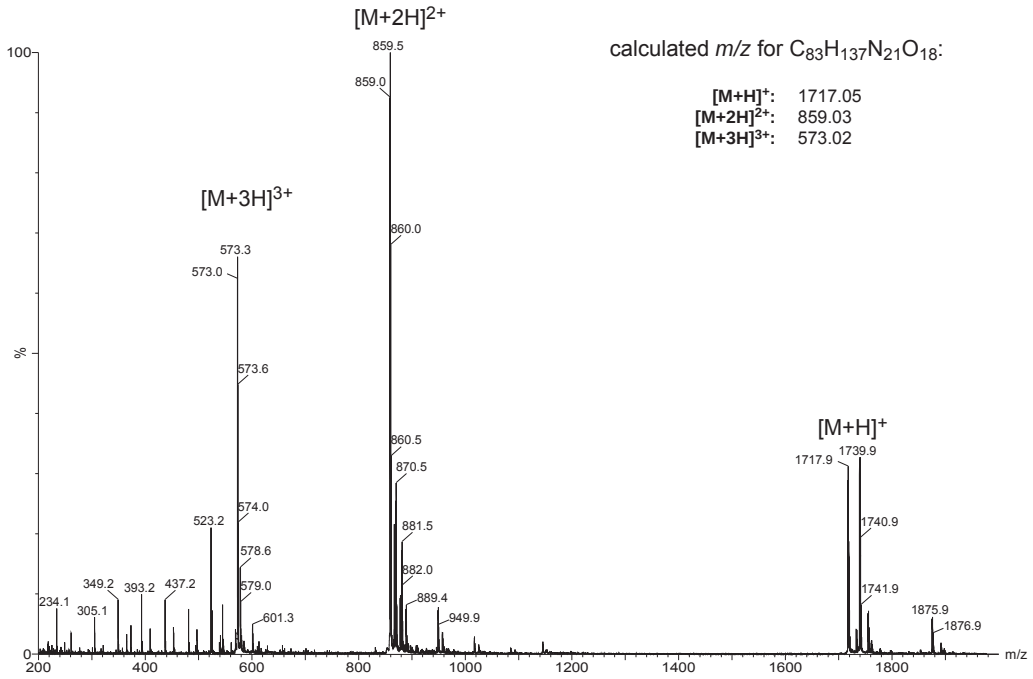

calculated *m/z* for $C_{83}H_{137}N_{21}O_{18}$:

$[M+H]^+$:	1717.05
$[M+2H]^{2+}$:	859.03
$[M+3H]^{3+}$:	573.02

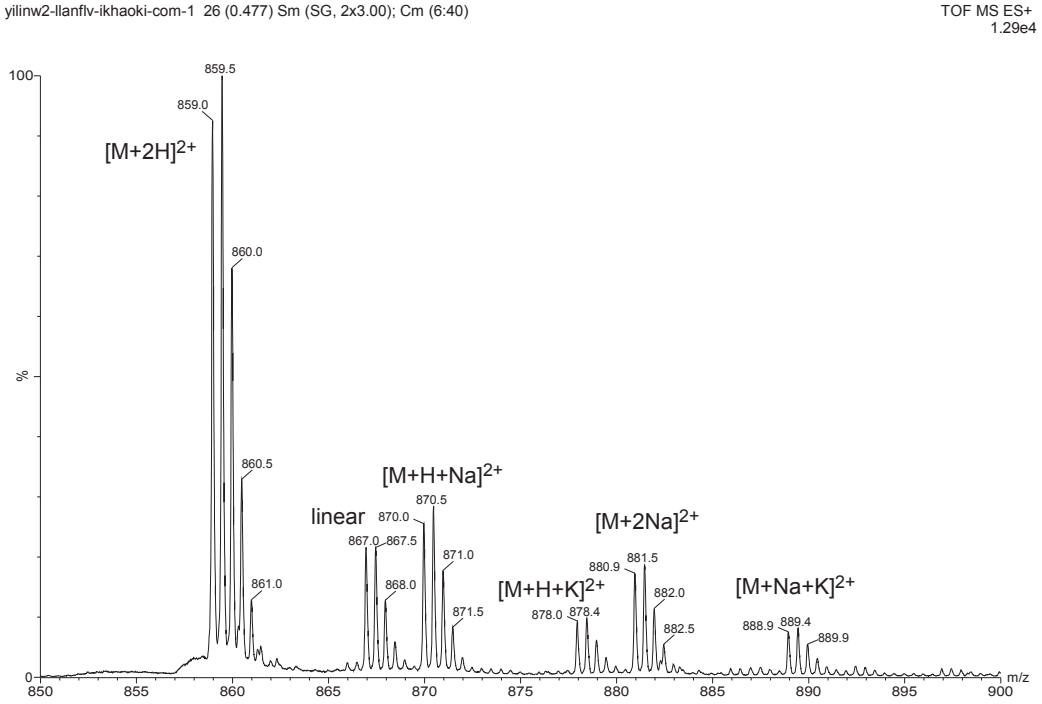
yilinw2-llanflv-ikhaoki-com-1 26 (0.477) Sm (SG, 2x3.00); Cm (6:40)
TOF MS ES+
1.29e4
100
%
0
[M+2H]2+
[M+H+Na]2+
linear
[M+2Na]2+
[M+H+K]2+
[M+Na+K]2+
859.5
859.0
860.0
860.5
861.0
870.0
870.5
867.0
867.5
871.0
868.0
871.5
880.9
881.5
882.0
878.0
878.4
882.5
888.9
889.4
889.9
850
855
860
865
870
875
880
885
890
895
900
m/z

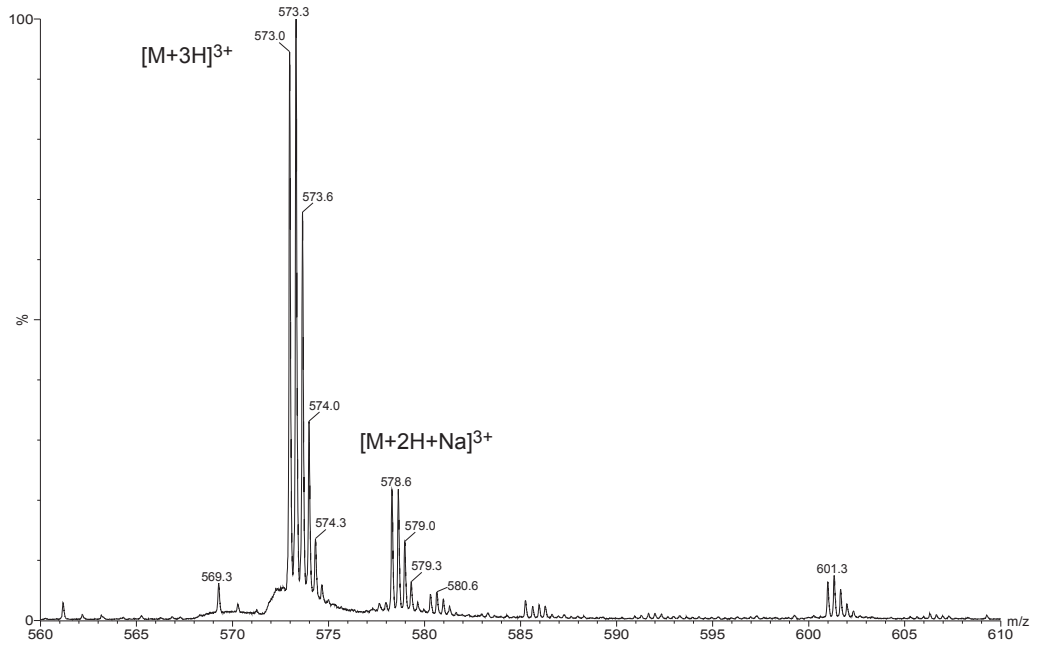
yilinw2-llanflv-ikhaoki-com-1 26 (0.477) Sm (SG, 2x3.00); Cm (6:40)
TOF MS ES+
8.55e3
100
%
0
[M+3H]3+
[M+2H+Na]3+
573.3
573.0
573.6
574.0
574.3
576.6
579.0
579.3
580.6
569.3
601.3
560
565
570
575
580
585
590
595
600
605
610
m/z

^{1}H NMR of macrocyclic β-sheet peptide **1Leu**, 1 mM in 100 mM deuterioacetate buffer in D_2O at 500 MHz and 298 K

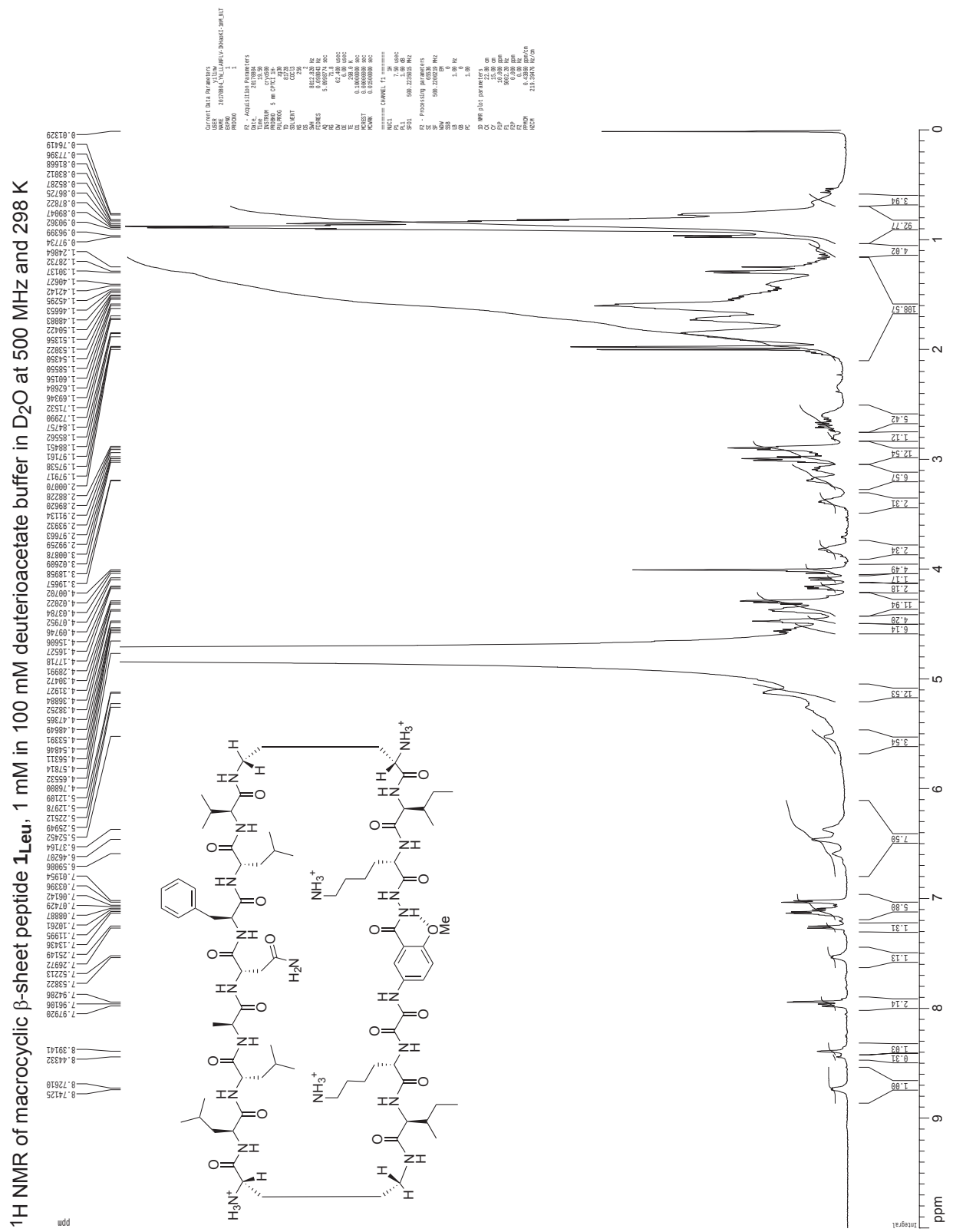

^{1}H NMR of macrocyclic β-sheet peptide **$\mathbf{1}_{\mathbf{Leu}}$**, 1 mM in 100 mM deuterioacetate buffer in D_2O at 500 MHz and 298 K

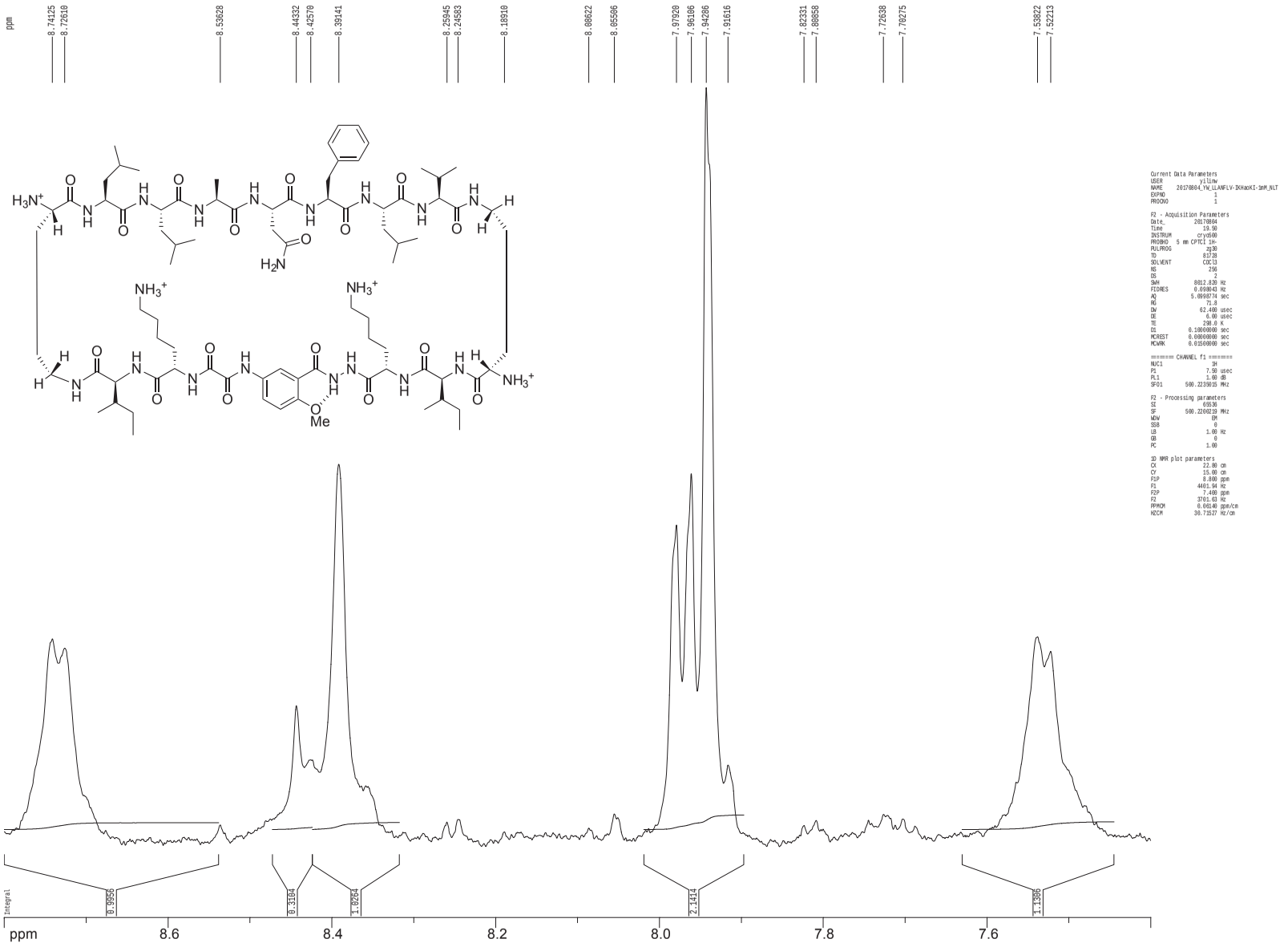

Current Data Parameters
USER vilinw
NAME 20170804_YW_LLAVFLV-IKHackI-1mM_NLT
EXPNO 1
PROCNO 1

F2 - Acquisition Parameters
Date_ 20170804
Time 19.50
INSTRUM cryo500
PROBHD 5 mm CPTCI 1H-
PULPROG zg30
TD 81728
SOLVENT CDCl3
NS 256
DS 2
SWH 8012.830 Hz
FIDRES 0.098043 Hz
AQ 5.0998774 sec
RG 71.8
DW 62.400 usec
DE 6.00 usec
TE 298.0 K
D1 0.10000000 sec
MCREST 0.00000000 sec
MCWRK 0.03500000 sec

====== CHANNEL f1 ======
NUC1 1H
P1 7.50 usec
PL1 1.00 dB
SFO1 500.2239035 MHz

F2 - Processing parameters
SI 65536
SF 500.2200219 MHz
WDW EM
SSB 0
LB 1.00 Hz
GB 0
PC 1.00

1D NMR plot parameters
CX 22.80 cm
CY 15.00 cm
F1P 8.800 ppm
F1 4401.94 Hz
F2P 7.400 ppm
F2 3701.63 Hz
PPMCM 0.08140 ppm/cm
HZCM 38.73527 Hz/cm

^{1}H NMR of macrocyclic β-sheet peptide **1$_{Leu}$**, 1 mM in 100 mM deuterioacetate buffer in D_2O at 500 MHz and 298 K

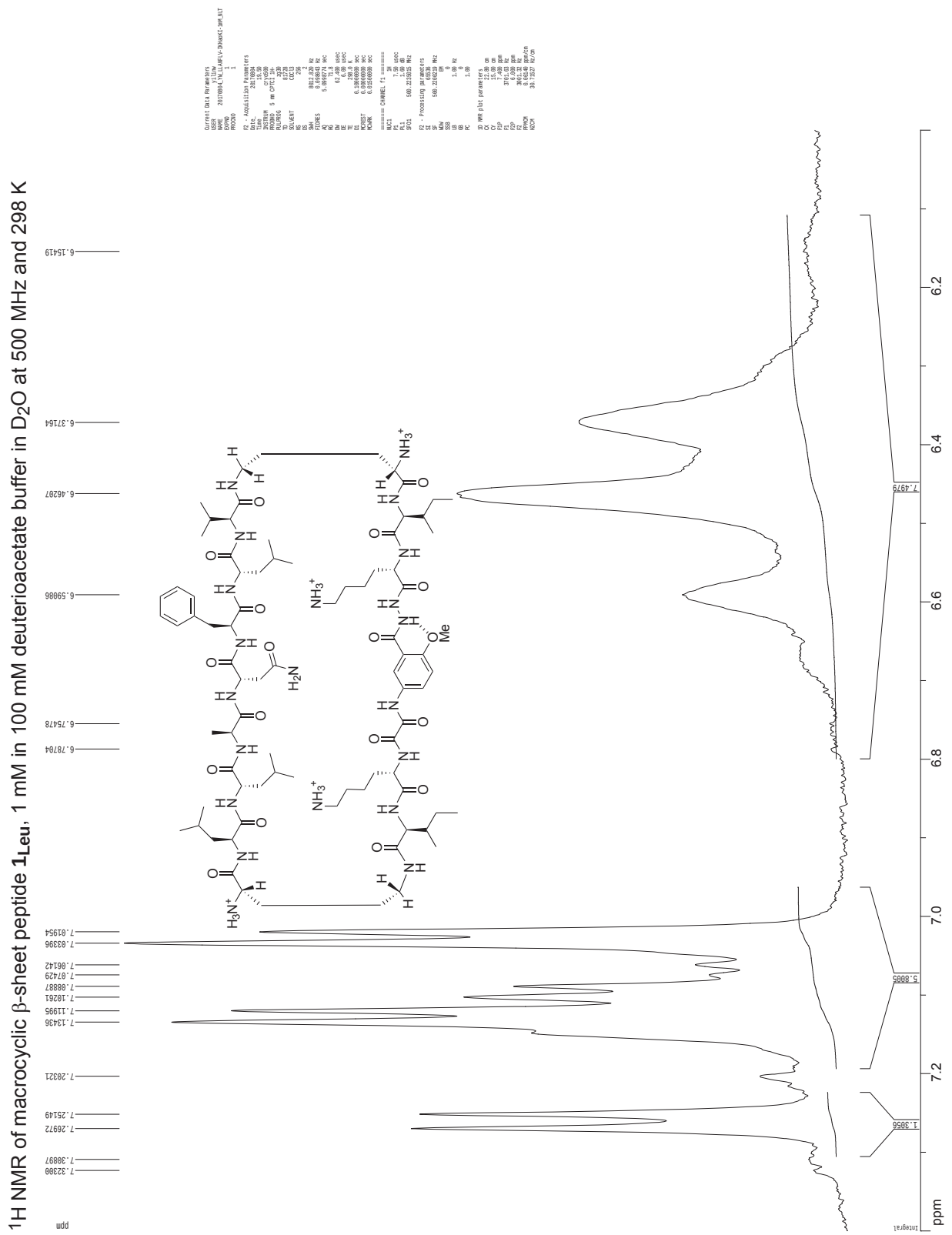

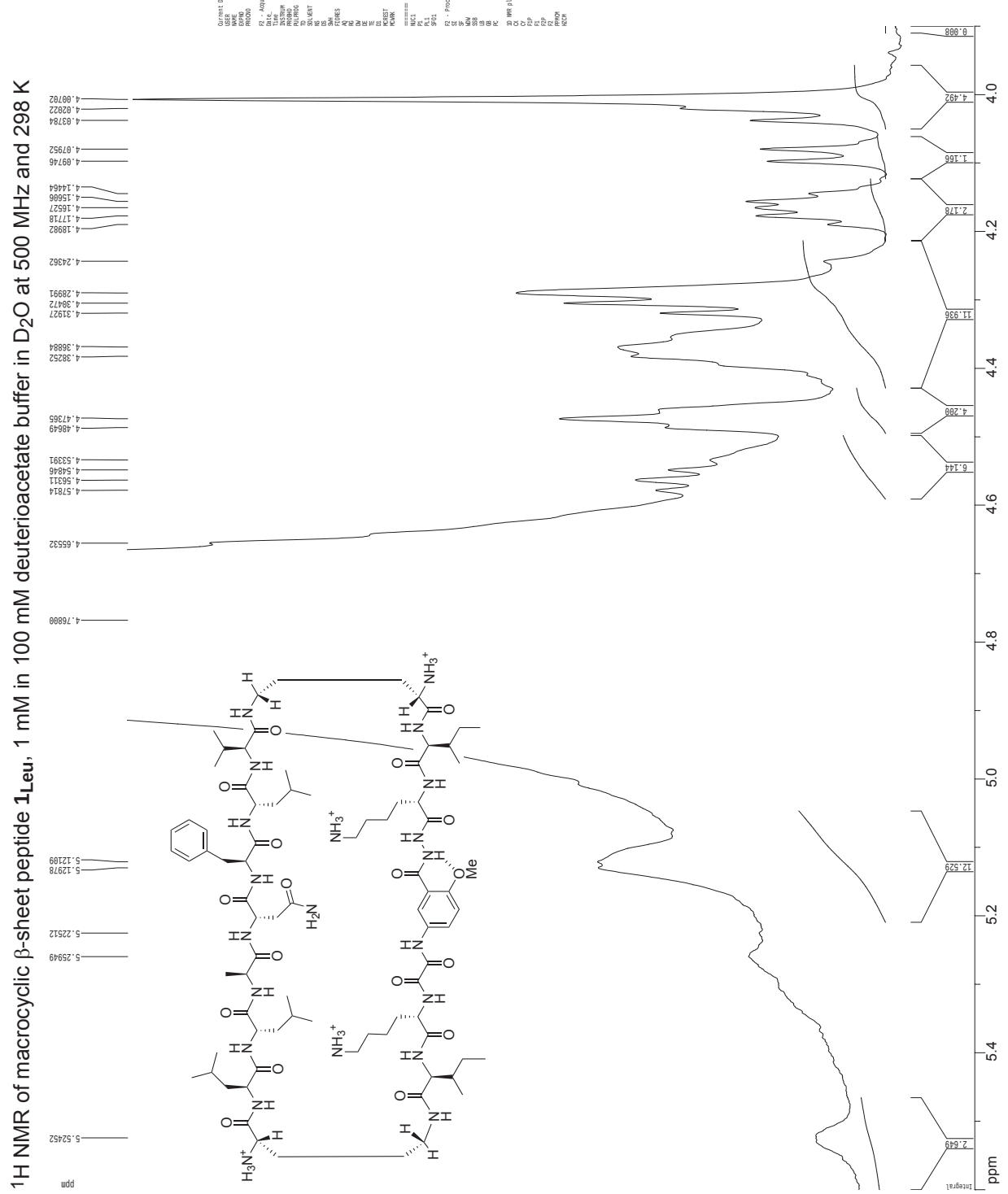
1H NMR of macrocyclic β-sheet peptide 1Leu, 1 mM in 100 mM deuterioacetate buffer in D2O at 500 MHz and 298 K
ppm
Integral
4.00702
4.02822
4.03784
4.07952
4.09746
4.14464
4.15606
4.16527
4.17718
4.18982
4.24362
4.28991
4.30472
4.31927
4.36884
4.38252
4.47365
4.48649
4.53391
4.54846
4.56311
4.57814
4.65532
4.76800
5.12109
5.12978
5.22512
5.25949
5.32452
2.649
12.529
6.144
4.200
11.936
2.178
1.166
4.492
0.088
5.0
5.2
5.4
4.8
4.6
4.4
4.2
4.0

^{1}H NMR of macrocyclic β-sheet peptide **$\mathbf{1_{Leu}}$**, 1 mM in 100 mM deuterioacetate buffer in D_2O at 500 MHz and 298 K

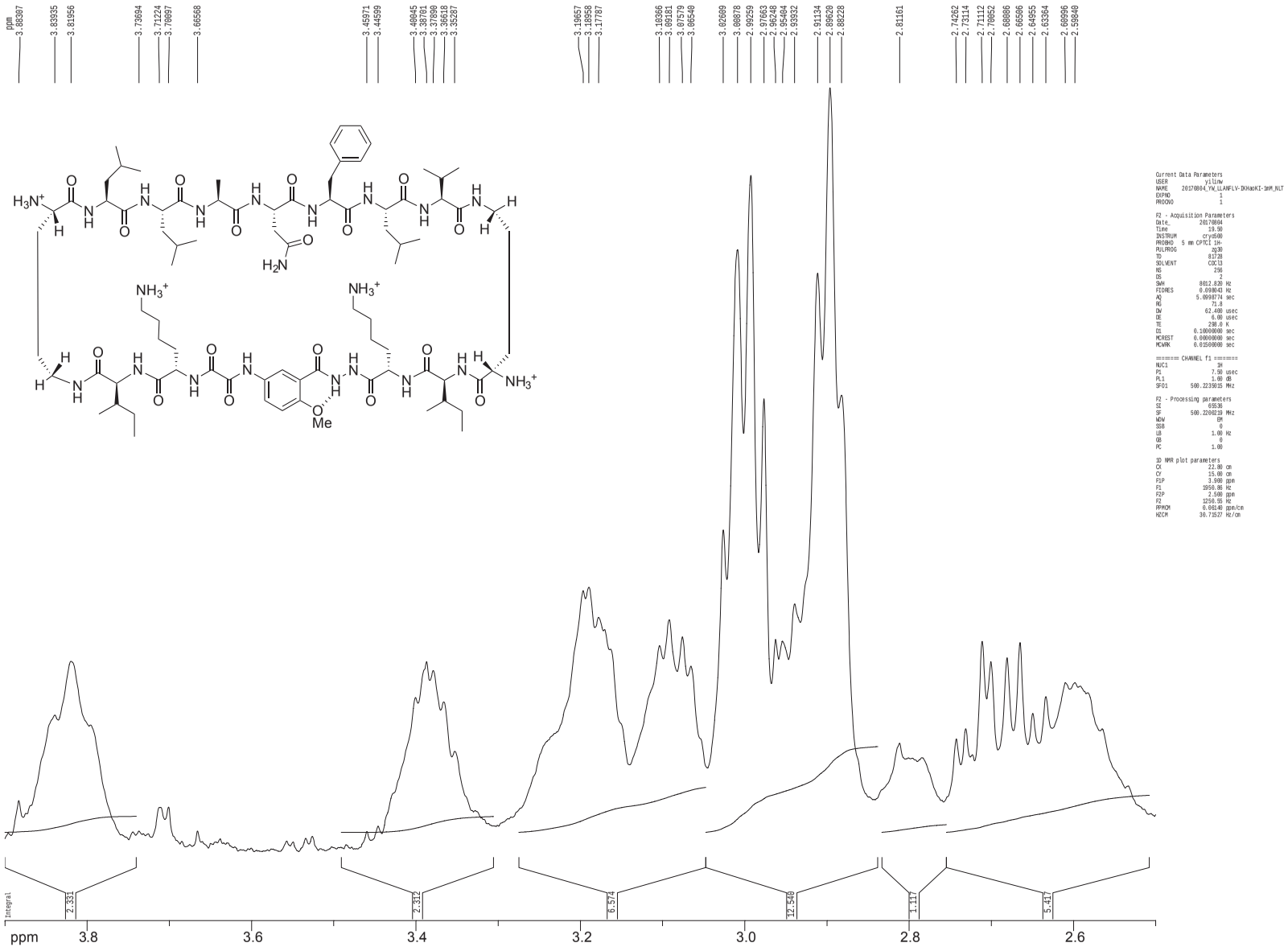

Current Data Parameters
USER vilinw
NAME 20170804_YW_LLAWFLV-IKHackI-1mM_NLT
EXPNO 1
PROCNO 1

F2 - Acquisition Parameters
Date_ 20170804
Time 19.50
INSTRUM cryo500
PROBHD 5 mm CPTCI 1H-
PULPROG zg30
TD 81728
SOLVENT CDCl3
NS 256
DS 2
SWH 8012.820 Hz
FIDRES 0.098043 Hz
AQ 5.0998774 sec
RG 71.8
DW 62.400 usec
DE 6.00 usec
TE 298.0 K
D1 0.10000000 sec
MCREST 0.00000000 sec
MCWRK 0.03500000 sec

====== CHANNEL f1 ======
NUC1 1H
P1 7.50 usec
PL1 1.00 dB
SFO1 500.2239035 MHz

F2 - Processing parameters
SI 65536
SF 500.2200219 MHz
WDW EM
SSB 0
LB 1.00 Hz
GB 0
PC 1.00

1D NMR plot parameters
CX 22.80 cm
CY 15.00 cm
F1P 3.900 ppm
F1 1950.86 Hz
F2P 2.500 ppm
F2 1250.05 Hz
PPMCM 0.08140 ppm/cm
HZCM 38.73527 Hz/cm

^{1}H NMR of macrocyclic β-sheet peptide **$\mathbf{1}_{\mathbf{Leu}}$**, 1 mM in 100 mM deuterioacetate buffer in D_2O at 500 MHz and 298 K

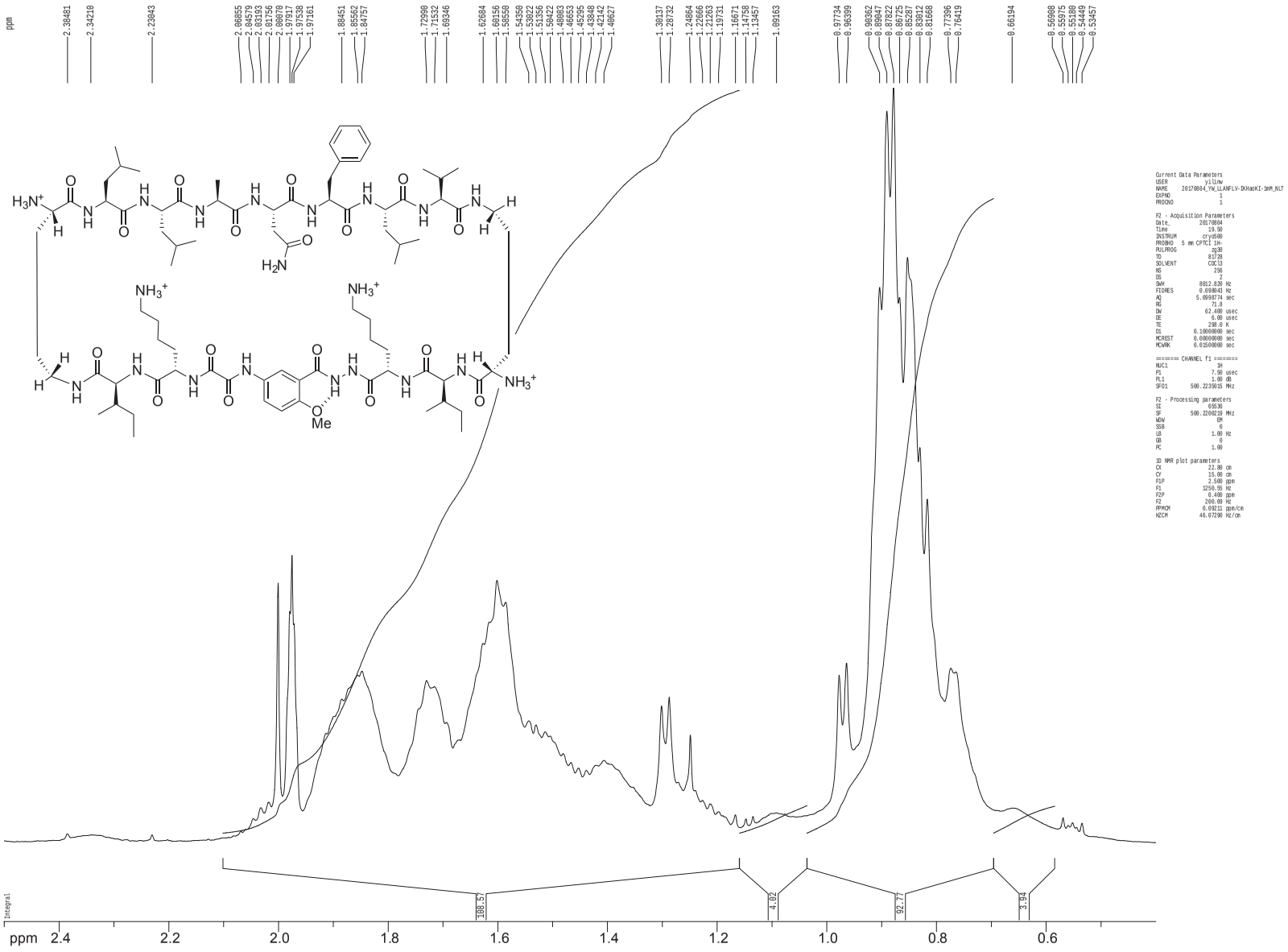

Current Data Parameters
USER vilinw
NAME 20170804_YW_LLAWFLV-IKHackI-1mM_NLT
EXPNO 1
PROCNO 1

F2 - Acquisition Parameters
Date_ 20170804
Time 19.50
INSTRUM cryo500
PROBHD 5 mm CPTCI 1H-
PULPROG zg30
TD 81728
SOLVENT CDCl3
NS 256
DS 2
SWH 8012.830 Hz
FIDRES 0.098043 Hz
AQ 5.0998774 sec
RG 71.8
DW 62.400 usec
DE 6.00 usec
TE 298.0 K
D1 0.10000000 sec
MCREST 0.00000000 sec
MCWRK 0.03500000 sec

====== CHANNEL f1 ======
NUC1 1H
P1 7.50 usec
PL1 1.00 dB
SFO1 500.2239035 MHz

F2 - Processing parameters
SI 65536
SF 500.2200219 MHz
WDW EM
SSB 0
LB 1.00 Hz
GB 0
PC 1.00

1D NMR plot parameters
CX 22.00 cm
CY 15.00 cm
F1P 2.500 ppm
F1 1250.55 Hz
F2P 0.400 ppm
F2 200.09 Hz
PPMCM 0.09211 ppm/cm
HZCM 46.07290 Hz/cm

^{1}H NMR 2D TOCSY of macrocyclic β-sheet peptide **$\mathbf{1_{Leu}}$** with 150-ms spin-lock mixing time
1 mM in 100 mM deuterioacetate buffer in D_2O at 500 MHz and 298 K

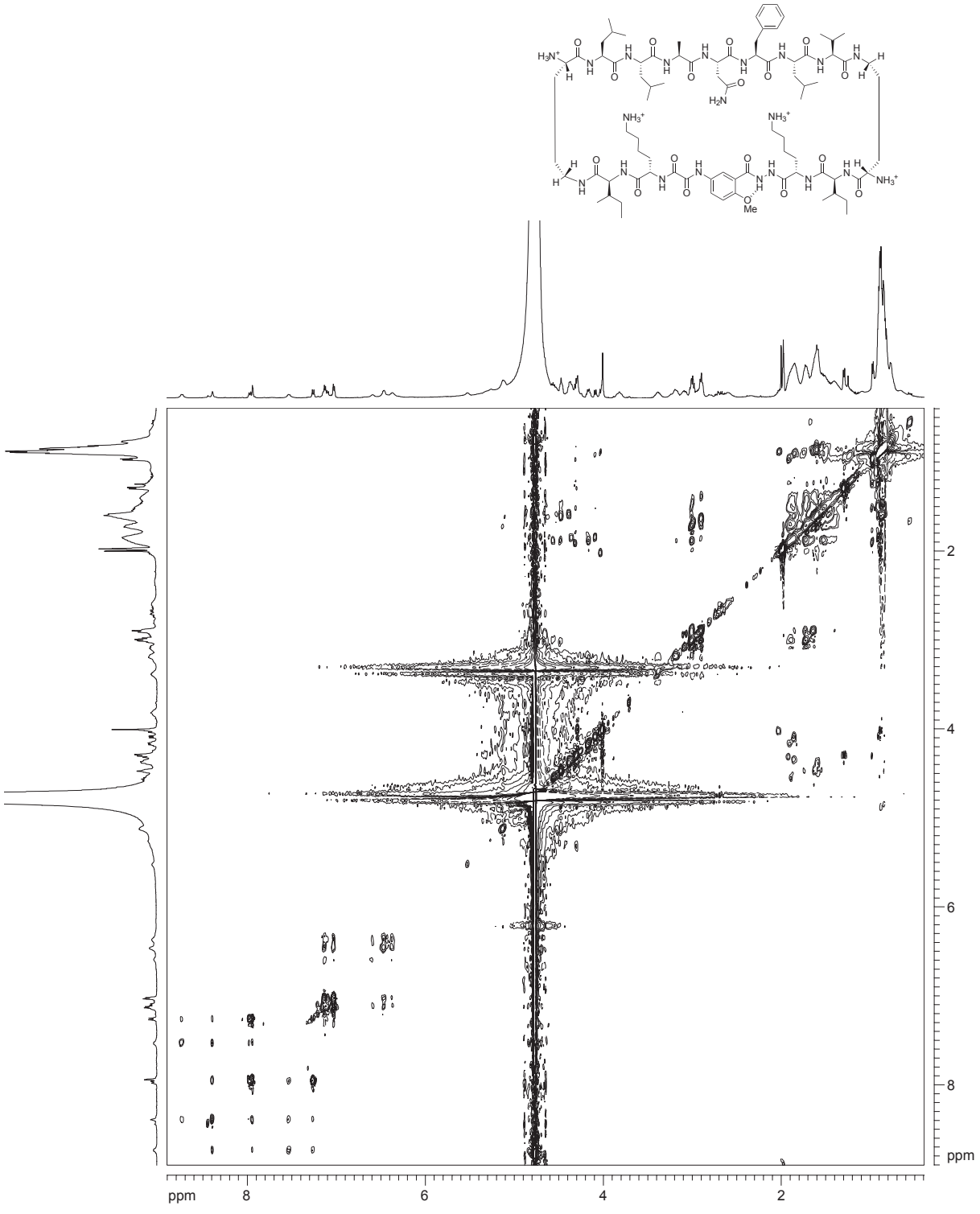

^{1}H NMR 2D TOCSY of macrocyclic β-sheet peptide **1$_{Leu}$** with 150-ms spin-lock mixing time
1 mM in 100 mM deuterioacetate buffer in D_2O at 500 MHz and 298 K

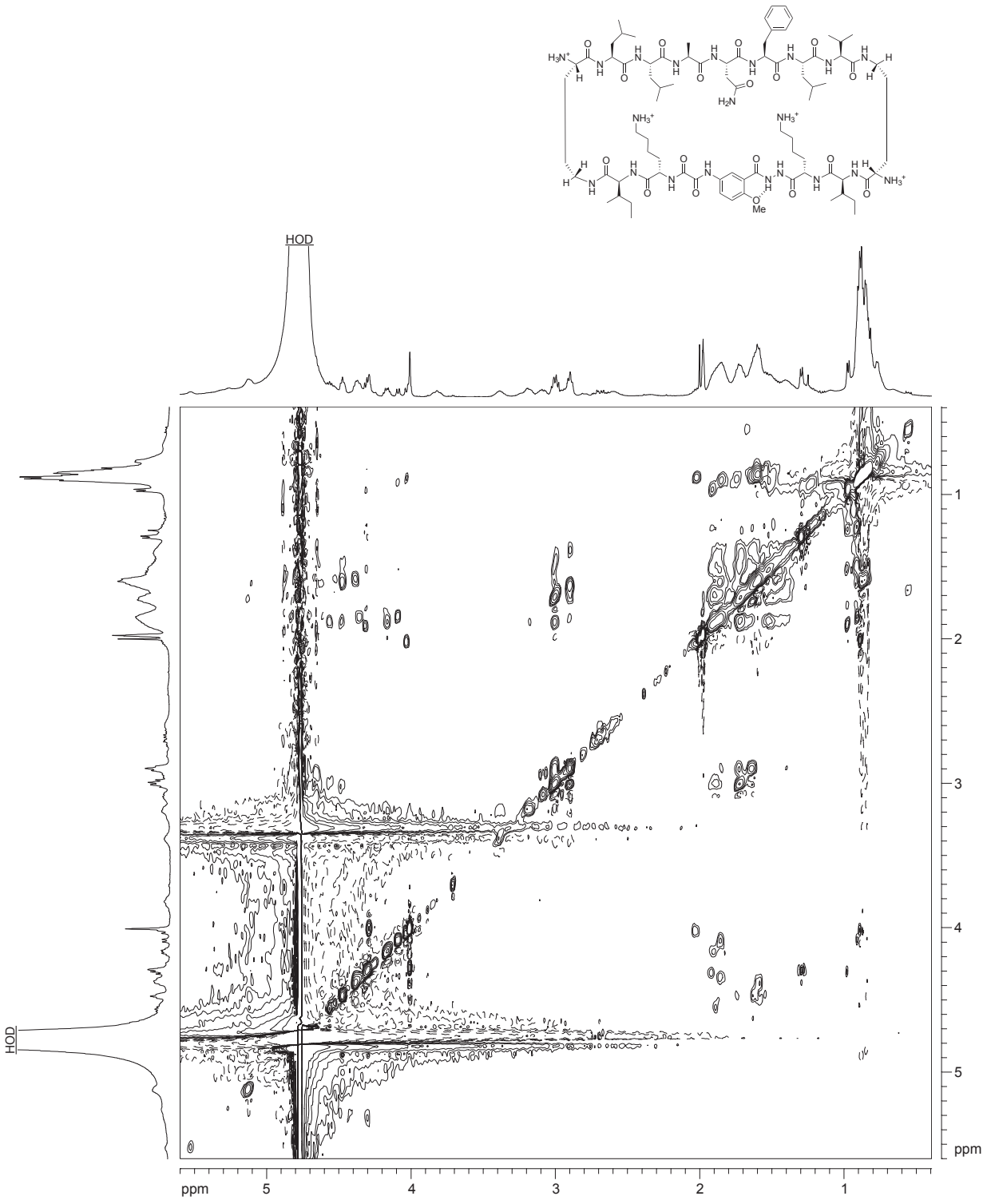

^{1}H NMR 2D NOESY of macrocyclic β-sheet peptide **$\mathbf{1_{Leu}}$** with 150-ms mixing time
1 mM in 100 mM deuterioacetate buffer in D_2O at 500 MHz and 298 K

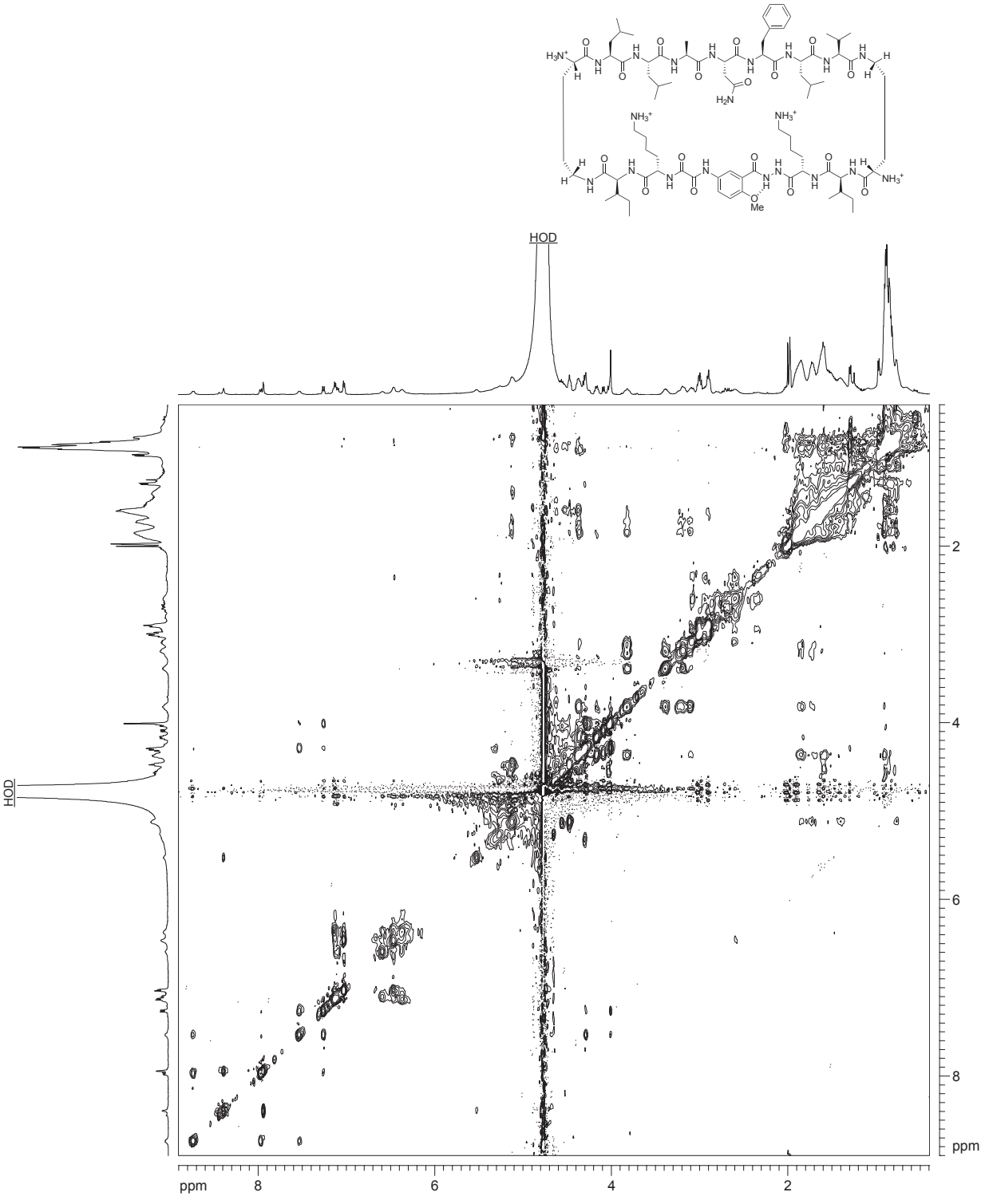

^{1}H NMR 2D NOESY of macrocyclic β-sheet peptide **1$_{Leu}$** with 150-ms mixing time
1 mM in 100 mM deuterioacetate buffer in D_2O at 500 MHz and 298 K

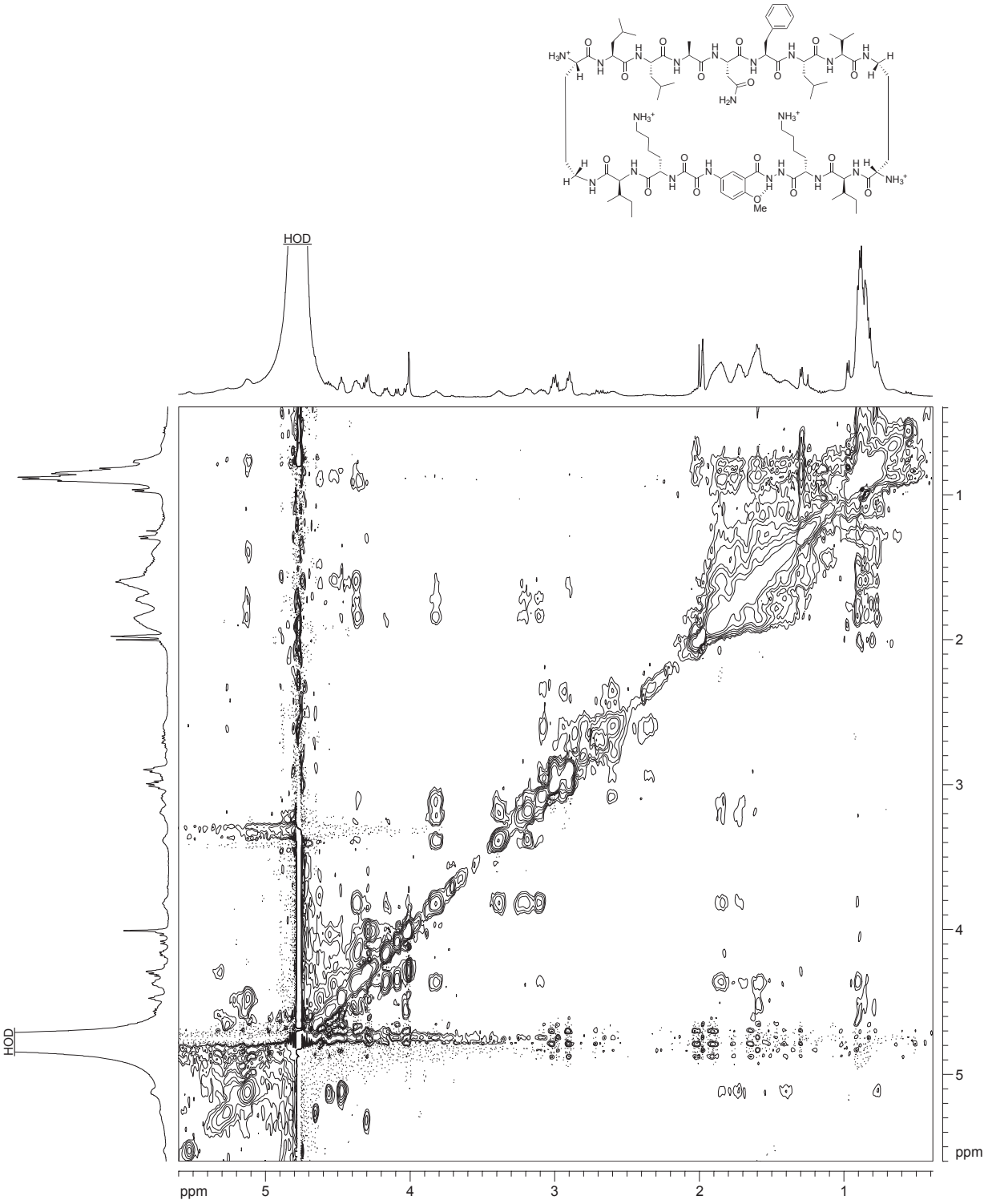

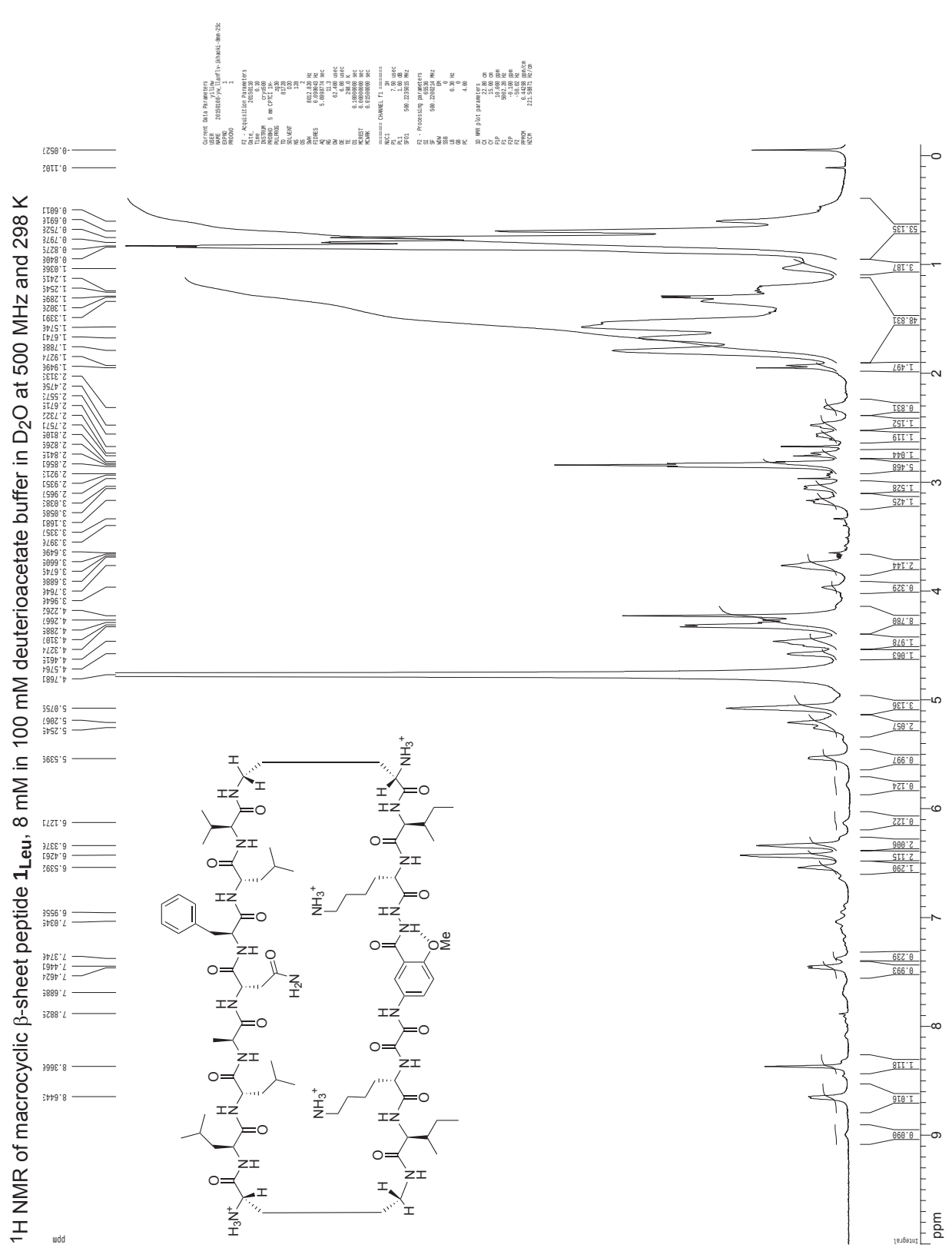
1H NMR of macrocyclic β-sheet peptide 1Leu, 8 mM in 100 mM deuterioacetate buffer in D2O at 500 MHz and 298 K
ppm
integral
Me
H2N
NH3+
H3N+

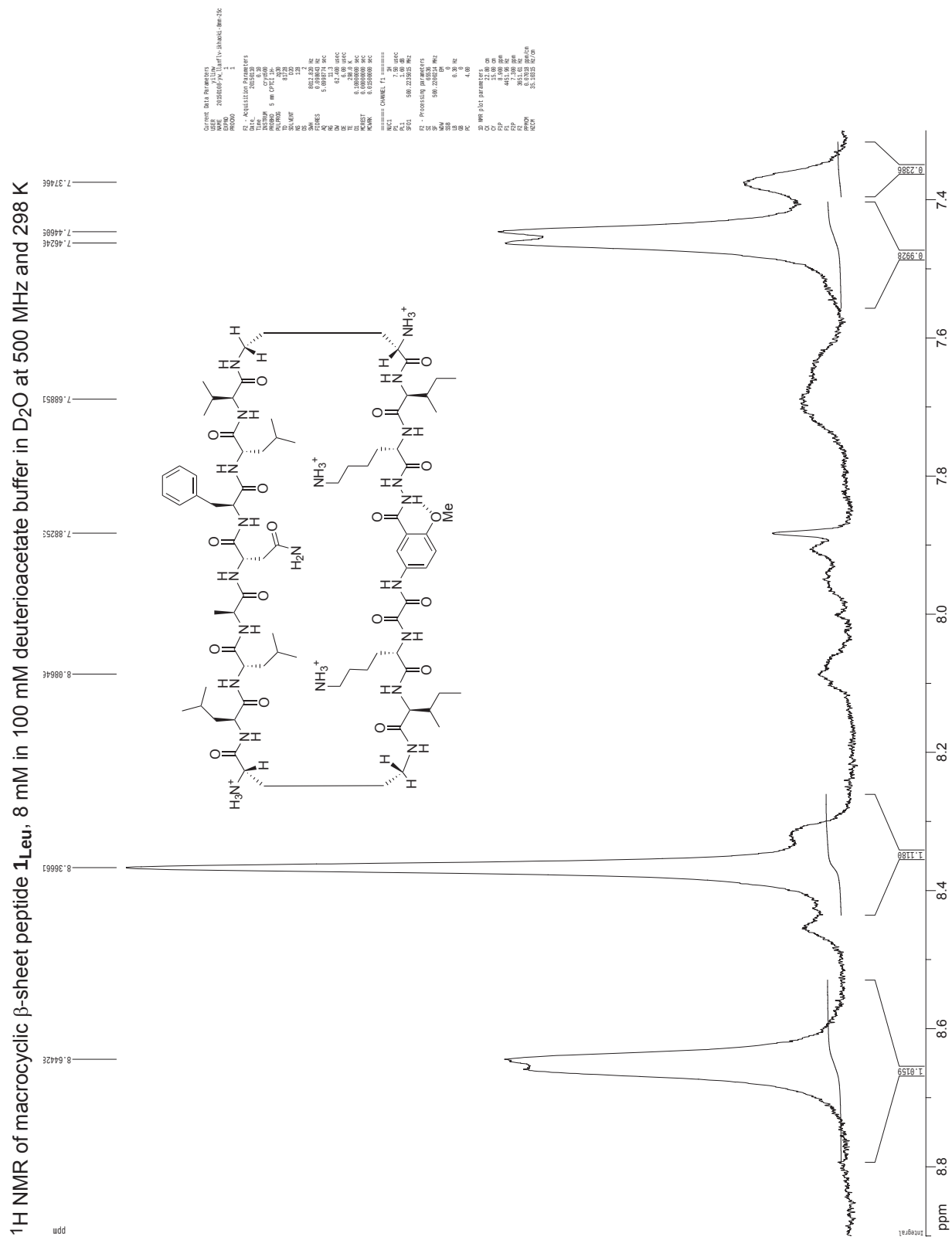
1H NMR of macrocyclic β-sheet peptide 1Leu, 8 mM in 100 mM deuterioacetate buffer in D2O at 500 MHz and 298 K
ppm
8.8
8.6
8.4
8.2
8.0
7.8
7.6
7.4
integral
1.0159
1.1180
0.9928
0.2386
8.64426
8.36651
8.08646
7.88252
7.68851
7.46246
7.44665
7.37466
Me

^{1}H NMR of macrocyclic β-sheet peptide **$\mathbf{1_{Leu}}$**, 8 mM in 100 mM deuterioacetate buffer in D_2O at 500 MHz and 298 K

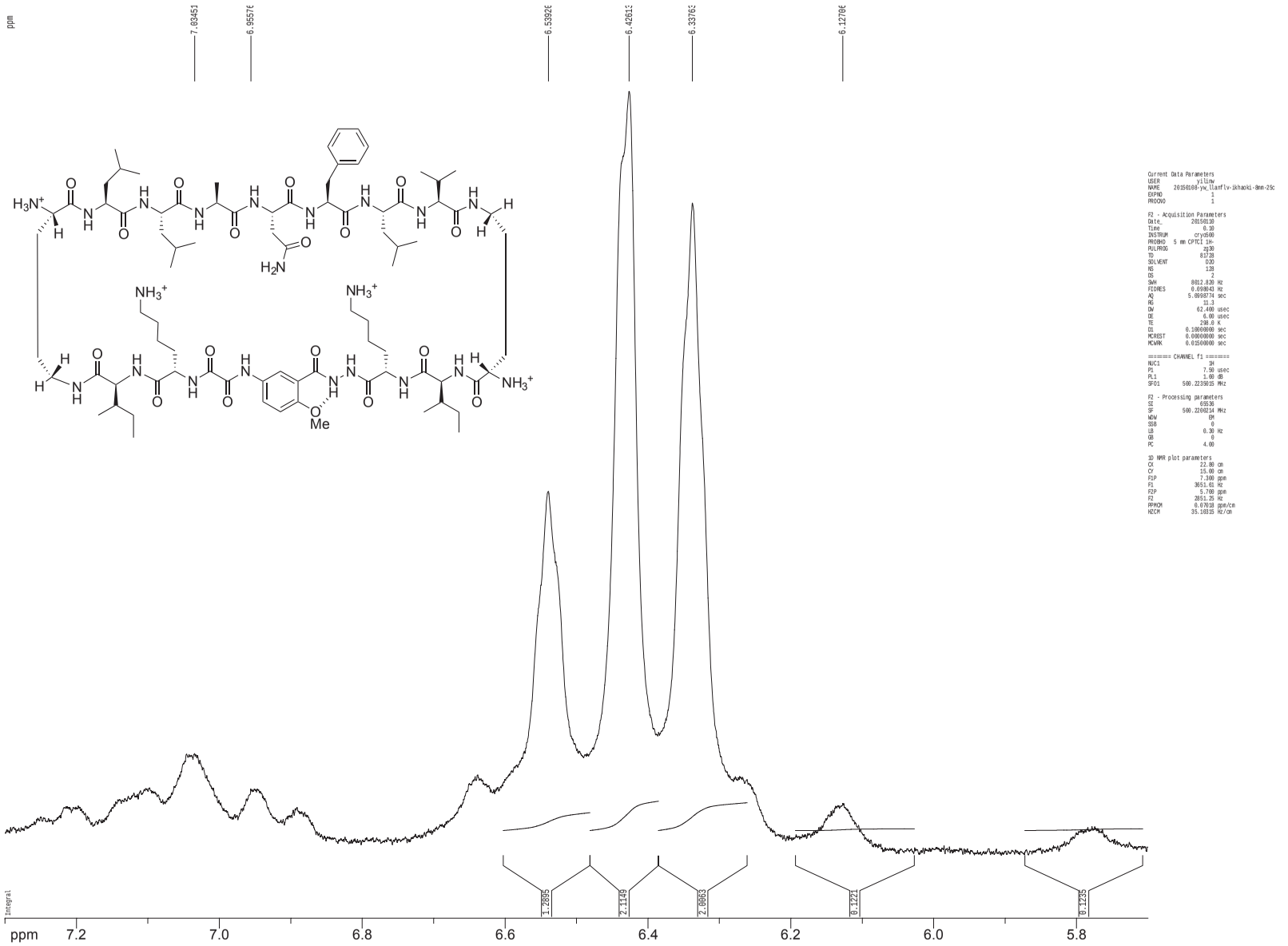

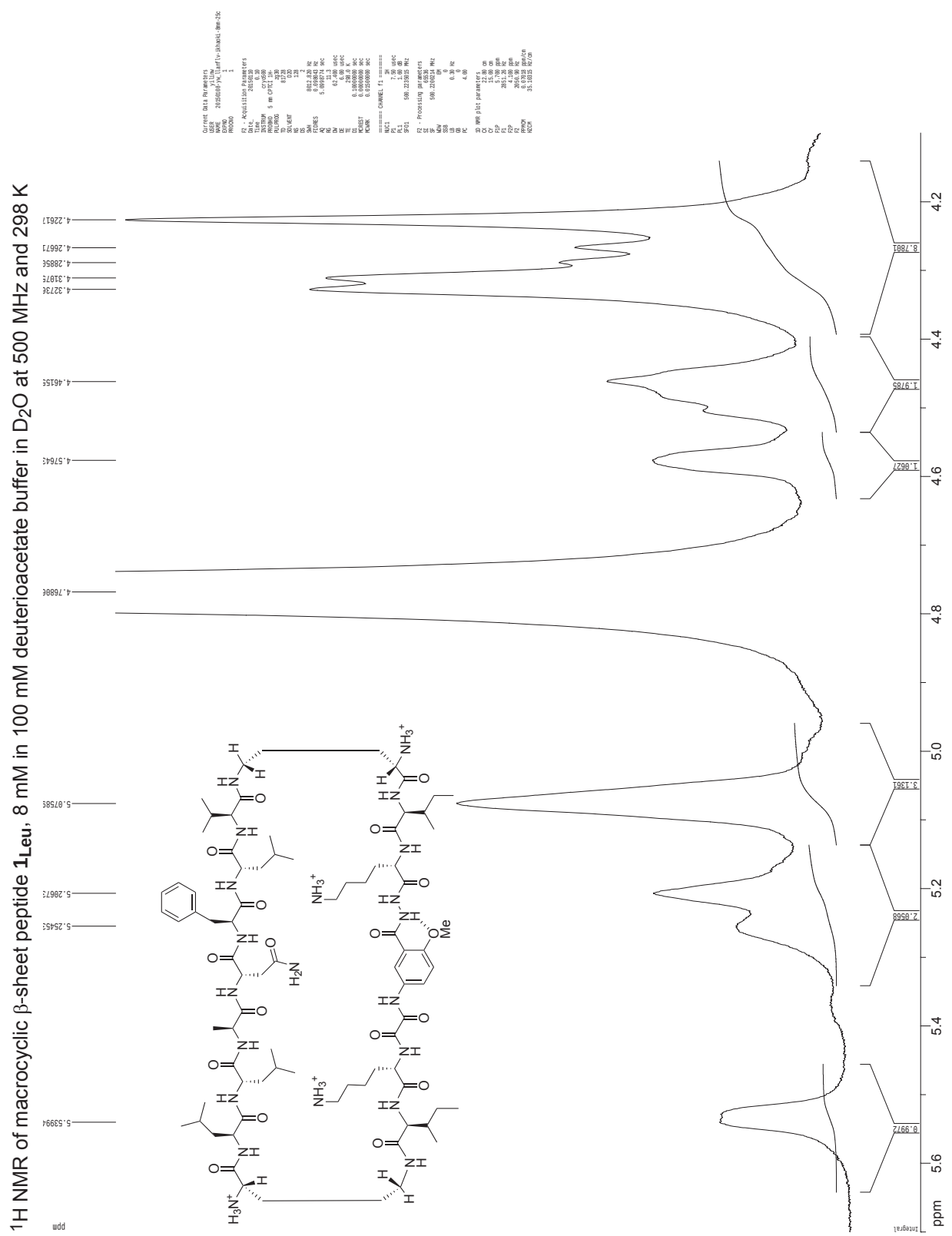
1H NMR of macrocyclic β-sheet peptide 1Leu, 8 mM in 100 mM deuterioacetate buffer in D2O at 500 MHz and 298 K
ppm
5.5399
5.2545
5.2067
5.0758
4.7680
4.5764
4.4615
4.3273
4.3107
4.2885
4.2673
4.2261
0.9972
2.0568
3.1361
1.0627
1.9785
8.7861
Integral
5.6
5.4
5.2
5.0
4.8
4.6
4.4
4.2

^{1}H NMR of macrocyclic β-sheet peptide **$\mathbf{1}_{\mathbf{Leu}}$**, 8 mM in 100 mM deuterioacetate buffer in D_2O at 500 MHz and 298 K

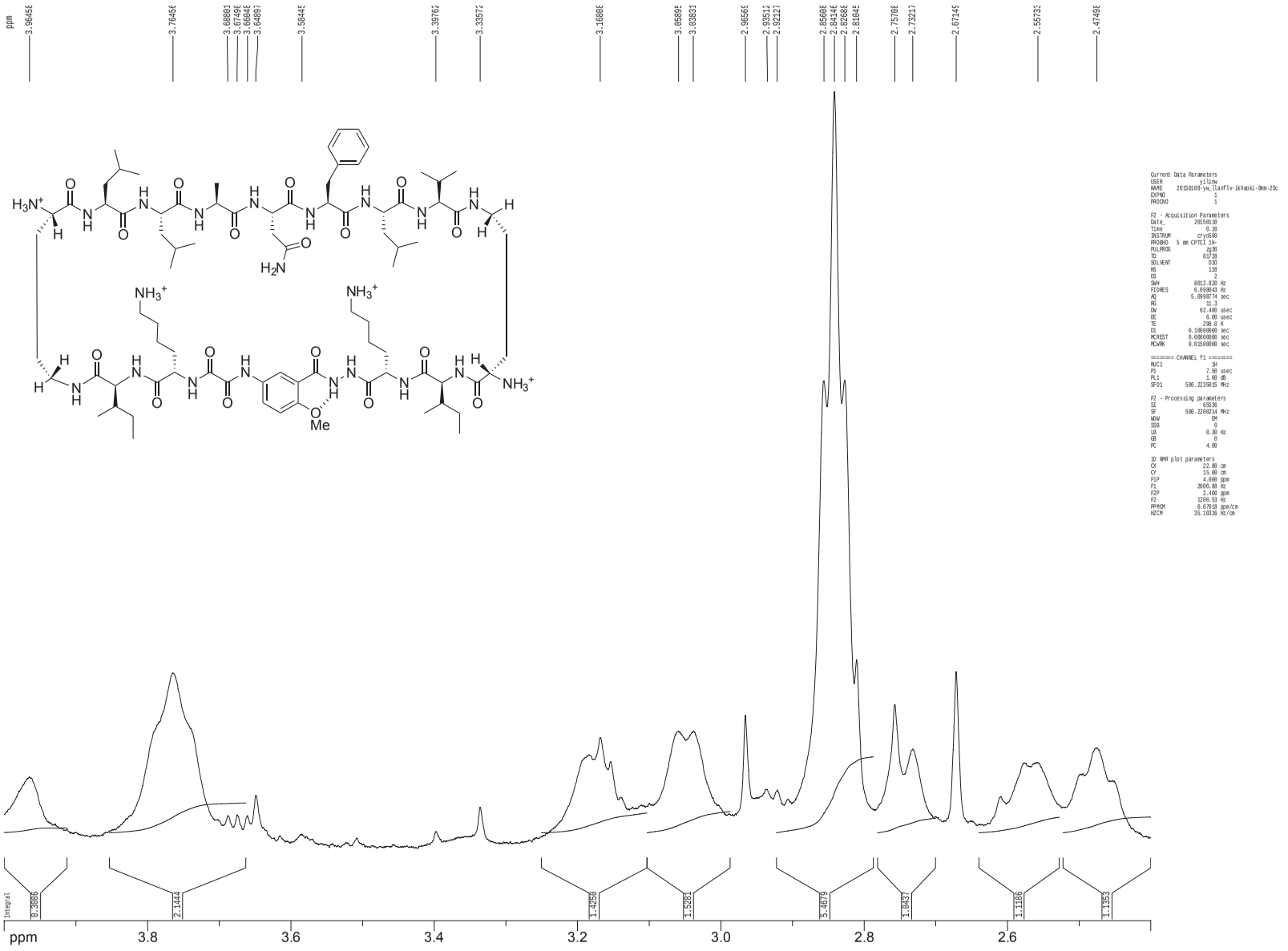

Current Data Parameters
USER villow
NAME 20150108-yw_11anflv-ikhaoki-8mm-25c
EXPNO 1
PROCNO 1

F2 - Acquisition Parameters
Date_ 20150110
Time 0.10
INSTRUM cryo500
PROBHD 5 mm CPTCI 1H-
PULPROG zg30
TD 81728
SOLVENT D2O
NS 128
DS 2
SWH 8012.820 Hz
FIDRES 0.098043 Hz
AQ 5.0998774 sec
RG 11.3
DW 62.400 usec
DE 6.00 usec
TE 298.0 K
D1 0.10000000 sec
MCREST 0.00000000 sec
MCWRK 0.03500000 sec

====== CHANNEL f1 ======
NUC1 1H
P3 7.50 usec
PL1 1.00 dB
SFO1 500.2235035 MHz

F2 - Processing parameters
SI 65536
SF 500.2200214 MHz
WDW EM
SSB 0
LB 0.30 Hz
GB 0
PC 4.00

1D NMR plot parameters
CX 22.80 cm
CY 15.00 cm
F1P 4.000 ppm
F1 2000.88 Hz
F2P 2.400 ppm
F2 1200.53 Hz
PPMCM 0.07018 ppm/cm
HZCM 35.10316 Hz/cm

^{1}H NMR of macrocyclic β-sheet peptide **1$_{Leu}$**, 8 mM in 100 mM deuterioacetate buffer in D_2O at 500 MHz and 298 K

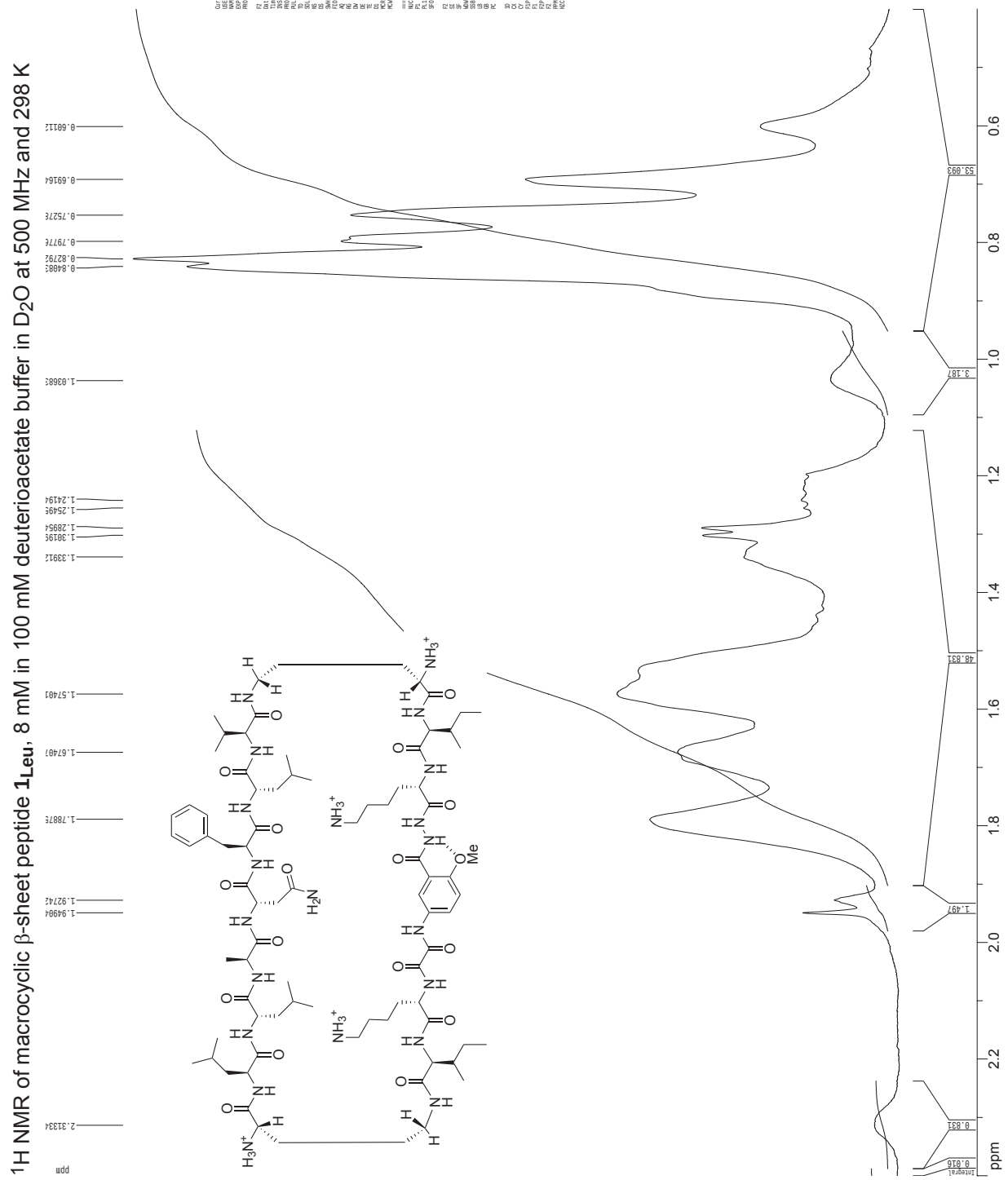

^{1}H NMR 2D TOCSY of macrocyclic β-sheet peptide **$\mathbf{1_{Leu}}$** with 150-ms spin-lock mixing time
8 mM in 100 mM deuterioacetate buffer in D_2O at 500 MHz and 298 K

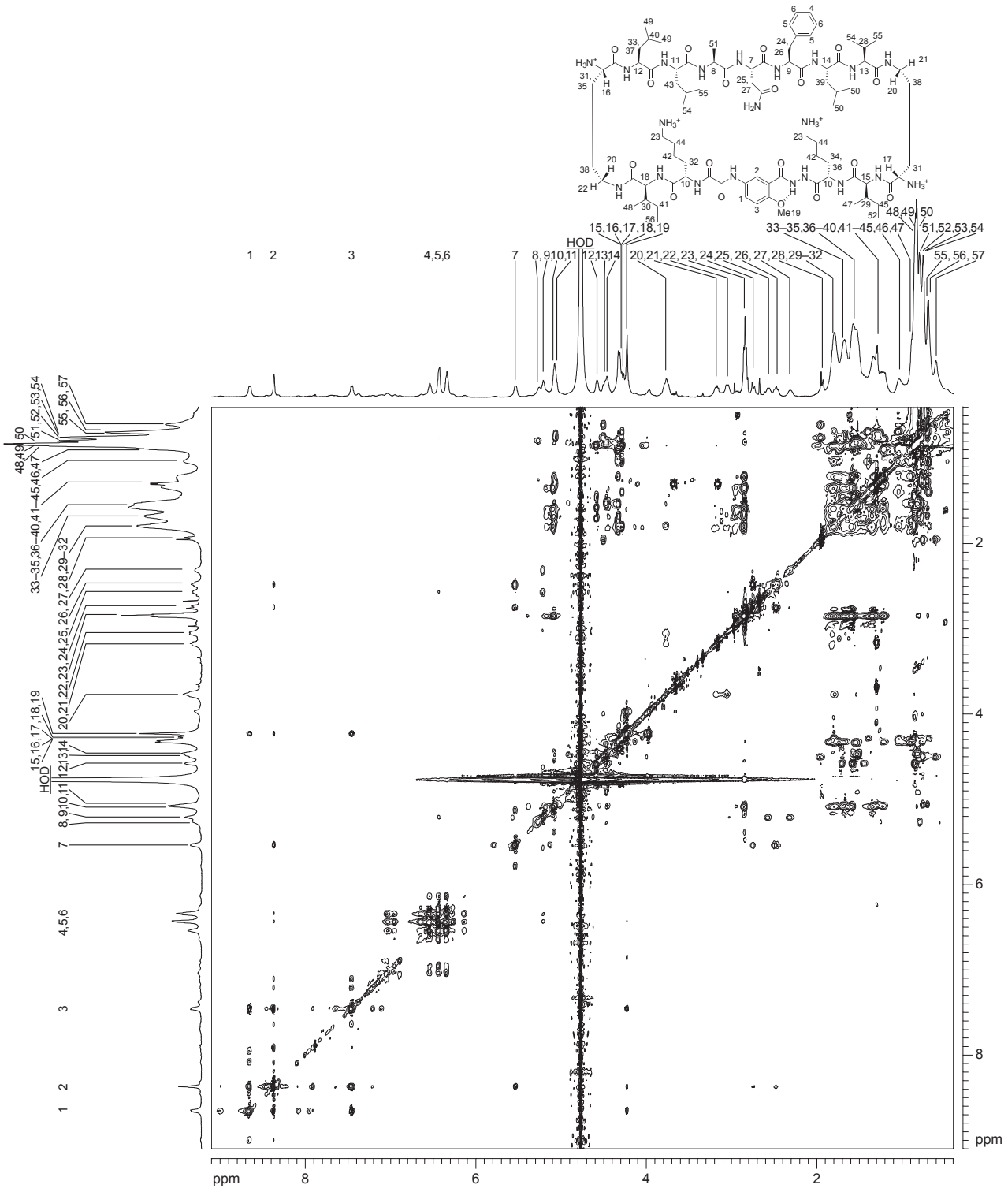

^{1}H NMR 2D TOCSY of macrocyclic β-sheet peptide **$\mathbf{1_{Leu}}$** with 150-ms spin-lock mixing time
8 mM in 100 mM deuterioacetate buffer in D_2O at 500 MHz and 298 K

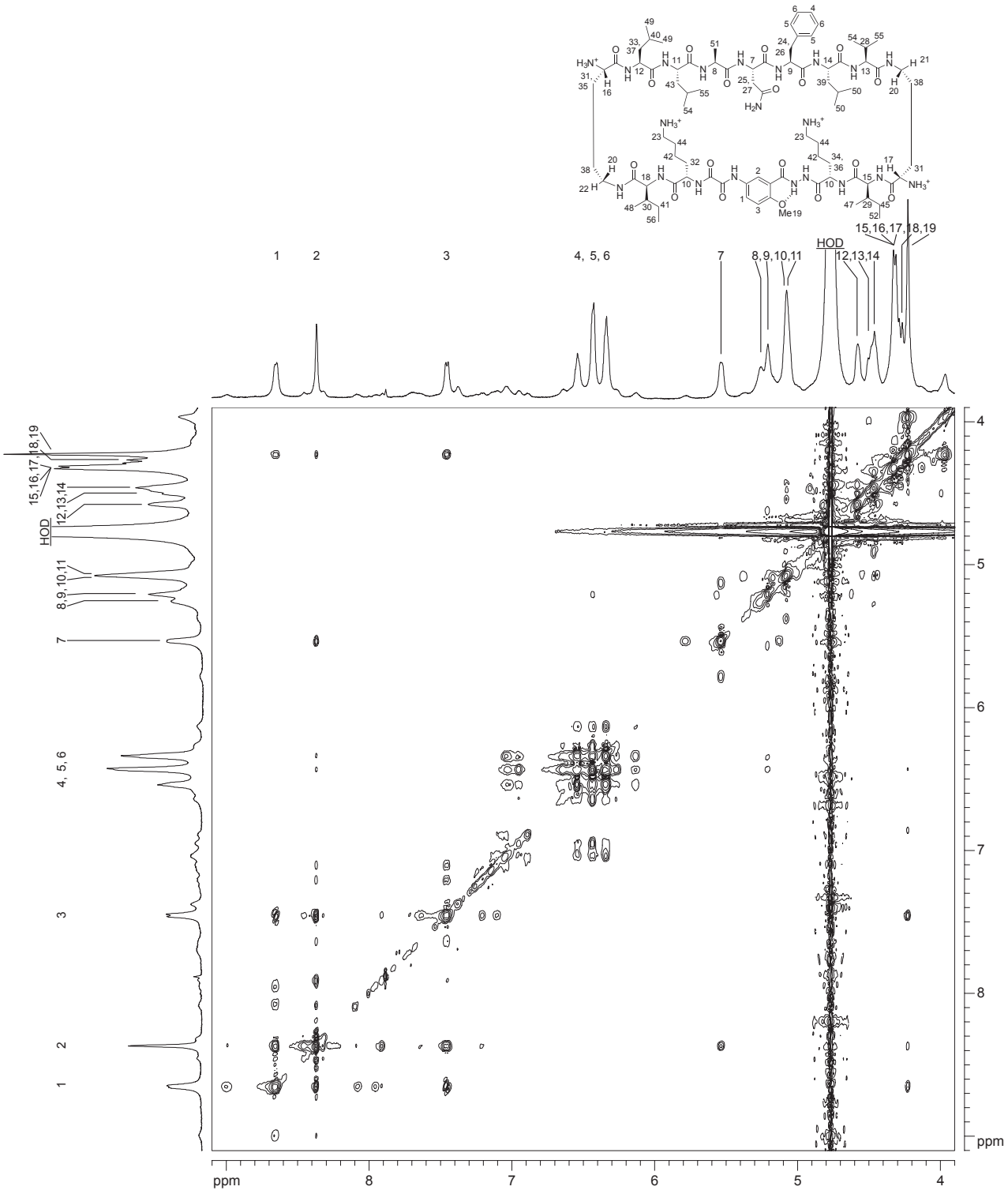

^{1}H NMR 2D TOCSY of macrocyclic β-sheet peptide **$\mathbf{1_{Leu}}$** with 150-ms spin-lock mixing time
8 mM in 100 mM deuterioacetate buffer in D_2O at 500 MHz and 298 K

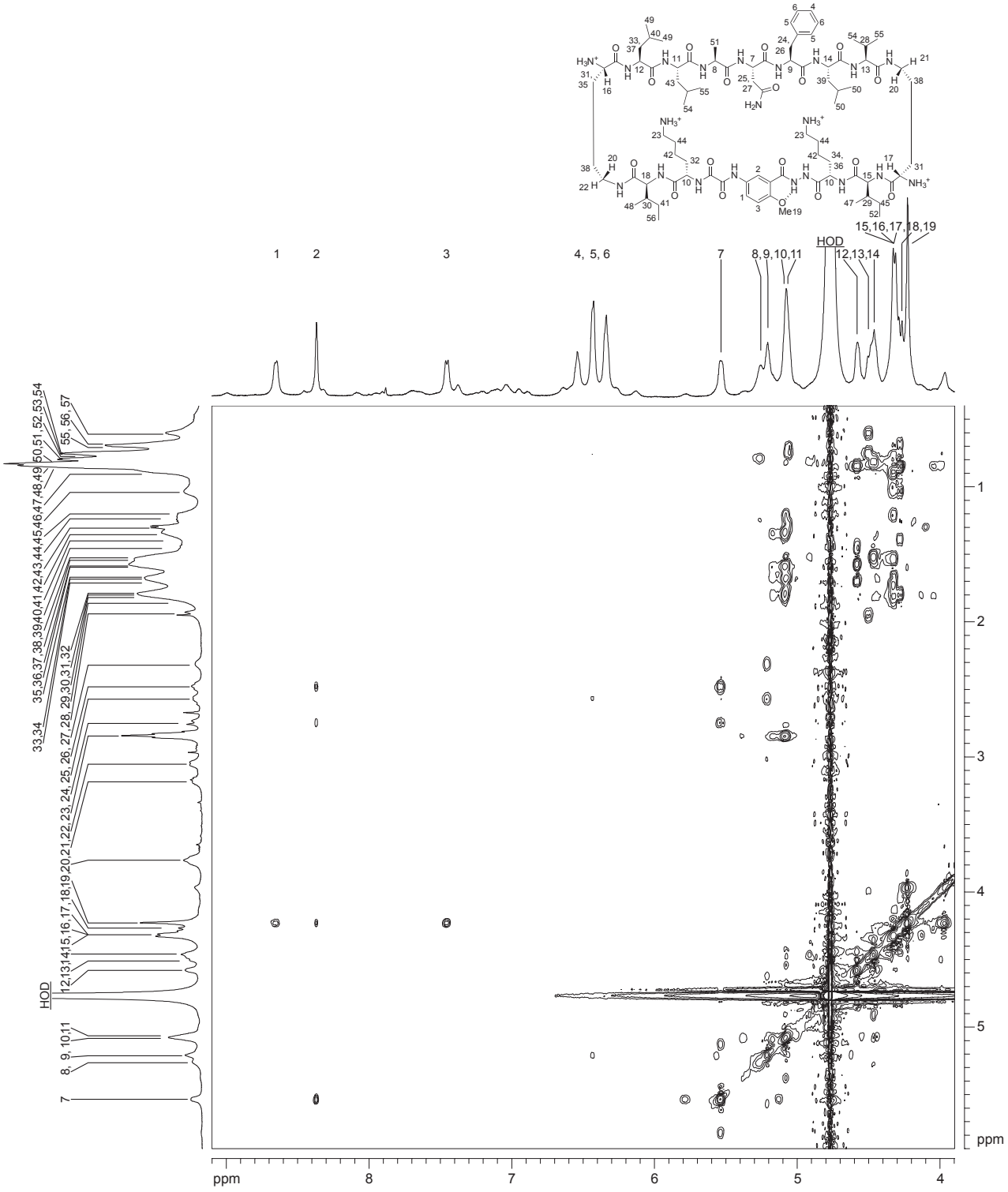

^{1}H NMR 2D TOCSY of macrocyclic β-sheet peptide **$\mathbf{1_{Leu}}$** with 150-ms spin-lock mixing time
8 mM in 100 mM deuterioacetate buffer in D_2O at 500 MHz and 298 K

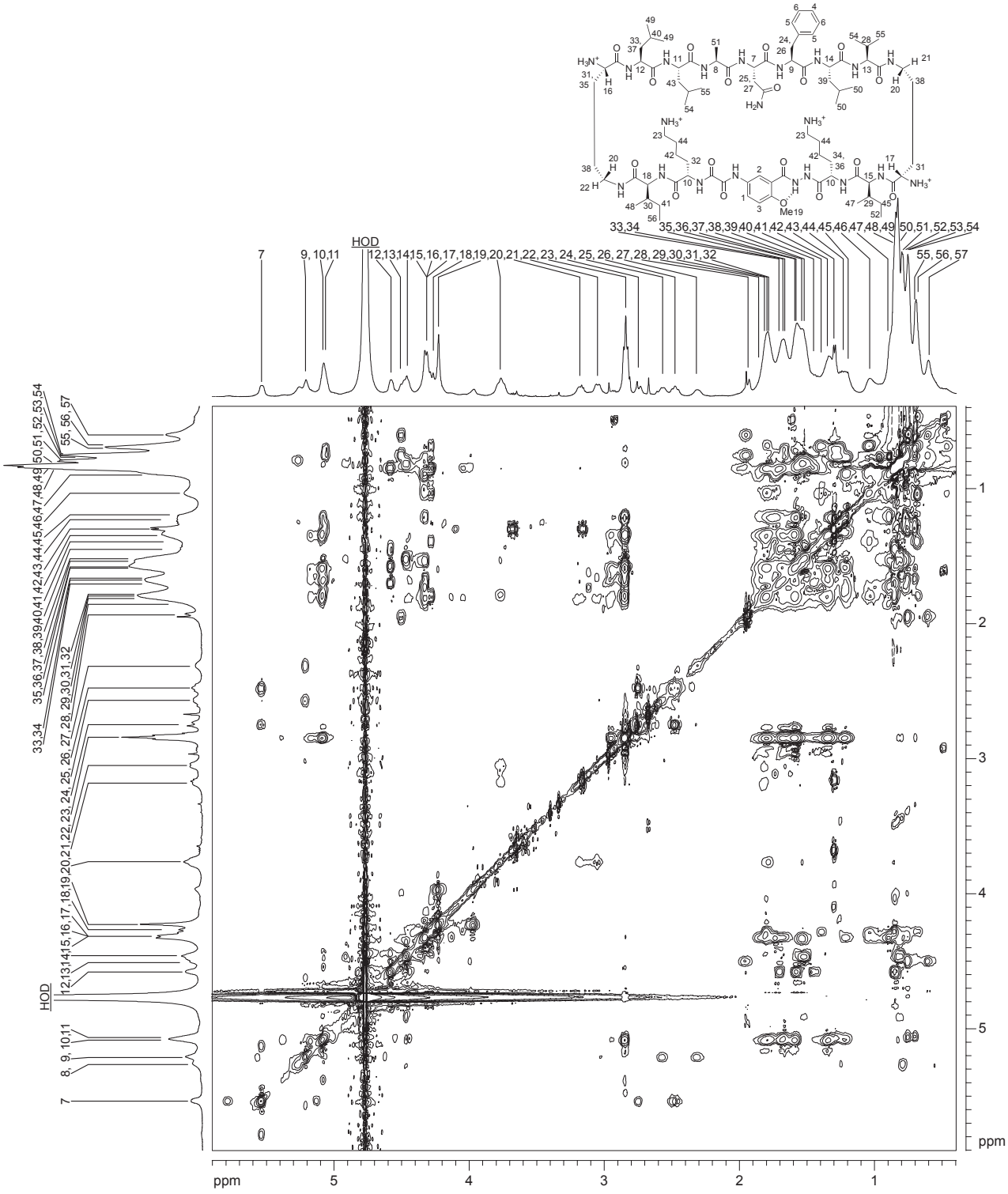

^{1}H NMR 2D NOESY of macrocyclic β-sheet peptide **$\mathbf{1_{Leu}}$** with 150-ms mixing time
8 mM in 100 mM deuterioacetate buffer in D_2O at 500 MHz and 298 K

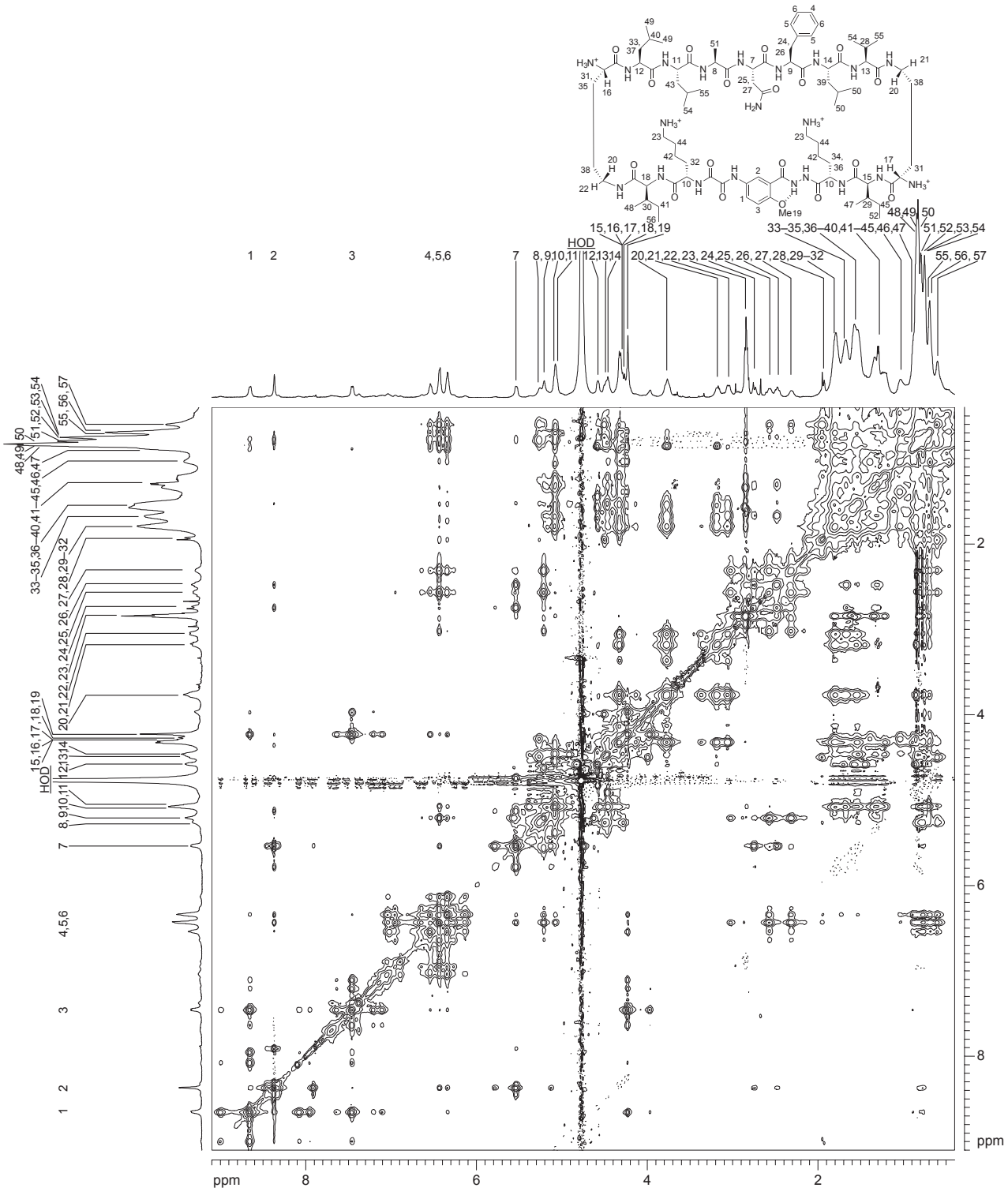

^{1}H NMR 2D NOESY of macrocyclic β-sheet peptide **1_{Leu}** with 150-ms mixing time
8 mM in 100 mM deuterioacetate buffer in D_2O at 500 MHz and 298 K

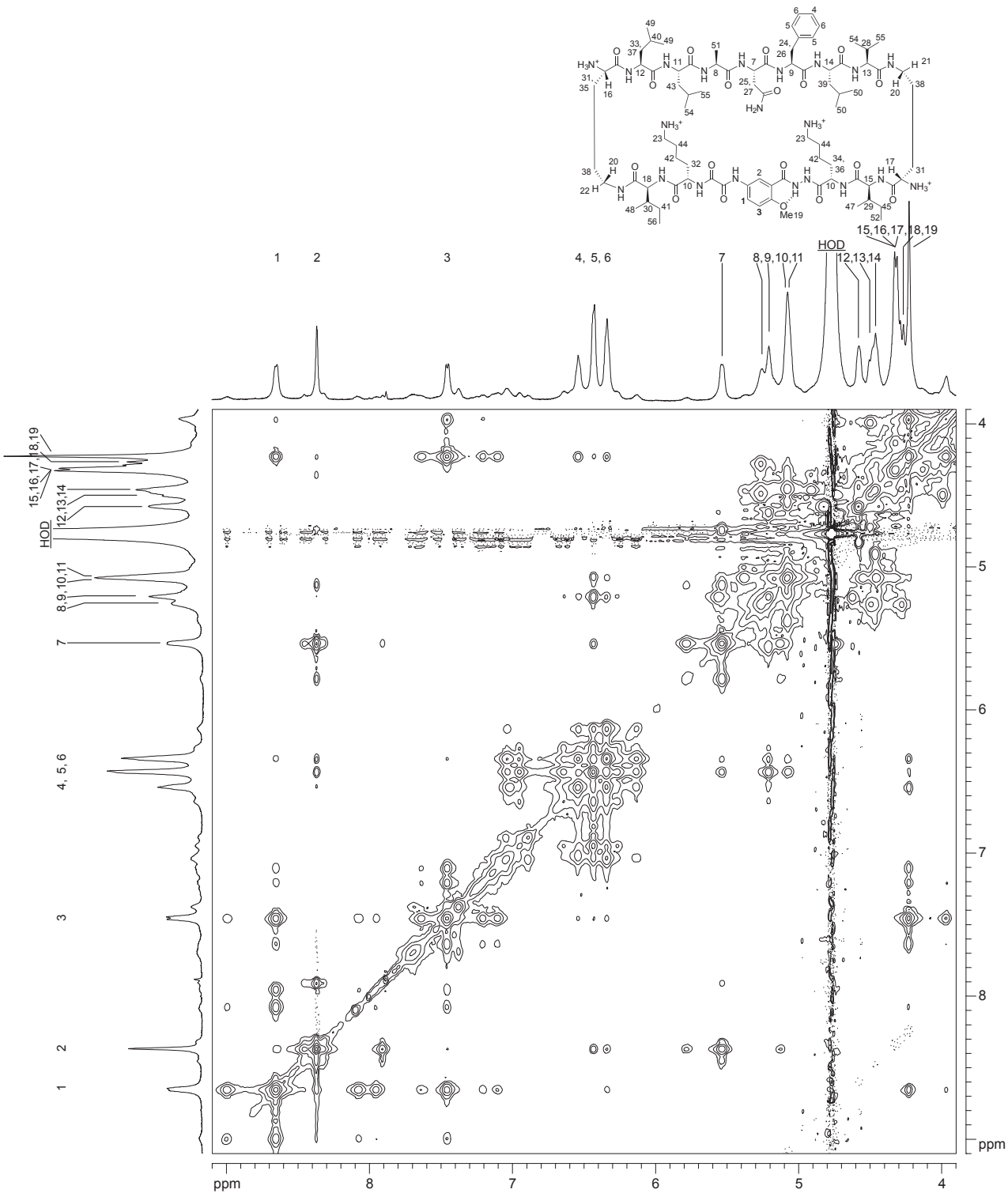

^{1}H NMR 2D NOESY of macrocyclic β-sheet peptide **1_{Leu}** with 150-ms mixing time
8 mM in 100 mM deuterioacetate buffer in D_2O at 500 MHz and 298 K

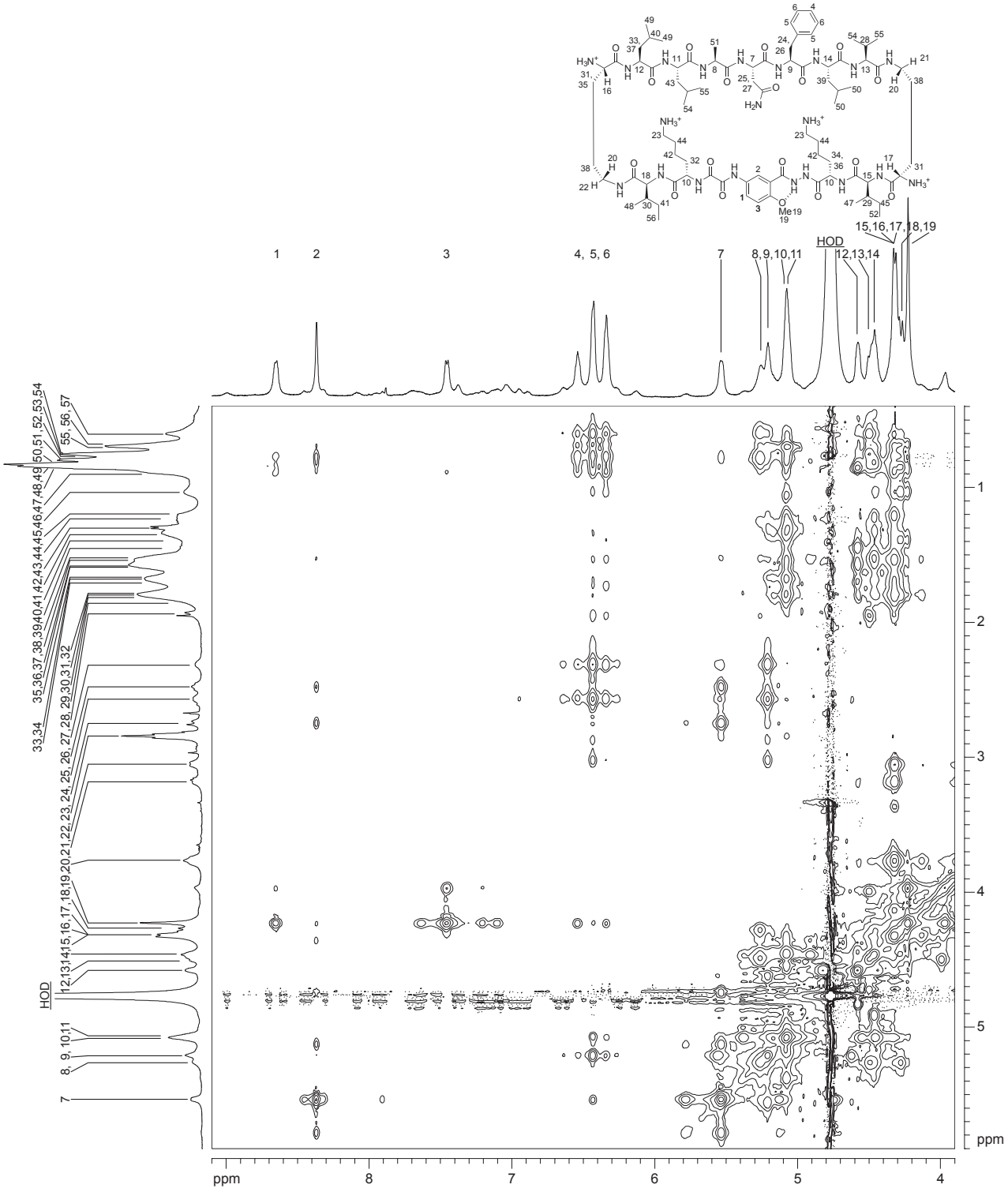

^{1}H NMR 2D NOESY of macrocyclic β-sheet peptide **$\mathbf{1_{Leu}}$** with 150-ms mixing time
8 mM in 100 mM deuterioacetate buffer in D_2O at 500 MHz and 298 K

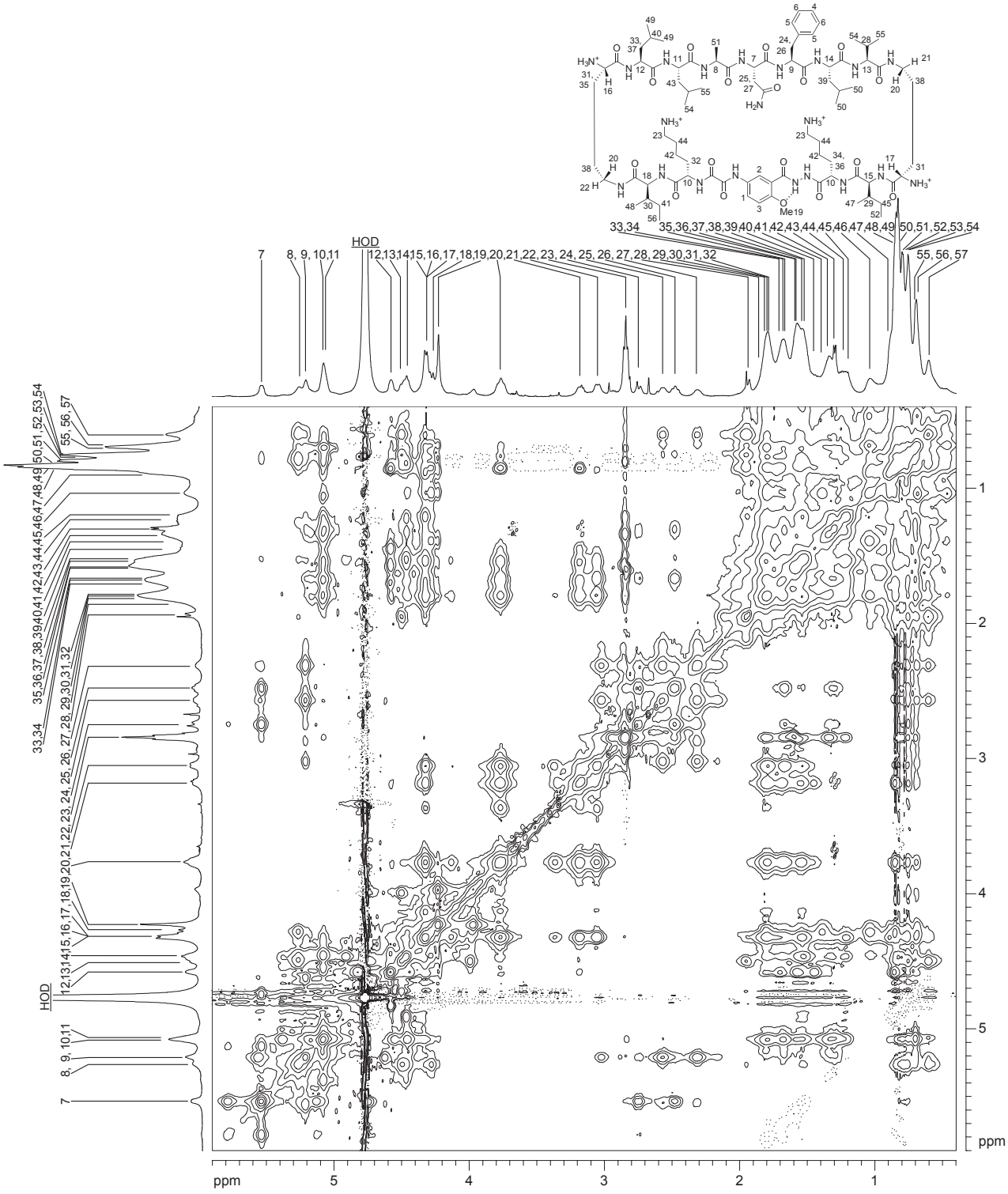

^{1}H NMR DOSY of macrocyclic β-sheet peptide **1$_{Leu}$** at 500 MHz and 298 K
16 mM in 100 mM deuterioacetate buffer in D_2O

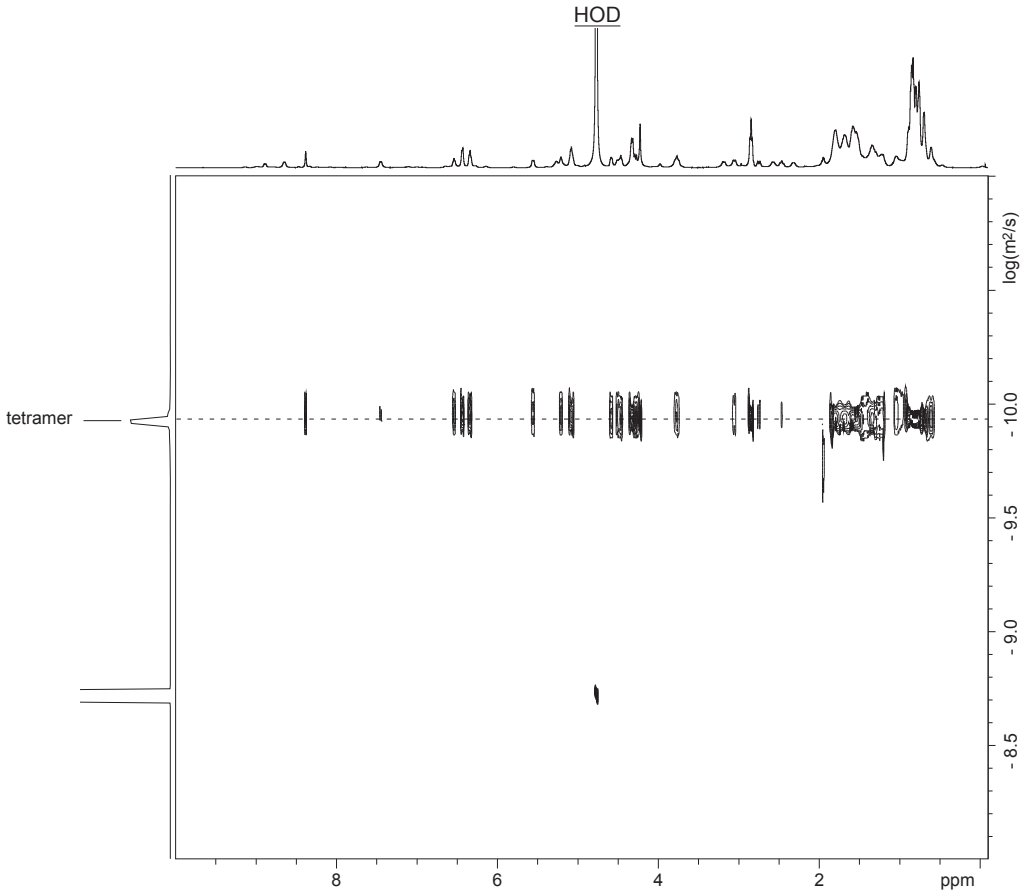

Calculations for macrocyclic β-sheet peptide **1$_{Leu}$** at 16 mM and pH 4.7

D_{HOD} = 19.0 x 10^{-10} m^2/s [a]
log (D_{HOD}) = -8.721

$D_{tetramer}$: log(D) = -9.943; D = $10^{-9.943}$ = 11.4 ± 0.5 x 10^{-11} m^2/s

[a]Longsworth, L. G. *J. Phys. Chem.* **1960**, *64*, 1914−1917.

^{1}H NMR DOSY of macrocyclic β-sheet peptide **1$_{Leu}$** at 500 MHz and 298 K
16 mM at pH 7.2 in D_2O

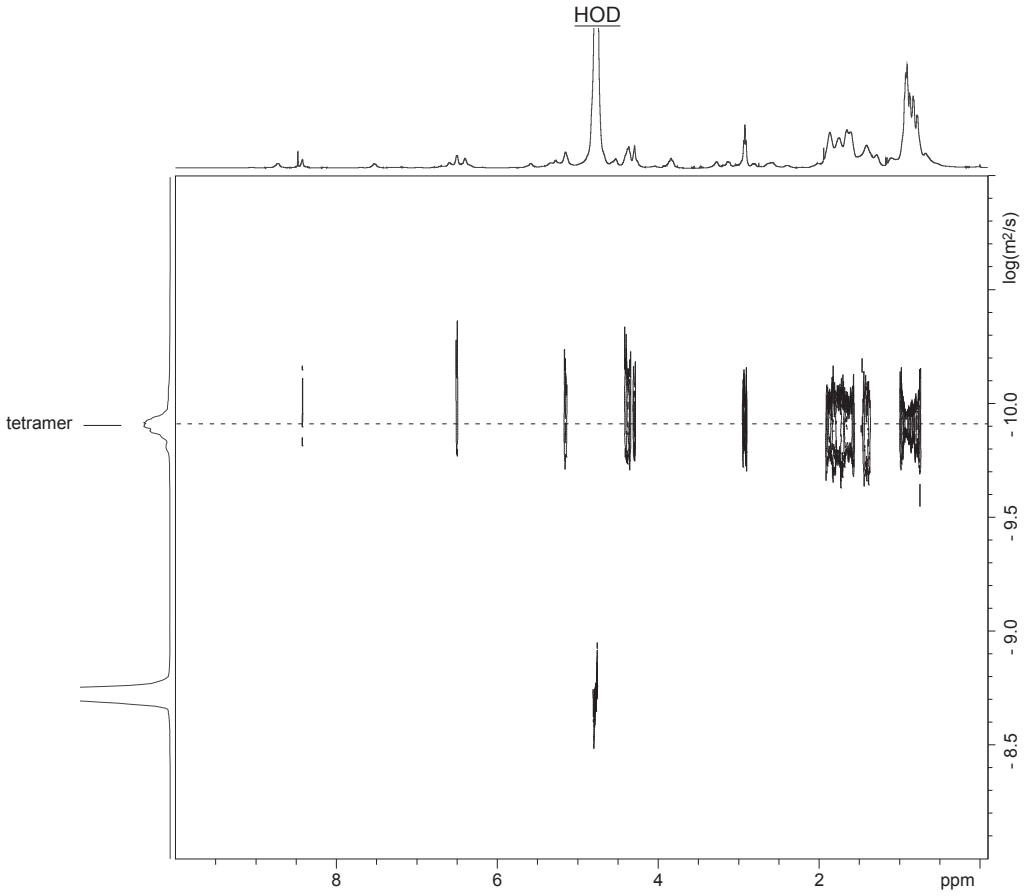

Calculations for macrocyclic β-sheet peptide **1$_{Leu}$** at 16 mM and pH 7.2

D_{HOD} = 19.0 x 10^{-10} m^2/s [a]
log (D_{HOD}) = -8.721

$D_{tetramer}$: log(D) = -9.909; D = $10^{-9.909}$ = 12.3 ± 1.3 x 10^{-11} m^2/s

[a]Longsworth, L. G. *J. Phys. Chem.* **1960**, *64*, 1914−1917.

RP-HPLC of Macrocyclic β-Sheet **1_{His}**

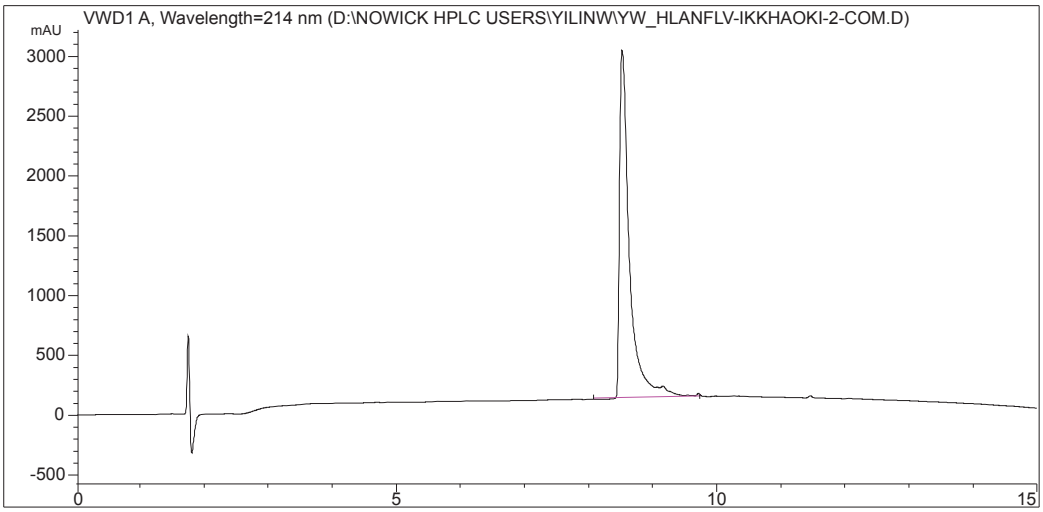

Peak #	RetTime [min]	Type	Width [min]	Area mAU *s	Height [mAU]	Area %
1	8.514	MM	0.1787	3.13333E4	2905.7468	100.000

column: Aeris XB-C18 2.6µ
dimensions: 150 mm x 4.6 mm
mobile phase: A: H_2O, 0.1% TFA
B: CH_3CN, 0.1% TFA
gradient: A/B (95:5) to (0:100) in 20 min
flow rate: 1.0 mL/min
detection: VWD, wavelength = 214 nm
temperature: 298 K

MS (ESI) of Macrocyclic β-Sheet **1_{His}**

yilinw3-hlanflv-ikhaoki-com-1 6 (0.110) Sm (SG, 2x3.00); Cm (5:52)

TOF MS ES+
2.13e4

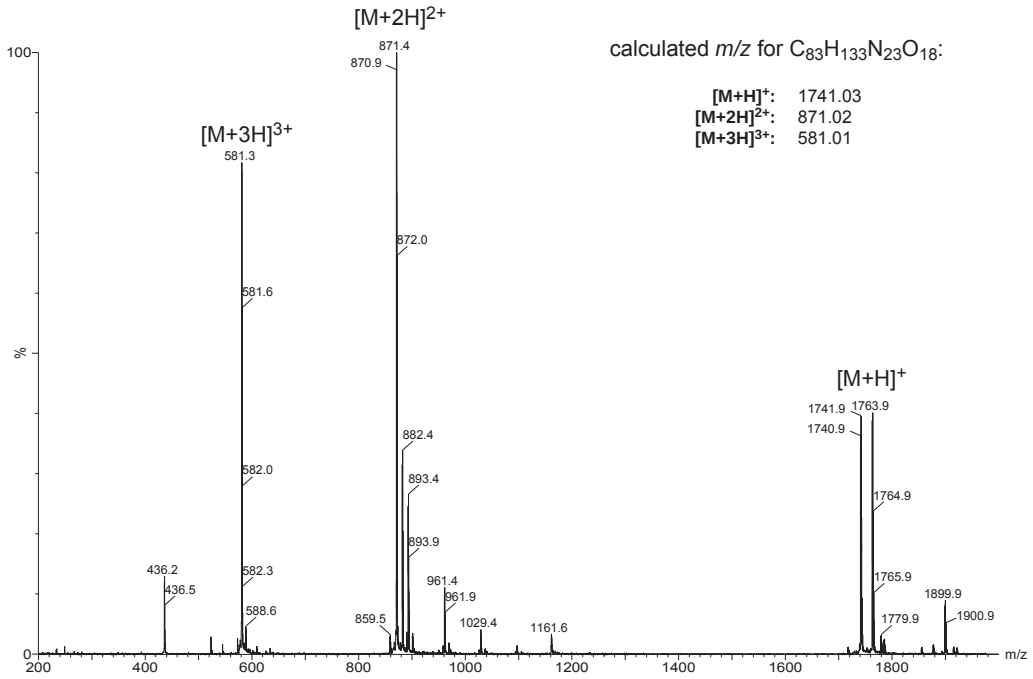

calculated *m/z* for $C_{83}H_{133}N_{23}O_{18}$:

$[M+H]^+$: 1741.03
$[M+2H]^{2+}$: 871.02
$[M+3H]^{3+}$: 581.01

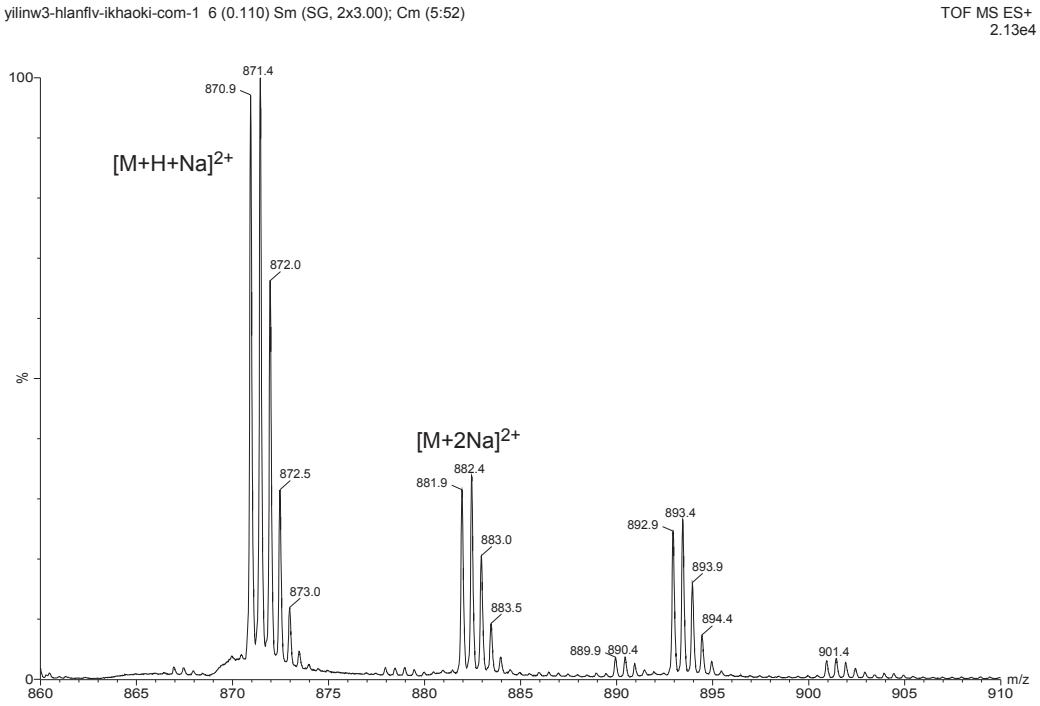
yilinw3-hlanflv-ikhaoki-com-1 6 (0.110) Sm (SG, 2x3.00); Cm (5:52)
TOF MS ES+
2.13e4
100
%
0
[M+H+Na]2+
[M+2Na]2+
871.4
870.9
872.0
872.5
873.0
881.9
882.4
883.0
883.5
889.9
890.4
892.9
893.4
893.9
894.4
901.4
860
865
870
875
880
885
890
895
900
905
910
m/z

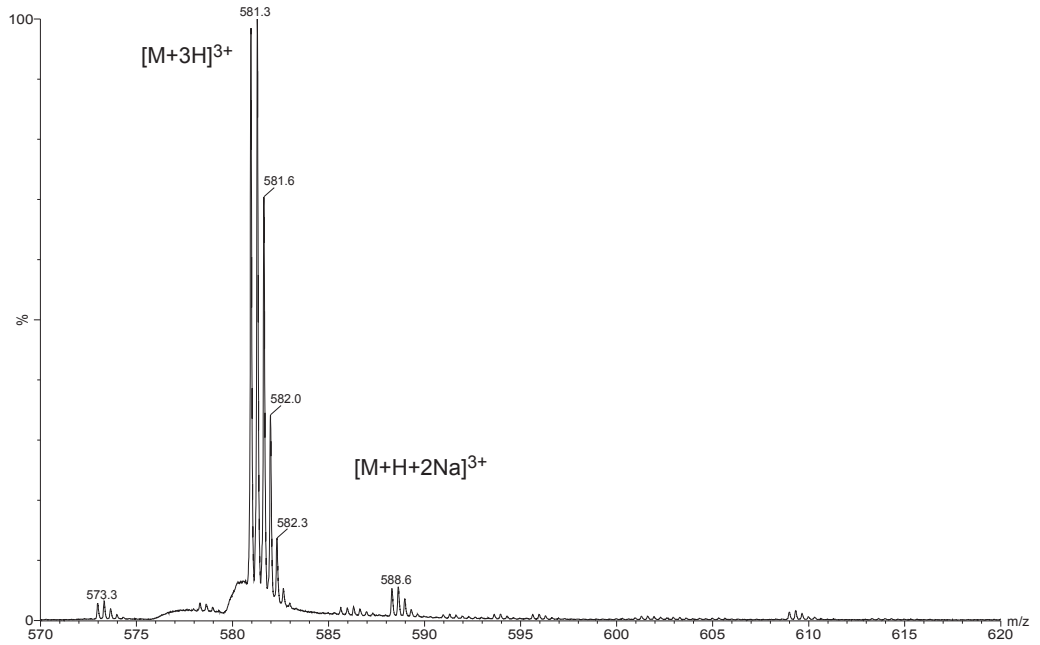
yilinw3-hlanflv-ikhaoki-com-1 6 (0.110) Sm (SG, 2x3.00); Cm (5:52)
TOF MS ES+
1.74e4
100
%
0
[M+3H]3+
[M+H+2Na]3+
581.3
581.6
582.0
582.3
573.3
588.6
570
575
580
585
590
595
600
605
610
615
620
m/z

^{1}H NMR of macrocyclic β-sheet peptide **1$_{His}$**, 16 mM at pH 2.5 in D_2O at 500 MHz and 293 K

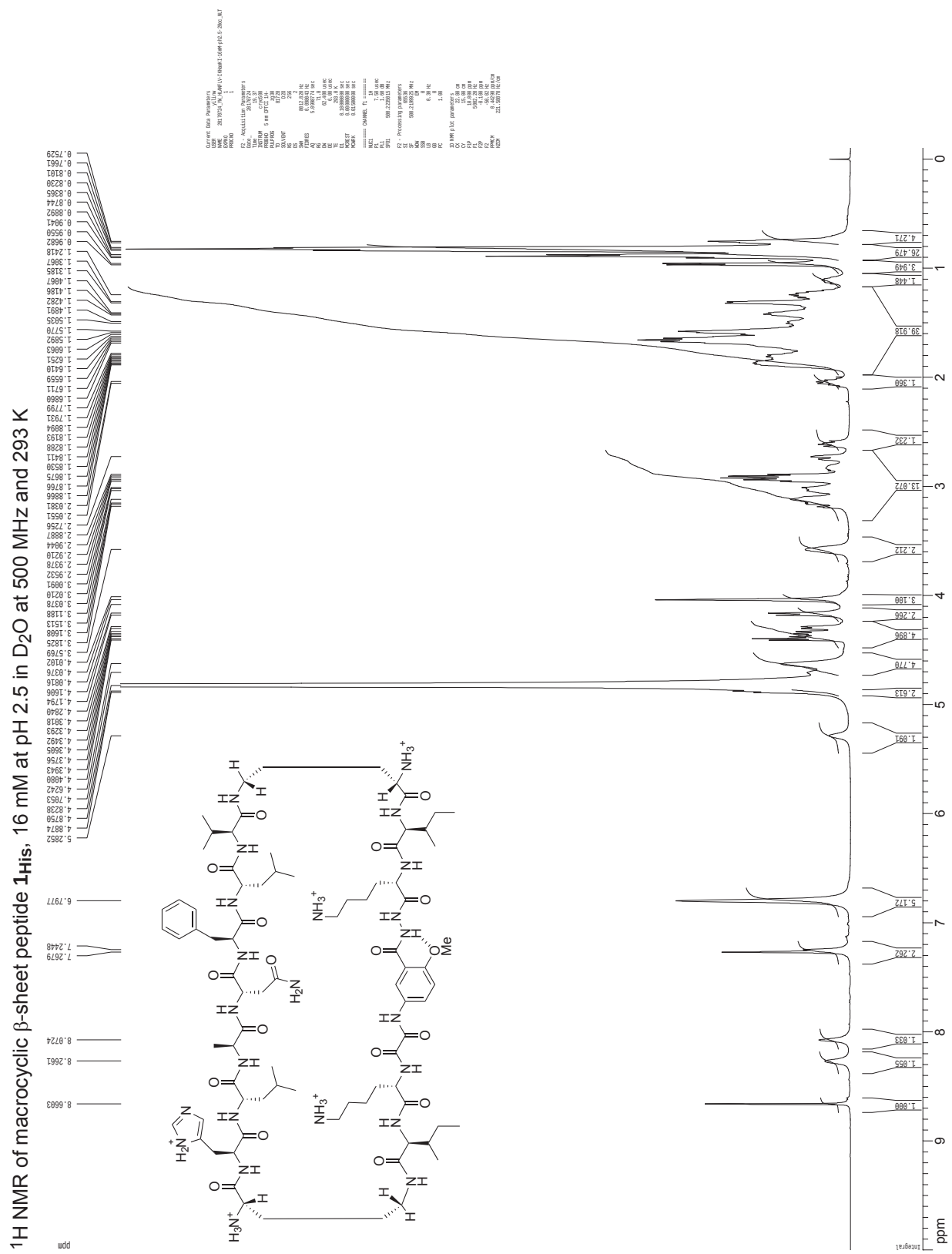

^1H NMR of macrocyclic β-sheet peptide $\mathbf{1_{His}}$, 16 mM at pH 2.5 in D_2O at 500 MHz and 293 K

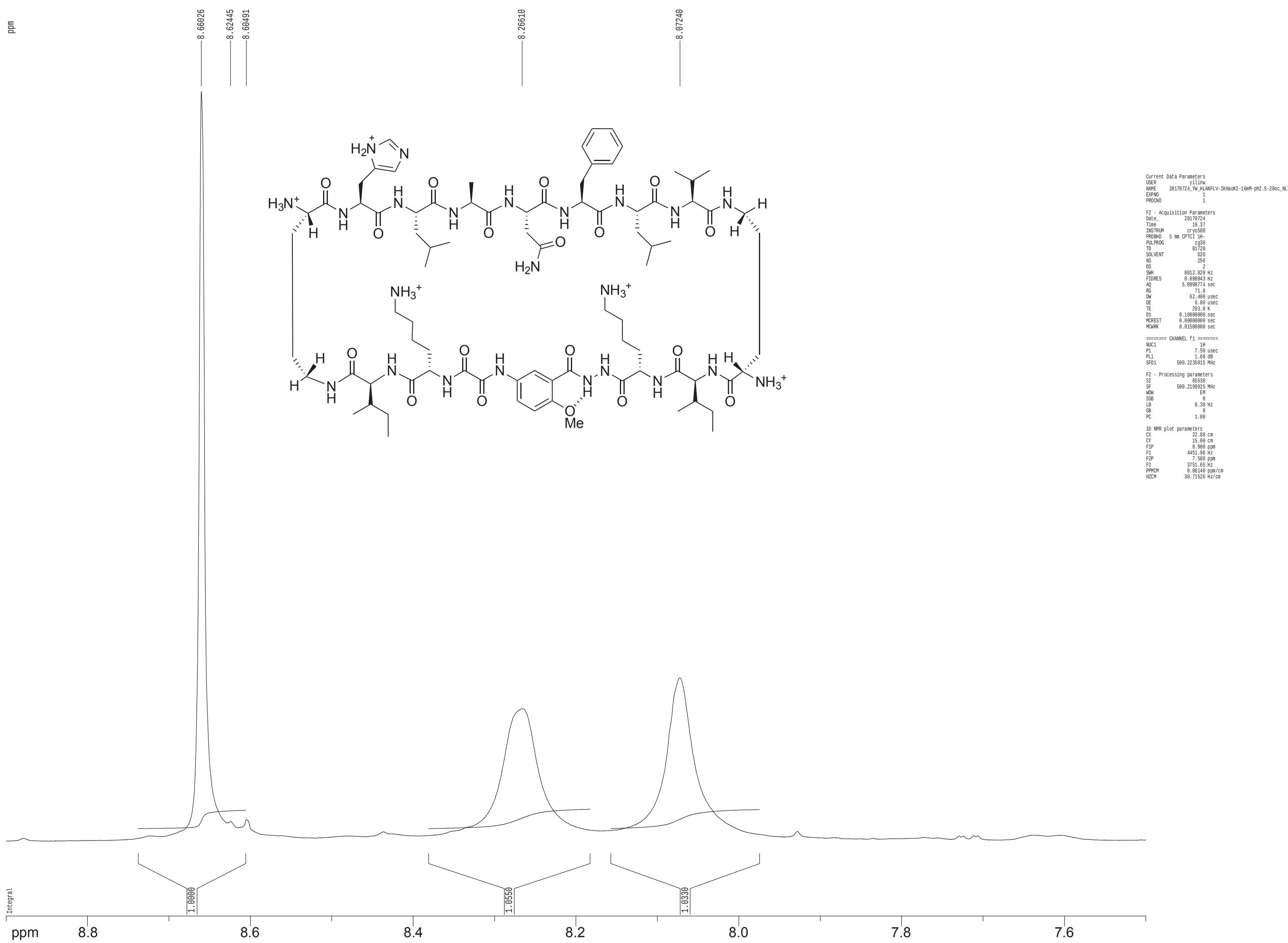

^{1}H NMR of macrocyclic β-sheet peptide **1$_{His}$**, 16 mM at pH 2.5 in D_2O at 500 MHz and 293 K

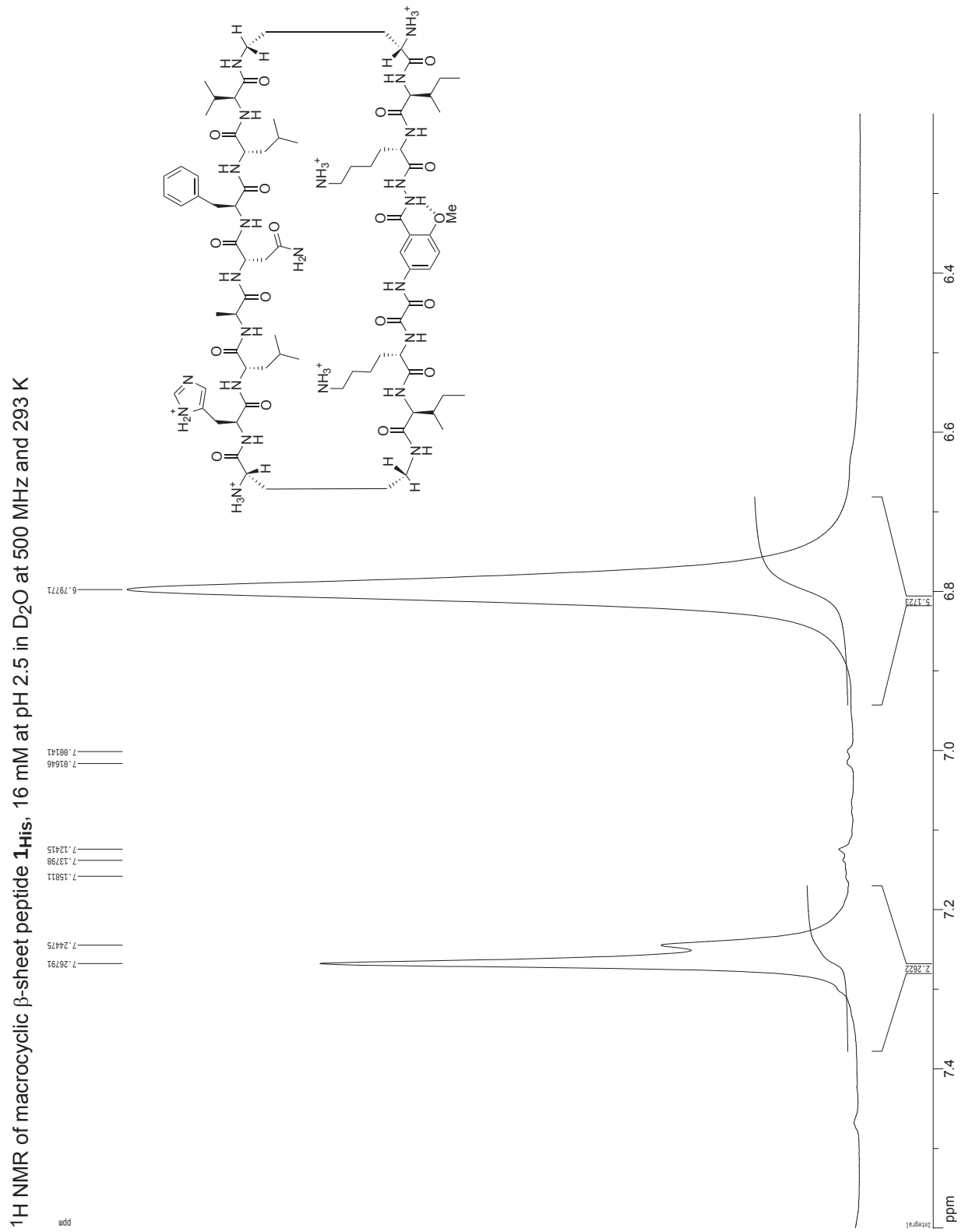

^{1}H NMR of macrocyclic β-sheet peptide **1$_{His}$**, 16 mM at pH 2.5 in D_2O at 500 MHz and 293 K

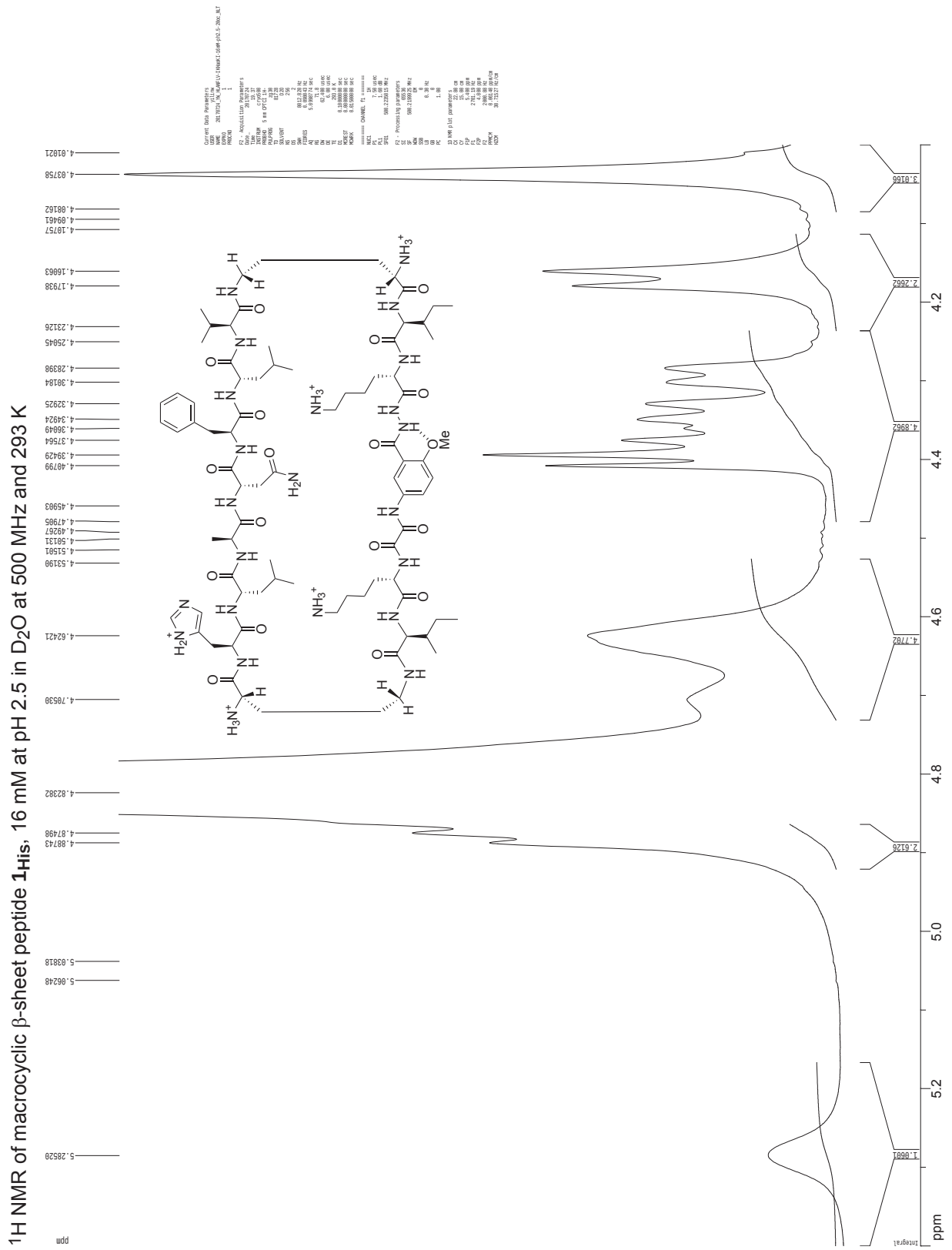

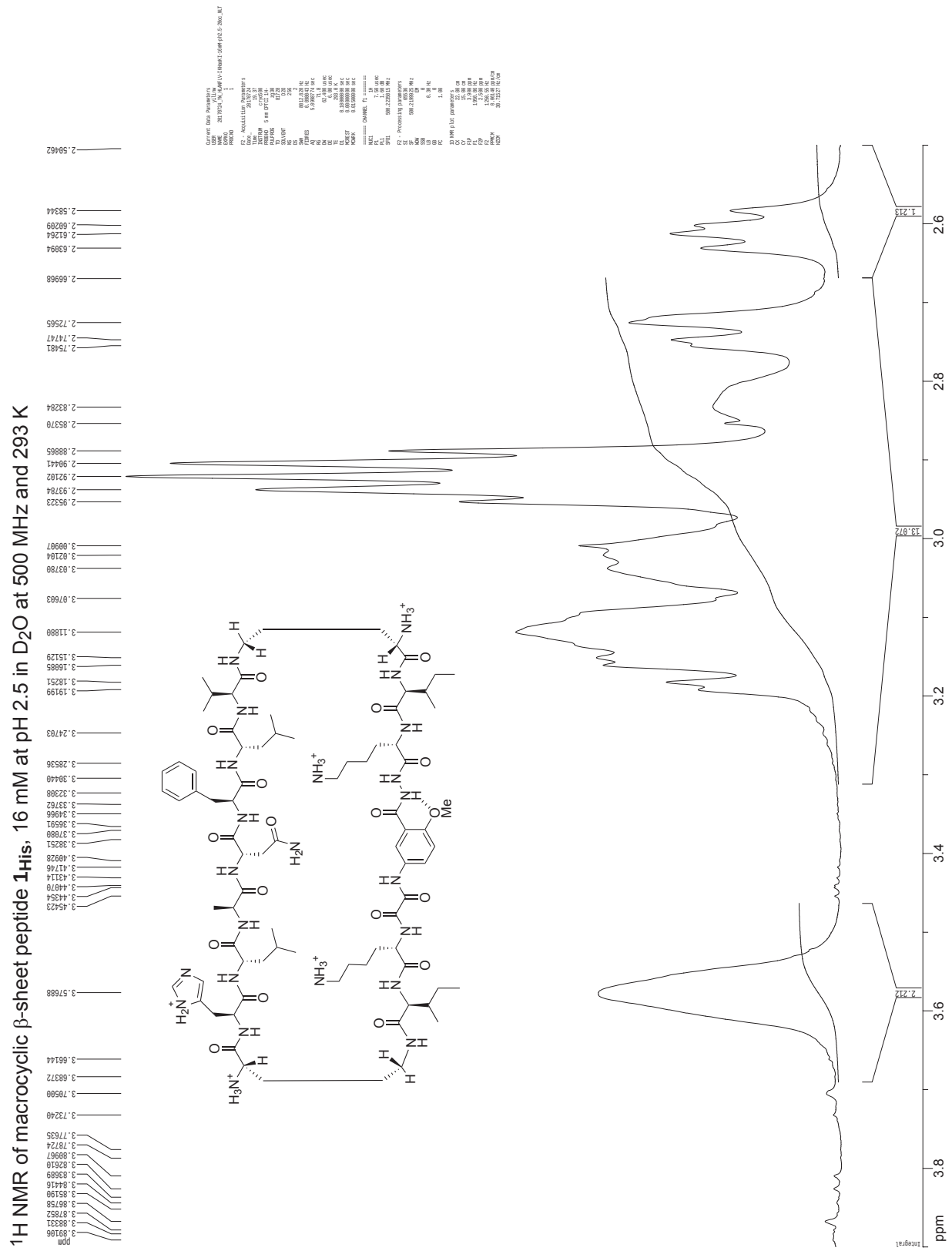
1H NMR of macrocyclic β-sheet peptide 1HisH, 16 mM at pH 2.5 in D2O at 500 MHz and 293 K
ppm
Integral
13.072
2.212
1.213

^{1}H NMR of macrocyclic β-sheet peptide **1$_{His}$**, 16 mM at pH 2.5 in D_2O at 500 MHz and 293 K

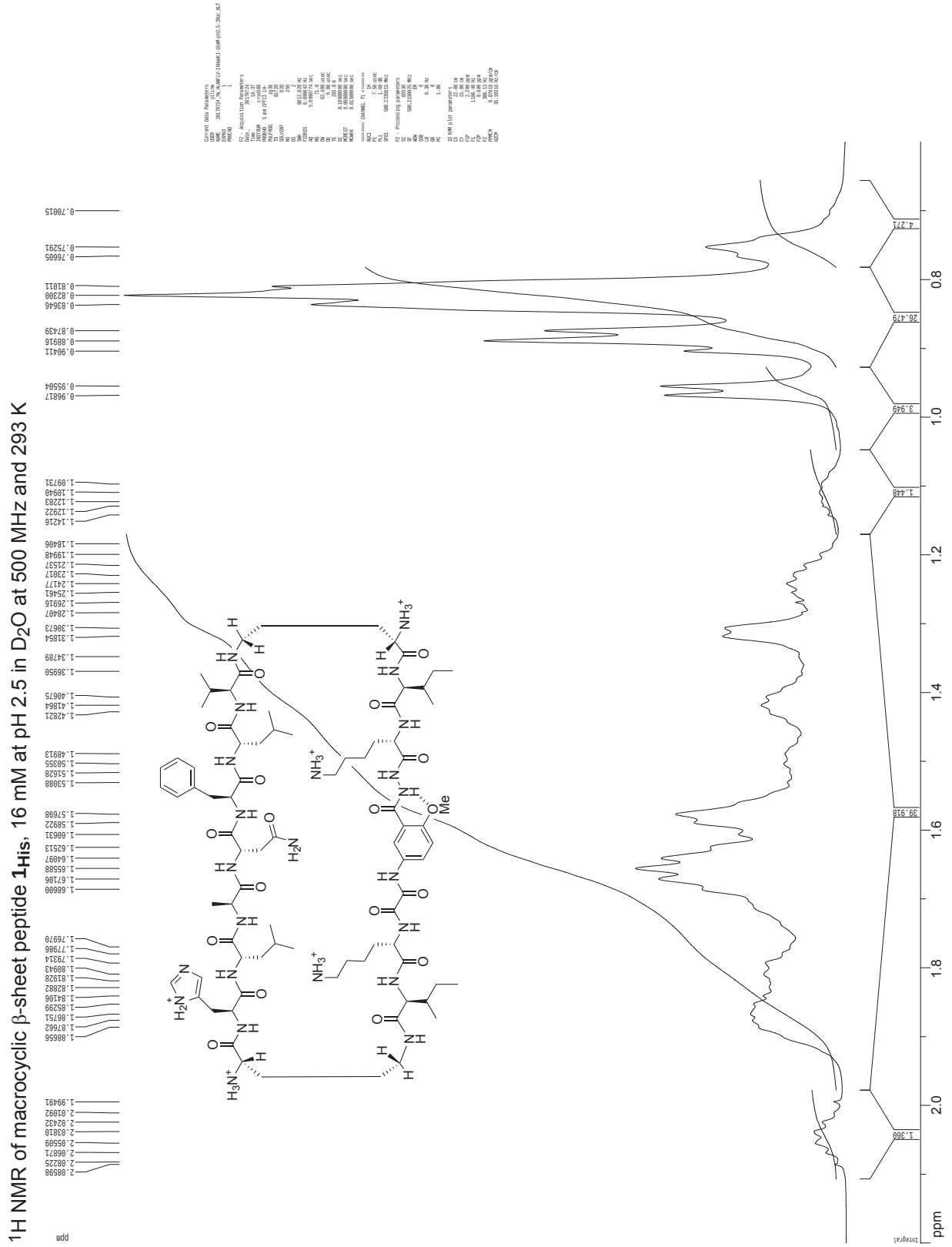

^{1}H NMR 2D TOCSY of macrocyclic β-sheet peptide **1$_{His}$** with 150-ms spin-lock mixing time
16 mM at pH 2.5 in D_2O at 500 MHz and 293 K

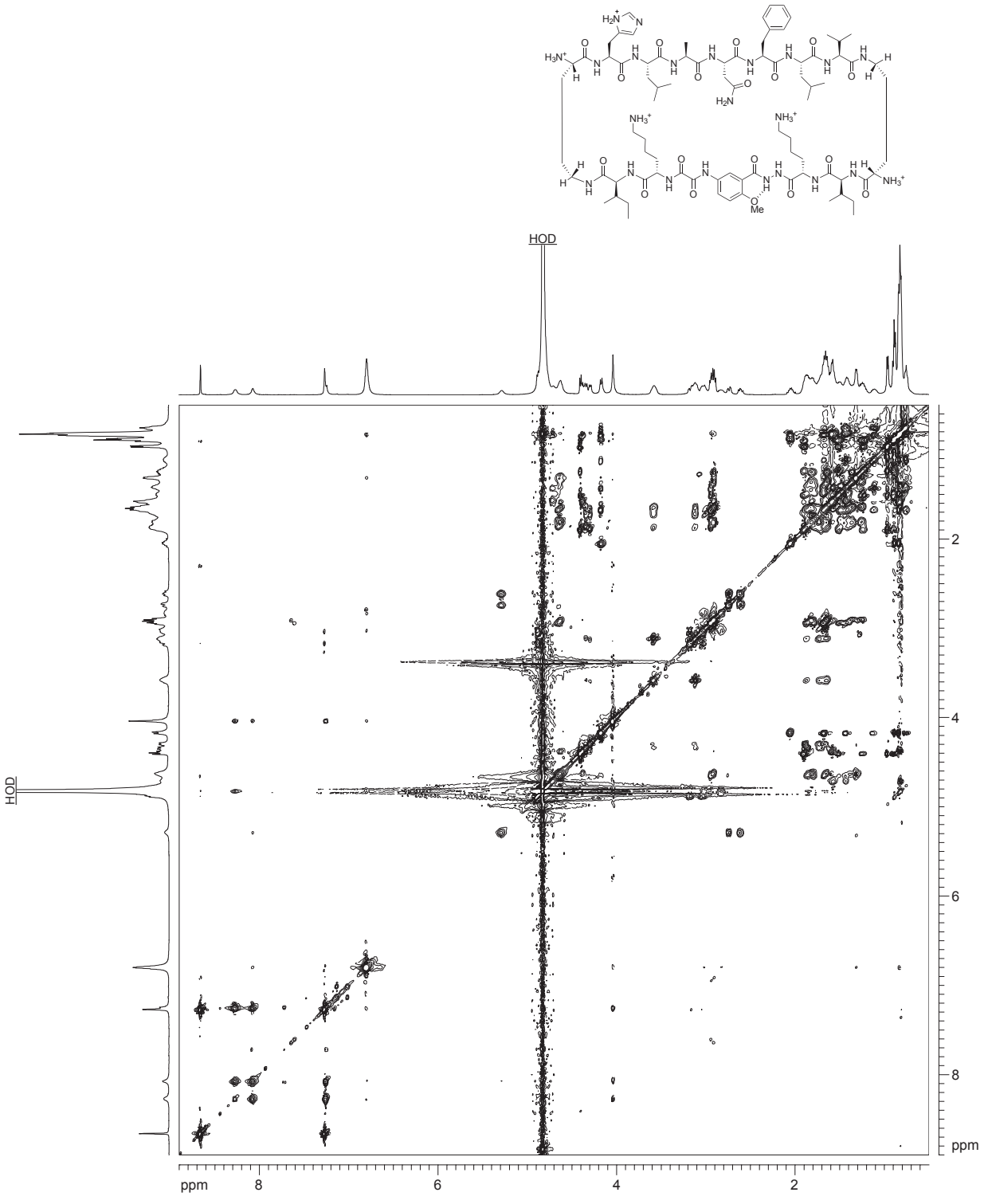

^{1}H NMR 2D TOCSY of macrocyclic β-sheet peptide **1$_{His}$** with 150-ms spin-lock mixing time
16 mM at pH 2.5 in D_2O at 500 MHz and 293 K

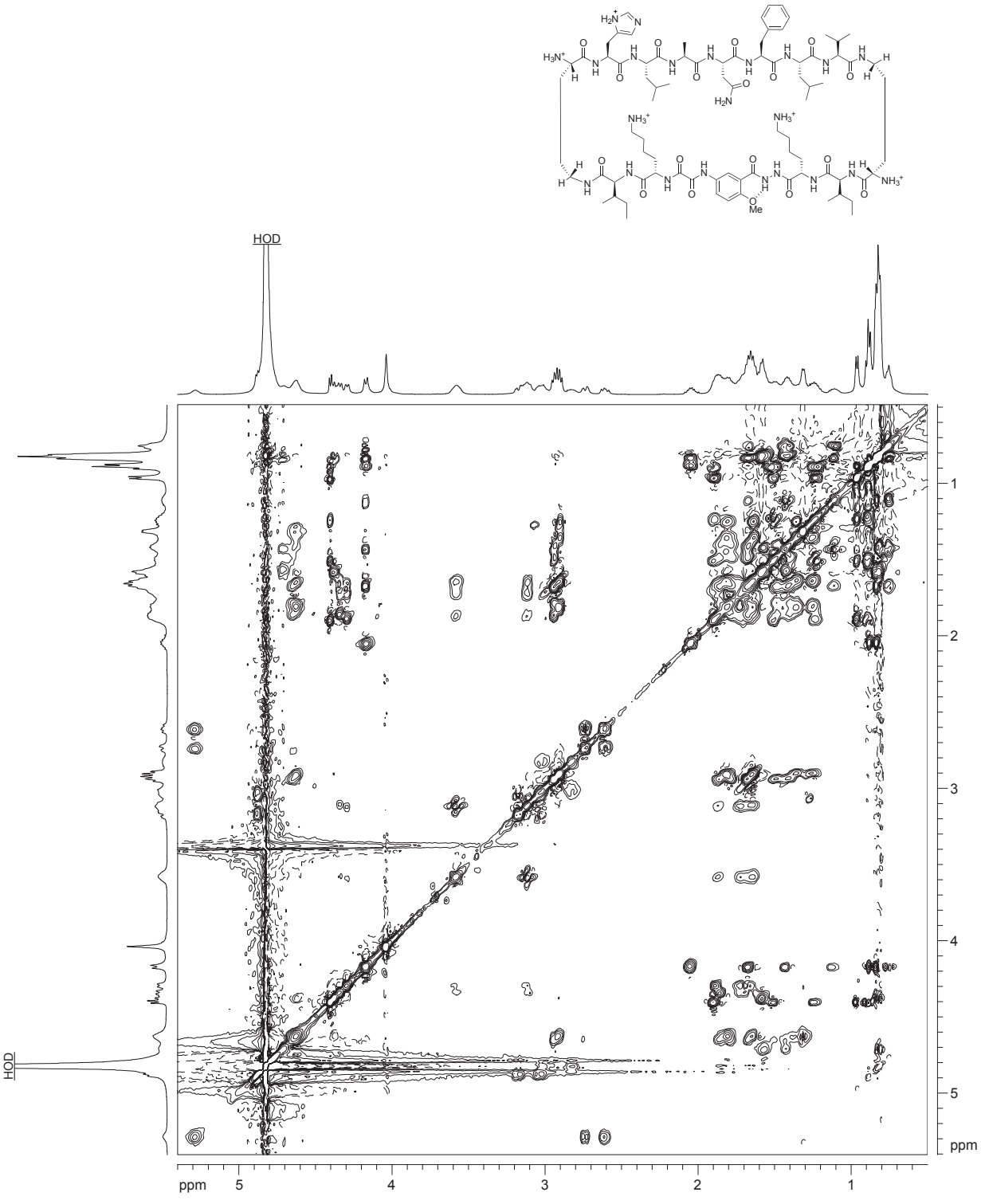

^{1}H NMR 2D NOESY of macrocyclic β-sheet peptide **1$_{His}$** with 150-ms mixing time
16 mM at pH 2.5 in D_2O at 500 MHz and 293 K

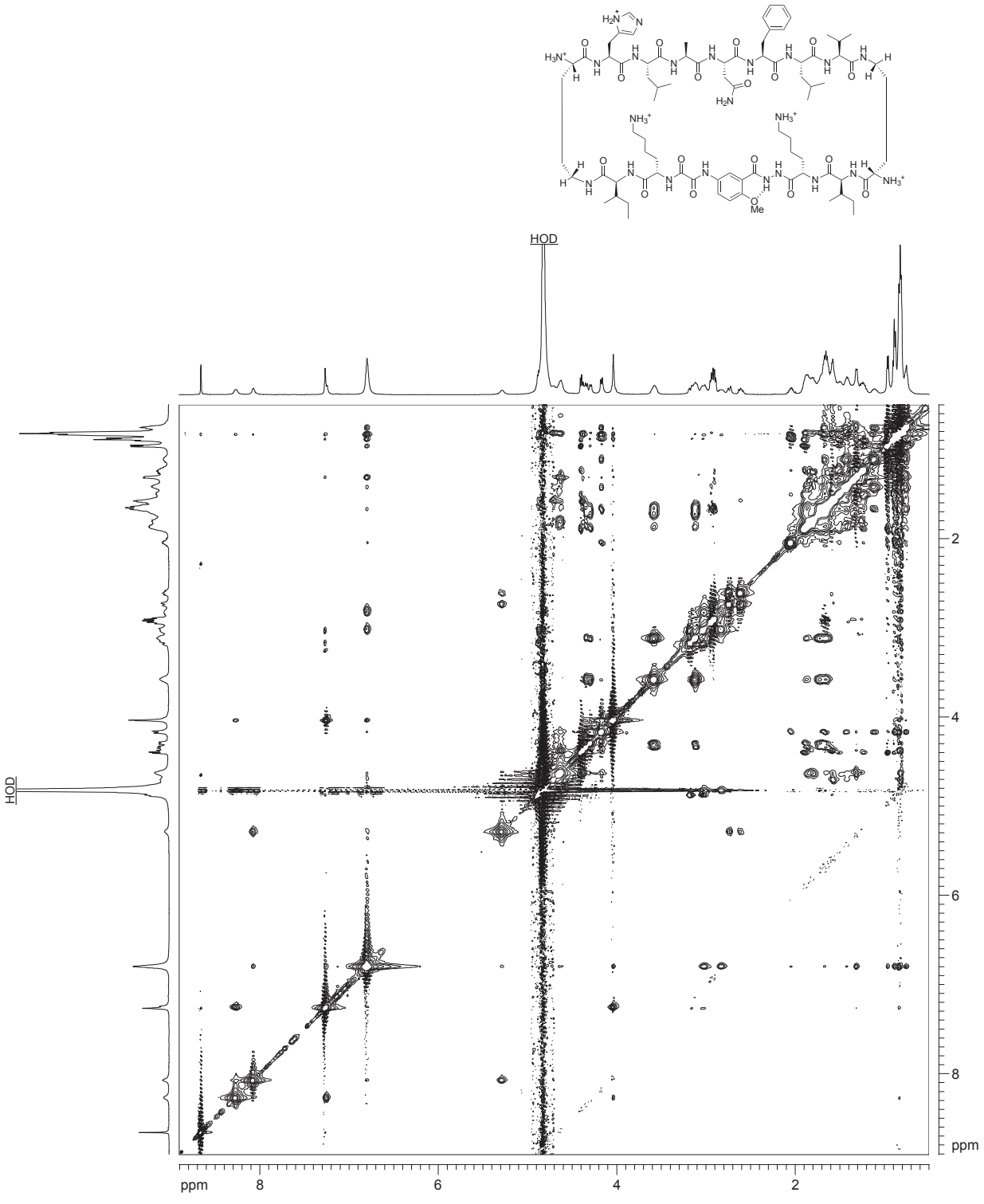

^{1}H NMR 2D NOESY of macrocyclic β-sheet peptide **1$_{His}$** with 150-ms mixing time
16 mM at pH 2.5 in D_2O at 500 MHz and 293 K

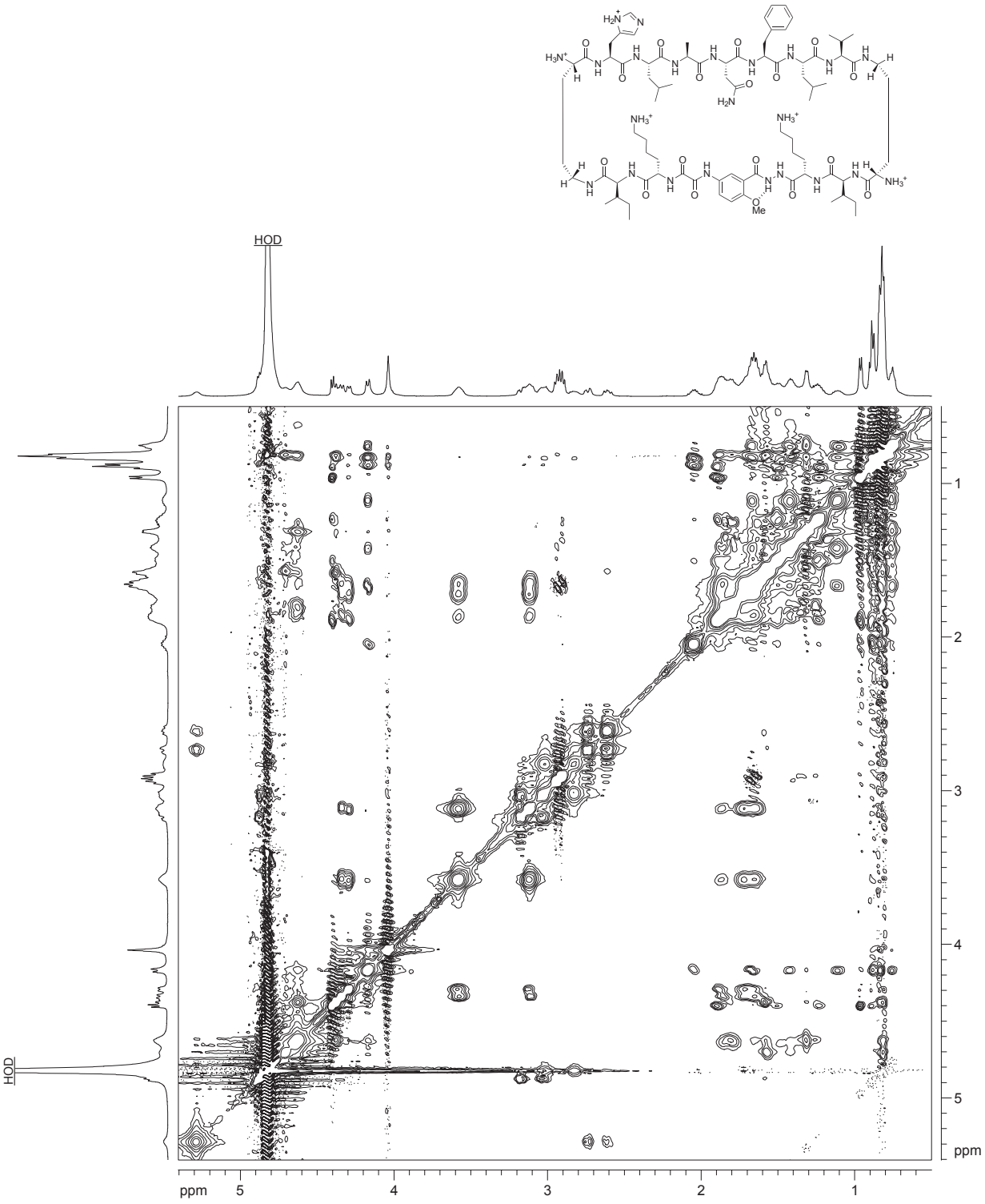

^{1}H NMR DOSY of macrocyclic β-sheet peptide **1$_{His}$** at 500 MHz and 298 K
1 mM at pH 2.5 in D_2O

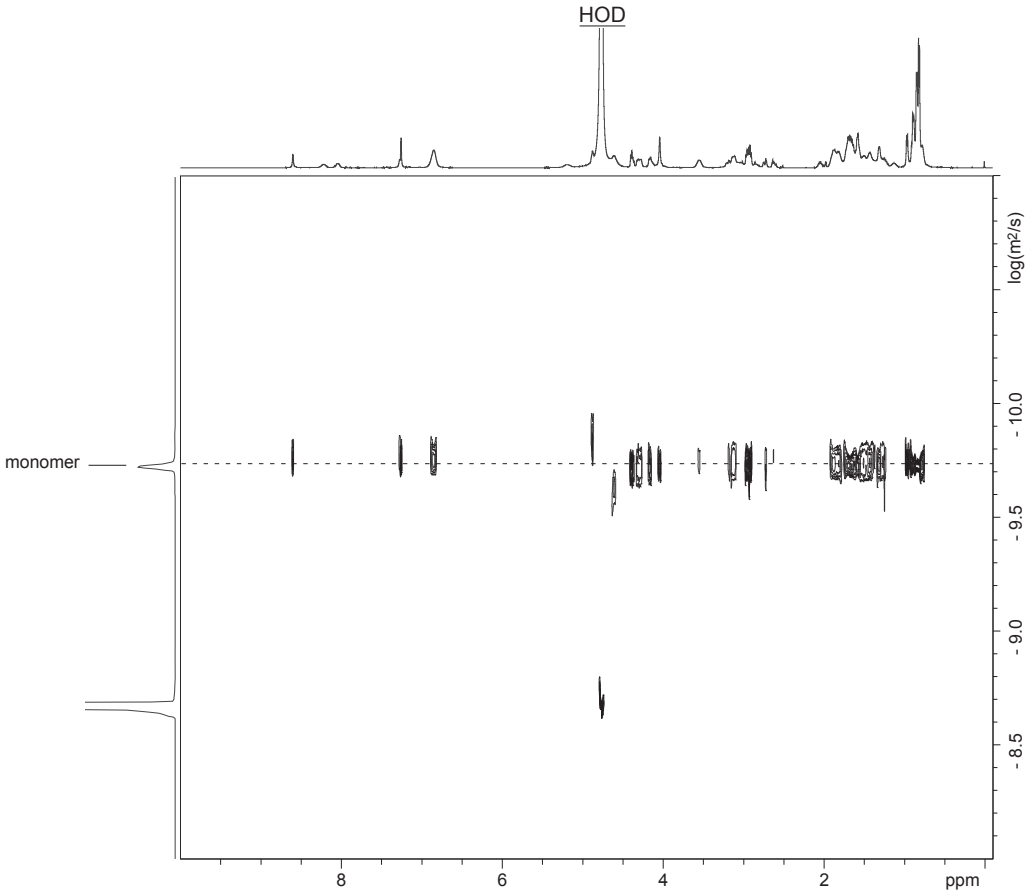

Calculations for macrocyclic β-sheet peptide **1$_{His}$** at 1 mM and pH 2.5

D_{HOD} = 19.0 x 10^{-10} m^2/s [a]
log (D_{HOD}) = -8.721

$D_{monomer}$: log(D) = -9.703; D = $10^{-9.703}$ = 19.8 ± 0.8 x 10^{-11} m^2/s

[a]Longsworth, L. G. *J. Phys. Chem.* **1960**, *64*, 1914−1917.

^{1}H NMR DOSY of macrocyclic β-sheet peptide **1$_{His}$** at 500 MHz and 298 K
4 mM at pH 2.5 in D_2O

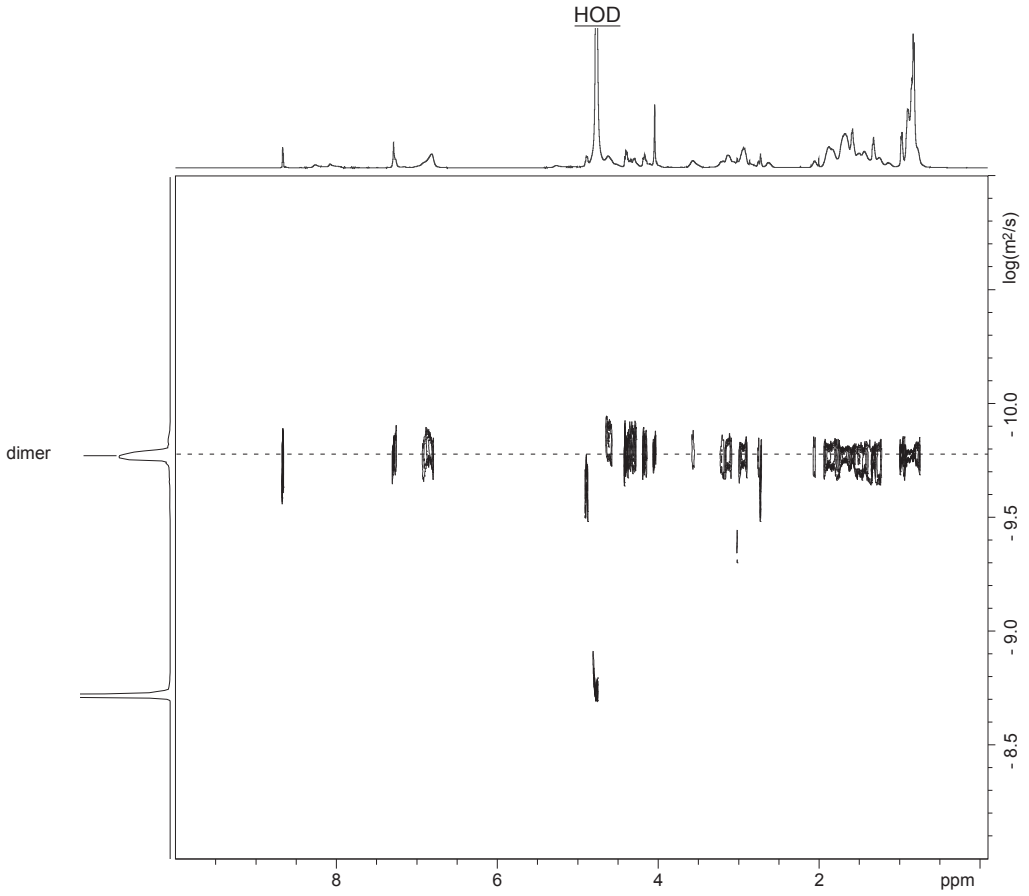

Calculations for macrocyclic β-sheet peptide **1$_{His}$** at 4 mM and pH 2.5

D_{HOD} = 19.0 x 10^{-10} m^2/s [a]
log (D_{HOD}) = -8.721

D_{dimer} : log(D) = -9.775; D = $10^{-9.775}$ = 16.8 ± 0.6 x 10^{-11} m^2/s

[a]Longsworth, L. G. *J. Phys. Chem.* **1960**, *64*, 1914−1917.

^{1}H NMR DOSY of macrocyclic β-sheet peptide **1$_{His}$** at 500 MHz and 298 K
8 mM at pH 2.5 in D_2O

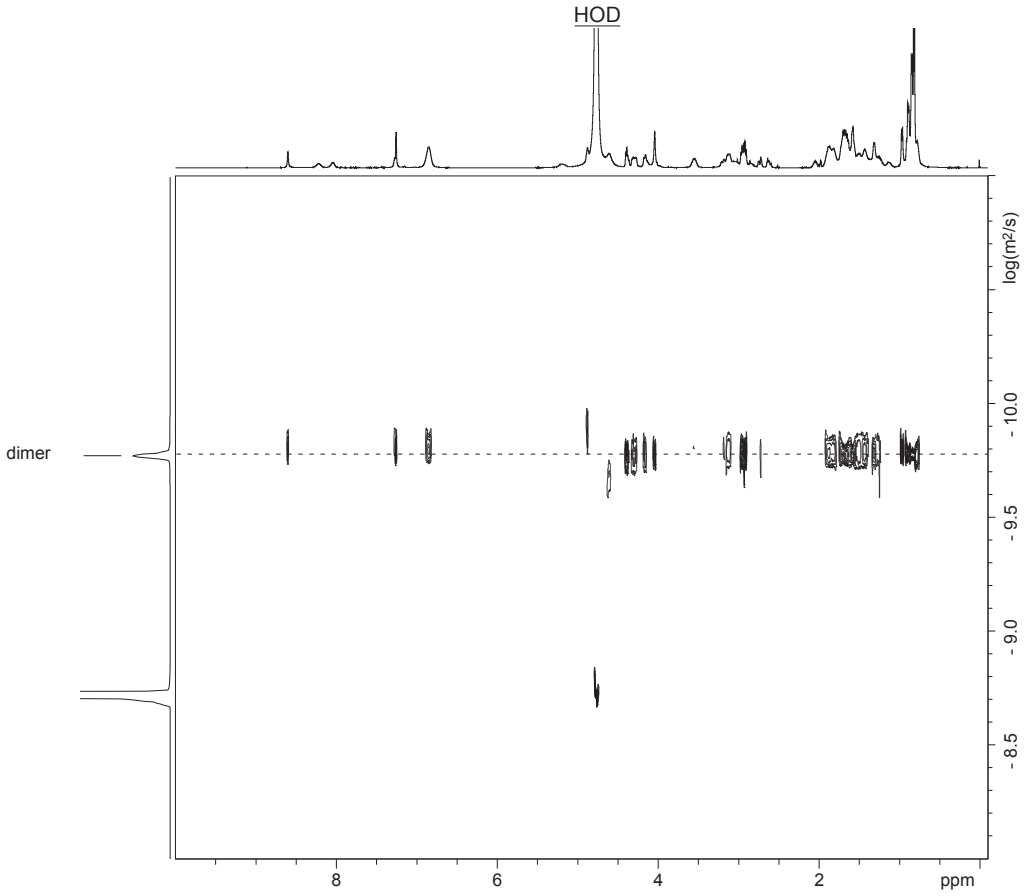

Calculations for macrocyclic β-sheet peptide **1$_{His}$** at 8 mM and pH 2.5

D_{HOD} = 19.0 x 10^{-10} m^2/s [a]
log (D_{HOD}) = -8.721

D_{dimer} : log(D) = -9.785; D = $10^{-9.785}$ = 16.4 ± 0.9 x 10^{-11} m^2/s

[a]Longsworth, L. G. *J. Phys. Chem.* **1960**, *64*, 1914−1917.

^{1}H NMR DOSY of macrocyclic β-sheet peptide **1$_{His}$** at 500 MHz and 298 K
16 mM at pH 2.5 in D_2O

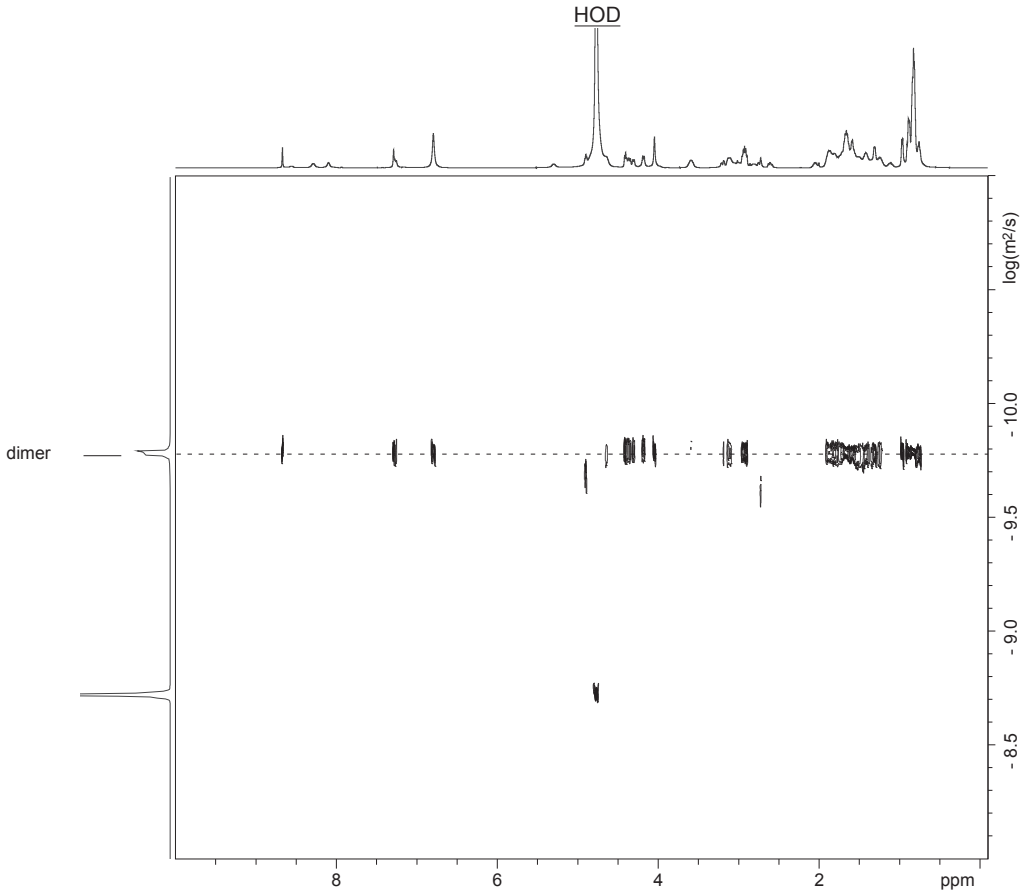

Calculations for macrocyclic β-sheet peptide **1$_{His}$** at 16 mM and pH 2.5

D_{HOD} = 19.0 x 10^{-10} m^2/s [a]
log (D_{HOD}) = -8.721

D_{dimer} : log(D) = -9.785; D = $10^{-9.785}$ = 16.4 ± 0.3 x 10^{-11} m^2/s

[a]Longsworth, L. G. *J. Phys. Chem.* **1960**, *64*, 1914−1917.

^{1}H NMR DOSY of macrocyclic β-sheet peptide **1$_{His}$** at 500 MHz and 298 K
16 mM at pH 4.7 in D_2O

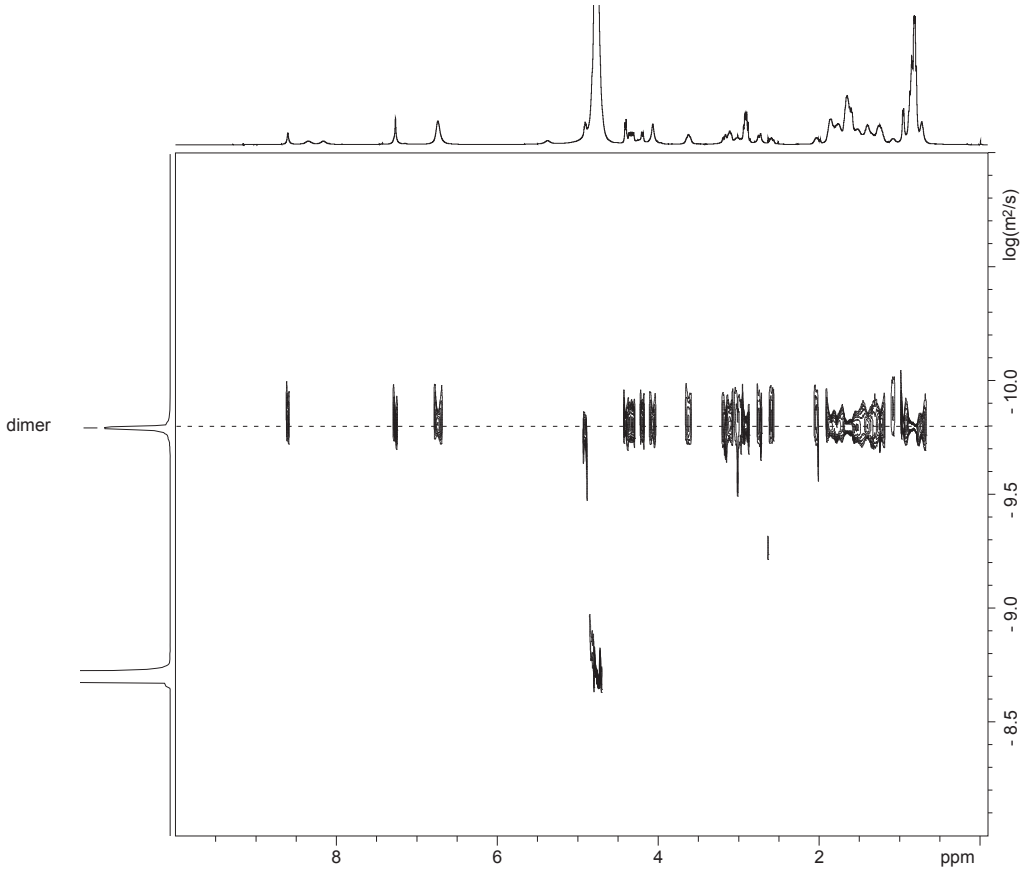

Calculations for macrocyclic β-sheet peptide **1$_{His}$** at 16 mM and pH 4.7

D_{HOD} = 19.0 x 10^{-10} m^2/s [a]
log (D_{HOD}) = -8.721

D_{dimer} : log(D) = -9.785; D = $10^{-9.785}$ = 16.4 ± 0.3 x 10^{-11} m^2/s

[a]Longsworth, L. G. *J. Phys. Chem.* **1960**, *64*, 1914−1917.

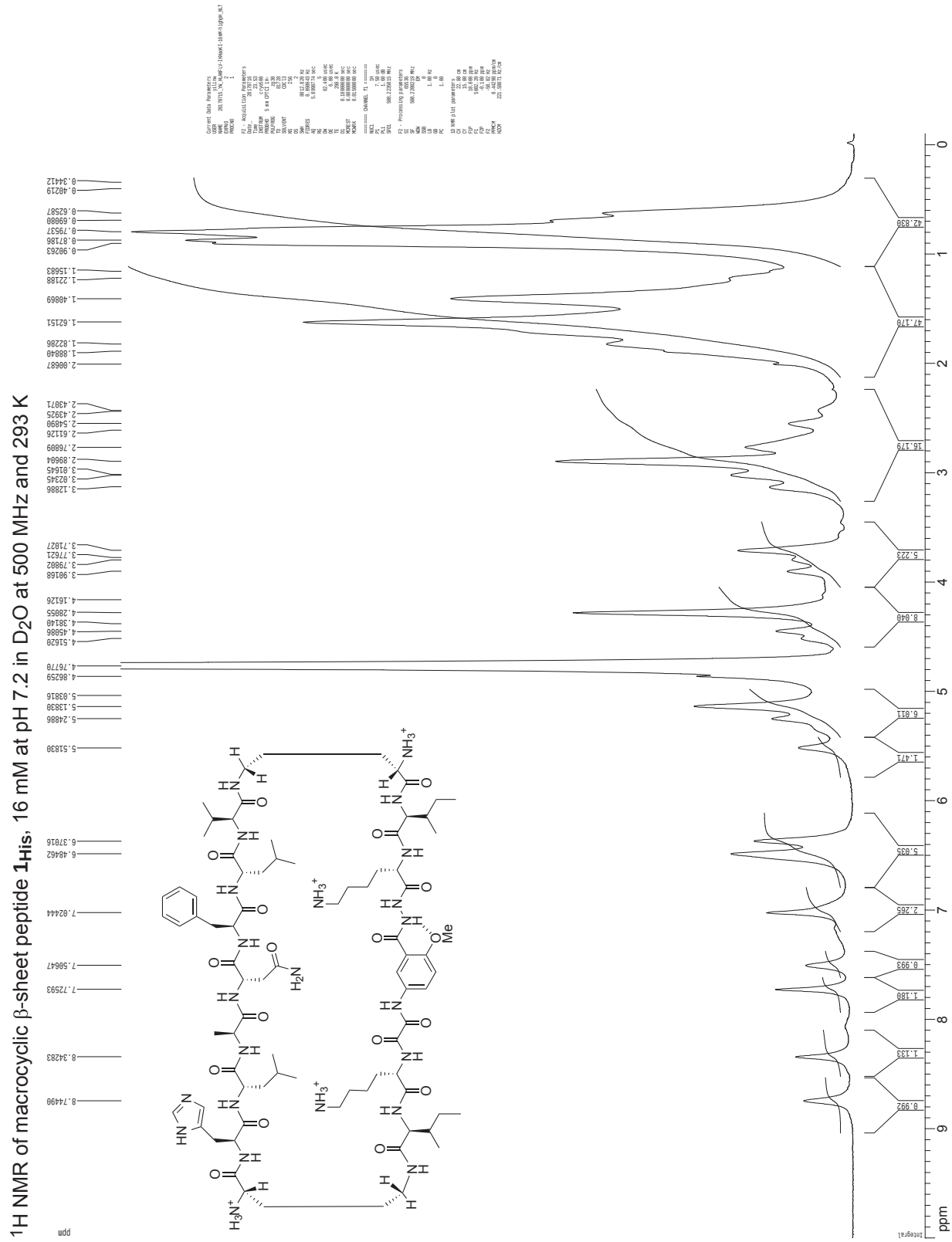
1H NMR of macrocyclic β-sheet peptide 1His, 16 mM at pH 7.2 in D2O at 500 MHz and 293 K
ppm
integral
NH3+
H2N
Me
HN

^{1}H NMR of macrocyclic β-sheet peptide $\mathbf{1_{His}}$, 16 mM at pH 7.2 in D_2O at 500 MHz and 293 K

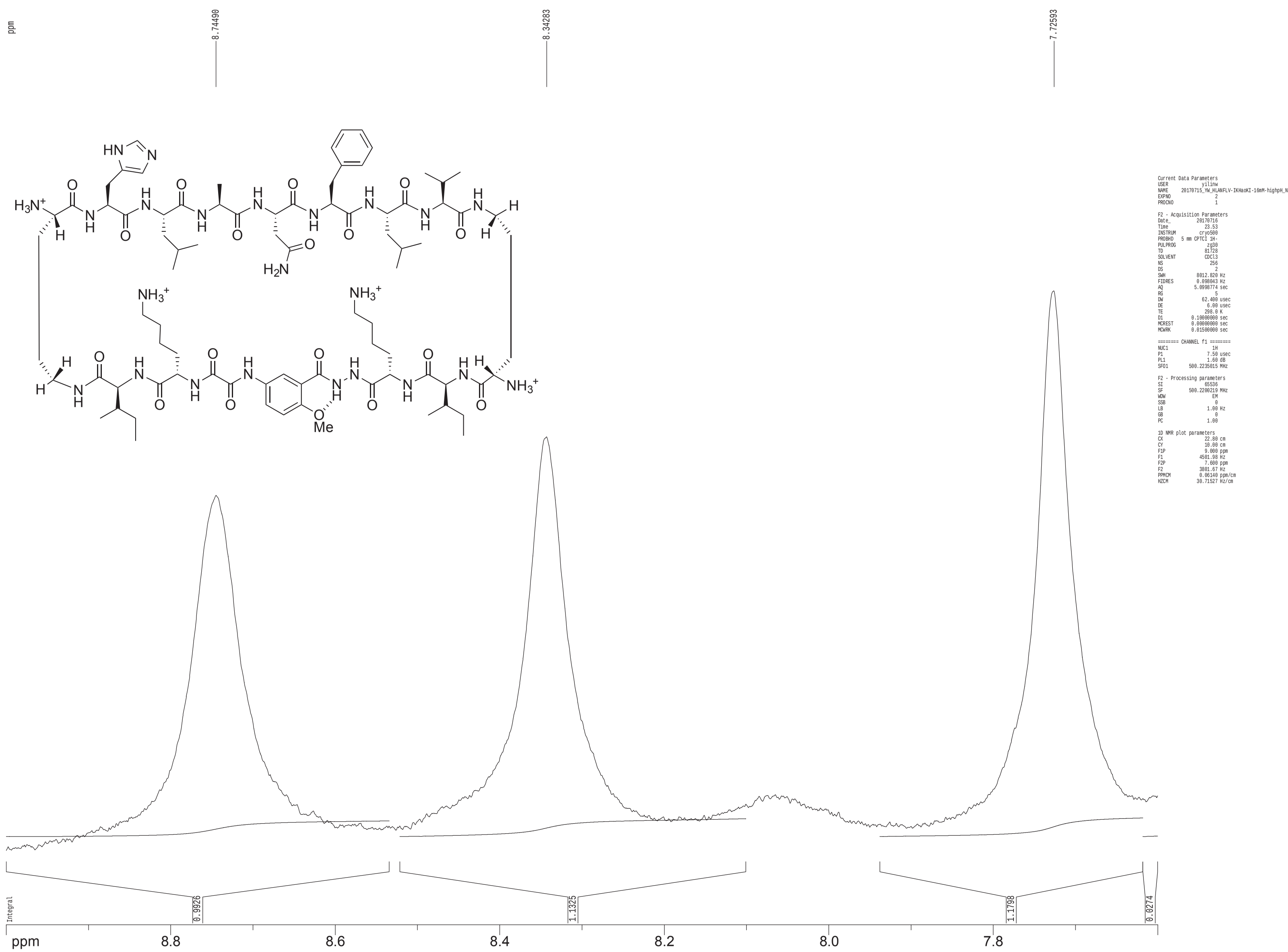

^{1}H NMR of macrocyclic β-sheet peptide **$\mathbf{1_{His}}$**, 16 mM at pH 7.2 in D_2O at 500 MHz and 293 K

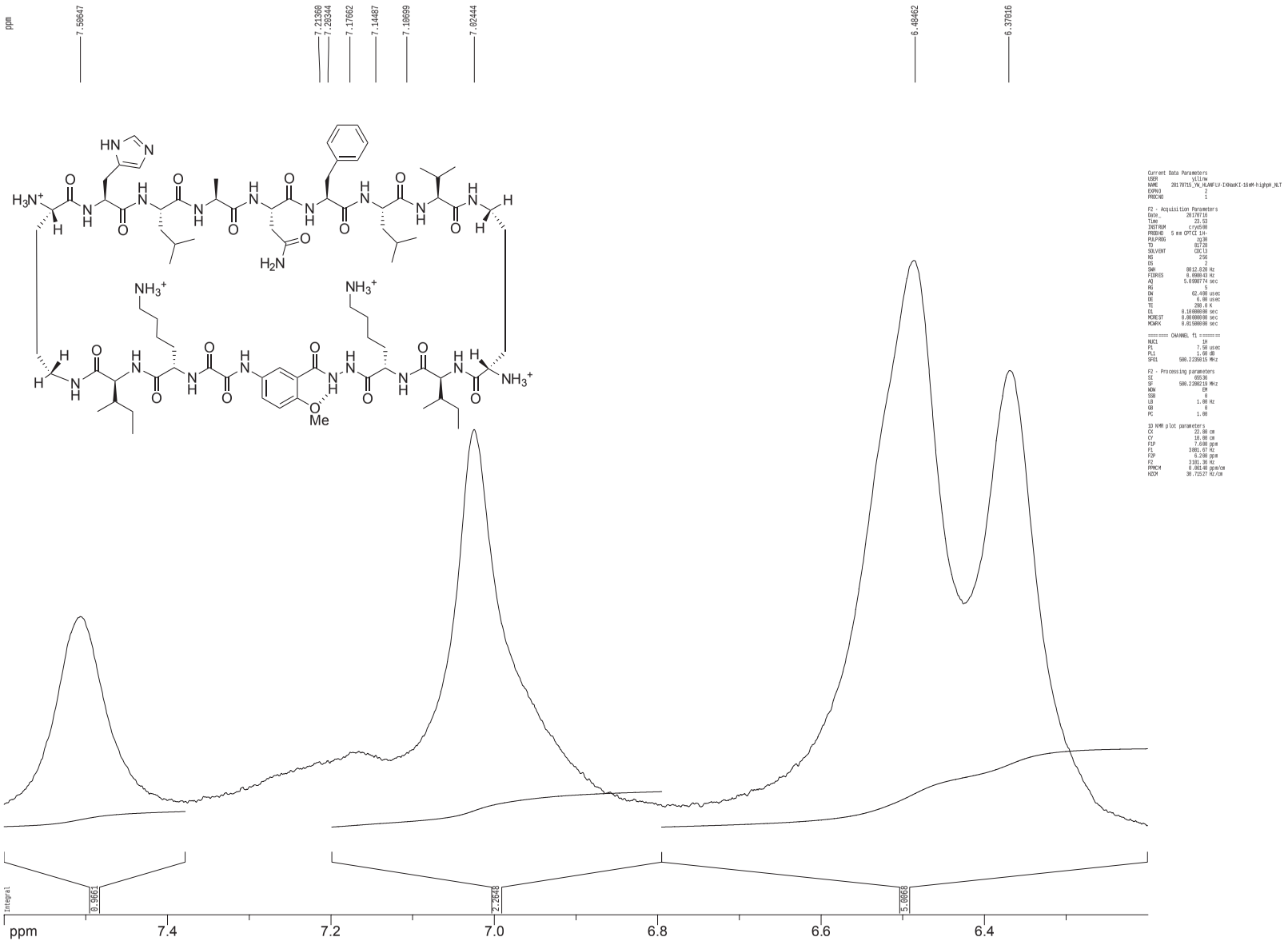

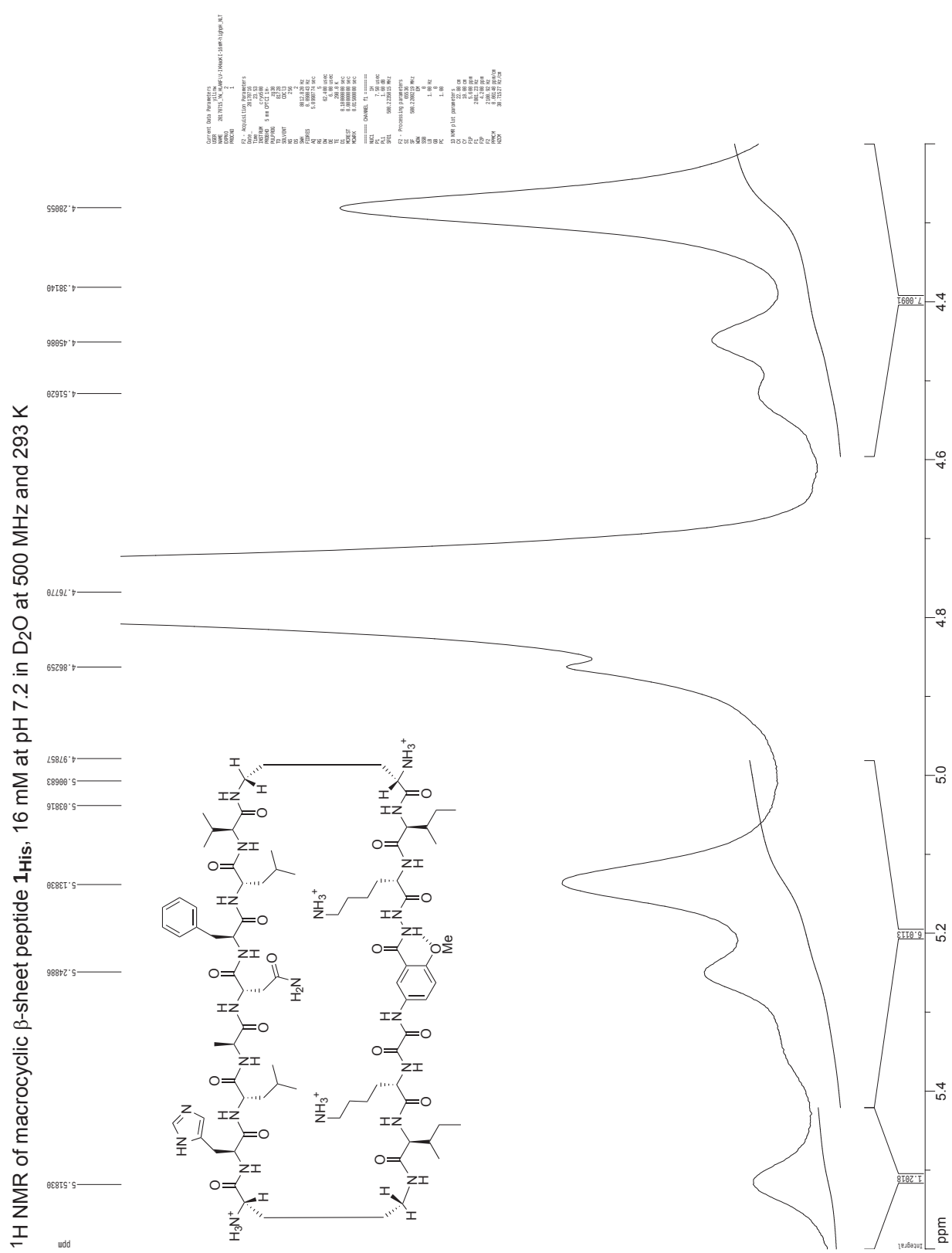
1H NMR of macrocyclic β-sheet peptide 1His, 16 mM at pH 7.2 in D2O at 500 MHz and 293 K
4.28055
4.38140
4.45086
4.51620
4.76770
4.86259
4.97857
5.00683
5.03816
5.13830
5.24886
5.51830
ppm
7.0091
6.0113
1.2018
Integral
4.4
4.6
4.8
5.0
5.2
5.4
ppm

^{1}H NMR of macrocyclic β-sheet peptide **$\mathbf{1_{His}}$**, 16 mM at pH 7.2 in D_2O at 500 MHz and 293 K

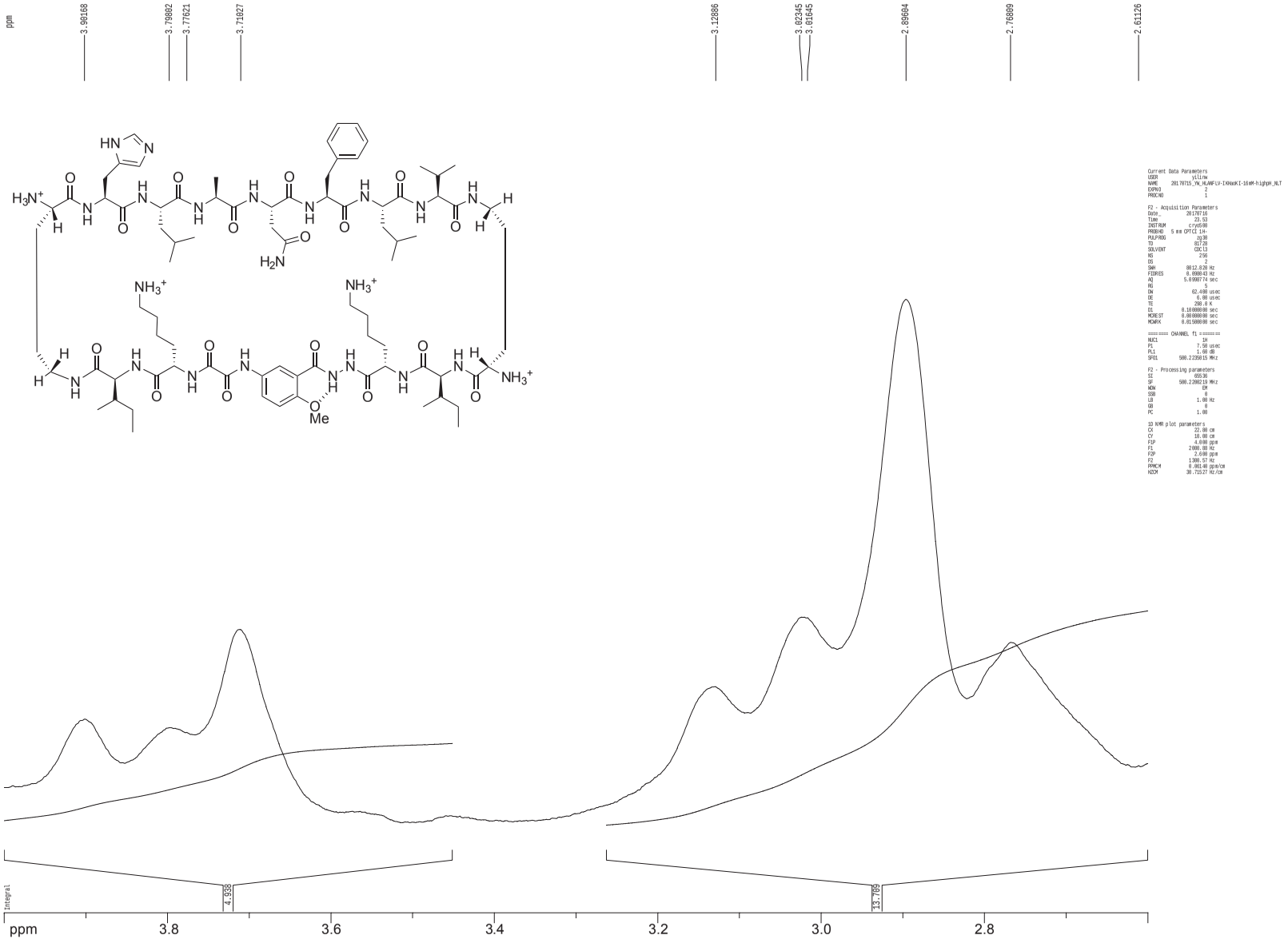

^{1}H NMR of macrocyclic β-sheet peptide **1$_{His}$**, 16 mM at pH 7.2 in D_2O at 500 MHz and 293 K

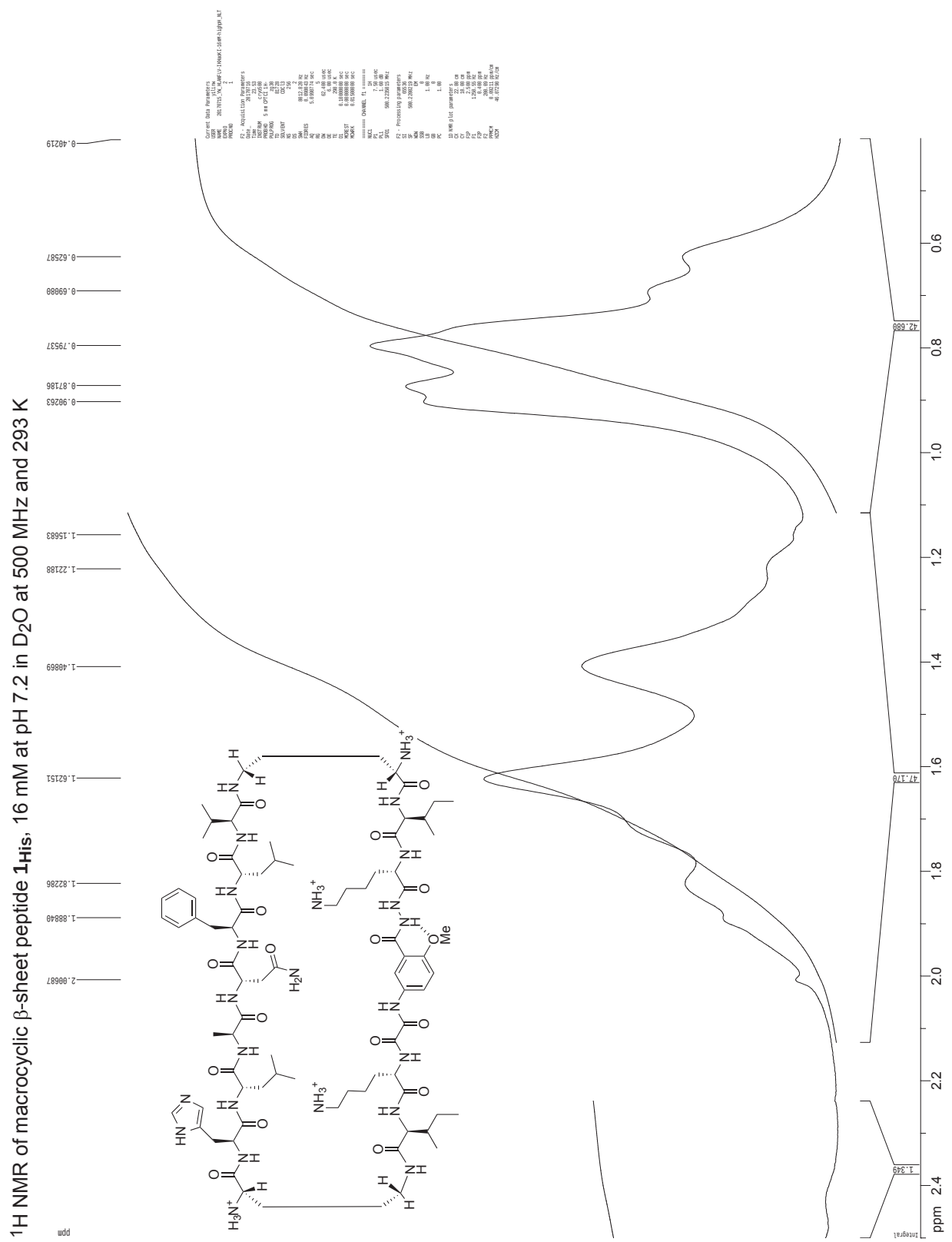

^{1}H NMR 2D TOCSY of macrocyclic β-sheet peptide **1$_{His}$** with 150-ms spin-lock mixing time
16 mM at pH 7.2 in D_2O at 500 MHz and 298 K

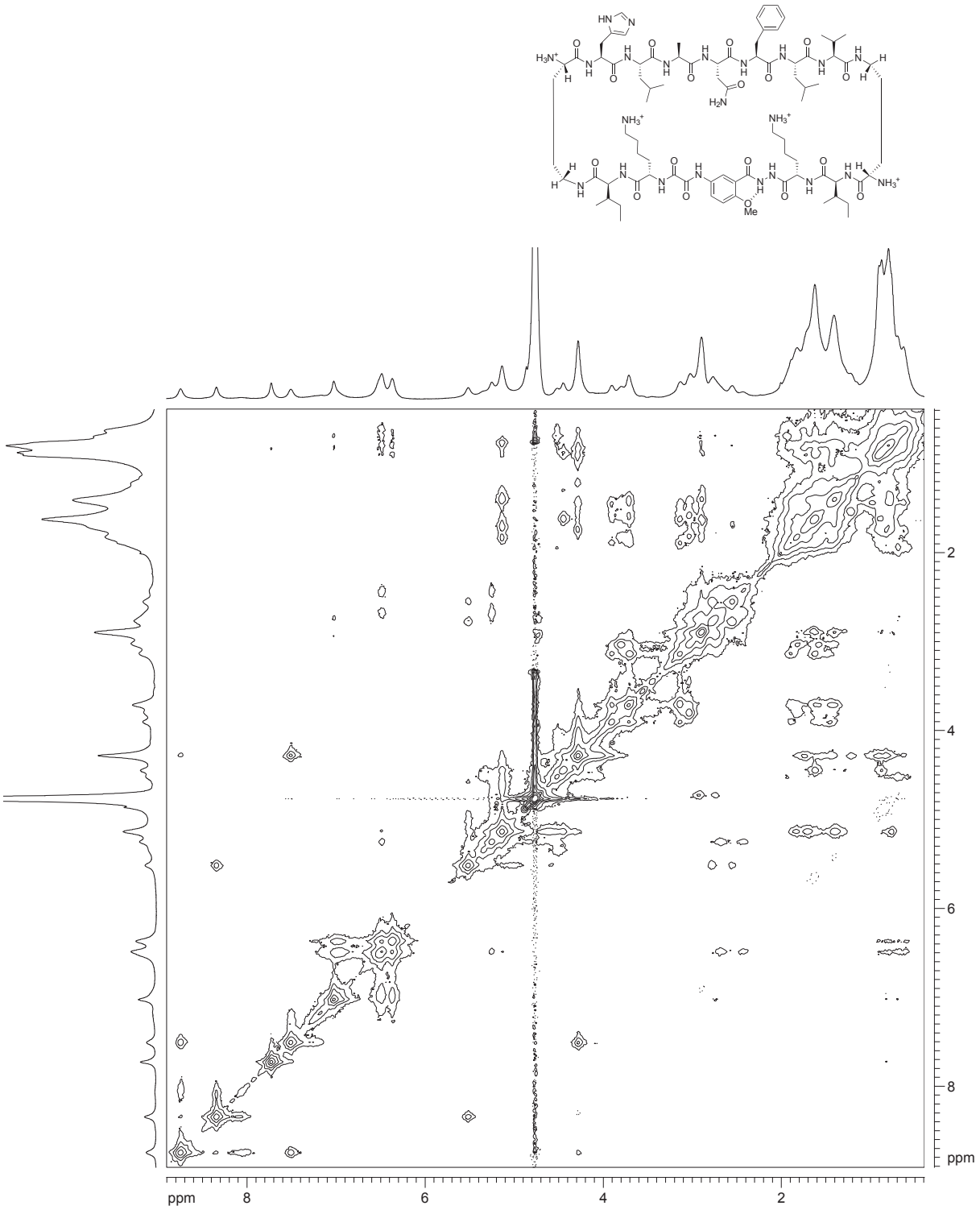

^{1}H NMR 2D TOCSY of macrocyclic β-sheet peptide **1_{His}** with 150-ms spin-lock mixing time
16 mM at pH 7.2 in D_2O at 500 MHz and 298 K

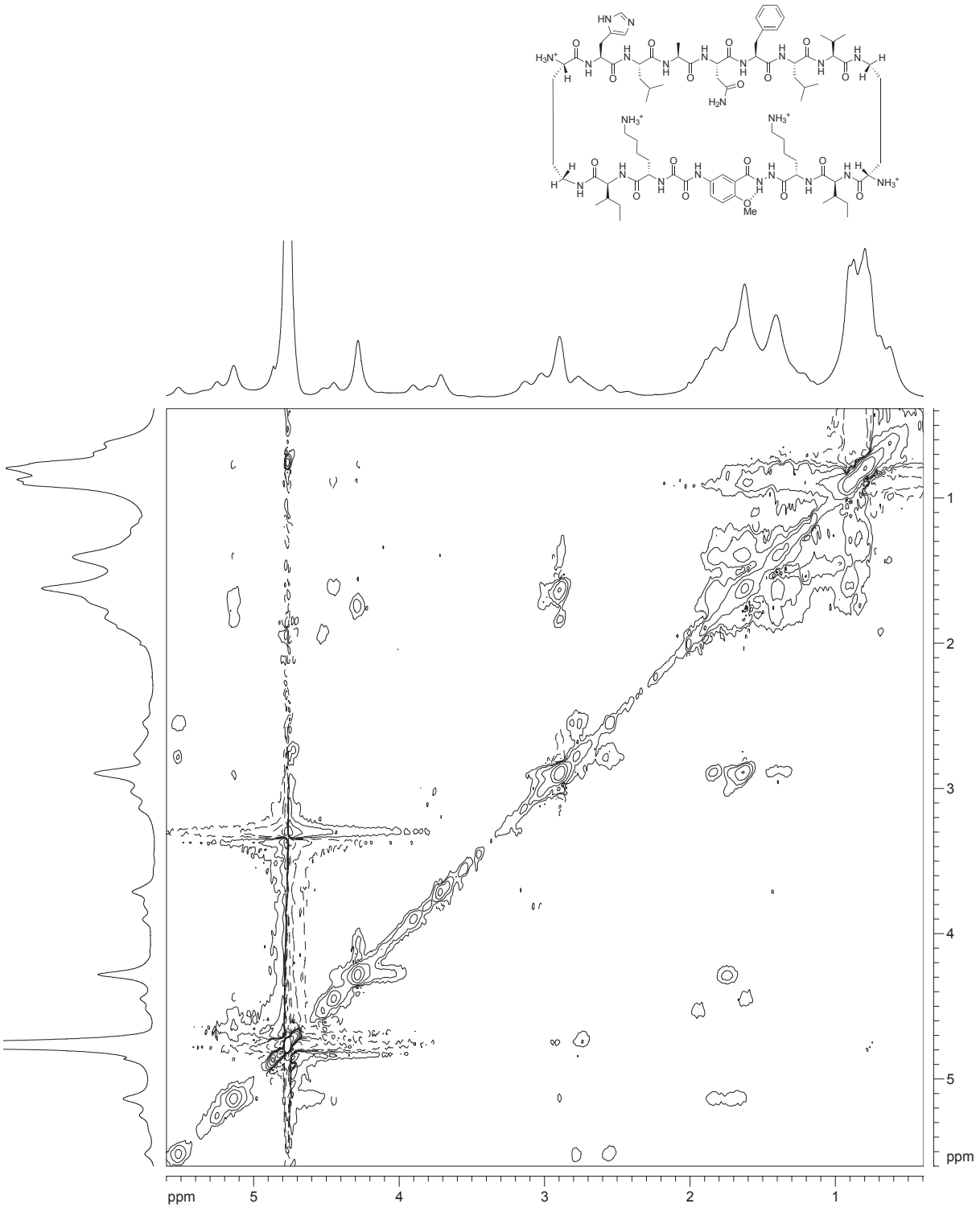

^{1}H NMR 2D NOESY of macrocyclic β-sheet peptide **1$_{His}$** with 150-ms mixing time
16 mM at pH 7.2 in D_2O at 500 MHz and 298 K

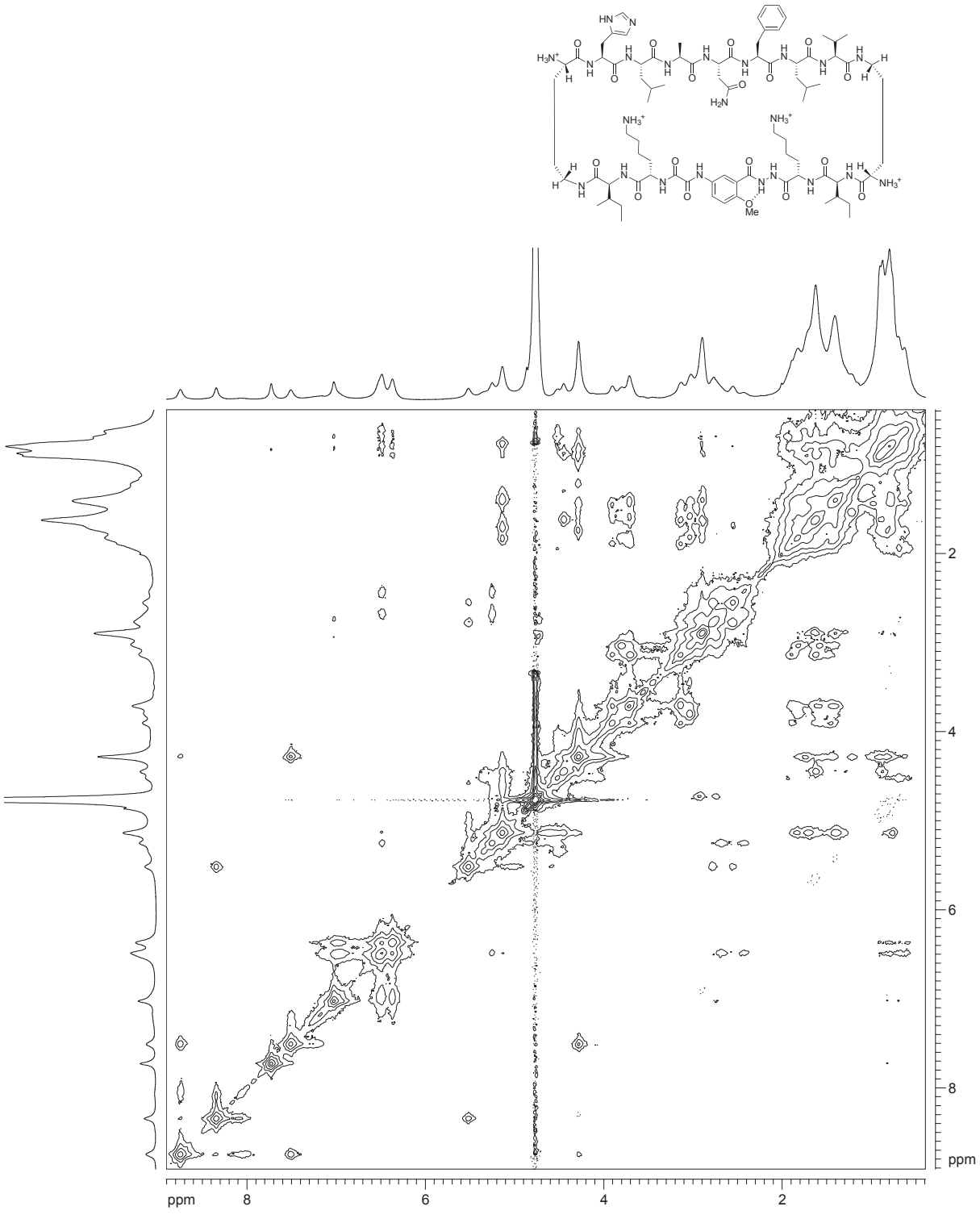

^{1}H NMR 2D NOESY of macrocyclic β-sheet peptide **1$_{His}$** with 150-ms mixing time
16 mM at pH 7.2 in D_2O at 500 MHz and 298 K

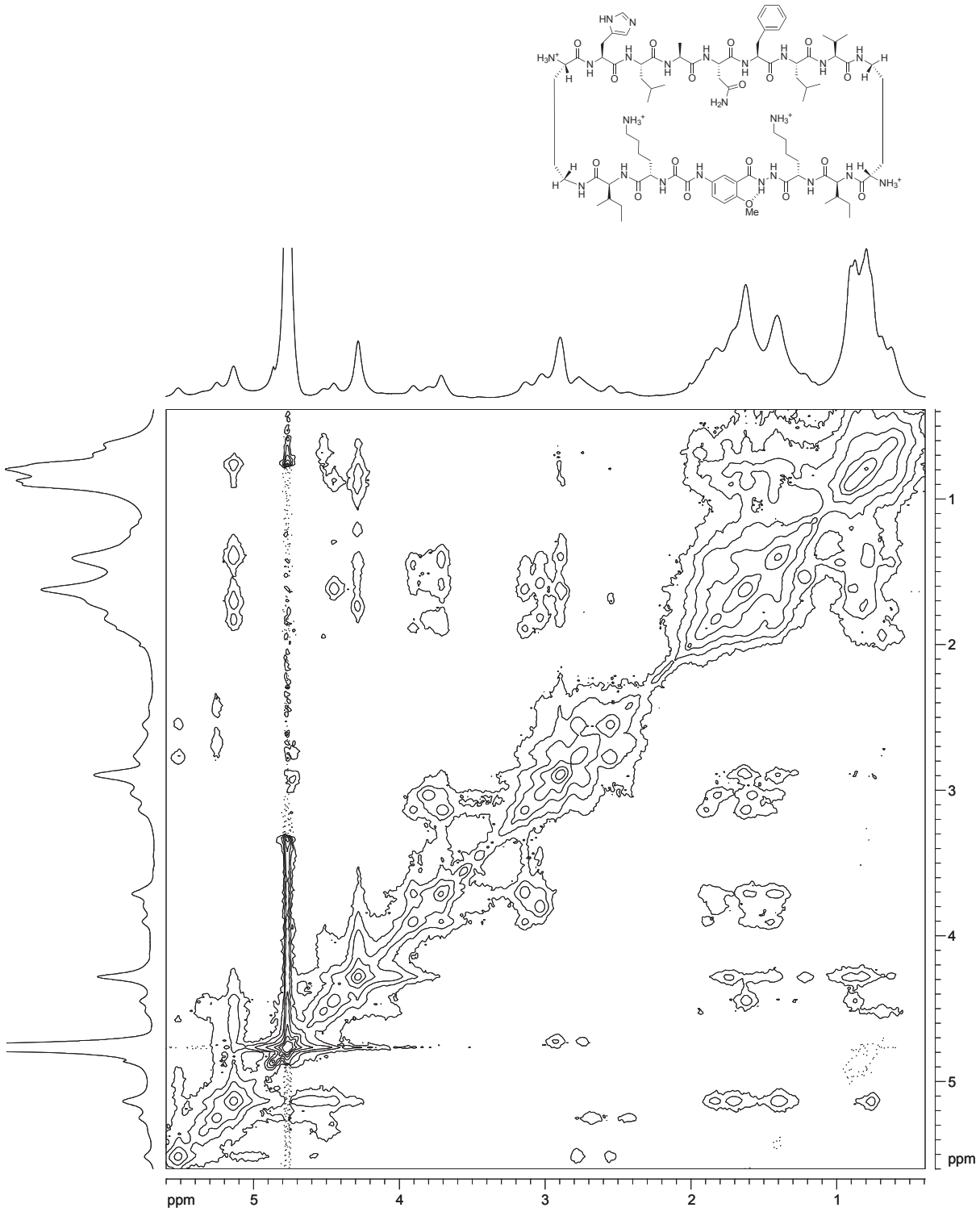

^{1}H NMR DOSY of macrocyclic β-sheet peptide **1$_{His}$** at 500 MHz and 298 K
16 mM at pH 7.2 in D_2O

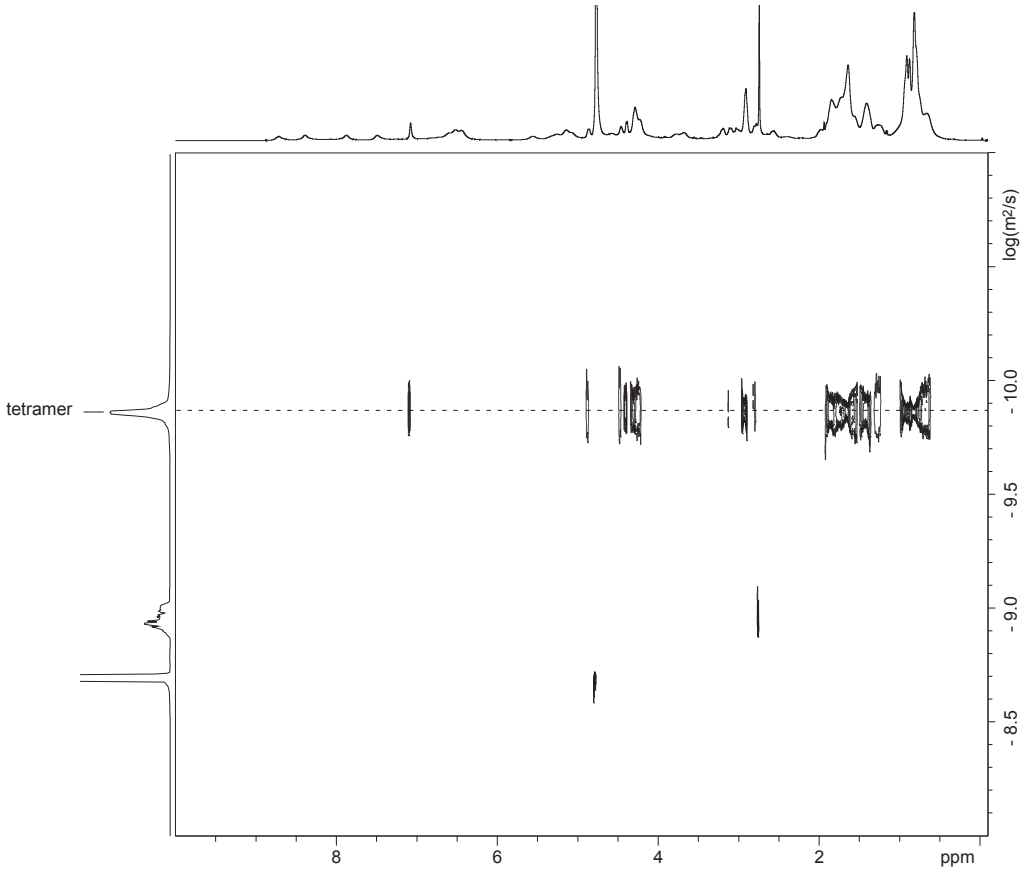

Calculations for macrocyclic β-sheet peptide **1$_{His}$** at 16 mM and pH 7.2

D_{HOD} = 19.0 x 10^{-10} m^2/s [a]
log (D_{HOD}) = -8.721

$D_{tetramer}$: log(D) = -9.910; D = $10^{-9.910}$ = 12.3 ± 1.2 x 10^{-11} m^2/s

[a]Longsworth, L. G. *J. Phys. Chem.* **1960**, *64*, 1914−1917.

Chapter 5

My Teaching Experiences

My transition from the Nowick lab to an instructor position was motivated by my desire to teach. I am excited at the prospect of engaging a diverse group of students in stimulating chemistry learning material, collaborating with colleagues, developing new effective curriculum, and improving and assessing student learning outcomes. I have always been excited about chemistry and I bring that energy into the classroom, encouraging students to discuss chemistry problems with each other as a dynamic way to develop their communication skills. As a recent Pedagogical Fellow (PF) undergoing advanced pedagogy training, I am eager to apply what I have learned to mentor my future students.

In the summer of 2016, I had the opportunity to instruct 30 students in an undergraduate course Chem 128, "Introduction to Chemical Biology." This position has given me valuable experience in lecturing and preparing course material. As a student, I always found that staying engaged is paramount to a better learning experience. Research shows that by incorporating active learning methods such as demonstration and questions, students reported fewer attention lapses.[1,2] To this end, I incorporated active learning techniques such as a modified *semi-flipped classroom* approach in my lectures.[2] Each class was set up such that a portion of the class was dedicated to lecturing and short 5-10 minute segments were set aside for students to tackle problems relevant to material covered. I adopted this approach as way for student self-assessment, so students have a chance to learn a concept and apply it to problem solving. This modified *semi-flipped classroom* approach helps students identify their knowledge gaps. During the lecture, I used formative assessment to track student learning and adjust the pacing of the class accordingly. Student evaluations showed that they liked the example problems as it helped them assess where they stood and what they needed to improve. My experience taught me that teaching is more than just communicating knowledge. Teaching, to me, is about inspiring

students to develop interest in the subject, which will in turn empower them to take ownership of their learning. In instructing Chem 128, I had the opportunity to teach a small group of students in an intimate setting.

Due to positive student evaluations from Chem 128, I was nominated to instruct an organic chemistry course with 370 students in the spring of 2017. I viewed this opportunity as a chance to incorporate and experiment with different teaching methods. One of the challenges of teaching such a big class is the perceived anonymity of the students, which can lead to lower class participation and student involvement.[3,4] This class also poses an added challenge of being an 8 AM class, which increases absenteeism and tardiness.[5,6] I discussed this with other PFs in my pedagogical program and tried to come up with various fun active learning activities that will work in a large lecture course and stimulate discussion amongst the students. For example, think-pair-share (TPS) is a collaborative learning strategy that can work with a class of any size. Students participate in TPS by (1) thinking individually about a topic or a question; and (2) sharing their ideas with classmates or the entire class. It is a great way for students to develop essential oral communication skills and build a learning community. Think-pair-share is also an efficient icebreaker for shy and quieter students to start speaking in class.

To complement the think-pair-share activities, I incorporated iClickers, a student response system that allows me to gauge student learning in the form of multiple-choice questions.[1,7-9] The questions are shown on the projector slide and the polling results are shown as bar graphs. The low-stake iClicker problems are purposefully spaced 10 to 15 minutes apart to refresh a student's attention span. Research shows that low-stake assignments effectively provide students with a realistic idea of their performance early on in the course and increase students' willingness to seek help.[10] When encountering iClicker problems where students are divided in

their solutions, I adopt TPS and have students discuss the question with their partners. The activity identifies misconceptions and gives every student a voice. Student evaluations showed that students found the iClicker problems useful in helping them understand the lecture material. In teaching this course, I learned the importance of incorporating effective active learning activities to increase motivation, engagement and community building.

Throughout my graduate career, I was a teaching assistant for over 10 chemistry lecture and laboratory courses. Similar to my experiences as an instructor, I strived to engage my students and have them engage with the material. In Spring 2013, I implemented collaborative learning activities in my organic chemistry discussion sections to foster an inclusive learning environment and increase student participation. I structured the discussion section such that the students began by working on a worksheet individually for a short period of time, 10-15 minutes, before they were divided into smaller groups of four or five students. The groups then had 25-30 minutes to discussed the worksheet before a student is selected at random to present a problem to the class. During this gap, I actively walked around the classroom to answer questions and address misconceptions. With small teams and a clear goal, I found that all students actively participated and even the shy, quieter students are not afraid to present problems to the class. This fostered a friendly and welcoming atmosphere, which further encouraged participation. I first learned about this technique through Professor David Van Vraken at UCI, who used it in his graduate course that I was enrolled in. In his course, the collaborative learning activities made students feel comfortable and included. I learned by example and direct experience that an inclusive environment will encourage students to interact with one another and even form study groups outside of class, building a strong sense of community.

In addition to active learning activities, I am also interested in incorporating technology in my classrooms. I have experience in using course management systems such as Canvas, which allows students to effectively navigate through course material and announcements. Another useful online tool I have experience with is Piazza, which is an online gathering space for students to ask questions and answer questions posted by other students. I look forward to learning about more technology tools in my pedagogy training.

Diversity arises from a wide range of experiences, backgrounds, and interests. In teaching a physical science subject such as Chemistry, socioeconomic status and language differences are diversity that needs to be addressed in the classroom. Unlike the social sciences subjects, topics of ethnicity, race, gender, sexual orientation, and religion are less likely to arise. Therefore, it is important to be compassionate and understanding when teaching. When teaching Chem 128, one of the students was unable to attend the final exam as she had recently been a victim of domestic abuse. It was an incredibly stressful time for her and I worked closely with the Campus Assault Resources and Education (CARE) counselors to minimize her trauma. We were able to schedule her exam at a much later time so that she is not disadvantaged because of her situation. If a student is performing adequately in class, I believe that it is important that the instructor is accommodating towards extenuating circumstances. With UCI being a minority-majority campus, half of my Chem 128 class was ESL and international students. When they were working on their final project of summarizing a research article, many struggled with comprehension. As I started learning English when I was six-years-old, I could relate to them and was able to offer useful advice on how to read a scientific article. As an instructor, I strive to maximize my students' learning potential by being empathetic and understanding.

As a recent PF, I have had the pleasure of working with like-minded individuals in the Pedagogical Fellows Program. The program provides an interdisciplinary community that provides professional and personal support. In one of the mandatory classes, University Studies 390A, PFs had the opportunity to discuss current and prominent literature in active learning, course design, inclusive teaching, assessment, instructional technology, and collaborative learning. The discussions were especially fruitful as PFs from different disciplines often had extremely different perspectives of the readings.

In conclusion, I am dedicated to providing a learning environment that is both engaging and supportive, one that empowers student learning. I implemented different active learning activities based on class sizes and assessed student learning outcomes by both formative and summative assessment. In the future, I hope to gain more experience as an instructor by teaching preparatory chemistry and general chemistry courses.

References

(1) Bunce, D. M.; Flens, E. A.; Neiles, K. Y. *J. Chem. Educ.* **2010**, *87*, 1438-1443.

(2) Hibbard, L.; Sung, S. N.; Wells, B. *J. Chem. Educ.* **2016**, *93*, 24-30.

(3) Exeter, D. J.; Ameratunga, S.; Ratima, M.; Morton, S.; Dickson, M.; Hsu, D.; Jackson, R. *Stud. High. Educ.* **2010**, *35*, 761-775.

(4) Mulryan-Kyne, C. *Teach. High. Educ.* **2010**, *15*, 175-185.

(5) Evans, M. D. R.; Kelley, P.; Kelley, J. *Front. Hum. Neurosci.* **2017**, *11*.

(6) Meltzer, L. J.; Shaheed, K.; Ambler, D. *Behav. Sleep Med.* **2016**, *14*, 140-154.

(7) Blasco-Arcas, L.; Buil, I.; Hernandez-Ortega, B.; Sese, F. J. *Comput. Educ.* **2013**, *62*, 102-110.

(8) Deslauriers, L.; Schelew, E.; Wieman, C. *Science* **2011**, *332*, 862-864.

(9) Caldwell, J. E. *CBE Life Sci. Educ.* **2007**, *6*, 9-20.

(10) Nicol, D. J.; Macfarlane-Dick, D. *Stud. High. Educ.* **2006**, *31*, 199-218.